Universidade de Aveiro Departamento de Geociências
2010

GIL MONTEIRO
JACINTO MACHADO

PALINOLOGIA E ESTRATIGRAFIA DO PZ SUPERIOR DA ZOM, NW E SW DE PORTUGAL

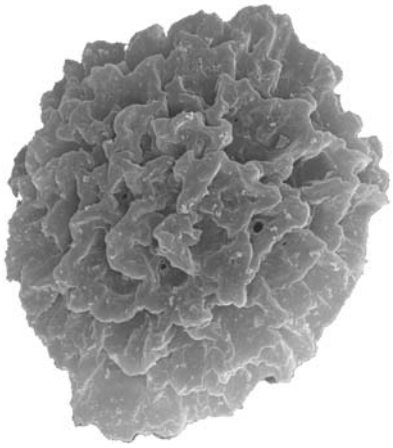

Universidade de Aveiro Departamento de Geociências
2010

GIL MONTEIRO JACINTO MACHADO

PALINOLOGIA E ESTRATIGRAFIA DO PZ SUPERIOR DA ZOM, NW E SW DE PORTUGAL

UPPER PALAEOZOIC STRATIGRAPHY AND PALYNOLOGY OF OMZ, NW AND SW PORTUGAL

Dissertação apresentada à Universidade de Aveiro para cumprimento dos requisitos necessários à obtenção do grau de Doutor em Geociências, realizada sob a orientação científica do Professor Doutor Fernando Joaquim Tavares Rocha, Professor Catedrático do Departamento de Geociências da Universidade de Aveiro e do Professor Doutor Paulo Emanuel Talhadas Ferreira da Fonseca, Professor Auxiliar com Agregação do Departamento de Geologia da Faculdade de Ciências da Universidade de Lisboa

Apoio financeiro da FCT (e FSE) no âmbito do POCI 2010 – Medida IV.3 e do QREN - POPH - Tipologia 4.1: SFRH / BD / 23787 / 2005

à Sara

o júri

presidente

Prof. Doutor Luís Filipe Pinheiro de Castro
Professor Catedrático da Universidade de Aveiro (Presidente do Júri)

Prof. Doutor Luís Carlos Gama Pereira
Professor Catedrático da Faculdade de Ciências e Tecnologia da Universidade de Coimbra

Prof. Doutora Deolinda Maria dos Santos Flores Marcelo da Fonseca
Professora Catedrática da Faculdade de Ciências da Universidade do Porto

Prof. Doutor Jorge Manuel Pessoa Girão Medina
Professor Auxiliar da Universidade de Aveiro

Doutora Zélia Pereira
Investigadora Auxiliar do Laboratório Nacional de Energia e Geologia

Prof. Doutor Geoff Clayton
Professor Associado do Trinity College de Dublin, Irlanda

Doutora Milada Vavrdová,
Investigadora Emérita do Instituto de Geologia da Academia de Ciências da Republica Checa

Prof. Doutor Fernando Joaquim Fernandes Tavares Rocha
Professor Catedrático da Universidade de Aveiro (orientador)

Prof. Doutor Paulo Emanuel Talhadas Ferreira da Fonseca
Professor Auxiliar com Agregação da Faculdade de Ciências da Universidade de Lisboa (co-orientador)

agradecimentos

A lista de agradecimentos é extensa, seja a pessoas, seja a instituições que me apoiaram durante o decorrer dos trabalhos. Considerando a estrutura modular desta tese, os agradecimentos relativos a partes ou capítulos da tese são feitos no fim de cada um desses capítulos. Deixo para esta secção os agradecimentos a apoios transversais ou de extrema importância.

Tive a sorte de integrar uma rede de investigadores já existente com um historial de colaboração em diversos aspectos da Geologia e em diversas áreas geográficas. Depois de me mostrar interessado em trabalhar em aspectos da Estratigrafia e Paleontologia ainda durante o curso de licenciatura, o Prof. Paulo Fonseca tornou esse interesse num projecto. Ele foi quem me apresentou a muitos dos investigadores que me apoiaram durante todo o tempo da tese. Ao Paulo agradeço o seu incansável apoio, paciência e discussão científica dos temas da tese, mesmo quando inundado em trabalho. Os seus vastos conhecimentos da Geologia de várias regiões de Portugal foram essenciais para o desenvolvimento da tese.

Ao Prof. Fernando Rocha, orientador principal, que na Universidade de Aveiro tornou possível a montagem de um laboratório de Palinologia funcional. A ele agradeço todas as portas que abriu, quer do ponto de vista científico quer da parte académica dentro da Universidade. Não obstante a sua função directiva na reitoria da Universidade durante grande parte da duração da tese, conseguiu, com a sua invejável capacidade de coordenação, gerir uma vasta equipa no seio de um centro de investigação, no qual me inseria.

Ao Prof. Hélder Chaminé por todo apoio dado, especialmente nas fases iniciais do projecto que me permitiram “entrar” de facto da área de estudo. O seu trabalho ao longo da zona de cisalhamento Porto-Tomar formaram a espinha dorsal sobre a qual o meu trabalho se desenvolveu.

Ao grupo de investigadores do Instituto de Geologia da Academia de Ciências da República Checa por todo o apoio desde o primeiro momento, em diversos campos da Geologia. As várias estadias em Praga foram extremamente enriquecedoras, pelo acolhimento logistico, científico e pessoal. Gostaria de destacar o apoio do Doutor Jindřich Hladil, Doutor Ladislav Slavik e a Doutora Leona Koptiková, que sempre, mesmo no meio de intenso trabalho, me apoiaram no decorrer dos trabalhos.

À Doutora Milada Vavrdová do mesmo Instituto que orientou o meu estágio antes do início do Doutoramento e continuou como orientadora no Doutoramento. A ela devo grande parte do conhecimento que hoje tenho de Palinologia do Paleozóico. Apesar da sua longa carreira e desejo de se dedicar aos membros mais novos da sua familia no descanso da casa de campo, adiou consecutivamente essa vontade (entre outras razões) para permitir a orientação desta tese.

À Prof. Deolinda Flores que em diversas situações me apoiou logistica e cientificamente na área da Petrologia Orgânica e me fez sentir benvindo no Departamento de Geologia da Faculdade de Ciências da Universidade do Porto.

Ao Prof. Geoff Clayton do Trinity College Dublin por ter sido quem, pela primeira vez, me falou em Palinologia e Petrologia Orgânica durante a estadia em Dublin ainda como aluno de licenciatura e ter continuado a dar apoio durante o decorrer da tese.

Ao Prof. Mário Cachão que foi um dos catalizadores do meu interesse em Estratigrafia desde tenra idade. No decorrer do Doutoramento sempre facilitou o uso do equipamento do Centro de Geologia da Universidade de Lisboa e com quem pude discutir temas relativos à tese.

Aos meus colegas do Departamento de Geociências da Universidade de Aveiro, com quem tive a oportunidade de partilhar experiências e conhecimento e permitiram fazer-me sentir em casa numa Universidade e cidade que não conhecia.

Aos meus colegas da Departamento de Geologia da Faculdade de Ciências da Universidade de Lisboa que fizeram das longas horas de trabalho uma experiência agradável pela sua boa disposição e amizade. Com eles beneficiei da troca de experiências e de conhecimento.

Vários colegas palinólogos com quem tive oportunidade de falar e discutir aspectos relevantes da Palinologia, quer durante congressos quer em visitas às suas instituições. De referir Rainer Brocke do Forschungsinstitut Senckenberg de Frankfurt; Olda Fatka da Universidade de Carlos, Praga; Jacques Verniers da Universidade de Gent; Maurice Streel da Universidade de Liège; José Pedro Fernandes do Departamento de Geologia, Faculdade de Ciências da Universidade do Porto; Thomas Servais da Universidade de Lille.

Aos meus pais pelo interesse e apoio que sempre demonstraram pela tese, apesar de muito distante das suas áreas de formação. O maior agradecimento é por terem feito de mim grande parte daquilo que sou hoje enquanto pessoa.
À Sara por todas as razões que são nossas, mas especialmente por ter tolerado a presença de um ermita em casa durante os meses que antecederam a entrega da tese.
Insititucionalmente devo agradecer em primeiro lugar à Fundação para a Ciência e a Tecnologia que proporcionou o apoio financeiro fundamental para a tese.
Ao Centro de Investigação Industriais e Argilas (MIA) agora incluido no GeoBioTec pelo apoio logístico e financeiro que proporcionou para grande parte do Doutoramento.
À Fundação Gulbenkian pela Bolsa de estágio de curta duração que permitiu a visita a vários laboratórios de Palinologia europeus durante 2006.
À Paleontological Association pelo apoio à participação em congresso durante 2008.
Ao Centro e Departamento de Geologia da Faculdade de Ciências da Universidade de Lisboa, ao Centro de Geologia da Faculdade de Ciências da Universidade do Porto, ao Instituto de Geologia da Academia de Ciências da República Checa e Departamento de Geologia do Trinity College Dublin pelo apoio logístico em diferentes fases do trabalho.

palavras-chave

Palinologia, Estratigrafia, Petrologia Orgânica, Carbónico, Devónico, esporos/pollen, acritarcas, Zona de Ossa-Morena, Zona de cisalhamento Porto-Tomar, Complexo Ígneo de Beja, Unidade de Albergaria-a-Velha, Bacia do Buçaco, Bacia de Santa Susana, Calcários de Odivelas, NW e SW de Portugal

resumo

Neste trabalho descreve-se e interpreta-se a estratigrafia e palinologia de rochas sedimentares e metassedimentos de idade devónica e carbónica aflorantes ao longo da zona de cisalhamento Porto-Tomar, a Sul na Bacia de Santa Susana e em vários locais onde afloram os Calcários de Odivelas.
Existe um registo de sedimentação descontínuo possivelmente associado a esta zona de cisalhamento desde o Devónico Superior até ao Pennsylvaniano. Desde o Devónico Superior até ao Mississippiano esta sedimentação é marinha, de carácter essencialmente turbiditico com uma tendência geral para se tornar mais proximal. A maturação térmica atingida por estas rochas (Unidade de Albergaria-a-Velha) é alta e a unidade é considerada pós-madura em termos de potencial gerador de hidrocarbonetos. O metamorfismo incipiente é acompanhado por intensa deformação.
A bacia do Buçaco é inteiramente terrestre e tem a sua idade restrita ao Gjeliano (Pennsylvaniano superior). O controlo da sedimentação pela actividade da zona de cisalhamento Porto-Tomar é evidente. A sua maturação térmica é relativamente baixa (dentro da catagénese) e a deformação menos intensa, contrastando com a Unidade de Albergaria-a-Velha com a qual parece ter uma relação geométrica complexa, de origem tectónica. As relações de campo e dados da maturação térmica permitem inferir um evento térmico e de deformação à escala regional entre o Serpukoviano e o Gjeliano e outro, essencialmente de deformação, entre o Gjeliano e o Carniano (Triássico Superior).
A bacia de Santa Susana tem características semelhantes à do Buçaco, visto estar enquadrada também numa zona de cisalhamento importante que neste caso separa a Zona de Ossa-Morena da Zona Sul Portuguesa. A sua idade é kasimoviana, possivelmente também moscoviana (Pennsylvaniano médio). A evolução térmica da bacia e a relação estrutural com as unidades circundantes permite inferir um evento térmico e de deformação regionalmente importante entre o Viseano e o (?)Moscoviano-Kasimoviano.
O estudo detalhado de vários locais onde afloram os Calcários de Odivelas permite desenhar uma paleogeografia regional durante o intervalo Emsiano terminal-Givetiano (fim do Devónico Inferior – Devónico Médio) para o sector Oeste da Zona de Ossa-Morena: Actividade vulcânica em regime marinho (e talvez subaéreo), formando edifícios vulcânicos no topo dos quais (e possivelmente também em altos fundos estruturais) se instalaram recifes, tendo a comunidade recifal, em termos de diversidade, persistido durante todo ou grande parte deste intervalo de tempo. O evento Choteč basal é observável num destes locais.

keywords

Palynology, Stratigraphy, Organic Petrology, Carboniferous, Devonian, spores/pollen, acritarchs, Ossa-Morena Zone, Porto-Tomar shear zone, Beja Igneous Complex, Albergaria-a-Velha Unit, Buçaco Basin, Santa Susana Basin, Odivelas Limestone, NW and SW Portugal

abstract

The Palynology and Stratigraphy of Devonian and Carboniferous sedimentary rocks and metasediments outcropping along the Porto-Tomar shear zone are described and interpreted. The Palynology and Stratigraphy of the Santa Susana Basin and of the Odivelas Limestone are also described and interpreted.

There is a discontinuous sedimentary record possibly associated with the Porto-Tomar shear zone extending from the Late Devonian to the Pennsylvanian. From the Late Devonian to the Mississippian, the sedimentation was marine, essentially turbiditic, with a general shallowing trend. The thermal maturation of these rocks (Albergaria-a-Velha Unit) is high, and the unit is considered to be post-mature in terms of hydrocarbon generation potential. The incipient metamorphism is accompanied by intense deformation.

The Buçaco basin is entirely terrestrial and its age is restricted to the Gzhelian (upper Pennsylvanian). The sedimentation is clearly controlled by the Porto-Tomar shear zone. Its thermal maturity is relatively low (within catagenesis range) and the deformation milder, contrasting with the Albergaria-a-Velha Unit. The contact between the two is tectonic. The field evidences and the thermal maturity data of the basin and surrounding units point to an important regional thermal and deformation event that took place between the Serpukovian and the Gzhelian and another, essentially tectonic, between the Gzhelian and the Carnian (Upper Triassic).

The Santa Susana basin has similarities with the Buçaco basin as it is also within an important shear zone, in this case separating the Ossa-Morena and South Portuguese Zones. Its age is kasimovian, and possibly moscovian (middle Pennsylvanian). The thermal evolution of the basin and the structural relations with the surrounding units point to a regional scale thermal and tectonic event occurring between the Viséan and the (?)Moscovian-Kasimovian.

The detailed study of several occurrences of the Odivelas Limestone allow an insight to the regional palaeogeography of the Western Ossa-Morena Zone during the latest Emsian – Givetian interval (latest lower Devonian – middle Devonian): marine (and possibly sub-aerial) volcanic activity forming volcanic buildings on top of which reef communities developed (and possibly on structural highs). The reef biota persisted, in terms of diversity, during all or most of this time interval. The basal Choteč event is recorded in one of these occurrences.

Index

Chapter 1 - Introduction

1.1 Purpose, scope and reasons for study 2
1.2 Geography and nature of outcrops 8
1.2.1 Espinho-Miranda do Corvo area 8
1.2.2 Odivelas reservoir, Santa Susana and surrounding areas. 9
1.3 General Geological setting 10
1.4 Abbreviations and notations 12
1.5 References 13

Chapter 2 - Procedure and Methods

2.1 Field work, stratigraphical procedure and general sampling methodology 19
2.2 Palynological procedure 19
2.2.1 Introduction 19
2.2.2 Sampling 20
2.2.3 Cleaning and crushing 20
2.2.4 Hydrochloric acid (HCl) 21
2.2.5 Hydrofluoric acid (HF) 21
Cold HF 22
Microwave 23
2.2.6 Second hydrochloric acid (HCl) attack 23
2.2.7 Centrifuging 24
2.2.8 Sieving 24
2.2.9 Watch Glass, pipetting, floating, specimen picking. 24
2.2.10 Oxidation 24
2.2.11 Acetolysis 25
2.2.12 Mounting 25
Mounting to observe with transmitted light 26
Mounting to observe with reflected light 26
2.2.13 Storage 26
2.2.14 Observation and documentation 27
Transmitted light 27
Reflected light 28
2.2.15 Image processing and plates 28
2.3 Palynofacies analysis 29
2.4 Conodont extraction procedure 30
2.4.1 Sampling 30
2.4.2 Cleaning and Crushing 30
2.4.3 Acetic acid dissolution 30
2.4.4 Sieving 30
2.4.5 Screening and picking 30
2.4.6 Observation and documentation 31

2.5 Clay mineralogy 31
2.5.1 Sampling 31
2.5.2 Crushing and mounting 31
2.5.3 Diffractometer 32
2.5.4 Diffractogram analysis 32
2.6 Organic Petrology 32
2.6.1 Sampling 32
2.6.2 Sample preparation 32
2.6.3 HF method 33
2.6.4 Heavy liquid separation 33
2.6.5 Mounting and polishing 33
2.6.6 Observation and measurement 34
2.7 Thin sections 34
2.7.1 Sampling 34
2.7.2 Sample preparation 34
2.7.3 Observation, measurements and documentation 35
2.8 Polished sections/surfaces 35
2.8.1 Sampling 35
2.8.2 Sample preparation 35
2.8.3 Observation and documentation 35
2.9 References 35
Personal Comunications 37

Chapter 3 - Palynology and Stratigraphy of the Upper Paleozoic metassedimentary basins along the Porto-Tomar major shear zone (Porto-Miranda do Corvo sector)

Abstract 40
3.1 Introduction 41
3.1.1 Geological setting 41
3.1.2 Factors controlling palynomorph preservation in metasediments and its application to the study of the AVU 43
3.1.2.1 Nature and characteristics of palynomorphs 43
3.1.2.2 Relevant Geological Variables 43
Sedimentation and diagenetic factors 43
Temperature and pressure 43
Compaction and Deformation 44
Fluid circulation and mineralization 45
3.2 Materials and methods 46
3.2.1 Stratigraphy 46
3.2.2 Provenance 46
3.2.3 Palynology and Palynofacies 48
3.2.4 Organic geochemistry and vitrinite reflectance 49

3.3 Results 50
3.3.1 Stratigraphy, Sedimentology and facies 50
3.3.2 Detrital framework analysis and provenance 54
3.3.3. Palynofacies 57
3.3.4 Palynology 59
3.3.4.1 Miospores 60
3.3.4.2 Organic-walled microplankton 62
3.3.5 Organic geochemistry, source rock potential and organic maturity 64
3.4 Discussion and Conclusions 67
3.5 Systematic Palynology 71
3.5.1 Miospores 71
3.5.2 Organic-walled microplankton 79
Acknowledgements 83
References 84
Plates 93

Chapter 4 - Stratigraphy, Palynology and clay mineralogy of the Pennsylvanian continental Buçaco Basin (NW Portugal)

Abstract 130
4.1 Local geological setting and structural outline 130
4.1.1 Previous work 131
4.1.2 Age of the basin 133
4.2 Materials and methods 133
4.3 Results 134
4.3.1 Description and definition of facies associations and formational units 134
4.3.2 Palaeocurrents and provenance of sediments 152
4.3.3 Organic Petrology and thermal history 153
4.3.4 Clay mineralogy analysis 155
4.3.5 Palynology 156
4.4 Discussion and conclusions 156
4.5 Systematic Palynology 162
Acknowledgements 172
References 172
Plates 177

Chapter 5 - Stratigraphy, Palynology and Palaeobotany of the Pennsylvanian continental Santa Susana Basin (SW Portugal)

Abstract 194
5.1 Introduction and Previous work 195
5.2 Methods and materials 197
5.3 Results 198
5.3.1 Lithostratigraphy 198
5.3.1.2 Santa Susana sections – SUS (Jongeis outlier) 200
Susana 5 200
Susana 6 200

5.3.1.3 Remeiras section - REM (Remeiras outlier) ... 202
5.3.1.3 Moinho da Ordem section - ORD (Vale de Figueira outlier) ... 202
5.3.1.4 Vale de Figueira Locality and sections - VFIG (Vale de Figueira outlier) ... 202
VFigueira 1 to 5 ... 204
VFigueira 6 ... 204
5.3.2 Geometry and architectural elements analysis ... 204
5.3.3 Palaeocurrents and provenance data ... 206
5.3.4 Clay fraction mineralogy ... 208
5.3.5 Palaeobotany ... 208
5.3.6 Palynology and age of the assemblages ... 211
VFigueira 1 to 5 sections ... 212
Susana 5 and 6 sections ... 213
5.3.7 Thermal and burial history ... 214
5.4 Discussion and Conclusions ... 216
5.5 Systematic Palynology ... 217
Acknowledgements ... 225
References ... 226
Plates ... 232
Plate 5.1 – Sporomorphs from the VFigueira 1 to 5 section ... 232

Chapter 6 - Lower and Middle Devonian Limestone units of Western Ossa-Morena Zone

Chapter Index

Abstract ... 250
6.1 Introduction ... 251
6.1.2 Upper Palaeozoic sedimentation in Ossa-Morena Zone ... 253
6.1.3 The Basal Choteč Event ... 254
6.2 Covas Ruivas Locality ... 255
6.2.1 Local Geological setting and previous work ... 255
6.2.2 Materials and Methods ... 256
6.2.2.1 Conodonts ... 256
6.2.2.2 Reef fauna ... 256
6.2.2.3 Thin sections, XRD and palynology analysis ... 256
6.2.2.4 Magnetic susceptibility ... 257
6.2.3 Results ... 257
6.2.3.1 Litho- and bio-facies and TOC ... 257
6.2.3.2 Conodonts ... 262
6.2.3.3 Reef Fauna ... 263
6.2.3.4 Magnetic susceptibility stratigraphy ... 264
6.2.4 Discussion and conclusions ... 265
6.3 Cortes Locality ... 267
6.3.1 Local Geological setting ... 267
6.3.2 Previous work ... 268
6.3.3 Lithotypes and stratigraphy ... 268
6.3.3.1 Petrographic and geochemical analyses ... 268
6.3.3.2 Magnetic susceptibility ... 269

6.3.4 Palaeontological record 271
6.3.4.1 Macrofauna 271
6.3.4.2 Micropalaeontology 276
6.3.5 Discussion and conclusions 276
6.4 Limestone units included in the Toca da Moura Volcano-Sedimentary complex 277
6.4.1 Local geological setting 277
6.4.2 Monte da Pena locality 278
6.4.2.1 Macropalaeontology and facies 278
6.4.3 Caeirinha locality 280
6.4.3.1 Macropalaeontology, micropalaeontology and facies 280
6.4.4 Age and interpretation of Monte da Pena and Caeirinha localities 281
Acknowledgements 281
References 282
Plates 295

Chapter 7 - Discussion and final conclusions
Future work 325
References 326

Appendix 1 329

Chapter 1

Introduction

INTRODUCTION

Chapter index

1.1 Purpose, scope and reasons for study 2
1.2 Geography and nature of outcrops..... 8
1.2.1 Espinho-Miranda do Corvo area..... 8
1.2.2 Odivelas reservoir, Santa Susana and surrounding areas. 9
1.3 General Geological setting 10
1.4 Abbreviations and notations 12
1.5 References 13

1.1 Purpose, scope and reasons for study

The Porto-Tomar shear zone and the associated metamorphic belt have been studied for a long time (e.g. Sharpe, 1849; Ribeiro, 1860; Delgado & Choffat, 1899, 1901), but the scope of these studies was always restricted to metamorphic geology (e.g. Sousa-Brandão, 1914a, 1914b; Severo-Gonçalves, 1974; Mendes, 1988), tectonics and structural geology (e.g. Freire de Andrade, 1938-40; Ribeiro et al., 1980).

It was Hélder Chaminé during the course of his PhD work (Chaminé, 2000) who identified a different unit of shales and siltstones (later called Albergaria-a-Velha unit). The unit had not been differentiated from the Arada unit which was shown to be older and with a higher metamorphic grade (Beetsama, 1995, Chaminé et al., 2003). This newly differentiated unit seemed to have a much milder metamorphic grade (when compared with the remaining units of the metamorphic belt) and, in some localities, had preserved primary (sedimentary) structures. The immense lithological similarities and intricate geometrical relations of the Arada and Albergaria-a-Velha units precluded their cartographic differentiation, a problem that persists today. Although there are a few criteria to differentiate the two in the field (in the presence of fresh and non-mineralized outcrops) it is almost impossible to distinguish the two in weathered or mineralized outcrops or using loose boulders. Regrettably geomorphological criteria, soil colour, vegetation type, and other criteria are not applicable.

The palynological tests conducted by J.P. Fernandes (Porto University) on samples collected by H. Chaminé provided poorly preserved assemblages of spores and acritarchs (Fernandes, et al., 2001). This paper allowed a first glimpse on the sedimentation ages (Devonian and Carboniferous), palaeoenvironmental conditions and maturity of the Albergaria-a-Velha unit. It was clear that a broader, in-depth study of the unit was needed. The proper identification of the ages, sedimentary palaeoenvironments and thermal maturity and history would have significant consequences for the characterization of the geodynamics of the Porto-Tomar shear zone over time (see Chapter 3).

The Buçaco basin (Pennsylvanian, not metamorphosed) was also investigated due to its geodynamic setting: a pull-apart basin along the Porto-Tomar shear zone (Gama Pereira, et al, 2008; Flores et al., 2010). Its detailed study and the proper characterization of the contacts between the surrounding units would provide important data for the interpretation of the dynamics of the Porto-Tomar shear zone (see Chapter 4).

A similar reasoning led to the investigation of the Santa Susana basin (Pennsylvanian, not metamorphosed), which is not related to the Porto-Tomar shear

zone s.s. but rests along a dextral N-S shear zone in SW Portugal (Santa Susana shear zone) and is most probably a pull-apart basin (Almeida et al., 2006; Oliveira et al., 2007) (see Chapter 5).

Within this shear zone there are several occurrences of limestone bodies. These are scattered along the shear zone and also along the Ferreira-Ficalho fault (see Chapter 6) where they seem to be spatially connected with the Odivelas Limestones. The possible spatial and temporal connection of all these limestone occurrences is explored in this work as well as the implications for the dynamics of the Santa Susana shear zone.

Furthermore the Odivelas Limestone is one of the few examples of Middle Devonian sedimentation in Ossa-Morena Zone and provides a unique opportunity to constrain the ages of tectonic, magmatic and metamorphic events regionally. It also provides important elements for the local and regional palaeogeography and regional and global palaeobiogeography.

For each basin or unit, a group of fundamental objectives were defined and presented as scientific questions. The ways to answer these questions defined the methods to be used. These in turn defined the specific tasks to be performed (field work, literature check, palynology sampling and processing, etc.). These ideal work flow tables were not fully executed due to time and budget constraints. It should also be mentioned that some of the methods applied did not provide significant results (see each chapter for discussion).

The discussion whether the questions were answered or not and how well were they answered is debated in the appropriate section of each chapter. Naturally new questions appeared that remain unanswered. These are presented throughout the chapters.

Albergaria-a-Velha Unit work flow – Chapter 3		
Main scientific questions	**Methods to apply**	**Specific tasks**
What are the ages of the unit? Is it homogeneous in each locality? Is there a spatial variation?	Palynology in several places in each locality.	Sampling, lab processing, microscope observation.
	Stratigraphical constraints above and bellow.	Mapping, literature.
	Literature.	J. P. Fernandes et al. Papers.
	GIS.	ArcMap plotting of ages.
What are the palaeoenvironments? Is there an age variation? Is there a spatial variation?	Sedimentology.	Logging of preserved sequences, facies interpretation.
	Palynofacies.	Sampling, lab processing, microscope observation, counts.
	Rock eval.	Sampling, shipping, interpretation.
What is the hydrocarbon potential? Where is the oil?	Palynofacies.	Sampling, lab processing, microscope observation, counts.
	Rock eval.	Sampling, shipping, interpretation.
	Geological interpretation, structural geology, literature.	Uphoff's papers, Geological interpretation from maps and literature.
What was the original spatial extension of the basin(s)? How was the regional palaeogeography?	Mapping, structural geology.	Geological interpretation from maps and literature.
	Sedimentology and Stratigraphy.	Logging of preserved sequences, facies interpretation.
	Data from on shore and off shore wells that reach the basement.	Sampling, palynological processing.
	Palaeocurrents.	Logging of preserved sequences, facies interpretation, field measurements.
	Palaeobiogeography.	Sampling, lab processing, microscope observation, statistics on microplankton and spores and connections with other zones.
What's the thermal history of the basin?	VR of Albergaria unit, Triassic and other overlying strata.	Sampling, Dublin or Porto, microscope observation.
	TAI, AAI.	Sampling, lab processing, microscope observation.
	Apatite fission track.	Sampling, sample processing, sample observation (Prague).
	Combination of age data and maturation. GIS.	Graphs with age Vs maturation/depth, maps with maturation and ages. ArcMap.

Table 1.1 – Albergaria-a-Velha Unit work flow. Please note that not all methods were applied and consequently not all specific tasks executed (in grey).

Buçaco basin work flow - Chapter 4		
Main scientific questions	**Methods to apply**	**Specific tasks**
When did sedimentation start? Was it synchronous across the basin?	Palynostratigraphy of basal levels in several places of the basin. Literature.	Field work – field sampling and logging across the basin. Lab processing of samples. Microscope observation.
	Logging of the basal contacts and first levels.	Field work – photographing, logging and geometry of the basal contacts.
	Transverse and longitudinal profiles of the basin.	Data compiling, logs' graphical correlation.
When did sedimentation end? Did it last the same across the basin?	Palynostratigraphy of the uppermost levels in several places of the basin.	Field work – Sampling and logging across the basin. Lab processing of samples. Microscope observation.
	Logging of uppermost levels.	Field work – photographing, logging.
Which were the sedimentation environments? How long did each one last and where in the basin?	Sedimentology, field logs, facies description, Literature.	Field work – Logging of all the sequence in several places, facies and Sedimentology.
	Clay mineralogy.	Field sampling, Lab processing of samples, XRD analysis.
	Palynofacies, Palaeobotany, Literature.	Sampling, Lab processing of samples. Microscope observation. Lemos de Sousa's papers.
What's the thermal history of the basin and surrounding units?	VR of the palynology samples and overlying Triassic rocks. Literature.	Sampling, processing, observation. Flores et al. papers.
	TAI and AAI of basin and surrounding units.	Sampling, Lab processing of samples, microscope observation.
What's the time and geometrical relation of the bounding units with the basin's sediments?	Literature.	Ribeiro, Courbouliex, Palain, etc. papers.
	Critical outcrops, mapping.	Data compiling, logs' graphical correlation.
What's the palaeogeography of the basin? Which are the source areas and how important are they?	Structural geology – Literature.	Courbouliex, Lemos de Sousa papers.
	Palaeobotanical ecology.	Lemos de Sousa's papers.
	Palaeocurrents, conglomerate lithologies, XRD of silts and sands.	Field work – measurements, observation. Sampling of silts and sands. Lab processing and data acquisition.
	Palynology of the conglomerates' boulders.	Sampling, Lab processing of samples. Microscope observation.

Table 1.2 – Buçaco basin work flow. Please note that not all methods were applied and consequently not all specific tasks executed (in grey).

Santa Susana basin work flow - Chapter 5		
Main scientific questions	**Methods to apply**	**Specific tasks**
When did sedimentation start? Was it synchronous across the basin?	Palynostratigraphy of basal levels in several places of the basin. Literature.	Field work – field sampling and borehole sampling and logging across the basin. Lab processing of samples. Microscope observation. J. P. Fernandes' papers.
	Logging of the basal contacts and first levels.	Field work – photographing, logging and geometry of the basal contacts.
	Transverse and longitudinal profiles of the basin. Literature.	Data compiling, logs' graphical correlation. Borehole info from Geol. Survey; Andrade, 1955; Geol. Survey's unpublished reports.
When did sedimentation end? Did it last the same across the basin?	Palynostratigraphy of the uppermost levels in several places of the basin.	Field work – Sampling and logging across the basin. Lab processing of samples. Microscope observation.
	Logging of uppermost levels.	Field work – photographing, logging.
Which were the sedimentation environments? How long did each one last and where in the basin?	Sedimentology, field logs, facies description, borehole logs, Literature.	Field work – Logging of all the sequence in several places, facies and Sedimentology; Andrade 1955 paper, Geol. Survey's unpublished reports.
	Clay mineralogy.	Field sampling, borehole sampling, Lab processing of samples, XRD analysis.
	Palynofacies, Palaeobotany, palaeoecology.	Sampling, Lab processing of samples. Microscope observation. Lemos de Sousa & Wagner's papers.
What's the thermal history of the basin and surrounding units?	HT, TM and basin sediments. Literature.	Sampling, processing, observation. P. Fernandes and Z. Pereira data.
	TAI and AAI of basin and surrounding units.	Sampling, Lab processing of samples, microscope observation.
	Porphyry petrography. Literature.	Sampling, thin section, observation. Geochemical analysis?
	Toca da Moura and Horta da Torre literature.	Data from Z. Pereira and P. Fernandes.
What's the time and geometrical relation of the bounding units with the basin's sediments?	Palynology of the Toca da Moura and Horta da Torre.	Sampling. Lab processing of samples. Microscope observation.
	Literature.	Z. Pereira papers.
	Borehole profiles, mapping.	Data compiling, logs' graphical correlation. Borehole info from IGM; Andrade, 1955; Geol. Survey's unpublished reports.
What's the palaeogeography of the basin? Which are the source areas and how important are they?	Structural geology – Literature.	Oliveira, Silva and Almeida's papers; Domingos et al. papers.
	Palaeobotanical ecology.	Lemos de Sousa & Wagner's papers.
	Palaeocurrents, conglomerate lithologies, XRD of silts and sands.	Field work – measurements, observation. Sampling of silts and sands. Lab processing and data acquisition.
	Palynology of the conglomerates' boulders.	Sampling, Lab processing of samples. Microscope observation.

Table 1.3 – Santa Susana basin work flow. Please note that not all methods were applied and consequently not all specific tasks executed (in grey).

Odivelas limestone and other limestone occurrences in OMZ work flow - Chapter 6		
Main scientific questions	**Methods to apply**	**Specific tasks**
What is the age of the limestones? Top and bottom. Are they all synchronous?	Reef fauna.	Logging, photographing, thin sections.
	Conodonts.	Logging, sampling, processing.
	Palynology.	Logging, sampling, processing, microscope observation.
	Magnetic Susceptibility Stratigraphy.	Logging, sampling, measurement and data processing.
	Forams?	Logging, sampling, thin sections, microscope observation.
What is the time and palaeogeographical relation with the volcanic suite and other units? Are they calciturbidites? Is there a terrestrial influence?	Mesoscale geometrical relations.	Field work – mapping, logging, sedimentary structures.
	Lithofacies.	Sampling, thin section, microscope observation.
	XRD and geochemical analysis.	Sampling, lab processing and XRD analysis. Microprobe and/or geochemical analysis.
	Literature.	Andrade and Conde's and Santos et al. papers on the volcanic suite - Mineralogy and geochemistry.
What is the palaeobiogeographical relation of the faunas with the rest of Europe/World?	J. Hladil analysis.	Sampling, photographing, thin sections. Literature.
	Palynology.	Sampling, processing, microscope observation, comparison and statistics with other assemblages from SPZ, Iberia, Gondwana, NAmerica.
Can some of the sections be correlated with other locations and with global events?	Conodonts.	Logging, sampling, processing.
	Magnetic Susceptibility Stratigraphy.	Logging, sampling, measurement and data processing.
	Lithofacies.	Sampling, thin section, microscope observation.
What is the limestones' maturation?	Petrography, TAI, AAI, CAI, FTIR.	Sampling, sample processing, thin sections, microscope observation.

Table 1.4 – Odivelas limestone and other limestone occurrences in OMZ work flow. Please note that not all methods were applied and consequently not all specific tasks executed (in grey).

1.2 Geography and nature of outcrops

1.2.1 Espinho-Miranda do Corvo area

The area in which the metamorphic belt associated with the Porto-Tomar shear zone crops out corresponds to a relatively hilly region, contrasting with the generally more flat area to the West that corresponds to the Meso-Cenozoic sediments of the Lusitanian basin. This can be readily observed in any satellite or aerial photo of the region. Outcrops were located in altitudes between 5m (Angeja area) up to about 400m (Buçaco area), although most were between 50 and 200m (see Fig. 1.1B). To the East the Central Iberian Zone corresponds to a hilly to true mountainous region (see Fig. 1.1A and B).

Most of the area is covered either by native forest (restricted to some valleys – maquis and *Quercus* forest) or by extensive *Eucalyptus* cultivated forest as a consequence of the poor soils and orographic characteristics. In either case outcrops are scarce and often heavily degraded. In many areas loose boulders are the only available geological information.

The region is densely populated, especially North of Aveiro, where there is dense urban sprawl leaving few preserved natural or agricultural areas. To the South of Aveiro there are significant populated areas around cities like Coimbra, Águeda and Mealhada, but there are also extensive areas with farmland and natural or cultivated forest (see Fig. 1.1E).

The region has a good network of motorways, national, regional and city roads. Dirt roads abound in the more rural areas and are usually well kept. Nearly every geological locality can be accessed by car to usually less than 1km from it (see Fig. 1.1D). There is one major train line crossing N-S, taking trains from Lisbon to Porto, but also regional train lines connecting towns and villages to major cities like Coimbra, Aveiro and Porto. From Coimbra there are regional train lines to the E and NE that cross some of the studied areas around Coimbra and to the Buçaco area. The Vouga train line connects Águeda to Aveiro and from here to the N up to Espinho, passing by many of the small towns and villages referred in this work. Unfortunately trains in this line are very infrequent and the line is said to be deactivated in a near future.

For this study, the most suitable outcrops were found in road cuts and train line cuts. These are often relatively tall (>2m), fresh to moderately weathered outcrops. These were suitable to sample for palynology and organic petrology and to describe sedimentary and stratigraphic characteristics (when available).

Other types of outcrops such as dirt road floor, natural river banks, valley slopes, etc., were almost invariably too weathered to sample or to provide any sedimentary information. Structural data could, nevertheless, be obtained from many of these.

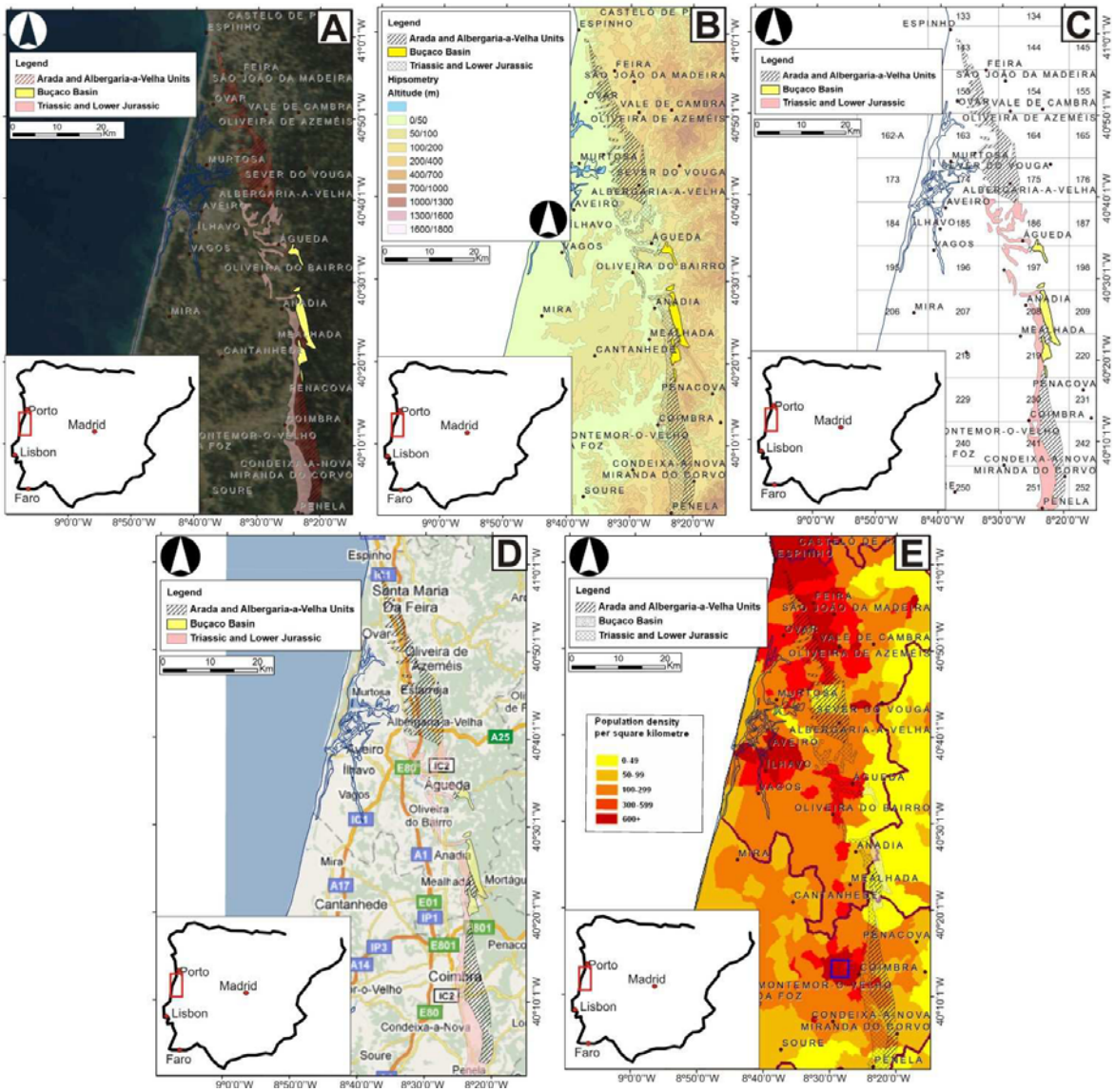

Fig. 1.1 – Albergaria-a-Velha and Arada units and Buçaco basin area maps (NW Portugal, Aveiro and Coimbra Districts) and approximate location within the Iberian Peninsula (lower left inlet). A – NASA MODIS (2002) satellite image; B – Hypsometry map; C – Cartogram of the military 1/25000 scale topographic maps used in this work; D – Road map from Google maps; E – Population density map (from Wikimedia commons).

1.2.2 Odivelas reservoir, Santa Susana and surrounding areas.

Nearly all the Alentejo region is considered to be a peneplain (e.g. Feio, 1951) with natural outcrops restricted to stream/river beds, banks and slopes. The Odivelas dam and the areas to the W and NW (including the Santa Susana area) are also peneplain areas, but there are important streams and rivers around which outcrops can be found. Vegetation is usually restricted to cultivated *Quercus* forest which has little influence on outcrop quality. Native forest (usually thick shrub forest) is restricted to more remote and incised valleys. Most outcrops are located between 50 and 100m of altitude.

There is a good network of motorways, national and regional roads. Dirt roads provide access to most of the localities within the distance of 1km. There are no relevant active train lines in the area.

Population density in very low and has little effect on the quality and quantity of the outcrops.

In the Odivelas area, the reservoir fills the relatively incised valley of the Ribeira de Odivelas which has abundant outcrops. Most are flooded during part of the year, but some are observable even during the wet season. Some abandoned quarries provide additional outcrop information. Loose boulders abound in many areas.

The Santa Susana area is relatively hilly, with Ribeira do Freixial and other streams' valleys providing fresh and continuous outcrops in its beds and banks. The Pego do Altar reservoir has similar characteristics to the Odivelas reservoir and several good outcrop areas can be found around its banks. Additional outcrops are found in some road cuts.

In the Monte da Pena and Caeirinha areas, outcrops are restricted to small abandoned quarries and more rarely to stream beds. Most of the information derives from loose boulders.

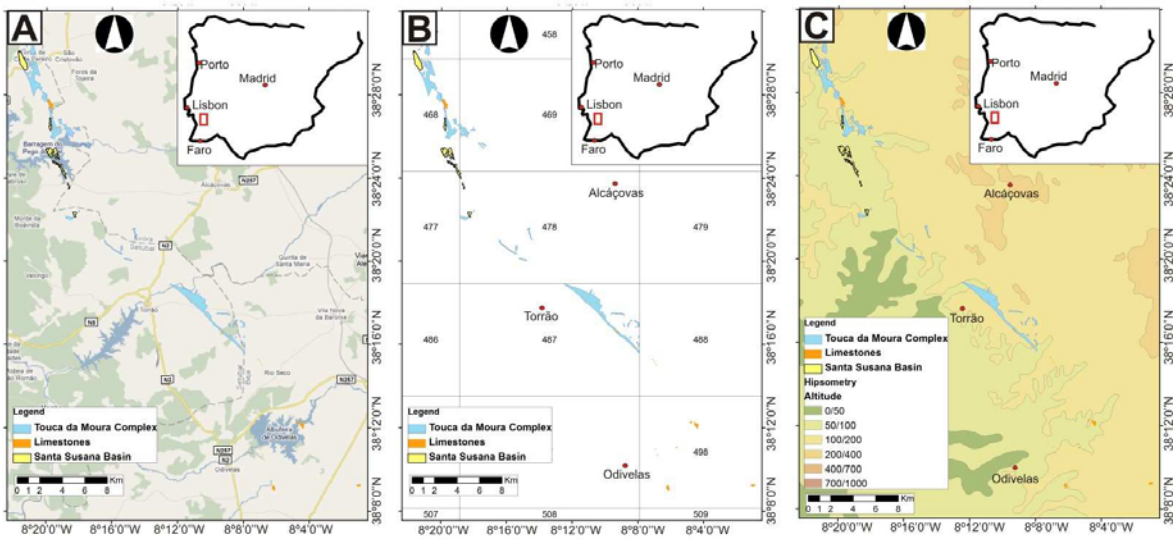

Fig. 1.2 – Odivelas Limestone and Santa Susana Basin basin area maps (Central South Portugal, Setúbal, Évora and Beja districts) and approximate location within the Iberian Peninsula (top right inlet). A – Road map from Google maps; B – Cartogram of the military 1/25000 scale topographic maps used in this work; C – Hypsometry map.

1.3 General Geological setting

The Iberian Massif (IM) constitutes the largest exposure of pre-Mesozoic rocks of the Iberian Peninsula and the largest exposed area of the European Variscides without significant (Alpine) reworking (Dallmeyer & Martinez Garcia, 1990).

The IM was divided into several zones according to their metamorphic, stratigraphical and structural characteristics. The zonation initially proposed by Lötze (1945) was later modified by Julivert & Martinez (1983) and Ribeiro et al. (1990). The northern branch (West Asturian-Leonese and Cantabrian Zones) and southern branch (South Portuguese Zone (SPZ)) generally show a milder deformation (upper crustal level), lower metamorphic degree and are essentially composed by Palaeozoic rocks. The central parts of the IM (Ossa-Morena (OMZ), Central Iberian and Galicia – Trás-os-Montes

Zones) have generally higher (although highly variable) metamorphic degrees, stronger tectonism (lower and upper crustal level) and are composed by pre-Cambrian and Palaeozoic rocks. Allochthonous terranes of oceanic nature border and are comprised within the central areas and reflect collision settings that occurred during the Cadomian and Variscan orogenies (e.g. Fonseca & Ribeiro, 1993; Ribeiro et al., 1990, 2009).

The OMZ is a major geotectonic unit located in the southern sector of the Iberian Massif (Lötze, 1945; Julivert & Martinez, 1983, see Fig.1.3). The OMZ southern border comprises highly deformed exotic terranes of oceanic nature (including the "Pulo do Lobo" Accretionary Terrane (PLAT) and the Beja-Acebuches Ophiolitic Complex (BAOC)), as complex tectonic melanges (Almeida et al., 2001; Araújo et al., 2005; Booth-Rea et al., 2006; Fonseca & Ribeiro, 1993; Fonseca et al., 1999; Figueiras et al. 2002; Mateus et al., 1999; Ribeiro et al., 2009). These formations are rimming an early main Variscan suture in the southwest of the Iberian Massif and they accreted to the OMZ before the Middle/Upper Devonian times (Fonseca & Ribeiro, 1993; Fonseca et al., 1999; Ribeiro et al., 2009). The BAOC separates the OMZ and SPZ, which is regarded as another exotic terrain, that accreted to the OMZ during Carboniferous times (Dallmeyer et al., 1993).

The OMZ is composed by several domains or units which have complex tectonic settings (Quesada, 1990; see Chapter 6). These domains were defined according to their stratigraphic, metamorphic and magmatic characteristics, although the division is not consensual (e.g. compare Oliveira et al., 1991 with Robardet & Gutiérrez-Marco, 1990, 2004).

The northern branch of the OMZ is composed by a metamorphic belt that rests along the NNW-SSE trending Porto-Tomar Shear Zone (PTSZ) (Chaminé, 2000; Chaminé et al., 2003; 2007; Gama Pereira, 1987). This belt comprises several autochthonous and parauthocthonous tectonostratigraphic units with low to high metamorphic grade (Beetsma, 1995; Chaminé, 2000; Chaminé et al., 2003; Gama Pereira, 1987). These units are essentially Proterozoic (Beetsma, 1995; Chaminé, 2000; Chaminé et al., 2003), but Upper Palaeozoic rocks are present (Albergaria-a-Velha unit) (Chaminé et al., 2003, Fernandes et al., 2001).

Recently Ribeiro et al. (2007) proposed a different "affinity" for this metamorphic belt. They describe this belt as "Finisterra continental slices" which would have been juxtaposed over the OMZ at the same time as the BAOC.

Further details of the Geology of each area are presented in the appropriate chapters.

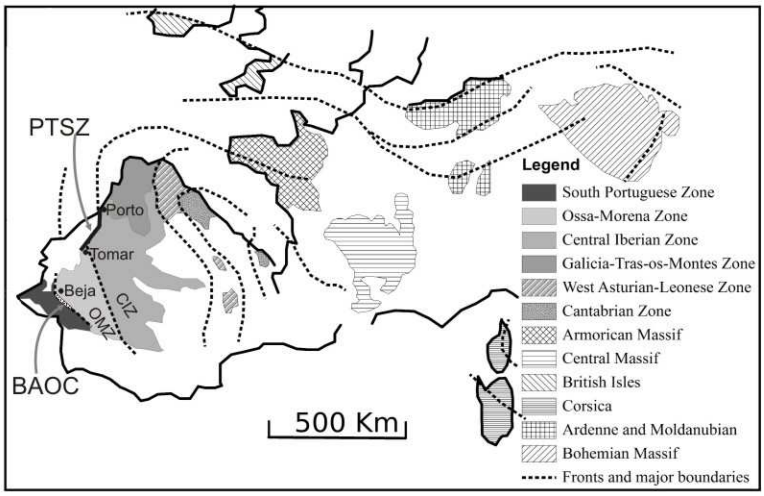

Fig. 1.3 –Geotectonic units of European Variscides and major fronts and boundaries with the indication of the BAOC (Beja-Acebuches Ophiolitic Complex) and the PTSZ (Porto-Tomar shear zone and associated metamorphic belt). Areas in white correspond to Meso-Cenozoic cover (adapted from Ribeiro et al, 1996).

1.4 Abbreviations and notations

SI units are used, otherwise noted. Graphical scales were preferred to numerical ones to allow the correct visualization of graphs, images and photos in several media (paper in different layouts or magnifications, computer screens, etc.).

BIC – Beja Igneous Complex
OMZ – Ossa Morena Zone
SPZ – South Portuguese Zone
CIZ – Central Iberian Zone
PTSZ – Porto-Tomar Shear Zone
AVU – Albergaria unit; Albergaria-a-Velha unit (used interchangeably)
OM – organic matter
AOM – Amorphous organic matter
Fm. – Formation
HCl – Hydrochloric acid
HF – Hydrofluoric acid
et al. – et alia (and others)
s.s. – sensu stricto
s.l. – sensu lato
km - kilometres
m – metres
dm - decimetres
cm – centimetres
mm – millimetres

1.5 References

ALMEIDA E., POUS J., SANTOS F.M., FONSECA P.E., MARCUELLO A., QUERALT P., NOLASCO R. & MENDES-VICTOR L., 2001. Electromagnetic imaging of a transpressional tectonics in SW Iberia. Geophysical Research Letters. AGU 28 (3): 439–442.

ALMEIDA, P., DIAS DA SILVA, I., OLIVEIRA, H. & SILVA, J. B., 2006. Caracterização Tectono-Estratigráfica da Zona de Cisalhamento de Santa Susana (ZCSS) no Bordo SW da Zona de Ossa Morena (ZOM), (Portugal). VII Congresso Nacional de Geologia. Estremoz, Portugal: 49 – 53.

ARAÚJO A., FONSECA P., MUNHÁ J., MOITA P., PEDRO P. & RIBEIRO A., 2005. The Moura Phyllonitic Complex: An accretionary complex related with obduction in the Southern Iberia Variscan Suture. Geodinamica Acta 18 (5): 375–388.

BEETSMA, J.J., 1995. The late Proterozoic/Paleozoic and Hercynian crustal evolution of the Iberian Massif, N Portugal, as traced by geochemistry and Sr-Nd-Pb isotope systematics of pre-Hercynian terrigenous sediments and Hercynian granitoids. Vrije Universiteit Amsterdam (unpublished PhD thesis): 223pp.

BOOTH-REA G., SIMANCAS J.F., AZOR A., AZAÑÓN J.M., GONZÁLEZ-LODEIRO F. & FONSECA P., 2006. HP–LT Variscan metamorphism in the Cubito-Moura schists (Ossa-Morena Zone, southern Iberia) Comptes Rendus Geoscience 338 (16): 1260–1267.

CHAMINÉ, H. I., 2000. Estratigrafia e estrutura da faixa metamórfica de Espinho-Albergaria-a-Velha (Zona de Ossa-Morena): implicações geodinâmicas. Universidade do Porto. Departamento de Geologia. Faculdade de Ciências da Universidade de Lisboa. PhD thesis. Porto: 497p.

CHAMINÉ, H. I., GAMA PEREIRA, L. C., FONSECA, P. E., MOÇO, L. P., FERNANDES, J. P., ROCHA, F. T., FLORES, D., PINTO DE JESUS, A., GOMES, C., SOARES DE ANDRADE, A. A. and ARAÚJO, A., 2003. Tectonostratigraphy of Middle and Upper Palaeozoic black shales from the Porto-Tomar-Ferreira do Alentejo shear zone (W Portugal): new perspectives on the Iberian Massif. Geobios 36(6): 649-663.

CHAMINÉ, H. I., FONSECA, P. E., PINTO DE JESUS, A., GAMA PEREIRA, L. C., FERNANDES, J. P., FLORES, D. MOÇO, L. P., DIAS DE CASTRO, R., GOMES, A., TEIXEIRA, J., ARAÚJO, M. A., SOARES de ANDRADE, A. A., GOMES C. & ROCHA, F. T., 2007. Tectonostratigraphic imbrications along strike-slip major shear zones: an example from the early Carboniferous of SW European Variscides (Ossa-Morena Zone, Portugal). In: Theo E. Wong (Ed.), XVth International Congress on Carboniferous and Permian Stratigraphy (Utrecht, 2003). Royal Dutch Academy of Arts and Sciences, Amsterdam, Edita NKAW: 405-416.

DALLMEYER, R.D. & MARTÍNEZ GARCÍA, E., 1990. Introduction to the Pre-Mesozoic Geology of Iberia In: DALLMEYER, R.D. & MARTÍNEZ GARCÍA, E. (Eds.) Pre-Mesozoic Geology of Iberia. Springer Verlag, Berlin Heidelberg: 3-5.

DALLMEYER R.D., FONSECA P.E., QUESADA C. & RIBEIRO A., 1993. 40Ar/39Ar mineral age constraints for the tectonothermal evolution of a Variscan Suture in SW Iberia. Tectonophysics 222: 177–194.

DELGADO, J. F. N. & CHOFFAT, P., 1899. Carta Geológica de Portugal, escala 1/500.000. 3ª ed. 2 folhas. Direcção dos Trabalhos Geológicos.

DELGADO, J. F. N. & CHOFFAT, P., 1901. La carte géologique du Portugal C.R. VIIIéme Congrés Géologique Internationale. Paris, France 2: 743-746.

FEIO, M., 1951. A evolução do relevo do Baixo Alentejo e Algarve. Comunicações dos Serviços Geológicos de Portugal 32 (2): 303-504.

FERNANDES, J. P., FLORES, D., ROCHA, F. T., GOMES, C., GAMA PEREIRA, L. C., FONSECA, P. E., PINTO DE JESUS, A. & CHAMINE, H. I., 2001. Devonian and Carboniferous palynomorph assemblages of black shales from the Ovar-Albergaria-a-Velha-Coimbra-Tomar region (W Portugal): tectonostratigraphic implications for the Iberian Terrane. Revista de Geociências Universidade de Aveiro 15 (1.2): 1-24.

FLORES, D., PEREIRA, L. C. G., RIBEIRO, J., PINA, B., MARQUES, M. M., RIBEIRO, M. A., BOBOS, I. & JESUS, A. P. D., 2010. The Buçaco Basin (Portugal): Organic petrology and geochemistry study. International Journal of Coal Geology 81 (4): 281-286

FONSECA P. & RIBEIRO A., 1993. Tectonics of the Beja-Acebuches Ophiolite: a major suture in the Iberian Variscan Foldbelt. Geologische Rundschau 82: 440–447.

FIGUEIRAS J., MATEUS A., GONÇALVES M., WAERENBORG J. & FONSECA P.E., 2002. Geodynamic evolution of the South Variscan Iberian Suture as recorded by mineral transformations. Geodinamica Acta 15 (1): 45–61.

FONSECA P., MUNHÁ J., PEDRO J., ROSAS F., MOITA P., ARAÚJO A. & LEAL N., 1999. Variscan ophiolites and high-pressure metamorphism in Southern Iberia. Ofioliti 24 (2): 259–268.

FREIRE de ANDRADE, C., 1938-40. Algumas considerações sobre a geologia dos arredores de Espinho e das Caldas de S. Jorge. Boletim do Museu e Laboratório Mineralógico e Geológico da Faculdade de Ciências da Universidade de Lisboa 3 (7-8): 23-35.

GAMA PEREIRA, L.C., 1987. Tipologia e evolução da sutura entre a Zona Centro Ibérica e a Zona Ossa Morena no sector entre Alvaiázere e Figueiró dos Vinhos (Portugal Central). Universidade de Coimbra PhD thesis: 331pp.

GAMA PEREIRA, L. C., PINA, B., FLORES, D. and ANJOS RIBEIRO, M., 2008. Bacia Permo-Carbónica do Buçaco: um modelo de Pull-Apart. 8ª Conferência Anual do CGET : resumos alargados. Sant'ovaia, H., Dória, A. and Ribeiro, M. D. A. Universidade do Porto. Faculdade de Ciências. Departamento de Geologia, Faculdade de Ciências da Universidade do Porto: 110-113.

JULIVERT, M. & MARTINEZ, F., 1983. Estructura de conjunto y vision global de la Cordillera Herciniana. Libro Jubilar J. M. Rios. Geologia de España 1: 607-630.

LOTZE F., 1945. Zur Gliederung der Varisziden in der Iberischen Meseta. Geotektonische Forschungen 6: 78–92.

MATEUS A., FIGUEIRAS J., GONÇALVES M. & FONSECA P.E., 1999. Evolving fluid circulation within the Beja-Acebuches Variscan Ophiolite Complex (SE, Portugal), Ofioliti 24 (2) (Sp. Iss.): 269–282.

MENDES, M. H., 1988. Contribuição para o estudo das rochas metamórficas aflorantes entre Ovar e Espinho. MsC thesis. Aveiro University. Geosciences Dept.: 186pp.

OLIVEIRA J.T., OLIVEIRA V. & PIÇARRA J.M., 1991. Traços gerais de evolução tectono-estratigráfica de Zona de Ossa-Morena em Portugal. Cuadernos Laboratorio Xeolóxico de Laxe 16: 221–250.

OLIVEIRA, H., SILVA, I. D. D. & ALMEIDA, P., 2007. Tectonic and Stratigraphic Description and Mapping of the Santa Susana Shear Zone (SSSZ), the SW Border of Ossa Morena Zone (OMZ), Barrancão – Ribeira de S. Cristóvão Sector (Portugal): Theoretical Implications. Geogaceta 41 (3-6): 151-156

QUESADA, C., 1990. Introduction of the Ossa-Morena Zone (part V). In: DALLMEYER, R.D. & MARTÍNEZ GARCÍA, E. (Eds.) Pre-Mesozoic Geology of Iberia. Springer Verlag, Berlin Heidelberg: 249–251.

RIBEIRO, A., PEREIRA, E., SEVERO GONÇALVES, L., 1980. Análise da deformação da zona de cisalhamento Porto-Tomar na transversal de Oliveira de Azeméis. Comunicações dos Serviços Geológicos de Portugal, 66: 3–9.

RIBEIRO, A., QUESADA, C. & DALLMEYER, R.D., 1990. Geodynamic Evolution of the Iberian Massif. In: DALLMEYER, R.D. & MARTÍNEZ GARCÍA, E. (Eds.) Pre-Mesozoic Geology of Iberia. Springer Verlag, Berlin Heidelberg: 398–409.

RIBEIRO A., SANDERSON D. & SW-Iberia Colleagues, 1996. SW Iberia: transpressional orogey in the Variscides. In: GEE, D. & ZEYEN, H.J. (Eds) Europrobe '96 - Litosphere Dynamics: Origin and Evolution of Continents. European Science Foundation. Uppsala Univ.: 91–98.

RIBEIRO, A., MUNHÁ, J., DIAS, R., MATEUS, A., PEREIRA, E., RIBEIRO, M. L., FONSECA, P. E., ARAÚJO, A., OLIVEIRA, J. T., ROMÃO, J., CHAMINÉ, H., COKE,

C. & PEDRO, J. C., 2007. Geodynamic evolution of the SW Europe Variscides. Tectonics 26: TC6009.

RIBEIRO, A., MUNHÁ, J., FONSECA, P. E., ARAÚJO, A., PEDRO, J. C., MATEUS, A., TASSINARI, C., MACHADO, G. & JESUS, A., 2009. Variscan ophiolite belts in the Ossa-Morena Zone (Southwest Iberia): Geological characterization and geodynamic significance. Gondwana Research 17 (2-3): 408-421.

RIBEIRO, C., 1860. Memória sobre o grande filão metalífero que passa ao nascente d'Albergaria a Velha e Oliveira de Azemeis. Memórias da Academia Real de Ciências. 2, II: 5-105.

SEVERO GONÇALVES, L. 1974. Geologie und petrologie des gebietes von Oliveira de Azeméis und Albergaria-a-Velha (Portugal). PhD thesis. Freien Universität Berlin: 261pp.

ROBARDET, M., GUTIÉRREZ-MARCO, J.C., 1990. Passive margin phase (Ordovician-Silurian-Devonian). In: DALLMEYER, R.D. & MARTÍNEZ GARCÍA, E. (Eds.) Pre-Mesozoic Geology of Iberia. Springer Verlag, Berlin Heidelberg: 249–251.

ROBARDET, M., GUTIÉRREZ-MARCO, J.C., 2004. The Ordovician, Silurian and Devonian sedimentary rocks of the Ossa-Morena Zone (SW Iberian Peninsula, Spain). Journal of Iberian Geology 30: 73-92

SHARPE, D., 1849. On the Geology of the neighbourhood of Oporto, including the Silurian Coal and Slates of Vallongo. Quarterly Journal of the Geological Society of London 5: 42–153.

SOUZA-BRANDÃO, V., 1914a. A faixa occidental das phyllites porphyroblásticas do precâmbrico do districto de Aveiro. Comunicações dos Servicos Geologicos de Portugal, 10: 78–143.

SOUZA-BRANDÃO, V., 1914b. Orientação óptica do chloritoide das phillites de Alcapedrinha (Arada, districto de Aveiro). Comunicações dos Serviços Geológicos de Portugal, 10: 144-158.

Chapter 2

Procedure and Methods

PROCEDURE AND METHODS

Chapter index

2.1 Field work, stratigraphical procedure and general sampling methodology..... 19
2.2 Palynological procedure 19
2.2.1 Introduction 19
2.2.2 Sampling..... 20
2.2.3 Cleaning and crushing 20
2.2.4 Hydrochloric acid (HCl)..... 21
2.2.5 Hydrofluoric acid (HF)..... 21
Cold HF 22
Microwave..... 23
2.2.6 Second hydrochloric acid (HCl) attack 23
2.2.7 Centrifuging..... 24
2.2.8 Sieving..... 24
2.2.9 Watch Glass, pipetting, floating, specimen picking. 24
2.2.10 Oxidation..... 24
2.2.11 Acetolysis 25
2.2.12 Mounting 25
Mounting to observe with transmitted light 26
Mounting to observe with reflected light 26
2.2.13 Storage..... 26
2.2.14 Observation and documentation..... 27
Transmitted light 27
Reflected light 28
2.2.15 Image processing and plates..... 28
2.3 Palynofacies analysis..... 29
2.4 Conodont extraction procedure 30
2.4.1 Sampling..... 30
2.4.2 Cleaning and Crushing 30
2.4.3 Acetic acid dissolution 30
2.4.4 Sieving..... 30
2.4.5 Screening and picking 30
2.4.6 Observation and documentation..... 30
2.5 Clay mineralogy 31
2.5.1 Sampling..... 31
2.5.2 Crushing and mounting 31
2.5.3 Diffractometer 31
2.5.4 Diffractogram analysis 32
2.6 Organic Petrology..... 32
2.6.1 Sampling..... 32
2.6.2 Sample preparation..... 32
2.6.3 HF method..... 32
2.6.4 Heavy liquid separation..... 33
2.6.5 Mounting and polishing..... 33
2.6.6 Observation and measurement..... 34
2.7 Thin sections..... 34
2.7.1 Sampling..... 34
2.7.2 Sample preparation..... 34
2.7.3 Observation, measurements and documentation 35

2.8 Polished sections/surfaces 35
2.8.1 Sampling 35
2.8.2 Sample preparation 35
2.8.3 Observation and documentation 35
2.9 References 35
Personal Comunications 37

2.1 Field work, stratigraphical procedure and general sampling methodology

Field work was conducted using rented vehicles and, in most instances, the author's own vehicle. Military topographic 1/25000 scale maps were used as a standard for field work. Frequently these were adapted to include geological information plotted with ArcGIS software and printed in the appropriate scale. The geological information derives from the Portuguese Geological Survey's 1/50000 scale geological maps, detailed maps from published literature and in the case of the Odivelas Limestones, from copies of field maps used by António Soares de Andrade in the course of his PhD work (Andrade, 1983).

Geological mapping was not part of the objectives of this thesis, but simplified geological maps of some areas were constructed (e.g. Covas Ruivas and Cortes localities, Odivelas Limestone, with the collaboration of an undergraduate student from FCUL).

Stratigraphical procedure was conducted regularly at the Buçaco and Santa Susana basins and at the Covas Ruivas locality of the Odivelas Limestone. Lithological columns were constructed using a metric tape measure and beds described taking into account lithology, fossil content, grain size, etc.. Samples were collected for several purposes (mostly for palynology) at regular intervals to ensure a representative sampling or to study specific aspects of a bed.

For other localities of the Odivelas Limestone loose boulders were sampled for corals, stromatoporoids and other fauna to be observed and more rarely as conodont samples.

For nearly all the areas and outcrops of the Albergaria-a-Velha unit, an adapted procedure was used. The strong deformation did not allow the construction of columns or, at best, these were limited to a few meters of vertical extent. Preserved sedimentary information (lithology, grain size, sedimentary structures) was described when available. Sampling methodology for palynology was adapted to ensure spatial representative coverage and that packages of rocks with different dominant lithologies (e.g. black shales vs. fine sandstones with rare shales) were not over or under sampled. Although the use of a grid would be desirable, the scarcity of outcrops with sufficient quality precluded its use.

2.2 Palynological procedure

2.2.1 Introduction

There is a great number of papers regarding palynological maceration techniques (e.g. Batten, 1999; Phipps and Playford, 1984; Traverse, 2007; Wood et al., 1996). All methods describe a series of steps with physical desegregation and chemical processing.

Most of them also include oxidation methods and other procedures that facilitate palynological observation.

In all of them the aim is to eliminate the mineral component of the sample and obtain a residue composed entirely of organic matter. This is based on the fact that organic matter is not attacked (or easily attacked) by neither Hydrochloric acid (HCl) nor Hydrofluoric acid (HF).

Usually a combination of acid attacks is used to eliminate all the mineral content of the rock and a set of physical separations of the resulting residue to obtain a concentrated organic residue with the correct particle size.

For each step a short description and discussion is made and the method used in this work is described. This text was richly improved with suggestions and contributions from many palynologists and palynology lab technicians (personal communications).

2.2.2 Sampling

Ideally, samples for palynological purposes should be taken from fresh surfaces, non-weathered and especially with no signs of oxidation (which destroys palynomorphs). The outermost parts of the outcrop should be discarded as they are probably oxidized and contaminated with living/recent organic debris. Depth of weathering varies with climate, time of exposure, lithology, among other factors (Rowe and Jones, 1999, Traverse, 2007). Ideally the sample should be taken from about 50cm into the outcrop to ensure minimal weathering. In practice for this work samples were taken from fresh or slightly weathered (most common situation) outcrops. These were very frequently road cuts. Evident mineralization, oxidation and deformation features were avoided. Fractures and other penetrating surfaces (including bedding planes) were avoided as these are preferential weathering "ways". Vegetated outcrops were not sampled. In some cases a big chunk of rock was detached from the outcrop and hammered to obtain fresh, non-mineralized, "not-too-deformed" pieces of rock

A few hundreds of grams were collected in most instances. Samples were labelled and bagged to avoid cross contamination and erroneous indexation. When collecting, samples were referenced with GPS coordinates and/or signalled in 1/25.000 scale topographic maps. Characteristics of the sample such as lithology, colour, weathering stage, mineralization, deformation, etc. were noted and transferred to a computer database using FILEMAKER software.

Borehole samples stored at the Portuguese Geological Survey and at the Geosciences department, Aveiro University were invariably washed cuttings. These were bagged and labelled the same way as for the remaining types of samples.

2.2.3 Cleaning and crushing

One or a few blocks (to be crushed) were cleaned with running water and washed with brushes and detergent if necessary. All the dust on the sample surface was removed as this is a source of contamination (other rocks, airborne dust, pollen fall, etc.) and consumes the acid for no purpose (Fatka pers. com.). Knives or scraping objects (Tongeren, pers. com.), compressed air and ultrasounds (Clayton, pers. com.) were used occasionally to clean the sample.

Theoretically, the greater the sample's surface area, the greater the efficiency of the acid reaction. This is limited by the size of palynomorphs (megaspores and chitinozoa are around 200μm) and the probability of breaking many palynomorphs with crushing. Jones (1998) suggested that the most efficient crushing size is between 0.7 and 1.71mm for consolidated lithologies, but many workers use pie-sized particles (e.g. Vavrdová, pers. com.; Riding & Kyffin-Hughes, 2004; Vecoli, pers. com.; Verniers,

pers. com.). Samples were wrapped with a plastic bag or foil and crushed with a hammer.

The amount of sample needed varies from worker to worker, but 5g is a standard amount referred by many (e.g. Eshet & Hoek, 1996; Jones, 1998; Riding & Kyffin-Hughes, 2004). The amount needed to have enough residue for several slides and to keep some for later studies will ultimately depend on the amount of organic matter initially present in the sample and the effectiveness of the processing technique. Thus the amount of sample used will depend on the lithology and the estimated organic matter content. For dark grey and black shales and fine siltstones about 5 to 10g were obtained from about 100g of initial cleaned sample, sieved to 0.7-1.7mm or 1-2mm sizes. For limestone samples up to 100g of pie-sized pieces were used.

2.2.4 Hydrochloric acid (HCl)

Hydrochloric acid is used to eliminate carbonates present in the sample. This step was not always used. Each sample was tested for carbonates and HCl attack was only used if the test is positive. HCl was observed to promote the release metal content of some rocks (apparently non-carbonated), especially Fe oxides, observed in the form of a green liquid. The amounts needed to dissolve a rock sample were indicated by Jones, 1998: 20ml of concentrated HCl (37%) is twice the amount need to, in theory, dissolve 5g of $CaCO_3$. This can serve as a basis for calculating corresponding amounts of rock, acid and concentrations.

Sample (grams)	10% HCl (ml)
5	54
10	108
15	162
20	220

Table 2.1– Proportion of sample weight and the amount of 10% HCl needed to theoretically dissolve it.

In all known published procedures and laboratories visited, reaction time is less than 24 hours, usually 3, 6 or 8 hours or simply “over night” (e.g. Fatka pers. com; Riding & Kyffin-Hughes, 2004; Vavrdová, pers. com.; Verniers, pers. com.)

Some published procedures indicate a complete neutralization before the HF attack (e.g. Eshet & Hoek, 1996). Theoretically the Ca ions are released into solution with the HCl attack and can be removed from the system by decanting this solution. To remove virtually all the Ca ions, 2 or 3 dilution-decanting cycles in 1L bottle (washing) are needed. If not properly removed, Ca and other ions will react with HF and form insoluble Ca fluorides that, although transparent, can effectively decrease the quality of the final residue. Complete neutralization is time consuming and unnecessary.

2.2.5 Hydrofluoric acid (HF)

HF is used to eliminate all silicates and other minerals (Langmyhr & Sveen, 1965). It is usually used after the HCl. According to Jones, 1998, 50ml of concentrated HF (37%) is twice the amount needed to dissolve 5g of SiO_2. The effectiveness of the reaction is improved by temperature increase (Langmyhr & Sveen, 1965). The dissolution of crystalline silica and silicates tends to form silica gels and precipitates that cover sample particles, decreasing the effectiveness of the reaction (Tongeren, pers.

com.). Langmyhr & Sveen, 1965 argued that for the complete dissolution of silicate minerals (not applied to palynology) stirring did not influence reaction times or efficiency. Brocke, pers. com and Fatka, pers. com. referred that stirring and the use of an orbital shaker reduced reaction times from a week to 1 or 2 days. Thus stirring, either mechanical or heat induced is generally recommended to ensure a complete reaction. The ions released by the acid reaction may form precipitates with the F ion which needs to be eliminated. Some minerals are particularly resistant to HF and HCl attack, namely zircons, tourmaline and other unidentified minerals. These are especially frequent in metamorphosed sediments. Reaction times vary greatly according to the lithology (minerals present), temperature, stirring, amount of acid and of sample. Fernandes (pers. com.) mentioned that the reaction can take only a few minutes for some black shales with no heating. Frequently reaction times are between a few days (e.g. Tongeren, pers. com.) up to 2 weeks (Clayton, pers. com.) with no heating. Orbital shakers are common in palynology laboratories to catalyse the reaction and remove silica gels from particle surfaces, especially during the first hours of the reaction (e.g. Tongeren, pers. com., Streel, pers. com., Brocke, pers. com.) and the reaction time is typically one or two days. Another method used is a static method with heating or no heating. This is used to process samples for megaspores or Pre-Cambrian samples (Streel, pers. com.) and chitinozoa (Ghent University). This reduces breakage of specimens to a minimal. It is probably also useful for high maturity and metamorphosed samples, when the palynomorphs loose their elasticity, but would be extremely laborious and time consuming. Heating is usually done using a water bath at 70 or 80ºC. Warming the residue in a hot plate can produce a differential heating of the residue and thus inappropriate catalysis of the reaction.

When adding HF it is advisable that the sample is at least humid so that the HF penetrates easily the rock pieces and it also makes the reaction milder (Fatka, pers. com.).

Two methods of HF attack were used in this study. Both are described bellow.

Cold HF

10 to 15g clean, crushed samples were placed in a 1L plastic bottle. 40% HF was added according to the amount of sample, using the following table as a reference (from Jones, 1998)

Sample (grams)	40%HF (ml)
5	50
10	100
15	150
20	200

Table 2.2 – Proportion of sample weight and the amount of 40% HF needed to theoretically dissolve it.

Each sample was left to react for periods up to 1 month, depending on the effectiveness of the reaction. The bottle is stirred frequently in the first minutes of reaction and then every 24h. Neutralization is done by successive dilution-decanting cycles until the liquid is apparently neutral (usually [HF] < 0.005%).

Microwave

The procedure used in this work followed very closely the one suggested in Ellin and Mclean, 1994. The microwave device available at Aveiro University is the CEM MDS-81D, exactly the one used in the referenced paper. This method increases the effectiveness of the reaction by heating the sample and HF in a pressurized environment.

The available vessels are different, allowing a set of 12 samples to be processed in each run. Each sample can be up to 2,5g, but for safety reasons and to ensure complete dissolution 2g were used in most instances. Duplicates of the 12 sample set were used in successive runs to obtain a total dissolved weight of 4 or 5g. Each vessel holds 13ml of 40% HF. The microwave device is activated for 20min at 100% power and left to cool down for 1h. This step is done for safety reasons, but also because reaction still takes place while the temperature is high. Neutralization was done in a similar way to the cold HF method.

The safety procedures and specifications for acid digestion of several kinds of minerals and rocks can be found at the CEM Co. website.

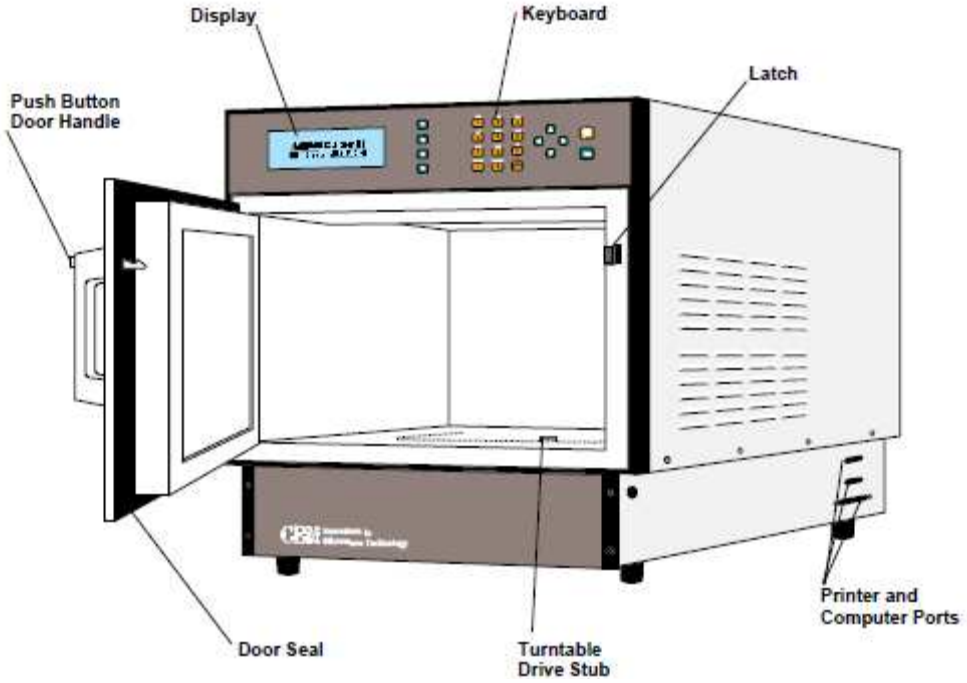

Fig. 2.1 – Microwave digestion MDS device (CEM) illustration showing its main components. Adapted from the operation manual.

2.2.6 Second hydrochloric acid (HCl) attack

Ca fluorides, other neo-formed crystals and undissolved minerals are very frequently present after HF attack. These can be removed with a second HCl attack. Often this is made using hot or boiling 10% HCl (Brocke, pers. com., Vecoli, pers. com., Streel, pers. com.) for a few minutes up to half an hour. Heating can be done using a water bath, Bunsen beaker or thermal plate. Alternatively another, milder, method is to use cold 10% HCl for a few hours (Tongeren, pers. com.). The "aggressiveness" of the attack will depend on the amount of undissolved minerals. More mature and metamorphosed samples tend to have more of these minerals.

The standard method used was to boil the residue in a 10%HCl solution over a thermal plate for a period of about 15min. This was found to be very effective in destroying most of the mineral fraction present after HF attack.

2.2.7 Centrifuging

Centrifuging is used in some laboratories to facilitate decanting and neutralization (using water or an acidic liquid). It is also used as a density separation of palynomorphs from other silt sized particles (Fatka, pers. com.). Heavy liquids are used in this case. The dried or humid residue is placed with the heavy liquid and palynomorphs will float and most minerals will sink. Centrifugation accelerates the process. This implies that the density of the liquid is very precisely known in order to eliminate also the lighter minerals. Centrifuging is used as an alternative to sieving in some cases. The applicability of this method for mature and metamorphosed samples is limited because palynomorphs may have pyrite and other minerals inside the chamber and attached to spines or growing around the wall. It may also be case that increased carbon content on the wall of palynomorphs may change its density. If any of these is the case, palynomorphs will sink along with the heavy minerals. This method was not used in this study.

2.2.8 Sieving

Spores and acritarchs are rarely smaller than 10μm and most of them are greater than 20μm (Traverse, 2007). Thus the pore size of the meshes should be between 10 and 20μm. Very frequently organic residues have significant amounts of very small particulate OM and AOM, and also film-like kerogen that tend to clog the sieve and can make observation of palynomorphs harder if they remain in significant proportions. If the residue is sieved in a 10μm mesh, the result is a very "close to original" organic assemblage but very "dirty", i.e. full of fine particles of kerogen. Sieving with a 20μm mesh produces a very clean residue but some organic content information is lost (Tongeren, pers. com.). This is especially important if palynofacies and kerogen typing is being made. A possible compromise is to use a 15μm mesh. Megaspores and chitinozoa are bigger and a 43 or 63μm size mesh is usually used to separate them from the rest of the residue.

For most samples a 15μm size mesh was used. For some samples with high concentration of very small (10μm and smaller) acritarchs, a 7μm size mesh was used. In all cases a small portion of the non-sieved residue was kept.

2.2.9 Watch Glass, pipetting, floating, specimen picking.

Acritarchs and other palynomorphs, if not highly carbonized or with minerals inside the chambers, will float on water and will remain floating due to water surface tension (Fatka, pers. com.). Using this principle, specimens can be pipetted out using a binocular microscope.

Another density/hydrodynamic behaviour separation technique consists on the usage of a rotating watch glass with the residue. Centrifugal force will segregate heavier and lighter organic particles allowing its separation (Clayton, pers. com.).

For megaspores and chitinozoa individual specimens are observed, usually not an assemblage in a slide. Thus they are usually pipetted out from a watch glass or a Petri dish under a binocular microscope (Verniers, pers. com.).

These methods were not used for this study.

2.2.10 Oxidation

Palynomorphs and most organic matter suffer a colour change with the increase of temperature (Bostick, 1971; 1979; Marshall & Yule, 1999). This is due to the loss of

volatiles and relative increase in carbon content (Marshall & Yule, 1999). This is a gradual and irreversible process (Marshall & Yule, 1999). Sporopollenin is the essential component of most spores and a similar compound makes up acritarch walls (Traverse, 2007). Although they react differently to temperature and geological time, the tendency is always towards grey or black colour and to loose transparency. This gradual darkening obscures many features and distinctive characteristics of palynomorphs and in extreme cases, only a rounded black opaque particle is observed. Elasticity is also gradually lost during this process (Vavrdová, pers. com.).

Several chemicals can be used to lighten palynomorphs and make them translucent so that their morphological characteristics can be observed. Mild products as H_2O_2, NaOCl (bleach) and stronger ones as HNO_3 alone or as Schultze's solution (HNO_3 1:3 $KClO_3$) are commonly used (Clayton, pers. com.; Colbath, 1985; Eshet & Hoek, 1996; Gray, 1965; Jones, 1998; Marshall, 1980). Heating catalyses the reaction (Jones, 1998). The use of these chemicals also has a dispersing action, especially useful for AOM and soluble kerogen which can obscure palynomorph observation (Eshet & Hoek, 1996).

Residues needing oxidation are typically black and oxidation has taken effect when they change to coffee brown or to a lighter colour (Fernandes, pers. com.; Pereira. pers. com.)

For the samples from the Buçaco and Santa Susana basins, a mild oxidation procedure using diluted NaOCl (house hold bleach) was used. A small portion of the organic residue (enough for one or two slides) was placed in a small glass container. About 100ml of (ca. [4%]) bleach were added and the mixture left to react. After the initial 18 hours a small amount of residue was pipetted out and checked for correct oxidation extent under a microscope. All samples were successfully oxidized after 18 to 36 hours. The method was ineffective for samples with higher maturation (Albergaria-a-Velha unit).

A strong oxidation procedure using Nitric acid and also Schultze's solution was tested with residues from the Albergaria-a-Velha unit. The results were poor and in most cases all the residue was lost, even after short periods of oxidation. As a second best option the residues were mounted to observe palynomorphs under a microscope with reflect light – see below.

2.2.11 Acetolysis

This is used to remove excessive OM in the form of organic acids. KOH and/or acetone are frequently used. Depending on the oxidation reactant used and the amount of fine kerogen in the residue, this step can be suppressed or not. Low quantities of fine kerogen and/or the use of an oxidizing agent that disperses OM may be sufficient to obtain a clean residue after sieving. If acetolysis is needed, the reactant should be applied during sieving or immediately prior to sieving.

This method was not used for this study.

2.2.12 Mounting

Two methods were used to mount the organic residues. One was used to observe palynomorphs under the microscope with transmitted light (acritarchs, palynofacies, and sporomorphs with low TAI) and the other with reflected light (sporomorphs with TAI > 4).

Mounting to observe with transmitted light

Mounting the final OM residue should be made using the thinnest slides (1mm thick) and cover slips (no. 0 or 1). This allows proper observation under the microscope, especially when focusing is concerned. Accordingly the mounting medium must be kept to the lowest amount (and thus its thickness) between the cover slip and the slide. It is advisable that the entire residue is in the same plane to allow proper focus. This can be achieved by drying the residue either on the slide or on the cover slip before applying the mounting medium. A humid residue or in solution is usually not mixable with mounting mediums.

Suitable mounting mediums should have ca. 1,5 refractive index. Several ones are available. **Glycerine Jelly** is very popular but it was found to be not stable after 10-15 years, as it becomes yellow and opaque (Fatka, pers. com.). It needs sealing with nail varnish or another hardening product. **Canada balsam** is also used but it is also not permanent. **Neo-mount** from MERCK is also used, but the refractive index is slightly bellow 1,5. Otherwise it is very effective and does not need sealing. **Entellan** from MERCK or **Entellan new** is permanent and doesn't need sealing. It is very sticky and viscous which makes mounting more difficult, but it can be diluted with Xylol which makes it more liquid and equally effective. **Eukite** is also used but it takes a long time to dry and needs the mixture of two compounds. It is not completely colourless, it's slightly yellow.

Megaspores and chitinozoa are usually mounted as specimens in especially prepared slides and glued or simply prepared for SEM observation.

For this study residues were dried on cover slips (24x32mm) using a low temperature thermal plate and mounted in slides (26x76mm) with Entellan new, ensuring the entire surface is covered and removing excess resin from the edges. If by any chance the surface was not completed covered with resin, nail varnish can be used to seal the mounted slide and avoid desiccation.

Mounting to observe with reflected light

A small amount of the >20µm fraction of the organic residue was placed over a thin 7x2cm acrylic slide and left to dry. Each slide was previously marked with the sample reference. When completely dry, a few drops of ethyl acetate were added, just enough to cover the entire slide surface. This ensures organic particles are "glued" to the slide and allows microscopic observation with both transmitted and reflected light – see below.

2.2.13 Storage

Small vials or flasks, glass or plastic are appropriate for storing residues. The capacity will depend on the amount and concentration of the residue, but usually 20ml is more than enough. In the moment of storage, prior to mounting, an anti-fungal/bacterial agent should be added. Phenol is highly toxic and thus highly effective (Tongeren, pers. com.). It should be used in very small amounts and with very low concentrations. Glycerine water is used as a storage medium and is effective at least for 15 years (Vecoli, pers. com.). Copper Sulphate is also used in very low concentrated solution, adding 1 or 2 drops to the final residue (Verniers, pers. com.).

Low concentrated phenol (~1%) solution was dropped (less than 1ml) to every flask immediately after filling with residue.

2.2.14 Observation and documentation

Transmitted light

For this study a NIKON E600 Pol and an OLYMPUS BX-40 were used to scan the slides and to photograph them. With the NIKON microscope a NIKON D50 camera attached to an F-Mount was used to photograph slides. With the OLYMPUS BX-40 a OLYMPUS DP20 camera was used.

Palynological slides can be observed in several magnifications. **Eye Pieces** have a fixed magnification and can be rotated to adjust to the observer's dioptre level. Additionally they can be adjusted to a specific inter-eye distance.

For a general look of the slide (e.g. visual estimation of the proportion of the kerogen types) the 10X objective can be used, but for any observation of a particular specimen, the 40X must be used and for detailed observation and for photography the 100X oil immersion objective is mandatory.

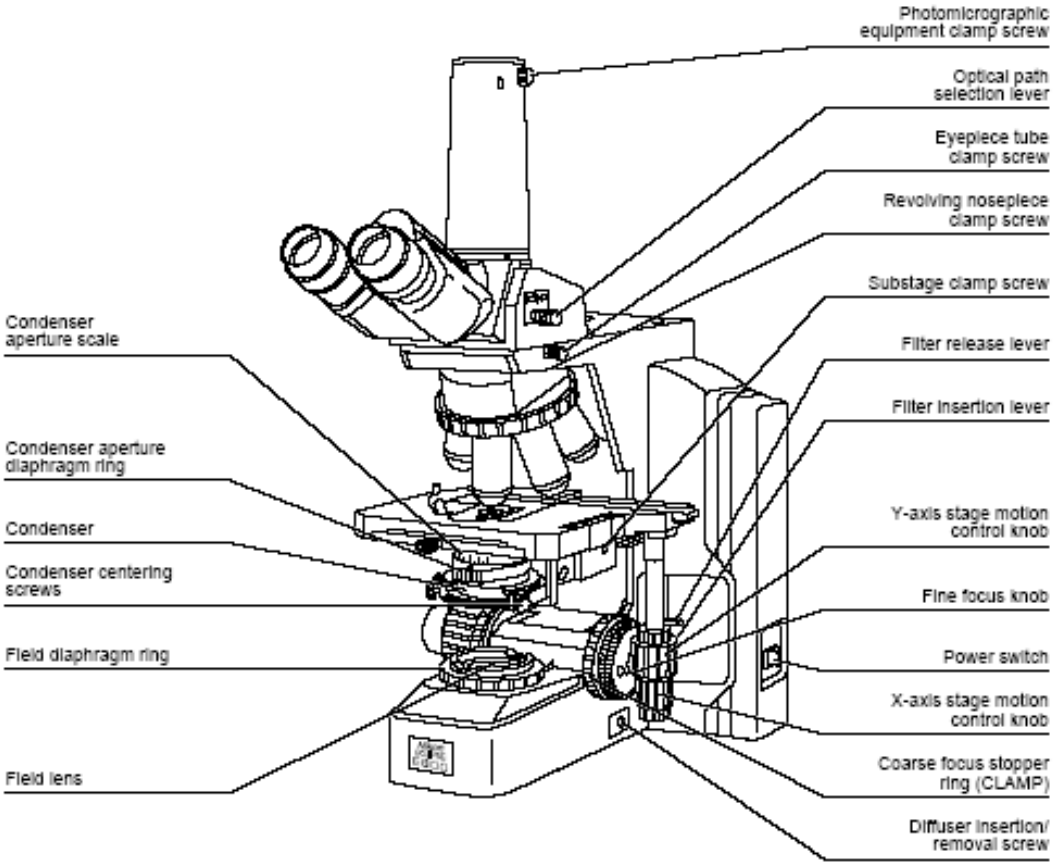

Fig. 2 - Nikon E600Pol microscope (transmitted light) diagram and nomenclature from the user manual. The Olympus BX40 used in this work has a very similar structure and components.

The light source (**brightness adjuster**) should always be kept near to the maximum. Light intensity can be adjusted with other parts. The **field diagram ring** should also be kept close to maximum. Only when a big depth of field is needed this can be stopped down, but it will most certainly compromise the brightness. The **condenser aperture diaphragm** determines the amount of light that reaches the slide, the depth of field and also the contrast. When photographing, the aperture should be stopped to about 70 or 80% of the numerical aperture of the objective (the other number on the surface besides the magnification). To have increased contrast, the aperture

should be even lower. However, if the specimen is dark the brightness might be deteriorated, so a compromise must be achieved.

The **auto-photo switch** allows that a Nomarski effect is introduced. This is particularly relevant to very dark and partially opaque specimens as it apparently increases transparency and creates a relief appearance.

The **swing out achromatic condenser** adds brightness to the field of view. This is important for dark specimens, but it introduces a light fringe around the specimen and sometimes chromatic aberration. The choice of using the condenser will depend on the transparency and colour of each specimen.

The polars (**polarizer and analyzer**) are most frequently set parallel, except if distinction between minerals and palynomorphs is necessary. Interference contrast may be achieved by manipulating the angle between the two.

Reflected light

The acrylic slides were observed with the Olympus BX60 microscope and documentation done with an Olympus C3030 camera. The thin layer of ethyl acetate allows the observation of fine detail of palynomorphs. The classical glass slide and glass cover slip mounts produce significant light diffraction which precludes proper observation. This method was used essentially to observe and document sporomorphs, but acritarchs could also be observed. The most significant disadvantage is that only one side of palynomorphs is observable (either distal or proximal) and internal features are usually not discernable. The main advantage is that literally all palynomorphs of a residue derived from a highly mature rock can be mounted, observed and documented. An additional advantage (provided that microwave HF digestion was not used) is that, after polishing, the same slides can be used for vitrinite reflectance measurements.

Considering the unrelenting high maturity of the Albergaria-a-Velha unit and the ineffectiveness of the tested oxidation techniques, this method becomes the main feasible way for the palynological characterization of this unit.

2.2.15 Image processing and plates

The images of palynomorphs obtained under the microscope are frequently unfocused and 2 or more microphotographs are needed to have a complete focused specimen. HELICON FOCUS is shareware image software that “glues” several partially unfocused images together to make a composite focused image without loosing or adding information to it. It is very user friendly and no special training is necessary. Many images can be glued, but the quality decreases. Two or three are best.

Photomicrographs of selected specimens for illustration were edited to remove debris that could decrease plate quality. When palynomorphs and debris could not be positively differentiated the latter were not removed to avoid artificial alteration of morphological features. For scaling and measurement of specimens the software AXIOVISION from ZEISS was used. For plate mounting COREL DRAW was used.

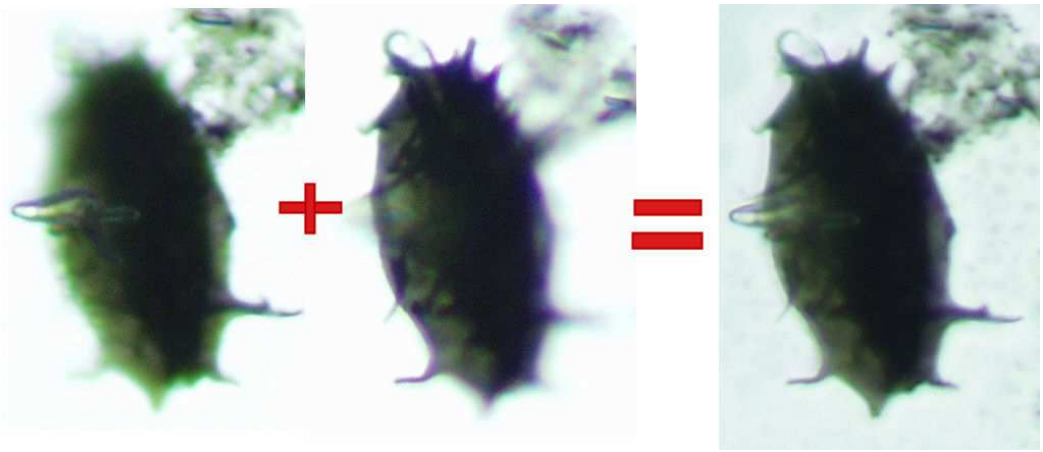

Fig. 2.3 - Example of merger of two partially unfocused images and the focused composite.

2.3 Palynofacies analysis

For palynofacies analysis random images of unsieved residue slides were photographed with the 40X objective. The area occupied by the several components in each image was then measured using AXIOVISION software. These values were transferred to an Excel sheet and proportions of the several components calculated in order to use them in ternary diagrams, coastal proximity indices, etc. (see Chapter 3).

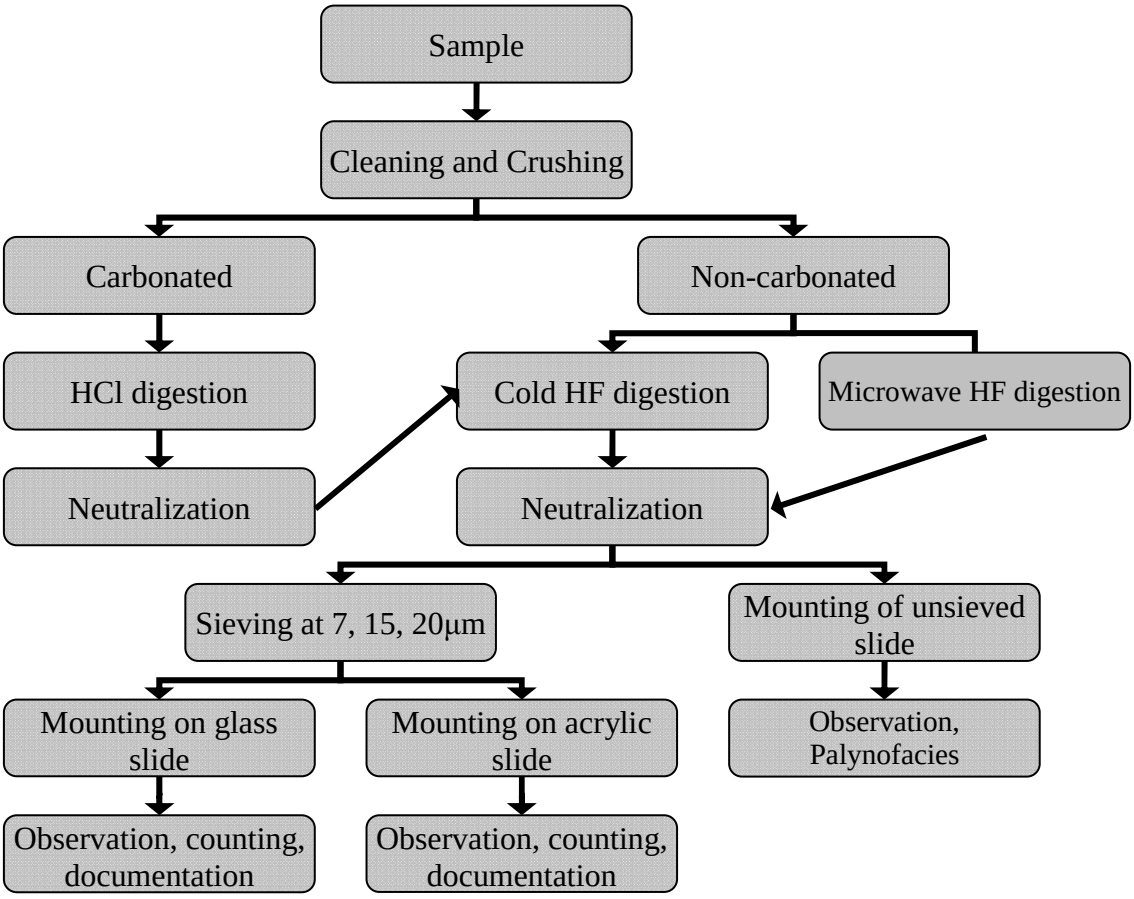

Flow chart for the palynological processing

2.4 Conodont extraction procedure

2.4.1 Sampling

Although many types of sediment contain conodont elements, only carbonate samples are suitable for extraction (Lindström, 1964). Limestone samples with bioclastic sand-sized grains were preferably chosen, especially if these were crinoidal. Weathered surfaces may show an irregular surface which is often indicative of the presence of bioclasts, but most of the times these are only recognizable after sectioning.

Sample weight varied from 1kg up to 5kg. When sampling a preserved sequence, outcrop samples were taken in regular intervals. When the limestone area was composed of deformed and/or metamorphosed rocks, the most suitable lithologies were selected, and these were often loose boulders.

2.4.2 Cleaning and Crushing

Samples were cleaned with running water and brushed to remove dirt, algae and lichen.

After cleaning they were crushed to pieces of approximately chestnut size.

2.4.3 Acetic acid dissolution

Crushed samples were placed in 10L plastic buckets and filled with 10% acetic acid. According to sample weight, 3 or 4L of 10% acetic acid was added. To enhance the reaction, the dilution of the acid (from glacial 100% to 10%) was done using hot water. The samples were left to react for a period of about 1 month after which the dissolved fraction smaller than 1mm was removed (see sieving). Another 3 or 4L of 10% acetic acid was added and left to react. This step was repeated until the sample was completely dissolved or enough conodont elements were picked from the residue.

2.4.4 Sieving

The dissolved fraction was removed from the buckets to a set of sieves with meshes 1mm and 125µm. The <125µm fraction was discarded. The >1mm fraction was put back into the bucket and the intermediate fraction retained and dried.

2.4.5 Screening and picking

The sieved and dried residue was thoroughly observed under a binocular microscope Olympus SZX-10 and conodont elements were picked using a thin iron spindle.

In some samples a magnetic separation of conodonts was attempted following the procedure described in Dow (1960). The Franz magnetic separator available was the same model used in the referred paper and the parameters obtained experimentally to differentiate minerals by its magnetic susceptibility were very similar. The method was only partially successful and about half of the residue was effectively separated. Additionally the oxidation method described in Carls & Slavík (2007) was tested, but it was totally ineffective, producing a residue which was very difficult to segregate using the magnetic separator and unsuitable to observe under the binocular microscope.

2.4.6 Observation and documentation

The best preserved and representative conodont elements were selected from the picked specimens. These were photographed with a binocular microscope before being

mounted over a double-sided sticky tape glued to a small glass slide. The arrangement of conodonts and its taxonomic identification (even if preliminary) was noted. The conodont elements were photographed using a SEM CAMECA SX 100 at the Institute of Geology of the Academy of Sciences of the Czech Republic. The images obtained were used for definitive taxonomic identification and are illustrated in the appropriate chapter.

2.5 Clay mineralogy

For the samples with little or no metamorphism, XRD analysis was performed to obtain palaeoclimatic and palaeogeographical information (in the case of the Buçaco and Santa Susana basins). The fine fraction (<4µm) was used for these samples. Some samples from the Covas Ruivas limestone area were also analyzed to obtain data on the mineralogical composition of the tuffites and limestones, but the <63µm whole rock fraction was used.

2.5.1 Sampling

Samples for the fine fraction analysis were collected from shale beds, usually with some striking colour (e.g. red – possible desert climate; dark grey – possible stagnant pond), but also from coarser sediments with obvious clayey matrix.

For the whole rock fraction analysis, no special care was taken and many samples are duplicates of conodont samples.

In both cases weathered and/or oxidized surfaces were avoided.

2.5.2 Crushing and mounting

For both types of samples (whole rock and clay fraction), crushing was performed using a plastic foil around the sample and crushed with a hammer. A small amount of sample (ca. 100g) was used.

For the clay fraction samples, the crushed sediment was placed in small glass cups with indication of the height (in centimetres). Distilled water was added to the top of the cup and the mixture stirred thoroughly. Using Stokes' law, the time that particles <4µm take to sink 1cm was calculated. After this time the upper centimetre was pipetted out to a glass slide (labelled accordingly) and left to dry. Occasionally the amount of sediment on the slide was not enough after the first pipetting in which case the procedure was repeated.

Dark samples often contained a considerable amount of organic matter which can deform the diffractogram if not removed prior to mounting. For these samples, before decanting, 10% H_2O_2 was added to the crushed sample and left to react for several days. The 10% H_2O_2 was replaced several times until no reaction was observed and the sample was later neutralized by successive decanting.

For the whole rock analysis, the crushed samples was dry-sieved using a <63µm mesh and the finer fraction diluted with distilled water and mounted on a labelled glass slide.

2.5.3 Diffractometer

The X-ray diffraction pattern was recorded with a copper anode X-ray tube (Cu-Kα radiation) using a Philips PW1710, powder diffractometer and X´Pert software PC-APD, 3.6 at the Tropical Research Institute (IICT) Department of Natural Sciences

(DCN)/ Global Development (DES) in Lisbon and with a Philips X'Pert PW3040/60 powder diffractometer with Cu-Kα radiation of the Diffractometry lab at the Geosciences Department of the University of Aveiro.

For each sample 3 runs were performed: air dried, glycoled and heated to 500ºC. Although laborious this allows an appropriate identification of the minerals present and the determination of their proportions. In all cases a 60º 2θ analysis was done.

2.5.4 Diffractogram analysis

Having a diffractogram for each sample, the computer file (.rd format) was analyzed with PANALYTICAL software which allowed a semi-automatic peak determination and quantification of each mineral.

2.6 Organic Petrology

2.6.1 Sampling

The sampling for organic petrology studies (metasediments) followed a similar procedure to the one described for palynology, without microwave digestion. Fresh, non-vegetated, non-mineralized, not "too deformed" outcrops were sampled. Considering that organic matter particles suitable for proper reflectance determination under the microscope should be at least 50 µm in diameter, dark grey silty and sandy samples were preferably taken while shales (suitable for palynology) were avoided. Nevertheless many shale samples processed for palynology provided sufficiently big and abundant vitrinite particles to be measured. The effectiveness of this method was reduced because petrographic information is lost when using palynological residues.

For the Triassic and Pennsylvanian (Buçaco and Santa Susana basins) silty and sandy samples with macroscopic plant remains were sampled. Coal samples were not collected.

2.6.2 Sample preparation

About 100g of metasediment cleaned sample (same standard cleaning as for palynology) were crushed and sieved to obtain about 10g of the <1mm fraction and about 10g of the <212µm fraction. The latter fraction is assumed to be composed of mono-component grains, either mineral or maceral. Additionally the darker fragments of the <500 µm fraction of silty samples were picked under a binocular microscope to a separate container for later mounting.

For the Triassic and Pennsylvanian samples the crushed samples were observed under a binocular microscope and plant remains (or coaly particles) were picked to a separate container for later mounting.

2.6.3 HF method

The organic residue from the samples deriving from the Buçaco and Santa Susana basins (processed for palynology) was sieved with a 53µm mesh and stored for later mounting.

Some samples from the Albergaria-a-Velha Unit were also processed with this method.

2.6.4 Heavy liquid separation

The procedure described here closely follows the one usually performed in the Organic Petrology Lab of the Geology Department of the Faculty of Sciences of the University of Porto. This step was performed only for the metasediment samples of the Albergaria-a-Velha unit.

The previously separated <212µm fraction is placed in a centrifuge flask (ca. 500ml capacity). 10g were used for most samples, but when the sample was expected to be poor on vitrinite particles up to 15g were used. About 200ml of bromoform diluted with alcohol (to obtain a liquid with ca. 1,7g/cm^3 density) was added to each flask ensuring that each group of four samples had exactly the same weight (to be later placed in the centrifuge). The mixture was shaken and placed on an ultrasonic bath for 10min to avoid clumping of particles. 4 samples at a time were placed on a centrifuge for 10min at a 3000rpm speed. After this step the supernatant should have a concentrate of organic mater and the decanted residue should be mostly mineral.

The supernatant is sieved using a 4cm diameter milipore filter within an apparatus composed of a Büchner flask attached to a vacuum pump which facilitates the sieving. The filter with the residue is placed over a small acrylic plate. A few drops of ethyl acetate are added which destroys the filter and glues the residue to the acrylic plate.

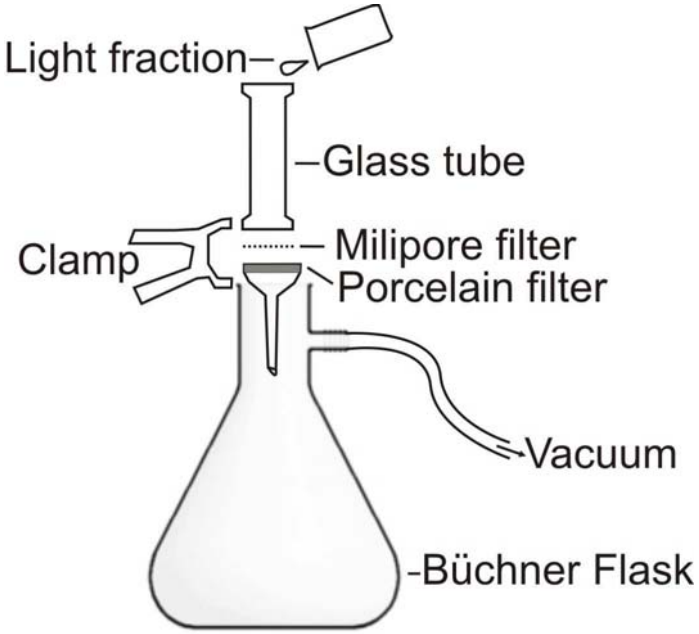

Fig. 2.4 – Sieving apparatus used to concentrate the light fraction of the heavy liquid separation.

2.6.5 Mounting and polishing

The <1mm fraction of metasediments, picked dark fragments and the picked plant remains were mounted in Epoxy resin. The particles were placed on the bottom of small flexible silicon gel containers and the epoxy resin (mix of resin and hardener) poured into the container just enough to completely cover the particles. Gentle stirring with a spindle ensured that no air bubbles remained attached to the particles. A small piece of paper with the reference of the sample was placed on top of the resin while it was liquid.

They were left to dry and harden in a lab oven at ca. 50ºC overnight. When the resin was completely hard, the reference of each sample was scratched with a knife on the back of each block to ensure correct indexation.

The epoxy blocks were removed from the containers and several steps of polishing were performed. #320 and #1000 sand paper were used in turn washing the block between each step. Some samples required an intermediate or final polishing step using the #500 and #4000 sand papers respectively.

The acrylic plates with the residue were gently polished over a glass surface using the #600 and #1200 SiC wet powders.

All samples had a final polish using a PlanoPol rotating disk machine over a fine tissue plate with 0,3µm and 0,05µm sized alumina abrasive gel.

All samples were examined under a reflected light microscope between each polishing stage and checked for important scratches or irregular surface areas and re-polished if necessary.

2.6.6 Observation and measurement

All polished samples were observed and measured with a reflected light microscope Leitz ORTHOPLAN. Measurements were obtained with the image analysis software FOSSIL and DISKUS. The software produced an EXCEL file and a histogram as the measurements were being made.

2.7 Thin sections

2.7.1 Sampling

For metasediments associated to the Porto-Tomar shear zone, coarse silt and sand sized samples were collected, avoiding significant weathering, mineralization and preferably choosing outcrops were bedding was preserved and sedimentary features were observable. Additional samples of fine siltstones and shales were collected to fully characterize turbidite beds or other specific sedimentary features.

For limestones of the Southern part of the Ossa-Morena zone, samples without significant mineralization and veining and relatively fresh were chosen. Samples with visible or suspected sand sized or coarser bioclasts (in weathered surfaces) were preferably chosen as these usually allow the identification of macrofossils either in thin section or polished sections.

Additional samples were taken from tuffites and cherts from the Odivelas Limestone localities for petrographic description and to determine the presence of some microfossils (radiolarians and tentaculites).

2.7.2 Sample preparation

All samples were cut in the LabPol of the Geology Department of the Faculty of Sciences of the University of Lisbon. The standard size is 31x23mm with a thickness of 20mm. Thin sections are produced with a final thickness of 0.02mm by a specialized technician.

2.7.3 Observation, measurements and documentation

Thin sections were observed in several binocular and petrographic microscopes. Sedimentary features, identification of bioclasts, quantification of the several types of particles present and other features were noted. When necessary, photographs were taken, always in digital format. The methods used to count particles and plot the results are described and discussed in the appropriate section of Chapter 3.

2.8 Polished sections/surfaces

2.8.1 Sampling

Several types of lithologies were sampled. Most of the samples collected were processed both for thin and polished sections. Samples were usually 10x10cm or bigger.

2.8.2 Sample preparation

Samples were initially cut at a specific angle either to allow maximum observation area and/or to have sections parallel or perpendicular to bedding, depending on the desired objective. Selected sections were then polished in 2 steps, the first with a rotating plate and wet #400 SiC powder and the second over a still glass surface with #600 or #800 SiC powder. This produced a surface with a *matte* shine and not glossy, thus appropriate for observation and photography.

2.8.3 Observation and documentation

The polished sections were observed with naked eye and with a binocular microscope and details of sedimentary features, identification of bioclasts and other characteristics noted. The whole surface of the sections and some details were photographed in a small studio.

2.9 References

ANDRADE, A. A. S., 1983. Contribution à l'analyse de la suture hercynienne de Beja (Portugal): perspectives métallogéniques. Laboratoire de Métallogénie I Nancy, Institut National Polytechnique de Lorraine. PhD: 137pp.

BATTEN, D. J., 1999. Small palynomorphs. In: JONES, T.P. & ROWE, N. P. (Eds). Fossil Plants and Spores: modern techniques. Geological Society, London: 15-19.

BOSTICK, N.H., 1971. Thermal alteration of clastic organic particles as an indicator of contact and burial metamorphism in sedimentary rocks. Geoscience and Man 3: 83–92.

BOSTICK, N.H., 1979. Microscopic measurement of the level of catagenesis of solid organic matter in sedimentary rocks to aid exploration for petroleum and to determine former burial temperatures — a review. SEPM Special Publications 26: 17–43.

CARLS, P. & SLAVÍK, L., 2007. Upgrading of magnetic susceptibility of conodont sample residues before magnetic separation. Lethaia 38 (2): 171 - 172.

COLBATH, G.K., 1985. A comparison of palynological extraction techniques using samples from the Silurian Bainbridge Formation, Missouri, U.S.A. Review of Palaeobotany and Palynology 44: 153-164.

DOW, V. E., 1960. Magnetic Separation of Conodonts. Journal of Paleontology, 34 (4): 738-743.

ELLIN, S. & MCLEAN, D., 1994. The use of microwave heating in hydrofluoric acid digestions for palynological preparations. Palynology 18(1): 23-31.

ESHET, Y. & HOEK, R., 1996. Palynological processing of organic-rich rocks, or: How many times have you called a palyniferous sample barren? Review of Palaeobotany and Palynology 94 (1-2): 101.

GRAY, J., 1965. Extraction techniques. In: B. KUMMEL & D. RAUP (Editors), Handbook of Paleontological Techniques. Freeman, San Francisco, CA: 530-587.

JONES, R. A., 1998. Focused microwave digestion and oxidation of palynological samples. Review of Palaeobotany and Palynology 103 (1-2): 17.

LANGMYHR, F. J. & SVEEN, S. 1965. Decomposability in Hydrofluorica acid of the main and some minor and trace minerals of silicate rocks. Analytica Chimica Acta 32: 1-7.

LINDSTRÖM, S., 1964. Conodonts. Elsevier Publishing Company: 196pp.

LPP Laboratory of Palynology and Palaeobotany. Utrecht University Palynology lab safety book. Geoscience Dept. Utrecht.

MARSHALL, J. E. A., 1980. A method for the successful oxidation and subsequent stabilisation of highly carbonised spore assemblages. Review of Palaeobotany & Palynology 29 (3-4): 313-319.

MARSHALL, J. E. A. & YULE, B. L., 1999. Spore colour measurement. In: JONES, T.P. & ROWE, N. P. (Eds). Fossil Plants and Spores: modern techniques. Geological Society, London: 165-168.

PHIPPS, D. & PLAYFORD, G., 1984. Laboratory techniques for the extraction of palynomorphs from sediments. Department of Earth Sciences. University of Queensland Papers 11 (1): 1-23.

RIDING, J., KYFFIN, B., HUGHES, J., 2004. A review of the laboratory preparation of palynomorphs with a description of an effective non-acid technique. Revista Brasileira de Paleontologia 7 (1): 13-44.

ROWE, N. P. & JONES, T.P., 1999. Locating and collecting. In: JONES, T.P. & ROWE, N. P. (Eds). Fossil Plants and Spores: modern techniques. Geological Society, London: 15-19.

TRAVERSE, A., 2007. Paleopalynology: Topics in Geobiology, 28. Springer: 813pp.

WOOD, G. D., GABRIEL, A. M. & LAWSON, J. D., 1996. Palynological Techniques - Processing and microscopy. In: JANSONIUS, J. & MCGREGOR, D. C. Palynology: Principles and Applications. American Association of Stratigraphic Palynologists Foundation 1: 29-50.

Personal Comunications

BROCKE - Rainer Brocker. Senckenberg Forschungsinstitut und Naturmuseum Senckenberganlage 25 60325 Frankfurt a.m. Deutschland

CLAYTON – Geoff Clayton. Department of Geology Trinity College. Dublin 2, Ireland

FATKA – Olda Fatka. Institue of Geology and Paleontology. Charles University. Albertov 6, Praha 2 - 128 43. Czech Republic.

FERNANDES – José Pedro Fernandes. Departamento de Geologia. Faculdade de Ciências da Universidade do Porto. Praça Gomes Teixeira 4099 - 002 Porto. Portugal.

PEREIRA – Zélia Pereira. Departamento de Geologia. Laboratório Nacional de Energia e Geologia. Rua da Amieira Apartado 1089 4466-956 S. Mamede de Infesta. Portugal.

STREEL – Maurice Streel. Géologie - B20, Université de Liège, Sart Tilman, B-4000 Liège. Belgium.

TONGEREN – Jan van Tongeren. Laboratory of Palynology and Palaeobotany. Utrecht University. Biology Dept. Budapestlaan 4. 3584 CD. Utrecht. The Netherlands.

VAVRDOVÁ – Milada Vavrdová. Institute of Geology, Academy of Sciences of the Czech Republic. Rozvojová 269, 165 00 Praha 6 – Lysolaje. Czech Republic

VECOLI – Marco Vecoli. Université de Lille 1. U F R Sciences de la Terre. Laboratoire LP3 - Bâtiment SN5. 59655 Villeneuve d'Ascq Cedex. France

VERNIERS – Jacques Verniers. Universiteit Gent. Vakgroep Geologie en Bodemkunde (Campus De Sterre). Krijgslaan 281, S8. 9000 Gent. Belgium.

Chapter 3

Palynology and Stratigraphy of the Albergaria-a-Velha metasedimentary unit - Porto-Tomar major shear zone (Espinho-Miranda do Corvo sector)

This chapter includes work published in
MACHADO, G., VAVRDOVÁ, M., ROCHA, F.T., FONSECA, P.E., CHAMINÉ, H.I., 2009. Dating and differentiation of geological units in highly deformed and metamorphosed rocks – Can palynology help? Examples from the Ossa- Morena Zone (W Portugal). *Trabajos de Geologia* (in press).

MACHADO, G., VAVRDOVÁ, M., FONSECA, P.E., CHAMINÉ, H.I. & ROCHA, F. T., 2008. Overview of the Stratigraphy and initial quantitative biogeographical results from the Devonian of the Albergaria-a-Velha Unit (Ossa-Morena Zone, W Portugal). *Acta Mus. Nat. Pragae, Ser. B, Hist. Nat.* 64 (2-4): 109-113.

MACHADO, G., VAVRDOVÁ, M., ROCHA, F.T., FONSECA, P.E., CHAMINÉ, H.I., 2008. Organic-walled microplankton from the Upper Devonian of the Albergaria-a-Velha black shales (W Portugal) and its palaeobiogeographical implications: preliminary results. 12th International Palynological Congress, 8th International Organisation of Palaeobotany Conference Bonn, Germany. Abstract Volume. *Terra Nostra* 2008/2. August 30 – September 5, 2008: 176.

MACHADO, G., VAVRDOVÁ, M., FONSECA, P.E., ROCHA, F.T. & CHAMINÉ, H.I., 2007. Palynomorphs from the metasediments of the Bemposta-Minhoteira sector (Albergaria-a-Nova area, Ossa-Morena Zone, NW Portugal). Portugal, INETI. In: Pereira, Z., Oliveira, J. T., Wicander, E. R. (Eds). Abstracts of the joint meeting of Spores/Pollen and Acritarch subcommissions CIMP. Lisbon, Portugal, 25-28.

PALYNOLOGY AND STRATIGRAPHY OF THE ALBERGARIA-A-VELHA METASEDIMENTARY UNIT - PORTO-TOMAR MAJOR SHEAR ZONE (ESPINHO-MIRANDA DO CORVO SECTOR)

Chapter Index

Abstract ... 40
3.1 Introduction ... 41
3.1.1 Geological setting ... 41
3.1.2 Factors controlling palynomorph preservation in metasediments and its application to the study of the AVU ... 43
3.1.2.1 Nature and characteristics of palynomorphs ... 43
3.1.2.2 Relevant Geological Variables ... 43
Sedimentation and diagenetic factors ... 43
Temperature and pressure ... 43
Compaction and Deformation ... 44
Fluid circulation and mineralization ... 45
3.2 Materials and methods ... 46
3.2.1 Stratigraphy ... 46
3.2.2 Provenance ... 46
3.2.3 Palynology and Palynofacies ... 48
3.2.4 Organic geochemistry and vitrinite reflectance ... 49
3.3 Results ... 50
3.3.1 Stratigraphy, Sedimentology and facies ... 50
3.3.2 Detrital framework analysis and provenance ... 54
3.3.3. Palynofacies ... 57
3.3.4 Palynology ... 59
3.3.4.1 Miospores ... 60
3.3.4.2 Organic-walled microplankton ... 62
3.3.5 Organic geochemistry, source rock potential and organic maturity ... 64
3.4 Discussion and Conclusions ... 67
3.5 Systematic Palynology ... 71
3.5.1 Miospores ... 71
3.5.2 Organic-walled microplankton ... 80
Acknowledgements ... 83
References ... 84
Plates ... 94

Abstract

The Albergaria-a-Velha Unit is one of the several tectonostratigraphic out-of-sequence units of the metamorphic belt associated with the Porto-Tomar strike-slip shear zone. It is composed by considerably deformed metasediments, namely shales, siltstones and rare fine sandstones. The sedimentological, stratigraphical and palynological data suggest that the Albergaria-a-Velha Unit was deposited from the (?)Early Frasnian to the Serpukovian in a distal marine environment, where turbiditic and basinal sedimentation prevailed, adjacent to a deltaic system. The collected data also suggests a gradual increase

of terrestrial input, indicating a prograding system. Detrital framework data points to a stable cratonic sediment source area composed by low grade metamorphic rocks. This unit is within the dry gas window in terms of hydrocarbon generation ranges.

Key-words: Ossa-Morena Zone, Porto-Tomar shear zone, Albergaria-a-Velha Unit, miospores, acritarchs, palynofacies, provenance, Late Devonian, Mississippian.

3.1 Introduction

3.1.1 Geological setting

The Iberian massif, in its northwestern region, is transected by a NNW-SSE major dextral deep-crustal shear zone, separating the Ossa-Morena Zone – OMZ (to East) and the Central Iberian Zone – CIZ (to West) (Chaminé, 2000; Chaminé et al., 2003, 2007; Dias & Ribeiro, 1993; Gama Pereira, 1987). This shear zone (Porto-Tomar shear zone – PTSZ) comprises a narrow metamorphic belt that extends from Tomar area (western central Portugal) (Gama Pereira, 1987) to South of Porto area (NW Portugal) (Chaminé, 2000; Chaminé et al., 2003, 2007; Pereira et al., 1998). The inclusion of this metamorphic belt in the OMZ has been assumed by most authors based on some lithological and chronological similarities between units of the PTSZ and units of the southern part of the OMZ, especially along other shear zones (Chaminé, 2000). Recently a revised interpretation of the geodynamic evolution of the Iberian variscides refers a Finisterra affinity for the metamorphic belt associated with the PTSZ (Ribeiro et al., 2007). The general dextral sense movement of this shear zone was considered to have started during the "Westphalian", based on the evident tectonosedimentary control of the Pennsylvanian Buçaco basin (e.g. Lefort & Ribeiro, 1980; Ribeiro et al., 1980; Gama Pereira et al., 2008; Pinto de Jesus et al., 2010), but was reinterpreted using structural data from the CIZ, as being already active during the early stages of the Variscan orogeny by Dias & Ribeiro (1993). The post-Mesozoic geodynamic evolution of Iberia has been dominated by reactivating inherited crustal structures, which induce stress activity of the Porto-Tomar fault zone segments since the end of the Variscan orogeny until the present-day (e.g., Gomes et al., 2007; Gomes, 2008; Vicente & Vega, 2009).

This metamorphic belt comprises several relative autochthonous and parautochthonous tectonostratigraphic units with high to very low metamorphic degrees, as well as allochthonous units of medium to high metamorphic degrees (Severo Gonçalves, 1974; Gama Pereira, 1987, 1998; Chaminé, 2000; Chaminé et al., 2003a,b, and references there in). The substratum of this belt comprises a Late Proterozoic unit (Beetsma, 1995) composed by black, grey and greenish phyllites and amphibolites (Chaminé, 2000, Fernández et al., 2003) – Arada unit and its equivalents further South to the region of Coimbra and Tomar (Chaminé et al., 2003; Gama Pereira, 1987). The Albergaria-a-Velha Late Paleozoic very-low black metasediments was initially reported by Chaminé (2000) and later proposed the Albergaria-a-Velha unit (AVU) by Chaminé et al. (2000). This is one of the several tectonostratigraphic out-of-sequence units of Porto–Coimbra–Tomar metamorphic belt. This metapelitic unit is tectonically imbricated with the Arada unit and its metapelitic equivalents further South to the region of Coimbra and Tomar (Gama Pereira, 1998; Chaminé et al., 2003a,b), unit making the cartographic differentiation of the two units extremely difficult. The AVU has been dated by Fernandes et al. (2001) and subsequently by Chaminé et al. (2003, 2007) as being Givetian-Frasnian to "Namurian" in age, using miospores. The thermal history of this unit has been investigated by Moço et al. (2001) and Chaminé et al. (2003) using vitrinite reflectance data, indicating a relatively low maturity, within catagenesis. The examination of phyllosilicate crystallographic parameters from this unit indicated higher palaeo-

temperatures and pressures, ranging the high anchizone – epizone, i.e., maximum temperatures >200ºC and pressures between 1 and 2 Kbar (Chaminé et al., 2003; Vázquez, et al., 2007). The AVU is overlaid unconformably by Late Triassic sediments of the Lusitanian basin (Grés de Silves Fm.) (Corboulieux, 1974; Palain, 1976), but not by the sediments of the Pennsylvanian Buçaco Basin. These contact the AVU by faults and both are overlain unconformably by the Grés de Silves Fm. (Ribeiro, 1853).

This work is a further contribution to the biostratigraphy (using palynology) and to the stratigraphical and sedimentological characterization of the AVU. The source rock potential and thermal history of this unit are also addressed.

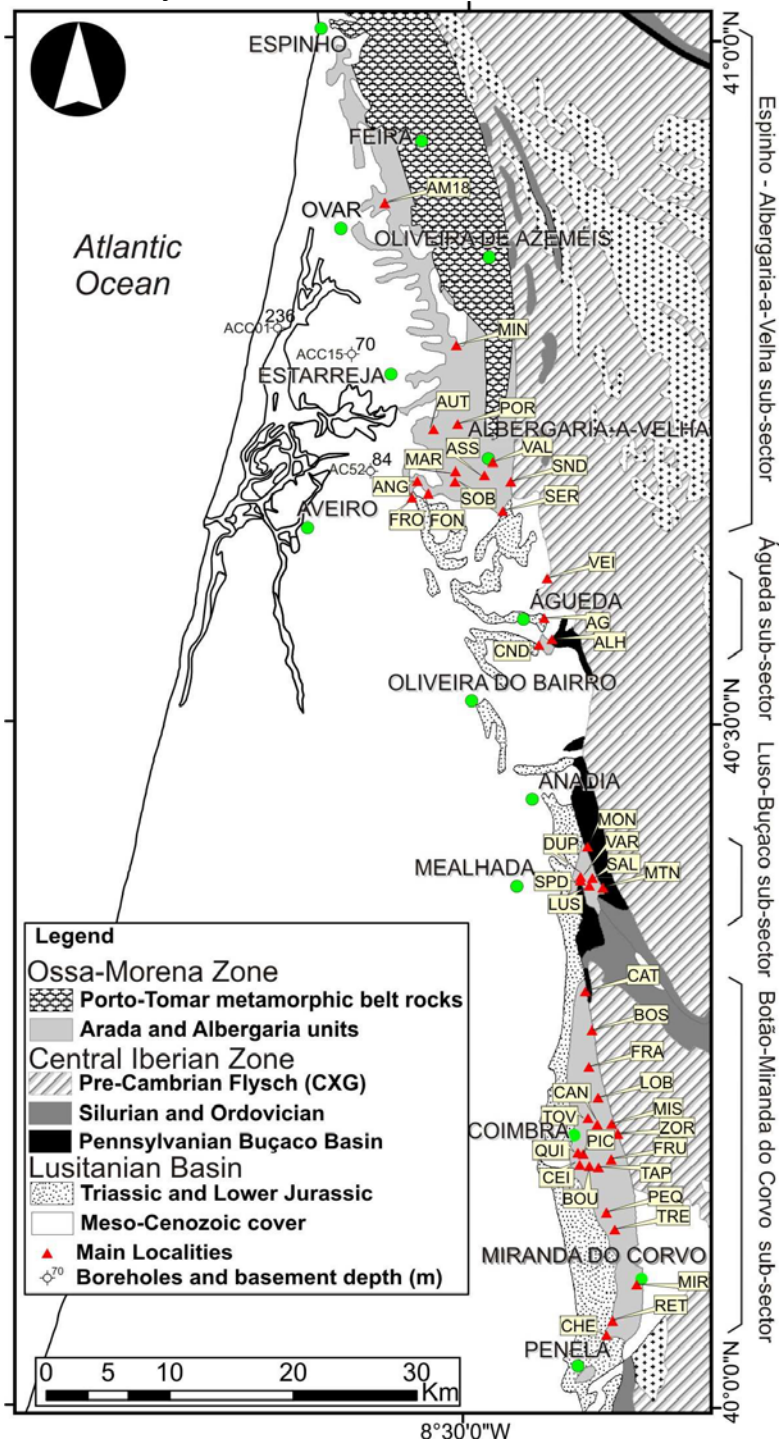

Fig. 3.1 – Simplified Geological map of the Espinho-Miranda do Corvo sector of the Porto-Tomar shear zone and associated metamorphic belt. Studied localities are shown in yellow square balloons. See Appendix 1 for exact location of samples.

3.1.2 Factors controlling palynomorph preservation in metasediments and its application to the study of the AVU

3.1.2.1 Nature and characteristics of palynomorphs

Due to the solubility of the mineral substances that make up most macrofossils and microfossils, they are very frequently absent or dramatically modified in sedimentary rocks that have been subjected to metamorphism. The main variables involved are temperature and pressure which are often associated with deformation and fluid circulation. Palynomorphs have sizes from a few micrometers (small acritarchs) up to a few hundreds of micrometers (larger chitinozoans and megaspores). The wall is composed of different organic substances according to their nature. It is usually very resistant to abrasion, breakage and can maintain its overall shape in a wide range of temperatures and pressures, showing a gradual and irreversible darkening with temperature. (e.g. Yule et al., 1998, 1999, 2000). Palynomorphs are found in rocks from the Precambrian (first acritarchs) up to recent. They are usually obtained by maceration of sedimentary rocks (HCl + HF attacks) and mounting of the organic residue on a microscopy slide. They can also be observed in thin sections, but this is done only when the organic wall has been replaced by mineral matter or when fragmentation precludes taxonomic identification in an organic residue observation.

3.1.2.2 Relevant Geological Variables

Sedimentation and diagenetic factors

Due to their size and hydrodynamic characteristics palynomorphs tend to be concentrated in pelitic sediments (e.g. Traverse, 2007). Coarser grained rocks may provide palynomorphs but usually in a much lower quantity and quality. Carbonates rarely provide good palynological assemblages (e.g. Wicander and Wright, 1983) due to the alkalinity of their sedimentation setting and usual low concentration of organic matter (Gehman, 1962; Traverse, 2007). Anoxic and dysoxic environments during both sedimentation and diagenesis favor organic matter preservation and thus of palynomorphs (Traverse, 2007; Tiwari et al., 1994). An extensive discussion with examples of the effects of physical variables during deposition and diagenesis is given in Tiwari et al. (1994).

Temperature and pressure

With increasing temperature and pressure palynomorphs progressively and irreversibly change colour and loose transparency. The effect of lithostatic pressure has been shown to retard organic maturation, but its effect is drastically reduced over 1Kbar (Sajgo et al.; 1986; SenGupta, 1975).

For the most mature and metamorphosed spores, little differentiation can be made as they reach a black and transmitted-light-opaque stage. They become more brittle and are thus more easily broken by deformation but their overall shape is frequently preserved and taxonomic identification is possible using strong oxidizing agents or SEM observation (e.g. Traverse, 2007).

Acritarchs respond differently and thin walled ones can remain translucent up to low-grade metamorphic conditions after which they start to disaggregate (especially when associated with deformation) and frequently produce skeletal structures with relicts of

their original ornamentation (Fig. 3.2). Thick walled acritarchs become dark in a similar way as spores and are destroyed in the same way as thin walled acritarchs.

Chitinozoans are probably the most resistant palynomorphs. They can be partially preserved as graphitized particles in mylonitic gneisses with estimated peak temperatures between 300 and 500ºC (Hanel et al., 1999). In all of these cases palynomorphs still provide useful palaeoenvironmental data and in some cases crude biostratigraphical bracketing.

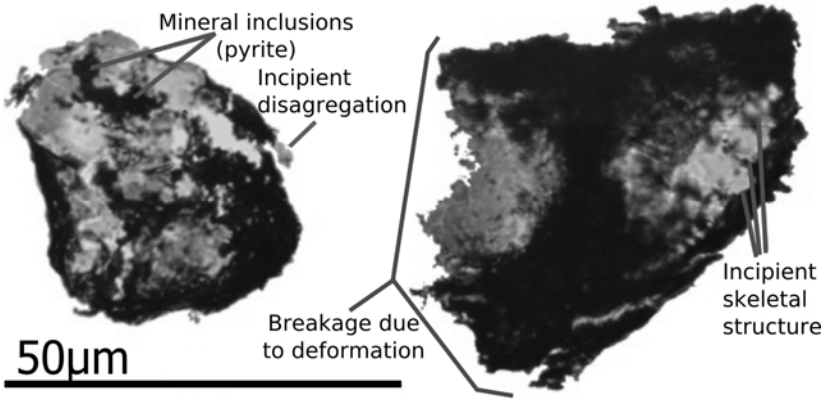

Fig. 3.2 - Example of partially destroyed thin-walled ?prasinophytes from a Frasnian highly deformed metasediment comprised in the AVU.

Compaction and Deformation

Compaction due to lithostatic pressure, especially in shales, causes flattening and consequent folding of the wall of palynomorphs (e.g. Clayton, 1972). Due to their elastic wall, the overall shape and ornamentation is usually preserved. Sedimentary rocks and their fossil content preserve most of their characteristics when subjected to gentle folding and minor faulting. Other deformation features such as penetrative foliation, grain boundary sliding, closely packed folding and bedding-parallel shear movement can destroy the entire macrofossil content and a significant part of the millimetre-sized microfossils. Due to their minute size and organic wall, palynomorphs can be preserved even in metasediments with millimetre scale foliation and closely packed kink folds. This is frequently observed in the AVU (Fig.3.3).

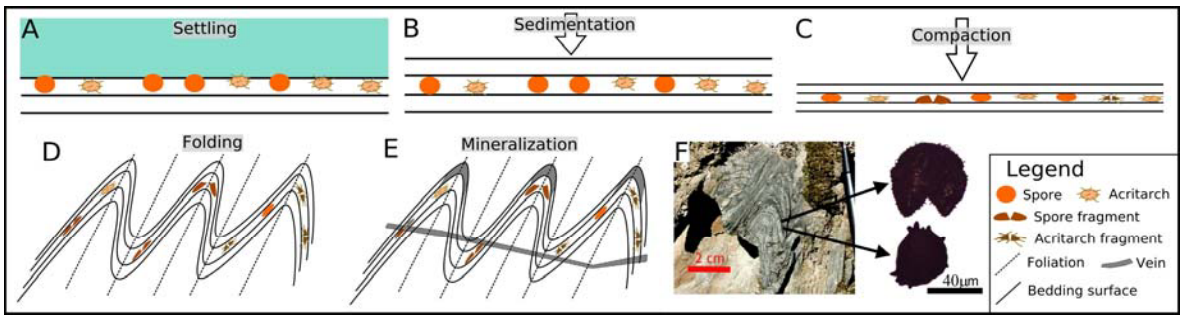

Fig. 3.3 - Schematic illustration of a hypothetical sequence of palynomorph destruction/preservation and a real case of a deformed and metamorphosed rock that provided both acritarchs and spores. A - sedimentation of palynomorphs in a marine setting; B - sedimentation of overlying strata; C - compaction due to overburden and destruction of some palynomorphs; D - Folding and associated foliation with further destruction of palynomorphs; E – Mineralization during or posterior to deformation with minor effect on palynomorphs; F - Real case of a deformed and mineralized metasediment that provided moderately preserved palynomorphs

Fluid circulation and mineralization

It is widely known among palynologists and organic petrologists that oxidation (positive Eh values), resulting either from weathering, diagenesis or metamorphism alters or destroys organic-matter (e.g. Tiwari et al., 1994). Metasediments that have extensive mineralization or veining with oxides are almost invariably barren. On the other hand exceptionally preserved palynomorphs can be found in pisolitic ironstones, in both matrix and pisoliths (Vavrdová, 1999). Sulphide mineralization, when restricted to veins or not completely replacing the host rock has a milder effect. Palynomorphs frequently have pyrite crystals growing inside of the wall or attached to the processes, but are generally preserved (Fig.3.2).

Silicification in early diagenesis stages can actually increase the fossilization potential of palynomorphs preserving them in their original 3D form as observed in the Rhynie chert. Silicification (either extensive or veining) in late diagenesis and during metamorphism usually decreases the preservation quality, but it is usually not a determining factor, except when there is a significant replacement of the host rock by silica. Samples of Upper Devonian black shales with mm-thick quartz veins and very near to thick (ca. 50cm) quartz + complex carbonates ± pyrite ± chalcopyrite ± dickite/kaolinite veins (Chaminé, 2000; Chaminé et al., 2003) were equally as fossiliferous as samples from the same locality with no mineralization, although more undissolved minerals remained after HF attack.

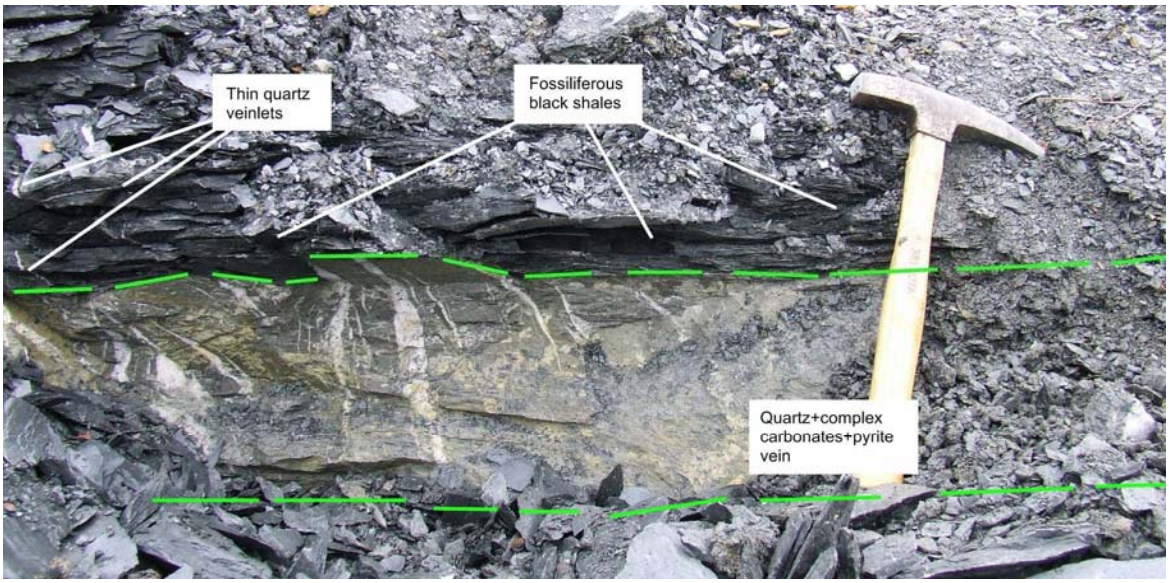

Fig. 3.4 - Fossiliferous black shale samples affected by mineralization.

It is difficult or even impossible to determine well defined limits of physical and chemical variables under which palynomorphs are preserved. In the case of the AVU sediments exposed to temperatures higher than 200ºC and pressures up to 2Kbar (Vázquez et al., 2007) provide diversified and moderately preserved palynomorphs that allow biostratigraphical bracketing to the stage level and sound palaeoenvironmental determinations. Strong deformation and some types of mineralization have a limited detrimental effect on the quality of the assemblages. The more deformed and heated, the worse the quality of the microfossils, but at least in some cases palynomorphs can be preserved in mylonitic gneisses exposed to temperatures between 300 and 500ºC and which still provide useful sedimentary and stratigraphical information (Hanel et al., 1999).

The potential of many metasedimentary units around the World is probably greater than currently considered by many palynologists and geologists. Although laborious and

sometimes unsuccessful, palynological processing of metasediments can provide information that would otherwise be unattainable.

3.2 Materials and methods

3.2.1 Stratigraphy

A few short undeformed sequences can be observed, up to ca. 24m thick in localities FON (3 sections – Espinho-Albergaria-a-Velha sub-sector), MON (1 section – Buçaco-Luso sub-sector) and BOS (1 section - Botão-Miranda do Corvo sub-sector) – see Fig. 3.1 and Appendix 1 for locations. These were logged and sampled for palynology, thin sections and polished surfaces to observe relevant sedimentary features. All other known localities may have a few relatively undeformed beds, but are invariably bounded by faults and are usually folded, making it impossible properly describe and interpret the sequence.

3.2.2 Provenance

The application of quantified modal compositions of sandstones to the study of provenance of sediments and geodynamic setting started with the seminal work of Dickinson (1970) and was later developed and refined by Basu et al. (1975) and Dickinson & Suczek (1979). Using the modal composition of sandstones from well-known and constrained geodynamic settings, they defined several fields of characteristic compositions in Quartz-Feldspar-Lithic fragments ternary diagrams. The method has been successfully used in several marine settings (e.g. Valloni & Maynard, 1981; Valloni, 1985; Packer & Ingersoll, 1986) and also with fluvial sandstones (e.g. Arribas & Arribas, 1991. Ingersoll, 1990; Garzanti et al., 2004; Pera & Arribas, 2004). This method is particularly useful to study ancient sedimentary rocks and metasediments, when the source areas and most of the evidences of the plate-tectonic setting prevailing during their deposition are not available or cannot be directly inferred (Bhatia, 1983). This is clearly the case of the AVU.

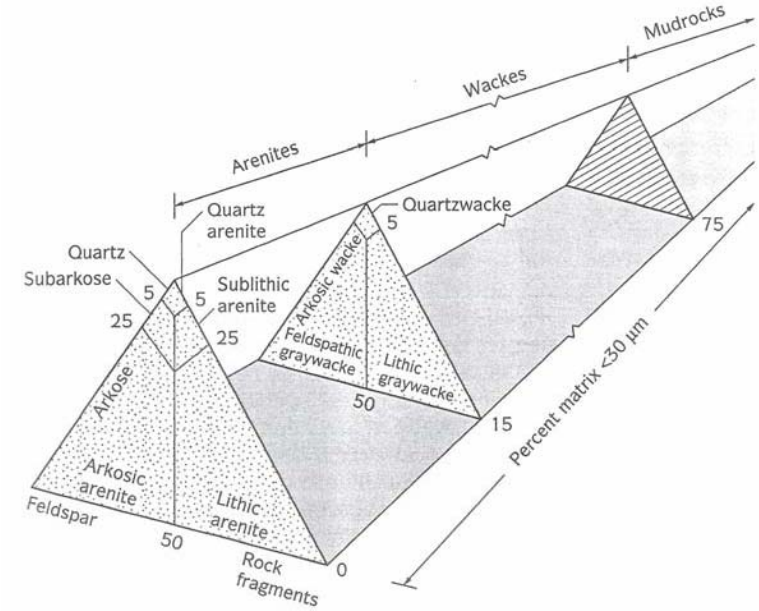

Fig. 3.5 – Classification scheme for sandstones. Adapted from Prothero & Schwab (1996).

The AVU is composed essentially by pelitic metasediments. Fine sand-sized rocks are generally rare, but are available is some areas, at the base of turbidite beds. The

samples used in this work derive from such beds from localities FON (1 sample – Espinho-Albergaria-a-Velha sector); MON (1 sample, Buçaco-Luso sub-sector); ALH and CND (3 samples - Águeda sub-sector); BOS, QUI and ZOR (4 samples – Botão-Miranda do Corvo sub-sector) – see Fig. 3.1 for locations and Appendix 1 for details.

The samples were thin sectioned preferentially parallel to bedding in order to obtain a homogenous grain size within the thin section. The grain packing index (*i*) (Kahn, 1956) was determined using the following equation:

$$i = \frac{Nc}{L} \times D$$

Where *Nc* is the number of grain-grain contacts along the length (*L*) and *D* the average grain diameter. Samples were classified using the classification scheme in Fig. 3.5.

300 particles were counted in each thin section using a semi-automated Swift point counter coupled to a Leitz Orthoplan microscope. Observation and counting were performed with crossed polars. The Gazzi-Dickinson counting method was used (Gazzi, 1966 in Ingersoll et al., 1984). Particles smaller than 0,00625mm (silt-sized and smaller) were counted as matrix. Recrystallization of the matrix, the presence of metamorphic minerals and also silicification were observable in some samples which often made difficult the recognition of individual grains. Grains of doubtful origin (probably metamorphic or from matrix recrystallization) were not considered. For quantification purposes, the Gazzi-Dickinson method considers the mineral of a polymineralic particle (lithic fragment) and not the lithic fragment itself, except where the grain-size of the lithic fragment is smaller than fine-sand (see Fig.3.6). Naturally the proportion of lithic fragments is reduced when compared with the classical method which does not discriminate minerals within lithic fragments. It does, however, reduce the effect of variable grain size which is often the case in sandstones. The following table summarizes the several categories of grains counted and some of their main characteristics.

Grains		Code	Main features
Quartzose monocrystalline		Qm	Fresh, commonly with undulatory extinction pattern
Quartzose polycrystalline		Qp	Mostly chert grains, minor fine-grained quartzites
Plagioclase		P	Typically slightly weathered and small. Characteristic polysynthetic twinning
K Feldspar		K	Typically slightly weathered and small
Undifferentiated Feldspars		Fx	Typically slightly weathered and small
Lithic fragments		L	Black, cryptocrystalline occasionally with very fine micas
Dense minerals		D	Very rare, mostly pyroxenes(?)
Uncertain		Misc	Too weathered of difficult to distinguish from matrix
Matrix		M	Generally siliceous, often with small micas
Groups of grain categories considered for QFL and QmFLt ternary plots			
QFL	Total Quartz	Q	Qm+Qp
	Feldspars s.l.	F	P+K+Fx
	Lithic fragments	L	L
QmFLt	Monocrystaline Quartz	Qm	Qm
	Feldspars s.l.	F	P+K+Fx
	Total lithics	Lt	L+Qp

Table 3.1 – Grain categories considered for this study, their main characteristics and groups of grain categories used for ternary plots.

Lithoclasts were initially differentiated according to their nature (volcanic, sedimentary and metamorphic) but the reduced number of grains and their cryptic nature did not allow the desired differentiation. The results were plotted in ternary diagrams and compared with the previously defined plots (Dickinson & Suczek, 1979 and Dickinson et al., 1983) using Grapher 4.0 software.

The number of undulatory and non-undulatory quartz grains and also the number of crystals of each polymineralic quartz grain were counted using the parameters defined in Basu et al. (1975). The counts were made on successive randomly chosen fields of view, counting all the grains greater than 0,0125mm. Due to the low grade metamorphism and deformation, only 5 samples were suitable for this analysis. The results were plotted in a diamond diagram using the fields proposed by Basu et al. (1975) as indicators of rock types in the source areas.

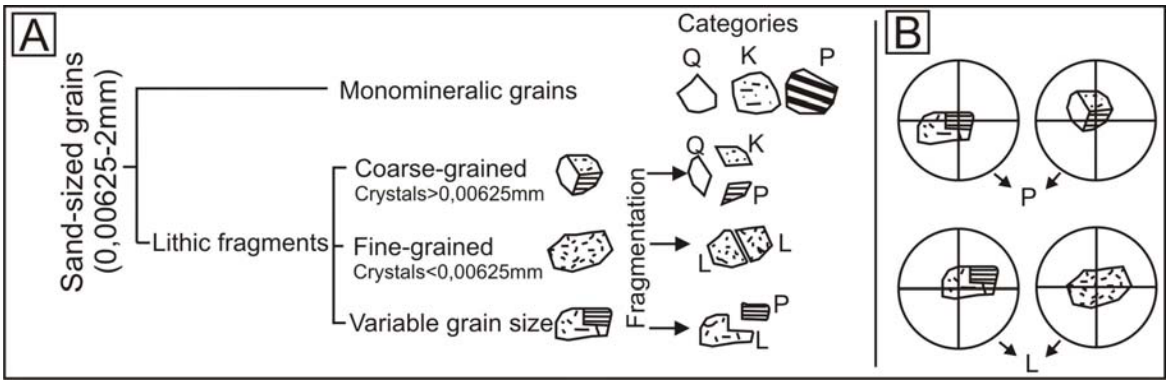

Fig. 3.6 – Schematic representation of the Gazzi-Dickinson method. A – Discrimination between monomineralic grains and lithic fragments and theoretical consequences of fragmentation. B – Practical categorization of grains when counting under the microscope. Modified from Zuffa (1985).

3.2.3 Palynology and Palynofacies

Several hundreds of dark grey and black shale and siltstone samples were collected. Of these about 250 were processed for palynology using the methods described in Chapter 2. Most of the processed samples produced considerable amounts of organic residue, but only about 100 had observable palynomorphs (called here productive samples). The slides produced from the productive residues were observed in transmitted light microscopes. Documentation of observable palynomorphs was conducted using a digital camera apparatus attached to the microscope. Selected productive residues were mounted in acrylic plates, air-dried and observed (and photographed) using a reflected light microscope (see Chapter 2).

The term palynofacies was introduced by Combaz (1964) and the concept has been successfully used for palaeoenvironmental interpretations and source rock assessment since then (see Batten, 1996a, b; Traverse, 2007 and Tyson, 1987, 1993 for revision of methods and applications). Palynofacies is based on the study, usually quantified, of particulate organic matter (or palynological matter) obtained by maceration of sedimentary rocks (Traverse, 2007; Tyson, 1993), as observed under transmitted light microscopy. The relative and absolute percentages of land- and marine-derived palynomorphs provide valuable information for the determination of sedimentary facies. Similarly the quantification of oil- and gas-prone organic particles allows a rapid and semi-quantitative assessment of source rocks.

Due to the generally poor quality of the organic residues obtained from the AVU the palynofacies analysis was limited to a few fundamental categories of palynomorphs. About 30 samples of known age were used. For each sample, two types of analysis were performed:

1) total particulate organic matter content analysis as observed on slides made from a non-sieved residue (see Chapter 2 for details). The following table summarizes the categories considered:

Category	Palaeonvironmental significance	Source rock
AOM	Stratified water column or deep basin. Anoxic-suboxic conditions.	Oil-prone
Phytoclasts	Exclusively land-derived, proxy for shore proximity.	Gas-prone
Palynomorphs	Variable.	Oil-prone

Table 3.2 – Summary table of the selected categories used for the palynofacies analysis on non-sieved slides. Compiled from Tyson (1987, 1993) and Batten (1996a, b).

2) non-AOM analysis observed on slides produced from a 7μm-sieved organic residue. Table 3.3 summarizes the categories considered:

Category	Origin	Palaeonvironmental significance	Source rock
Spores	Terrestrial	Exclusively land-derived, proxy for shore proximity	Oil-prone
Phytoclasts		Exclusively land-derived, proxy for shore proximity	Gas-prone
Zooclasts		Benthic marine arthropods, but also land derived debris	Inert
Chitinozans	Marine	Exclusively marine, relatively deep environments.	?
Acritarchs		Exclusively marine, proxy for organic productivity under "normal" marine conditions	Oil-prone
Prasinophytes		Dominant in abnormal marine conditions (salinity, temperature, oxygenation, etc.)	Highly Oil-prone

Table 3.3 - Summary table of the selected categories used for the palynofacies analysis on 7μm-sieved slides. Compiled from Tyson 1987, 1993; Miller, 1996 and Batten 1996a, b.

Other approaches to palynofacies analysis such as the differentiation of long- and short-spined acritarchs and spore morpho groups were not attempted as the studied palynomorphs were probably preferentially preserved or destroyed by metamorphism and deformation.

Most categories can be easily recognized under transmitted light microscopy. Chitinozoans and zooclasts were grouped because their differentiation is often difficult due to the considerable maturity of the organic matter. Phytoclasts could be differentiated in most instances by their overall morphology, but smaller and heavily-degraded particles were sometimes doubtfully assigned to this category, although they could also be classified as degraded zooclasts. Thus there is an inherent uncertainty associated with this method.

3.2.4 Organic geochemistry and vitrinite reflectance

Twelve selected samples were analyzed by Rock-Eval 6 pyrolysis. The samples were gently pulverized, homogenized and sieved through a 1 mm mesh. All samples were subjected to elemental analysis of total organic and inorganic carbon (TOC, TIC, respectively) using an Eltra Metalyt CS 100/1000S apparatus at the Organic Geochemistry

lab of the Czech Geological Survey (Brno). The Rock-Eval 6 pyrolysis (Espitalié et al. 1985, Lafargue et al. 1998) was carried out in nitrogen at a programmed temperature of 300-550 °C with heating rate of 25 °C/min. Several organic geochemical parameters were obtained, namely S1 – free hydrocarbons (mg HC/g rock); S2 – bound (pyrolytic) hydrocarbons (mg HC/g rock); pyrogenic CO_2 and CO (S3) and peak temperature of pyrolysis (T_{max}); HI – hydrogen index (mg HC/g TOC) and OI – oxygen index (mg CO2/g TOC).

Heavy liquid concentrates and selected palynological residues obtained by cold HF dissolution of mineral matter were mounted using the methods described in Chapter 2. Both types of residues were observed under a microscope Leitz ORTHOPLAN. (reflected light) of the Organic Petrology lab of the Geology Department of the Faculty of Sciences of the University of Porto. Reflectance measurements and photomicrographs were obtained with the image analysis software FOSSIL and DISKUS.

3.3 Results

3.3.1 Stratigraphy, Sedimentology and facies

The AVU is composed of several dispersed outcrops of pelitic metasediments and rare fine sandstones. Most of the sedimentary information is obliterated by an intense deformation and very low to low grade metamorphism. Due to the different rheologic behaviour of lithologies to deformation, most of the sedimentary information is preserved on siltstones and sandstones while shales seldom allow the observation of sedimentary structures. This difference is visible at the outcrop scale, down to millimetre scale, as observed in thin sections. Outcrops dominated by shales or fine siltstones are consistently heavily deformed. Original bedding and fine lamination are occasionally observed as S_0 surfaces between S_1 (foliation) penetrative surfaces.

The sand/mud ratio varies greatly, but seems to be fairly similar within a group of outcrops over areas of few Km^2. This ratio was visually estimated for localities and groups of outcrops. It is typically between 30%/70% to 20%/80% and the total average is close to 30%/70%. The longest preserved sequences are sandstone- (and sometimes siltstone-) dominated and thus have a higher-than-average ratio.

Very rare cm-thick oil shale beds can be observed in some sections dominated by shales (and more rarely also siltstones and fine sandstones). More commonly the same type (presumably) of oil shales is found within fault gauges.

During the course of this work not a single macrofossil or trace fossil was found, despite a persistent and systematic search in every outcrop with preserved sedimentary features. The chances of finding fossils at a macroscopic scale are considerably reduced by the metamorphism and deformation of this unit.

The vast majority of non-weathered outcrops had rocks of light to dark grey or black colour. Notable exceptions are some, but not all, siltstone and fine sandstone beds, which had yellow to light brown colours.

Considering the localities where sedimentary information can be obtained, three main lithofacies can be defined. These should be, however, considered end members of a range. The main characteristics are defined in table 3.5. The laminated grey shale facies is very commonly observed and can be recognized even with considerably deformed rocks, as the striking contrast of light grey and dark grey mm-thick laminae is often preserved. The lamination is defined by darker and finer laminae alternating with lighter and slightly coarser laminae. This is observed at hand sample and thin section scales (Pl. 3.16F, G).

Sub-sector	Locality/Group of outcrops	Age	Mud %	Sand %
Espinho – Albergaria-a-Velha	MIN	Early Frasnian	100	0
	AUT	Famennian?	100	0
	ASS	Early Tournaisian	100	0
	VAL	Late Famennian -Early Tournaisian	100	0
	FRO	Serpukovian?	90	10
	FON F (preserved section)	Early Serpukovian	60	40
	FON N	Early Serpukovian	90	10
	FON G (preserved section)	Early Serpukovian	20	80
	FON I (preserved section)	Early Serpukovian	50	50
	SND-B	Early Serpukovian	20	80
	SER	Serpukovian	100	0
Luso – Buçaco	MON (preserved section)	Serpukovian	90	10
	SPD-DUP	?	90	10
	MTN	Famennian?	100	0
Botão – Miranda do Corvo	BOS2 (preserved section)	?	10	90
	BOS	?	20	80
	FRA	Tournaisian-Viséan	50	50
	LOB	Early Tournaisian	100	0
	QUI-TOR	Serpukovian	30	70
	QUI	Serpukovian	40	60
	ZOR	?	80	20
	CEI-TAP-FRU	Late Famennian?	80	20
	BOU	Late Famennian -Early Tournaisian	20	80
	SEN	?	20	80
	TRE	?	80	20
	MIR2	?	80	20
	MIR3	?	30	70
	RET	Early Frasnian	90	10
	CHE	Early Viséan	80	20

Table 3.4 – Visual estimates of sand/mud ratio in several localities and groups of outcrops. Localities are listed roughly from North to South.

The black shale facies can be found in localities such as VAL, ASS, SER, AUT and LOB which are entirely composed by shales (Pl. 3.17B) with an extremely reduced fine siltstone component. Pyrite is frequently observed in these and other shale-dominated localities. Lamination is faint and only seldom seen between very penetrative foliation planes.

Of all the studied localities, only five sections showed a deformation degree that allowed the description of relatively continuous stratigraphic sequences and the examination of details of sedimentary features. All of them are bounded by faults which do not allow the recognition of the sequence between the two sides of the fault. All can be included in the sand-silt-shale lithofacies. Three of these sections are at the Fontão locality, Espinho - Albergaria-a-Velha sub-sector (FON – see Fig.3.1), along road cuts between the village of Angeja and Fontão and are Serpukovian in age; one at Monsarros (locality MON2 – see Fig.3.1), Luso-Buçaco sub sector, also Serpukovian in age and one at Bostelim (locality BOS2 – see Fig.3.1), Botão – Miranda do Corvo sub sector, age unknown.

Lithofacies	Description	Associated palynofacies (shales)	Stratigraphical Occurrence	Interpretation
Laminated grey shales	Grey shales with mm- to cm-thick darker and lighter laminae.	Very high AOM; acritarchs and prasinophytes rare, spores common.	Frasnian to Serpukovian.	Basinal sedimentation with seasonal control (?)
Black shales	Black shales with minimal coarser or lighter material. Lamination seldom visible.	Very high AOM; acritarchs and prasinophytes may be common. Spores very common.	Essentially Famennian-Early Tournaisian, but some Viséan and Serpukovian occurrences.	Basinal sedimentation in anoxic conditions
Sand-silt-shale beds	Successive cm- to m- thick beds with normal grading. Massive base, laminated top, occasional cross beds.	Few or none acritarchs and prasinophytes; abundant spores; phytoclasts occasionally frequent.	Restricted to the Serpukovian	Low density turbidites and (?) pro delta deposits

Table 3.5 – The 3 end-members of the lithofacies defined for the AVU, their summarized description, associated palynofacies, stratigraphical occurrence and interpretation of the prevailing sedimentary environment.

At Fontão, sections FON I and FON G are composed by dm- to m-thick (rarely cm-thick) successive beds of fining-upward cycles. Most beds are composed dominantly by siltstones that fine up to shales, but some fine sandstone-dominated beds also occur. These beds typically have a coarser, massive or crudely bedded base and a finer laminated top. Occasionally cross-beds can be observed in a cm- to mm-thick intermediate interval. These correspond to parts $a \pm b \pm c + d \pm e$ of Bouma sequences (Bouma, 1962). Generally thicker beds are also coarser, but some thin beds have relatively coarse beds (fine sandstones). Within these two sections, some intervals are composed solely of very fine siltstone and shales (e.g. 5,5 to 8m at FON I and 3 to 4m at FON G) and no granulometric differences can be distinguished macroscopically within each bed, but analogous fining-upward cycles may be present at a smaller scale. Alternatively these shale dominated intervals can represent basinal deposition occurring between turbidity current events (level *e* of Bouma sequences).

Some general fining and coarsening-upward cycles can be distinguished at the meter scale, but these trends do not seem to be associated with any other sedimentological variation.

These two sections are interpreted as successive low density turbidite beds. The variations in thicknesses and granulometry can be explained by the magnitude of the turbidity event that originated each bed, the position of the sedimentation area in relation to the source area and the granulometry of the sediment available at the source area.

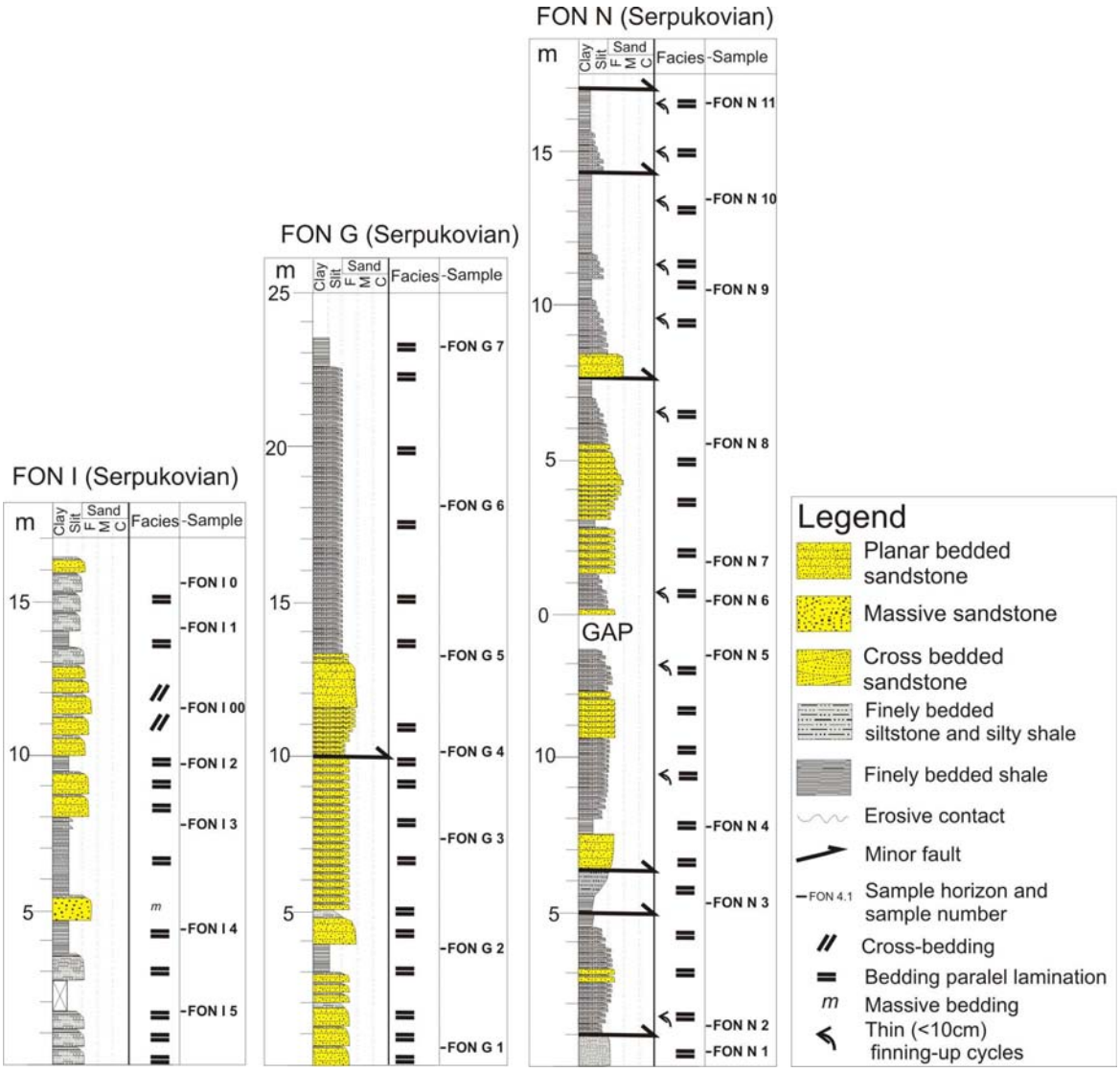

Fig. 7 – Lithological columns of the Fontão (FON) locality.

Section FON N is similar to FON I and FON G and many of its beds can also be interpreted as low-density turbidites. However the section is generally finer grained and the fining-upward cycles are not as well defined and some beds even show inverted grading. Additionally some siltstone beds do not show significant changes in granulometry and lack the massive - cross bed - laminated sequence observed elsewhere. This type of succession of dm-thick fine sandstone and siltstone beds associated with thin shale beds (occasionally even mm-thick oil shale beds) can be observed in a nearby locality (ANG – see Fig.3.1) and possibly in other localities where deformation precludes detailed observation of the sedimentology. This section is interpreted as succession of low density turbidite beds deposited in a considerably distal setting interbedded with basinal sediments represented by the shale dominated intervals, but can also represent pro-delta deposits not necessarily associated with turbidity currents.

The Monsarros 2 section shows a sequence of siltstone-dominated turbidite beds with fairly regular thicknesses, although some very fine fining-upward cycles can be observed (ca. 9m). Cross bedding is seldom observed, although this feature may be obscured by the substantial oxidation of this section. Most beds correspond to levels *a* and *d* of Bouma sequences. Level *e* (shales at the top of each cycle) is very poorly developed in this sequence.

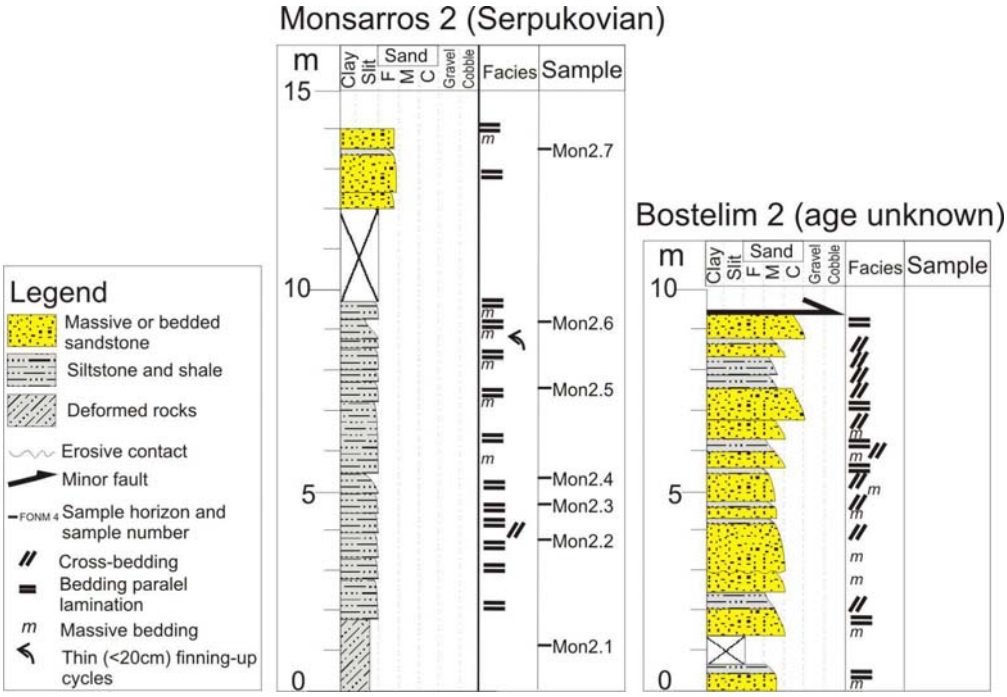

Fig. 8 - Lithological columns of the Monsarros (MON2) and Bostelim (BOS) locality.

The Bostelim 2 (BOS) section is the coarsest sequence observed in all known AVU outcrops. At least in one of the cycles the base is defined by an erosive surface. The fining-upward cycles are dm- to m-thick and commonly have medium to coarse sand-grained bases that grade to siltstones and more rarely shales. Some thinner beds can be observed (Pl. 3.16D). Fairly complete Bouma sequences can be observed, with a thick coarse massive base (level *a*), a crudely to well bedded interval of medium sands (level *b*), cross laminated sands (level *c*) and parallel laminated siltstone top (level *d*). Shales are seldom present at the top of cycles. Palynological samples from this locality were barren.

3.3.2 Detrital framework analysis and provenance

The absence of coarse-grained metasediments in the AVU precludes the direct and precise identification of transported lithologies and thus the interpretation of the source areas.

The collected point-counting data set shows that samples are all wackes, either quartz, sublithic or subarkose wackes, due to their high matrix/cement contents. The arenites have high matrix/cement contents, between 18 and 47%. The original dataset used by Dickinson & Suczek (1979) included only samples with matrix/cement proportion less than 25% which can limit the significance of the collected data.

Quartzose grains, both mono- and polymineralic, dominate all analysed frameworks. Most were monomineralic quartz grains, ranging from 64 to 95% of all grains. Undulatory extinction was commonly observed, although the extinction pattern differed between grains, suggesting that the deformation episode that originated the undulatory extinction affected the units in the source areas and not the AVU itself. Quartzite grains were frequently observed (but counted as monomineralic grains following the methodology described above). Cherts grains are also frequently observed. Feldspars s.l. are quite rare (0 to 3,3%), considerably smaller than other grains and frequently weathered. Plagioclase is the most common feldspar s.l.. Lithic fragments (excluding Qp) are usually rare, ranging from 0 to 6%. These are in most instances black

cryptocrystalline, occasionally with very small mica crystals. They may be volcanic derived lithoclasts, but their true nature is uncertain.

Category / Sample	Qm	Qp	P	K	Fx	L	M	D	Misc	Classification
ALH3.3	51,7%	11,7%	0,0%	0,0%	0,3%	2,0%	32,3%	0,7%	1,3%	Quartz wacke
ALH3.2	52,3%	22,3%	1,0%	0,0%	0,7%	3,3%	18,3%	0,3%	1,7%	Quartz wacke
BOS3.2	35,7%	13,0%	1,0%	0,0%	0,0%	6,0%	39,0%	1,7%	3,7%	(sub)lithic wacke
BOS4.1	36,0%	6,0%	0,0%	0,0%	0,0%	6,0%	47,3%	2,7%	2,0%	(sub)lithic wacke
CND1.2	44,3%	12,7%	0,3%	0,0%	0,0%	2,3%	37,0%	0,7%	2,7%	Quartz wacke
FON I 00	30,7%	7,3%	3,3%	0,0%	1,3%	4,0%	47,3%	1,0%	5,0%	(sub)arkosic wacke
MON2.8c	51,3%	3,3%	1,7%	0,0%	0,7%	0,7%	40,0%	0,7%	1,7%	Quartz wacke
QUI3.1	31,3%	2,7%	0,3%	0,3%	1,3%	2,7%	51,0%	0,3%	10,0%	(sub)lithic wacke
ZOR1.2	31,3%	1,0%	0,3%	0,0%	0,3%	0,0%	60,0%	2,7%	4,3%	Quartz wacke

Table 3.6 – Framework modes, grain packing index and classification of the sandstones from the AVU.

One single sample group is visible, plotting in the craton interior and recycled (quartzitic) orogen fields. The average modal composition of the sample group is $Q_{91,4}F_{2,9}L_{5,7}$ and $Qm_{76,5}F_{2,9}Lt_{20,6}$. The considerable proportion of polycrystalline quartz grains (Qp) accounts for the "shift" from the Qm vertex.

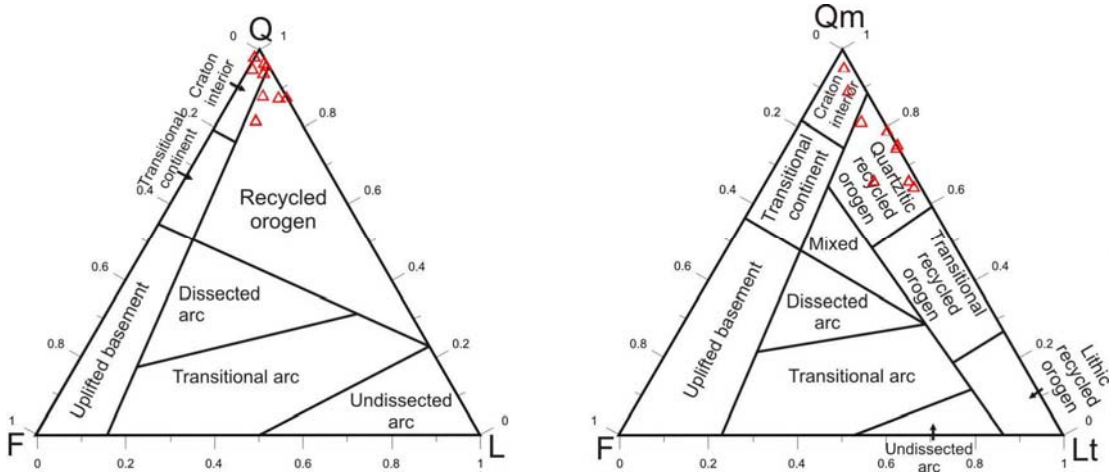

Fig. 3.9 – Ternary QFL (left) and QmFLt (right) plots showing framework modes of the AVU samples. Fields defined by Dickinson et al. (1983) and Dickinson (1985). Redrawn from a Grapher 4.0 output.

All the analyzed samples contained a dominant proportion of undulatory quartz (sensu Basu et al., 1975), from 58 to 67%. The proportions of non-undulatory quartz and polycrystalline quartz varied (between 10 and 27%), but in most cases, the latter was more frequent than the former.

Sample	Qz undulatory	Qz non undulatory	Qz polycrystalline	>3 crystals	<3 crystals
ALH3.2//	63,8%	10,9%	25,3%	86,4%	13,6%
BOS3.2	64,2%	19,1%	16,8%	89,7%	10,3%
BOS4.1	58,0%	20,5%	21,6%	73,7%	26,3%
CND1.2	67,1%	13,2%	19,7%	83,3%	16,7%
ALH3.3B	62,8%	10,4%	26,8%	88,6%	11,4%

Table 3.7 – Percentages of undulatory, non-undulatory and polycrystalline quartz in the analyzed samples.

Among polycrystalline quartz grains, the ones with 3 or more crystal units per grain were clearly dominant, (between 73 and 90%), corresponding to chert (s.l.) grains and more rarely to very-fine quartzite grains.

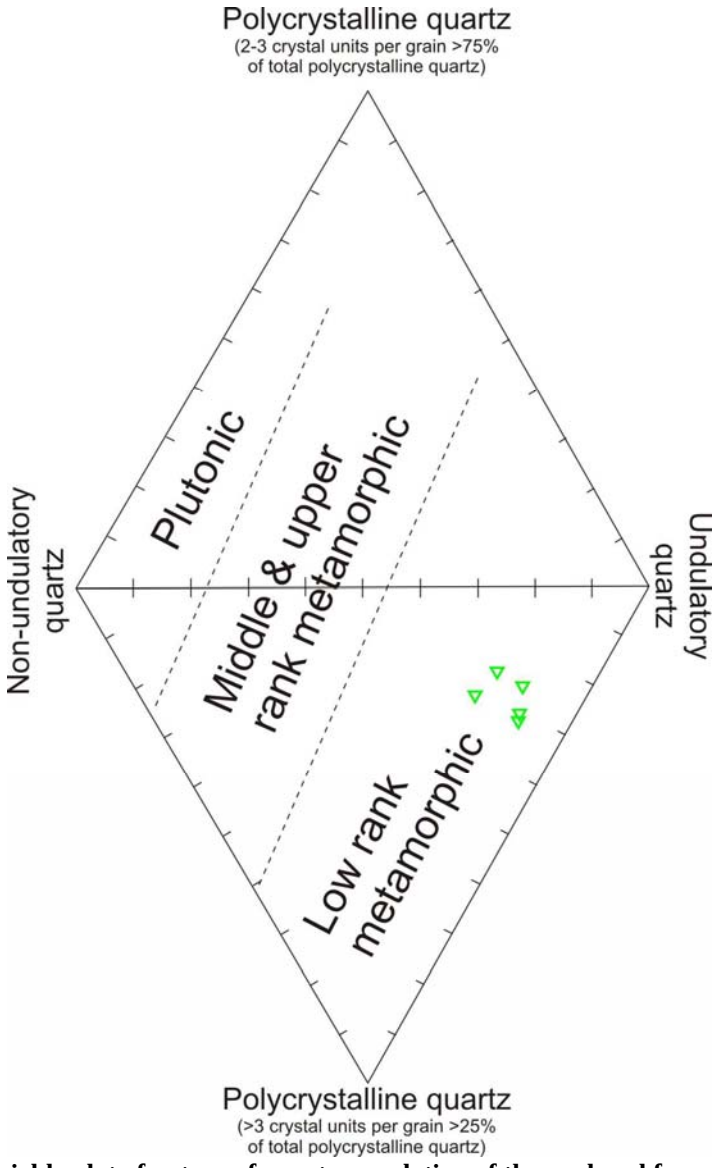

Fig. 3.10 – Four variable plot of nature of quartz population of the analyzed frameworks of the AVU. Plot structure and fields redrawn from Basu et al. (1975)

Apart from the undulosity, there were no relevant petrographic differences between undulose and non-undulose quartz grains. These were characteristically fresh, with variable roundness: from very angulose to well rounded, typically sub-angulose or sub-rounded (Pl. 3.17C, D). One single sample group is visible in the diamond plot of Basu et al. (1975) (Fig.3.10), plotting within the low rank metamorphic field. This is in accordance with the composition of the lithoclastic component of the frameworks which was dominated by chert and quartzite grains.

3.3.3. Palynofacies

The palynofacies analysis allowed the graphical representation of the several categories and group of categories in ternary plots and bi-dimensional plots with a time axis.

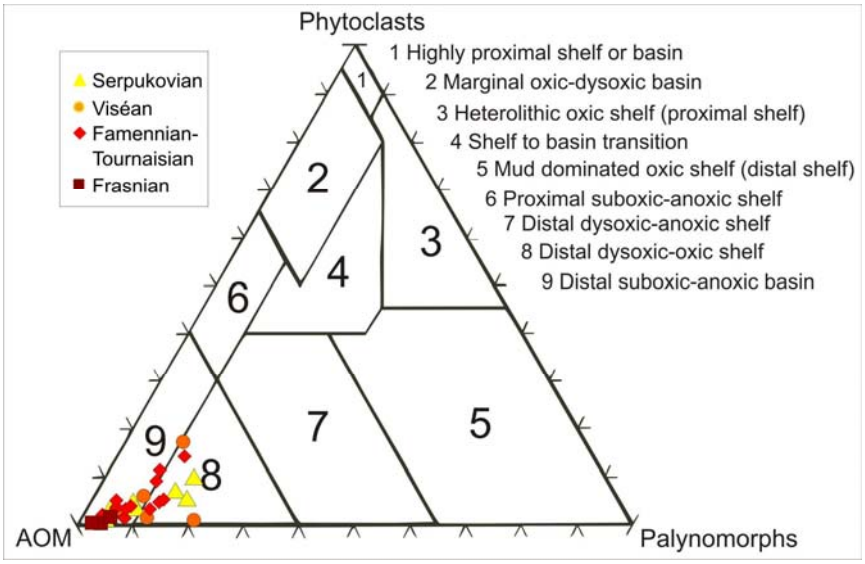

Fig. 3.11 – Ternary Tyson diagram showing the distribution of selected samples from the AVU according to their palynological content. Base diagram adapted from Tyson (1993).

The Tyson diagram shows a single sample group plotting near the AOM vertex, corresponding to the distal suboxic-anoxic basin and distal dysoxic-oxic shelf fields. There is little differentiation between samples according to their age. Nevertheless there is a badly defined trend away from the AOM vertex from older to younger samples. This corresponds to an increase in the proportion of palynomorphs (spores and organic-walled microplankton) and to a lesser extent an increase of phytoclast content. Frasnian samples plot closely together, very near the AOM vertex. Palynomorphs are observable but are statistically irrelevant. Phytoclasts are extremely rare. Famennian-Tournaisian samples are concentrated very close to the AOM vertex, but extend into the distal dysoxic-oxic shelf field. This is mainly due to the presence of acritarchs and prasinophytes (even though highly fragmented) up to 13% in some samples. Spores are also frequent, but never as common as acritarchs and prasinophytes. Viséan samples are dispersed, with some plotting very near the AOM vertex (AOM around 90%) while others plot within the distal dysoxic-oxic shelf field, corresponding to samples with higher palynomorph or phytoclast content. Serpukovian samples are also dispersed, but can be separated in two groups, one within the distal dysoxic-oxic shelf field, corresponding to samples with higher spore content (up to 17%) and another plotting near the AOM vertex. The second group can also be identified in the terrestrial-marine palynomorphs Vs age and spore-organic-walled microplankton Vs age plots (Figs. 3.12 and 3.13).

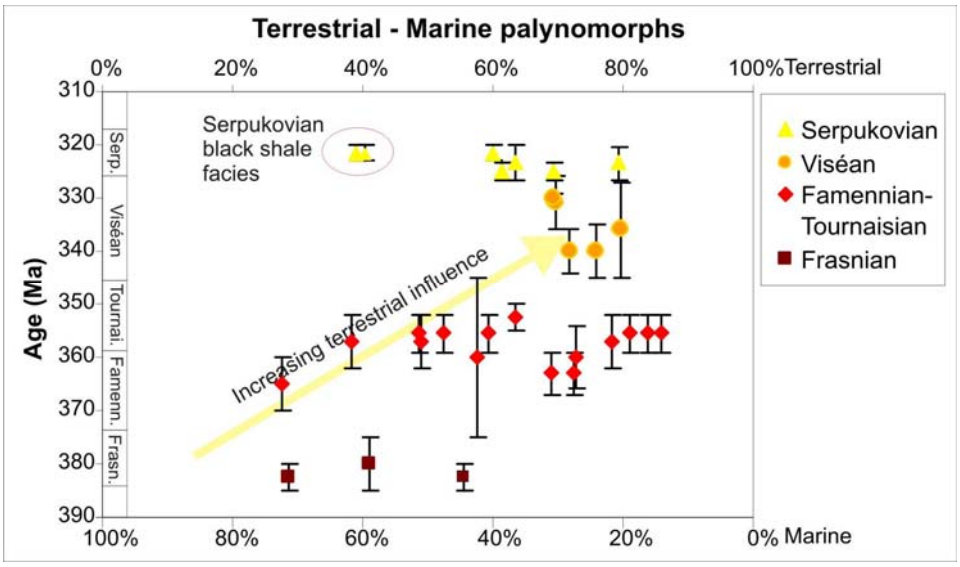

Fig. 3.12 – Terrestrial/Marine palynomorphs Vs Age plot. See table 3.3 for the grouping of categories. Error bars on Y-axis based on the uncertainty of the biostratigraphical determination of each sample. Ages compiled from Time Scale Creator software (Geologic Time Scale 2004).

Similarly to the Tyson diagram, the palynofacies analysis of the sieved residues shows some dispersal of data, but some trends are observable. The terrestrial-marine palynomorphs Vs age and spore-organic-walled microplankton Vs age plots (Figs. 3.12 and 3.13) show a progressive and irregular increase of terrestrial palynomorphs' content form older to younger samples. Frasnian samples show some dispersal of data, but both organic-walled microplankton and total marine palynomorphs are dominant. This reflects the dominance of highly fragmented acritarchs in the residues, over the spores. Lithologically all Frasnian samples correspond to grey shales, often finely laminated. Famennian-Tournaisian samples cover a wide range of proportions in both plots, but most samples show a higher proportion of spores and total terrestrial palynomorphs. This reflects the general abundance of spores in the residues of this age. It should be mentioned, however, that some residues were particularly rich in acritarchs and occasionally also in prasinophytes. Both types of residues (spore- and acritarch-rich) correspond to black shale lithologies.

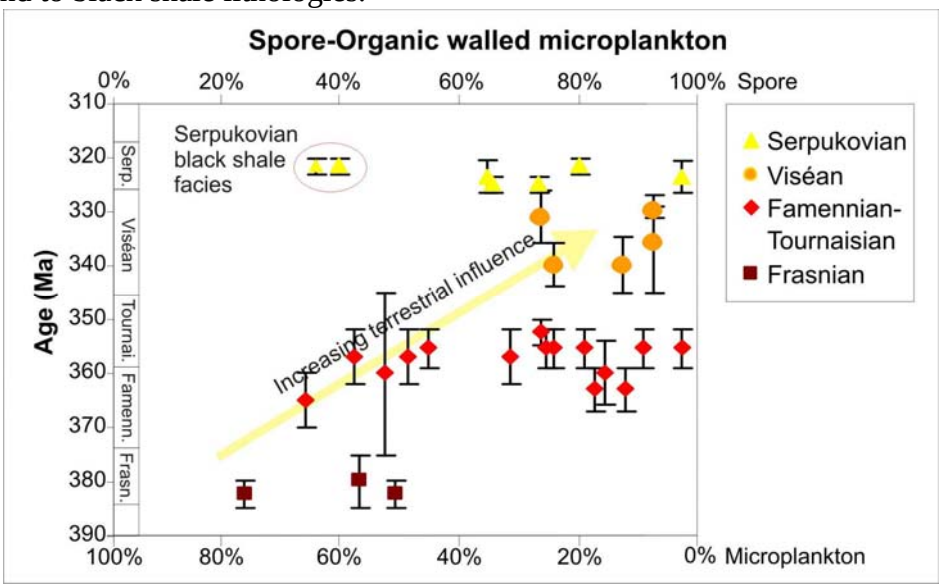

Fig. 3.13 – Spore/organic walled microplankton (acritarch and prasinophytes) Vs Age plot. Error bars on Y-axis based on the uncertainty of the biostratigraphical determination of each sample. Ages compiled from Time Scale Creator software (Geologic Time Scale 2004).

Viséan samples are characterized by the abundance of spores in sieved residues. Phytoclasts become more frequent. This is reflected in both plots, where single sample groups are observed, around the 90% spores and 75% terrestrial palynomorph axes. Lithologically Viséan samples correspond to grey shales and some highly deformed silt-shale outcrops (possibly turbidites?). Serpukovian samples are divided in two groups, similarly to the Tyson diagram. One shows similar characteristics to the Viséan samples; with high spore contents and generally high content of terrestrial palynomorphs (phytoclasts are relatively frequent). It corresponds to the sand-silt-shale beds, interpreted as turbidites. The second group has a relatively high content of organic walled microplankton, few spores and very rare phytoclasts. Organic-walled microplankton seems to correspond to simple polygonomorphs and very small prasinophytes, although identification is difficult as specimens are highly fragmented. Lithologically these samples correspond to black shales, apparently identical to the Famennian-Tournaisian ones.

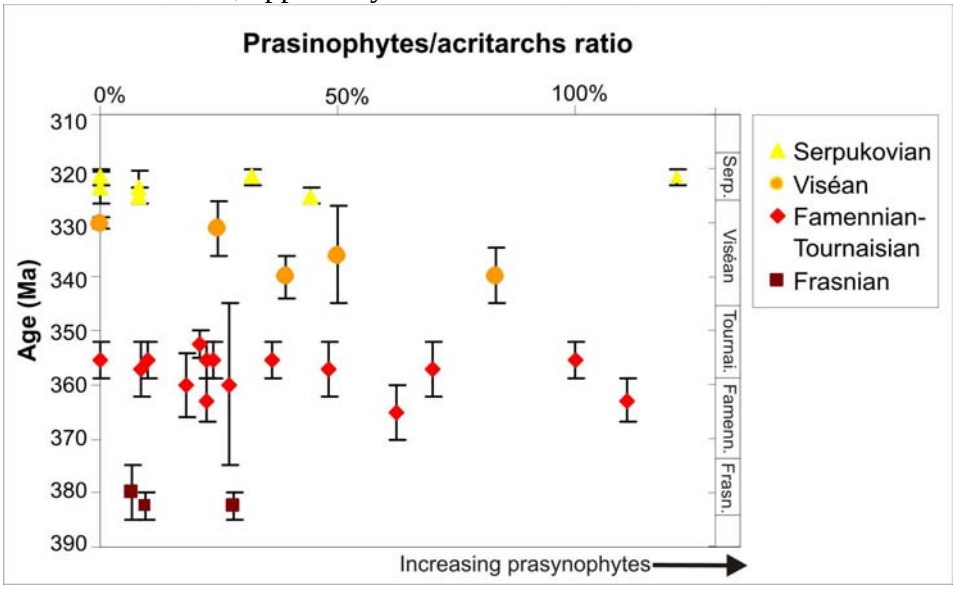

Fig. 3.14 – Prasinophyte/acritarch ratio Vs Age plot. Error bars on Y-axis based on the uncertainty of the biostratigraphical determination of each sample. Ages compiled from Time Scale Creator software (Geologic Time Scale 2004).

The prasinophyte/acritarch ratio Vs age plot has limited statistical significance as many samples had very few organic-walled microplankton specimens that could be positively identified as belonging to one group. Samples plotting along the 0% axis indicate that either acritarch or prasinophyte counts were 0. Generally acritarchs seem to be more common than prasinophytes, although some samples, especially Famennian and Tournaisian ones have residues where prasinophytes are particularly abundant. Samples from one locality, SOB, (not used for this quantification) had abundant and moderate to well preserved prasinophytes (especially *Cymatiosphaera* spp. and *Dictyotidium* spp.) and virtually no acritarchs.

3.3.4 Palynology

The palynological content is invariably heavily matured, although the maturity seems to be considerably variable. In at least two localities, the spores are translucent with grey hues. For the remaining localities spores are generally black and opaque, although some thin walled ones retain some translucency. The organic residue was composed, in most instances, by semi-translucent dark grey to black AOM with subordinate amounts of

sporomorphs and acritarchs (s.l.), which were very often fragmented and unsuitable for taxonomic determination and by black opaque relatively large organic particles. The latter could frequently be identified as phytoclasts, chitinozoa and more rarely as zooclasts. Acritarchs and prasinophytes are present in most samples with ages from the Frasnian to the Early Tournaisian. These are frequently translucent, although commonly fragmented. Phytoclasts are generally rare.

Many non-productive samples allowed, however, simple kerogen typing and quantification of the organic components (see Palynofacies section).

The overwhelming majority of the productive samples from the AVU provided poorly preserved palynomorphs. Complete recognizable palynomorphs were scarce and ornamentation was frequently destroyed (distal part of processes, fine sculpture, etc.). The operculum in prasinophytes was commonly absent and internal cyst coherence was often degraded and incipient fragmentation was present in many cases. Relevant characteristics of miospores such as the existence of layers (opposed to simple flanges), nature of cingulum/zona, details of trilete mark, etc. were very often difficult to observe. Few localities allowed the observation and taxonomic identification of palynomorphs with transmitted light. In most instances palynomorphs were black and opaque, occasionally partly translucent. Most organic residues were observed under a reflected light microscope. Thus, most of the taxa reported here are left in open nomenclature. Nevertheless most of the samples could be assigned to a stage and occasionally to one or to a group of biozones established for Devonian and Carboniferous of Western Europe (e.g. Clayton et al., 1977; Streel et al., 1984).

3.3.4.1 Miospores

The spore assemblage recovered from Minhoteira (MIN locality) derives from 4 productive samples from which several dozens of slides were made. This is one of the few localities that allowed the observation and documentation of palynomorphs using transmitted light.

Most of the specimens could not be identified and the total number of identified grains is too low to allow a quantitative approach. Nevertheless it is clear that spores assignable to *Apiculiretusispora*, *Geminospora*, *Grandispora* and to a lesser extent to *Leiotriletes* and *Retusotriletes* genera were dominant. Stratigraphically relevant taxa include *Aneurospora extensa* morphon (*A. extensa – A. goensis*) Turnau 1999; *Aneurospora* cf. *greggsii* (McGregor) Streel 1974; *Chelinospora concinna* Allen, 1965; *Contagisporites optivus* var. *vorobjevensis* (Chibrikova) Owens 1971; *Cristatisporites triangulatus* (Allen) McGregor & Camfield 1982; cf. *Densosporites devonicus* Richardson 1960; *Geminospora lemurata* Balme 1962 and *Geminospora micromanifesta* (Naumova) Arkhangelskaya 1985. Two specimens of *Lophozonotriletes media* Taugourdeau-Lantz, 1967 were found in one of the samples, but not *Cirratriradites jekhowskyi* Taugourdeau-Lantz, 1967; *Hystricosporites multifurcatus*, (Winslow) Mortimer & Chaloner, 1967; *Pustulatisporites rugulatus*, (Taugourdeau-Lantz) Loboziak & Streel, 1981 and *Verrucosisporites bulliferus* Richardson & Mcgregor, 1986. In fact, characteristic species that could be expected to appear together with the described assemblage such as *Ancyrospora* spp.; *Emphanisporites* spp. and *Hystricosporites* spp. were not found.

It is worth referring the presence of taxa more commonly found in Eastern Europe and Central Asia such as *Geminospora* cf. *aurita* Arkhangelskaya, 1985; *Geminospora micromanifesta* (Naumova) Arkhangelskaya 1985; *Geminospora notata* (Naumova) Obukhovskaya 1993; *Kedoesporis imperfectus* (Naumova) Obukhovskaya & Obukhovskaya, 2008; aff. *Lophotriletes multiformis* Tchibrikova, 1977; *Retusotriletes* cf.

scabratus Turnau 1986 (see for example Obukhovskaya & Obukhovskaya, 2008; Obukhovskaya et al., 2000).

Other taxa usually found in older Devonian strata such as *Apiculiretusispora* cf. *perfectae* Steemans, 1989; *Retusotriletes warringtonii* Richardson & Lister, 1969; *Latosporites* cf. *ovalis* Breuer, Al-Ghazi, Al-Ruwaili, Higgs, Steemans & Wellman, 2007 represent a small fraction of the assemblage and are interpreted as reworked.

Considering the presence of *Chelinospora concinna* Allen, 1965 and *Cristatisporites triangulatus* (Allen) McGregor and Camfield 1982, the Minhoteira assemblage can be assigned to the TCo miospore biozone of Streel et al. (1987), equivalent to the *optivus-triangulatus* miospore biozone of Richardson & McGregor (1986): uppermost Givetian – lowermost Frasnian. The presence of *Lophozonotriletes media* Taugourdeau-Lantz, 1967 would suggest the BM biozone of Streel et al. (1987), but none of the defining species of this and previous BJ biozones were recorded. Some of the taxa reported here more commonly found in Eastern Europe and Central Asia also indicates a younger age, equivalent to the EI subzone of the DE biozone as defined in Obukhovskaya et al. (2000): middle-upper Frasnian.

The taxa usually found in older Devonian strata may have been reworked, although there was no visible difference in their preservation. Reworked acritarchs possibly of Early Devonian age were found in this locality (Machado et al., 2007).

The stratigraphical relevance in Western Europe of taxa used to define and characterize biozones in Eastern Europe is uncertain. The Minhoteira assemblage is thus considered to be Early Frasnian in age (TCo biozone possibly extending to BM biozone of Streel et al. (1974)).

Nearly all other samples produced residues containing palynomorphs not observable by standard transmitted light methods. Occasionally spores with a relatively thin wall could be successfully observed and photographed. All oxidation methods tested resulted in the partial or total destruction of the organic residue. Oxidation methods were, however, successfully used by Fernandes et al., (2001) with samples from the AVU. In most instances residues were only properly observed using reflected light microscopy. This allowed taxonomical work to be conducted although with some limitations. A single (proximal or distal) surface could be observed and frequently the true nature and dimensions of flanges, cingula/zoni could not be described appropriately. Documentation of specimens using this method was possible in some cases, but often the resulting images were too blurred to be used in any type of illustration.

Stratigraphical palynology in most cases was based on first known occurrence of Genera and Species. Standard miospore biozonation for the Devonian and Carboniferous was not directly applicable not only due to the poor preservation but also due to the lack of continuous sections were miospore assemblage successions could be observed.

Famennian and Early Tournaisian miospore assemblages are characterized by the presence of *Grandispora* cf. *echinata* Hacquebard, 1957; *Grandispora* aff. *cornuta* Higgs 1975; *Grandispora* cf. *famenensis* (Naumova) Streel, 1974 in Becker et al. 1974 var. *minuta* Nekriata, 1974 and especially by *Grandispora gracilis* (Kedo) Streel in Becker et al., 1974 which is present in nearly every sample of this age and also appears as a reworked form in Viséan samples. Other characterizing taxa are *Corbulispora cancellata* (Waltz) Bharadwaj & Venkatachala, 1961; rarely *Cyrtospora cristifer* (Luber) Van der Zwan, 1979 and *Emphanisporites rotatus* (McGregor) McGregor 1973; *Rugospora* cf. *flexuosa* (Jushko) Streel in Becker et al., 1974 and *Verrucosisporites nitidus* morphon (sensu Van der Zwan, 1980). Late Famennian/Early Tournaisian assemblages commonly contain a number of taxa which are probably reworked from (?)Frasnian sediments such as *Hymenozonotriletes* spp. and *Archaeoperisaccus* aff. *ovalis* Naumova, 1953.

Viséan assemblages are difficult to identify positively but the presence of *Apiculatisporis* cf. *hacquebardi* Playford, 1964; *Densosporites annulatus* (Loose) Smith & Butterworth, 1967; *Lycospora* spp.; *Schulzospora* spp.; *Stenozonotriletes lycosporoides* (Butterworth & Williams) Smith & Butterworth, 1967; *Triquitrites* spp.; *Verrucosisporites baccatus* Staplin, 1960 are indicative of this stage. It is difficult to match each sample to a specific biozone within the Viséan as frequently only one or two characteristic taxa are present.

Serpukovian assemblages are relatively diversified and several taxa allow the attribution of samples to this stage. Identified taxa include *Acanthotriletes* cf. *aculeolatus* (Kosanke) Potonié & Kremp, 1955; *Apiculatisporis* cf. *variocorneus* Sullivan, 1964; *Crassispora* aff. *kosankei* (Potonié & Kremp) Smith & Butterworth, 1967; *Dictyotriletes castaneaeformis* (Horst) Sullivan, 1964; *Grumosisporites inaequalis* (Butterworth & Williams) Smith & Butterworth 1967 and other species of this genus; *Leiotriletes* spp.; *Lycospora* cf. *subtriquetra* (Luber) Potonié & Kremp, 1956; *Proprisporites laevigatus* Neves, 1961; cf. *Savitrisporites nux* (Butterworth & Williams) Smith & Butterworth, 1967. It is possible that some samples are actually Early Bashkirian as some of the identified taxa have ranges that extend into the Bashkirian, although none is restricted to this stage. Assemblages assigned to the Serpukovian usually include several forms which are most likely reworked such as *Apiculatasporites wapsipiniconensis* Peppers, 1969; aff. *Geminospora* spp.; *Grandispora* spp.; *Lophozonotriletes* spp.; *Rugospora* spp. and *Samarisporites* sp.

3.3.4.2 Organic-walled microplankton

The preservation of the palynological assemblages is usually poor to moderate, but some assemblages contain particularly abundant and diversified acritarchs. The better studied assemblages originate from the Upper Devonian black shales of the classical locality of the Albergaria-a-Velha area (VAL locality), along with other black shale outcrops of Famennian and Early Tournaisian age (namely localities ASS, DUP, SER, SOB – see Fig. 3.1 and Appendix 1 for details). The diversified assemblage contains over 50 different acritarch and prasinophyte species. Prasinophyte phycomata are invariably small or very small (5 to 15µm), except for some *Dictyotidium* spp. which may be up to 40µm. Acritarchs were not used as a biostratigraphical tool (despite the existence of some acritarch based biozonation of the Frasnian and Famennian - e.g. Vanguestaine, 1986; Vanguestaine et al., 1983) as spores were present in all samples that contain acritarchs and could be used for biostratigraphical purposes.

Qualitative analysis of the assemblage points to a close affinity with the Laurussian late Devonian marine Realm, in contrast with the Late Devonian assemblages from the South Portuguese Zone which show clear affinities with North Gondwana, as suggested by Clayton et al. (2002). Previous work by Vavrdová and Isaacson (1999) included late Devonian acritarch assemblages of the Represa and Phyllite-Quartzite Formations described in Cunha & Oliveira (1989) as belonging to the Gondwanan Realm. The affinity of the Albergaria-a-Velha shales is indicated by the presence of *Cymatiosphaera perimembrana* Staplin, 1961; *Uncinisphaera* (*Villosacapsula*) *ceratioides* (Stockmans & Willière) Colbath, 1990; *Winwaloeusia* cf. *ranulaeforma* Martin, 1984 and other acritarch genera and species described from Central and Northern Europe (especially Belgium – Ardennes-Rhenish massif) and Eastern USA and a complete absence, so far, of species of *Horologinella* and *Schizocystia* (common Gondwanan genera). Other common Gondwanan genera such as *Umbellasphaerdium* and *Crassiangulina* are possibly present

in the Albergaria shales, but only one fragmented specimen of each taxon was found, making the identification tentative.

Cluster analysis

Previous work conducted by Clayton et al. (2002) and Colbath (1990) on Late Devonian organic-walled microplankton suggested the existence of a cluster with Gondwanan affinities and another with Laurussian affinities (apart from other areas – see Colbath, 1990), coherent with the idea proposed by Vanguestaine (1986) and later by Vavrdová and Isaacson (1999). As discussed by Colbath (1990), any attempt to quantify the statistical proximity of assemblages is limited by several factors, namely the different criteria between workers, uneven amount of publications between regions and of course the natural phenotypic variability of acritarchs and prasinophytes and local and regional ecological variability.

With the aim of testing the initial qualitative results a cluster analysis was performed using the data obtained so far from the Albergaria-a-Velha black shales and data available in the literature from the following areas:

- Belgium: Martin (1981, 1985) and Stockmans and Willière (1969, 1974);
- Eastern USA: Clayton et al. (2002); Molyneaux et al. (1984); Wicander (1974, 1983); Wicander and Loeblich (1977) and Wicander and Playford (1985);
- Libya: El-Mehdawi (1998); Clayton et al. (2002); Moreau-Benoit (1984); Paris et al. (1985) and Streel et al. (1988);
- Algeria: Clayton et al. (2002) and Jardiné et al. (1972, 1974);
- South Portuguese Zone: Clayton et al. (2002); Cunha and Oliveira (1989); Gonzalez et al. (2005) and Pereira (1999).

PAST – Palaeontological Statistics Freeware was used to perform the analysis and the Paired group algorithm with Jaccard similarity measure was chosen.

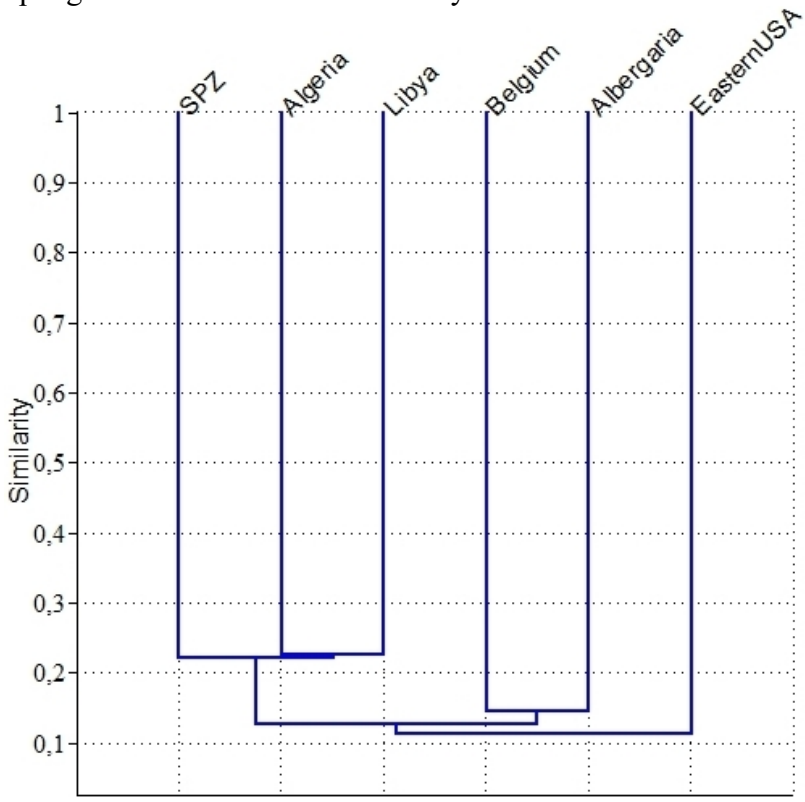

Fig. 3.15 - Cluster diagram of the considered acritarch assemblages. Paired group, Jaccard measure.

	EasternUSA	SPZ	Algeria	Libya	Belgium	Albergaria
EasternUSA	1	0,14554	0,094527	0,13089	0,1124	0,080808
SPZ	0,14554	1	0,22222	0,21649	0,16667	0,13861
Algeria	0,094527	0,22222	1	0,22368	0,10811	0,11111
Libya	0,13089	0,21649	0,22368	1	0,11806	0,11538
Belgium	0,1124	0,16667	0,10811	0,11806	1	0,14493
Albergaria	0,080808	0,13861	0,11111	0,11538	0,14493	1

Table 3.8 - Similarity and distance indices matrix for the considered assemblages

The similarity cluster diagram (Fig. 3.15) and correlation matrix (Table 3.8) show a very close relation between the Libyan and Algerian assemblages, as already reported in Clayton et al. (2002). The similarity of the South Portuguese Zone with these two areas is evident and even higher than suggested earlier by Clayton et al. (2002). The Albergaria-a-Velha assemblage clusters closely with the Belgium assemblages and to a lesser extent to those of Eastern USA. In general the Albergaria-a-Velha assemblage shows closer similarity to the Laurussian Realm, contrasting with the North Gondwanan assemblages.

It has to be mentioned that all the clusters' cut-off points are close to the base of the diagram which suggests a low degree of diversification. This is probably an artefact of the chosen algorithm, but also a result of an (still) incomplete database. Nevertheless general groups of assemblages can be defined and thus palaeobiogeographical interpretations can be attempted.

3.3.5 Organic geochemistry, source rock potential and organic maturity

The rock-eval parameters of the twelve analysed samples are summarized in the following tables.

Sample	T max [°C]	S1 [mgHC/ g rock]	S2 [mgHC/ g rock]	S3 [mgCO_2/ g rock]	PI [S1/ (S1+S2)]	S4 CO_2 [mgCO_2/ g rock]	S4 CO [mgCO/ g rock]	S5 [mgCO_2/ g rock]
ANG16	422	0,04	0,05	0,04	0,44	6,2	1,1	4
VAL4	354	0,03	0,05	0,07	0,38	4,3	0,2	3
MIN16.3	333	0,04	0,04	0,13	0,50	1,2	0,6	3
LOB1.1	329	0,02	0,02	0,02	0,50	11,5	2,8	3
MIR4.3	337	0,03	0,02	0,09	0,60	2,3	0,3	3
CAT5.1	353	0,05	0,04	0,08	0,57	9,4	1,9	2
CHE1.1	343	0,02	0,04	0,13	0,33	5,7	2,0	3
ALH1.4	324	0,04	0,05	0,09	0,44	2,1	0,8	2
SAL3.1	328	0,01	0,01	0,00	0,50	6,0	2,6	9
GOL1.1	351	0,01	0,02	0,06	0,33	1,6	2,0	2
SER2	326	0,01	0,02	0,02	0,33	1,7	2,1	2
TRE1.1	343	0,02	0,04	0,05	0,33	1,8	2,0	4

Table 3.9 – Rock-eval parameters of the analyzed samples from the AVU.

Sample	PC [%]	RC [%]	TOC [%]	HI [mgHC/ g TOC]	OI [mgCO_2/ gTOC]	pyro MINC[%]	oxi MINC[%]	total MINC[%]	Age
ANG16	0,01	0,22	0,23	22	17	0,00	0,11	0,11	Serpuk.
VAL4	0,01	0,13	0,14	36	50	0,04	0,08	0,12	L. Famenn.
MIN16.3	0,01	0,06	0,07	57	186	0,01	0,08	0,09	E. Frasn.
LOB1.1	0,01	0,43	0,44	5	5	0,00	0,08	0,08	E. Tournai.
MIR4.3	0,01	0,07	0,08	25	113	0,00	0,08	0,08	?
CAT5.1	0,01	0,34	0,35	11	23	0,01	0,05	0,06	Viséan
CHE1.1	0,01	0,25	0,26	15	50	0,02	0,08	0,10	E. Viséan
ALH1.4	0,01	0,09	0,10	50	90	0,10	0,05	0,15	?
SAL3.1	0,01	0,27	0,28	4	0	0,00	0,25	0,25	?
GOL1.1	0,01	0,13	0,14	14	43	0,10	0,05	0,15	?
SER2	0,01	0,14	0,15	13	13	0,01	0,05	0,06	Serpuk.
TRE1.1	0,01	0,14	0,15	27	33	0,00	0,11	0,11	?

Table 3.10 – Rock-eval parameters of the analyzed samples from the AVU and their ages.

All samples are characterized by considerably low TOC values and by an apparent high maturity. There seems to be little or no differentiation of samples according to their age.

The high maturity is indicated by the low S1 and S2 values (see Fig. 3.16). Production index (PI) is also very low and indicates high thermal maturity equivalent to dry gas generation zone. This is coherent with the observed maturation in palynological slides where all the organic matter is dark grey to black. The vast majority of the analyzed organic residues have slightly translucent to opaque, black spores, indicating a TAI > 4+. A few localities, however, show translucent grey spores. Previous work conducted on the AVU, regarding the illite crystallinity and other crystallographic parameters of phyllosilicates indicated that the AVU had undergone metamorphic conditions of high anchizone – epizone, with palaeotemperatures >200ºC and pressures between 1 and 2 Kbar, (Vázquez et al., 2007). Measurements of vitrinite reflectance obtained from heavy liquid concentrates indicate Rr% values between 1 and 1,3% (Chaminé et al., 2003; Moço et al., 2001). Palynological residues from the AVU mounted on acrylic plates and polished were observed for this study. Very few particles could be positively identified as being vitrinite, since petrologic information is lost in palynological residues. Nevertheless all measured particles resulted in values higher than 3 Rr%.

The T_{max} values below 400 °C do not represent kerogen maturity and are related to residual bitumen or exsudatinite.

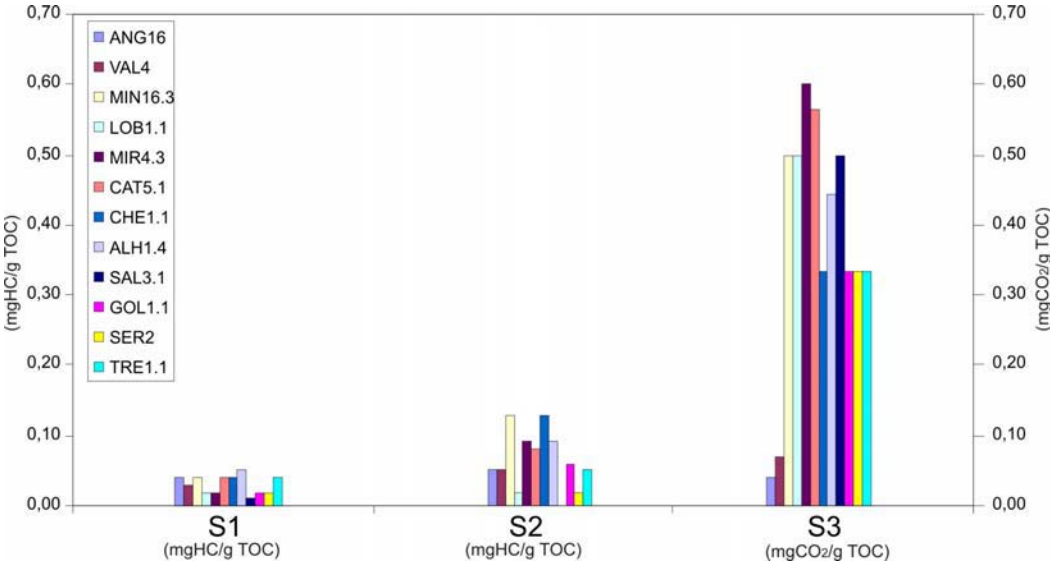

Fig. 3.16 – S1, S2 and S3 values for the analyzed samples from the AVU.

Kerogen typing can usually be performed using Hydrogen and Oxygen indices (HI/OI) ratios plotted on van Krevelen diagram (Tissot et al., 1974). This application is limited with increasing temperature and consequent reduction of both HI and OI.

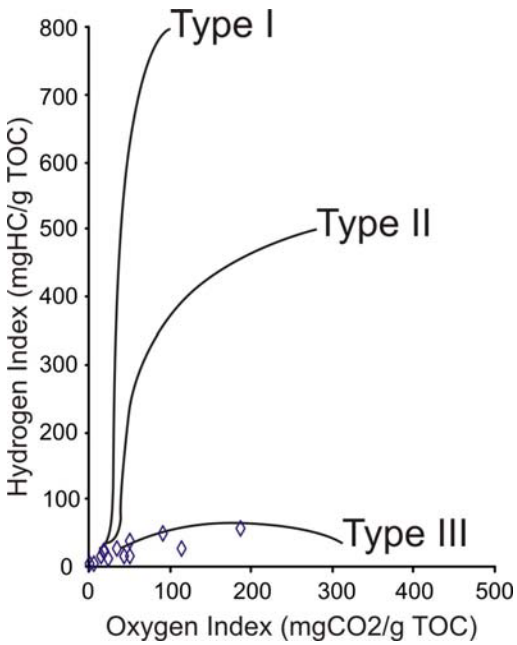

Fig. 3.17 – van Krevelen diagram with 3 main types of kerogen and the HI/OI ratios of the AVU samples. Original diagram from Tissot et al., 1974.

The AVU samples have considerably low values of HI (<60 mgHC/g TOC) and OI (<190 $mgCO_2$/g TOC), thus most of them plot in the area where the 3 types of kerogen lines merge, rendering kerogen typing impossible (Fig. 3.17). However 3 samples (MIN16.3, MIR4.3 and ALH1.4) plot within the kerogen type III field, i.e., of essentially terrestrial origin and thus gas-prone. The palynofacies data indicate that terrestrial influence was scarce, even for the more proximal environments recorded in some rocks of Serpukovian age. The organic residues of the AVU are typically marine AOM-rich (>85% of total organic residue) with accessory amounts of organic-walled microplankton, spores and generally rare or very rare phytoclasts.

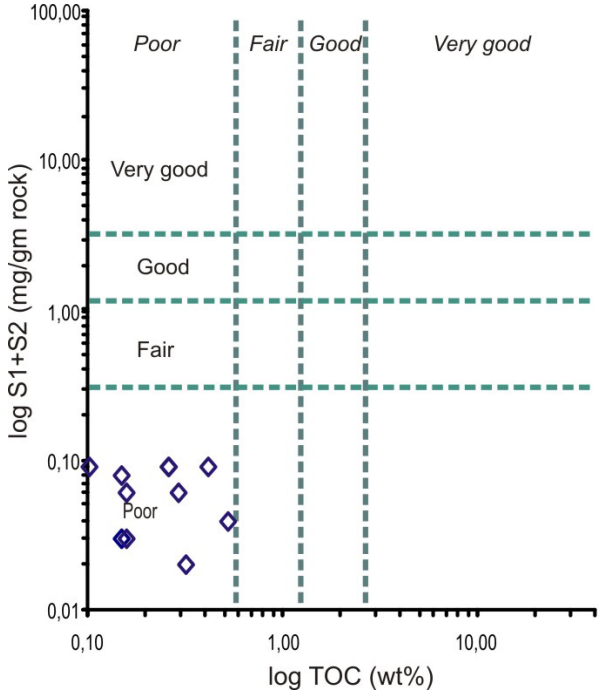

Fig. 3.18 - log TOC Vs log S1+S2 plot. Redrawn from Maky & Ramadan, 2008.

The source rock potential of the analyzed samples seems limited. This is readily indicated by the low TOC values (<0,5wt%) and also by the low S1 and S2 values (≤0,05 mgHC/g rock). The palynofacies analysis on shale samples of the AVU invariably indicates oil-prone source rocks, although this method does not give an estimate of the proportion of the hydrocarbon-prone material per weight or volume of rock.

3.4 Discussion and Conclusions

The dominant presence of quartz (and quartzose clasts – cherts and quartzites) imply that the observed framework modes derive from significantly mature detritus (e.g. Prothero and Schwab, 1996). The high proportion of matrix/cement in all samples would indicate otherwise (sensu Folk, 1951), but this textural characteristic may have been substantially altered by the low grade metamorphic conditions to which this unit was exposed. Such changes in the matrix's nature are observable in some of the samples (Pl. 3.17C). In addition the textural characteristics may be related to the type of sediment reaching the shelf areas (which was very likely mud-rich) and later transported by turbidity currents.

The distribution of the data-set within the craton interior and quartzitic recycled orogen fields may reflect a drainage basin located on an essentially stable cratonic area (Central Iberian Zone?) which may have a collisional or transcurrent character along its margin; it has been suggested (Chaminé et al., 2003, 2007) that the Porto-Tomar shear zone was already active during the Late Devonian and Mississippian, controlling the regional sedimentation by forming scattered pull-apart like and/or fault-wedge basins in a marine setting near a continental block. The results presented here suggest that such tectonic activity may have been affecting the continental block where the source areas were located, but probably were not affecting the shelf and basin floor where sedimentation was occurring. Neither intraclasts nor clasts from the closely associated Arada unit where found in the analysed frameworks. These would be expected if significant tectonic activity (and consequent recycling) was occurring within the

sedimentation area (compare for example Burnett & Quirk, 2001; McCann, 1991). It should be mentioned, however, that shale clasts were observed at the outcrop scale in one locality (SND – see Fig. 3.1). The same locality presented relatively large (>1cm diameter) quartzite grains within fine-sandstone beds. The significance of this shale and quartzite clasts is uncertain.

The results from the undulosity of quartz, although restricted to a few samples, clearly indicate that the sediments of the AVU derive from rocks with a low metamorphic grade. This is coherent with the observed presence of quartzite and chert grains. The CIZ can be a potential source area. This zone is adjacent to the AVU and composed essentially by low grade metasediments of Late Proterozoic–Cambrian age ("Complexo Xisto-Grauváquico", i.e., *Schist-Greywacke Complex* – e.g., Carríngton da Costa, 1950; Medina et al., 1989, 1993) overlain by Ordovician to Lower Devonian (e.g. Cooper, 1980; Oliveira et al., 1992; Paris, 1981) very low grade metasediments. The timing of the metamorphic event (or events) that affected the CIZ and the time at which these metasediments were exposed and eroded is certainly pre-Late Pennsylvanian (see Chapter 4; Gama Pereira, 1987). It is uncertain, however, if they were already exposed by Late Devonian times.

The sand/mud ratio varies greatly, but, with few exceptions, mud clearly dominates and the sand is usually medium to fine. Most of the available relatively undeformed sections (sand-silt-shale facies) show a turbiditic character and possibly a (distal?) prodelta setting. The textural maturity of the sandstones and the general dominance of mud over sand imply the existence of a considerably large and essentially low relief drainage area and also the presence of a deltaic system where most of the coarser sediments are trapped (Bouma, 2000). A similar sedimentary setting, associated with a large deltaic system was described by Ahrens (1936) and Stets & Shäfer (2008) from the Central Facies Belt of the Devonian of the Rhenohercynian basin. Although deformed and slightly metamorphosed in some areas, the gradual passage from deltaic subaerial (to NW) to shallow marine and to deeper marine settings (to SE) is clearly observed in this basin. In the case of the AVU, only the distal parts of a similar sedimentary system were preserved. This implies that the post-sedimentary tectonic evolution of the area, clearly associated with the Porto-Tomar shear zone (Chaminé et al., 2003a, b, 2007), destroyed most of the sedimentary record and preserved only a few discrete portions of a much larger basin, as nappes over older rocks. The sedimentary information collected strongly suggests that a turbidite system close to the fine-grained end member (sensu Bouma, 2000) is represented by the metasediments of the AVU. The observed turbidite sequences can be generally included in facies association V and more rarely IV (BOS section) of Mutti and Normark (1987), indicating distal (rarely intermediate) lobe depositional elements. The sedimentary packages composed essentially or entirely by shales (black shale and laminated grey shale facies) within this unit are volumetrically important and are not always associated (at least spatially) with packages identified as turbidites. These shale packages may represent the distal parts of lobes formed by turbidite deposition and/or hemipelagic deposits.

The palynofacies analysis, coupled with the lithological and sedimentological characteristics of the metasediments of the AVU show some palaeoenvironmental variations through time. A single sedimentation environment seems to be recorded from Frasnian sediments (laminated grey shales). A marine, most likely basinal setting is indicated by the finely laminated grey shales with a typical marine palynological association. The constant presence of organic matter and significant proportion of AOM, shown by palynological analysis, along with the cm- to mm-lamination and the absence of bioturbation (although the macro-scale observational evidence is strongly limited by deformation) implies that, generally, the marine organic productivity in the water column

was considerably high, but also that the oxygen minimum was near or below the sediment-water interface where sedimentation was taking place (Calvert, 1987, Curtis, 1980). A similar setting with laminated sediments forming in areas where the oxygen minimum intersected the ocean floor was described by Calvert (1964) and Donegan & Schrader (1982) in the Gulf of Mexico.

The characteristics of the palynological content of Frasnian samples are in accordance with this interpretation. The lighter and darker laminae commonly found suggest can be interpreted as rhythmites. The origin and processes responsible for this rhythmical sedimentation are difficult to determine. A distal deltaic suspension fall out sedimentation type with a seasonal control can tentatively explain the observed sedimentary features. This lithofacies is also observed in the Viséan and Serpukovian (more rarely in Tournaisian-Famennian rocks) and, presumably, the sedimentary setting where these facies is formed prevailed through time.

The Tournaisian and Famennian rocks are, in most instances, black shales, with a characteristic palynological content; AOM-rich along with a diversified organic-walled microplankton assemblage. The terrestrial influence is increased, indicated by the greater presence of spores and slightly higher phytoclast content.

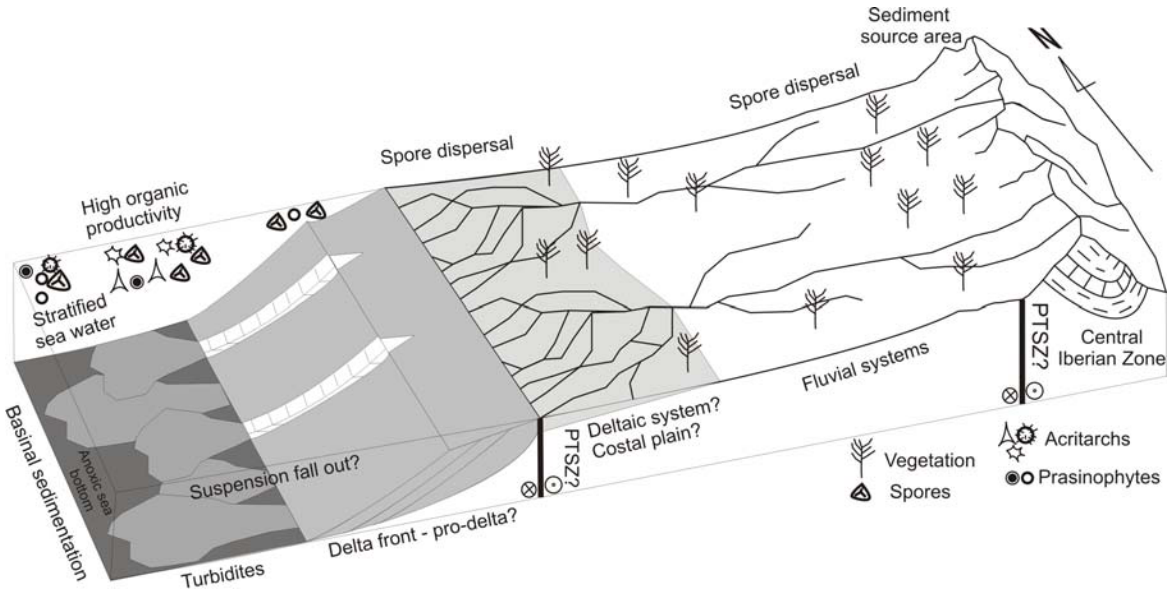

Fig. 3.19 – General schematic representation of the hypothetical tectonic and sedimentation setting of the AVU.

Viséan and Serpukovian sediments are generally more coarse grained, with the appearance of turbidite and (?)pro-delta sediments, but the black shale and laminated grey shale facies persist, indicating a diversification of sedimentary environments. The amount of terrestrial input is greater, indicated by the generally coarser-grained sediments but also the greater amount of spores and, to a lesser extent, the amount of phytoclasts. AOM proportions decrease slightly. It should be mentioned that acritarch diversity and abundance decreases globally in the latest Devonian and especially during the Mississippian (see Strother, 2008 for a revision of previous work and causes) which could have influenced the results obtained from palynofacies analyses. Nevertheless other palynological and lithological "proxies" point to the same conclusions.

Overall it seems the sedimentary system has a general prograding tendency, from basinal distal deposits during the Frasnian to more proximal settings in the Viséan and especially during the Serpukovian where turbidites seem to prevail.

The thermal and burial history of the AVU as a whole started after the Serpukovian (youngest sediments) and lasted, in a first phase, to the Lower Triassic. This is indicated by the outcrop-scale observation of Lower Triassic sediments of the Lusitanian basin (Grés de Silves Fm.) resting unconformably over the AVU in several localities and associated ferruginization (see Pl. 3.16A). The intramontane Late Pennsylvanian Buçaco basin (Wagner et al., 1983; Pinto de Jesus et al., 2010; see Chapter 4) does not overlay the AVU stratigraphically; the contacts are invariably tectonic. This indicates that the exhumation of the AVU happened in post-Late Pennsylvanian and pre-Late Triassic times. It also indicates that the thermal and generally the geological history of the basin represented by the AVU in this region were significantly controlled by the PTSZ which was active at least from the Late Pennsylvanian. The potential oil play system formed by the AVU, Buçaco basin sediments and the Lusitanian basin lacks the correct timing of events within and near this shear zone. However, the basin represented by the AVU most probably extended far beyond the influence of the PTSZ (see Capdevila & Mougenot, 1988, Moço et al., 2001) and may be preserved as basement under the Lusitanian basin, both on- and off-shore. Indeed samples from shallow wells located in the Lusitanian basin (Estarreja and Ovar area) that reached the basement (A. Cavaco hydrogeology company internal reports) analysed by us indicate the presence of shales with similar palynological content (regarding age and palynofacies) to the AVU. Additional interest on the pre-Triassic source rocks and the associated oil play was shown by Uphoff (2005). Based on a deep exploration well (Aljubarrota 1) that reached the basement and presented oil shows within the Triassic sediments and additional geophysical and organic geochemical results he considers at least two Palaeozoic units as source rocks and a Triassic-Jurassic reservoir and seal (Uphoff, 2005). The source rock units are considered to be 1) the lateral, distal, extension of the Buçaco basin and 2) Silurian shales (Vale da Ursa and Sazes Fms.) (Uphoff, 2005). The significance of the Silurian shales as part of the oil play is considered here as limited or non-existent since these are Central Iberian Zone units, which most probably does not extend to the West, below the Lusitanian basin (Capdevila & Mougenot, 1988).

It is worth mentioning the possible interest of the AVU as a shale gas source rock. It is within the dry gas generation zone; it is volumetrically quite important both at the surface and subsurface (although its true volume and extension are still unknown) and it is highly fractured. It is uncertain if the low TOC values present here are representative of the AVU preserved in the subsurface. The van Krevelen diagram points to a gas-prone rock which is in contrast with the palynological content of this unit (which clearly indicates an oil-prone source rock). This can be explained by the current thermal maturity of the AVU – dry gas generation zone – which would result in the observed OI/HI ratios.

Notes on the cartographic differentiation of the AVU and Arada unit

As mentioned before the differentiation of the two units is extremely difficult. Nevertheless some criteria may be used in the field and when analyzing samples in the lab. This is a compilation of the author's experience and shared knowledge of the area with Hélder Chaminé and Paulo Fonseca.

AVU	Arada Unit
Black, dark grey, light grey shales.	Light grey, occasionally dark grey and very commonly greenish shales
No green shales	No black shales
Light and dark yellow and rarely greenish siltstones and fine sandstones	No siltstones or sandstones

Weathering produces purple, yellow and brown hues; white hues in extreme cases	Weathering produces purple and yellow hues. Other colors may be present, but were not directly observed
Bedding and lamination are commonly visible, although usually folded, even in weathered outcrops	Bedding or other clear sedimentary features were never observed
1 tectonic foliation and 1 folding phase, usually genetically connected. Usually does not form slaty cleavage that disaggregates in well defined planes.	Commonly more than 1 tectonic foliation and more than 1 folding. Highly penetrative cleavage produces well defined (planar) slate pieces.
Quartz veins oblique or parallel to bedding/lamination planes and on hinge areas. Iron oxides accumulate on foliation planes.	Quartz veins may have iron oxides
Quartz veins with greenish carbonates and sulphides (py±cpy)	Sulphides and greenish carbonates never observed on veins
Scattered py is common in darker lithologies, frequently altered to iron oxides, resulting in small red spots	Garnet (red coloured) is occasionally observed, apparently very similar to the oxidized py spots. Can be distinguished using a hand lens.

Table 3.11 – Practical criteria to differentiate the AVU and Arada unit.

During the course of this work, hundreds of outcrops were examined. It became clear that the vast majority of them could be positively considered to belong to the AVU. The initial suspicion in the field was later confirmed by the analysis of the palynological residues from the samples taken. The initial representations of the AVU as discrete, restricted and scattered groups of outcrops within the Arada unit (with much greater cartographic extension) e.g. Chaminé et al. (2003; 2007) should probably be revised, although the way to correctly represent the AVU remains uncertain.

The area mapped as AVU between the villages of Valongo do Vouga and Carvoeiro (Gomes et al., 2007 and the eastern basin referred in Vázquez et al., 2007), bordering the contact between the CIZ and the OMZ most probably is not AVU. This is indicated by the lithologies found along this area (non-laminated light grey shales) and by the palynological content which did not produced palynomorphs. The rocks present in this area are tentatively assigned to the Ordovician grey shales and phyllites that crop out further N and S of this area.

The Sernada-do-Vouga unit or sub-unit referred in some papers (e.g. Chaminé et al. 2007; Gomes et al., 2007) can be tentatively correlated with the Viséan and Serpukovian coarser sediments (sand-silt-shale beds lithofacies) of the AVU.

3.5 Systematic Palynology

3.5.1 Miospores

The turmal division used here is modified from Potonié (1958, 1970) in Traverse (2007) with additional subturmal divisions by Oshurkova & Paschkevich, 1990.

Anteturma SPORITES Potonié, 1893

Turma TRILETES (Reinsch) Dettmann, 1963

Subturma AZONOTRILETES (Luber) Dettmann, 1963

Infraturma LAEVIGATI (Bennie & Kiston) Potonié, 1956

Genus *Leiotriletes* (Naumova) Ischchenko, 1952
Leiotriletes aff. *balapucensis* di Pasquo, 2007 (Pl. 3.7w)
Leiotriletes cf. *devonicus* Naumova, 1953 (Pl. 3.5p)
Leiotriletes aff. *devonicus* Naumova, 1953 (Pl. 3.3c)
Leiotriletes inermis (Waltz) Ischenko, 1952 (Pl. 3.9k)
Leiotriletes cf. *microgranulatus* Playford, 1962 (Pl. 3.9l)
Leiotriletes ornatus Ischenko, 1956 (Pl. 3.9m)
Leiotriletes aff. *pagius* Allen, 1965 (Pl. 3.3d)
Leiotriletes aff. *trivialis* Naumova, 1953 (Pl. 3.3e)
Leiotriletes spp. (Pl. 3.3f, Pl. 3.5o; Pl. 3.9n)

Genus *Punctatisporites* (Ibrahim) Potonié & Kremp, 1954
Punctatisporites cf. *glaber* (Naumova) Playford, 1962 (Pl. 3.9u)
Punctatisporites minutus Kosanke, 1950 (Pl. 3.5y)
Punctatisporites irrasus Hacquebard, 1957 (Pl. 3.5z; Pl. 3.9v)
Punctatisporites lucidulus Playford & Helby, 1968 (Pl. 3.5aa; Pl. 3.9w)
Punctatisporites planus Hacquebard, 1957
Punctatisporites cf. *reticulopunctatus* Hoffmeister, Staplin & Malloy, 1955 (Pl. 3.9x)
Punctatisporites solidus Hacquebard, 1957 (Pl. 3.3l)
Punctatisporites springsurensis Playford, 1978 (Pl. 3.3m)
Punctatisporites spp. (Pl. 3.3n; Pl. 3.5ab; Pl. 3.7z; Pl. 3.9z)

Genus *Retusotriletes* (Naumova) Streel, 1964
Retusotriletes cf. *communis* Naumova, 1953 (Pl. 3.3o)
Retusotriletes cf. *dubius* (Eisenack) Richardson, 1965 (Pl. 3.5ac)
Retusotriletes incohatus Sullivan, 1964 (Pl. 3.7aa)
Retusotriletes minor Kedo, 1963 (Pl. 3.3p)
Retusotriletes cf. *pychovii* Naumova, 1953 (Pl. 3.3q)
Retusotriletes cf. *scabratus* Turnau, 1986 (Pl. 3.3r)
Retusotriletes warringtonii Richardson & Lister, 1969 (Pl. 3.3s)
Retusotriletes sp.1 (Pl. 3.3t)
Description: Sub-triangular general outline. Trilete mark slightly sinuous extending to spore margin, with narrow (2µm wide) lips. The exine is smooth, except in the equatorial part of the trilete mark where badly defined verrucae, broad-based cones and spines are observable. This irregularly arranged ornamentation makes the outline in these areas appear dentate or spinose.
Dimensions: 30µm long and 23µm wide.
Remarks: a single specimen was observed and the preservation is, as most of the assemblage, poor. The specimen closely resembles *R. warrangtonii*, but curvaturae is not observed and it has significant localized ornamentation which is not observed in *R. warrangtonii*.
Retusotriletes spp. (Pl. 3.3u; Pl. 3.5ad; Pl. 3.7ab; Pl. 3.9ac)

Infraturma APICULATI (Bennie & Kidston) Potonié, 1956

Subinfraturma GRANULATI Dybová & Jachowicz, 1957

Genus *Cyclogranisporites* Potonié & Kremp, 1954
Cyclogranisporites sp. (Pl. 3.4s)

Genus Geminospora Balme, 1952
Geminospora cf. *aurita* Arkhangelskaya, 1985 (Pl. 3.2f)
Geminospora lemurata Balme, 1962 (Pl. 3.2g)
Geminospora micromanifesta (Naumova) Arkhangelskaya, 1985 (Pl. 3.2h)
Remarks: The distinction between *G. lemurata* and *G. micromanifesta* seems to rely solely on fine details of the ornamentation which are very similar. It is likely that these two species are conspecific. The preservation of the present material does not allow a detailed study of this topic.
Geminospora notata (Naumova) Obukhovskaya, 1993 (Pl. 3.2i)
Geminospora spp. (Pl. 3.2j; Pl. 3.5b; Pl. 3.7n; Pl. 3.8ac)

Genus *Granulatisporites* (Ibrahim) Schopf, Wilson & Bentall, 1944
Granulatisporites sp.

Genus *Tricidarisporites* Sullivan & Marshall, 1966
Tricidarisporites fasciculatus (Love) Sullivan & Marshall, 1966 (Pl. 3.10f)

Subinfraturma VERRUCATI Dybová & Jachowicz, 1957

Genus *Grumosisporites* Smith & Butterworth, 1967
Grumosisporites inaequalis (Butterworth & Williams) Smith & Butterworth, 1967 (Pl. 3.9c)
Grumosisporites cf. *verrucosus* (Butterworth & Williams) Smith & Butterworth, 1967 (Pl. 3.9d)
Grumosisporites sp. (Pl. 3.9e)

Genus *Verrucosisporites* (Ibrahim) Smith, 1971
Verrucosisporites baccatus Staplin, 1960 (Pl. 3.7ag)
Verrucosisporites nitidus morphon (sensu Van der Zwan, 1980) (Pl. 3.6f)
Verrucosisporites tumulentus Clayton & Graham, 1974 (Pl. 3.6g)
Verrucosisporites cf. *scurrus* (Naumova) McGregor & Camfield, 1982 (Pl. 3.10i, j)
Verrucosisporites spp. (Pl. 3.3t; Pl. 3.6h; Pl. 3.7ah; Pl. 3.10k)

Subinfraturma NODATI Dybová & Jachowicz, 1957

Genus *Acanthotriletes* (Naumova) Potonié & Kremp, 1954
Acanthotriletes cf. *aculeolatus* (Kosanke) Potonié & Kremp, 1955 (Pl. 3.8a)
Acanthotriletes aff. *echinatus* Hoffmeister, Staplin & Malloy, 1955 (Pl. 3.8b)
Acanthotriletes spp. (Pl. 3.7a; Pl. 3.8c)

Genus *Aneurospora* (Streel) Richardson, Streel, Hassan & Steemans, 1982
Aneurospora (*Geminospora*) *extensa* morphon (*A. extensa – A. goensis*) Turnau 1999 (Pl. 3.1b, c)
Aneurospora cf. *greggsii* (McGregor) Streel, 1974 (Pl. 3.1d)

Aneurospora sp. (Pl. 3.1e)

Genus *Apiculatisporis* (Ibrahim). Potonié & Kremp, 1956
Apiculatisporis cf. *porosus* Williams in Neves et al., 1973 (Pl. 3.8f)
Apiculatisporis cf. *hacquebardi* Playford, 1964 (Pl. 3.4c)
Apiculatisporis cf. *variocorneus* Sullivan, 1964 (Pl. 3.8g)
Apicultisporis spp. (e.g. Pl. 3.8h)

Genus *Apiculatisporites* Potonié & Kremp, 1956
Apiculatasporites davenportensis Peppers, 1969 (Pl. 3.1f; Pl. 3.4b)
Apiculatasporites wapsipiniconensis Peppers, 1969 (Pl. 3.8i)
Apiculatasporites sp.

Genus *Apiculiretusispora* (Streel) Streel 1977
Apiculiretusispora cf. *arenorugosa* McGregor, 1973 (Pl. 3.1g)
Apiculiretusispora cf. *gaspiensis* McGregor, 1973 (Pl. 3.1h)
Apiculiretusispora cf. *perfectae* Steemans, 1989 (Pl. 3.1i)
Apiculiretusispora cf. *plicata* (Allen). Streel, 1967 (Pl. 3.1j)
Apiculiretusispora cf. *synorea* Richardson & Lister, 1969 (Pl. 3.k)
Apiculiretusispora spp. (Pl. 3.1l; Pl. 3.4d)

Genus *Grandispora* (Hoffmeister, Staplin & Malloy) McGregor, 1973
Grandispora aff. *cornuta* Higgs, 1975 (Pl. 3.5c)
Grandispora cf. *echinata* Hacquebard, 1957 (Pl. 3.5d)
Grandispora cf. *famenensis* (Naumova) Streel, 1974 in Becker et al. 1974 var. minuta Nekriata, 1974 (Pl. 3.5e)
Grandispora gracilis (Kedo) Streel in Becker et al., 1974 (Pl. 3.5f)
Grandispora cf. *gracilis* (Kedo) Streel in Becker et al., 1974 (Pl. 3.7o)
Grandispora cf. *micronulata* (Kedo) Avkhimovitch, 2000 (Pl. 3.2k)
aff. Grandispora microseta (Kedo) Streel in Becker et al., 1974
Grandispora minuta (Kedo) Avkhimovitch, 2000 (Pl. 3.2l)
Grandispora permulta (Daemon) Loboziak, Streel & Melo, 1999 (Pl. 3.2m)
Grandispora tamarae Loboziak in Higgs et al., 2000 (Pl. 3.2n)
Grandispora aff. *tamarae* Loboziak in Higgs et al., 2000 (Pl. 3.9b)
Grandispora aff. *velata* (Eisenack) McGregor, 1973 (Pl. 3.2o)
Grandispora sp.1 (Pl. 3.2p)
Description: Trilete camerate spores with triangular to roundly triangular outline. Intexine outline generally conformable with exine outline. Trilete mark usually damaged, straight or slightly sinuous extending to 4/5 of intexine body radius. Laesurae with narrow (ca. 2µm wide) lips. Intexine with densely packed grana and small verrucae. Exoexine thinner than intexine, laevigate, with few, very broad-based coni around the equator.
Dimensions: Maximum width: 87 to 110µm; Maximum length: 90 to 133µm. Intexine body diameter is 75 to 80% of total spore diameter.
Remarks: Only 3 badly preserved specimens were observed. The specimens could also belong to Genus *Auroraspora*, considering that the exine could actually be a flange, however the simple connate ornamentation is more indicative of *Grandispora*.
Grandispora spp. (Pl. 3.2q; Pl. 3.5f; Pl. 3.7p; Pl. 3.9a)

Genus *Lophotriletes* (Naumova) Potonié & Kremp, 1954
Lophotriletes atratus Naumova, 1953 (Pl. 3.5p)

aff. *Lophotriletes multiformis* Tchibrikova, 1977 (Pl. 3.3g)
Lophotriletes sp.1 (Pl. 3.5q, r)
Description: Rounded trilete miospores. Trilete mark extending to or near to the equator, simple or with slightly raised lips with ca. 1µm total width, often obscured by the ornamentation. Surface irregularly covered by verrucae and baculae with ca. 1µm width and variable length. The verrucae occasionally coalesce and rarely form lumina. 50% or less of the surface is covered by ornamentation.
Dimensions: Diameter 35 to 40µm
Lophotriletes sp. (Pl. 3.5s)

Genus *Spinozonotriletes* (Hacquebard) Neves & Owens, 1966
Spinozonotriletes sp. (Pl. 3.10c)

Subinfraturma BACULATI Dybová & Jachowicz, 1957

Genus *Ancyrospora* Richardson, 1960
cf. *Ancyrospora*? *andevalensis* González, Playford & Moreno, 2005 (Pl. 3.8d)
Ancyrospora sp. (Pl. 3.4a; Pl. 3.8e)

Genus *Raistrickia* (Schopf, Wilson & Bentall) Potonié & Kremp, 1954
Raistrickia imbricate Kosanke, 1950
Raistrickia sp. (Pl. 3.9ab)

Infraturma MURORNATI Potonié & Kremp, 1954

Genus *Acinosporites* Richardson, 1965
Acinosporites sp. (Pl. 3.1a; Pl. 3.7b)

Genus *Convolutispora* Hoffmeister, Staplin & Malloy, 1955
Convolutispora cf. *ampla* Hoffmeister, Staplin & Malloy, 1955 (Pl. 3.4e; Pl. 3.8m)
Convolutispora cerebra Butterworth & Williams, 1958 (Pl. 3.4f; Pl. 3.8n)
Convolutispora cf. *cerebra* Butterworth & Williams, 1958 (Pl. 3.7g)
Convolutispora circumvallata Clayton, 1971 (Pl. 3.4h; Pl. 3.8o)
Convolutispora aff. *disparalis* Allen, 1965 (Pl. 3.4g; Pl. 3.7h; Pl. 3.8p)
Convolutispora florida Hoffmeister, Staplin, & Malloy 1955
Convolutispora jugosa Smith & Butterworth, 1967 (Pl. 3.8q)
Convolutispora paraverrucata McGregor 1964 (Pl. 3.4i)
Convolutispora subtilis Owens, 1971 (Pl. 3.4j; Pl. 3.8r)
Convolutispora varicosa Butterworth & Williams, 1958 (Pl. 3.4k)
Convolutispora cf. *vermiformis* Hughes & Playford, 1961 (Pl. 3.4l)
Convolutispora spp. (Pl. 3.4m; Pl. 3.7i; Pl. 3.8s)

Genus *Corbulispora* Bharadwaj & Venkatachala, 1961
Corbulispora cancellata (Waltz) Bharadwaj & Venkatachala, 1961 (Pl. 3.4n)

Genus *Cordylosporites* Playford & Satterthwait, 1985
Cordylosporites sp. (Pl. 3.4o)

Genus *Dictyotriletes* (Naumova) Smith & Butterworth, 1967
Dictyotriletes cf. *aequalis* Staplin, 1960 (Pl. 3.8x)

Dictyotriletes castaneaeformis (Horst) Sullivan, 1964 (Pl. 3.8y)
Dictyotriletes cf. *densoreticulatus* Potonié & Kremp, 1955 (Pl. 3.8z)
Dictyotriletes submarginatus (Playford) Van der Zwan, 1980 (Pl. 3.4v)
Dictyotriletes spp. (Pl. 3.2d; Pl. 3.4w; Pl. 3.7m; Pl. 3.8aa)

Genus *Emphanisporites* McGregor, 1961
Emphanisporites rotatus (McGregor) McGregor, 1973 (Pl. 3.5a)
Emphanisporites sp. (Pl. 3.8ab)

Genus *Microreticulatisporites* (Knox) Potonié & Kremp, 1954
Microreticulatisporites concavus Butterworth & Williams, 1958 (Pl. 3.9s)

Genus *Rugospora* Neves & Owens, 1966
Rugospora cf. *flexuosa* (Jushko) Streel in Becker et al., 1974 (Pl. 3.6a; Pl. 3.9ad)
Rugospora polyptycha Neves & Ioannides, 1974 (Pl. 3.9ae)
Rugospora spp. (Pl. 3.6b; Pl. 3.9af)

Suprasubturma CAVATITRILETES Oshurkova & Paschkevich, 1990

Subturma ZONOCAVATITRILETES Oshurkova & Paschkevich, 1990

Genus *Kedoesporis* (Naumova) Obukhovskaya & Obukhovskaya, 2008
Kedoesporis imperfectus (Naumova) Obukhovskaya & Obukhovskaya, 2008 (Pl. 3.2u)

Subturma ZONOTRILETES Waltz, 1935

Genus *Triquitrites* Wilson & Coe, 1940
Triquitrites aff. *bucculentus* Guennel, 1958 (Pl. 3.10g)
Triquitrites sp. (Pl. 3.7ae; Pl. 3.10h)

Infraturma CINGULATI (Potonié & Klaus) Dettmann 1963

Genus *Archaeozonotriletes* (Naumova) Allen 1965
Archaeozonotriletes chulus cf. *var. chulus* (Cramer) Richardson & Lister, 1969 (Pl. 3.1m)
aff. *Archaeozonotriletes divellomedium* (Chibrikova) Burgess & Richardson, 1991 (Pl. 3.1n)
Archaeozonotriletes sp. (Pl. 3.1o)

Genus *Camptozonotriletes* Staplin, 1960
Camptozonotriletes cf. *verrucosus* Butterworth & Williams, 1958 (Pl. 3.8k)

Genus Contagisporites Owen 1971
Contagisporites optivus var. vorobjevensis (Chibrikova) Owens, 1971 (Pl. 3.1u)

Genus Knoxisporites (Potonié & Kremp) Neves, 1961
Knoxisporites concentricus (Byvscheva) Playford & McGregor, 1993
Knoxisporites aff. *concentricus* (Byvsheva) Playford & McGregor, 1993 (Pl. 3.7t)
Knoxisporites ruhlandii Doubinger & Rauscher, 1966 (Pl. 3.5l)
Knoxisporites cf. *ruhlandii* Doubinger & Rauscher, 1966 (Pl. 3.7u)
Knoxisporites cf. *triradiatus* Hoffmeister, Staplin & Malloy, 1955 (Pl. 3.9h)

Knoxisporites spp. (Pl. 3.5m; Pl. 3.7v; Pl. 3.g)

Genus *Lophozonotriletes* (Naumova) Potonié, 1958
Lophozonotriletes cf. *Convolutispora insulosa* Playford, 1978 (Pl. 3.9o)
Lophozonotriletes bellus Kedo, 1963 (Pl. 3.5t)
Lophozonotriletes cf. *bouckaertii* Loboziak & Streel, 1989 (Pl. 3.5u)
Lophozonotriletes cf. *lebedianensis* Naumova, 1953 (Pl. 3.5v)
Lophozonotriletes cf. *grandis* (Naumova) Arkhangelskaya, 1985 (Pl. 3.3h)
Lophozonotriletes media Taugourdeau-Lantz, 1967 (Pl. 3.3i)
Lophozonotriletes tuberosus Sullivan, 1964 (Pl. 3.5w)
Lophozonotriletes spp. (Pl. 3.3j; Pl. 3.5x; Pl. 3.7x; Pl. 3.9p)

Genus *Savitrisporites* Bharadwaj, 1955
cf. *Savitrisporites nux* (Butterworth & Williams) Smith & Butterworth, 1967 (Pl. 3.10b)

Genus *Stenozonotriletes* (Naumova) Potonié, 1958
Stenozonotriletes cf. *bracteolus* (Butterworth & Williams) Smith & Butterworth, 1967 (Pl. 3.10d)
Stenozonotriletes lycosporoides (Butterworth *&* Williams) Smith & Butterworth, 1967 (Pl. 3.7ad)
Stenozonotriletes spp. (Pl. 3.10e)

Genus *Tumulispora* Staplin & Jansonius, 1964
aff. *Tumulispora rarituberculata* (Luber) Potonié, 1966 (Pl. 3.7af)

Subturma ZONOLAMINATITRILETES Smith & Butterworth, 1967

Infraturmae CRASSITI (Bharadwaj & Venkatachala) Smith & Butterworth, 1967 and CINGULICAVATI Smith & Butterworth, 1967

Genus *Crassispora* (Bharadwaj) Sullivan, 1964
Crassispora aff. *kosankei* (Potonié & Kremp) Smith & Butterworth, 1967 (Pl. 3.8t)
Crassispora spp. (Pl. 3.4q; Pl. 3.7j)

Genus *Cristatisporites*
Cristatisporites aff. *echinatus* Playford, 1963 (Pl. 3.4p)
aff. *Cristatisporites inaequus* (McGregor) Gao, 1975 (Pl. 3.1w)
Cristatisporites triangulatus (Allen) McGregor & Camfield, 1982 (Pl. 3.1x)
Cristatisporites spp. (Pl. 3.1y; Pl. 3.8u)

Genus *Cristicavatispora* González, Playford & Moreno, 2005
Cristicavatispora dispersa González, Playford & Moreno, 2005 (Pl. 3.4r)

Genus *Densosporites* (Berry) Butterworth, Jansonius, Smith & Staplin, 1964
Densosporites annulatus (Loose) Smith & Butterworth, 1967 (Pl. 3.7k; Pl. 3.8v)
cf. *Densosporites devonicus* Richardson, 1960 (Pl. 3.2c)
Densosporites spinifer Hoffmeister, Staplin & Malloy, 1955 (Pl. 3.4u)
Densosporites spp. (Pl. 3.7l; Pl. 3.8w)

Genus *Hymenozonotriletes* (Naumova) Potonié, 1958

Hymenozonotriletes cristatus Menendez & Pöthe de Baldis, 1967 . (Pl. 3.2r)
Hymenozonotriletes cf. *cristatus* Menendez, 1967 (Pl. 3.5h; Pl. 3.7q)
Hymenozonotriletes (*Samarisporites*) cf. *inaequus* (McGregor) Owens, 1971 (Pl. 3.5i; Pl. 3.7r)
Hymenozonotriletes cf. *incisus* Naumova, 1953 (Pl. 3.5j)
Hymenozonotriletes spp. (Pl. 3.5k; Pl. 3.7s; Pl. 3.9f)
Hymenozonotriletes sp.1 (Pl. 3.2s)
Description of specimens: Spores trilete, outine rounded stellate. Equatorial flange thin and laevigate with very irregular width, forming a stellate general spore outline. Central body roundly triangular, slightly thicker than flange, apparently laevigate. A darker (thicker?) ring is observed in the equatorial region, conformable with the central body outline. Laesure indistinct due to poor preservation.
Dimensions: Maximum width: 60-65µm. Central body maximum with: 35-40µm.
Remarks: Two poorly preserved specimens were observed that do not allow the proper description of the central body.
Hymenozonotriletes sp. (Pl. 3.2t)

Genus *Lycospora* (Schopf, Wilson & Bentall) Potonié & Kremp, 1954
Lycospora cf. *subtriquetra* (Luber) Potonié & Kremp, 1956 (Pl. 3.9q)
Lycospora spp. (Pl. 3.7y; Pl. 3.9r)

Genus Samarisporites Richardson, 1965
Samarisporites spp. (Pl. 3.6c; Pl. 3.10a)

Infraturma PATINATI (Butterworth & Williams) Playford & Dettman, 1996

Genus *Chelinospora* Allen, 1965
Chelinospora concinna Allen, 1965 (Pl. 3.1t)
Chelinospora spp. (e.g. Pl. 3.8l)

Genus *Camarozonotriletes* (Naumova) Naumova, 1953
Camarozonotriletes cf. *antiquus* (Naumova) Kedo, 1955 (Pl. 3.1r)
Camarozonotriletes spp. (Pl. 3.1s; Pl. 3.8j)

Genus *Cymbosporites* Allen, 1965
Cymbosporites cyathus Allen, 1965 (Pl. 3.2a)
Cymbosporites sp. (Pl. 3.2b)

Genus *Cyrtospora* Winslow, 1962
Cyrtospora cristifer (Luber) Van der Zwan, 1979 (Pl. 3.4t)

Supersubturma PSEUDOSACCITRILETES Richardson, 1965

Infraturma MONOPSEUDOSACCITI Smith & Butterworth, 1967

Genus *Auroraspora* Hoffmeister, Staplin & Malloy, 1955
Auroraspora cf. *asperella* (*Kedo*) Van der Zwan, 1980 (Pl. 3.7e)
Auroraspora asperella variant B (Kedo) Van der Zwan, 1979 (Pl. 3.1p)
Auroraspora micromanifesta (Hacquebard) Richardson, 1960 (Pl. 3.1q)
Auroraspora spp. (e.g. Pl. 3.4d; Pl. 3.7f)

Genus *Diducites* Van Veen, 1981
Diducites sp. (Pl. 3.2e)

Genus Spelaeotriletes Neves & Owens, 1966
aff. *Spelaeotriletes balteatus* (Playford) Higgs, 2006 (Pl. 3.6d)

Subturma PERINOTRILETES Erdtman, 1947

Genus *Perotrilites* (Erdtman) Couper, 1953
aff. *Perotriletes tessellatus* (Staplin) Neville in Neves et al., 1973
Perotrilites sp. (Pl. 3.3k)

Genus *Proprisporites* Neves, 1958
Proprisporites laevigatus Neves, 1961 (Pl. 3.9t)

Turma MONOLETES Ibrahim, 1933

Subturma AZONOMONOLETES Luber, 1935

Infraturma LAEVIGATOMONOLETI Dybová & Jachowicz, 1957

Genus *Laevigatosporites* (Ibrahim) Schopf, Wilson & Bentall, 1944
Laevigatosporites spp. (Pl. 3.9i, j)

Genus *Latosporites* Potonié & Kremp, 1954
Latosporites cf. *ovalis* Breuer, Al-Ghazi, Al-Ruwaili, Higgs, Steemans & Wellman, 2007 (Pl. 3.3a)
Latosporites sp. (Pl. 3.3b)

Anteturma POLLENITES Potonié, 1931

Turma SACCITES Erdtman, 1947

Subturma MONOSACCITES Potonié & Kremp, 1954

Infraturma TRILETESACCITI Leschik, 1955

Genus *Schulzospora* Kosanke, 1950
Schulzospora sp. (Pl. 3.7ac)

Infraturma VESICULOMONORADITI Pant, 1954

Archaeoperisaccus aff. *ovalis* Naumova, 1953 (Pl. 3.4c)

INCERTAE SEDIS

Genus *Corystisporites* Richardson, 1965
Corystisporites sp. (Pl. 3.1v)

Genus *Radialetes* Playford, 1963
aff. *Radialetes* sp. (Pl. 3.9aa)

3.5.2 Organic-walled microplankton

Division CHLOROPHYTA Pascher, 1914

Class PRASINOPHYCEAE Christensen, 1962

Family LEIOSPHAERIDIA (Timofeev) Mädler, 1958

Genus *Leiosphaeredia* (Eisenack) Turner, 1984
Leiosphaeredia spp. (Pl. 3.11g; Pl. 3.13l, m, n)

Family CYMATIOSPHAERACEAE Mädler, 1963

Genus *Cymatiosphaera* (O. Wetzel) Deflandre, 1954
Cymatiosphaera chelina Wicander & Loeblich, 1977 (Pl. 3.12f)
Cymatiosphaera cf. *fritilla* Wicander & Loeblich, 1977 (Pl. 3.12g)
Remarks: The Albergaria specimens closely resemble the type material but the ornament in the centre of each lumina seems to form, at least in some cases, a small pila and not a simple granule.
Cymatiosphaera melikera Wicander & Loeblich, 1977 (Pl. 3.12h)
Cymatiosphaera nebulosa Deunff, 1956 (Pl. 3.12i)
Cymatiosphaera perimenbrana Staplin, 1961 (Pl. 3.12j)
Cymatiosphaera cf. *subtrita* Playford, 1981 (Pl. 3.12k)
Cymatiosphaera sp. (Pl. 3.12l)

Genus *Dictyotidium* (Eisenack) Staplin, 1961
Dictyotidium cf. *craticulum* (Wicander & Loeblich) Wicander & Playford,1985 (Pl. 3.12q)
Dictyotidium cf. *confragum* Playford in Playford & Dring, 1981 (Pl. 3.12r)
Dictyotidium cf. *defectivum* Colbath, 1990 (Pl. 3.12s)
Remarks: The Albergaria specimens closely resemble the type material but the diameter is between 13 to 23μm, smaller than originally described by Colbath, 1990.
Dictyotidium litum Colbath, 1990 (Pl. 3.12u)
Dictyotidium cf. *polygonium* Staplin, 1961 (Pl. 3.12v)
Dictyotidium senticogremium Hashemi & Fahimi, 2006 (Pl. 3.12w)
Dictyotidium cf. *senticogremium* Hashemi & Fahimi, 2006 (Pl. 3.12x)
Remarks: The Albergaria specimens are similar to the type material of *Dictyotidium senticogremium* described by Hashemi & Fahimi, 2006, but the ornament in the centre of each lumina is a simple broad-based cone. This ornament is developed only in some lumina. Occasionally the muri connecting the vertices of the pentagonal fields are absent, but this may be a preservational feature.
Dictyotidium spp. (e.g. Pl. 3.12y)

Family PTEROSPERMELLACEAE Eisenack, 1972

Genus *Maranhites* Brito, 1965
Maranhites perplexus Wicander & Playford, 1985 (Pl. 3.11h)

Maranhites sp. (Pl. 3.11i)

Genus *Pterospermella* Eisenack, 1972
aff. *Pterospermella hermosita* (Cramer) Fensome et al., 1990 (Pl. 3.14q)
Pterospermella cf. *helios* (Sarjeant) de Coninck, 1975 (Pl. 3.14r)
Pterospermella cf. *malaca* Loeblich & Wicander, 1976 (Pl. 3.14s)
Remarks: In his original description Loeblich & Wicander, 1976 include the reference to at least one specimens with a quadrate shaped flanged, although it was not illustrated.
Pterospermella tenellula Playford, 1981 (Pl. 3.14t)
Pterospermella aff. *timofeevii* Deunff in Eisenack et al., 1973 (Pl. 3.14u)
Pterospermella sp.1 (Pl. 3.14v)
Description: Oval to elipsiodal outline. Central body is darker with an irregular surface (minutely scabrate?). A slit (excystment?) is observed to extend the full legth of the central body. Flange is lighter with a regular width, aparently laevigate, with minor folds around the perifery. Dimensions: 13µm maximum width, 16µm maximum length. Central body 8,5µm maximum width, 12µm maximum length. Flange 1,5 to 2µm wide.
Pterospermella spp. (e.g. Pl. 3.14w)

Group ACRITARCHA Evitt, 1963

Genus *Ammonidium* (Lister) Sarjeant & Vavrdová, 1997
aff. *Ammonidium alloiteaui* Deunff , 1955 (Pl. 3.12a)
Ammonidium cf. *microcladum* (Downie) Lister, 1970 (Pl. 3.11a)
Ammonidium sp.

Genus *Baltisphaeridium* (Eisenack) Eiserhardt, 1989
Baltisphaeridium urticans Stockmans & Willière, 1974 (Pl. 3.12b)
Baltisphaeridium sp. (Pl. 3.12c)

Genus *Buedingiisphaeridium* (Schaarschmidt) Sarjeant & Stancliffe, 1994
Buedingisphaeridium sp. (Pl. 3.12d)

Genus *Crassiangulina* (Jardiné) Wauthoz, Dorning & Le Hérissé, 2003
aff. *Crassiangulina* sp. (Pl. 3.12e)

Genus *Dactylofusa* (Brito & Santos) Cramer, 1970
Dactylofusa cf. *maranhensis* (Pl. 3.12m)
Description: vesicle fusiform 30 to 45µm in length. A longitudinal slit (excystement?) extendending from pole to pole is frequently observed. Processes short (few µm) of uniform width, simple or terminating with short bifurcation or small bulb. Comunicating freely (or apparently so) with vesicle interior. They are randomly distributed on the vesicle surface or roughly aligned with the length.

Genus *Daillydium* Stockmans & Willière, 1969
Daillydium pentaster (Staplin) Playford in Playford & Dring, 1981 (Pl. 3.12n, o)
Daillydium sp. (Pl. 3.11b)

Genus *Deltotosoma* Playford in Playford & Dring, 1981
Deltotosoma sp. (Pl. 3.12p)

Genus *Estiastra* (Eisenack) Sarjeant & Stancliffe, 1994
Estiastra sp. (Pl. 3.13a)

Genus *Florisphaeridium* Lister, 1970
aff. Florisphaeridium (Baltisphaeridium) guillermii (Cramer) Fensome et al., 1990 (Pl. 3.13b)
Florisphaeridium sp.

Genus *Geron* (Cramer) Cramer, 1969
Geron sp. (Pl. 3.13c)

Genus *Goniosphaeridium* (Eisenack) Turner, 1984
Goniosphaeridium polygonale (Eisenack) Eisenack, 1969 (Pl. 3.11c)

Genus *Gorgonisphaeridium* Staplin, Jansonius & Pocock, 1965
Gorgonisphaeridium anasillos Colbath, 1990 (Pl. 3.13d, d')
Gorgonisphaeridium caningensis Colbath, 1990 (Pl. 3.13e)
Gorgonisphaeridium evexispinosum Wicander, 1974 (Pl. 3.13f)
Gorgonisphaeridium ohioense (Winslow) Wicander, 1974 (Pl. 3.13g)
Gorgonisphaeridium plerispinosum Wicander, 1974 (Pl. 3.13h, h')
Gorgonisphaeridium (*Baltisphaeridium*) *rakoae* (Stockmans & Willière) Sarjeant & Vavrdová, 1997 (Pl. 3.13i)
Gorgonisphaeridium sp. (Pl. 3.11d, e)

Genus *Helosphaeridium* Lister, 1970
Helosphaeridium aff. *clavispinulosum* Lister, 1970

Genus *Histopalla* Playford in Playford & Dring, 1981
Histopalla sp. (Pl. 3.13j)

Genus *Leiofusa* (Eisenack) Cramer, 1970
Leiofusa sp. (Pl. 3.11f; Pl. 3.13k)

Genus *Lophosphaeridium* (Timofeev) Downie, 1963
Lophosphaeridium coniferum Colbath, 1990 (Pl. 3.14a)
cf. *Lophosphaeridium deminutum* Playford in Playford & Dring, 1981 (Pl. 3.14b)
cf. *Lophosphaeridium incultum* Colbath, 1990 (Pl. 3.14c)
cf. *Lophosphaeridium papilatum* (Staplin) Martin, 1969 (Pl. 3.14d)
Lophosphaeridium pelicanense Playford, 1981 (Pl. 3.14e)
Lophosphaeridium spp. (e.g. Pl. 3.14f)

Genus *Micrhystridium* Deflandre, 1937
Micrhystridium aff. *castanoideum* Stockmans & Willière, 1969 (Pl. 3.14g)
Micrhystridium deconinckii Stockmans & Willière, 1969 (Pl. 3.14h)
Micrhystridium mametii Stockmans & Willière, 1974 (Pl. 3.14i)
Micrhystridium nannacanthum Deflandre, 1945 (Pl. 3.14j)
Micrhystridium aff. *stellatum* Deflandre, 1945 (Pl. 3.11j; Pl. 3.14k)
Micrhystridium vulgare Stockmans & Willière, 1962 (Pl. 3.14l)
Micrhystridium spp. (Pl. 3.11k, l; Pl. 3.14m, n)

Genus *Multiplicisphaeridium* (Staplin) Staplin, Jansonius & Pocock, 1965
Multiplicisphaeridium cf. *fisherii* (Cramer) Lister, 1970 (Pl. 3.11m)
Multiplicisphaeridium sp. (Pl. 3.14o)

Genus *Navifusa* Combaz, Lange & Pansart, 1967
Navifusa sp. (Pl. 3.11n; Pl. 3.14p)

Genus *Solisphaeridium* (Staplin) Moczydlowska, 1998
Solisphaeridium sp. (Pl. 3.14x)

Genus *Stellinium* Jardiné, Combaz, Magloire,. Peniguel & Vachey, 1972
Stellinium micropolygonale (Stockmans & Willière) Playford, 1977 (Pl. 3.14y)

Genus *Umbellasphaeridium* Jardiné, Combaz, Magloire, Peniguel & Vachey, 1972
aff. *Umbellasphaeridium* sp. (Pl. 3.11p)

Genus *Uncinisphaera* Wicander, 1974
Uncinisphaera (*Villosacapsula*) *ceratioides* (Stockmans & Willière) Colbath, 1990 (Pl. 3.14z)

Genus *Unellium* Rauscher, 1969
Unellium cornutum Wicander & Loeblich, 1977 (Pl. 3.15a)
Unellium cf. *piriforme* Rauscher, 1969 (Pl. 3.15b)
Unellium aff. *winslowiae* Rauscher, 1969 (Pl. 3.15c)
Unellium sp. (Pl. 3.11o)

Genus *Veryhachium* (Deunff) Sarjeant & Stancliffe, 1994
Remarks: The idea of Wicander & Wood, 1981 is favoured here, in that *Veryhachium* spp. should be considered a group or complex composed of forms with laevigate wall, vesicle with triangular outline (more or less convex/concave sides) and wide range of sizes and 3 short or long processes in the corners of the vesicle, within the same plane. *Veryhachium europaeum* possibly corresponds better to the concept of *Dorsennidium*. For taxonomic purposes, species that seem to be morphologically distinct, i.e., without transitional forms between them are considered.
Veryhachium (*Dorsennidium*) *europaeum* (Stockmans & Willière) Sarjeant & Stancliffe, 1994 (Pl. 3.15d)
Veryhachium cf. *pannuceum* Wicander & Loeblich, 1977 (Pl. 3.15e)
Veryhachium reductum Deunff, 1954 (Pl. 3.15f)
Veryhachium trispinosoides (de Jekhowsky) Wicander, 1974 (Pl. 3.15g)
Veryhachium trispinosum (Eisenack) Deunff, 1954 (Pl. 3.15h)
Veryhachium sp. (Pl. 3.11q)

Genus *Winwaloeusia* Deunff, 1977
Winwaloeusia cf. *ranulaeforma* Martin, 1984 (Pl. 3.15i)
Winwaloeusia sp. (Pl. 3.11r)

Acknowledgements

Álvaro Pinto and Raúl Jorge from Creminer- FCUL and Mário Cachão from Centro de Geologia-FCUL for the logistical support; Luís Gama Pereira, Dept. Ciências

da Terra –UC for the constructive discussions and practical aspects in the field; Hélder Chaminé – ISEP who mentored the initial stages of the field work and significantly contributed to the interpretation of this area; Deolinda Flores Centro de Geologia – FCUP, for all the support with the organic petrology part of this study; Eva Franců, Czech Geological Survey for the support with the organic geochemistry results and interpretation. Eugénio Soares and Lina Carvalho – Aveiro University are acknowledged for their technical support with the microwave digestion system; Alberto Gomes from FLUL for the logistical support in the early stages of the work. Alberto Verde – FCUL for the support with the thin sections.

References

AHRENS, W., 1936. Erläuterungen zur geologischen Karte v. Pressen u. benachbarten dt. Ländern, Bl. Mayen. 47S.; Berlin.

ARRIBAS, J. & ARRIBAS, M. E., 1991. Petrographic evidence of different provenance in two alluvial fan systems (Palaeogene of the northern Tajo Basin, Spain) In: MORTON, A. C., TODD, S. P. & HAUGHTON, P. D. W. (eds), Developments in Sedimentary Provenance Studies. Geological Society Special Publication 57: 263-271.

BASU, A., YOUNG, S. W., SUTTNER, L. J., JAMES, W. C. & MACK, G. H., 1975. Re-evaluation of the use of undulatory extinction and polycrystallinity in detrital quartz for provenance interpretation. Journal of Sedimentary Research 45 (4): 873-882.

BATTEN, D., J., 1996a. Chapter 26A - Palynofacies and Palaenvironmental interpretation. In: JANSONIUS, J. & MCGREGOR, D. C. (eds), Palynology: principles and applications. American Association of Stratigraphic Palynologist Foundation 3: 1011-1064.

BATTEN, D., J., 1996b. Chapter 26B - Palynofacies and Petroleum potential. In: JANSONIUS, J. & MCGREGOR, D. C. (eds), Palynology: principles and applications. American Association of Stratigraphic Palynologist Foundation 3: 1065-1084.

BHATIA, M. R., 1983. Plate tectonics and geochemical composition of sandstones: Journal of Geology 91: 611–627.

BEETSMA, J. J., 1995. The late Proterozoic/Paleozoic and Hercynian crustal evolution of the Iberian Massif, N Portugal, as traced by geochemistry and Sr-Nd-Pb isotope systematics of pre-Hercynian terrigenous sediments and Hercynian granitoids. Vrije Universiteit Amsterdam (unpublished PhD thesis): 223pp.

BERNARD, S., BENZERARA, K., BEYSSAC, O., MENGUY, N., GUYOT, F., BROWN Jr, G.E. & GOFFE, B., 2007. Exceptional preservation of fossil plant spores in high-pressure metamorphic rocks. Earth Planet. Sc. Lett. 262 (1-2): 257-272.

BOUMA, A. H., 1962. Sedimentology of some Flysch deposits: A graphic approach to facies interpretation, Elsevier:168 pp.

BOUMA, A. H., 2000. Coarse-grained and fine-grained turbidite systems as end member models: applicability and dangers. Marine and Petroleum Geology, 17: 137-143.

BURNETT D. J. & QUIRK D. G., 2001. Turbidite provenance in the Lower Palaeozoic Manx Group, Isle of Man: implications for the tectonic setting of Eastern Avalonia. Journal of the Geological Society 158 (6): 913-924.

CALVERT, S. E., 1964. Factors affecting distribution of laminated diatomaceous sediments in the Gulf of California. In: VAN ANDEL, T. H. & SHOR, G. G. (eds), Marine Geology of the Gulf of California, Memories AAPG 3: 311-330.

CALVERT, S. E., 1987. Oceanographic controls on the accumulation of organic matter in marine sediments. Geological Society, London, Special Publications, 26 (1): 137-151.

CAPDEVILA, R. & MOUGENOT, D., 1988. Pre-Mesozoic basement of the western Iberian continental margin and its place in the Variscan Belt. In: BOILLOT, G. & WINTERER, E.L. (eds). Proceedings of the Ocean Drilling Program, Scientific Results 103: 3-12.

CARRÍNGTON da COSTA J. 1950. Notícia sobre uma carta geológica do Buçaco, de Nery Delgado. Serviços Geológicos de Portugal: 27 pp.

CHAMINÉ, H.I., 2000. Estratigrafia e estrutura da faixa metamórfica de Espinho-Albergaria-a-Velha (Zona de Ossa-Morena): implicações geodinâmicas. Universidade do Porto: 497 pp. (unpublished PhD thesis).

CHAMINÉ H. I., FONSECA P. E., ROCHA F., MOÇO L. P., FERNANDES J. P., GAMA PEREIRA L. C., GOMES C.; LEMOS de SOUSA M. J. & RIBEIRO A., 2000. Unidade de Albergaria-a-Velha (faixa de cisalhamento de Porto–Tomar–Ferreira do Alentejo): principais resultados de um estudo geológico pluridisciplinar. Geociências, Revista da Universidade de Aveiro 14 (1/2): 49-60.

CHAMINÉ H. I., GAMA PEREIRA L. C., FONSECA P. E., NORONHA F. & LEMOS de SOUSA M. J.,2003a. Tectonoestratigrafia da faixa de cisalhamento de Porto–Albergaria-a-Velha–Coimbra–Tomar, entre as Zonas Centro-Ibérica e de Ossa-Morena (Maciço Ibérico, W de Portugal). Cadernos Laboratorio Xeoloxia Laxe 28: 37-78.

CHAMINÉ, H. I., GAMA PEREIRA L. C., FONSECA P. E., MOÇO L. P., FERNANDES J. P., ROCHA F T., FLORES D., PINTO de JESUS A., GOMES C., SOARES de ANDRADE A. A. & ARAÚJO, A., 2003b. Tectonostratigraphy of middle and upper Palaeozoic black shales from the Porto–Tomar–Ferreira do Alentejo shear zone (W Portugal): new perspectives on the Iberian Massif. Geobios 36 (6): 649-663.

CHAMINÉ, H. I., FONSECA, P. E., PINTO DE JESUS, A., GAMA PEREIRA, L. C., FERNANDES, J. P., FLORES, D. MOÇO, L. P., DIAS DE CASTRO, R., GOMES, A., TEIXEIRA, J., ARAÚJO, M. A., SOARES de ANDRADE, A. A., GOMES C. & ROCHA, F. T., 2007. Tectonostratigraphic imbrications along strike-slip major shear zones: an example from the early Carboniferous of SW European Variscides (Ossa-Morena Zone, Portugal). In: Theo E. Wong (Ed.), Proceedings. XVth International Congress on Carboniferous and Permian Stratigraphy (Utrecht, 2003). Royal Dutch Academy of Arts and Sciences, Amsterdam, Edita NKAW: 405-416.

CLAYTON, G., 1972. Compression structures in the Lower Carboniferous miospore Dictyotriletes admirabilis Playford. Palaeontology 15(1): 121-124.

CLAYTON, G., COQUEL, R., DOUBINGER, J., GUEINN K.J., LOBOZIAK, S., OWENS, B. & STREEL, M., 1977. Carboniferous miospores of Western Europe: illustration and zonation. Meded. Rijks Geol. Dienst 29: 1-71.

CLAYTON, G., WICANDER, R. & PEREIRA, Z., 2002. Palynological evidence concerning the relative positions of Northern Gondwana and Southern Laurussia in latest Devonian and Mississippian times. - In: WYSE JACKSON, P. & PARKES, M.A. (eds). Studies in Palaeozoic palaeontology and biostratigraphy in honour of Charles Hepworth Holland. Special Papers in Palaeontology 67: 45-56.

CLAYTON, G., MCCLEAN, D. & OWENS, B., 2003. Carboniferous palinostratigraphy: recent developments in Europe (Abstract 103). International Congress on Carboniferous and Permian Stratigraphy, Utrecht, August 2003.

CLAYTON, G., HIGGS, K., MCCLEAN, D. & OWENS, B., 2008. Carboniferous miospore biostratrigraphy in Western Europe. 12th International Palynological Congress, 8th International Organisation of Palaeobotany Conference Bonn, Germany. Terra Nostra, 2. Abstract no. 117: 51-52.

COMBAZ, A. 1964. Les palynofacies. Revue de Micropaleontologie 7: 205 18.

COOPER A., 1980. The Stratigraphy and Palaeontology of the Ordovician to Devonian rocks of the area North of Dornes (near Figueiró dos Vinhos), central Portugal. University of Sheffield (unpublished PhD thesis): 378pp.

COURBOULEIX, S., 1974. Étude géologique des régions de Anadia et de Mealhada : le socle, le Primaire et le Ttrias. Comunicações dos Serviços Geológicos de Portugal LVIII: 5-37

CUNHA, T.A. & OLIVEIRA, J. T., 1989. Upper Devonian palynomorphs from the Represa and phyllite-quartzite formations, Mina de São Domingos region, Southeast Portugal; tectonostratigraphic implications. - Bulletin de la Societe Belge de Geologie 98: 295-309.

CURTIS, C. D., 1980. Diagenetic alteration in black shales. Journal of the Geological Society 137 (2): 189.

DIAS, R. & RIBEIRO, A., 1993. Porto-Tomar shear zone, a major structure since the beginning of the Variscan orogeny. Comunicações do Instituto Geológico e Mineiro 79: 31–40.

DICKINSON, W. R., 1970. Interpreting detrital modes of graywacke and arkose. Journal of Sedimentary Research 40 (2): 695-707.

DICKINSON, W. R. & SUCZEK, C. A., 1979. Plate tectonics and sandstone compositions. AAPG Bulletin 63(12): 2164-2182.

DICKINSON, W. R., BEACH, L. S., BRACKENRIDGE, G. R., ERJAVEC, J. L., FERGUSON, R. C., KNEPP, R. A., LINDBERG, F. A. & RYBERG, P. T., 1983. Provenance of North American Phanerozoic sandstones in relation to tectonic setting. Geological Society of America Bulletin 94: 222-235.

DICKINSON, W.R., 1985. Interpreting provenance relations from detrital modes of sandstones. In: ZUFFA, G.G. (ed.), Provenance of Arenites. Reidel Publ., Dordrecht: 333–361.

DONEGAN, D. & SCHRADER, H., 1982. Biogenic and abiogenic components of laminated hemipelagic sediments in the central Gulf of California. Marine Geology 48: 215 237.

EL-MEHDAWI, A.D., 1998. Palynology of the Upper Tahara Formation in Concession NC7A, Ghadames Basin in Geological Exploration in Murzuq Basin. - In: Sola, M.A. & Worsley, D. (Eds) Elsevier B.V. National Oil Corporation and Sebha University: 273-294.

ESPITALIÉ J., DEROO G. & MARQUIS F., 1985. La pyrolyse Rock-Eval et ses applications. Revue de l´Institute Français du Pétrole 40(5): 563-579.

FERNANDES, J.P., FLORES, D., ROCHA, F.T., GOMES, C., GAMA PEREIRA, L.C., FONSECA P.E. & CHAMINÉ, H.I., 2001. Devonian and Carboniferous palynomorph assemblages of black shales from the Ovar–Albergaria-a-Velha–Coimbra–Tomar (W Portugal): tectonostratigraphic implications for the Iberian Terrane. Geociências - Revista da Universidade de Aveiro 15: 1-23.

FERNÁNDEZ, F.J., CHAMINÉ, H.I., FONSECA, P.E., MUNHÁ, J.M., RIBEIRO, A., ALLER, J., FUERTES-FUENTES, M., BORGES, F.S., 2003. High-temperature fabrics in garnetiferous quartz-tectonites fromW Portugal: geodynamic implications for the Iberian Variscan Belt. Terra Nova 15 (2): 96–103.

FOLK R. L., 1951. Stages of textural maturity in sedimentary rocks: Journal of Sedimentary Petrology 21: 127-130

GAMA PEREIRA, L.C., 1987. Tipologia e evolução da sutura entre a Zona Centro Ibérica e a Zona Ossa Morena no sector entre Alvaiázere e Figueiró dos Vinhos (Portugal Central). Universidade de Coimbra (unpublished PhD thesis): 331pp

GAMA PEREIRA L. C., 1998. A faixa de cisalhamento Porto–Tomar, no sector entre o Espinhal e Alvaiázere (Portugal Central). In: CHAMINÉ H. I. et al. (coords), Geologos, Revista Departamento de Geologia da Universidade do Porto 2: 23-27.

GAMA PEREIRA L. C., PINA B., FLORES D. &RIBEIRO M. A., 2008. Tectónica distensiva: o exemplo da Bacia Permo-Carbónica do Buçaco. In: Conferência Internacional Geociências no Desenvolvimento das Comunidades Lusófonas. Memórias e Notícias Nova Série 3: 199-205.

GARZANTI, E., VEZZOLI, G., ANDO, S., FRANCE-LANORD, C., SINGH, S. K. & FOSTER, G., 2004. Sand petrology and focused erosion in collision orogens: the Brahmaputra case. Earth and Planetary Science Letters 220: 157-174.

GEHMAN, H. M., Jr., 1962. Organic matter in limestones. Geochimica et Cosmochimica Acta 26: 885-897.

GOMES, A., CHAMINÉ, H. I., TEIXEIRA, J., FONSECA, P. E., GAMA PEREIRA, L. C., JESUS, A. P., PEREZ ALBERTÍ, A., ARAÚJO, A., COELHO, A., SOARES de ANDRADE, A. & ROCHA, F. T., 2007. Late Cenozoic basin opening in relation to major strike-slip faulting along the Porto-Coimbra-Tomar fault zone (Northern Portugal). In: Nichols G., Williams E., Paola C. (eds.) Sedimentary Processes, Environments and Basins: A Tribute to Peter Friend, IAS Special Publication, Blackwell Publishing: 137-153.

GOMES A., 2008. Evolução Geomorfológica da plataforma litoral entre Espinho e Águeda. Universidade do Porto (unpublished PhD thesis): 337p.

GONZÁLEZ, F., MORENO, C. & PLAYFORD, G., 2005. Upper Devonian biostratigraphy of the Iberian Pyrite Belt, southwest Spain - Part two: Organic-walled microphytoplankton. Palaeontographica, Abt. B 273: 1-51.

HANEL, M., MONTENARI, M. & KALT, A. 1999. Determining sedimentation ages of high-grade metamorphic gneisses by their palynological record; a case study in the northern Schwarzwald (Variscan Belt, Germany). International Journal of Earth Science 88 (1): 49-59.

INGERSOLL, R.V., 1990. Actualistic sandstone petrofacies: discriminating modern and ancient source rocks: Geology 18: 733–736.

INGERSOLL, R. V., FULLARD, T. F., FORD, R. L., GRIMM, J. P., PICKLE, J. D. & SARES, S. W., 1984. The effect of grain size on detrital modes: a test of the Gazzi-Dickinson point-counting method. Journal of Sedimentary Research 54 (1): 103-116.

JARDINÉ, S., COMBAZ, A., MAGLOIRE, L., PENIGUEL, G. & VACHET, G., 1972. Acritarches du Silurien et du Dévonien du Sahara Algérien. - 7th Congrès International de Stratigraphie et de Géologie du Carbonifére, Krefeld C.R.: 347-353.

JARDINE, S., COMBAZ, A., MAGLOIRE, L., PENIGUEL, G. & VACHEY, G. (1974): Distribution stratigraphique des Acritarches dans le Paleozoique du Sahara Algerien. Review of Palaeobotany and Palynology 18 (1-2): 99-129.

KAHN, J. S., 1956. The analysis and distribution of the properties of packing in sand size sedimentes. Journal of Geology 64: 385-395.

LAFARGUE E., MARQUIS F. & PILLOT D., 1998. Rock-Eval 6 applications in hydrocarbon exploration, production, and soil contamination studies. Oil & Gas Science and Technology. Revue de l´Institute Français du Pétrole 53: 421-437.

LEFORT J. P. & RIBEIRO A., 1980. La faille Porto–Badajoz–Cordoue a-t-elle contrôllé l'evolution de l'ocean paleozöique sud-armoricain? Bulletin de la Societé Géologique de France 22(3): 455-462.

MARTIN, F., 1981. Acritarches du Famennien inférieur a Villers-sur-Lesse (Belgique). Bulletin de l'Institut Royal des Sciences Naturelles de Belgique, sciences de la Terre, 52 (2): 1-55.

MARTIN, F., 1981. Acritarches du Famennien inférieur a Villers-sur-Lesse (Belgique). Bulletin de l'Institut Royal des Sciences Naturelles de Belgique, sciences de la Terre, 52 (2): 1-55.

MARTIN, F. (1985): Acritarches du Frasnian supérieur et du Famennien inférieur du bord méridional du Bassin de Dinant (Ardenne belge). - Bulletin de l'Institut Royal des Sciences Naturelles de Belgique, sciences de la Terre, 55: 1-57.

MAKY, A. B. F. & RAMADAN, M. A. M., 2008. Nature of Organic Matter, Thermal Maturation and Hydrocarbon Potentiality of Khatatba Formation at East Abu-gharadig Basin, North Western Desert, Egypt Australian Journal of Basic and Applied Sciences 2(2): 194-209

McCANN T., 1991. Petrological and geochemical determination of provenance in the southern Welsh Basin. In: MORTON A. C., TODD S. P. & HAUGHTON P. D. W. (eds). Developments in Sedimentary Provenance Studies. Geological Society Special Publications. 57: 215-230

MEDINA, J., RODRIGUEZ ALONSO, M. D., BERNARDES, C. A., 1989. Litoestratigrafia e estrutura do complexo xisto-grauváquico na região do Caramulo – Portugal. Revista da Universidade de Aveiro - Geociências 4(1): 51-73.

MEDINA, J., TASSINARI, C. C., PINTO, M. S., 1993. Idades Rb-Sr no complexo xisto-grauváquico na região de Mortágua, Portugal Central. In: NORONHA F., MARQUES M. & NOGUEIRA, P. (eds). Actas IX Semana de Geoquímica e II Congresso de Geoquímica dos Países de Língua Portuguesa. FCUP: 399-403.

MILLER, M. A., 1996. Chitinozoa. In: JANSONIUS, J. & MCGREGOR, D. C., (eds) Palynology: principles and applications. American Association of Stratigraphic Palynologists Foundation 1: 307-336.

MOÇO, L. P., CHAMINE, H. I., FERNANDES, J. P., LEMOS DE SOUSA, M. J., FONSECA, P. E. & RIBEIRO, A., 2001. Organic Metamorphism level of Devonian Black shale from Albergaria-a-Velha region (NW Portugal): Tectonostratigraphic implications. Gaia 16 195-197.

MOLYNEUX, S.G., MANGER, W. L. & OWENS, B., 1984. Preliminary account of Late Devonian palynomorph assemblages from the Bedford Shale and Berea Sandstone formations of central Ohio, U.S.A. Journal of Micropalaeontology 3(2): 41-51.

MOREAU-BENOIT, A., 1984. Acritarches et Chitinozoaires du Devonien moyen et superieur de Libye occidentale. Review of Palaeobotany and Palynology, Alfred Eisenack memorial issue I 43(1-3): 187-216.

MUTTI E. & NORMARK W. R., 1987. Comparing examples of modern and ancient turbidite systems: problems and concepts. In: LEGGETT J. K. & ZUFFA G. G. (eds).

Marine Clastic Sedimentology: Concepts and Case Studies. Graham & Trotman, London: 1-38.

OBUKHOVSKAYA, T. G., AVKHIMOVITCH, V. I., STREEL, M. & LOBOZIAK, S., 2000. Miospores from the Frasnian-Famennian boundary deposits in Eastern Europe (the Pripyat Depression, Belarus and the Timan-Pechora Province, Russia) and comparison with Western Europe (Northern France). Review of Palaeobotany and Palynology 112 (4): 229.

OBUKHOVSKAYA, V. Y. & OBUKHOVSKAYA, T. G., 2008. Miospores of the genus *Kedoesporis* gen. nov. from Devonian deposits of Belarus LITHOSPHERE 2 (29): 61 - 65. (in Russian)

OLIVEIRA, J. T., PEREIRA, E., PICARRA, J. M., YOUNG, T. & ROMANO, M., 1992. O Paleózoico inferior de Portugal; síntese da estratigrafia e da evolução paleogeográfica. Paleozóico inferior de Ibero-America. LISO RUBIO, M. J. Badajoz, Spain, Universidad de Extremadura: 359-376.

PACKER, B.M., & INGERSOLL, R.V., 1986. Provenance and petrology of Deep Sea Drilling Project sands and sandstones from the Japan and Mariana forearc and backarc regions Sedimentary Geology 51 (1-2): 5-28.

PALAIN, C., 1976. Une série détritique terrigène. Les «grès de Silves»: Trias et Lias Inférieur du Portugal. Memórias dos Serviços Geológicos de Portugal (Nova série). 25: 363pp.

PARIS, F., RICHARDSON, J. B., RIEGEL, W., STREEL, M. & VANGUESTAINE, M., 1985. Devonian (Emsian-Famennian) palynomorphs. Palynostratigraphy of North-east Libya. - In: Thusu, B. and Owens, T. London, United Kingdom, British Micropalaeontological Society 4 (1): 49-82.

PARIS, F., 1981. Les chitinozoaires dans le Paleózoïque du SW de l'Europe. Memoires de la Sociète Géologique e Mineralógique de Bretagne, 26: 412pp.

PERA, E. L. & ARRIBAS, J., 2004. Sand composition in an Iberian passive-margin fluvial course: the Tajo River. Sedimentary Geology 171: 261-281.

PEREIRA E., ROMÃO J. & CONDE L. N., 1998. Geologia da Transversal de Tomar - Mação: Sutura entre a Zona Centro Ibérica (ZCI) e Zona de Ossa-Morena (ZOM). In: OLIVEIRA J. T. & DIAS R. (eds), Livro Guia das Excursões do V Congresso Nacional de Geologia, Lisbon, Portugal: 159-188.

PEREIRA, Z., 1999. Palinoestratigrafia do Sector Sudoeste da Zona Sul Portuguesa. - Comunicações Instituto Geológico e Mineiro de Portugal 86: 25-58.

PINTO DE JESUS A., LEMOS DE SOUSA M. J., CHAMINÉ H. I., DIAS R., FONSECA P. E. & GOMES A., 2010. O Carbonífero em Portugal. In: COTELO NEIVA J.M. et al. (eds), Ciências Geológicas: Ensino e Investigação e sua História I, Geologia Clássica. Associação Portuguesa de Geólogos / Sociedade Geológica de Portugal: 341-355.

POTONIÉ, R., 1970. Synopsis der Gattungen der Sporae dispersae V. Nachträge zu allen Gruppen (Turmae). Beihefte zum Geologischen Jahrbuch 87: 1–22

PROTHERO, D.R. & SCHWAB, F., 1996. Sedimentary Geology. W.H. Freeman and Company: 575p.

RIBEIRO, A., PEREIRA, E. & SEVERO GONÇALVES, L., 1980. Análise da Deformação da Zona de Cisalhamento Porto-Tomar na Transversal de Oliveira de Azeméis. Comunicações Instituto Geológico e Mineiro de Portugal, 66: 3-9.

RIBEIRO, A., MUNHÁ, J., DIAS, R., MATEUS, A., PEREIRA, E., RIBEIRO, M. L., FONSECA, P. E., ARAÚJO, A., OLIVEIRA, J. T., ROMÃO, J., CHAMINÉ, H.I., COKE, C. & PEDRO, J. C., 2007. Geodynamic evolution of the SW Europe Variscides. Tectonics, 26 (TC6009)

RIBEIRO, C., 1853. On the Carboniferous and Silurian formations of the neighbourhood of Bussaco in Portugal. (With notes and a description of the animal remains by DANIEL SHARPE, J. W. SALTER & T. RUPERT JONES, and an account of the vegetable remains by CHARLES J. F. BUNBURY). Quarterly Journal Geological Society London (London): 135-160.

RICHARDSON J. B. & MCGREGOR D. C., 1986. Silurian and Devonian spore zones of the Old Red Sandstone continent and adjacent regions. Bulletin of the Geological Survey of Canada 365: 79pp.

SAJGO, C., J. MCEVOY, WOLFF, G. A. & HORVATH, Z. A., 1986. Influence of temperature and pressure on maturation processes - I. Preliminary report. Organic Geochemestry 10(1-3): 331.

SENGUPTA, S., 1975. Experimental alterations of the spores of lycopodium clavatum as related to diagenesis. Review of Palaeobotany and Palynology 19: 173-192.

SEVERO GONÇALVES, L., 1974. Geologie und petrologie des Gebietes von Oliveira de Azeméis und Albergaria-a-Velha (Portugal). Freien Universität Berlin. (unpublished PhD thesis): 261 pp.

STETS, J. & SCHÄFER, A., 2008. The Early Devonian Rhenohercynian Basin (Middle Rhine Valley, Rheinisches Schiefergebirge). In: KÖNIGSHOF P. & LINNEMANN U. (eds), The Rheno-Hercynian, Mid-German Crystalline and Saxo-Thuringian Zones (Central European Variscides) Excursion Guide. Final Meeting of IGCP 497 and IGCP 499. Frankfurt-Dresden, Germany: 16-54.

STOCKMANS, F. & WILLIÈRE, Y., 1969. Acritarches du Famennien Inférieur. - Académie Royale des Sciences, des Lettres et des Beaux Artes de Belgique, Classe des sciences, Mémoires 38 (6): 1-63.

STOCKMANS, F. & WILLIÈRE, Y., 1974. Acritarches de la "Tranchée de Senzeille" (Frasnien supérieur et Famennien inférieur). - Académie Royale des Sciences, des Lettres et des Beaux Artes de Belgique, Classe des sciences, Mémoires 41: 3-79.

STREEL, M., PARIS, F., RIEGEL, W. & VANGUESTAINE, M., 1988. Acritarchs, Chitinozoan and spore stratigraphy from the Middle and Late Devonian of northeast Libya. - In: A. EL ARNAUTI et al. (Eds) Subsurface palynostratigraphy of Northeastern Libya: 111-128.

STROTHER, P. K., 2008. A speculative review of factors controlling the evolution of phytoplankton during Paleozoic time. Revue de Micropaleontologie 51(1): 9-21.

TIWARI, R. S., VIJAYA & MISHRA, B.K., 1994. Taphonomy of spores and pollen in Gondwana sequence of India. The Palaeobotanist 42: 108-119.

TRAVERSE, A., 2007. Paleopalynology. (2nd edition). Topics in Geobiology. (Landman, N. & Jones, D. Eds). Springer. Dordrecht, The Netherlands: 813 pp.

TYSON, R. V., 1987. The genesis and palynofacies characteristics of marine petroleum source rocks. Geological Society, London, Special Publications 26 (1): 47-67.

TYSON, R. V., 1993. Palynofacies analysis. In: JENKINS, D. G. (ed). Applied micropaleontology. Kluwer Academic Publishers, Dordrecht, The Netherlands: 153–191

TISSOT, B., DURAND B., ESPITAlLIE, J. & COMBAZ, A., 1974. Influence of nature and genesis of organic matter in the formation of petroleum. AAPG Bulletin 58: 499-506.

VALLONI, R., MAYNARD, B., 1981. Detrital modes of recent deep-sea sands and their relation to tectonic setting: a first approximation. Sedimentology 28: 75–83.

VALLONI, R., 1985. Reading provenance from modern marine sands. In: ZUFFA, G.G. (Ed.), Provenance of Arenites. D. Reidel, Dordrecht: 309– 332.

VANGUESTAINE, M., 1986. Late Devonian and Carboniferous acritarch stratigraphy and paleogeography. Annales - Societe Geologique de Belgique 109 (1): 93.

VANGUESTAINE, M., DECLAIRFAYT, T., ROUHART, A. & SMEESTERS, A., 1983. Zonation par Acritarches du Frasnien superieur - Famennien inferieur dans les bassins de Dinant, Namur, Herve et Campine (Devonien superieur de Belgique). Annales - Societe Geologique de Belgique 106 (1): 121.

VAVRDOVÁ, M. & ISAACSON, P. E., 1999. Late Famennian phytogeographic provincialism; evidence for a limited separation of Gondwana and Laurentia. North Gondwana; mid-Palaeozoic terranes, stratigraphy and biota. - Geologische Bundesanstalt, 54: 453-463.

VAVRDOVA, M., 1999. The acritarch succession in the Klabava and Sarka Formations (Arenig-Llanvirn): evidence for an ancient upwelling zone? Acta Universitatis Carolinae: Geologica 43(1-2): 263-265.

VÁZQUEZ, M., I. ABAD, JIMÉNEZ-MILLÁN, J., ROCHA, F. T., FONSECA, P. E. & CHAMINÉ, H. I., 2007. Prograde epizonal clay mineral assemblages and retrograde alteration in tectonic basins controlled by major strike-slip zones (W Iberian Variscan chain). Clay Mineralogy 42(1): 109-128.

WAGNER R. H., LEMOS de SOUSA M. J. & SILVA F. G., 1983. Stratigraphy and fossil flora of the Upper Stephanian C of Buçaco, north of Coimbra (Portugal). In: LEMOS de SOUSA M .J. (ed), Contributions to the Carboniferous Geology and Palaeontology of the Iberian Peninsula, Univiversiade do Porto, Faculdade de Ciências, Mineralogia e Geologia: 127-156.

WICANDER, R., 1974. Upper Devonian-Lower Mississippian acritarchs and prasinophycean algae from Ohio, U.S.A. - Palaeontographica, Abt. B, 148(1-3): 9-43.

WICANDER, R. & LOEBLICH, A.R., 1977. Organic-walled microphytoplankton and its stratigraphic significance from the Upper Devonian Antrim Shale, Indiana, U.S.A. Palaeontographica, Abt. B 160 (4-6): 129-165.

WICANDER, R, 1983. A Catalog and Biostratigraphic Distribution of North American Devonian Acritarchs. - AASP Foundation Contributions Series, 10: 133pp.

WICANDER, R. & WRIGHT, R. P., 1983. Organic-walled microphytoplankton abundance and stratigraphic distribution from the middle devonian columbus and delaware limestones of the hamilton quarry, marion county, Ohio. Ohio Journal of Science 83(1): 2-13.

WICANDER, R. & PLAYFORD, G., 1985. Acritarchs and spores from the Upper Devonian Lime Creek Formation, Iowa, U.S.A. Micropaleontology 31(2): 97-138.

YULE, B. L., ROBERTS, S., MARSHALL, J.E.A. & MILTON, J.A., 1998. Spore colour scale using colour image analysis. Organic Geochemestry 28: 139-149.

YULE, B., CARR, A. D., MARSHALL, J. E. A. & ROBERTS, S., 1999. Spore transmittance (% St): a quantitative method for spore colour analysis. Organic Geochemestry 30 (7): 567-581.

YULE, B. L., ROBERTS, S. & MARSHALL, J. E. A., 2000. The thermal evolution of sporopollenin. Organic Geochemestry 31(9): 859- 870.

ZUFFA, G.G., 1985. Optical analyses of arenites: influence of methodology on compositional results. In: ZUFFA, G.G. (Ed.), Provenance of Arenites. D. Reidel, Dordrecht: 165–189.

Plates

Plate 3.1 – Lower (Middle?) Frasnian Miospore assemblage. All are transmitted light photomicrographs.

a *Acinosporites* sp.
b, c *Aneurospora* (*Geminospora*) *extensa* morphon (*A. extensa – A. goensis*) Turnau 1999
d *Aneurospora* cf. *greggsii* (McGregor) Streel, 1974
e *Aneurospora* sp.
f *Apiculatasporites davenportensis* Peppers, 1969
g *Apiculiretusispora* cf. *arenorugosa* McGregor, 1973
h *Apiculiretusispora* cf. *gaspiensis* McGregor, 1973
i *Apiculiretusispora* cf. *perfectae* Steemans, 1989
j *Apiculiretusispora* cf. *plicata* (Allen). Streel, 1967
k *Apiculiretusispora* cf. *synorea* Richardson & Lister, 1969
l *Apiculiretusispora* sp.
m *Archaeozonotriletes chulus* cf. *var. chulus* (Cramer) Richardson & Lister, 1969
n aff. *Archaeozonotriletes divellomedium* (Chibrikova) Burgess & Richardson, 1991
o *rchaeozonotriletes* sp.
p *Auroraspora asperella* variant B (Kedo) Van der Zwan, 1979
q *Auroraspora micromanifesta* (Hacquebard) Richardson, 1960
r *Camarozonotriletes* cf. *antiquus* (Naumova) Kedo, 1955
s *Camarozonotriletes* sp.
t *Chelinospora concinna* Allen, 1965
u *Contagisporites optivus* var. *vorobjevensis* (Chibrikova) Owens, 1971
v *Corystisporites* sp.
w aff. *Cristatisporites inaequus* (McGregor) Gao, 1975
x *Cristatisporites triangulatus* (Allen) McGregor & Camfield, 1982
y *Cristatisporites* sp.

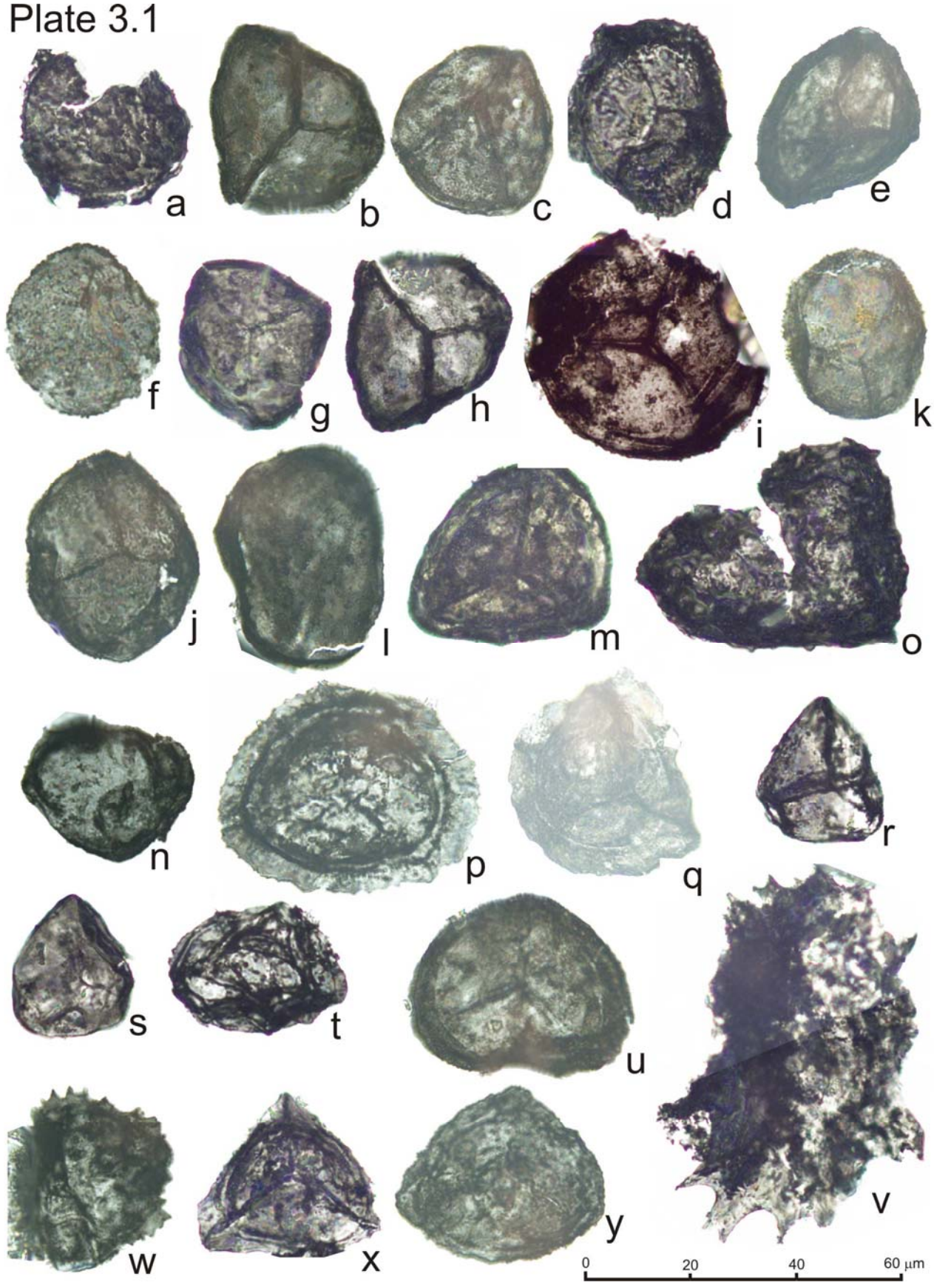
Plate 3.1
a
b
c
d
e
f
g
h
i
k
j
l
m
o
n
p
q
r
s
t
u
v
w
x
y
0
20
40
60 µm

Plate 3.2 – Lower (Middle?) Frasnian Miospore assemblage. All are transmitted light photomicrographs.

a *Cymbosporites cyathus* Allen, 1965
b *Cymbosporites* sp.
c cf. *Densosporites devonicus* Richardson, 1960
d *Dictyotriletes* sp.
e *Diducites* sp.
f *Geminospora* cf. *aurita* Arkhangelskaya, 1985
g *Geminospora lemurata* Balme 1962
h *Geminospora micromanifesta* (Naumova) Arkhangelskaya, 1985
i *Geminospora notata* (Naumova) Obukhovskaya, 1993
j *Geminospora* sp.
k *Grandispora* cf. *micronulata* (Kedo) Avkhimovitch, 2000
l *Grandispora minuta* (Kedo) Avkhimovitch, 2000
m *Grandispora permulta* (Daemon) Loboziak, Streel & Melo, 1999
n *Grandispora tamarae* Loboziak, 2000
o *Grandispora* aff. *velata* (Eisenack) McGregor, 1973
p *Grandispora* sp.1
q *Grandispora* sp. p aff. *Lophotriletes multiformis* Tchibrikova, 1977
r *Hymenozonotriletes cristatus* Menendez & Pöthe de Baldis, 1967
s *Hymenozonotriletes* sp.1
t *Hymenozonotriletes* sp.
u *Kedoesporis imperfectus* (Naumova) Obukhovskaya & Obukhovskaya, 2008

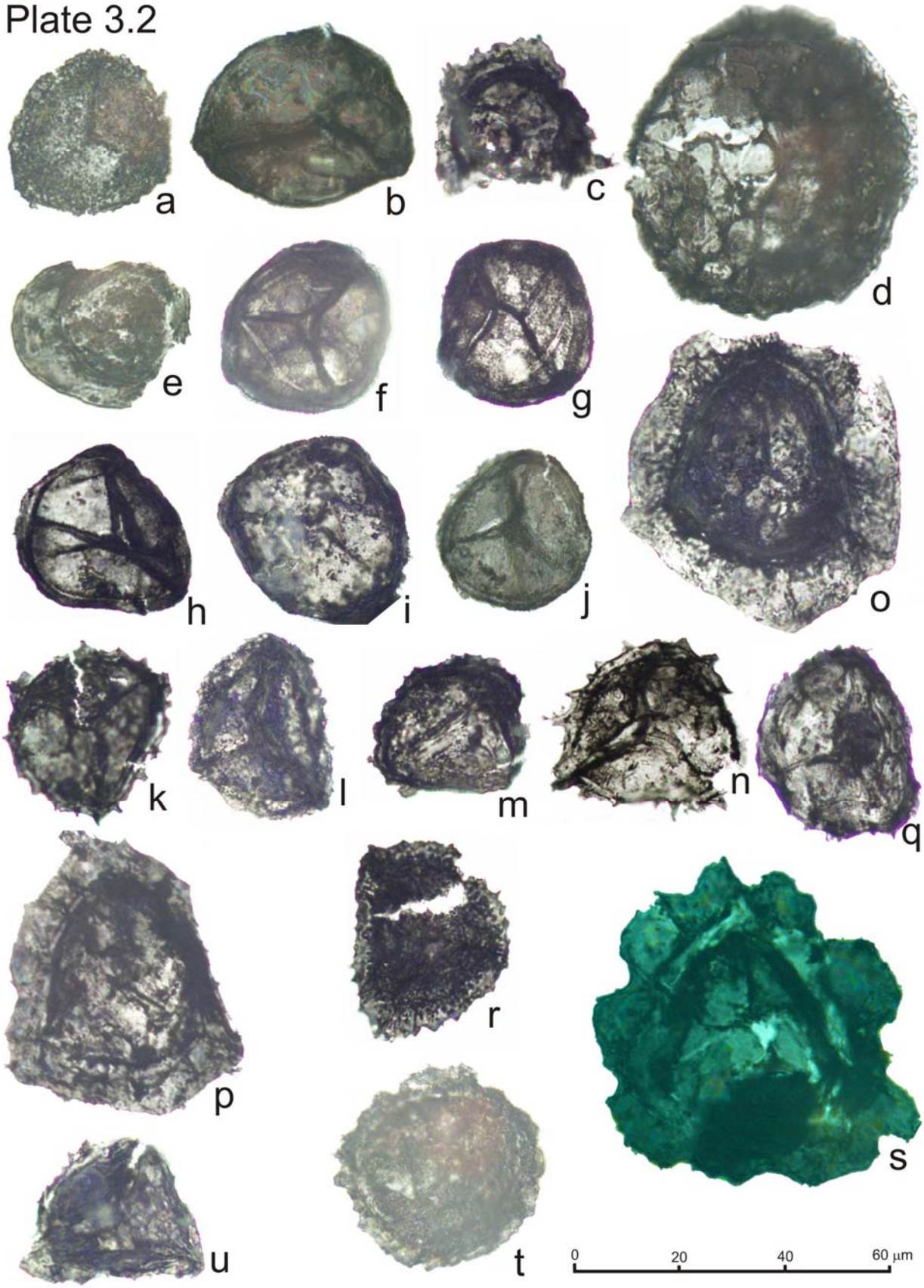
Plate 3.2
a
b
c
d
e
f
g
h
i
j
o
k
l
m
n
q
p
r
s
u
t
0
20
40
60 µm

Plate 3.3 – Lower (Middle?) Frasnian Miospore assemblage. All are transmitted light photomicrographs.

a *Latosporites* cf. *ovalis* Breuer, Al-Ghazi, Al-Ruwaili, Higgs, Steemans & Wellman, 2007
b *Latosporites* sp.
c *Leiotriletes* aff. *devonicus* Naumova, 1953
d *Leiotriletes* aff. *pagius* Allen, 1965
e *Leiotriletes* aff. *trivialis* Naumova, 1953
f *Leiotriletes* sp.
g aff. *Lophotriletes multiformis* Tchibrikova, 1977
h *Lophozonotriletes* cf. *grandis* (Naumova) Arkhangelskaya, 1985
i *Lophozonotriletes media* Taugourdeau-Lantz, 1967
j *Lophozonotriletes* sp.
k *Perotrilites* sp.
l *Punctatisporites solidus* Hacquebard, 1957
m *Punctatisporites springsurensis* Playford, 1978
n *Punctatisporites* sp.
o *Retusotriletes* cf. *communis* Naumova, 1953
p *Retusotriletes minor* Kedo, 1963
q *Retusotriletes* cf. *pychovii* Naumova, 1953
r *Retusotriletes* cf. *scabratus* Turnau, 1986
s *Retusotriletes warringtonii* Richardson & Lister, 1969
t *Retusotriletes* sp.1
u *Retusotriletes* sp.
v *Verrucosisporites* sp.
w, x Phytoclast

Plate 3.3

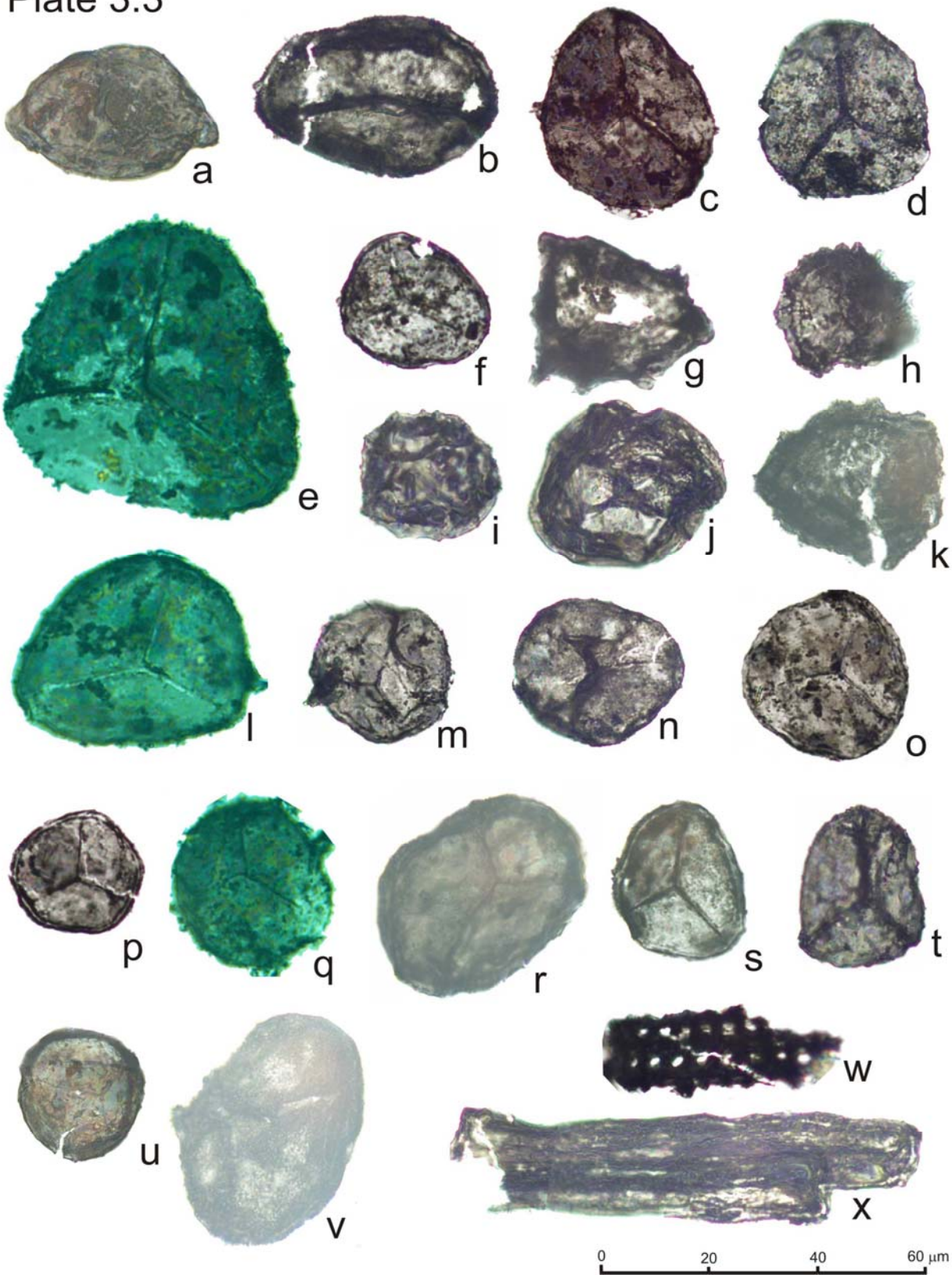

Plate 3.4 - Famenian-Tournaisian miospore assemblage. a to t and v to w are reflected light photomicrographs; u is a transmitted light photomicrograph.

a *Ancyrospora* sp.
b *Apiculatasporites davenportensis* Peppers, 1969
c *Archaeoperisaccus* aff. *ovalis* Naumova, 1953
d *Auroraspora* sp.
e *Convolutispora* cf. *ampla* Hoffmeister, Staplin & Malloy, 1955
f *Convolutispora cerebra* Butterworth & Williams, 1958
g *Convolutispora circumvallata* Clayton, 1971
h *Convolutispora* aff. *disparalis* Allen, 1965
i *Convolutispora subtilis* Owens, 1971
j *Convolutispora paraverrucata* McGregor, 1964
k *Convolutispora varicosa* Butterworth & Williams, 1958
l *Convolutispora* cf. *vermiformis* Hughes & Playford, 1961
m *Convolutispora* sp.
n *Corbulispora cancellata* (Waltz) Bharadwaj & Venkatachala, 1961
o *Cordylosporites* sp.
p *Cristatisporites* aff. *echinatus* Playford, 1963
q *Crassispora* sp.
r *Cristicavatispora dispersa* González, Playford & Moreno, 2005
s *Cyclogranisporites* sp.
t *Cyrtospora cristifer* (Luber) Van der Zwan, 1979
u *Densosporites spinifer* Hoffmeister, Staplin & Malloy, 1955
v *Dictyotriletes submarginatus* (Playford) Van der Zwan, 1980
w *Dictyotriletes* sp.

Plate 3.4

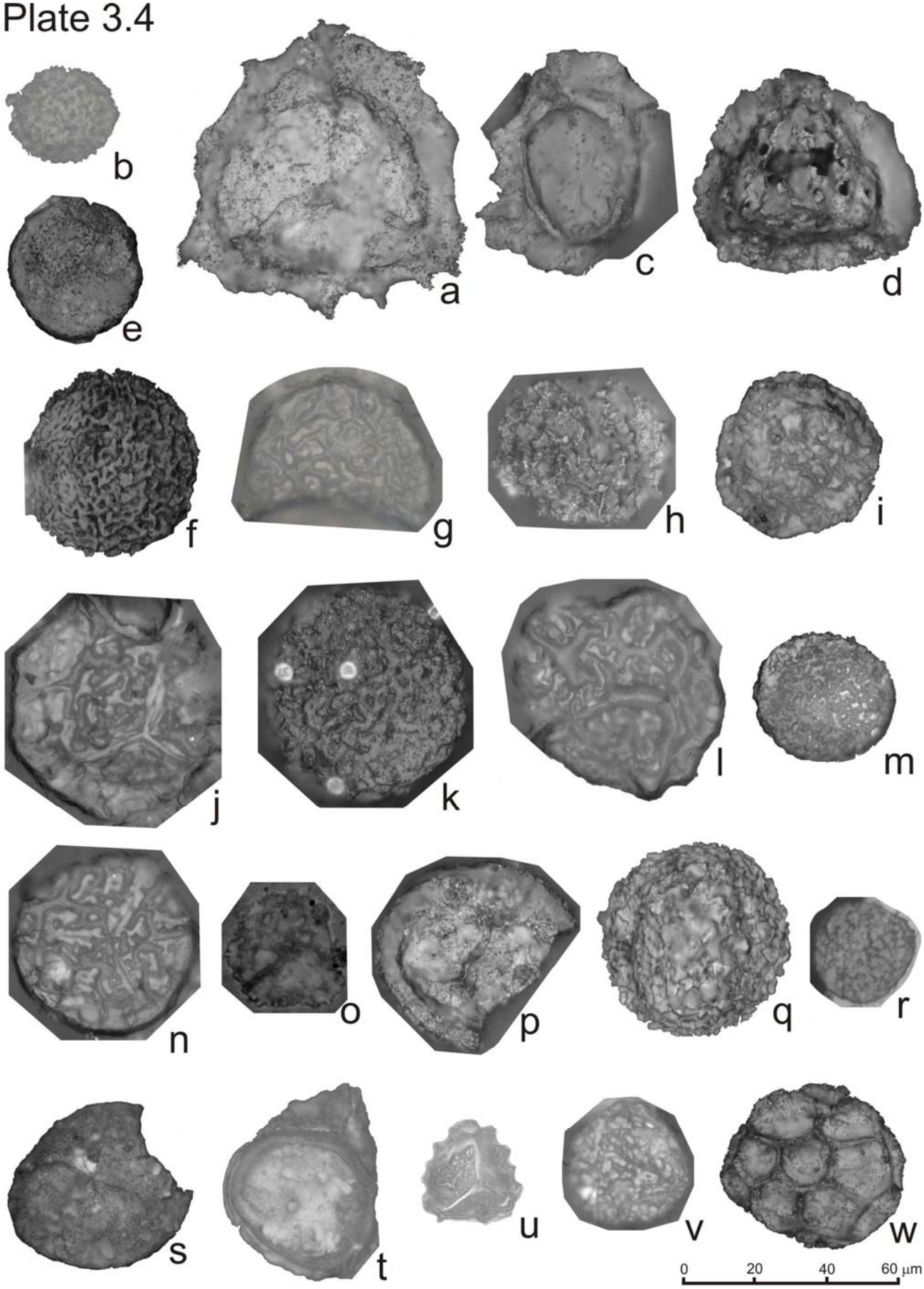

Plate 3.5 – Famenian-Tournaisian miospore assemblage. a to c and e to ad are reflected light photomicrographs; d is a transmitted light photomicrograph.

a *Emphanisporites rotatus* (McGregor) McGregor, 1973
b *Geminospora* sp.
c *Grandispora* aff. *cornuta* Higgs, 1975
d *Grandispora* cf. *echinata* Hacquebard, 1957
e *Grandispora* cf. *famenensis* (Naumova) Streel, 1974 in Becker et al., 1974 var. minuta Nekriata, 1974
f *Grandispora gracilis* (Kedo) Streel in Becker et al., 1974
g *Grandispora* sp.
h *Hymenozonotriletes* cf. *cristatus* Menendez, 1967
i *Hymenozonotriletes* (*Samarisporites*) cf. *inaequus* (McGregor) Owens, 1971
j *Hymenozonotriletes* cf. *incisus* Naumova, 1953
k *Hymenozonotriletes* sp.
l *Knoxisporites ruhlandii* Doubinger & Rauscher, 1966
m *Knoxisporites* sp
n *Leiotriletes* cf. *devonicus* Naumova, 1953
o *Leiotriletes* sp.
p *Lophotriletes atratus* Naumova, 1953
q, r *Lophotriletes* sp.1
s *Lophotriletes* sp.
t *Lophozonotriletes bellus* Kedo, 1963
u *Lophozonotriletes* cf. *bouckaertii* Loboziak & Streel, 1989
v *Lophozonotriletes* cf. *lebedianensis* Naumova, 1953
w *Lophozonotriletes tuberosus* Sullivan, 1964
x *Lophozonotriletes* sp.
y *Punctatisporites irrasus* Hacquebard, 1957
z *Punctatisporites lucidulus* Playford & Helby, 1968
aa *Punctatisporites minutus* Kosanke, 1950
ab *Punctatisporites* sp.
ac *Retusotriletes* cf. *dubius* (Eisenack) Richardson, 1965
ad *Retusotriletes* sp

Plate 3.5

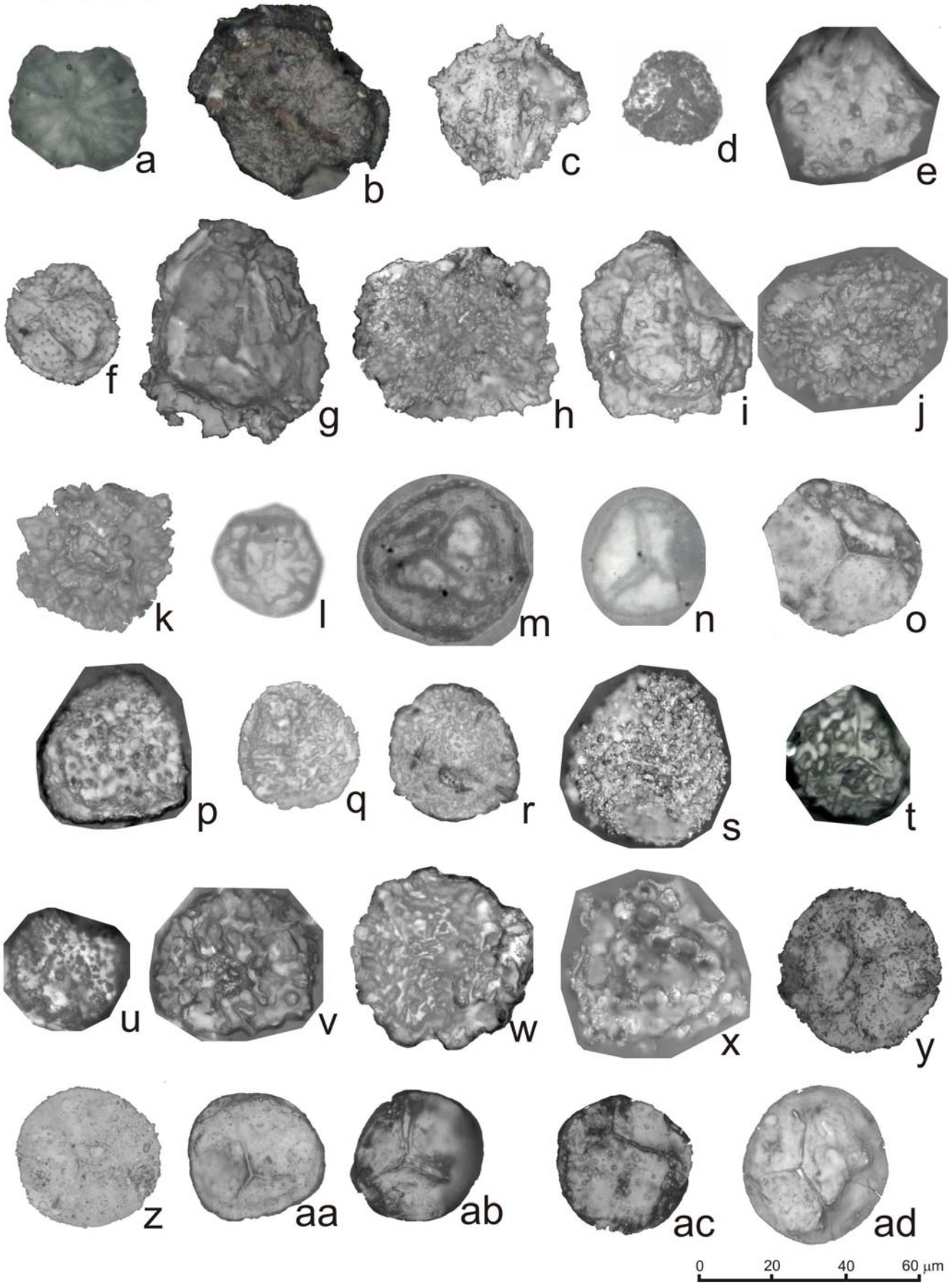

Plate 3.6 – Famenian-Tournaisian miospore assemblage. a to c and e to k are reflected light photomicrographs; d and l to ag are transmitted light photomicrographs.

a *Rugospora* cf. *flexuosa* (Jushko) Streel in Becker et al., 1974
b *Rugospora* sp.
c *Samarisporites* sp.
d aff. *Spelaeotriletes balteatus* (Playford) Higgs, 2006
e *Stenozonotriletes* sp.
f *Verrucosisporites nitidus* morphon (sensu Van der Zwan, 1980)
g *Verrucosisporites tumulentus* Clayton & Graham, 1974
h *Verrucosisporites* sp.
k to ag Reworked(?) chitinozoans

Plate 3.6

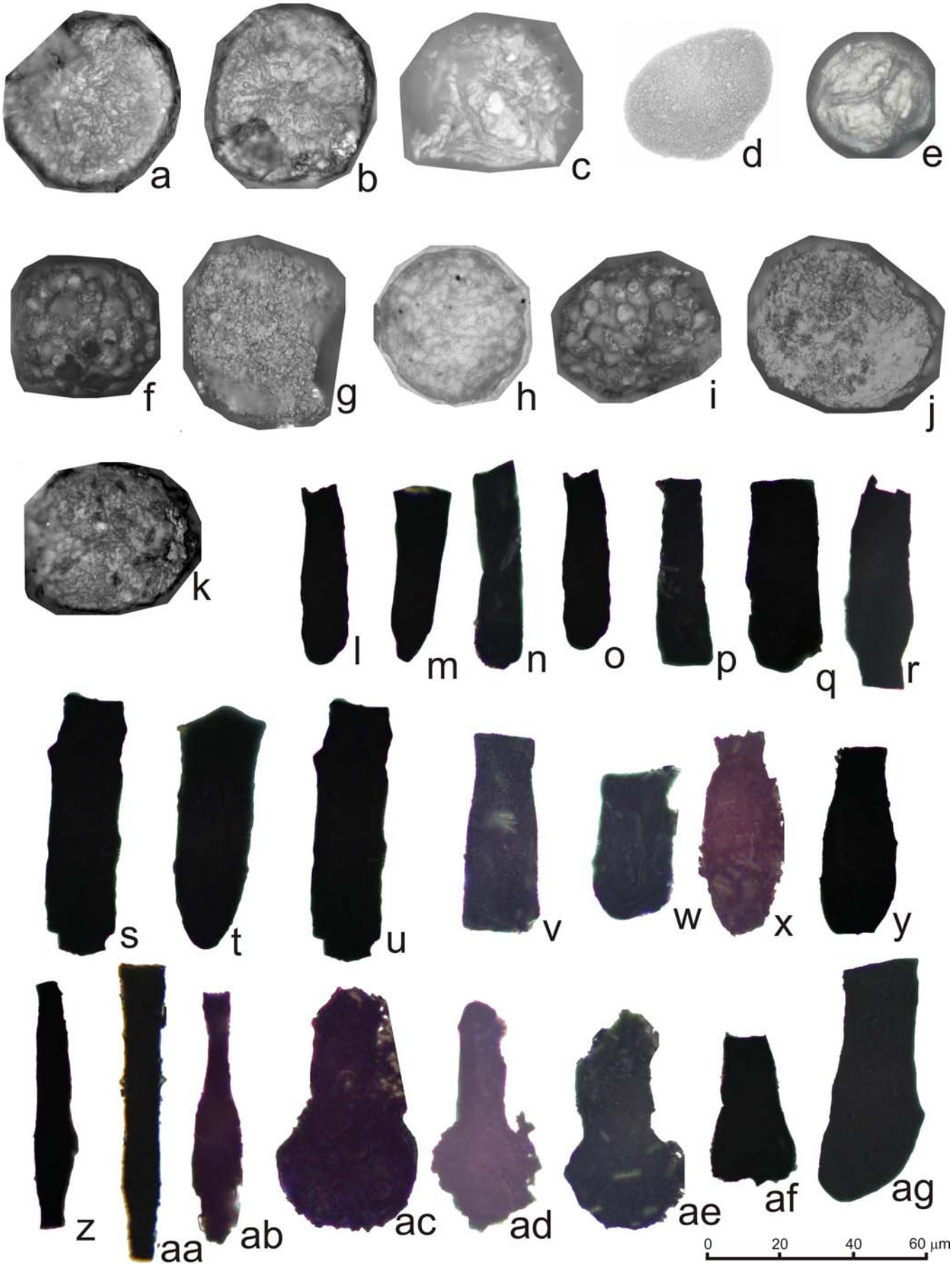

Plate 3.7 – Viséan miospore assemblage. a to b and d to ah are reflected light photomicrographs; c is a transmitted light photomicrograph.

a *Acanthotriletes* sp.
b *Acinosporites* sp.
c, c' *Apiculatisporis* cf. *hacquebardi* Playford, 1964
d aff. *Apiculiretusispora* sp.
e *Auroraspora* cf. *asperella* (*Kedo*) Van der Zwan, 1980
f *Auroraspora* sp.
g *Convolutispora cf. cerebra* Butterworth & Williams, 1958
h *Convolutispora* cf. *disparalis* Allen, 1965
i *Convolutispora* sp.
j *Crassispora* sp.
k *Densosporites anulatus* (Loose) Smith & Butterworth, 1967
l *Densosporites* sp.
m *Dictyotriletes* sp.
n *Geminospora* sp.
o *Grandispora* cf. *gracilis* (Kedo) Streel in Becker et al., 1974
p *Grandispora* sp.
q *Hymenozonotriletes* aff. *cristatus* Menendez, 1967
r *Hymenozonotriletes* (*Samarisporites*) *inaequus* (McGregor) Owens, 1971
s *Hymenozonotriletes* sp.
t *Knoxisporites* aff. *concentricus* (Byvsheva) Playford & McGregor, 1993
u *Knoxisporites* cf. *ruhlandii* Doubinger & Rauscher, 1966
v *Knoxisporites* sp.
w *Leiotriletes* aff. *balapucensis* diPasquo, 2007
x *Lophozonotriletes* sp.
y *Lycospora* sp.
z *Punctatisporites* sp.
aa *Retusotriletes incohatus* Sullivan, 1964
ab *Retusotriletes* sp.
ac *Schulzospora* sp.
ad *Stenozonotriletes lycosporoides* (Butterworth & Williams) Smith & Butterworth, 1967
ae *Triquitrites* sp.
af aff. *Tumulispora rarituberculata* (Luber) Potonié, 1966
ag *Verrucosisporites baccatus* Staplin, 1960
ah *Verrucosisporites* sp.

Plate 3.7

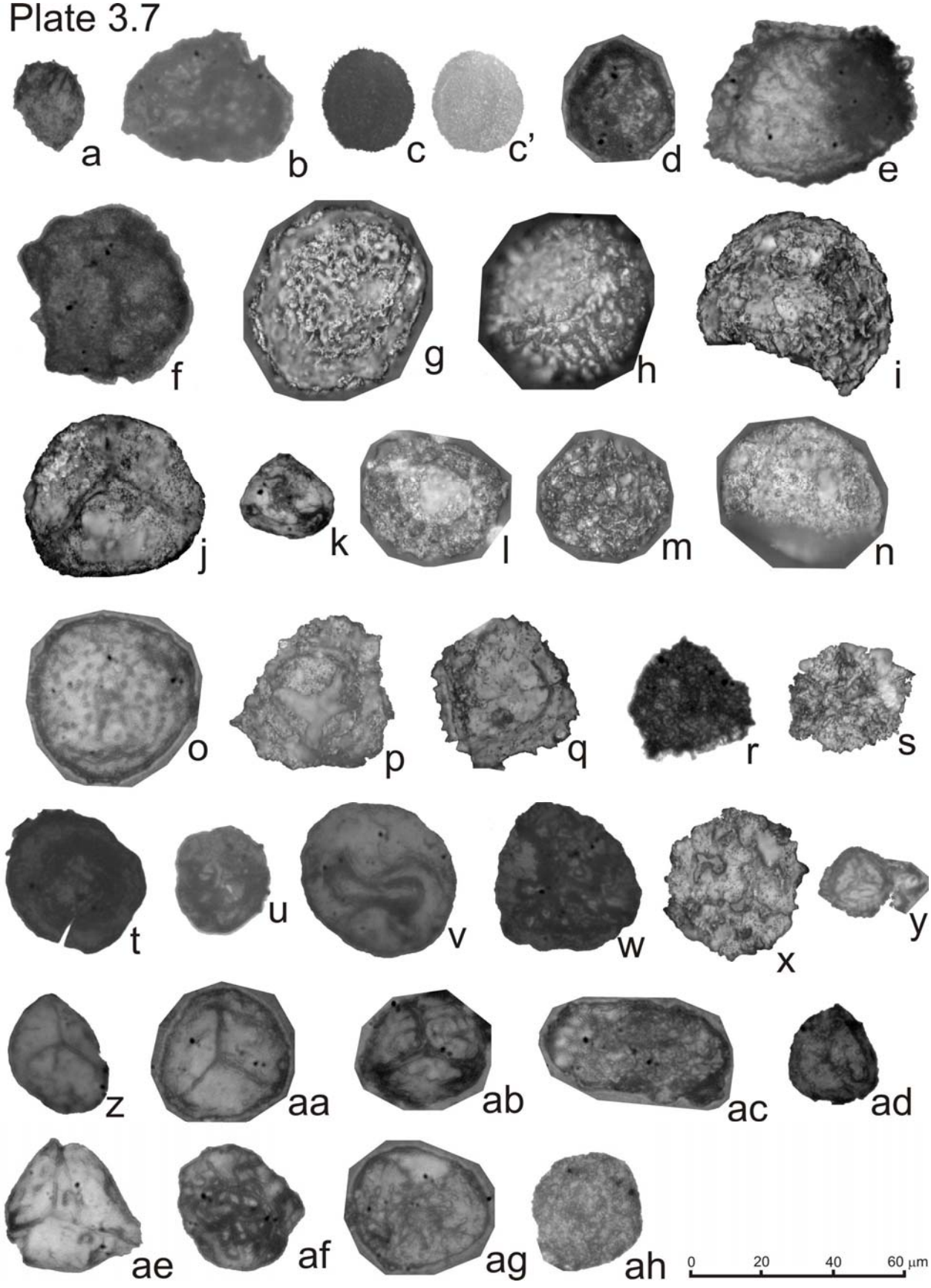
a
b
c
c'
d
e
f
g
h
i
j
k
l
m
n
o
p
q
r
s
t
u
v
w
x
y
z
aa
ab
ac
ad
ae
af
ag
ah
0
20
40
60 µm

Plate 3.8 – Serpukovian miospore assemblage. a to e, g to n and q to ac are reflected light photomicrographs; f, o and p are SEM photomicrographs.

a *Acanthotriletes* cf. *aculeolatus* (Kosanke) Potonié & Kremp, 1955
b *Acanthotriletes* aff. *echinatus* Hoffmeister, Staplin & Malloy, 1955
c *Acanthotriletes* sp.
d cf. *Ancyrospora*? *andevalensis* González, Playford & Moreno, 2005
e *Ancyrospora* sp
f *Apiculatisporis* cf. *porosus* Williams in Neves et al., 1973
g *Apiculatisporis* cf. *variocorneus* Sullivan, 1964
h *Apicultisporis* sp.
i *Apiculatasporites wapsipiniconensis* Peppers, 1969
j *Camarozonotriletes* sp
k *Camptozonotriletes* cf. *verrucosus* Butterworth & Williams, 1958
l *Chelinospora* sp.
m *Convolutispora* cf. *ampla* Hoffmeister, Staplin & Malloy, 1955
n *Convolutispora cerebra* Butterworth & Williams, 1958
o *Convolutispora circumvallata* Clayton, 1971
p *Convolutispora disparalis* Allen, 1965
q *Convolutispora jugosa* Smith & Butterworth, 1967
r *Convolutispora subtilis* Owens, 1971
s *Convolutispora* sp.
t *Crassispora* aff. *kosankei* (Potonié & Kremp) Smith & Butterworth, 1967
u *Cristatisporites* sp.
v *Densosporites anulatus* (Loose) Smith & Butterworth, 1967
w *Densosporites* sp.
x *Dictyotriletes* cf. *aequalis* Staplin, 1960
y *Dictyotriletes castaneaeformis* (Horst) Sullivan, 1964
z *Dictyotriletes* cf. *densoreticulatus* Potonié & Kremp, 1955
aa *Dictyotriletes* sp.
ab *Emphanisporites* sp.
ac aff. *Geminospora* sp

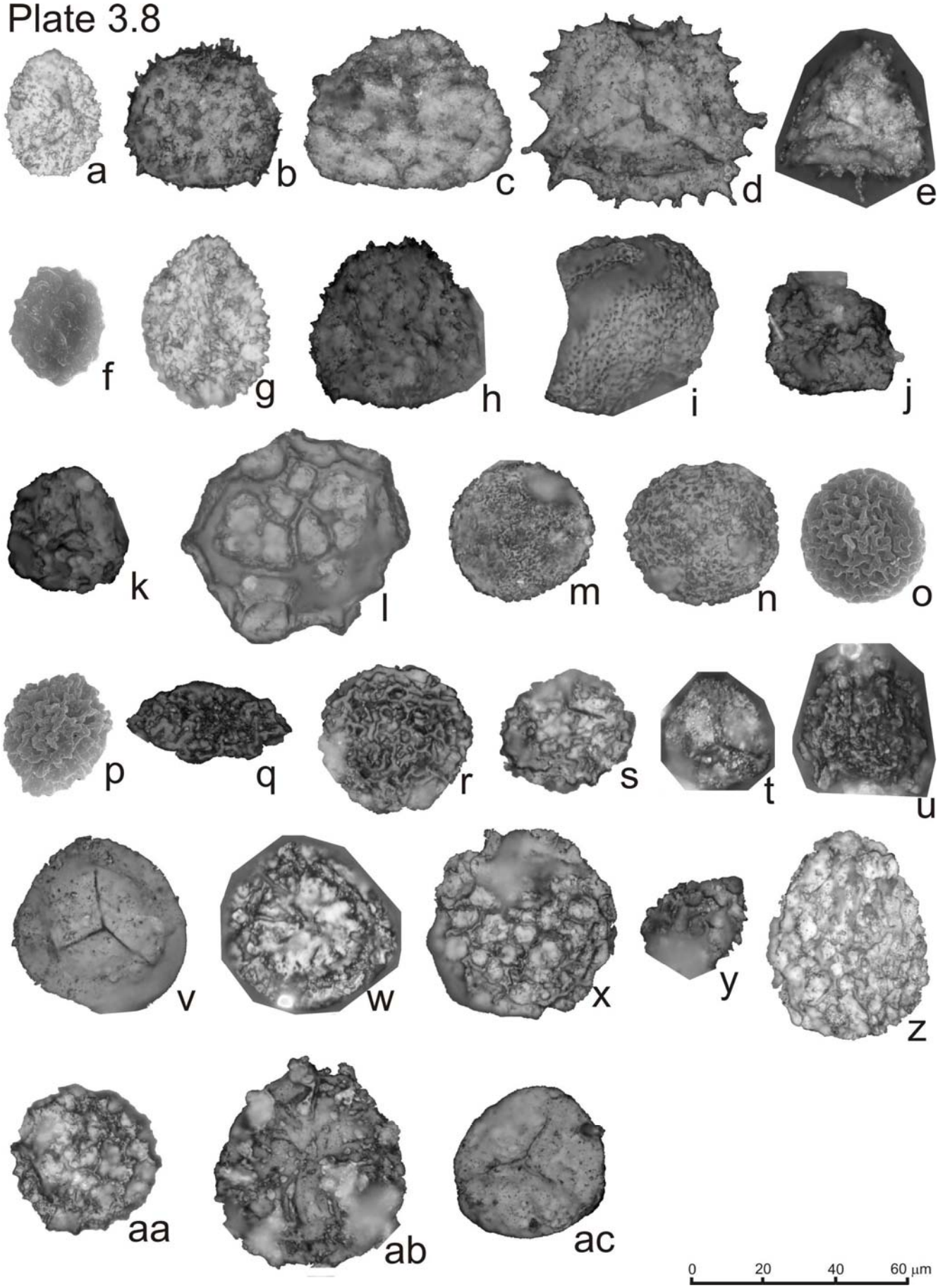
Plate 3.8
a
b
c
d
e
f
g
h
i
j
k
l
m
n
o
p
q
r
s
t
u
v
w
x
y
z
aa
ab
ac
0
20
40
60 µm

Plate 3.9 – Serpukovian miospore assemblage. a to b, d to j and n to af are reflected light photomicrographs; c and ac are SEM photomicrographs; k to m are transmitted light photomicrographs.

a *Grandispora* sp.
b *Grandispora* aff. *tamarae* Loboziak in Higgs et al., 2000
c *Grumosisporites inaequalis* (Butterworth & Williams) Smith & Butterworth, 1967
d *Grumosisporites* cf. *verrucosus* (Butterworth & Williams) Smith & Butterworth, 1967
e *Grumosisporites* sp
f *Hymenozonotriletes* sp.
g *Knoxisporites* sp.
h *Knoxisporites* cf. *triradiatus* Hoffmeister, Staplin & Malloy, 1955
i, j *Laevigatosporites* sp.
k *Leiotriletes inermis* (Waltz) Ischenko, 1952
l *Leiotriletes* cf. *microgranulatus* Playford, 1962
m *Leiotriletes ornatus* Ischenko, 1956
n *Leiotriletes* sp.
o *Lophozonotriletes* cf. *Convolutispora insulosa* Playford, 1978
p *Lophozonotriletes* sp.
q *Lycospora* cf. *subtriquetra* (Luber) Potonié & Kremp, 1956
r *Lycospora* sp.
s *Microreticulatisporites concavus* Butterworth & Williams, 1958
t *Proprisporites laevigatus* Neves, 1961
u *Punctatisporites* cf. *glaber* (Naumova) Playford, 1962
v *Punctatisporites irrasus* Hacquebard 1957
w *Punctatisporites* cf. *lucidulus* Playford & Helby, 1968
x *Punctatisporites* cf. *nitidus* Hoffmeister, Staplin & Malloy, 1955
y *Punctatisporites* cf. *reticulopunctatus* Hoffmeister, Staplin & Malloy, 1955
z *Punctatisporites* sp.
aa aff. *Radialetes* sp.
ab *Raistrickia* sp.
ac *Retusotriletes* sp.
ad *Rugospora flexuosa* (Jushko) Streel in Becker et al., 1974
ae *Rugospora polyptycha* Neves & Ioannides, 1974
af *Rugospora* sp.

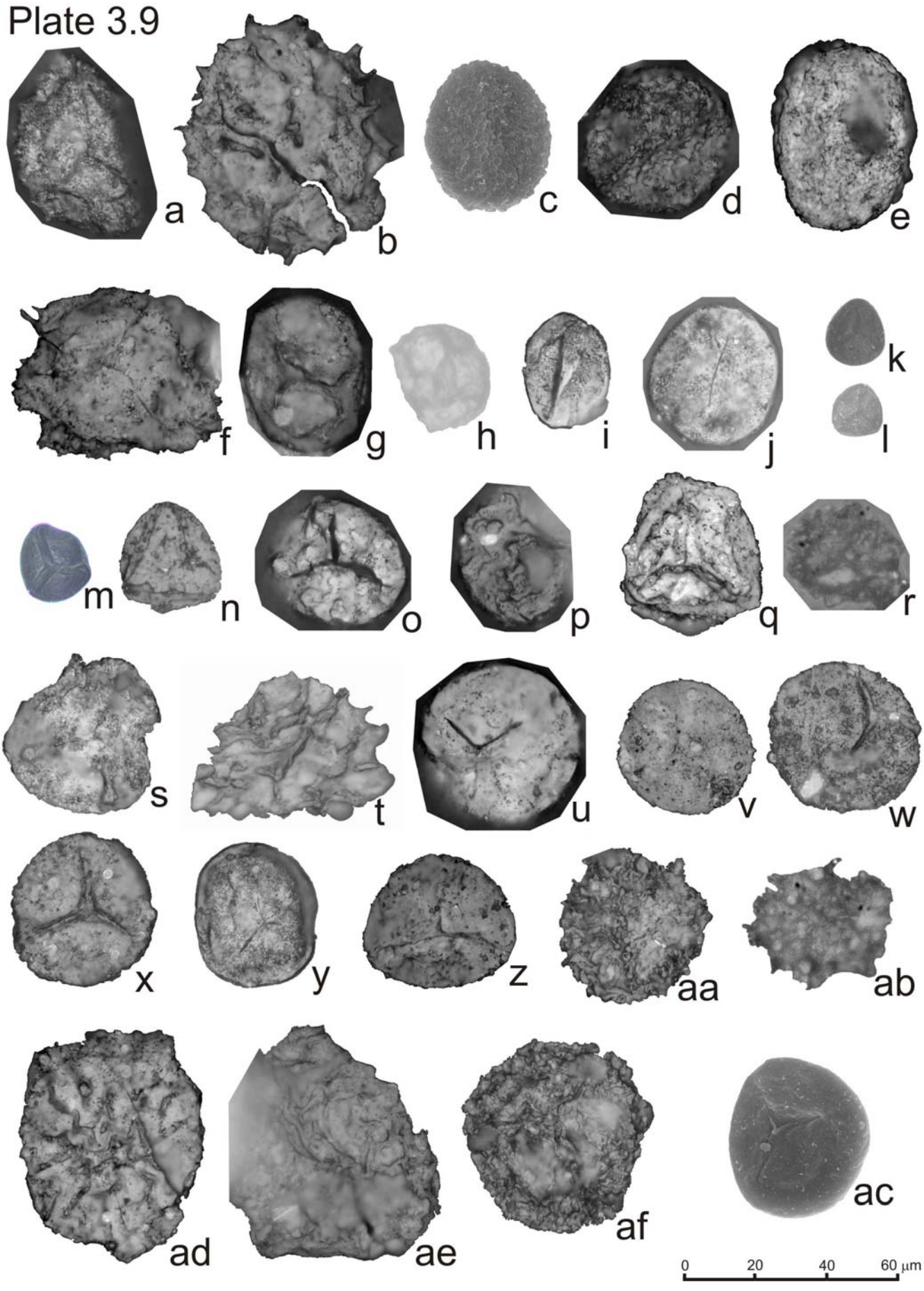
Plate 3.9
a
b
c
d
e
f
g
h
i
j
k
l
m
n
o
p
q
r
s
t
u
v
w
x
y
z
aa
ab
ad
ae
af
ac
0
20
40
60 µm

Plate 3.10 – Serpukovian miospore assemblage and examples of non-sieved slides used for Palynofacies analysis. a to k are reflected light photomicrographs. l to m are transmitted light photomicrographs. aom – amorphous organic matter; ac. – acritarch (s.l.); spo. – spore; phytoc. – Phytoclast; frag. – fragment.

a *Samarisporites* sp.
b cf. *Savitrisporites nux* (Butterworth & Williams) Smith & Butterworth, 1967
c *Spinozonotriletes* sp.
d *Stenozonotriletes* cf. *bracteolus* (Butterworth & Williams) Smith & Butterworth, 1967
e *Stenozonotriletes* sp.
f *Tricidarisporites fasciculatus* (Love) Sullivan & Marshall, 1966
g *Triquitrites* aff. *bucculentus* Guennel, 1958
h *Triquitrites* sp.
i, j *Verrucosisporites* cf. *scurrus* (Naumova) McGregor & Camfield, 1982
k *Verrucosisporites* sp.
l Example of a Frasnian non-sieved residue (RET2.1 sample)
m Example of a Famennian non-sieved residue (VAL9.1 sample)
n Example of a Viséan non-sieved residue (FRA3.1 sample)
o Example of a Serpukovian non-sieved residue (FONG5 sample)

Plate 3.10

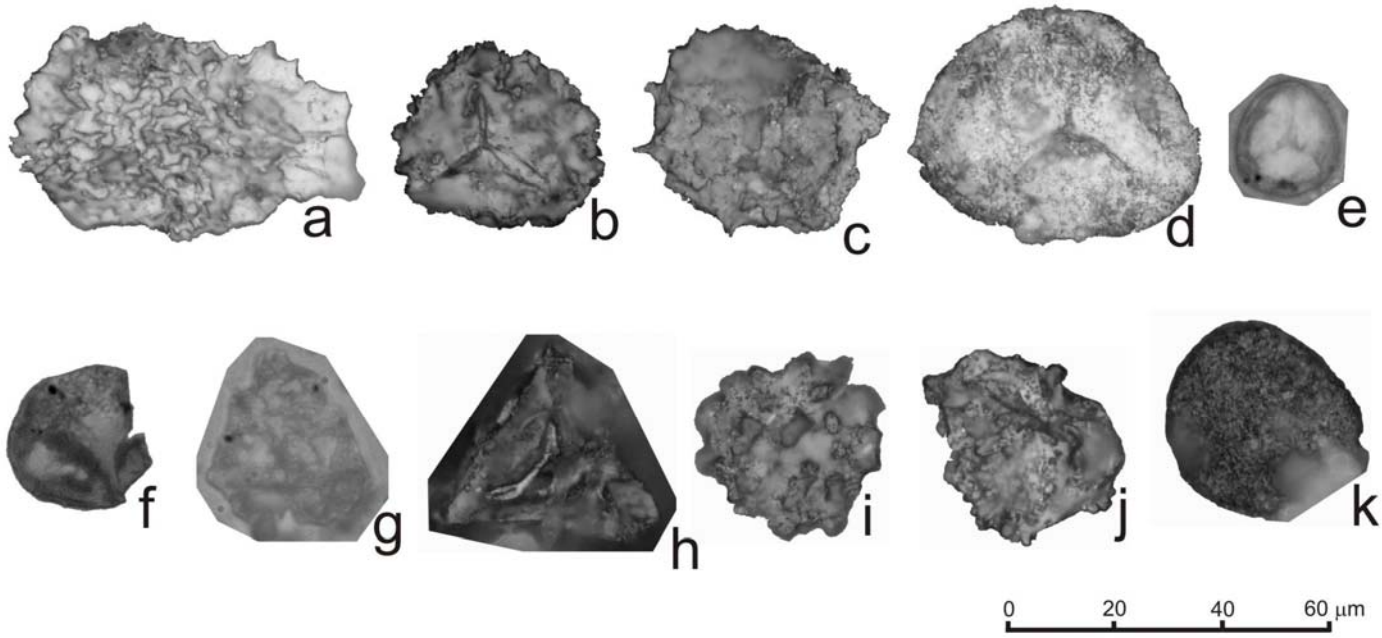
a
b
c
d
e
f
g
h
i
j
k
0
20
40
60 µm

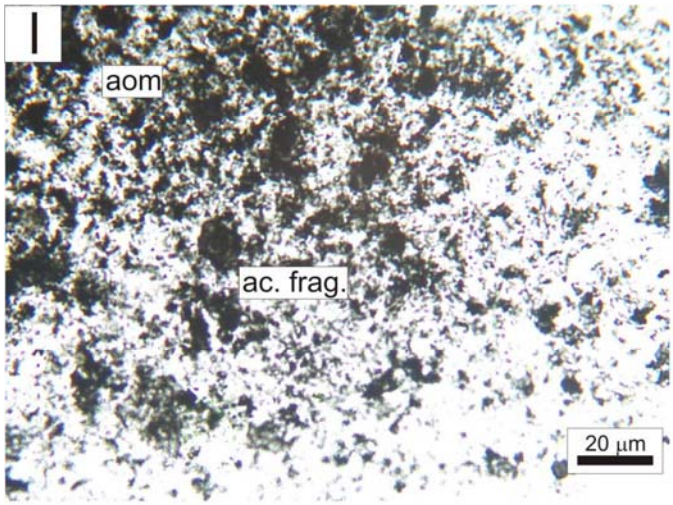
l
aom
ac. frag.
20 µm

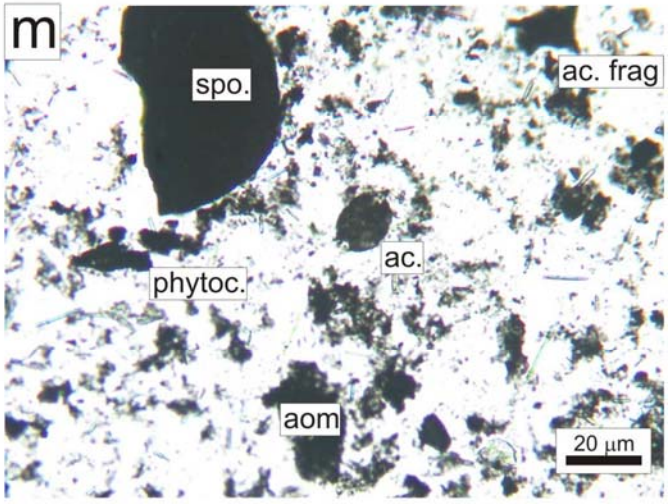
m
spo.
ac. frag
ac.
phytoc.
aom
20 µm

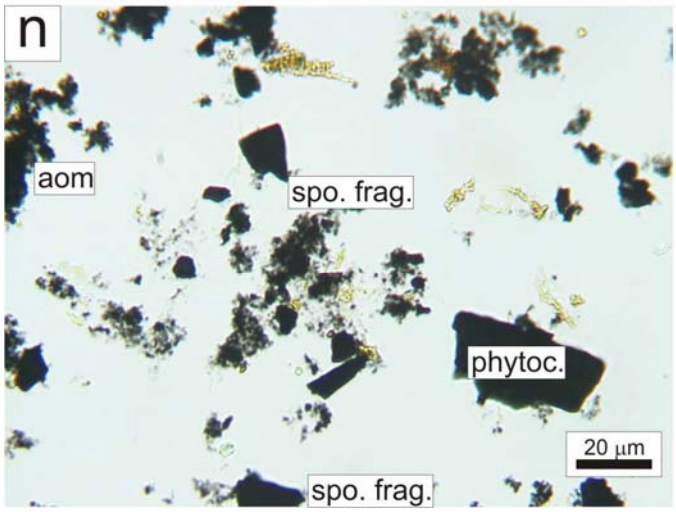
n
aom
spo. frag.
phytoc.
20 µm
spo. frag.

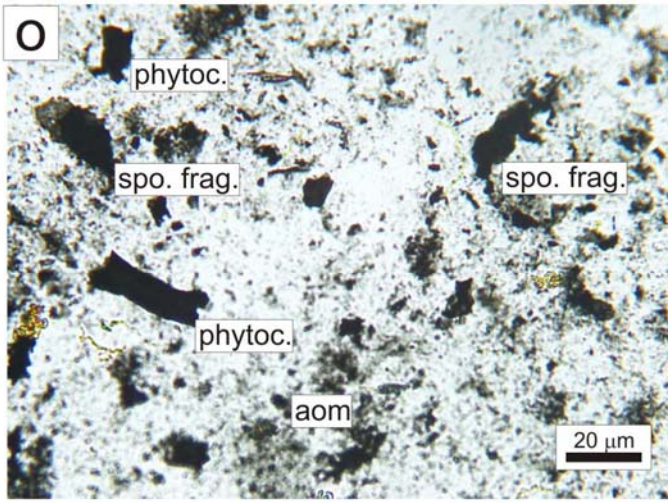
o
phytoc.
spo. frag.
spo. frag.
phytoc.
aom
20 µm

Plate 3.11 – Lower (Middle?) Frasnian organic-walled microplankton assemblage. All are transmitted light photomicrographs.

a *Ammonidium* cf. *microcladum* (Downie) Lister, 1970
b *Daillydium* sp.
c aff. *Goniosphaeridium polygonale* (Eisenack) Eisenack, 1969
d, e *Gorgonisphaeridium* sp
f *Leiofusa* sp.
g *Leiosphaeridia* sp.
h *Maranhites perplexus* Wicander & Playford, 1985
i *Maranhites* sp.
j *Micrhystridium* cf. *stellatum* Deflandre, 1945
k, l *Micrhystridium* sp.
m *Multiplicisphaeridium* cf. *fisheri* (Cramer) Lister, 1970
n *Navifusa* sp.
o *Unellium* sp.
p aff. *Umbellasphaeridium* sp.
q *Veryhachium* sp.
r *Winwaloeusia* sp.

Plate 3.11

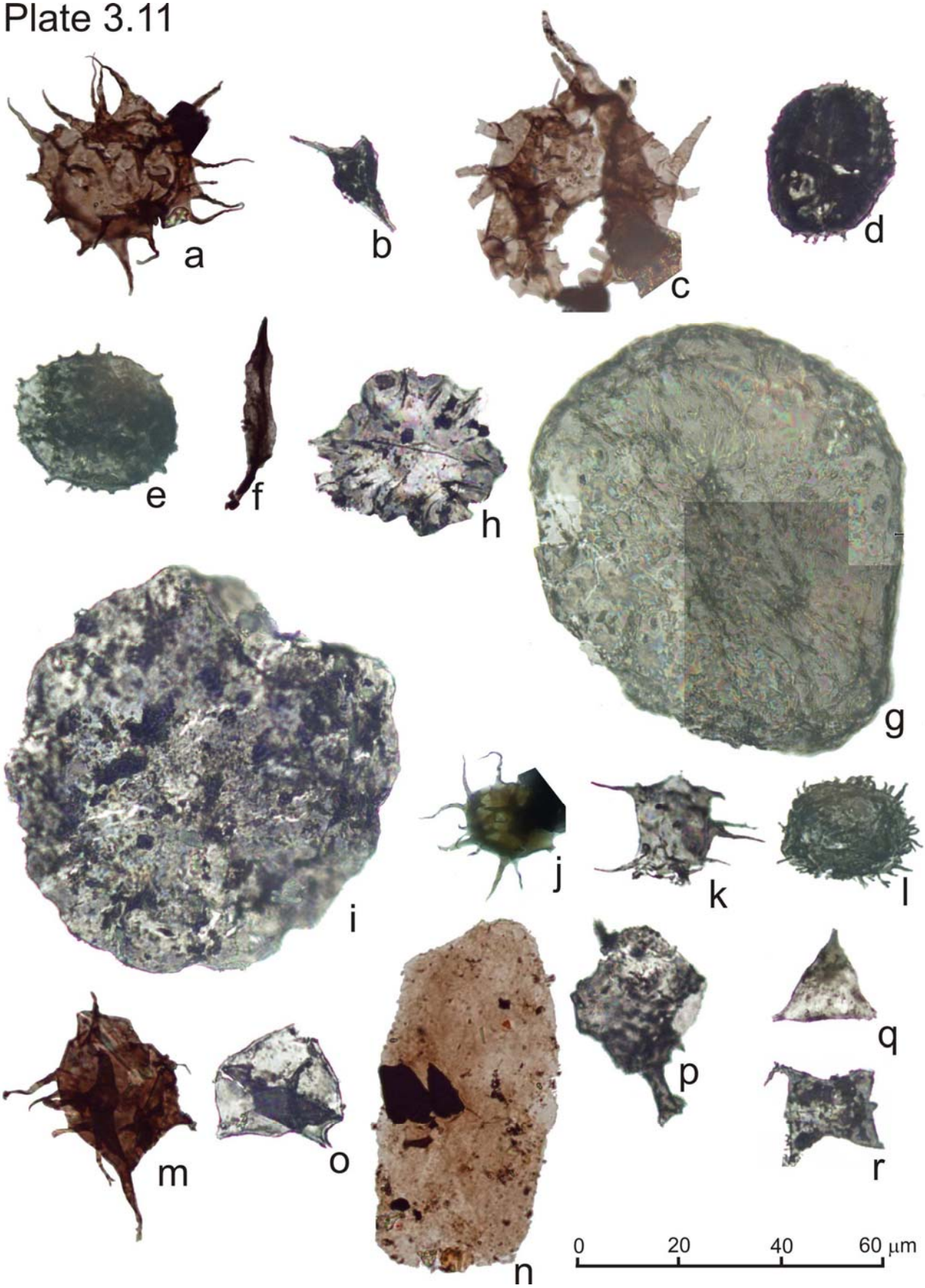

Plate 3.12 – Famennian and Lower Tournaisian organic-walled microplankton assemblage. All are transmitted light photomicrographs.

a aff. *Ammonidium alloiteaui* Deunff, 1955
b *Baltisphaeridium urticans* Stockmans & Willière, 1974
c *Baltisphaeridium* sp.
d *Buedingiisphaeridium* sp.
e aff. *Crassiangulina* sp.
f *Cymatiosphaera chelina* Wicander & Loeblich, 1977
g *Cymatiosphaera fritilla* Wicander & Loeblich, 1977
h *Cymatiosphaera melikera* Wicander & Loeblich, 1977
i *Cymatiosphaera nebulosa* Deunff, 1956
j *Cymatiosphaera perimenbrana* Staplin, 1961
k *Cymatiosphaera* cf. *subtrita* Playford, 1981
l *Cymatiosphaera* sp.
m *Dactylofusa* cf. *maranhensis*
n, o *Daillydium pentaster* (Staplin) Playford in Playford & Dring, 1981
p *Deltotosoma* sp.
q *Dictyotidium* cf. *craticulum* (Wicander & Loeblich) Wicander & Playford, 1985
r *Dictyotidium* cf. *confragum* Playford in Playford and Dring, 1981
s *Dictyotidium* cf. *defectivum* Colbath, 1990
t *Dictyotidium* aff. *granulatum* Playford in Playford and Dring, 1981
u *Dictyotidium litum* Colbath, 1990
v *Dictyotidium* cf. *polygonium* Staplin, 1961
w *Dictyotidium senticogremium* Hashemi & Fahimi, 2006
x *Dictyotidium* cf. *senticogremium* Hashemi & Fahimi, 2006
y *Dictyotidium* sp.

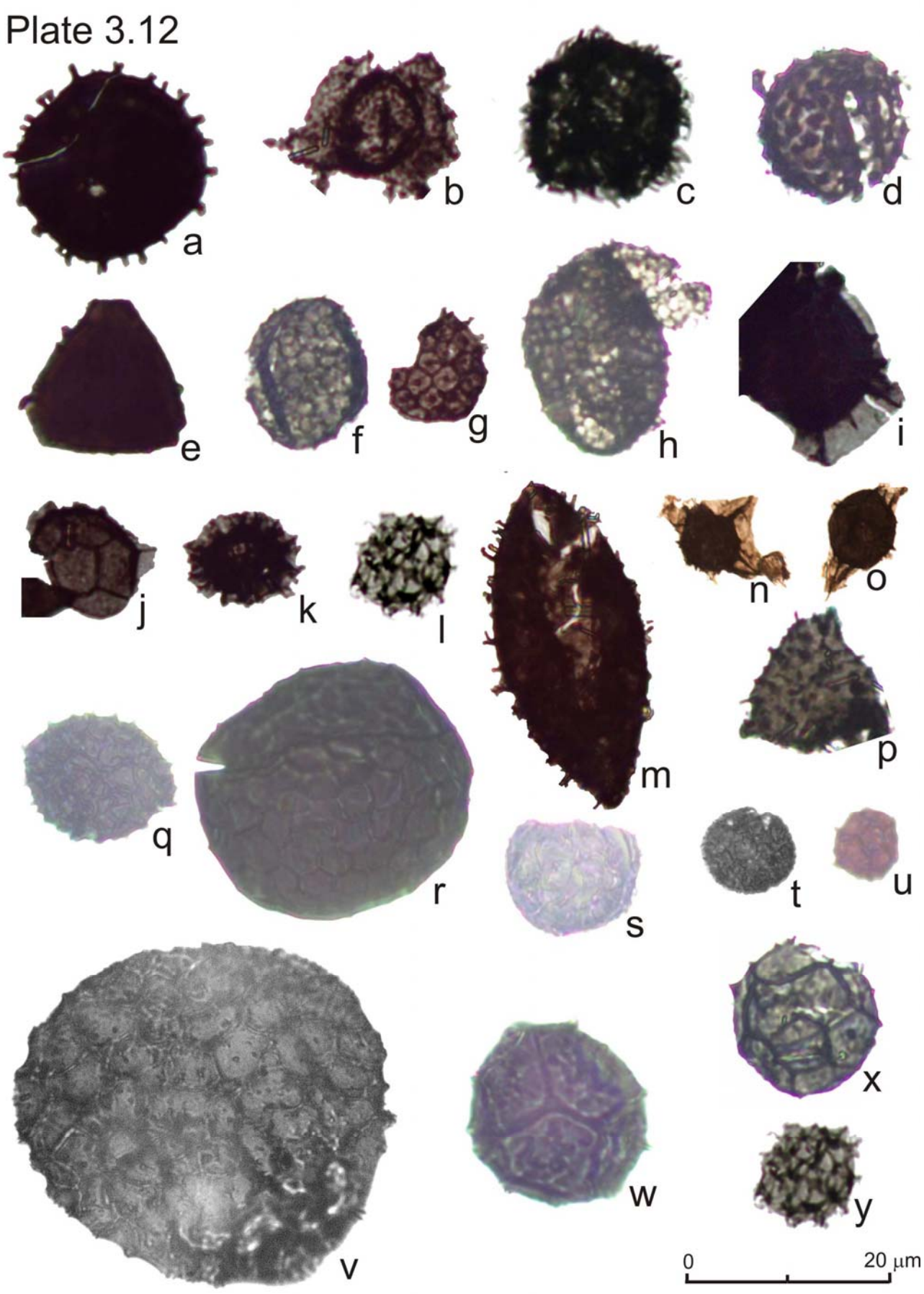
Plate 3.12
a
b
c
d
e
f
g
h
i
j
k
l
m
n
o
p
q
r
s
t
u
v
w
x
y
0
20 µm

Plate 3.13 – Famennian and Lower Tournaisian organic-walled microplankton assemblage. All are transmitted light photomicrographs.

a	*Estiastra* sp.
b	aff. *Florisphaeridium* (*Baltisphaeridium*) *guillermii* (Cramer) Fensome et al., 1990
c	*Geron* sp.
d, d’	*Gorgonisphaeridium anasillos* Colbath, 1990
e	*Gorgonisphaeridium caningensis* Colbath, 1990
f	*Gorgonisphaeridium evexispinosum* Wicander, 1974
g	*Gorgonisphaeridium ohioense* (Winslow) Wicander, 1974
h, h’	*Gorgonisphaeridium plerispinosum* Wicander, 1974
i	*Gorgonisphaeridium* (*Baltisphaeridium*) *rakoae* (Stockmans & Willière) Sarjeant & Vavrdová, 1997
j	*Histopalla* sp.
k	*Leiofusa* sp.
l, m, n	*Leiosphaeredia* spp.

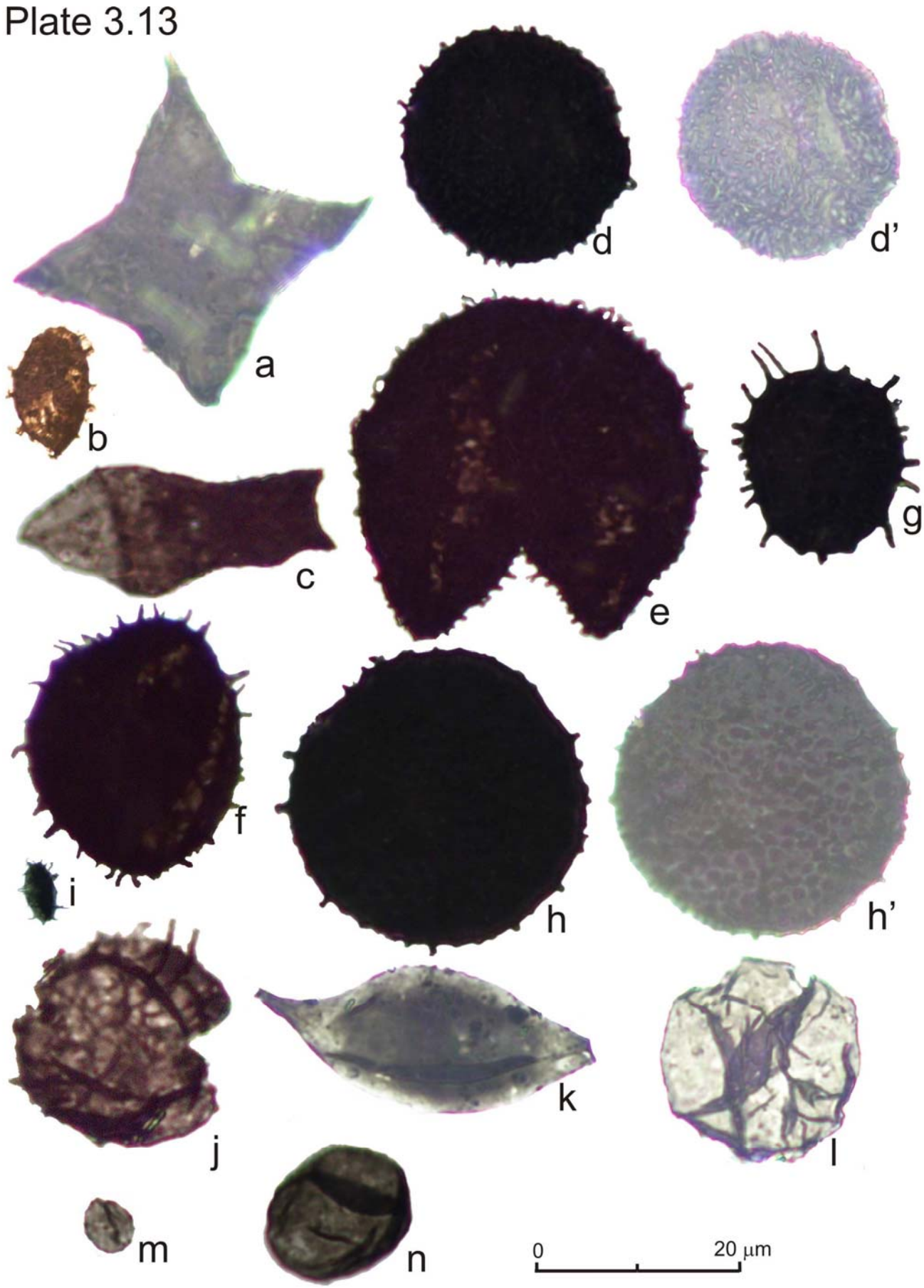
Plate 3.13
a
b
c
d
d'
e
g
f
i
h
h'
j
k
l
m
n
0
20 µm

Plate 3.14 – Famennian and Lower Tournaisian organic-walled microplankton assemblage. All are transmitted light photomicrographs.

a *Lophosphaeridium coniferum* Colbath, 1990
b cf. *Lophosphaeridium deminutum* Playford in Playford & Dring, 1981
c cf. *Lophosphaeridium incultum* Colbath, 1990
d cf. *Lophosphaeridium papilatum* (Staplin) Martin, 1969
e *Lophosphaeridium pelicanense* Playford, 1981
f *Lophosphaeridium* sp.
g *Micrhystridium* aff. *castanoideum* Stockmans & Willière, 1969
h *Micrhystridium deconinckii* Stockmans & Willière, 1969
i *Micrhystridium mametii* Stockmans & Willière, 1974
j *Micrhystridium nannacanthum* Deflandre, 1945
k *Micrhystridium* aff. *stellatum* Deflandre, 1945
l *Micrhystridium vulgare* Stockmans & Willière, 1962
m, n *Micrhystridium* spp.
o *Multiplicisphaeridium* sp.
p *Navifusa* sp.
q *Pterospermella* cf. *helios* (Sarjeant) de Coninck, 1975
r aff. *Pterospermella hermosita* (Cramer) Fensome et al., 1990
s *Pterospermella* cf. *malaca* Loeblich & Wicander, 1976
t *Pterospermella tenellula* Playford, 1981
u *Pterospermella* aff. *timofeevii* Deunff in Eisenack et al., 1973
v *Pterospermella* sp.1
w *Pterospermella* sp.
x *Solisphaeridium* sp.
y *Stellinium micropolygonale* (Stockmans & Willière) Playford, 1977
z *Uncinisphaera* (*Villosacapsula*) *ceratioides* (Stockmans & Willière) Colbath, 1990

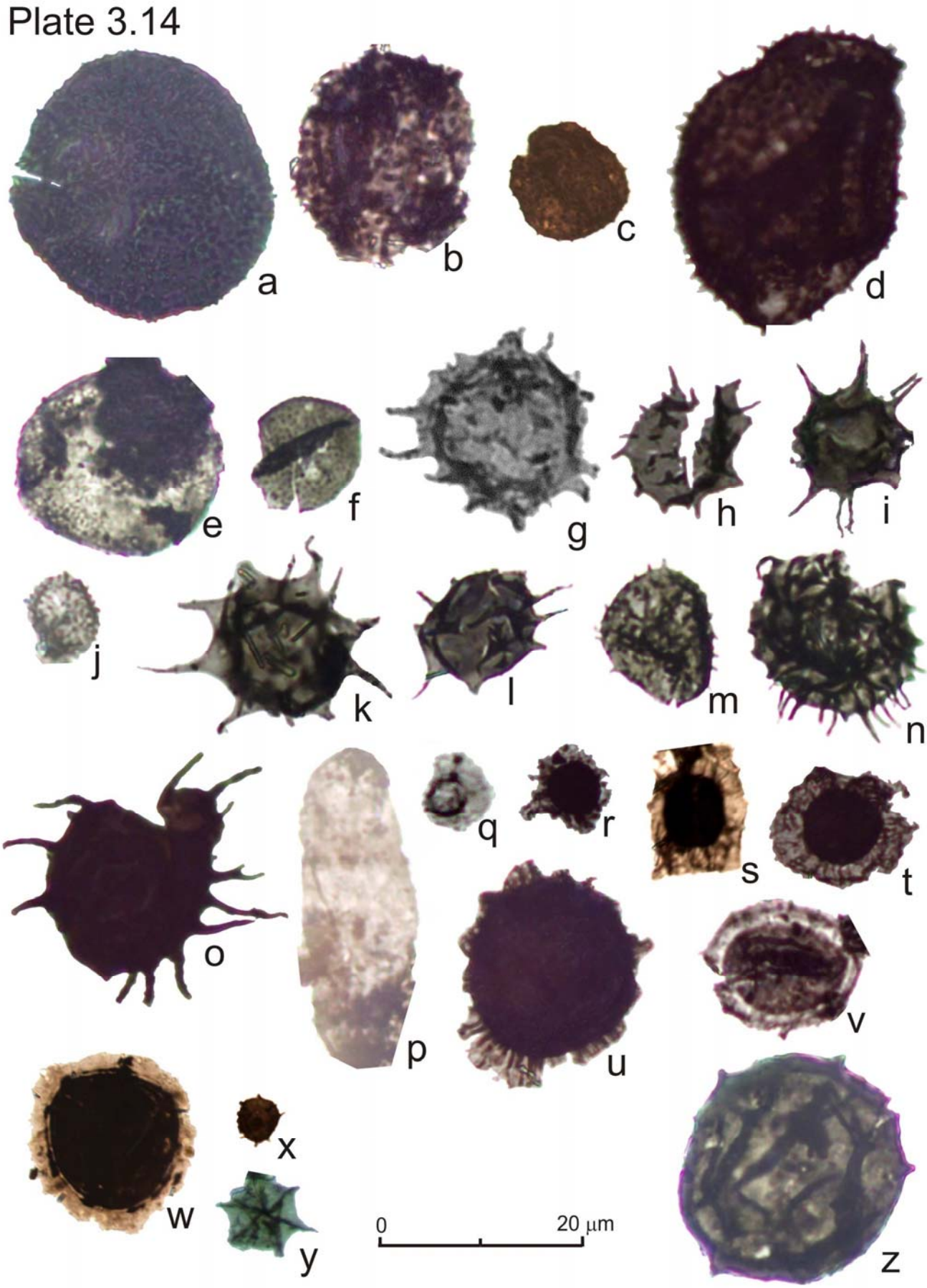
Plate 3.14
a
b
c
d
e
f
g
h
i
j
k
l
m
n
o
p
q
r
s
t
u
v
w
x
y
z
0
20 µm

Plate 3.15 – Famennian and Lower Tournaisian organic-walled microplankton assemblage. All are transmitted light photomicrographs.

a *Unellium cornutum* Wicander & Loeblich, 1977
b *Unellium* cf. *piriforme* Rauscher, 1969
c *Unellium* aff. *winslowiae* Rauscher, 1969
d *Veryhachium* (*Dorsennidium*) *europaeum* (Stockmans & Willière) Sarjeant & Stancliffe, 1994
e *Veryhachium* cf. *pannuceum* Wicander & Loeblich, 1977
f *Veryhachium reductum* Deunff, 1954
g *Veryhachium trispinosoides* (de Jekhowsky) Wicander, 1974
h *Veryhachium trispinosum* (Eisenack) Deunff, 1954
i *Winwaloeusia* cf. *ranulaeforma* Martin, 1984

Plate 3.15

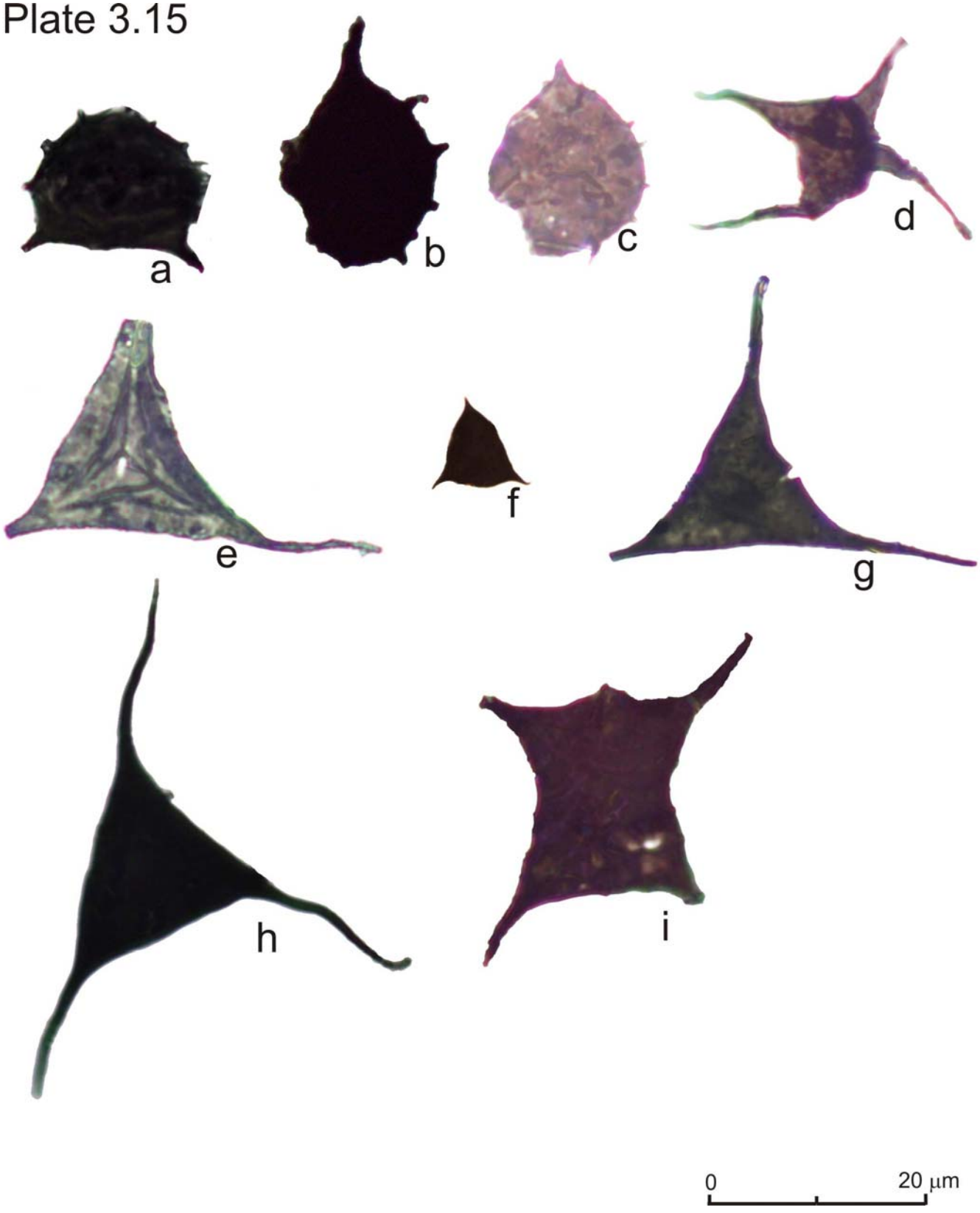

Plate 3.16 – Selected images of the AVU at the outcrop and hand sample scales

A Unconformity of the Late Triassic sediments over the AVU. Note the intense ferruginization of the AVU. IP3 road, near Coimbra

B Outcrop with successive (near vertical) turbidite beds. Way-up to left. ALH locality, near Águeda

C Detail of one of the beds from B showing one fining-upward cycle. Polished surface.

D Detail of locality BOS2, showing several fining-upward cycles with different thicknesses (incomplete Bouma sequences).

E Syn-sedimentary deformation structure. Laminated grey shale facies. FRA locality.

F Example of the finely laminated grey shale facies. Note the hinge of a tight fold in the centre. SND locality, near Sernada-do-Vouga.

G Example of the finely laminated grey shale facies. Polished surface. Note the alternation of lighter, slightly coarser laminae and darker, finer laminae. SND locality, near Sernada-do-Vouga.

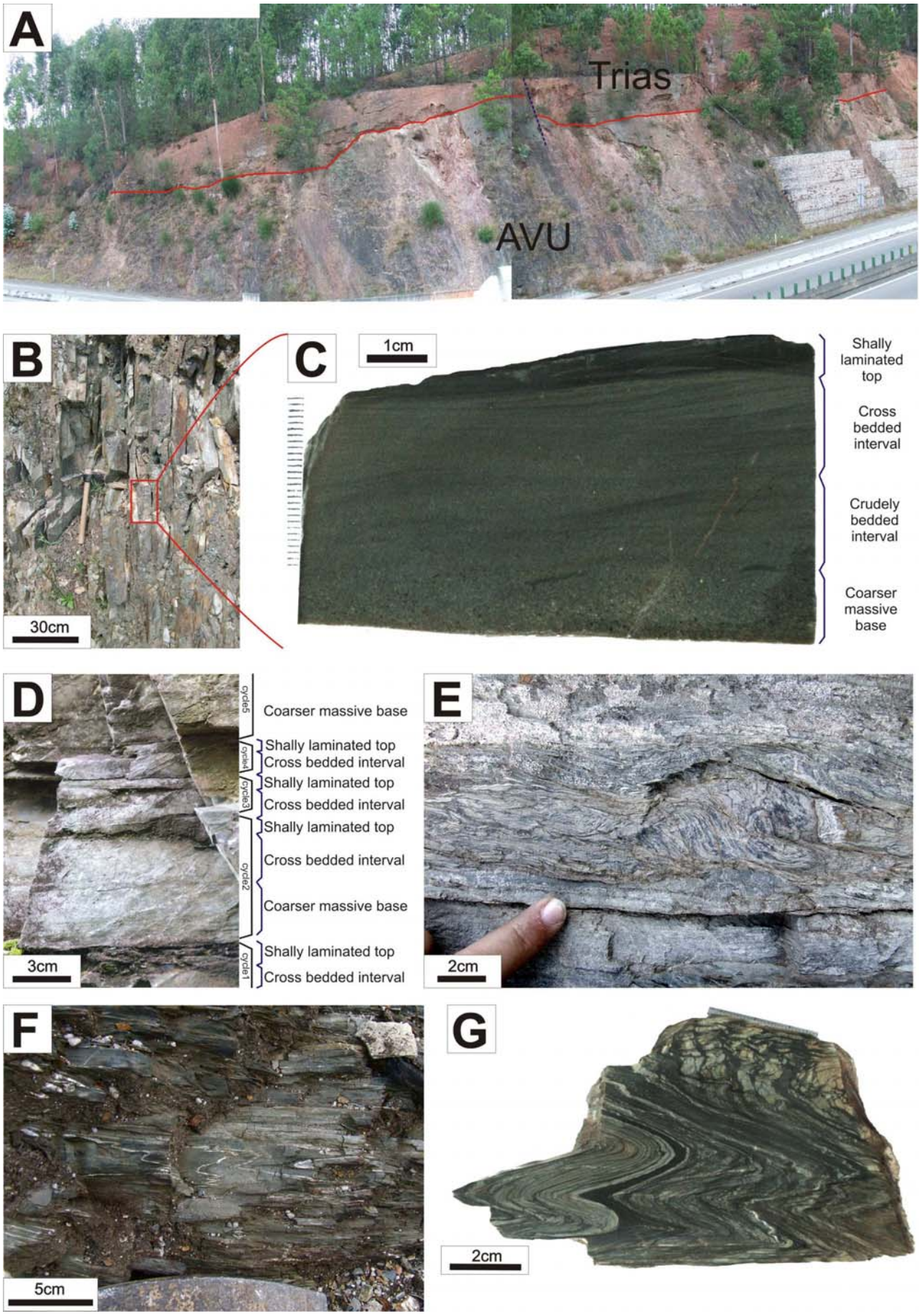
A
Trias
AVU
B
30cm
C
1cm
Shally laminated top
Cross bedded interval
Crudely bedded interval
Coarser massive base
D
cycle5
cycle4
cycle3
cycle2
cycle1
Coarser massive base
Shally laminated top
Cross bedded interval
Shally laminated top
Cross bedded interval
Shally laminated top
Cross bedded interval
Coarser massive base
Shally laminated top
Cross bedded interval
3cm
E
2cm
F
5cm
G
2cm

Plate 3.17 – Selected images of the AVU at the outcrop and thin section scales. Qz-Quartz; Qzite – quartzite; fp – feldspar.

A, A' Composite photomicrograph of thin sections from base to top of a thin turbidite bed (same sample as Pl. 3.17B and C).

B Fresh outcrop of the black shale facies. ASS locality (near the type locality of Albergaria-a-Velha). Hammer on centre for scale.

C Photomicrograph of a thin section from the base of a turbidite bed. ALH locality near Águeda. Crossed polars.

D Photomicrograph of a thin section from the base of a turbidite bed. BOS locality. Note the metamorphic growth of phillosilicates (multicolour tints) replacing the original matrix. Crossed polars.

E Photomicrograph of a thin section from silty shale bed. Note the common quartz clasts (white) and oxides (black) (and particulate organic matter?) in a phyllosilicate (sericitic?) background. Orientation of minerals sub-paralel to bedding. Paralel polars.

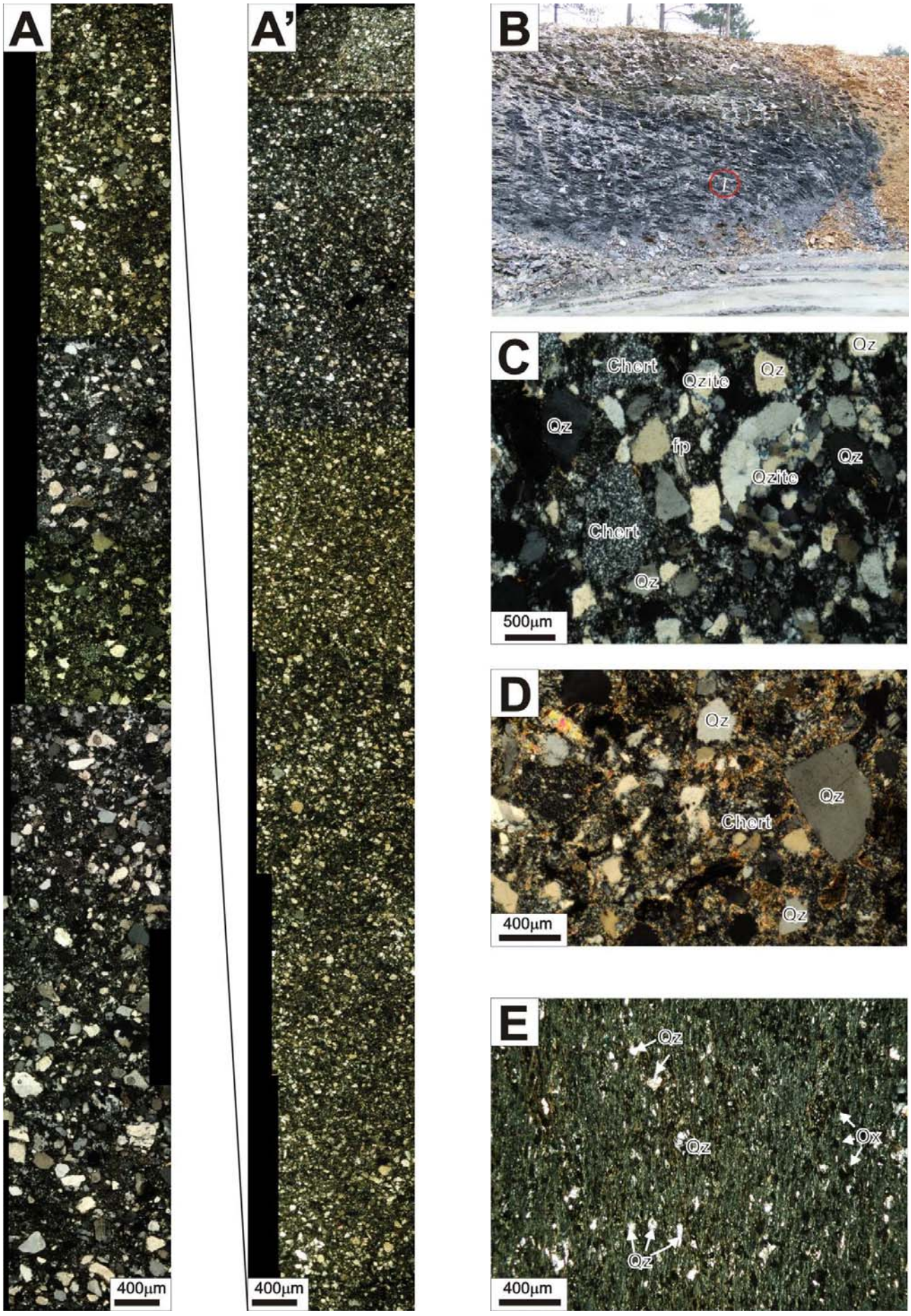
A
400µm
A'
400µm
B
C
Chert
Qzite
Qz
Qz
fp
Qz
Qzite
Chert
Qz
Qz
500µm
D
Qz
Qz
Chert
Qz
400µm
E
Qz
Qz
Qx
Qz
400µm

Chapter 4

Stratigraphy, Palynology and clay mineralogy of the Pennsylvanian continental Buçaco Basin (NW Portugal)

STRATIGRAPHY, PALYNOLOGY AND CLAY MINERALOGY OF THE PENNSYLVANIAN CONTINENTAL BUÇACO BASIN (NW PORTUGAL)

Abstract 130
4.1 Local geological setting and structural outline 130
4.1.1 Previous work 131
4.1.2 Age of the basin 133
4.2 Materials and methods 133
4.3 Results 134
4.3.1 Description and definition of facies associations and formational units 134
4.3.2 Palaeocurrents and provenance of sediments 152
4.3.3 Organic Petrology and thermal history 153
4.3.4 Clay mineralogy analysis 155
4.3.5 Palynology 156
4.4 Discussion and conclusions 156
4.5 Systematic Palynology 162
Acknowledgements 172
References 172
Plates 177

Abstract

The Buçaco basin is a Pennsylvanian continental basin located along an important NNW-SSE strike shear zone that separates the Ossa-Morena and Central Iberian Zones in central western and NW Portugal. The shear zone controlled the basin's sedimentation and probably its post-sedimentary evolution. Sedimentation is initially alluvial with characteristic red sandstones breccias and conglomerates. A gradual change to fluvial (and possibly lacustrine) type of sedimentation is observed. Palynological data indicate that the sedimentation took place during the Gzhelian (NBM Miospore Biozone of Clayton et al., 1977). "Autunian" (early Permian) assemblages were not found. The provenance of sediments and the thermal history is discussed as well as the geometrical and chronological relations of the basin with the surrounding units.
Key-words: Buçaco Basin, Gzhelian, spores/pollen, Continental sedimentation, Ossa-Morena Zone, Central Iberian Zone, SW Portugal.

4.1 Local geological setting and structural outline

The Pennsylvanian Buçaco basin crops out in several areas for nearly 30km along a N-S trend between the villages of Bolfiar (Northernmost outcrops) and Monte Redondo (Southernmost outcrops) Northeast of Coimbra. The width is highly variable due to the irregular contact (sedimentary and tectonic) with neighbouring formations. The maximum width is approximately 2km. To the S it pinches out and locally the W and E edges are limited by faults associated with the Porto-Tomar shear zone. Caenozoic sediments cover

the basin to the N, and the basin's rocks are only visible along relatively deep valleys that cut the Caenozoic cover. Its western edge is very frequently limited by faults that put it in direct contact with the Albergaria-a-Velha and Arada units of the Ossa-Morena Zone (Chaminé et al., 2003; Gama-Pereira et al., 2008) or the Upper Triassic (Adloff et al., 1974; Palain, 1976, Palain et al., 1977) sediments of the Lusitanian basin (Grés de Silves Fm.). The contact of the basin's rocks with the Grés de Silves Fm. is seldom exposed. It is invariably materialized by a fault or by a high angle angular unconformity (Luso area). The eastern edge is defined by faults in the southernmost sector, but for the most part the basin, the basal unit (Algeriz Fm. – see bellow) rests unconformably over the units of the Central Iberian Zone (CIZ): Cambrian - Pre-Cambrian metasediments of the "Complexo Xisto-Grauváquico" (CXG) and Ordovician sedimentary rocks (Ribeiro, 1853; Courbouliex, 1974; Domingos et al., 1983; Flores et al., 2010)

The structure of the basin has been generally presented by Domingos et al. (1983) and described in more detail by Gama-Pereira et al. (2008) and Flores et al. (2010). The basin forms a highly asymmetrical syncline with a long, normal eastern flank and an overturned to vertical short western flank (Domingos et al., 1983; Wagner and Sousa, 1983; Flores et al., 2010). Based on the current outcrop pattern, field structural evidence and the relation with the Porto-Tomar shear zone (PTSZ) Gama-Pereira et al. (2008) and Flores et al., (2010) interpret this as a pull-apart basin with a subsiding western block. In their model the pulses of the Porto-Tomar dextral shear zone control the major sedimentary phases of the basin as the Eastern block was uplifted and eroded.

4.1.1 Previous work

The first published work about this basin dates back to the 1800's when Carlos Ribeiro (Ribeiro, 1853) identified Carboniferous rocks in this area. He correctly identified and distinguished the several units that crop out in this area and described the geometrical relations between them. A lithological map and several schematic cross-sections were also presented. Bernardino Gomes and later Wenceslau de Lima (Gomes, 1865; Lima, 1888/1892; 1894) reported and described fossil plants from several sites and discussed the age of the assemblages. The basin has been studied by several authors during the last century, namely Teixeira (1941a, 1944, 1945, 1947, 1949) dealing mostly with palaeontological aspects, Corboulieux (1972, 1974) dealing with regional geology and stratigraphy; Pires (1972) briefly studied the sedimentology of a few small sections and Sousa & Wagner (1983); Wagner & Sousa (1983) and Wagner et al. (1983) dealt with the stratigraphy and palaeobotany of the basin. The latter work defined 3 formations of the basin according to sedimentological and palaeobotanical criteria (see Table 4.3). This definition is the one used in most of the subsequent studies. Two short papers on the nature and characteristics of the clasts of the conglomerates have been published by Neiva (1943) and Carvalho (1949). One paper (Gomes et al., 2005) was published on the palynology and palaeomagnetism of the basin and overlying Grés de Silves Fm. (Upper Triassic) but only poorly preserved pollen/spore assemblages were found. The sedimentology and the prevailing sedimentary environments of the basin were addressed in a conference paper by Dinis & Reis (2007) who concluded that lacustrine sedimentation was a common feature, both vertically and laterally, and not restricted to the coaly shale-siltstone dominated Vale da Mó Fm. (see Table 4.3). More recently two studies on the organic facies and petrology with some data on the basin's structure have been published (Gama-Pereira et al., 2008; Flores et al., 2010).

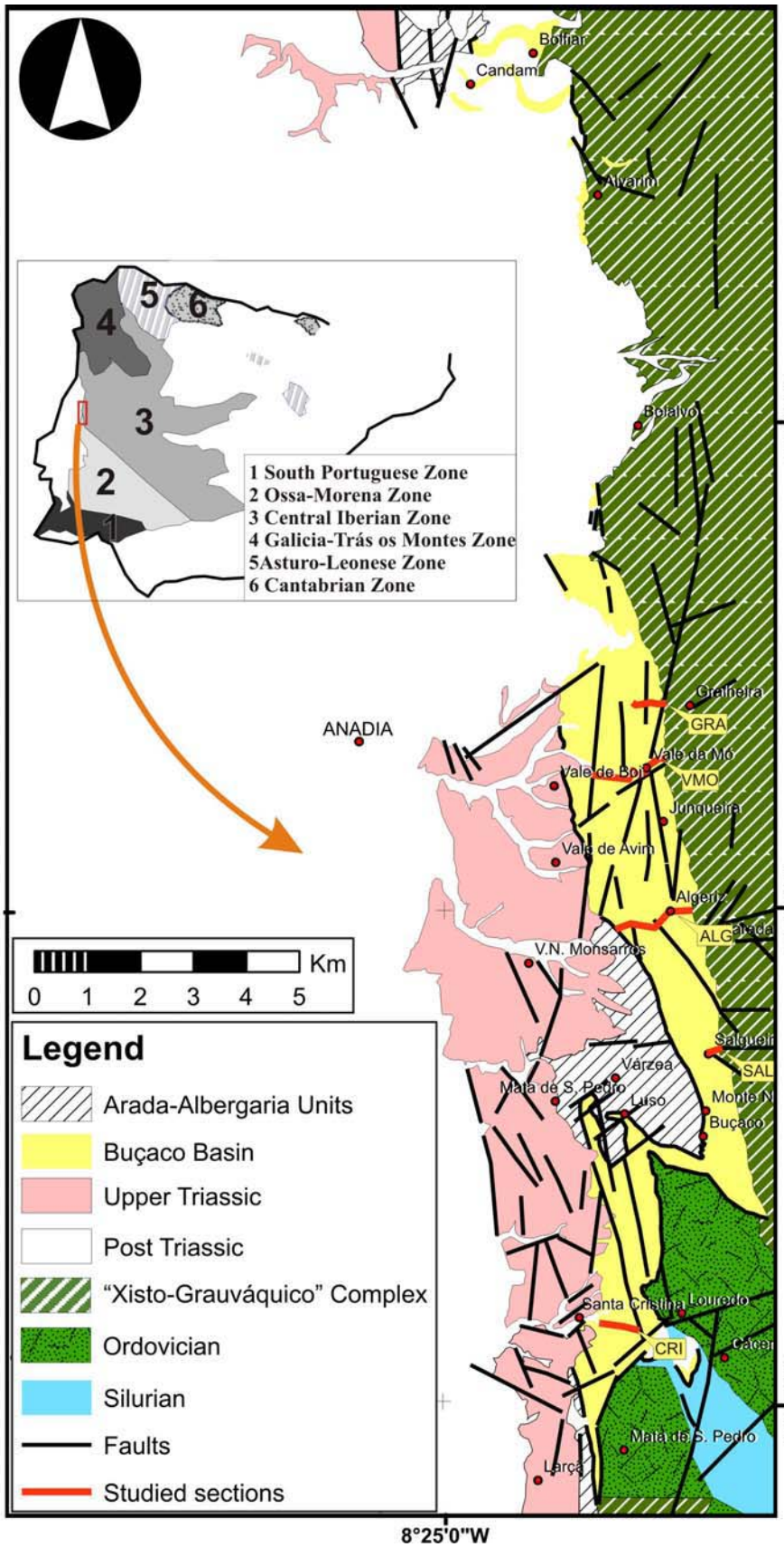

Fig. 4.1 Geological map of the Buçaco Basin and surrounding units. Adapted from Courbouliex (1974), Flores et al. (2010) and data from Pires (1972).

4.1.2 Age of the basin

The age of the macrofloral assemblages as been discussed since the first palaebotanical studies conducted by Gomes and Lima (Gomes, 1865; Lima, 1888/1892; 1894). Lima considered the assemblages to be comparable with the ones from Rotliegend in Germany and Autun in France (then lower Permian), although he mentioned in his correspondence with Zeiller (Teixeira, 1941b) that other taxa would correspond to the "houiller supérieur" (Pennsylvanian). Lima also considered that there were no significant differences between the assemblages found in different stratigraphic levels (Lima, 1888/1892) although these different levels were not identified. Florin (1940) considered the assemblage to be typically Permian due to the presence, among others, of *Lebachia laxifolia* Florin, 1939. Later Teixeira (1941a, 1944, 1945, 1947 and 1949) persisted the idea that the assemblages could be late Stephanian C or early Autunian. Courbouliex (1974) reported two new palaeobotanical localities which, according to P. Corsin's identification and interpretation, would be Stephanian C in age and concluded that sedimentation in the basin lasted from the Stephanian C to the Autunian. The most recent work by Wagner and Sousa (1983) and Wagner et al. (1983) is based on the collections available in several Portuguese museums, the published work and collection of new specimens. They concluded that all the assemblages (including the ones referenced by Courbouliex, 1974) can be placed in the late Stephanian C – early Autunian interval and that no taxon has a range restricted to either of these stages. The work by Gomes et al. (2005) recovered *Potonieisporites novicus* (Bharadwaj) Poort & Veld, 1997 from the Santa Cristina area (Monsarros Fm.) which again did not restrict the age to a particular stage.

4.2 Materials and methods

The sections available are relatively continuous E-W road cuts in the Vale da Mó – Vale de Boi road (Northern part – called here VMO section), Parada-Algeriz-Monsarros (central area – called here ALG section) and Santa Cristina (Southern part, called here CRI section) (Fig. 4.1). Additional sections are available in the Gralheira area, especially around the Gralheira reservoir (GRA section) and at Salgueiral (SAL section) but these cover only the basal formation. The ALG section is the most complete and the one used by most authors to describe the basin. Road cuts are typically ca. 3m tall except for some conglomeratic levels that can reach more than 10m. Strata dip from 20 to ca 60º to W which seriously limits the observation of lateral facies variations. Other sections are available in ~N-S roads but these have limited vertical extents. The current structure of the basin and the available sections result in the construction of lithological columns that go not only from basal to higher levels, but also from proximal to distal facies as the observer moves away from the source area (see following sections).

Several sections were described and sampled for palynology (and duplicates for XRD and organic petrology): ALG section, Parada-Algeriz-Monsarros road cuts, (all formations well exposed); the southern section in the road East of Santa Cristina – CRI section (parts of the Monsarros Fm. exposed); the Vale da Mó-Vale de Boi road section - VMO section (Algeriz Fm. badly exposed, but very fresh road cuts for the Monsarros Fm.); the Gralheira area – GRA section (Algeriz Fm. well exposed) and Salgueiral – SAL section (part of the Algeriz Fm and a small part of the Monsarros Fm.).

Miall's facies code system was applied (Miall, 1996, see table 4.1), although the poor exposure and weathering limited its application in numerous occasions. The reduced extent of the outcrops did not allow the proper identification and interpretation of groups of facies as architectural elements. The same problem was encountered when defining ranks of bounding surfaces.

Facies code	Facies	Sedimentary structures
Gmm	Matrix-supported massive gravel	Weak grading
Gmg	Matrix-supported gravel	Inverse to normal grading
Gci	Clast-supported gravel	Inverse grading
Gcm	Clast-supported massive gravel	Massive
Gh	Clast-supported crudely bedded gravel	Horizontal bedding, imbrication
Gt	Gravel stratified	Trough cross-beds
Gp	Gravel stratified	Planar cross-beds
St	Sand, fine to very coarse, may be pebbly	Solitary or grouped planar cross beds
Sp	Sand, fine to very coarse, may be pebbly	Solitary or grouped planar cross beds
Sr	Sand, fine to coarse	Ripple cross-lamination
Sh	Sand, fine to very coarse, may be pebbly	Horizontal lamination, parting or streaming lineation
Sl	Sand, fine to very coarse, may be pebbly	Low-angle (<15º) cross-beds
Ss	Sand, fine to very coarse, may be pebbly	Broad shallow scours
Sm	Sand, fine to coarse	Massive or faint lamination
Fl	Sand, silt, mud	Fine lamination, very small ripples
Fsm	Silt, mud	Massive
Fm	Mud, silt	Massive, desiccation cracks
C	Coal, carbonaceous mud	Plant, mud films

Table 4.1 – Miall's lithofacies code system. Adapted from Miall, 1996, excluding the facies codes not recorded in the Buçaco Basin.

4.3 Results

4.3.1 Description and definition of facies associations and formational units

As mentioned before the basin's sediments have been divided into 3 Formations by Wagner et al., (1983). Other subdivisions have been proposed, namely by Courbouliex, (1972, 1974). Table 4.3 is a tentative summarization of the proposed divisions and their correlation. It should be mentioned that all previous work was based almost exclusively on the ALG section. Other sections to the N and S show appreciable differences in vertical thicknesses and some lateral facies changes are significant.

The Algeriz Fm. (basal unit) was logged (from N to S) at the GRA, VMO, ALG (Algeriz-Parada road) and SAL sections. Exposure at the CRI section is very poor. The most complete section of the Algeriz Fm. is at the GRA section, where the sequence can be observed from its erosive contact with the CIZ units to the first grey measures of the overlying Formation. In this section, the total thickness is estimated to be ca. 145m with some degree of uncertainty due to observational gaps and small faults.

This Formation is characterized by a basal group of beds composed of red coloured, massive, matrix-supported, coarse grained (up to 20cm clasts) breccias beds up to 6m thick (usually 1 to 2m) – facies association SG1. Miall's facies codes associated with this facies association are Gmm, Gmg and more rarely Gcm and Gci (see Fig. 4.2, 4.3, 4.7 and 4.11

and Pl. 4.6A). Rarely Ss and Sm occur on top of breccia beds. Schists and other metapelites derived from the CXG and possibly from other schistose units of the CIZ are characteristic clasts of these breccias. These can constitute up to 90% of the clasts in some breccia beds, but in most cases they range from 10 to 30%. These beds usually exhibit chaotic arrangement of clasts, with weak normal to inverse grading. The basal breccia beds are restricted to the initial ca. 5m, except at the SAL section where they are about 15m thick. These are followed by a thick sequence of red coloured, clast-supported, massive to crudely bedded conglomerates – facies association SG2. Miall's facies codes associated with this facies association are Gcm and more rarely Gmg and Gci (see Fig. 4.2, 4.3, 4.7 and 4.11). To the top Gh occurs. Maximum clast size varies from bed to bed, but it is rarely above 20cm. Sandstones and finer grained lithologies are extremely rare and restricted to the top of some of the conglomeratic beds. At the ALG section there are a few organic matter-rich fine sandstone and mudstone layers within this subunit. The basal contact of each conglomeratic bed is erosional in most instances. The amount of schist and metapelite clasts gradually diminishes to the top of the subunit, but in some beds there are "abundance peaks". This gradual and irregular change probably reflects equivalent changes of catchment areas. Other clast lithologies are quartzites and quartz. These are common to abundant since the first breccia beds and increase their abundance as the schist diminishes. In the first few meters, all transported clasts have a red patina and most of them have an oxidized (reddish) core. To the top, the patina persists but the proportion of clasts with reddish core diminishes gradually. The roundness changes gradually but very irregularly from very angulose/angulose clasts at the base to sub-angulose/sub-rounded at the top of the conglomerate subunit. This reflects not only the decreasing proportion of schist clasts (which tend to be more angulose) but also the effective better roundness of quartz and quartzite clasts. Although no palaeocurrent data was obtained from this subunit the source area is easily determinable. All recognizable clast lithologies from the breccias and conglomerates can be positively identified as belonging to the CXG and Ordovician units of the CIZ. Furthermore, near the contact area all these older units have an extensive ferruginization which is also observed in most clasts of the breccia beds (Pl. 4.6A). This basal part of the Algeriz Fm. was briefly described by Wagner et al. (1983), but not differentiated as a subunit. Courboulieux (1972, 1974) refers to this subunit as the unit 1 - conglomerát de base (Table 4.3).

The thickness of this basal subunit seems to decrease from N to S. It is over 55m thick at the GRA section – the type section, less than 20m at the VMO section (top not observed), over 34 at Salgueiral and corresponds to the first 10m of the ALG section.

In terms of formal units the basal breccias and conglomerates can be designated as a member, provisionally called Gralheira Member. Its most characteristic features are the presence of red coloured matrix- or clast-supported breccias and conglomerates and the very rare occurrence of sandstone or mudstone interbeds.

The overlying subunit is composed of red coloured massive to faintly laminated, often pebbly sandstones (Pl. 4.6D, F) and red coloured, clast-supported, massive to crudely bedded conglomerates. The latter are composed mostly of quartzite and quartz clasts, with schist and metapelite making up 10 to 20% (rarely 40%) of the clasts (Pl. 4.6B and C). Roundness changes gradually from sub-rounded/sub-angulose at the base to rounded/well rounded at the top. Clast size reaches a maximum of ca. 50cm in the thickest beds. These conglomerates are generally similar to facies association SG2. Conglomerates are dominant over the sandstones at the GRA and VMO sections and subordinate at the ALG section. Sandstones and more rarely mudstones appear at the top of and within

conglomerate beds from which they grade into, but also as separate beds, usually with sharp basal contacts. Sandstone scour fills within conglomerate packages are much more abundant than in the underlying subunit. Sandstone beds are initially thick (>2m) massive, often pebbly, usually with a coarser base (occasionally gravelly) and grade to medium sized sand at the top (74 to 104m at the GRA section; undefined at the VMO section; 10 to 55m at the ALG section). Frequently (especially at the GRA section) these beds grade from conglomerates (described above) and seem to be genetically related. Some of these are associated as couplets, a few decimetres thick, forming tabular packages with sharp contacts (Pl. 4.6E, G). These sandstones ± conglomerates (some similar to facies association SG2) are defined as facies association SG3. Miall's facies codes associated with this facies association are Gh and Sh and more rarely Gcm, Gci and Ss (see Fig. 4.2, 4.3 and 4.7). To the top of the unit sandstone beds tend to be thinner (<2m), with horizontal lamination (although often crude), each bed grading from coarse/medium sand at the base to fine sand at the top, occasionally topped by a massive or laminated grey mudstone layer – facies association SG4 (Pl. 4.6E). These mudstone layers are, especially at the ALG section, organic matter-rich and some contain recognizable plant remains (as described by Wagner et al., 1983). Associated Miall's facies codes are Sh, Fsm and more rarely Fl and Ss (see Fig. 4.2, 4.3 and 4.7).

The characteristic red colour of the sandstones may in fact be, at least partially, a result of recent weathering and/or diagenesis. Commonly the red colour is restricted to an outer centimetrical layer of rock while its core is grey or whitish.

This subunit is ca. 70m at the GRA section; over 140m at the VMO section (top not observed) and over 64m at the ALG section – the type section (top not observed).

In terms of formal units the above described subunit can be considered the second member of the Algeriz Formation, provisionally called Parada Member (best exposed along the road from Algeriz to Parada). The lower limit is arbitrarily defined as the first relatively thick (>1m) sandstone bed. The most characteristic features are the red coloured sandstones interbedded, in different proportions, with red coloured clast-supported conglomerates with rounded clasts. The upper limit is defined as the first thick (>5m) grey mudstone bed (first grey measure of the Vale da Mó Member of the Monsarros Fm. – see below).

The Algeriz Fm., composed by the Gralheira and Parada Members, is 143m thick at the GRA section; over 160m thick at the VMO section; over 72m at the ALG section and over 32m at the SAL section.

Wagner et al. (1983) defined the Vale da Mó Fm. based on a ca. 40m long section near the village of Algeriz and named it after another village around which outcrops of this formation are common (Vale da Mó). No other sections were presented. Within the Monsarros Fm. several sections up to 20m thick composed of finely laminated, organic matter-rich mudstones can be observed, especially at the VMO section. These sections are extremely similar to the Vale da Mó Fm. in terms of facies association and differ essentially in their vertical extent. The identification and differentiation of the Vale da Mó Fm. outside its type area is thus difficult, especially when detailed mapping of the basin is performed and may even lead to erroneous structural interpretations. Thus it is proposed to redefine the Vale da Mó Fm. as a Member of the Monsarros Fm (Table 4.3). The vertical extent is badly constrained as there is no section where its base and top are visible. It is probably restricted to less than 100m.

Facies association	Short description	Miall's facies codes	Distribution
SG1	Red massive, matrix-supported, coarse grained breccias	Gmm, Gmg and more rarely Gcm and Gci	First meters of the Gralheira Member
SG2	Red clast-supported, massive to crudely bedded conglomerates/breccias	Gcm and more rarely Gmg, Gci and Gh	Top of the Gralheira Member and basal Parada Member
SG3	Massive, often pebbly sandstones ± conglomerates	Gh and Sh and more rarely Gcm, Gci and Ss	Parada Member
SG4	Crudely bedded sandstones ± grey mudstone	Sh, Fsm and more rarely Fl and Ss	Parada Member, especially the top
FP1	Laminated or massive grey fine sandstone to claystone	Fl, Fsm and more rarely C and Sm	Vale da Mó and Serradinho Members
FP2	Cycles of sand grading to shale topped by a thin coal layer	Fl, C and more rarely Sl(?)	Serradinho Member (only in the southern areas)
GR1	Cycles of clast supported conglomerates with rounded quartzose clasts that fine up to sandstones	Gh, Gt, Gp, Sp and Sr and more rarely Gcm and Ss	Serradinho Member
GR2	Cycles of clast supported conglomerates with clasts with red patina and reddish sandstone tops	Gh and Sr, but also Gcm and Gci	Top of Serradinho Member

Table 4.2 – Facies associations defined for the Buçaco basin sediments and their main characteristics and vertical and lateral distribution.

The Vale da Mó Member was only positively identified in this work along a road cut outside the village of Algeriz (road to Junqueira). It is uncertain if this is the same section described by Wagner et al. (1983). About 20m were logged and the remaining section showed only a repetition of the same sequence (Fig. 4.7). The base of this Member can be observed at the GRA section. The thin sand-mud tops of conglomeratic beds of the Algeriz Fm. become increasingly thicker and richer in organic matter. The first thick (>5m) mudstone bed is considered to define the base of this Member (at 144m of the GRA section - see Fig. 4.2). The facies association of this Member can be generally included in type FP1: grey to dark grey fine sandstone to claystone beds, usually finely laminated, but occasionally massive. Plant-derived debris are common, from small coal fragments up to decimetrical, well preserved plant fragments (Pl. 4.7A and C). Thin (<20cm) fining-upward cycles are very common. Thin coal seams are occasionally observed at the top of these cycles. Coarser grained lithologies are rare, but may be observed at the base of thicker cycles. This facies association is observed throughout the Monsarros Fm., at the ALG section and more commonly at the VMO section. Associated Miall's facies codes are Fl, Fsm and more rarely C and Sm (see Fig. 4.2, 4.3, 4.4, 4.6, 4.7, 4.8, 4.9, 4.10, 4.12). The CRI section shows a slightly different type of fine grained lithofacies. Very thin cycles (10 to 20cm) of sand (coarse to medium) grading to shale or silt, frequently topped by an extremely thin coal layer: facies association FP2. These are interbedded with thick conglomeratic beds but apparently are not grading from them (see Fig. 4.12 and Pl. 4.7B). It is only observed in the Monsarros Fm.

The subunit overlying the Vale da Mó Member is composed of a long sequence of considerably monotonous coarse fluvial sediments. In both VMO and ALG sections, the sequence is characterized by successive m-thick fining-upward cycles. The base of the cycles is almost invariably conglomeratic, usually with erosive basal contacts which sometimes erode significant parts of the underlying cycle. The conglomerates fine up to sandstones and are frequently topped by mudstones occasionally with coal seams (facies

association FP1). The proportion of conglomerate/sandstone/mudstone varies from cycle to cycle. The sequence is generally coarser at the ALG section than at the VMO section where sandstones and mudstones are more abundant. The conglomerates are almost invariably clast-supported, composed by quartz and quartzite clasts, although other lithologies occur such as black schist, meta-sandstones and mafic rocks. The proportion of black schist is low for most of the sequence (ca. 5%), but there are "abundance peaks" in several parts of the ALG section. The abundance of these clasts shifts progressively from very rare to about 20% and then suddenly increases, from one cycle to the next, up to 100% total clast components. The peak is usually followed by a sharp decline, but the proportion of schist clasts can remain relatively high (ca. 20%) in the following cycles (see Fig. 4.13 and Pl. 4.7E and F). It is interesting to note that at least in two occasions the increased proportion of schist clasts is preceded by an increase in maximum clast size. The same is observed in the basal part (Gralheira Member) of the VMO section. This part of the sequence is defined as the Serradinho Member of the Monsarros Fm. (small group of houses named Serradinho where the type section is located, W of Algeriz village). It is over 500m thick at the VMO section, 460m at the ALG section and over 400m at the CRI section.

There are two main facies associations that can be defined in this member (apart from the FP1 and FP2 described above): GR1 and GR2. GR1 is characterized by clast supported conglomerates, usually with rounded to well-rounded quartzite and quartz clasts, that fine up to sandstones which are usually restricted to a relatively thin interval. The conglomeratic part is massive, with crude bedding-parallel lamination or with planar or trough cross beds (observed solely in gravel-conglomerates).

<table>
<tr><th>Author / Short description</th><th>Courbouliex (1972, 1974)</th><th>Wagner et al. (1983)</th><th colspan="3">This work</th><th>Type section</th></tr>
<tr><td>Red, matrix- or clast-supported breccias and conglomerates and very sst or mudst</td><td>1. Conglomerát de base</td><td rowspan="2">Algeriz Fm.</td><td rowspan="2">Algeriz Fm.</td><td colspan="2">Gralheira Member</td><td>Gralheira reservoir area</td></tr>
<tr><td rowspan="2">Red sst and red clast-supported conglomerates with rounded clasts</td><td>2. Les grès "lie de vin"</td><td colspan="2" rowspan="2">Parada Member</td><td rowspan="2">Road cut Algeriz-Parada</td></tr>
<tr><td>3. Les grès "lie de vin" avec petits bancs conglomératics</td><td rowspan="5">Monsarros Fm.</td></tr>
<tr><td>Grey coaly Siltst and mudst</td><td>?</td><td>Vale da Mó Fm.</td><td colspan="2">Vale da Mó Member</td><td>Road cut Algeriz-Junqueira</td></tr>
<tr><td>Conglomerates, sst and mudst with thin coal seams</td><td>4. Les conglomérats et schistes gris</td><td rowspan="2">Monsarros Fm.</td><td rowspan="3">Serradinho Member</td><td>Serradinho Member</td><td>Road cut Algeriz-Monsarros</td></tr>
<tr><td>Conglomerates, sst and mudst with ferric staining</td><td>5. Les conglomérats à interbancs gris ou rouges</td><td>Serradinho Member (Up. Facies)</td><td>Road cut Algeriz-Monsarros</td></tr>
<tr><td>Fluviatile conglomerates and sst of the overturned flank</td><td>6. Les conglomerates à interbancs schisto-gréseux du flanc ouest</td><td>Not considered</td><td>Repetition of part of Serradinho Member</td><td>Best exposed at the road cut Algeriz-Monsarros</td></tr>
</table>

Table 4.3 – Comparison of the several schemes for the subdivision of the basin. All previous work based on the ALG section.

Imbrication of clasts is seldom seen (Pl. 4.7E). Associated Miall's facies codes are Gh, Gt, Gp, Sp and Sr and more rarely Gcm and Ss. The colour of the beds is white, yellow or light brown. Clast surfaces are clean. Maximum clast size is usually about 10cm, but beds with coarser elements exist. This facies association is observed at the CRI, ALG and VMO sections. The lower part of the Serradinho Member were this facies association is dominant, along with FP1, probably corresponds to unit 4 of Courbouliex (1972, 1974) - Les conglomérats et schistes gris. GR2 is quite similar but differs in having generally higher maximum clast size (although highly variable between and within cycles); a red patina on clast surfaces (and frequently reddish core, especially schist clasts) and reddish sandstone tops; worse roundness (and especially mixing of rounded and angular clasts); massive or inverse grading and generally higher matrix/clast ratio (Pl. 4.7G). Associated Miall's facies codes are Gh and Sr, but also Gcm and Gci. This facies association is restricted to the uppermost part of the Monsarros Fm (referred to here as Monsarros Fm. upper facies). It is observed at the ALG and VMO sections and possibly at the CRI section (only sandstones are observable). Similarly to the Algeriz Fm. the origin of the ferric staining seems, at least partially, due to diagenesis or recent weathering. However the red patina of the clasts seems to be originated by surface processes prior to burial. The upper part of the Serradinho Member were this facies association is dominant probably corresponds to unit 5 of Courbouliex (1972, 1974) - Les conglomérats à interbancs gris ou rouges. These differences are not considered to be relevant enough to erect a new Member for the Monsarros Fm. Both GR1 and GR2 commonly grade upwards to facies association FP1.

The following lithological columns from sections in the Buçaco basin are presented from N to S. Base of the sequence is always on the lower left and top on the upper right. The number of meters between parts of the columns or at their base represent the estimated thickness of sequence missing. Va, a, sa, sr, r, wr refer to the visual estimated roundness of the clasts in the conglomerates: very angulose, angulose, sub-angulose, sub-rounded, rounded, well rounded, respectively.

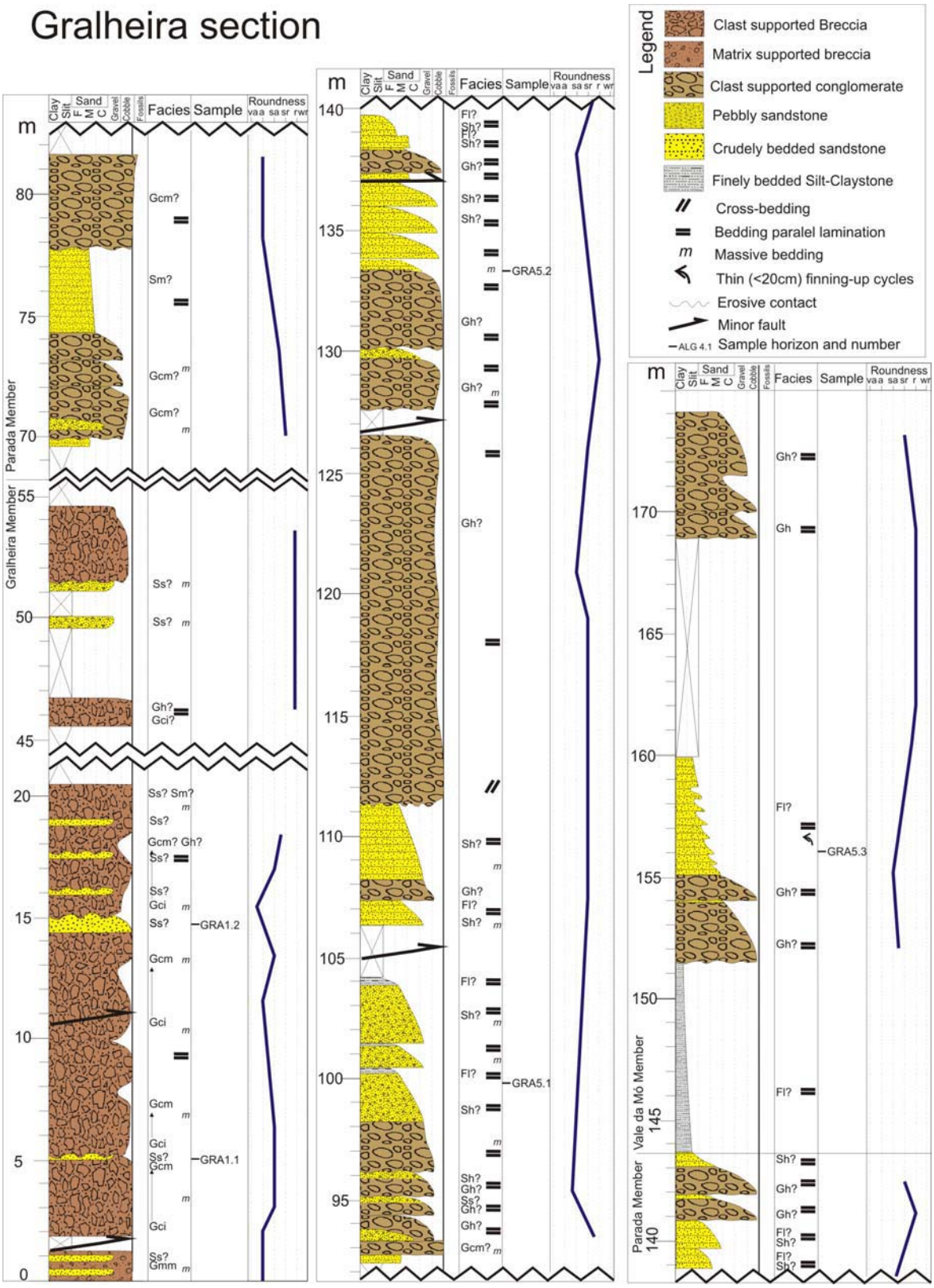

Fig. 4.2 – Lithological column of the GRA section. Parada and Gralheira Members (Algeriz Fm.) are represented as well as the base of the Vale da Mó Member (Monsarros Fm.).

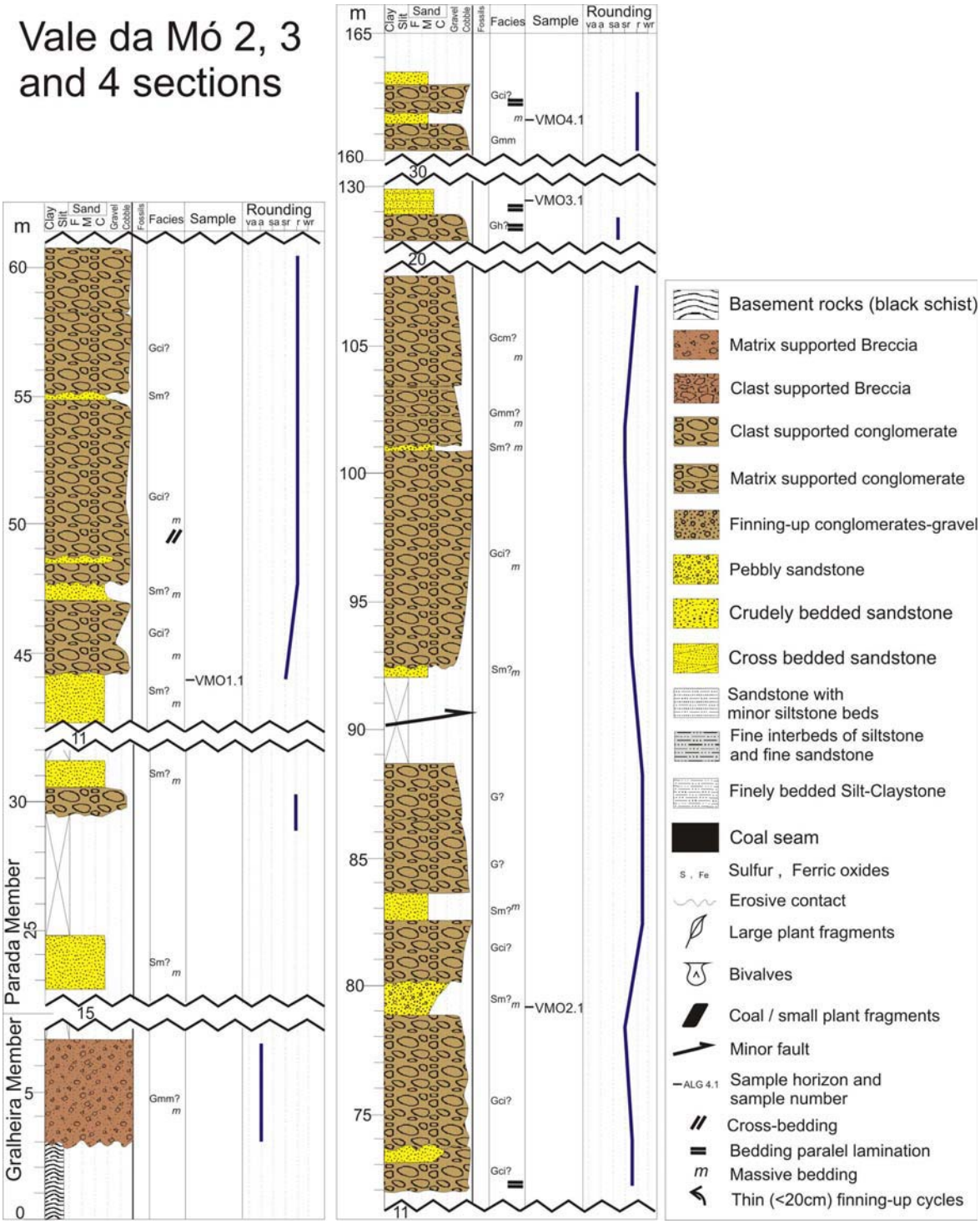

Fig. 4.3 - Lithological column of the basal part of the VMO section. Parada and Gralheira Members (Algeriz Fm.) are represented.

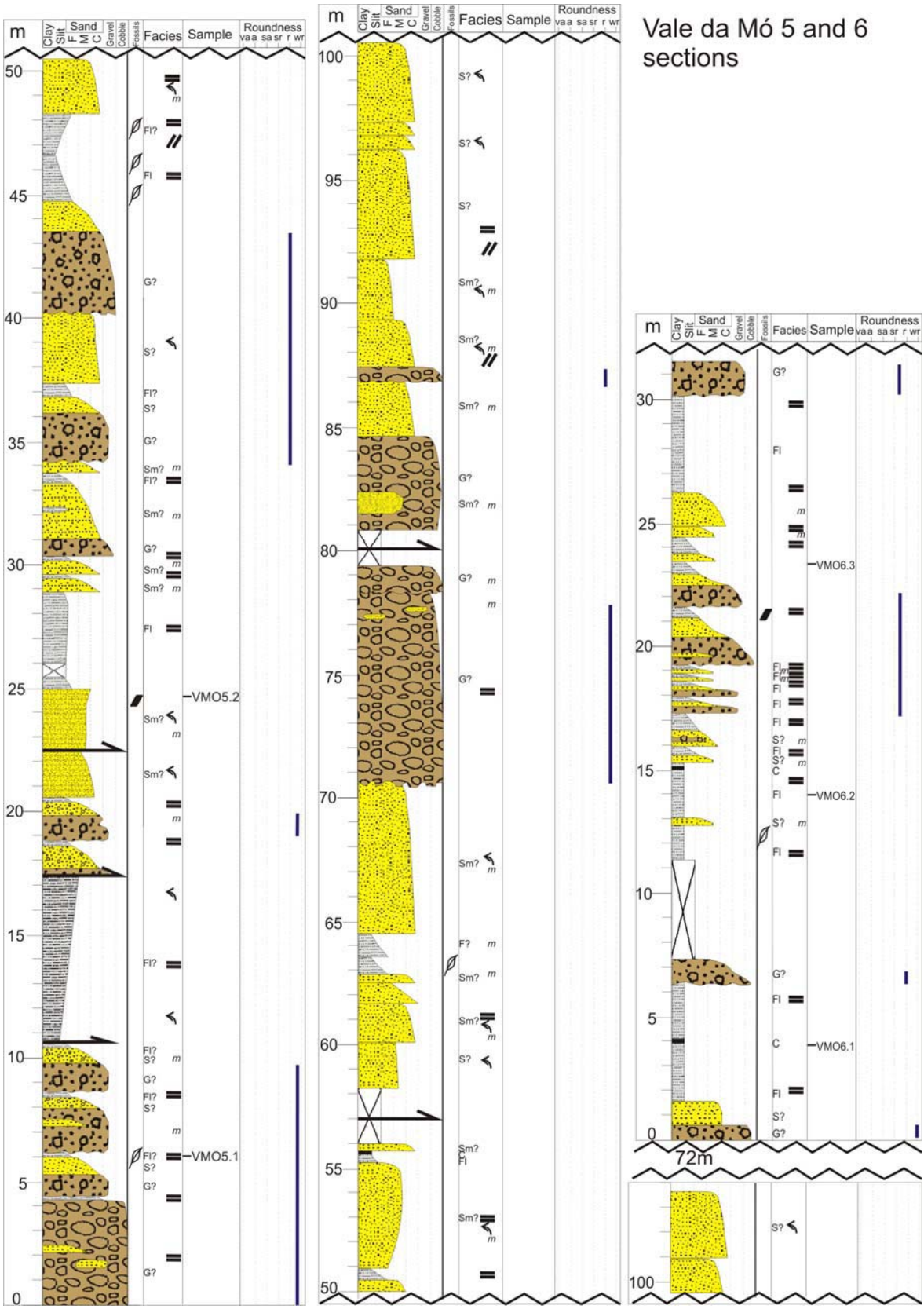

Fig. 4.4 - Lithological column of the lower middle part of the Vale da Mó section. Serradinho Member (Monsarros Fm.) is represented. Same legend as in Fig. 4.3.

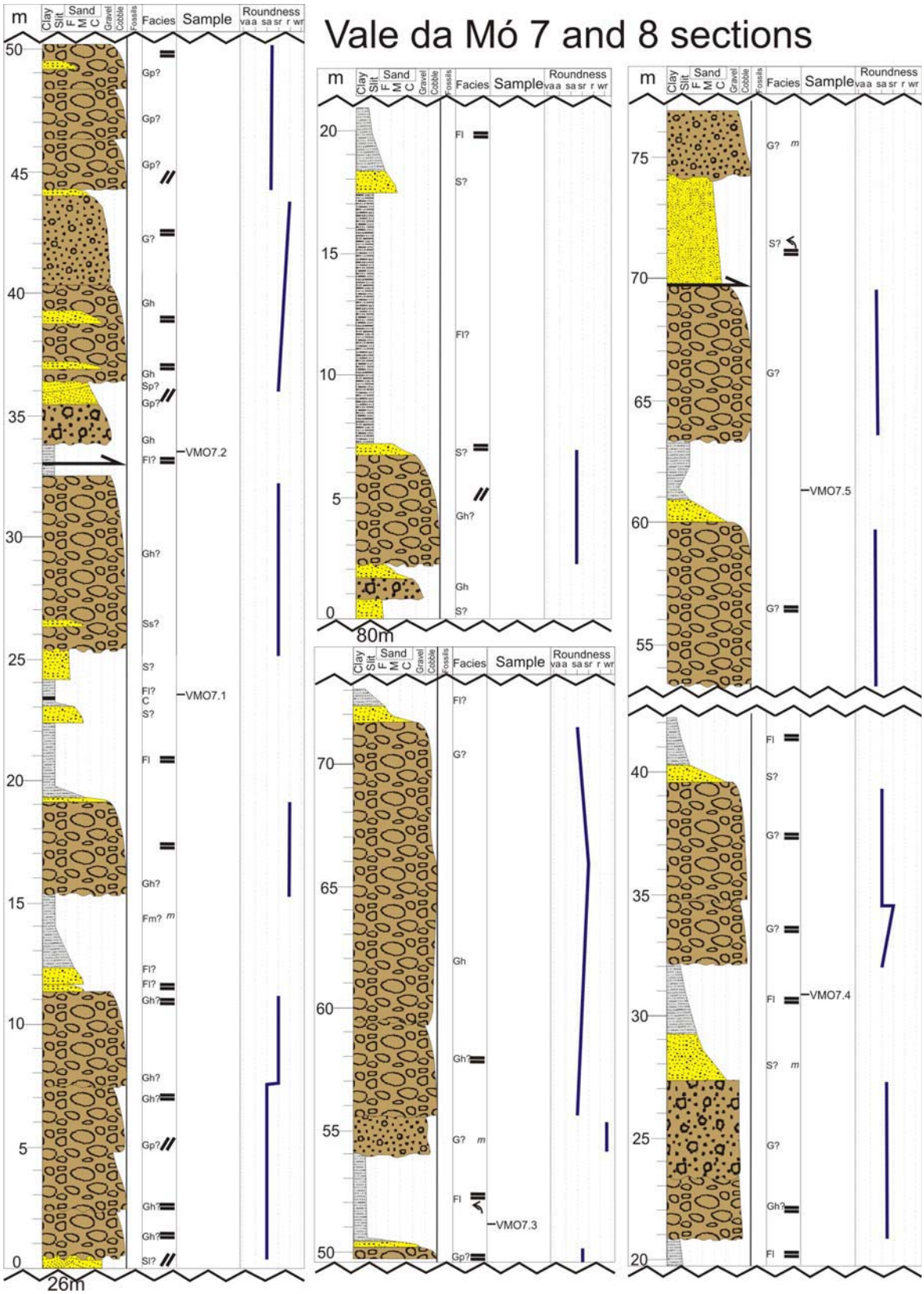

Fig. 4.5 - Lithological column of the middle part of the VMO section. Serradinho Member (Monsarros Fm.) is represented. Same legend as in Fig. 4.3.

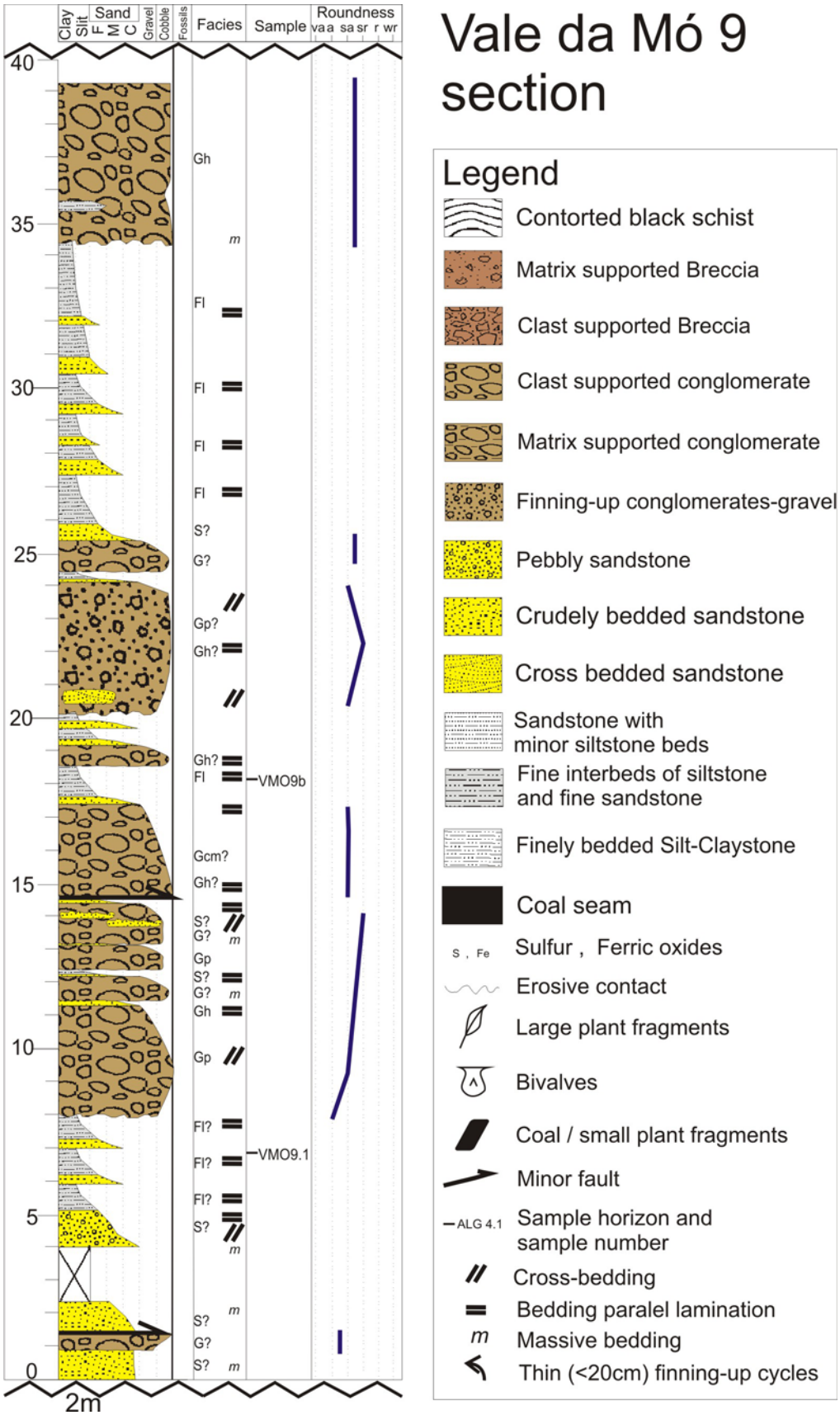

Fig. 4.6 - Lithological column of the upper part of the VMO section. Serradinho Member (Monsarros Fm.) is represented.

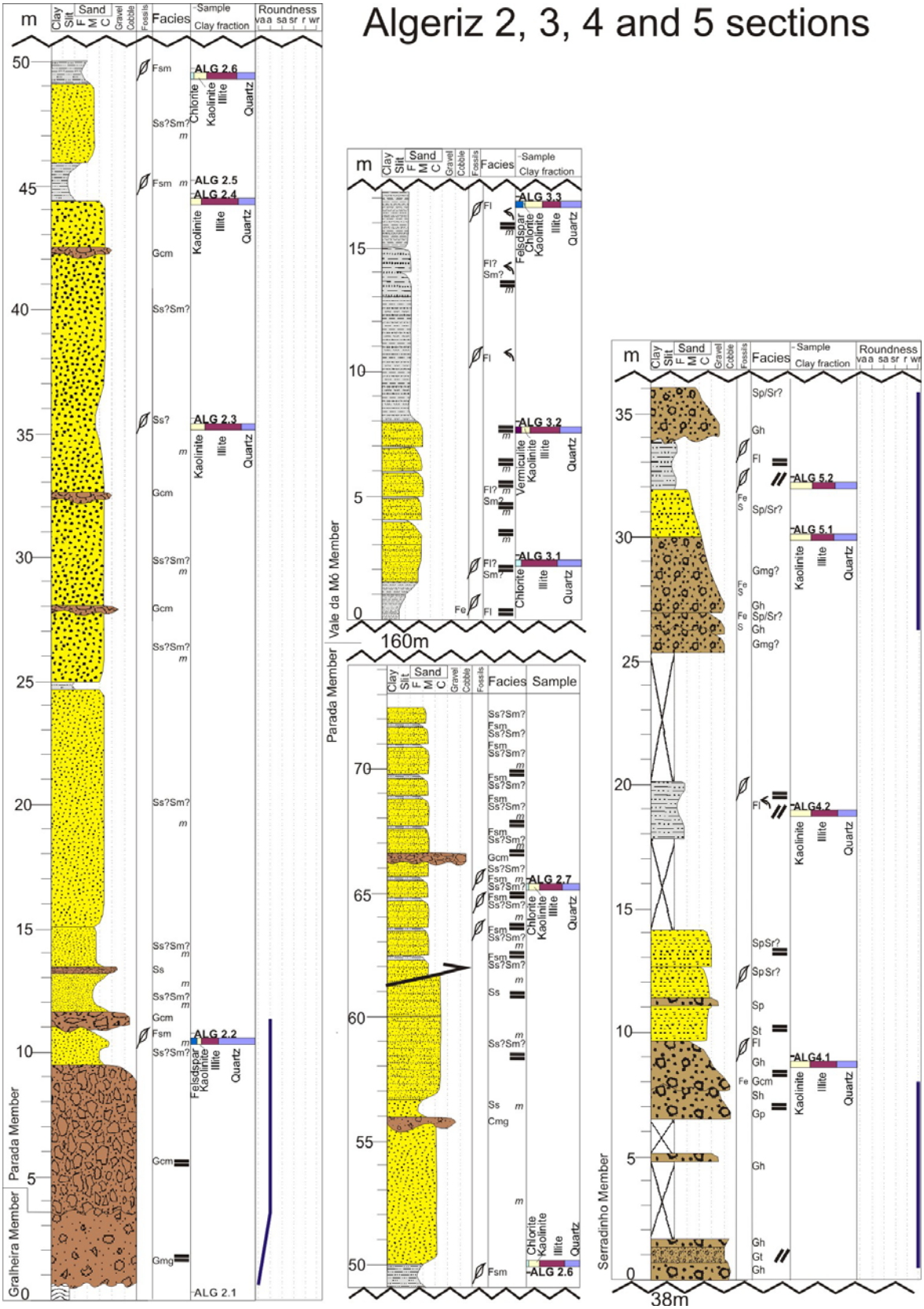

Fig. 4.7 – Lithological column of the basal part of the ALG section. Parada and Gralheira Members (Algeriz Fm.) and Vale da Mó and Serradinho Members (Monsarros Fm.) are represented. Variation of the proportions of the clay fraction components is shown. Same legend as in Fig. 4.10.

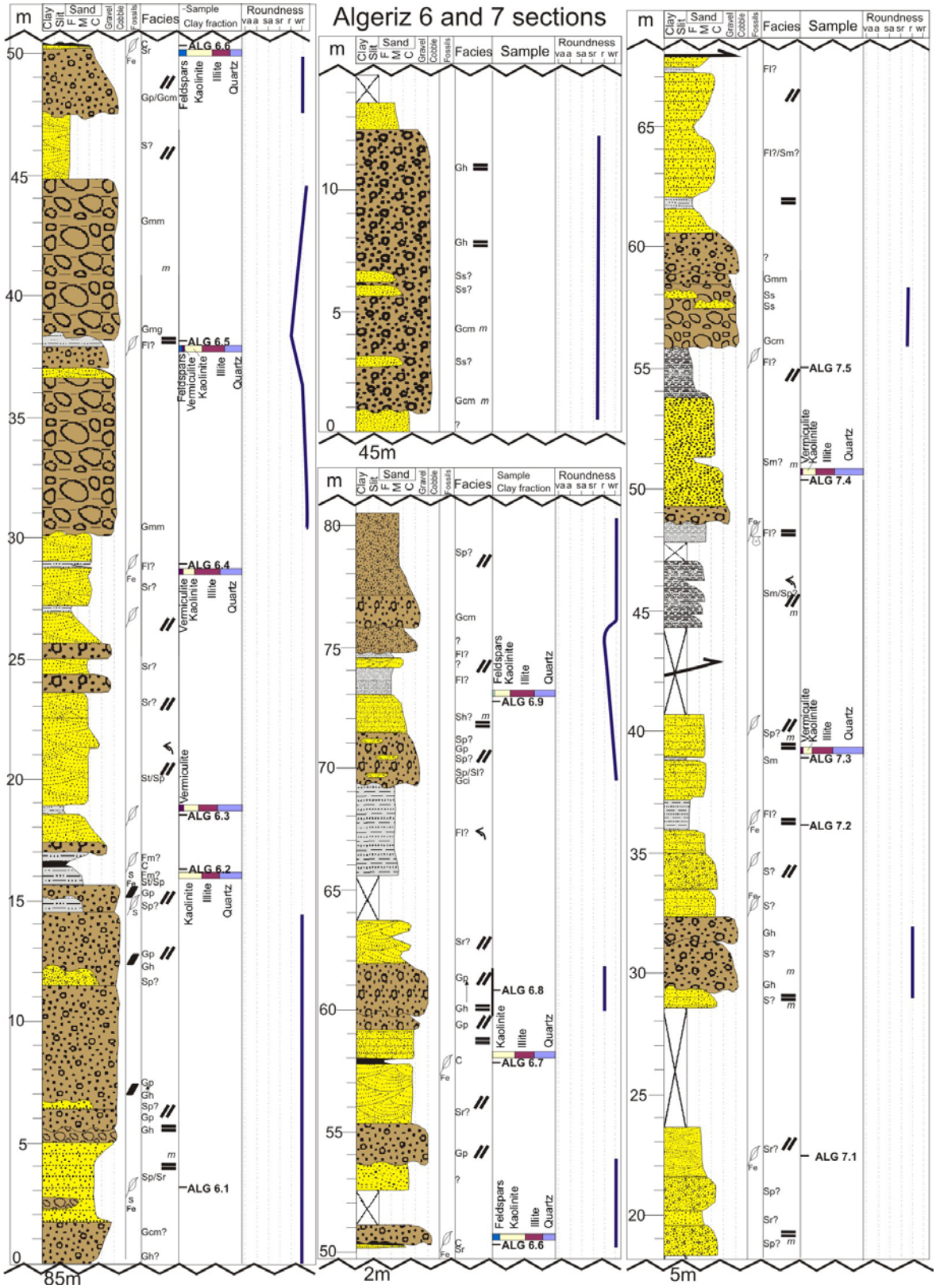

Fig. 4.8 - Lithological column of the middle part of the ALG section. Serradinho Member (Monsarros Fm.) is represented. Variation of the proportions of the clay fraction components is shown. Same legend as in Fig. 4.10.

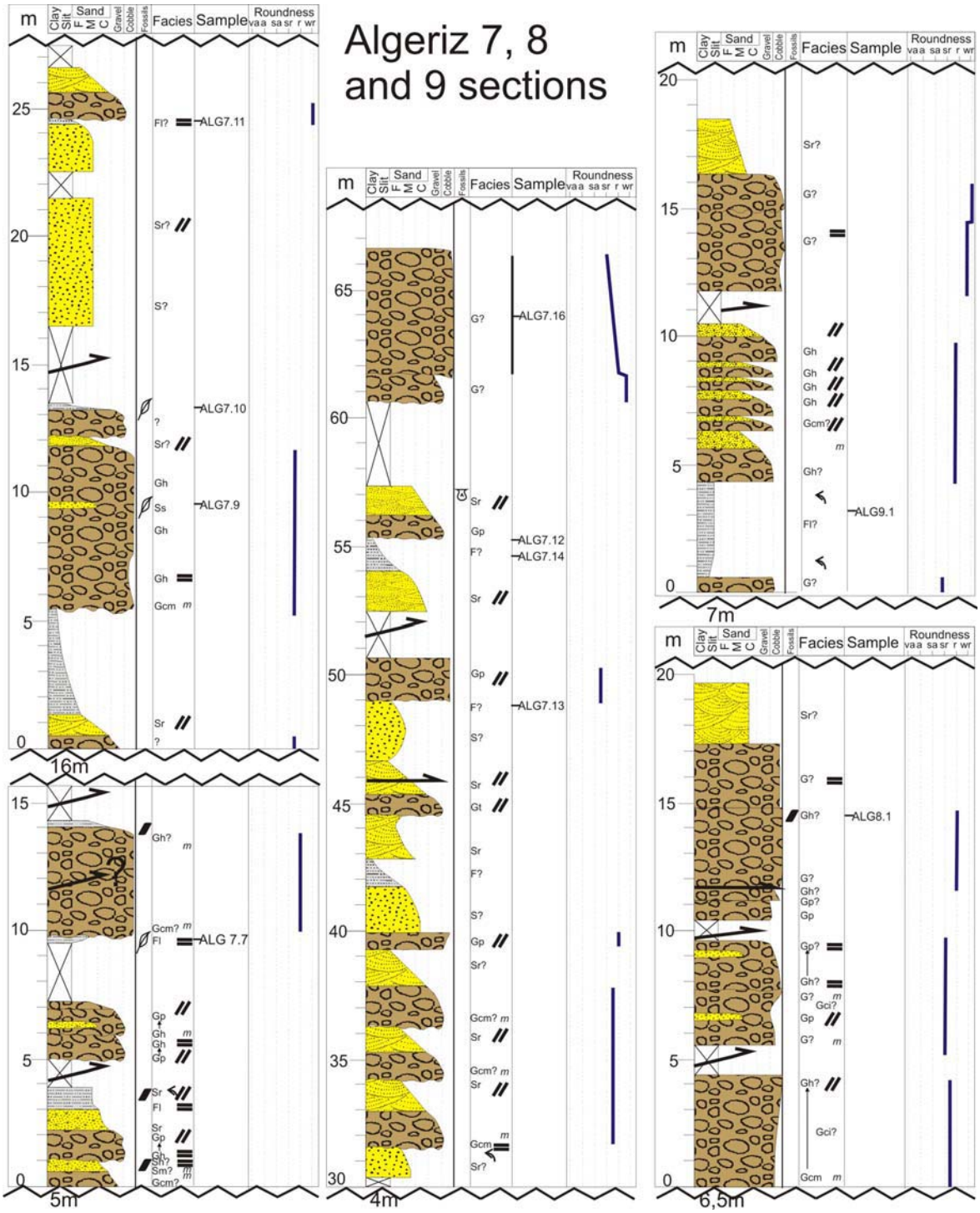

Fig. 4.9 - Lithological column of the middle upper part of the ALG section. Serradinho Member (Monsarros Fm.) is represented. Same legend as in Fig. 4.10.

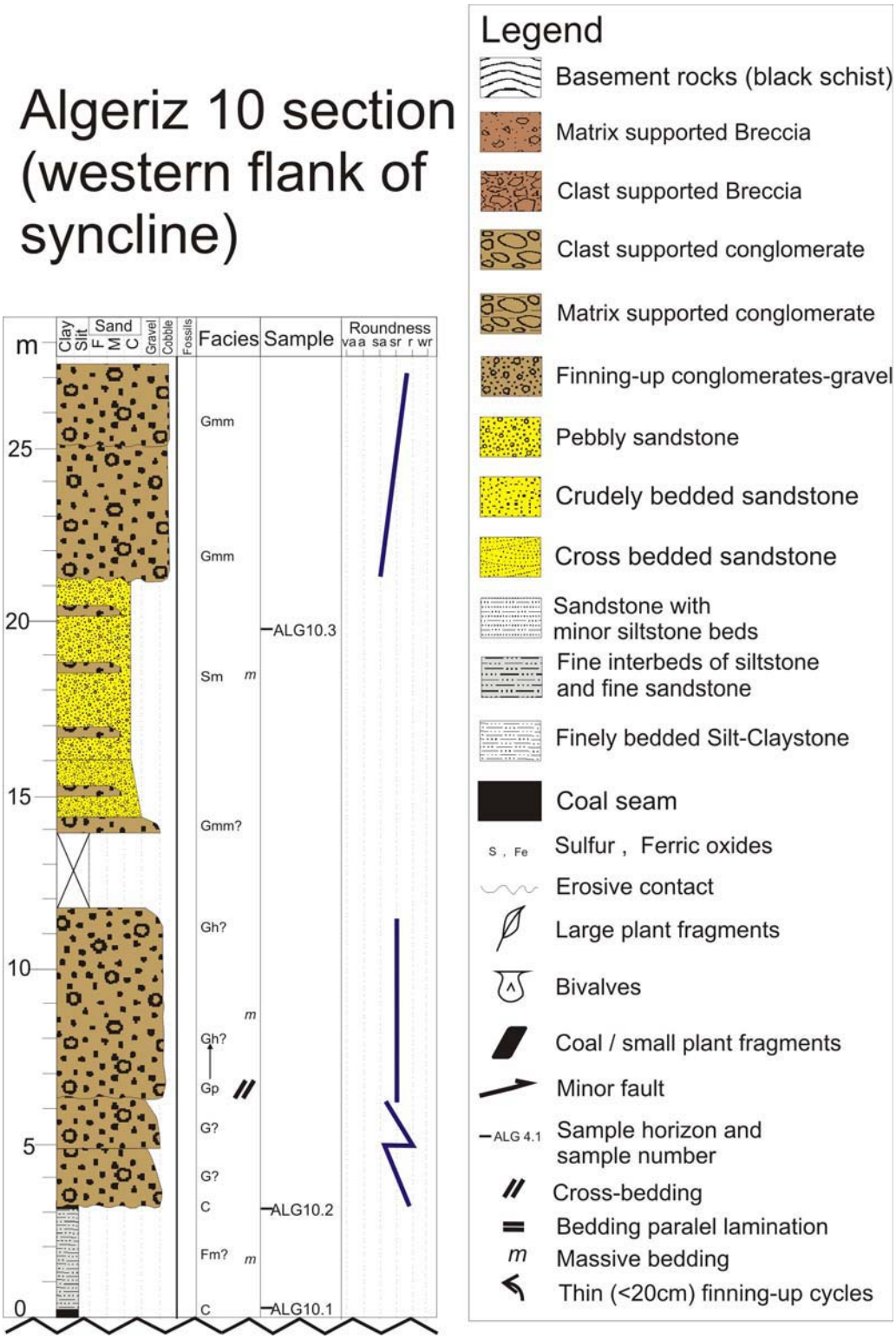

Fig. 4.10 - Lithological column of the upper part of the ALG section. Serradinho Member (Monsarros Fm.) is represented.

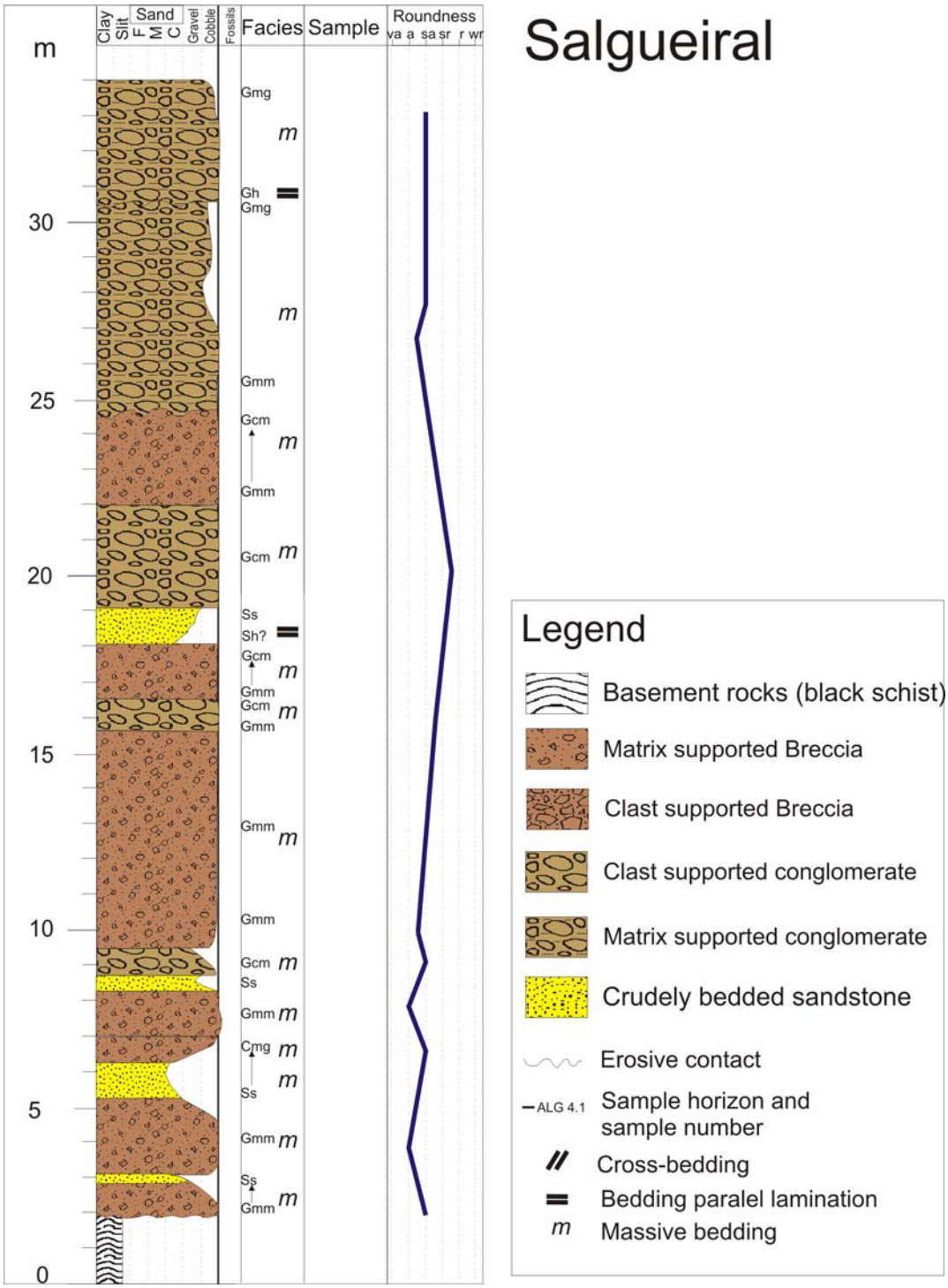

Fig. 4.11 - Lithological column of the basal part of the Salgueiral section. Parada Member (Algeriz Fm.) is represented.

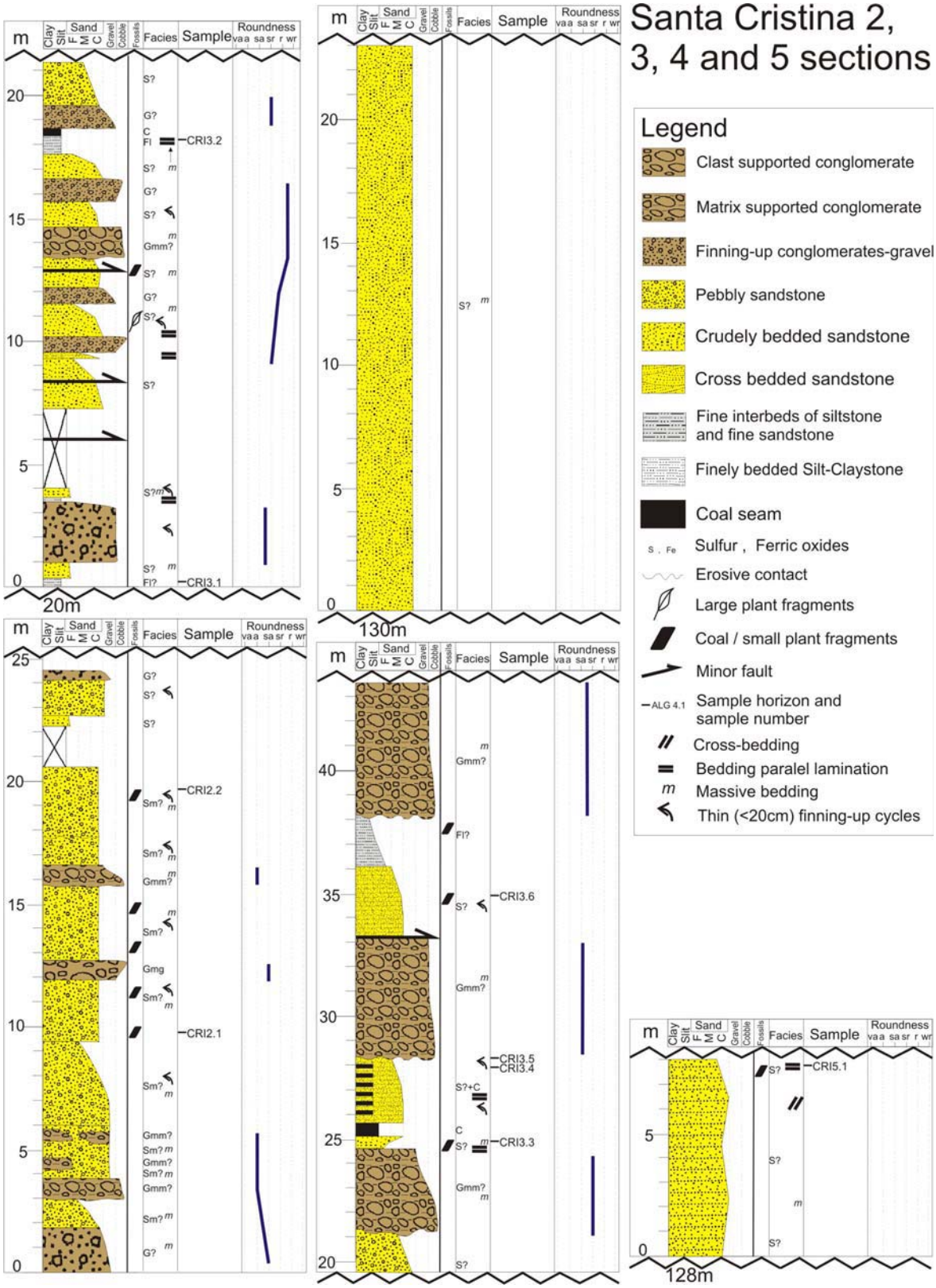

Fig. 4.12 - Lithological column of the CRI section. Serradinho Member (Monsarros Fm.) is represented.

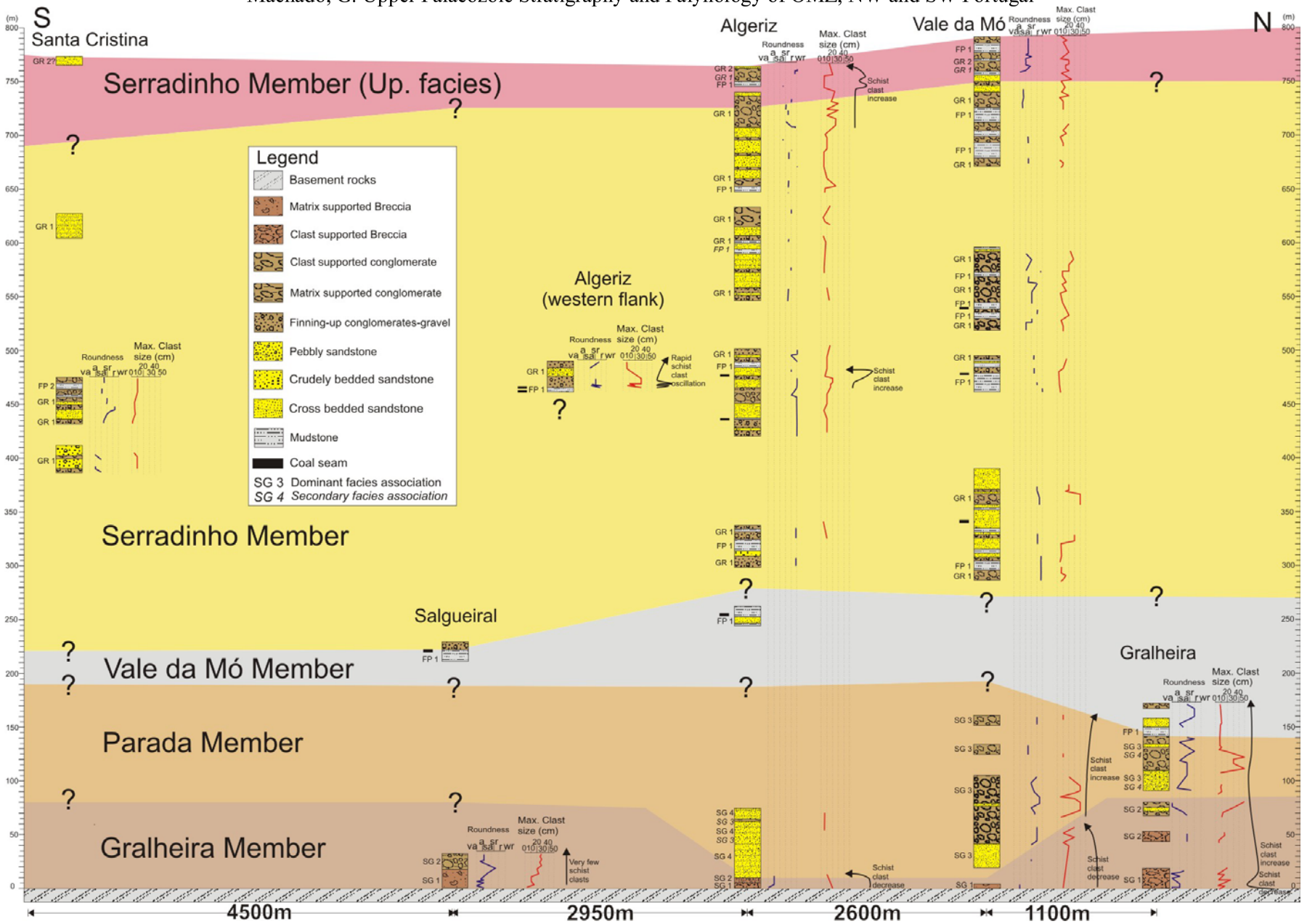

Fig. 4.13 – S-N scheme of the Buçaco Basin. Simplified lithological columns of the studied sections are shown along with the corresponding conglomerate clast roundness (blue line), maximum diameter (red line) and overall schist clast variation (black line).

4.3.2 Palaeocurrents and provenance of sediments

Palaeocurrent directions were measured at the ALG and VMO sections (exclusively from the Serradinho Member). Most of the measurements were made in sandstones or gravel conglomerates, predominantly on cross bedding structures but also in ripple marks observed on bedding planes. At the ALG section these show very consistent directions mainly to SW and S. The measurements made on imbricated clasts of coarser conglomeratic beds (e.g. Pl. 4.7E) showed a considerable dispersal of directions, essentially discordant with the directions obtained from the finer beds (see Fig. 4.14). A similar dispersal of data was observed at the VMO section where most of the measurements were made on imbricated clasts of coarse conglomerates. The main directions are to the S and ESE, closer to the basin's main trend, but still highly disperse (see Fig. 4.14).

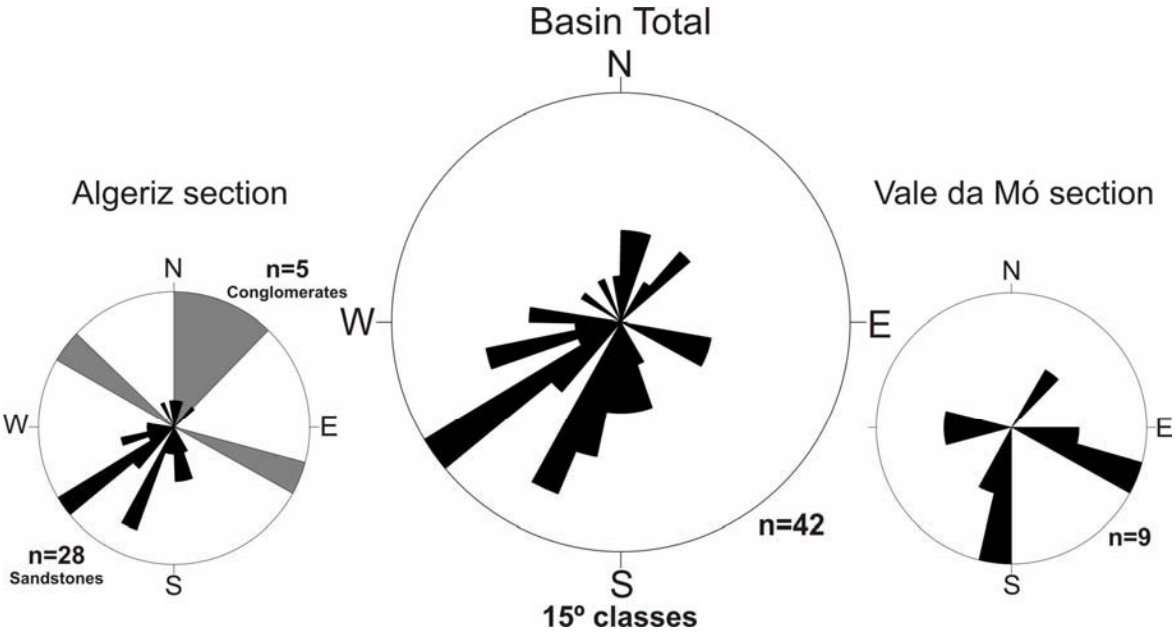

Fig. 4.14 – Rose diagrams showing palaeocurrent directions of Algeriz and VMO sections and basin total. The averages of multiple measurements from the same horizon where considered as single measurements when plotting data. For the Algeriz section the grey denotes measurements of imbricated clasts and black for cross bedding and ripples on sandstones. The VMO section measurements are mostly from imbricated clasts.

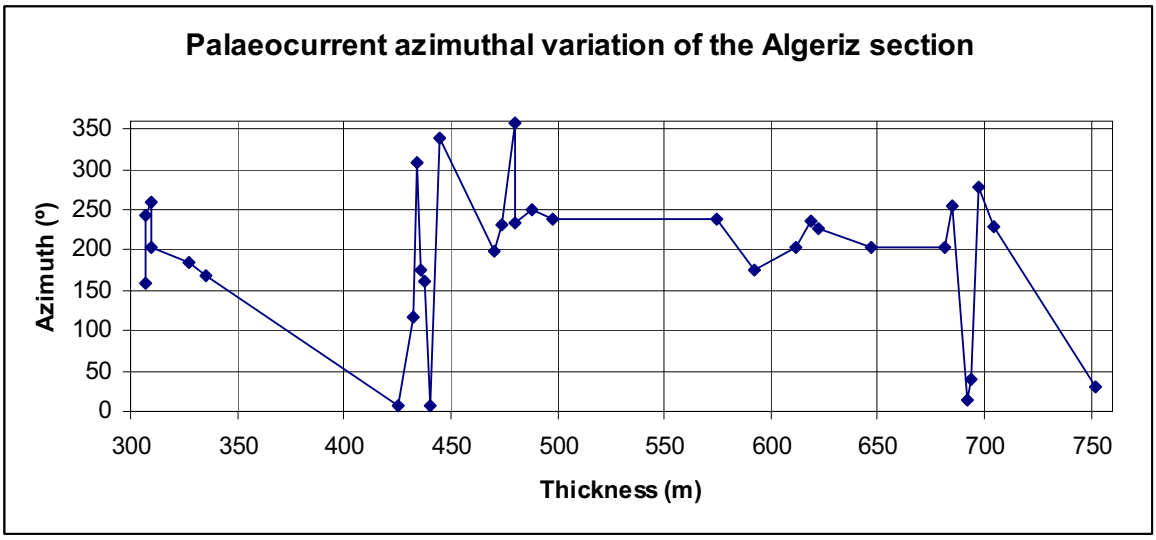

Fig. 4.15 – Distribution of palaeocurrent measurements through the ALG section (Serradinho Member) and its azimuthal variation. Note the concentration of azimuthal directions between ca. 160 to 250º (SSE to WSW), despite the considerable dispersal. Thickness (x axis) is correlatable with the thickness (y axis) of Fig. 4.13.

The azimuthal variation of palaeocurrent directions is significant, but a consistent mode between ca. 160 to 250º (SSE to WSW) is observed at the ALG section (Serradinho Member). No significant changes or shifts are identified and thus the main transport direction seemed to have remained essentially unchanged for the whole duration of the deposition of the Serradinho Member.

4.3.3 Organic Petrology and thermal history

Several palynological residues and picked coal fragments were mounted in epoxy blocks, polished, observed and measured using the methods described in Chapter 2. Vitrinite particles were abundant in all samples which allowed a good number of measurements to be made (Table 4.4). Inertinite particles were common in several samples (semifusinite, micrinite and more rarely macrinite and fusinite) and often difficult to distinguish petrographically from vitrinite. These frequently plotted as a separate group with reflectance values between 1,3 and 1,5% Rr (Pl. 4.7H). Some samples had vitrinite particles showing evidences of oxidation, especially around the edges and occasionally the entire surface (irregular, sometimes pitted surface). Measurements on these particles were avoided. Most vitrinite particles can be classified as collotelinite. Preserved cellular structures were seldom observed. Sporinite was rare in most samples. Polymaceralic particles were very rare. Alginite particles were not observed.

Measurements of Random Vitrinite Reflectance (Rr) show that most samples have averages around 1%. It should be mentioned that frequently the histograms showed a bimodal distribution, usually with a dominant population around 1% and another close to 0,8% (which seems to dominate is samples ALG4.1, 6.1, 8.1 and VMO7.6). The same bimodal distribution was described by Flores et al. (2010) although they found the 0,8% Rr population to be dominant in their samples.

	Sample	Thickness (m)	Counts	Rr (%)	Stand. Dev. (%)	Max Temp. Baker (1988)	Max Temp. Barker & Pawliewicz (1986)	Max Temp. Barker & Goldstein (1990)
Parada Member	ALG22hf	10	93	1,07	0,10	154,74	162,16	169,74
	ALG2.7hf	55	107	1,41	0,14	183,73	197,90	202,91
Vale da Mó Member	ALG3.1hf	244	75	1,23	0,12	169,12	179,88	186,19
	ALG3.3hf	261	105	0,99	0,24	147,26	152,93	161,18
Serradinho Member	ALG4.1hf	307	98	0,86	0,31	131,95	134,06	143,67
	ALG5.2hf	328	103	0,99	0,17	147,06	152,69	160,95
	ALG6.1hf	422	73	0,70	0,31	111,18	108,45	119,89
	ALG6.5hf	457	94	1,07	0,21	154,90	162,35	169,92
	ALG7.2hf	582	103	1,11	0,15	158,57	166,88	174,12
	ALG7.5sed	601	97	1,16	1,16	163,53	172,99	179,79
	ALG7.6hf	622	100	1,02	0,21	150,43	156,85	164,81
	ALG8.1hf	735	97	0,85	0,47	130,90	132,77	142,47
Serradinho Member	VMO6.1hf	467	97	1,08	0,15	156,13	163,86	171,32
	VMO6.2hf	477	100	0,96	0,14	144,21	149,17	157,69
	VMO6.3hf	487	49	0,96	0,09	143,45	148,24	156,82
	VMO7.1hf	542	55	1,03	0,12	151,28	157,88	165,77
	VMO7.6hf	732	27	0,86	0,09	132,79	135,10	144,63
	VMO9bhf	767	86	1,02	0,10	150,50	156,93	164,89

Table 4.4 – Samples from the Vale da Mó (VMO) and Algeriz-Monsarros (ALG) sections, covering the Algeriz and Monsarros Formations. "sed" denotes picked coal fragments and "hf" palynological residue obtained from HF dissolution. Thickness corresponds to the position of the sample in the compiled lithological columns of Fig. 4.13. Equations used to estimate maximum temperatures (Tp) are: Barker (1988): Tp = ((LnRr)x104)+148; Barker & Pawliewicz (1986): Tp = ((LnRr)+1.2)/0.0078; Barker & Goldstein (1990): Tp = (((LnRr)+1.26)/0.00811)*0.965)+12.1.

Additional samples were processed from the CRI section, and from an isolated outcrop of the (?)Monsarros Fm. in the GRA section (not shown here). Most of the samples were too oxidized to be measured. Two samples however, one from CRI and another from the GRA section provided enough measurable particles. The mean vitrinite reflectance values obtained are also around 1%.

Tentatively the results could be used to determine palaeogeothermal gradients, by plotting thickness Vs Rr% or Maximum palaeotemperature. There is a badly defined trend with similar values in both VMO and ALG sections, but correlation values (R^2) are extremely low (around 0,1) due to the significant dispersal of mean values. Additional samples covering the whole sequence are needed to be able to properly estimate palaeogeothermal gradients.

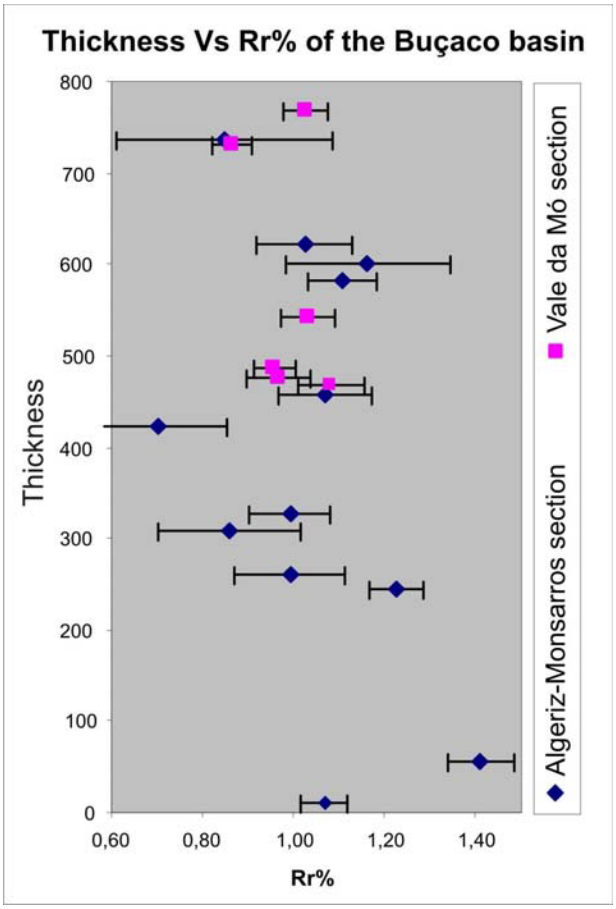

Fig. 4.16 – Rr% values and corresponding thicknesses for the samples from the ALG and VMO sections. Error bars based on standard deviation values.

4.3.4 Clay mineralogy analysis

Samples were collected extensively from the ALG section (identical to the palynology samples) and its <4μm fraction analyzed in an X-ray diffractometer (see methods section and Chapter 2). Additional samples were collected and analyzed from the GRA section (mostly red sandstones), VMO section (red sandstones and siltstones and grey shales and siltstones – palynology samples) and from the CRI section (one red sandstone and one grey siltstone).

Nearly all samples were composed of varying amounts of quartz, kaolinite and illite (mostly $2M_1$ polytype, occasionally muscovite). Chlorite occurs in vestigial amounts (<5%) rather consistently in samples of the Algeriz formation (especially at the ALG section) and more sparsely in the Monsarros Fm. A single sample from the most basal part (near the contact with the basement) of the VMO section had ca. 30% chlorite group minerals and no kaolinite. A few samples of the basal formation also had vestigial amounts of oxides (hematite), gypsum and nepouite (genthite). Feldspars (s.l.) occur sparsely in the Algeriz Fm. (up to 10%) and very rarely in the overlying Formation. The proportion of quartz/kaolinite/illite varies considerably within the Algeriz Fm., with quartz and illite (and sometimes muscovite) usually dominating the mineralogical composition, while within the Monsarros Fm. this proportion remains very constant throughout the section. The illite/kaolinite (I/K) ratio is high and highly oscillating within the Algeriz Fm. and

gradually decreases until it reaches 0 at the base of the Vale da Mó Member. From that point it gradually increases until around 1 and oscillates gently to the top of the Monsarros Fm.

Another relevant finding is the presence of vermiculite up to ca. 8% in several successive levels of the Monsarros Fm.

4.3.5 Palynology

Samples were collected preferably from grey or dark grey shally siltstones or shales. These occurred at the top of fining-upward cycles, frequently just bellow thin coal seams that occasionally topped the cycles. All collected samples provided a good amount of organic residue from which several slides of the unsieved and >53µm fractions were produced. Residues were observed un-oxidized and with mild oxidation using low concentrated bleach. All of the assemblages were dominated by phytoclasts. Most of them showed some degree of corrosion, probably originated from weathering and sparse Fe-oxide mineralization observed at the outcrop and possibly from sedimentary transport and early diagenesis (?bacterial decay). 11 samples from the ALG section provided observable sporomorphs, although samples from the Algeriz Fm. only showed rare and poorly preserved sporomorphs. Over 100 taxa were identified in total, although many restricted to generic level. This limitation was particularly evident for grains attributable to genera *Potonieisporites*, *Florinites* and *Schopfipollenites* which were the most abundant palynomorphs. 6 samples from the Serradinho and Vale da Mó Members of the ALG section provided determinable sporomorphs. 4 of them had relatively common, moderately to poorly preserved sporomorphs and 2 had very abundant, moderately to well preserved sporomorphs. 3 samples from the Serradinho Member of the VMO section and one form the CRI section provided rare and very poorly preserved sporomorphs. Rare reworked acritarchs were recorded in some of the samples from the ALG section.

The samples providing diversified assemblages were dominated by *Potonieisporites* spp., *Florinites* spp., *Schopfipollenites* spp. and *Laevigatosporites* spp. Other common genera are *Cheiledonites* spp., *Densosporites* spp. (decreasing abundance towards the top), *Crassispora* spp. (not present in the uppermost sample), *Dictyotriletes*-like sporomorphs (mostly fragments), *Lycospora* spp. (slight decrease towards the top), *Thymospora* spp., *Verrucosisporites* spp. and *Wilsonites* spp.

The presence of *Potonieisporites novicus*, *P. bhardwajii* and *Cheiledonites major* along with the considerable abundance of the two genera are indicative of the *Potonieisporites novicus-bhardwajii – Cheiledonites major* (NBM) miospore biozone of Clayton et al., 1977. The decrease of the frequency of *Densosporites* spp. and the disappearance of *Crassispora konsakei* (and all *Crassispora* spp.) to the top of the sequence are further indications of this biozone. Other relevant genera such as *Spinosporites, Thymospora* and *Triquitrites* have fairly constant frequencies throughout the sequence. *Vittatina* spp. and *Disaccites* non *striatti* are also present throughout but always rare to frequent.

4.4 Discussion and conclusions

The Gralheira Member is composed solely of continental gravity-driven sedimentary deposits. It seems to have all the characteristic features of alluvial fans formed at a distinct break in topography in a sub-aerial setting (see Nichols, 1999; Prothero & Schwab, 1996 for a revision). The sequence starts with matrix-supported breccias and

conglomerates (SG1 facies association) with very rare sandstone intercalations, indicative of plastic to pseudo-plastic debris-flows (Fritz & Moore, 1988). The overlying conglomerates are mostly clast-supported (SG2 facies association). The transport mechanism remains essentially gravitational, with more water- and clast-rich material being transported in an essentially pseudo-plastic flow (Fritz & Moore, 1988). The increase of quartzite and quartz clasts over the schist along with the improvement of the roundness and the decrease of ferruginization suggests that the material available in the drainage basin changed gradually from local deeply weathered rocks with little or no transport to mildly weathered, transported and moderately sorted material.

The Parada Member continues to have pseudo-plastic debris-flow deposits, but it probably includes another type of gravitational transport mechanism. The sandstones with gravelly bases and fine sand to mudstone tops may be indicative of sheet-flood events (SG4 facies association) (Fritz & Moore, 1988; Nichols, 1999). The characteristic gravel (or coarser)-sand couplets are observed in facies association SG3 and the meter scale beds with normal grading and horizontal lamination are common in this member, especially towards the top. Antidune cross-stratification was not observed. The basal massive and pebbly sandstones are probably associated with debris-flow events that grade to sheet flood- or even stream-flow type of transport that deposits the finer material (SG3 facies association) (Fritz & Moore, 1988; Nichols, 1999). Both SG3 and SG4 facies associations occur throughout at the GRA section, while SG4 facies association dominates most of the basal part of the ALG section. The mudstone top of some of the sandstone beds indicates that towards the end of sheet-flood and even some debris-flow events there was a calmer, probably stream flow-dominated transport and deposition phase (Fritz & Moore, 1988; Nichols, 1999; Wells & Harvey, 1987). Where these mudstone layers are organic matter-rich and laminated (mostly at the ALG section), a standing water body must have remained for a considerable amount of time. These are possibly incipient abandoned channel and possibly flood plain deposits which are greatly developed in the overlying formation. Overall there is a clear trend indicating an increase of the amount of water in the sedimentary system. Rather than a climatic change, this trend can be easily explained by an expansion of the catchment area as erosion took place.

The overlying Monsarros Fm. shows evidences of sedimentation where stream-flow type of transport prevailed (Fritz & Moore, 1988). The Vale da Mó Member as well as other parts of the sequence where FP1 facies association is observed seem to have been deposited in an environment with a standing water body to allow the deposition of m-thick, often laminated mudstones. The nature of this water body is uncertain and may vary depending of the characteristics and vertical extent of the mudstone intervals. The short intervals of finely laminated mudstone interbedded with coarse conglomerates may be associated with flood deposits/overbank fines that deposited in the final stages of flooding events (Brookfield, 2004). The thicker, usually organic matter-rich, mudstone intervals probably result from longer periods of lacustrine-type of sedimentation, not restricted to one event or season. The possible basin-wide extent and lateral correlation of these intervals is difficult to assess confidently. It is possible that these deposits correspond to back swamp/abandoned channel sediments where peat could form. The fact that most of the coal seams are at the top of these FP1 facies association intervals, directly bellow the base of another conglomeratic cycle, is indicative of an autogenic control (sensu Miall, 1996), related with the fluvial dynamics (e.g. channel avulsion – Catuneanu, 2006; Jones & Schumm, 1999) and not with external factors such as tectonism.

Seasonal events probably controlled the development of the intrabed thin cycles (<20cm). The surfaces bounding these cycles probably correspond to 3rd order bounding surfaces sensu Miall (1996). The FP2 facies association identified at the CRI section has several characteristics of turbidity current type of sedimentation. The thin cycles commonly have a coarser massive base followed by a cross bedded fine sand/silt interval and topped by finely bedding parallel laminated organic matter-rich shale or coal. If truly turbidites, this would imply the existence of a perennial lake. It is difficult to explain the sharp lower and upper contacts of these intervals with the coarse conglomeratic beds. Dinis & Reis (2007) interpreted these conglomerates and lake shoreface deposits, but no significant differences were found between these and other conglomeratic beds of the VMO and ALG sections which are clearly of fluvial nature.

Within the Serradinho Member the dominant GR1 facies association is indicative of fluvial type of sedimentation, probably a braided system (Prothero & Schwab, 1996). The meter scale fining-upward cycles may reflect lateral shifts of the main channels of the fluvial system. The erosional surfaces bounding these cycles probably correspond to 4th or 5th order bounding surfaces, sensu Miall (1996). To the top of the Monsarros Fm., the appearance of GR2 facies association is indicative of an increased importance of gravity driven sediment transport. Several fining-upward cycles have matrix-supported conglomerates and inverse grading can be observed in several instances. GR2 facies association shows some similarities with SG2 facies association although the main transport mechanism is probably stream-flow. The red patina is indicative of more intense weathering of the rocks prior to their burial. This change can be tentatively explained by renewed tectonic activity in the catchment areas. The mixing of rounded and well rounded clasts (dominant in the underlying sequence) and sub-angulose to angulose clasts suggests that the previously available catchment areas are still supplying sediments, but others became available as the surrounding relief was renewed.

The influence of tectonism on the Buçaco basin can be detected in two main scales of events. The appearance of a trench along an important fault zone, either by a simple fault escarpment or a fully developed releasing bend (originating a pull-apart basin – see Flores et al., 2010 and Gama Pereira et al., 2008) promoted the onset of sedimentation. The same scale of events probably originated the end of sedimentation as the basin and surrounding areas were compressed and deformed, leading to the current synclinal structure (Domingos et al., 1983; Gama Pereira et al., 2008). These compressive events may explain the increased relevance of gravity driven sedimentation of the uppermost part of the Monsarros Fm. Another scale of tectonic events is probably related to the sudden shifts of transported lithologies. These could be related with small fault movements exposing different lithologies in the catchment areas subsequently eroded and deposited in the basin (compare for example Wagreich & Strauss, 2005). Only the peaks of schist clasts abundance described above can be used to trace these events although they were probably more frequent. Fault movements exposing yet more quartzite- or quartz-bearing rocks would not result in detectable changes in the basin's sedimentary record. Both scales of events seem to be non-periodic. The meter scale fining-upward cycles and especially the significant changes in maximum clast size could suggest some tectonic influence, but are easily explained by simple fluvial system dynamics processes such as channel avulsion (Catuneanu, 2006; Jones & Schumm, 1999)

The palaeocurrent data show an overall trend of flow direction to the S and SW which is concordant with the provenance data obtained from the lithologies identified on the conglomerates: Quartzite and quartz dominating throughout and variable amounts of

black schist and other metapelites and metasandstones and rare mafic igneous rocks. All of these can be correlated with CXG and Ordovician units presently exposed to the E, in the CIZ. The Algeriz Fm. has the same transported lithologies. The pre-Pennsylvanian units presently cropping out to the W of the basin (Albergaria-a-Velha and Arada units –referred to as "Complexo Cristalofílico" in older literature) were probably not exposed during the deposition of the Buçaco Basin. Although there are black schist clasts that could be potentially correlated with these units, after extensive sampling of schist-rich conglomeratic beds not a single clast could be positively identified as belonging to the Albergaria-a-Velha unit. The differentiation of the several schistose units outcropping in this area is certainly difficult, but after the examination of hundreds of outcrops of the Albergaria-a-Velha and Arada units in the course of this work a critical eye is capable of such differentiation. In addition several clasts of these schists (the most similar with the Albergaria-a-Velha unit) were processed for palynology. The amount of organic matter was negligible, similar to palynology samples collected from dark grey and black schists of the CXG in this area and further North. The Albergaria-a-Velha unit consistently produces residues with considerable amounts of amorphous organic matter and commonly spores and microplankton (even if only fragmentary).

The source of sediments is clearly from the E (current coordinates) but the sediment transport in the basin seems to be closer to the main strike (N-S). Thus it is likely that the fluvial systems had catchment areas developing in the CIZ, eroding and transporting sediments to W (and SW?) into the basin and deflected to SW and S within the basin.

The dextral sense of the PTSZ (e.g. Chaminé et al., 2003; 2007) very likely altered the original orientation of the measured planes and lineaments. The amount of rotational (clock-wise) movement is uncertain.

Wagner et al. (1983) reported a schist-rich breccia bed at the ALG section resting unconformably over the "Complexo Cristalofílico". This outcrop was not observed. Additionally the contact between the two units in this area corresponds to a valley with no outcrops. The contact of the two units has been investigated in several sections in the area. Although outcrop conditions are poor, the contact is invariably materialized by a fault (visible along a road trench near Monte Novo and along road cuts near Buçaco). Ribeiro (1893) describes the same type of contact. He states that the "Complexo Cristalofílico" thrusts over the Pennsylvanian-Permian sediments prior to the deposition of the Triassic sediments (which lie unconformably over both units). Our observations are consistent with this interpretation.

The XRD results allow a differentiation of two main groups of clay mineralogy compositions. The first, corresponding to the Algeriz Fm., is characterized by varying proportions of illite and quartz, significant amounts of kaolinite, sparse occurrence of feldspars and chlorite, and vestigial and rare presence of gypsum, oxides (hematite) and nepouite. The presence of muscovite, $2M_1$ illite and quartz are indicative that at least an important part of the clay fraction is inherited (Weaver, 1989). Wagner et al. (1983) suggest that the basal formation includes a significant proportion of soil, eroded during high-energy transport episodes. The presence of oxides and nepouite could indicate the presence of Oxisols in the source area (Dixon, 1998; Weaver, 1989), thus a prevailing hot, humid palaeoclimate (e.g. Soil Survey Staff, 1998). The main erosional products of low relief areas covered by oxisols, transported by fluvial systems, are solutes and very fine grained material (Weaver, 1989). In the case of the Buçaco basin the source area is suspected to be at a considerably higher ground (Wagner et al., 1983, Wagner and Sousa, 1983) and specifically for the Gralheira and Parada Members, the type of sedimentation is

clearly gravitational, with little water (debris-flows and sheet-floods). The red beds of the Algeriz Fm. could, at first glance, indicate a hot arid palaeoclimate (see, for example, a review of arid continental depositional environments in Nichols, 1999). A closer look reveals the presence of thin, dark grey, organic matter-rich, siltstones and sandstone beds within the Algeriz Fm., probably resulting from ponds formed between the debris-flow and sheet-flood events. These ponds probably would not develop with a prevailing hot and dry palaeoclimate (Nichols, 1999)

Higher in the sequence (Monsarros Fm.), the clay fraction mineralogy shifts gradually to a fairly constant pattern of similar amounts of quartz, illite and kaolinite. The more regular and less diversified composition of the clay fraction is indicative of a greater chemical and physical sorting of the transported rocks/minerals (Weaver, 1989). The decrease of the I/K ratio possibly reflects an increase of the amount of weathering in the source area and thus the amount of kaolinite transported by fluvial systems into the basin, considering that kaolinite is frequently the dominant component of soils derived from metamorphic rocks (Jonhson, 1970). Correlation between the relative amount of transported and sedimented kaolinite and intensity of weathering has been described for recent rivers (see Weaver, 1989 p. 200-205). The vertical sampling intervals are too wide to infer on specific causes for the observed trends.

The palynology results indicate that the sediments of the Buçaco basin most likely range from the middle to upper NBM miospore biozone of Clayton et al., 1977, corresponding to late Stephanian (Late Stephanian C – Stephanian D in older literature (e.g. Clayton et al., 1977); Stephanian C in more recent literature). Considering the new division of the Carboniferous system (Heckle & Clayton, 2006) the age is probably Early Gzhelian. The definitive correlation of the global and west European divisions of the Carboniferous has not been achieved; compare for example the table in Heckle & Clayton (2006) and the correlation of the Time Scale Creator software based on data from the International Commission on Stratigraphy. Thus there is some uncertainty regarding the ascription of the Buçaco basin's sediments to a globally-defined stage or part of a stage. The assemblages show no evidence of "Autunian" rocks being present in the basin (sensu lowermost Permian).

The thermal history of this area, including the underlying lower Palaeozoic rocks and the overlying Lusitanian basin sequence was addressed by Uphoff (2005) who also discussed the possible oil play formed by these units. He considered that there were no considerable gaps and no erosion from the end of Buçaco basin sedimentation (Late Pennsylvanian) to the beginning of the sedimentation of the Mesozoic Lusitanian basin (Carnian (Late Triassic) – Grés de Silves Fm.). The angular unconformity separating the Buçaco basin rocks and the Grés de Silves Fm. indicates that the former was exposed by Late Triassic times. However the thermal maturity by that time in not known nor the depth to which it was buried. The data collected from the thin impure coal seams and palaeobotanical sites of the Grés de Silves Formation in the neighbouring area (Anadia and Lograssol) show Rr values between 0,85 and 1,1%. This is consistent the interpretation of Uphoff (2005) who considers that the maximum burial depth (and maximum temperature attained) of the Buçaco basin rocks occurred during the Mesozoic as the Lusitanian basin developed. However, the geodynamic setting of the Buçaco basin along an important shear zone and its plausible pull-apart structure (Gama Pereira et al., 2008; Flores et al., 2010) may suggest a pre-Late Triassic burial and exhumation history. The high heat flow and thus high geothermal gradients recorded and estimated in pull-apart basins, such as Pennsylvanian alluvial-fluvial basins of Northern Spain (e.g. Frings et al., 2004) would

result in an increased maturation at relatively shallow depths. Considering an extremely high geothermal gradient such as 85ºC/Km estimated for pull-part basins, it would require ca.2km of sediments to be deposited and completely eroded during a time interval of ca. 72Ma (latest Pennsylvanian – Carnian) for the Buçaco basin rocks to reach their current maturation (Fig. 4.17 and 4.18). Alternatively the thrusting and later erosion of older rocks (Arada and Albergaria-a-Velha units – Ossa-Morena Zone) over the basin would produce the same effect (Fig. 4.17 and 4.18), but nappe structures of this magnitude are unknown for this area. Thus it is probable that the Buçaco basin underwent a burial and exhumation process prior to Late Triassic, but never reached the temperatures attained during the Mesozoic.

A simple thermal and burial history model was constructed using Petromod1D by constructing a hypothetical well. The input data is compiled in table 4.5 and is based on Palain (1976) for the thicknesses and lithologies of the Upper Triassic and Lower Jurassic sequences (A1, A2, B1, B2, C1 and C2) and Adloff et al. (1974) for the corresponding ages. Calibration data for Triassic and Pennsylvanian rocks (temperature) derives from vitrinite reflectance data presented in this chapter.

Name	Top	Base	Thickness	Eroded	Sedim. Age		Erosion age		Lithology
					From	To	From	To	
Jurassic+Cretaceous	0	5000	5000		189,6	92			SAND&LIME
C2	5000	5080	80		196,5	189,6			LIMEmarly
C1	5080	5088	8		197	196,5			SHALEevap
B2	5088	5106	18		198	197			DOLOMITE
B1	5106	5171	65		203	198			SAND&SHALE
Hiatus?	5171	5171	0		215	203			none
A2	5171	5421	250		217	215			SAND&SHALE
A1	5421	5671	250		228	217			SANDcongl
Hiatus+erosion?	5671	5671	0	1600	258	228	258	228	none
Unknown Permian unit	5671	7271	0 (or 1600)	1600	298	258	258	228	SANDSTONE
Serradinho Member	7271	7821	550		299	298			SANDcongl
Vale da Mó Member	7821	7921	100		299,5	299			SHALE&SILT
Parada Member	7921	8021	100		300	299,5			SANDcongl
Gralheira Member	8021	8071	50		300,5	300			SANDcongl

Table 4.5 – Input data for the Petromod 1D basin modelling of Figs. 4.17 and 4.18. The Jurassic and Cretaceous thicknesses and ages are part of the model merely to include a post-Triassic overburden.

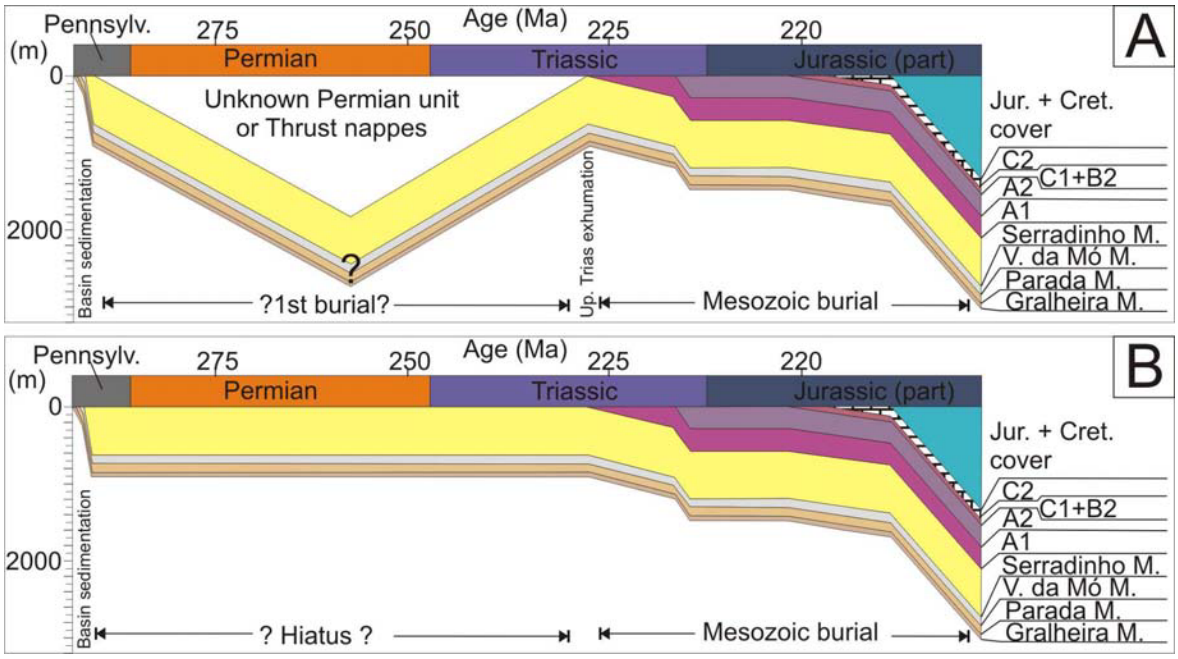

Fig. 4.17 – Simplified Lopatin Burial depth Vs Age diagrams. Redrawn from a Petromod 1D model output. A – Buçaco basin rocks with pre-Late Triassic burial and exhumation. B – Buçaco basin rocks with a single, essentially Mesozoic, burial history.

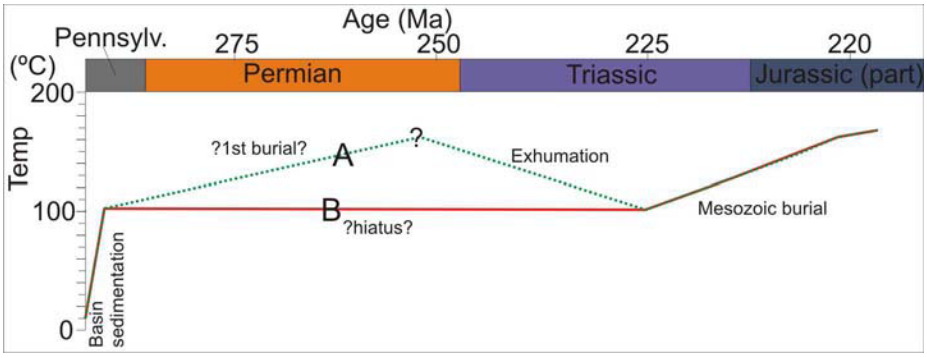

Fig. 4.18 – Hypothetic thermal history of the Buçaco basin. Redrawn from a Petromod 1D output. A – Thermal history with pre-Late Triassic burial and exhumation. B – Thermal history with long hiatus (latest Pennsylvanian – Early Triassic) and Mesozoic burial.

4.5 Systematic Palynology

For the systematic palynology the turmal division used here is modified from Potonié (1970) in Traverse (2007). The frequency of each taxon is indicated. The frequency ranges of Smith and Butterworth (1967) were applied and are summarized in the following table:

Rare	<0,5%
Frequent	0,5-2%
Common	2,1-5%
Very common	5,1-10%
Abundant	>10%

Anteturma SPORITES Potonié, 1893

Turma TRILETES (Reinsch) Dettmann, 1963

Subturma AZONOTRILETES (Luber) Dettmann, 1963

Infraturma LAEVIGATI (Bennie & Kiston) Potonié, 1956

Genus *Leiotriletes* (Naumova) Potonié & Kremp, 1954
Occurrence: frequent
Leiotriletes levis (Kosanke) Potonié & Kremp, 1955 (Pl. 4.1a)
Occurrence: rare
Leiotriletes sp. (Pl. 4.1b)
Occurrence: frequent

Genus *Punctatisporites* (Ibrahim) Potonié & Kremp, 1954
Occurrence: rare
Punctatisporites sp.
Occurrence: rare

Infraturma APICULATI (Bennie & Kidston) Potonié, 1956

Subinfraturma GRANULATI Dybová & Jachowicz, 1957

Genus *Granulatisporites* (Ibrahim) Potonié & Kremp, 1954
Occurrence: rare
Granulatisporites aff. *verrucosus* (Wilson & Coe) Schopf, Wilson & Bentall, 1944 (Pl. 4.1c)
Occurrence: rare
Granulatisporites sp.
Occurrence: rare

Subinfraturma VERRUCATI Dybová & Jachowicz, 1957

Genus *Columinisporites* Peppers, 1964
Occurrence: frequent
Columinisporites heyleri (Doubinger) Alpern & Doubinger, 1973 (Pl. 4.1d)
Occurrence: rare
Columinisporites sp.
Occurrence: frequent

Genus *Verrucosisporites* (Ibrahim) Smith & Butterworth, 1967
Occurrence: common
Verrucosisporites cf. *insuetus* Platford & Dino, 2000 (Pl. 4.1e)
Occurrence: rare
Verrucosisporites cf. *microverrucosus* Ibrahim, 1933 (Pl. 4.1f)
Occurrence: rare

Verrucosisporites cf. *morulatus* (Knox) Smith & Butterworth, 1967 (Pl. 4.1g)
Occurrence: rare
Verrucosisporites cf. *sifati* (Ibrahim) Smith & Butterworth, 1967 (Pl. 4.1h)
Occurrence: rare
Verrucosisporites cf. *verrucosus* (Ibrahim) Smith & Butterworth, 1967 (Pl. 4.1i)
Occurrence: rare
Verrucosisporites spp. (e.g. Pl. 4.1j)
Occurrence: common

Subinfraturma NODATI Dybová & Jachowicz, 1957

Genus *Apiculatisporites* Potonié & Kremp, 1956
Occurrence: rare
Apiculatisporites sp. (Pl. 4.1k)

Infraturma MURORNATI Potonié & Kremp. 1954

Genus *Convolutispora* Hoffmeister, Staplin & Malloy, 1955
Occurrence: frequent
Convolutispora sp. (Pl. 4.1l)
Occurrence: frequent

Genus *Dictyotriletes* (Naumova). Smith & Butterworth, 1967
Occurrence: common
Dictyotriletes bireticulatus (Ibrahim 1932) Potonié & Kremp, 1955 (Pl. 4.1m)
Occurrence: rare
Dictyotriletes aff. *densoreticulatus* Potonié & Kremp, 1955 (Pl. 4.1n)
Occurrence: rare
Dictyotriletes spp.
Occurrence:common

Subturma ZONOTRILETES Waltz, 1935

Infraturma AURICULATI (Schopf) Dettmann, 1963

Genus *Ahrensisporites* (Potonie & Kremp) Horst, (1955)
Occurrence: rare
Ahrensisporites sp.
Occurrence: rare

Genus *Tripartites* Schemel, 1950
Occurrence: rare
Tripartites sp. (Pl. 4.1o)
Occurrence: rare

Genus *Triquitrites* (Wilson & Coe) Potonié & Kremp, 1954
Occurrence: common
Triquitrites angulatus Kosanke, 1950 (Pl. 4.1p)

Occurrence: rare
Triquitrites desperatus Potonié & Kremp, 1955 (Pl. 4.1q)
Occurrence: rare
Triquitrites dividuus Wilson & Hoffmeister, 1956 (Pl. 4.1r)
Occurrence: rare
Triquitrites tribullatus (Ibrahim) Schopf, Wilson & Bentall, 1944 (Pl. 4.1s)
Occurrence: rare
Triquitrites cf. *triturgidus* (Loose) Schopf, Wilson & Bentall, 1944
Occurrence: rare
Triquitrites spp. (e.g. Pl. 4.1t)
Occurrence: frequent

Infraturma CINGULATI (Potonié & Klaus) Dettmann 1963

Genus *Reticulatisporites (*Ibrahim) Neves, 1964
Occurrence: rare
aff. *Reticulatisporites reticulatus* Ibrahim, 1933 (Pl. 4.2a)
Occurrence: rare

Genus *Knoxisporites* (Potonié & Kremp) Neves, 1961
Occurrence: rare
Knoxisporites sp. (Pl. 4.2b)
Occurrence: rare

Subturma ZONOLAMINATITRILETES Smith & Butterworth, 1967

Infraturmae CRASSITI (Bharadwaj & Venkatachala) Smith & Butterworth, 1967 and CINGULICAVATI Smith & Butterworth, 1967

Genus *Cirratriradites* Wilson & Coe, 1940
Occurrence: rare
Cirratriradites sp. (Pl. 4.2c)
Occurrence: rare

Genus *Crassispora* Bharadwaj, 1957
Occurrence: common
Crassispora kosankei (Potonié & Kremp) Bharadwaj, 1957 (Pl. 4.2d)
Occurrence: frequent
Crassispora spp. (e.g. Pl. 4.2e)
Occurrence: frequent

Genus *Densosporites* (Berry) Butterworth ‚Jansonius, Smith & Staplin, 1964
Occurrence: common
Densosporites cf. *anulatus* (Loose) Smith & Butterworth, 1967 (Pl. 4.2f)
Occurrence: rare
Densosporites cf. *dentatus* (Waltz) Potonié & Kremp, 1956 (Pl. 4.2g)
Occurrence: rare
Densosporites cf. *gracilis* Smith & Butterworth, 1967 (Pl. 4.2h)

Occurrence: rare
Densosporites cf. *sphaerotriangularis* Kosanke, 1950 (Pl. 4.2i)
Occurrence: rare
Densosporites variomarginatus Playford, 1962 (Pl. 4.2j)
Occurrence: rare
Densosporites spp. (e.g. Pl. 4.2k)
Occurrence: common

Genus *Lundbladispora* (Balme) Playford, 1965
Occurrence: rare
aff. *Lundbladispora gigantea* (Alpern) Doubinger, 1968 (Pl. 4.2l)
Occurrence: rare

Genus *Lycospora* (Schopf, Wilson & Bentall) Somers, 1972
Occurrence: common
Lycospora granulata Kosanke, 1950 (Pl. 4.2m)
Occurrence: rare
Lycospora cf. *parva* Kosanke, 1950 (Pl. 4.2n)
Occurrence: rare
Lycospora paulula Artüz, 1957 (Pl. 4.2o)
Occurrence: rare
Lycospora punctata Kosanke, 1950 (Pl. 4.2p)
Occurrence: frequent
Lycospora pusilla (Schopf, Wilson & Bentall) Somers, 1972 (Pl. 4.2q)
Occurrence: frequent
Lycospora sp. (Pl. 4.2r)
Occurrence: common

Supersubturma PSEUDOSACCITRILETES Richardson, 1965

Infraturma MONOPSEUDOSACCITI Smith & Butterworth, 1967

Genus *Endosporites* Wilson & Coe, 1940
Occurrence: frequent
Endosporites cf. *vesicatus* Kosanke, 1950 (Pl. 4.2s)
Occurrence: rare
Endosporites spp. (e.g. Pl. 4.2t)
Occurrence: frequent

Genus *Guthoerlisporites* Bhardwaj, 1954
Occurrence: common
Guthoerlisporites magnificus Bhardwaj, 1954 (Pl. 4.2u)
Occurrence: frequent
Guthoerlisporites sp. (Pl. 4.2v)
Occurrence: frequent

Genus *Nuskoisporites* Potonié & Klaus, 1954
Occurrence: rare

Nuskoisporites sp. (Pl. 4.2w)
Occurrence: rare

Subturma PERINOTRILETES Erdtman, 1947

Genus *Vestispora* (Wilson & Hoffmeister) Wilson & Venkatachala, 1963
Occurrence: rare
cf. *Vestispora fenestrata* (Kosanke & Brokaw) Spode, in Smith & Butterworth, 1967 (Pl. 4.3a)
Vestispora sp. A (Pl. 4.2x)
Description: Ellipsoidal outline, maximum 100 µm long and 70µm wide. Trilete mark small, often indistinct, rays less than 10 µm long. Slightly raised lips. Laevigate surface. Irregularly placed concentric rims or plications with varying width (1 to 6 µm) around equatorial area, occupying about half of the proximal surface area. Distal surface is seldom observed but appears to have the same rims or plications although restricted to the outermost part of the equatorial area.
Occurrence: frequent
Vestispora sp. (Pl. 4.2y)
Occurrence: rare

Turma MONOLETES Ibrahim, 1933

Subturma AZONOMONOLETES Luber, 1935

Infraturma LAEVIGATOMONOLETI Dybová & Jachowicz, 1957

Genus *Laevigatosporites* Ibrahim, 1933
Occurrence: very common
Laevigatosporites cf. *minimus* (Wilson & Coe) Schopf, Wilson & Bentall, 1944 (Pl. 4.3b)
Occurrence: rare
Laevigatosporites minor Loose, 1934 (Pl. 4.3c)
Occurrence: frequent
Laevigatosporites ovalis Kosanke, 1950 (Pl. 4.3d)
Occurrence: rare
Laevigatosporites cf. *perminutus* Alpern, 1958 (Pl. 4.3e)
Occurrence: rare
Laevigatosporites spp. (e.g. Pl. 4.3f)
Occurrence: very common

Infraturma SCULPTATOMONOLETI Dybová & Jachowicz, 1957

Genus *Cheiledonites* Doubinger, 1957
Occurrence: common
Cheiledonites gigantea (Alpern) Doubinger, 1968 (Pl. 4.3g)
Occurrence: frequent
Cheiledonites major Doubinger, 1957 (Pl. 4.3h)
Occurrence: rare
Cheiledonites potoniei Doubinger, 1957 (Pl. 4.3i)

Occurrence: rare
Cheiledonites sp.
Occurrence: common

Genus *Punctatosporites* Ibrahim, 1933
Occurrence: frequent
Puntactosporites cf. *minutus* Ibrahim, 1933 (Pl. 4.3j)
Occurrence: rare
Punctatosporites sp.
Occurrence: frequent

Genus *Spinosporites*
Occurrence: common
Spinosporites exiguus Upshaw & Hedlund, 1967 (Pl. 4.3k)
Occurrence: frequent
Spinosporites spinosus Alpern, 1958 (Pl. 4.3l)
Occurrence: frequent
Spinosporites sp. (Pl. 4.3m)
Occurrence: frequent

Genus *Torispora* Balme, 1952
Occurrence: rare
Torispora sp. (Pl. 4.3n)
Occurrence: rare

Genus *Thymospora* (Wilson & Venkatachala) Alpern & Doubinger, 1973
Occurrence: common
Thymospora obscura Wilson & Venkatachala, 1963 (Pl. 4.3o)
Occurrence: rare
Thymospora pseudothiessenii (Kosanke) Alpern & Doubinger, 1973 (Pl. 4.3p)
Occurrence: frequent
Thymospora thiessenii (Kosanke) Wilson & Venkatachala, 1963 (Pl. 4.3q)
Occurrence: frequent
Thymospora sp. (Pl. 4.3r)
Occurrence: common

Anteturma POLLENITES Potonié, 1931

Turma SACCITES Erdtmann, 1947

Subturma MONOSACCITES (Chitaley) Potonié & Kremp, 1954

Infraturma TRILETESACCITI Leschik, 1955

Genus *Cordaitina* (Samoilovich) Hart, 1965
Occurrence: frequent
Cordaitina uralensis (Luber) Dibner, 1971 (Pl. 4.3s)
Occurrence: rare

Cordaitina spp. (e.g. Pl. 4.3t)
Occurrence: frequent

Genus *Dyupetalum* Jansonius & Hills, 1979
Occurrence: common
Dyupetalum sp. (Pl. 4.3v)
Occurrence: common

Genus *Latensina* Alpern, 1958
Occurrence: frequent
Latensina trileta Alpern, 1958 (Pl. 4.3u)
Occurrence: frequent

Genus *Wilsonites* Kosanke, 1950
Occurrence: common
Wilsonites aff. *delicatus* Kosanke, 1950 (Pl. 4.4a)
Occurrence: rare
Wilsonites cf. *vagus* Inossova, 1976 (Pl. 4.3x)
Occurrence: rare
Wilsonites spp. (e.g. Pl. 4.3x)
Occurrence: common

Infraturma ALETESACCITI Leschik, 1955

Genus *Florinites* Schopf, Wilson & Bentall, 1944
Occurrence: very common
Florinites bederi Pittau et al, 2008 (Pl. 4.4b)
Occurrence: frequent
Florinites aff. *diversiformis* Kosanke, 1950 (Pl. 4.4c)
Occurrence: rare
Florinites sp. A (Pl. 4.4e)
Description: Oval to ellipsoidal overall shape 80 to 140μm long and 50 to 80μm wide. The saccus is often folded changing the overall shape and dimensions of the miospore. Corpus minute, less than 20μm in maximum dimension, usually centred, well defined and darker than saccus. Trilete mark not discernible. Saccus laevigate with (internal?) irregular and incomplete reticulate pattern.
Remarks: *Florinites* sp. specimens with similar morphology and very small corpus have also been recorded from the Kasimovian Santa Susana Basin in SW Portugal.
Occurrence: frequent
Florinites spp. (e.g. Pl. 4.4d)
Occurrence: very common

Infraturma VESICULOMONORADITI Pant, 1954

Genus *Potonieisporites* (Bharadwaj) Bharadwaj, 1964
Occurrence: very common
Potonieisporites bhardwajii Remy & Remy, 1961 (Pl. 4.4f)
Occurrence: very common

Potonieisporites clarus Shwartsman in Inossova et al., 1976 (Pl. 4.4g)
Occurrence: frequent
Potonieisporites novicus Bharadwaj, 1954 (Pl. 4.4h)
Occurrence: rare
Potonieisporites sp.A (Pl. 4.4i)
Description: Bilateral, monosaccate, monolete pollen grain. Oval to ellipsoidal outline 130-150µm X 50-10µm maximum dimensions. Very large corpus occupying over ¾ of the grain with an incomplete crassitude (ca. 6µm wide). Saccus often folded with a vermiculate to irregular and incomplete reticulate pattern. Monolete mark simple, extending from half to full width of the corpus.
Occurrence: frequent
Potonieisporites sp. (Pl. 4.4j)
Occurrence: very common

Subturma DISACCITES Cookson, 1947

Disaccites non striatti (Pl. 4.4k)
Occurrence: frequent

Infraturma DISACCIATRILETI (Leschik) Potonié, 1958

Genus *Vesicaspora* (Schemel) Wilson & Venkatachala, 1963
Occurrence: rare
Vesicaspora sp. (Pl. 4.4l)
Occurrence: rare

Infraturma DISACCITRILETI Leschik, 1955

Genus *Illinites* (Kosanke) Potonié & Kremp, 1954
Occurrence: rare
Illinites elegans Kosanke, 1950 (Pl. 4.4m)
Occurrence: rare
Illinites sp.
Occurrence: rare

Genus *Platysaccus* (Naumova) Potonié & Klaus, 1954
Occurrence: rare
Platysaccus sp. (Pl. 4.4n)
Occurrence: rare

Subturma STRIATITES Pant, 1954

Genus *Corisaccites* Venkatachala & Kar, 1966
Occurrence: rare
aff. *Corisaccites* sp. (Pl. 4.4o)
Occurrence: rare

Genus *Lueckisporites* Potonié & Klaus, 1959

Occurrence: rare
Lueckisporites sp. (Pl. 4.4p)
Occurrence: rare

Genus *Protohaploxypinus* (Samoilovich) Morbey, 1975
Occurrence: rare
Protohaploxypinus jacobii (Jansonius) Hart, 1964 (Pl. 4.5a)
Occurrence: rare

Subturma POLYSACCITES Cookson, 1947

Genus *Alatisporites* Ibrahim, 1933
Occurrence: rare
Alatisporites sp. (Pl. 4.4q)
Occurrence: rare

Turma PLICATES (Naumova) Potonié & Kremp, 1954

Subturma PRAECOLPATES Potonié & Kremp, 1954

Genus *Schopfipollenites* Potonié & Kremp, 1954
Occurrence: very common
Schopfipollenites ellipsoides (Ibrahim) Potonié & Kremp, 1954 (Pl. 4.5b)
Occurrence: frequent
Schopfipollenites ovalis Schwartsman, 1976 (Pl. 4.5c)
Occurrence: common
Schopfipollenites parvus Schwartsman, 1976 (Pl. 4.5d)
Occurrence: frequent
Schopfipollenites spp. (e.g. Pl. 4.5e)
Occurrence: common

Subturma POLYPLICATES Erdtman, 1952

Genus *Vittatina* (Luber) Wilson, 1962
Occurrence: frequent
Vittatina costabilis Wilson, 1962 (Pl. 4.5g)
Occurrence: rare
Vittatina simplex Jansonius, 1962 (Pl. 4.5f)
Occurrence: rare
Vittatina sp. (Pl. 4.5h)
Occurrence: frequent

Subturma MONOCOLPATES (Wodehouse) Iverson & Troels-Smith, 1950

Genus *Cycadopites* (Wodehouse) Wilson & Webster, 1946
Occurrence: rare
Cycadopites sp. (Pl. 4.5i)
Occurrence: rare

Acknowledgements

Deolinda Flores and the Centro de Geologia of the Faculty of Sciences of the Porto University are gratefully acknowledged for the logistical and scientific support on the organic petrology section. Geoff Clayton (Trinity College Dublin) for clarifying some aspects of miospore biostratigraphy. Luís Gama Pereira (Coimbra University) and Hélder Chaminé (Instituto Superior de Engenharia do Porto) for the helpful discussions on the geology of this area. Madalena Fonseca (Instituto Superior de Agronomia) for the logistical support on the XRD data and discussion of the results. Pedro Dinis of the Coimbra University for the discussions on the sedimentology of the basin.

References

ADLOFF, M. C., DOUBINGER, J. & PALAIN, C., 1974. Contribution à la Palynologie du Trias et du Lias Inférieur du Portugal, «Grès de Silves» du Nord du Tage. Comunicações dos Serviços Geológicos de Portugal 58: 48-91.

BARKER, C. E., 1988. Geothermics of petroleum systems: implications of the stabilisation of kerogen thermal maturation after a geologically brief heating duration at peak temperature. In: Magoon, L. B. (ed.) Petroleum systems of the United States. United States Geological Survey Bulletin 1870: 26 - 29.

BARKER, C.E. & GOLDSTEIN, R.H., 1990. Fluid-inclusion technique for determining maximum temperature in calcite and its comparison to vitrinite reflectance geothermometer. Geology 18: 1003–1006.

BARKER, C.E. & PAWLEWICZ, M.J., 1986. The correlation of vitrinite reflectance with maximum temperature inhumic organicmatter. In: Bunterbath, G., Stegena, L. (Eds.), Paleothermics. Springer-Verlag, Berlin, Heidelberg: 79–93.

BROOKFIELD, M. E., 2004. Principles of Stratigraphy. Blackwell Publishing: 342pp.

CARVALHO, G. S. D., 1949. Notícias sobre os seixos polidos do conglomerado Antracolítico da Serra do Buçaco. Memórias e Notícias Universidade de Coimbra 23: 29-31.

CATUNEANU, O., 2006. Principles of Sequence Stratigraphy. Elsevier: 386pp.

CHAMINÉ, H. I., GAMA PEREIRA, L. C., FONSECA, P. E., MOÇO, L. P., FERNANDES, J. P., ROCHA, F. T., FLORES, D., PINTO DE JESUS, A., GOMES, C., SOARES DE ANDRADE, A. A. and ARAÚJO, A., 2003. Tectonostratigraphy of Middle and Upper Palaeozoic black shales from the Porto-Tomar-Ferreira do Alentejo shear zone (W Portugal): new perspectives on the Iberian Massif. Geobios 36(6): 649-663.

CHAMINÉ, H. I., FONSECA, P. E., PINTO DE JESUS, A., GAMA PEREIRA, L. C., FERNANDES, J. P., FLORES, D. MOÇO, L. P., DIAS DE CASTRO, R., GOMES, A.,

TEIXEIRA, J., ARAÚJO, M. A., SOARES de ANDRADE, A. A., GOMES C. & ROCHA, F. T., 2007. Tectonostratigraphic imbrications along strike-slip major shear zones: an example from the early Carboniferous of SW European Variscides (Ossa-Morena Zone, Portugal). In: Theo E. Wong (Ed.), XVth International Congress on Carboniferous and Permian Stratigraphy (Utrecht, 2003). Royal Dutch Academy of Arts and Sciences, Amsterdam, Edita NKAW: 405-416.

CLAYTON, G., COQUEL, R., DOUBINGER, J., GUEINN K.J., LOBOZIAK, S., OWENS, B. & STREEL, M., 1977. Carboniferous Miospores of Western Europe: illustration and zonation. Meded. Rijks Geol. Dienst 29: 1-71.

COURBOULEIX, S., 1972. Etude géologique des régions de Anadia et de Mealhada, au Nord de Coimbra, Portugal. Diplome d'Etudes Supérieures Université Claude Bernard Lyon: 342 p

COURBOULEIX, S., 1974. Etude géologique des régions de Anadia et de Mealhada : le socle, le primaire et le trias. Comunicações dos Serviços Geológicos de Portugal 57: 5-37

DINIS, P. & REIS, R. P. D., 2007. The Permo-Carboniferous lake and lake margin environments of Buçaco Basin (West Portugal). IAS 2007, Patras.

DIXON, J. B., 1998. Roles of clays and oxide minerals in soils. In: Parker, A. & Rae, J. E. Environmental interactions of clays 2. Springer: 37-50.

DOMINGOS, L. C. G., FREIRE, J. L. S., GOMES da SILVA, F., GONÇALVES, F., PEREIRA, E. & RIBEIRO, A., 1983. The structure of the intramontane upper Carboniferous basins in Portugal. Memórias dos Serviços Geológicos de Portugal 29: 187-194.

FLORES, D., PEREIRA, L. C. G., RIBEIRO, J., PINA, B., MARQUES, M. M., RIBEIRO, M. A., BOBOS, I. & JESUS, A. P. D., 2010. The Buçaco Basin (Portugal): Organic petrology and geochemistry study. International Journal of Coal Geology 81 (4): 281-286

FLORIN, R., 1940. Publ. Mus. Lab. Min. Geol. Fac. Ciencias Porto. XVIII

FRINGS, K., LUTZ, R., WALL, H. and WARR, L., 2004. Coalification history of the Stephanian Ciñera-Matallana pull-apart basin, NW Spain: Combining anisotropy of vitrinite reflectance and thermal modelling. International Journal of Earth Sciences 93(1): 92-106.

FRITZ, W. & MOORE, J., 1988. Basics of physical Stratigraphy and Sedimentology. John Willey & sons. New York: 371pp

GAMA PEREIRA, L. C., PINA, B., FLORES, D. and ANJOS RIBEIRO, M., 2008. Bacia Permo-Carbónica do Buçaco : um modelo de Pull-Apart. 8ª Conferência Anual do CGET : resumos alargados. Sant'ovaia, H., Dória, A. and Ribeiro, M. D. A. Universidade do Porto.

Faculdade de Ciências. Departamento de Geologia, Faculdade de Ciências da Universidade do Porto: 110-113.

GOMES, B. A., 1865. Flora fóssil do terreno carbonífero das visinhanças do Porto, Serra do Bussaco e Moinho d'Ordem próximo de Alcácer do Sal. Commissão Geológica de Portugal. Memória. Lisboa.

GOMES, C. R., DIEZ, J. B., MOHAMED, K., VILLANUEVA, U., SOARES, A. F. & REY, D., 2005. Nuevos datos palinoestratigráficos y paleomagnéticos de los afloramientos estefano-pérmicos del Grupo Buçaco en el sinclinal de Santa Cristina (Norte de Coimbra, Portugal). MAGIBERIII. Barcelona, Spain, Universitat de Barcelona.

JOHNSON, L. J., 1970. Relation to lithology of the parent rock and other factors - I. Clays and Clay Minerals 18: 247-260.

JONES, L. S. & SCHUMM, S. A., 1999. Causes of avulsion: an overview. In: Dwight, N. S. & Rogers, J., Fluvial sedimentology. Special Pub. International Association of Sedimentologists 28: 171-178.

LIMA, W., 1888/1892. Notícia sobre as camadas da série permo-carbónica do Bussaco. Communicações da Commissão de Trabalhos Geológicos de Portugal (Lisboa) 2: 129-152.

LIMA, W., 1894. Sobre uma espécie critica do Rothliegendes. Revista Sci. Natur. Soc. (Porto) 3 (11): 1-4.

MIALL, A., 1996. The geology of fluvial deposits: sedimentary facies, basin analysis and petroleum geology. Springer-Verlag, Berlin. 582 p.

NEIVA, J. M. C., 1943. Os conglomerados antracolíticos e a idade de algumas formações eruptivas portuguesas. Boletim da Sociedade Geológica de Portugal 2(1-2): 71-80

NICHOLS, G., 1999. Sedimentology and Stratigraphy. Blackwell Publishing:: 335pp.

PALAIN, C., 1976. Une Série Détritique Terrigène. Les «grès de Silves»: Trias et Lias Inférieur du Portugal. Memórias dos Serviços Geológicos de Portugal (Nova série). 25: 363p.

PALAIN, C., J. DOUBINGER, ADLOFF, M C., 1977. La base du Mesozoique du Portugal et les problemes poses par la stratigraphie du Trias. Triasico y Permico de Espana. C. Virgili. Madrid, Spain, Consejo Superior de Investigaciones Cientificas, Universidad de Madrid. 77; 4: 269-280.

POTONIÉ, R., 1970. Synopsis der Gattungen der Sporae dispersae V. Nachträge zu allen Gruppen (Turmae). Beihefte zum Geologischen Jahrbuch 87: 1–22

PROTHERO, D. R. & SCHWAB, F., 1996. Sedimentary geology. An introduction to sedimentary rocks and Stratigraphy. W. H. Freeman and Company: 575pp

RIBEIRO, C., 1853. On the Carboniferous and Silurian formations of the neighbourhood of Bussaco in Portugal. (With notes and a description of the animal remains by Daniel Sharpe, J. W. Salter and T. Rupert Jones, and an account of the vegetable remains by Charles J. F. Bunbury). Quarterly Journal Geological Society London (London): 135-160.

SOIL SURVEY STAFF, 1998. Keys to Soil Taxonomy, 8th Edn. U. S. Department of Agriculture, Natural Resources Conservation Services: 327pp.

DE SOUSA M. J. & WAGNER, R. H., 1983. General description of the terrestrial Caboniferous basins in Portugal and history of investigations. Memórias dos Serviços Geológicos de Portugal. 29: 117-126.

SMITH, A. H. V. & BUTTERWORTH, M. A., 1967. Miospores in the coal seams of the Carboniferous of Great Britain. Special Papers in Palaeontology 1: 1-324.

TEIXEIRA, C., 1941a. O Antrocolítico do Bussaco e a sua flora fóssil. Comunicações dos Serviços Geológicos de Portugal 22: 19-28

TEIXEIRA, C., 1941b. W. de Lima e a flora fóssil do Permo-Carbónico português : fragmentos de uma monografia inédita, coordenadas. Comunicações dos Serviços Geológicos de Portugal 22: 3-17.

TEIXEIRA, C., 1944. O Antrocolítico Continental Português. (Estratigrafia e Tectónica). PhD Thesis. Universidade do Porto. Porto.

TEIXEIRA, C., 1945. O Antrocolítico Continental Português. (Estratigrafia e Tectónica). Boletim da Sociedade Geológica de Portugal 5 (1-2): 1-139

TEIXEIRA, C., 1947. Nota sobre um insecto fóssil do Autuniano do Buçaco. Comunicações dos Serviços Geológicos de Portugal 28: 107-110

TEIXEIRA, C., 1949. Plantas fósseis do Permo-Carbónico português. Comunicações dos Serviços Geológicos de Portugal 29: 177-186

TRAVERSE, A., 2007. Paleopalynology. Topics in Geobiology, 28. 2nd ed. Springer. 814p

UPHOFF, T. L., 2005. Subsalt (pre-Jurassic) exploration play in the northern Lusitanian Basin of Portugal. AAPG Bulletin 89(6): 699-714.

WAGNER, R. H. & DE SOUSA, M. J. & GOMES DA SILVA, F., 1983. Stratigraphy and fossil flora of the upper Stephanian C of Buçaco, North of Coimbra (Portugal). Contributions to the Carboniferous Geology and Palaeontology of the Iberian Peninsula. Sousa, M. J. L. D., Universidade do Porto, Faculdade de Ciencias, Mineralogia e Geologia. Volume dedicated to Wenceslau de Lima: 127-156.

WAGNER, R. H. & DE SOUSA, M. J., 1983. The Carboniferous Megafloras of Portugal – A revision of identifications and discussion of Stratigraphic ages. Memórias dos Serviços Geológicos de Portugal 29: 127-152.

WAGREICH, M., STRAUSS, P.E., 2005. Source area and tectonic control on alluvial fan development in the Miocene Fohnsdorf intramontane basin, Austria. In: HARVEY, A.M., MATHER, A.E. & STOKES, M. (Eds.): Alluvial Fans: Geomorphology, Sedimentology, Dynamics. Geological Society, London, Special Publications 251: 207-216.

WEAVER, R. (1989). Clays, Muds, and Shales, Elsevier. 837p.

WELLS, S. & HARVEY, A., 1987. Sedimentologic and geomorphic variations in storm generated alluvial fans, Hangill Fells, Northwest England. Bulletin Geological Society of America 98: 182-198.

Plates

Plate 4.1 – Sporomorphs of the Buçaco basin

a *Leiotriletes levis* (Kosanke) Potonié & Kremp, 1955
b *Leiotriletes* sp.
c *Granulatisporites* aff. *verrucosus* (Wilson & Coe) Schopf, Wilson & Bentall, 1944
d *Columinisporites heyleri* (Doubinger) Alpern & Doubinger, 1973
e *Verrucosisporites* cf. *insuetus* Platford & Dino, 2000
f *Verrucosisporites* cf. *microverrucosus* Ibrahim, 1933
g *Verrucosisporites* cf. *morulatus* (Knox) Smith & Butterworth, 1967
h *Verrucosisporites* cf. *sifati* (Ibrahim) Smith & Butterworth, 1967
i *Verrucosisporites* cf. *verrucosus* (Ibrahim) Smith & Butterworth, 1967
j *Verrucosisporites* spp.
k *Apiculatisporites* sp.
l *Convolutispora* sp.
m *Dictyotriletes bireticulatus* (Ibrahim 1932) Potonié & Kremp, 1955
n *Dictyotriletes* aff. *densoreticulatus* Potonié & Kremp, 1955
o *Tripartites* sp.
p *Triquitrites angulatus* Kosanke, 1950
q *Triquitrites desperatus* Potonié & Kremp, 1955
r *Triquitrites dividuus* Wilson & Hoffmeister, 1956
s *Triquitrites tribullatus* (Ibrahim) Schopf, Wilson & Bentall, 1944
t *Triquitrites* sp.

Plate 4.1

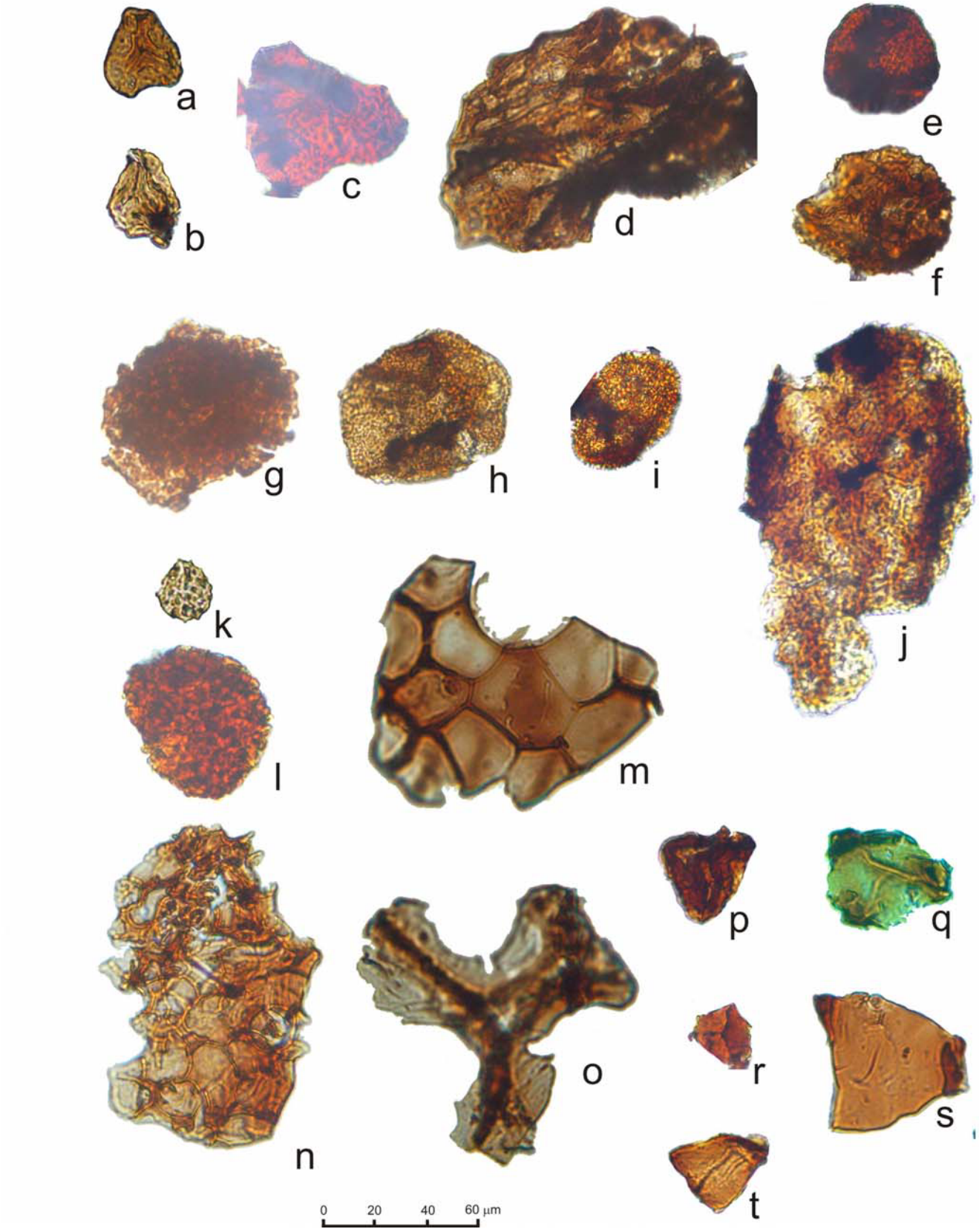

Plate 4.2 – Sporomorphs of the Buçaco basin

a aff. *Reticulatisporites reticulatus* Ibrahim, 1933
b *Knoxisporites* sp.
c *Cirratriradites* sp. *d*
d *Crassispora kosankei* (Potonié & Kremp) Bharadwaj, 1957
e *Crassispora* sp.
f *Densosporites* cf. *anulatus* (Loose) Smith & Butterworth, 1967
g *Densosporites* cf. *dentatus* (Waltz) Potonié & Kremp, 1956
h *Densosporites* cf. *gracilis* Smith & Butterworth, 1967
i *Densosporites* cf. *sphaerotriangularis* Kosanke, 1950 **/7**
j *Densosporites variomarginatus* Playford, 1962
k *Densosporites* sp.
l aff. *Lundbladispora gigantea* (Alpern) Doubinger, 1968
m *Lycospora granulata* Kosanke, 1950
n *Lycospora* cf. *parva* Kosanke, 1950
o *Lycospora paulula* Artüz, 1957
p *Lycospora punctata* Kosanke, 1950
q *Lycospora pusilla* (Schopf, Wilson & Bentall) Somers, 1972
r *Lycospora* sp.
s *Endosporites* cf. *vesicatus* Kosanke, 1950
t *Endosporites sp.*
u *Guthoerlisporites magnificus* Bhardwaj, 1954
v *Guthoerlisporites* sp.
w *Nuskoisporites* sp.
x *Vestispora* sp.A
y *Vestispora* sp.

Plate 4.2

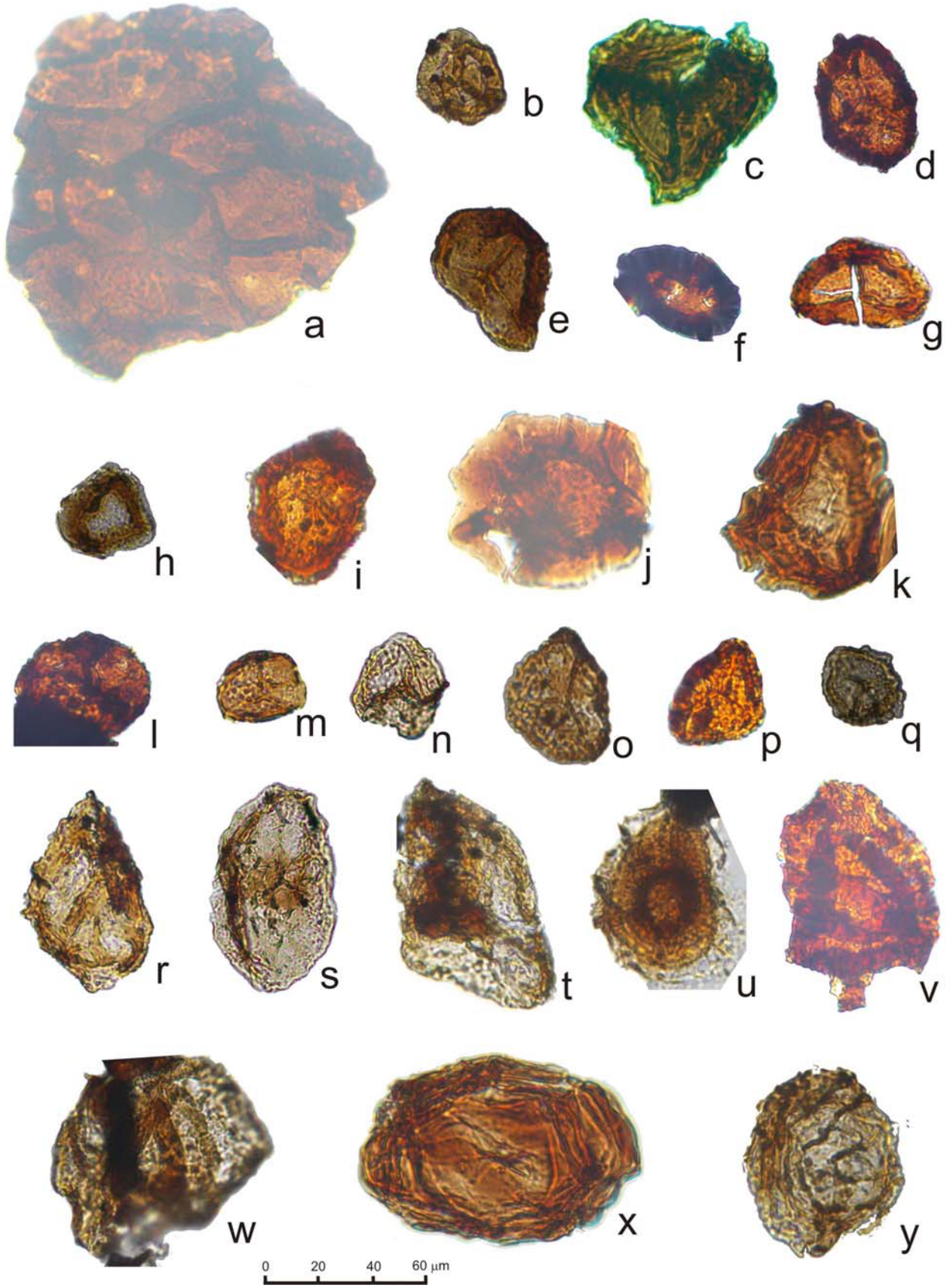

Plate 4.3 – Sporomorphs of the Buçaco basin

a cf. *Vestispora* fenestrata
b *Laevigatosporites* cf. *minimus* (Wilson & Coe) Schopf, Wilson & Bentall, 1944
c *Laevigatosporites minor* Loose, 1934
d *Laevigatosporites ovalis* Kosanke, 1950
e *Laevigatosporites* cf. *perminutus* Alpern, 1958
f *Laevigatosporites* sp.
g *Cheiledonites gigantea* (Alpern) Doubinger, 1968
h *Cheiledonites major* Doubinger, 1957
i *Cheiledonites potoniei* Doubinger, 1957
j *Puntactosporites* cf. *minutus* Ibrahim, 1933
k *Spinosporites exiguus* Upshaw & Hedlund, 1967
l *Spinosporites spinosus* Alpern, 1958
m *Spinosporites* sp.
n *Torispora* sp.
o *Thymospora obscura* Wilson & Venkatachala, 1963
p *Thymospora pseudothiessenii* (Kosanke) Alpern & Doubinger, 1973
q *Thymospora thiessenii* (Kosanke) Wilson & Venkatachala, 1963
r *Thymospora* sp.
s *Cordaitina uralensis* (Luber) Dibner, 1971
t *Cordaitina* sp.
u *Latensina trileta* Alpern, 1958
v *Dyupetalum* sp.
x *Wilsonites* cf. *vagus* Inossova, 1976
y *Wilsonites* sp.

Plate 4.3

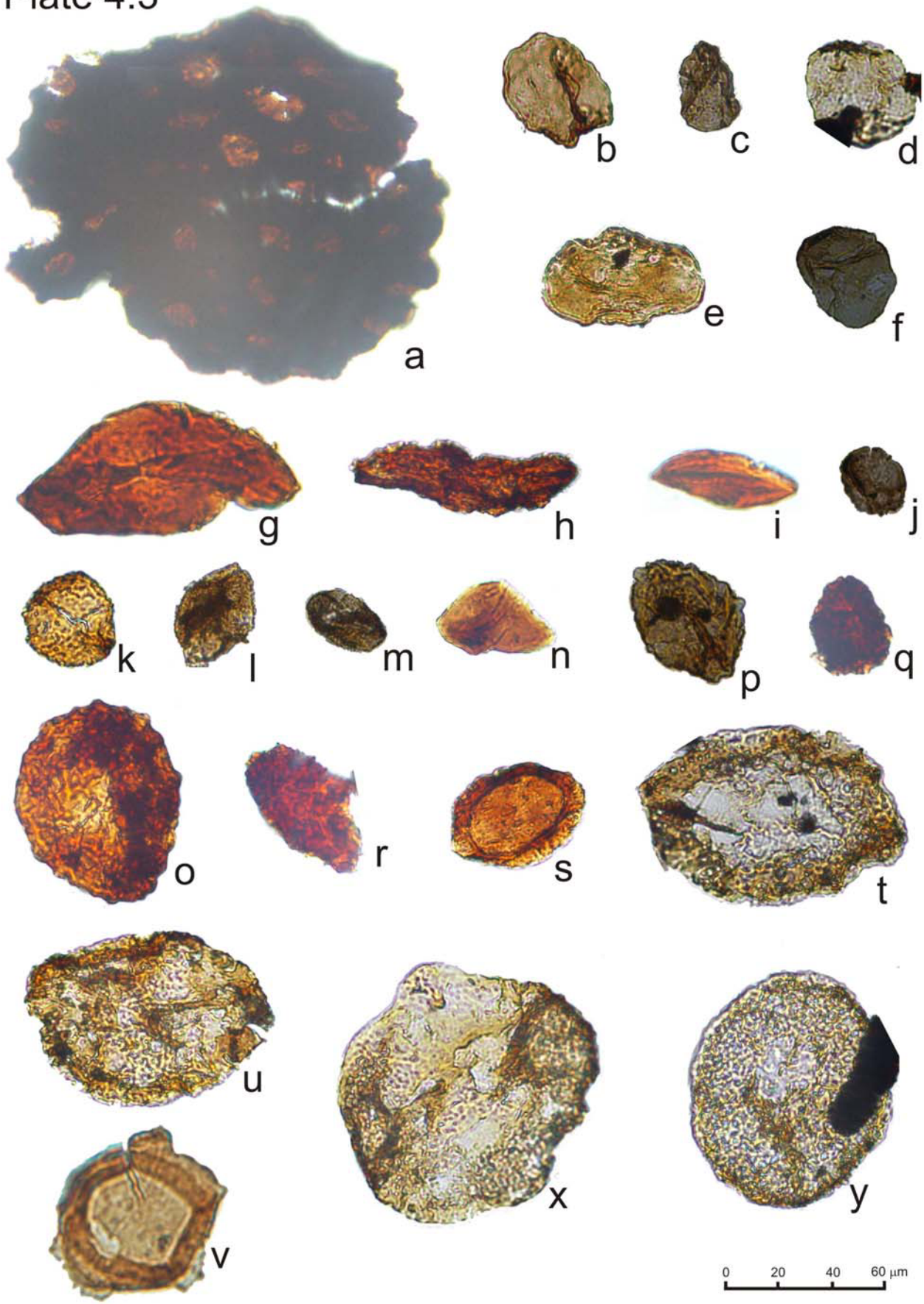

Plate 4.4 – Sporomorphs of the Buçaco basin

a *Wilsonites* aff. *delicatus* Kosanke, 1950
b *Florinites bederi* Pittau et al., 2008
c *Florinites* aff. *diversiformis* Kosanke, 1950
d *Florinites* sp
e *Florinites* sp. A
f *Potonieisporites bhardwajii* Remy & Remy, 1961
g *Potonieisporites clarus* Shwartsman in Inossova et al., 1976
h *Potonieisporites novicus* Bharadwaj, 1954
i *Potonieisporites* sp. A
j *Potonieisporites* sp.
k *Disaccites* non striatti
l *Vesicaspora* sp.
m *Illinites elegans* Kosanke, 1950
n *Platysaccus* sp.
o aff. *Corisaccites* sp.
p *Lueckisporites* sp.
q *Alatisporites* sp.

Plate 4.4

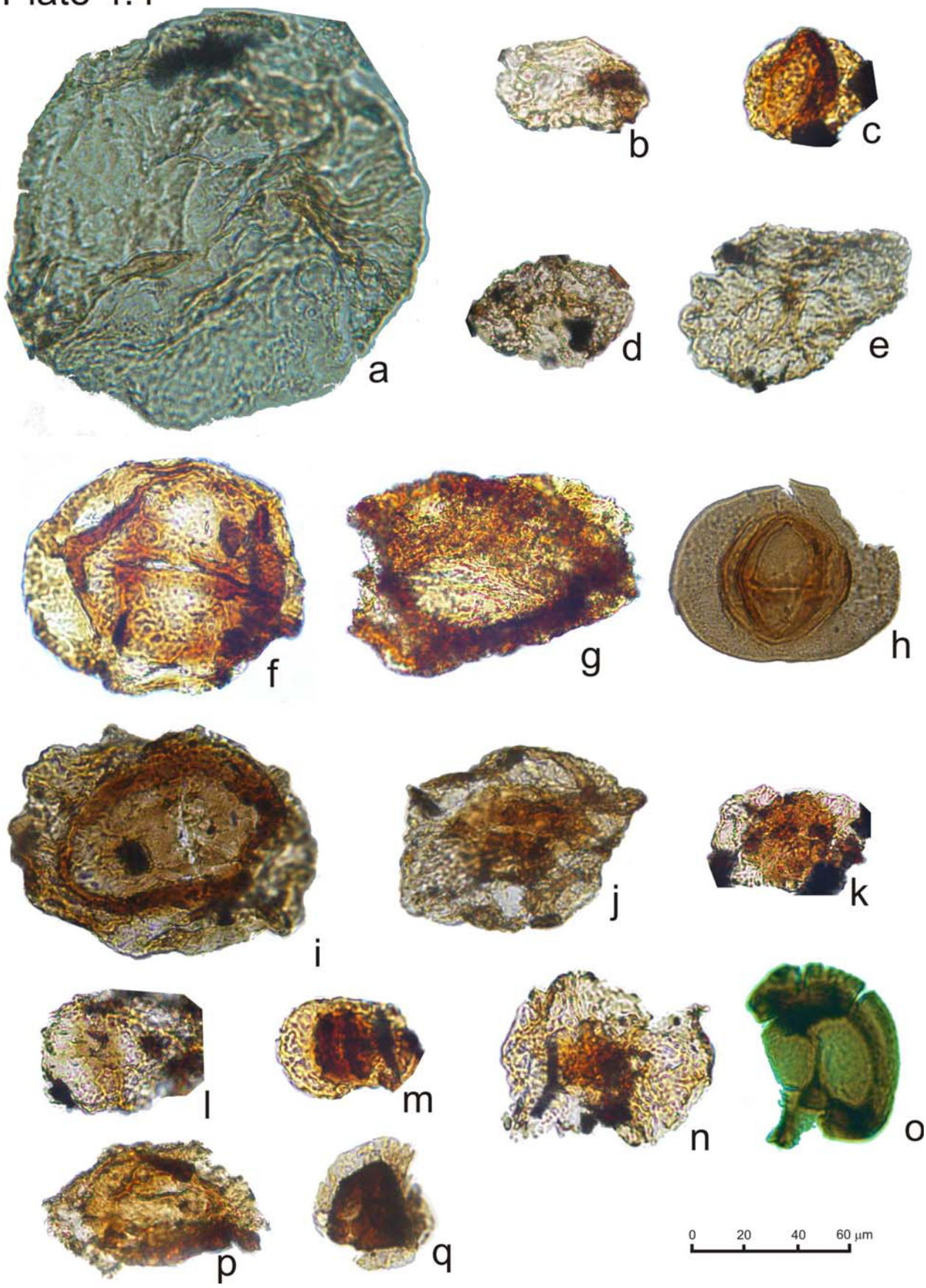

Plate 4.5 – Sporomorphs of the Buçaco basin

a *Protohaploxypinus jacobii* (Jansonius) Hart, 1964
b *Schopfipollenites ellipsoides* (Ibrahim) Potonié & Kremp, 1954
c *Schopfipollenites ovalis* Schwartsman, 1976
d *Schopfipollenites parvus* Schwartsman, 1976
e *Schopfipollenites* sp.
f *Vittatina simplex* Jansonius, 1962
g *Vittatina costabilis* Wilson, 1962
h *Vittatina* sp.
i *Cycadopites* sp.
j *Cymatiosphaera* sp. (reworked)
k *Gorgonisphaeridium* sp. (reworked)
l *Michrystridium* sp. (reworked)
m ?arthropod fragment
n General appearance of a slide under a transmitted light microscope (note different scale)

Plate 4.5

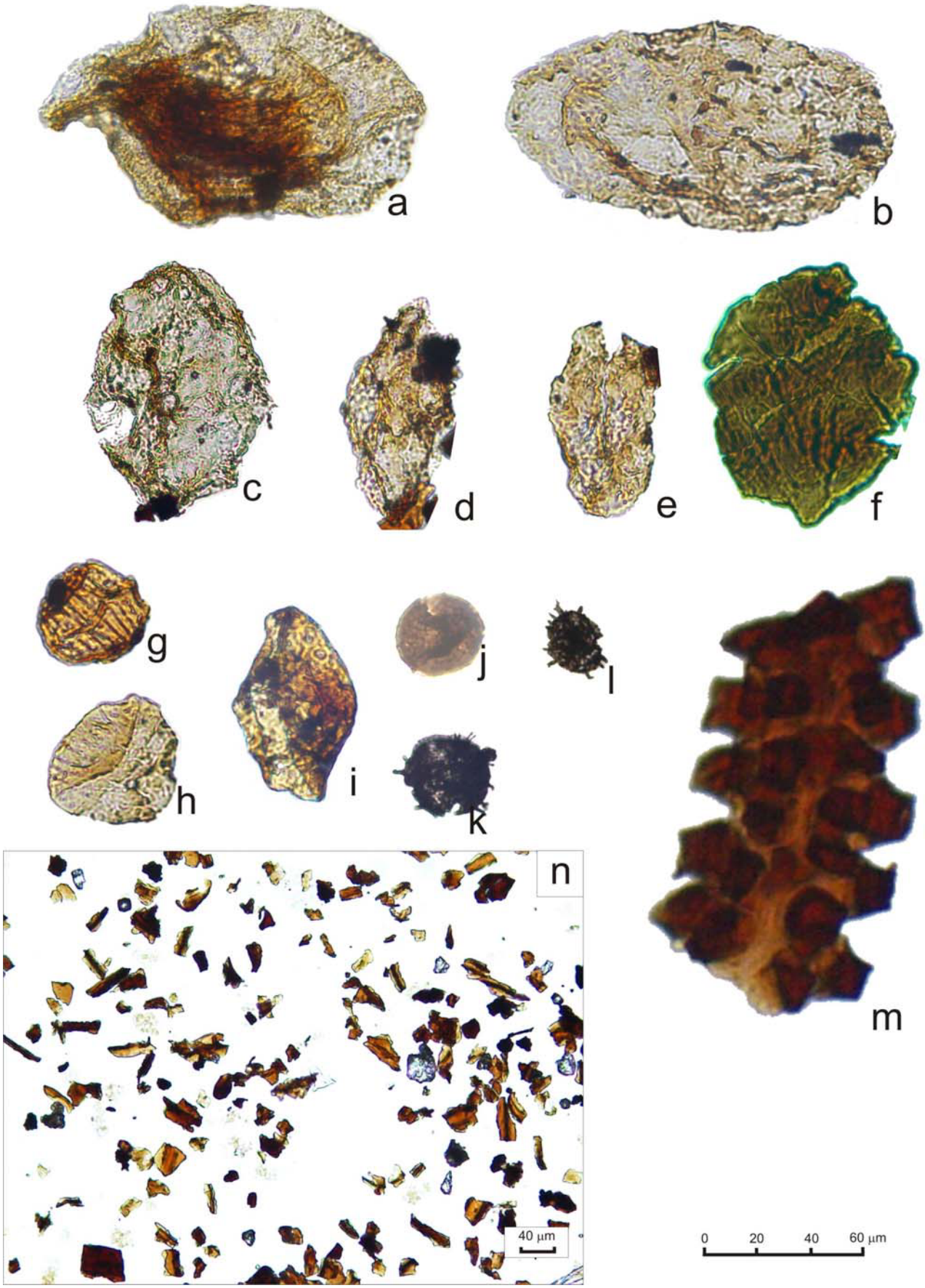

Plate 4.6 – Sedimentary features of the Algeriz Fm. Sst – sandstone; sh – shale; cong – conglomerate; Qzit – quartz/quartzite clast; sch – schist clast; intcl – intraclasts.

A Basal contact of the Algeriz Fm (Gralheira Member) with the underlying CXG schistose units. Note the intense ferruginization of the basement rocks. Compare the schist-rich matrix supported breccia with the B and C. Aprox. N-S orientation. Algeriz-Parada road.

B Detail of a breccia bed in the basal part of the Parada Member. Note the better roundness, increased clast content and more diversified lithologies when compared with the Gralheira Member. Aprox. W-E orientation. Algeriz-Parada road.

C Detail of a conglomeratic bed in the basal part of the Parada Member. Note the ferruginization affecting the surface and interior of the clasts. Aprox. W-E orientation. Road N of Vale da Mó village.

D Example of the relatively thick massive to crudely bedded sandstone beds of the Parada Member. Aprox. W-E orientation Algeriz-Parada road.

E Conglomerates, sandstones and shales of the Parada Member. A meter scale fining-upward cycle is bounded by erosive contacts. The upper conglomeratic bed has several sets of conglomerate-sandstone couplets (arrows). Aprox. NNW-SSW orientation. GRA section.

F Polished surface of sample GRA5.2 (GRA section), Parada Member. Pebbely massive sandstone. Arrows indicate pebbles.

G Sandstone-conglomerate couplets. GRA section.

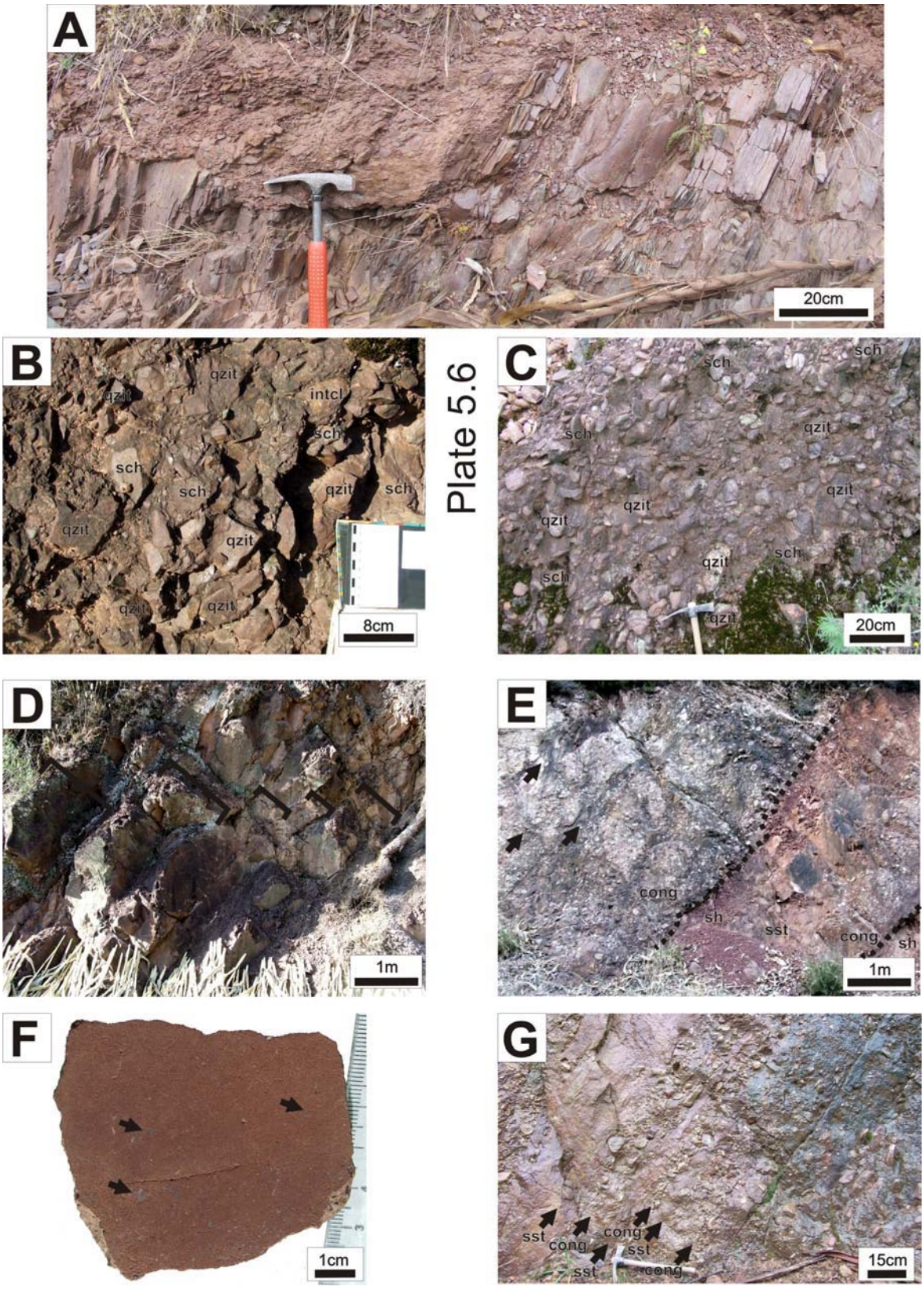
A
20cm
B
qzit
intcl
sch
8cm
C
sch
qzit
20cm
Plate 5.6
D
1m
E
cong
sh
sst
1m
F
1cm
G
sst
cong
15cm

Plate 4.7 – Sedimentary features of the Monsarros Fm. Large dashed arrow shows palaeocurrent direction. C – coal; cong – conglomerate.

A Bedding surface of a siltstone bed showing oriented plant remains (pl) and fresh water molluscs' internal moulds and shells (mol). Middle part of the Serradinho Member. ALG section.

B Turbidite-like cycles overlying a sheared coal seam (C). The truncations may in part be sedimentary, but most seem to be due to faulting. Serradinho Member. Aprox. W-E orientation. CRI section.

C Detail of a finely laminated mudstone. Serradinho Member. Aprox. W-E orientation. VMO section.

D Sandy channel fill cutting the underlying sandstone and mudstone beds. Serradinho Member. Aprox. E-W orientation. VMO section.

E Clast imbrication on a schist-rich conglomeratic bed. Serradinho Member (Upper facies). Aprox. Aprox. W-E orientation. ALG section.

F Several schist-rich conglomeratic beds with significant ferruginization (darker beds to the left) followed by a quartz/quartzite-rich conglomerate with very few schist clasts and little ferruginization (whitish beds to the right). Western flank, Serradinho Member (?)Upper facies. Aprox. W-E orientation. ALG section.

G Sandstones and conglomerates of the Serradinho Member Upper facies. Note the high angle oblique bedding of sandstone/conglomerate sets. Aprox. W-E orientation. VMO section.

H Reflected light microphotograph of the palynological residue sample ALG3.3. sf - semifusinite; vit – vitrinite (collotelinite).

Plate 5.7

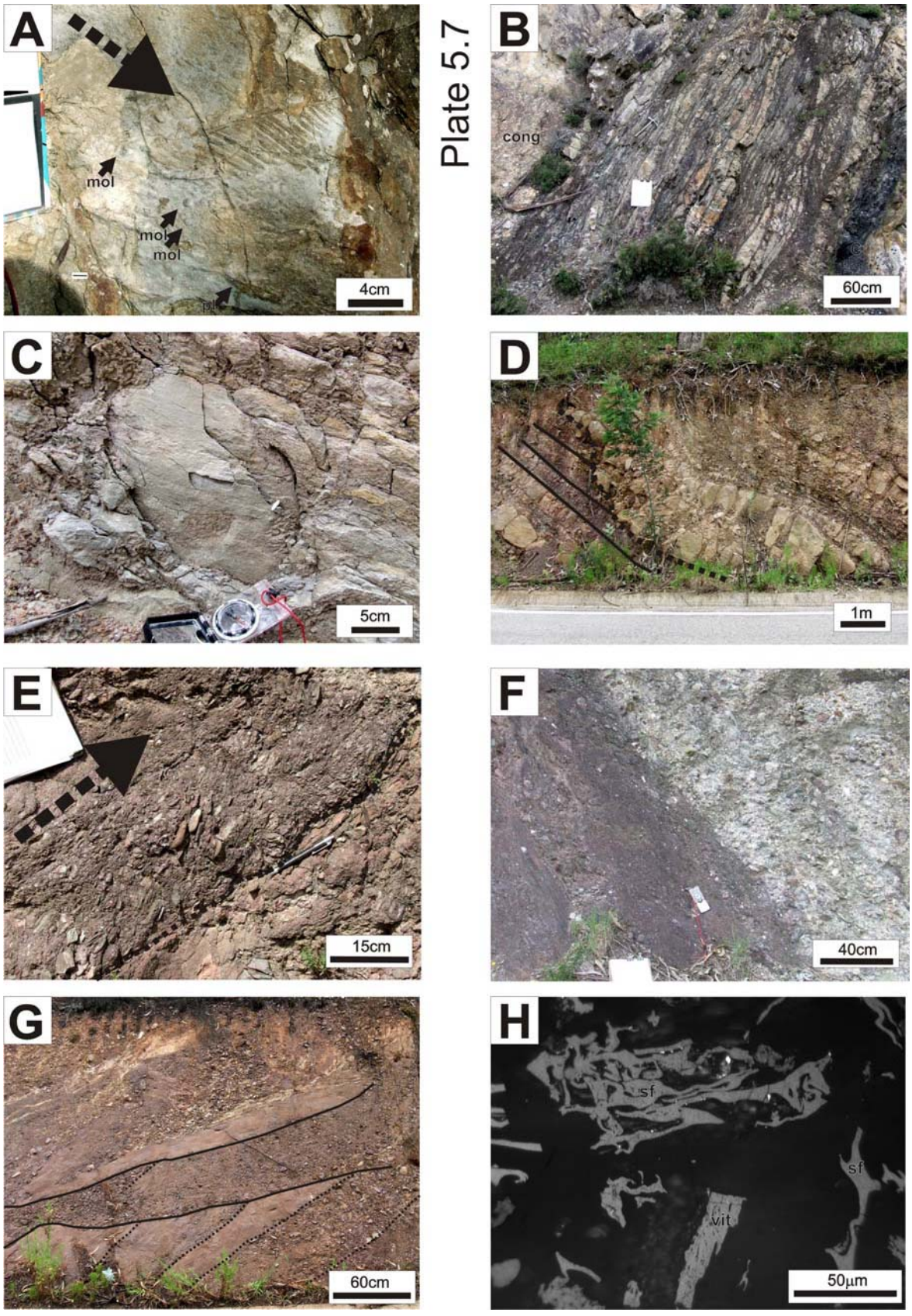
A
mol
mol
mol
4cm
B
cong
60cm
C
5cm
D
1m
E
15cm
F
40cm
G
60cm
H
sf
sf
vit
50µm

Chapter 5

Stratigraphy, Palynology and Palaeobotany of the Pennsylvanian continental Santa Susana Basin (SW Portugal)

This chapter includes work published in:

MATTIOLI, M., MACHADO, G., SILVA, I. & ALMEIDA, P., 2009. Revision of the stratigraphy and palaeobotany of the Moscovian (Upper Carboniferous intramontane Santa Susana Basin (SW Portugal). Paleolusitana 1: 269-275.

MACHADO, G., MATTIOLI, M., SILVA, I. & ALMEIDA, P., 2009. Initial biostratigraphical results from a ?Moscovian/Kasimovian paleobotanical site in Santa Susana basin (Alcácer do Sal, Portugal). CIMP Faro'09, II Joint Meeting of Spores/Pollen and Acritarch CIMP Subcommissions. Faro, Portugal: 69-72.

STRATIGRAPHY, PALYNOLOGY AND PALAEOBOTANY OF THE PENNSYLVANIAN CONTINENTAL SANTA SUSANA BASIN (SW PORTUGAL)

Chapter Index

Abstract 194
5.1 Introduction and Previous work 195
5.2 Methods and materials 197
5.3 Results 198
5.3.1 Lithostratigraphy 198
5.3.1.2 Santa Susana sections – SUS (Jongeis outlier) 200
Susana 5 200
Susana 6 200
5.3.1.3 Remeiras section - REM (Remeiras outlier) 202
5.3.1.3 Moinho da Ordem section - ORD (Vale de Figueira outlier) 202
5.3.1.4 Vale de Figueira Locality and sections - VFIG (Vale de Figueira outlier) 202
VFigueira 1 to 5 204
VFigueira 6 204
5.3.2 Geometry and architectural elements analysis 204
5.3.3 Palaeocurrents and provenance data 206
5.3.4 Clay fraction mineralogy 208
5.3.5 Palaeobotany 208
5.3.6 Palynology and age of the assemblages 211
VFigueira 1 to 5 sections 212
Susana 5 and 6 sections 213
5.3.7 Thermal and burial history 214
5.4 Discussion and Conclusions 216
5.5 Systematic Palynology 217
Acknowledgements 225
References 226
Plates 232
Plate 5.1 – Sporomorphs from the VFigueira 1 to 5 section 232

Abstract

The Santa Susana basin (SSB) is a Pennsylvanian continental basin located along an important N-S strike shear zone that separates the Ossa-Morena and South Portuguese Zones (SW Portugal). The shear zone controlled the basin's sedimentation and probably its post-sedimentary evolution. Fluvial sedimentation prevailed, but lacustrine sediments can be found in restricted areas in the basin's upper unit. Palynological and palaeobotanical data indicate that at least part of the sedimentation took place during the Kasimovian (lower Stephanian/Cantabrian) but the sporomorph content of different localities suggests that significantly older sediments (?Moscovian/Bashkirian - Westphalian B or C) may be present. The geometrical and temporal relations of the basin with the surrounding units are discussed.

Key-words: Ossa-Morena Zone, South Portuguese Zone, Santa Susana Basin, Kasimovian, spores/pollen, continental sedimentation, SW Portugal.

5.1 Introduction and Previous work

The Santa Susana Basin (SSB) is a Pennsylvanian continental basin, located along an important NNW-SSE to N-S shear zone separating the South Portuguese Zone (SPZ) to the East and the Ossa-Morena Zone (OMZ) to the West (Almeida et al., 2006; Domingos et al, 1983; Oliveira et al., 2007; Sousa and Wagner, 1983) (Fig. 5.2). The basin rests over older OMZ units, namely the Toca da Moura volcano-sedimentary complex (Gonçalves, 1983; Oliveira et al., 2006; Pereira et al., 2006; Santos et al., 1987) and the Grupo de Cuba rocks (microdiorites and porphyry rocks) (e.g. Gonçalves, 1983, 1984/5) (see Table 5.1). The basal parts of the basin have conglomerates that contain porphyry boulders (Pl. 5.8c), but it is also cut by porphyry dykes, indicating their contemporaneousness (Andrade et al. 1955; Gonçalves, 1983) (see Table 5.1).

To the West the basin is separated from the Pulo do Lobo Group units of the South Portuguese Zone by the Santa Susana shear zone (SSSZ), an important regional structure that runs NNW-SSE (Almeida et al., 2006; Oliveira et al., 2007), referred to as part of the Ferreira-Ficalho thrust in older literature (e.g. Gonçalves, 1983). Pulo do Lobo Group units (s.l.) include the Pulo do Lobo (phyllite, quartzite, acidic and basic metavolcanic), Ribeira de Limas (phyllites and metagreywackes), Santa Iria and Horta da Torre Formations (shales, siltstones and quartzites) (Garcia-Alcalde et al., 2002; Oliveira, 1983). This group of Formations is also referred to as Ferreira-Ficalho Group (e.g. Garcia-Alcalde et al., 2002).

The basin extends for over 15Km in length along a NNW-SSE direction and is 0.1 to 1km wide. Significant parts of the basin, especially in its southern part, are covered by Tertiary deposits, but the true extent of the basin was revealed in the 1950s by borehole data. The Pego do Altar water reservoir has covered yet another part of the basin in the early 1950s. Nowadays there are 3 main outliers, from North to South: Jongeis (SUS sections), Remeiras (REM section) and Vale de Figueira (VFIG and ORD sections) (Fig. 5.2). Other small areas exist to the South, but most are covered by Tertiary deposits and are known mainly from borehole data.

The basin has several coal seams that were explored until 1944 (Sousa and Wagner, 1983). The Jongeis exploration (Jongeis outlier) was the largest and longest, but another smaller exploration was conducted near Vale Figueira de Baixo – called Moinho da Ordem mine (Vale de Figueira outlier).

The study of this basin dates back to the 1800s when Bernardino Gomes first reported fossil plants from the basin and made the first taxonomic identifications (Gomes, 1865). Lima conducted a second palaeobotanical study of the basin (e.g. Lima, 1895/98) attributing an age to the fossil sites. Later, Carlos Teixeira worked on several Portuguese Carboniferous fossil plant sites, including the SSB (Teixeira, 1938/40; 1940; 1944, 1945) and revised some of the work by Gomes and Lima and compared the assemblages with others found in Spain and elsewhere in Europe. More recently a series of papers by Wagner and Sousa have revised the taxonomy, stratigraphic significance and palaeobiogeography of the Iberian Carboniferous fossil macroflora including the Santa Susana assemblages (e.g. Sousa and Wagner, 1983; 1985). These authors attributed the assemblage to the “very late Westphalian D or earliest Cantabrian”. Most of the specimens described and re-described by these workers were from the Vale de Figueira locality in the southern part of the basin. Unfortunately all of these studies were based on spot sampling

of palaeobotanical sites and the collections have not been enlarged since Teixeira collected some specimens. These are stored at the Natural History Museum in Lisbon (Bernardino Gomes Collection), Museum of the Geological Survey in Lisbon (Carlos Teixeira Collection and part of the Wenceslau de Lima collection) and in the Wenceslau de Lima Museum in the Faculty of Sciences of the Porto University. Based on the work by Sousa and Wagner (1983) regarding the Santa Susana and Ervedosa (Douro area, N Portugal) basins, and compiling data from other Euramerican basins, Cleal (2008a, b) considered the assemblages from Portugal and NW Spain as a discrete group with close affinities with the Rhine and Silesia Palaeoprovinces.

The basin's stratigraphy has only been summarily described in some of the previous palaeobotanical studies and also in specific studies (e.g. Andrade, 1927/30; Andrade et al., 1955; Neiva, 1943) dealing with borehole data and with the characteristics of clasts in the conglomerates. The scarcity of studies on the basin's stratigraphy can be explained by the paucity of continuous outcrops in the area except for some stream beds and reservoir banks.

Geotectonic Domain	Lithostratigraphy		Age
Ossa Morena Zone	Santa Susana Basin	Upper unit (sst, shales, coals	Kasimovian (this work)
		Basal Unit (polygenic conglomerates)	(?)Moscovian-Kasimovian (this work)
	Grupo de Cuba Felsics (Microdiorites and porphyry rocks)		Serpukhovain- (?)Kasimovian (Priem et al., 1976)
	Toca da Moura Complex (Slates, greywackes, limestones, basalts, tuffs)		Tournaisian-Viséan (Pereira et al., 2006)
South Portuguese Zone	Pulo do Lobo Group s.l. (Including Pulo do Lobo, Ribeira de Limas, Santa Iria and Horta da Torre Fms)		(?) Middle Devonian to Famennian (Pereira et al., 2008)

Table 5.1 – Synthesized table of the Geological units and Formations considered for this work and their age.

Facies analysis is difficult in most places due to the scarcity of outcrops and their poor continuity. Conglomerates (from boulder size to gravel) and dark grey siltstones and shales with occasional coal seams are quite common (e.g. Pl. 5.8b). Sandstones also appear in some localities. These have been interpreted as fluvial deposits by most authors, but a more detailed facies analysis was never performed.

Only two brief notes were published concerning the palynology of the basin: Fernandes (1998; 2001). Both refer to samples derived from borehole cuttings (Fernandes, pers. com.) and the relatively diversified spore assemblage allowed an attribution to the Miospore biozones *Angulisporites splendidus – Latensina trileta* (ST) and/or *Thymospora obscura – T. thiessenii* (OT) of Clayton *et al*., 1977.

The basin's geometry and tectonics have received little interest, despite the significant relevance of the area to the understanding of the whole region. Regional mapping conducted by the Geological Survey produced a short note (Carvalhosa & Zbyszewsky, 1994) and a glimpse of the structure was described in Domingos et al. (1983). More recently detailed structural and geological mapping of the northern area of the basin (Jongeis) and surrounding units has revealed a transtensive dextral tectonic style, along the SSSZ producing sedimentation in a pull-apart basin during the Pennsylvanian (Oliveira et al., 2007, Almeida et al., 2006). On-going work in the southern parts of the basin is showing a similar tectonic style.

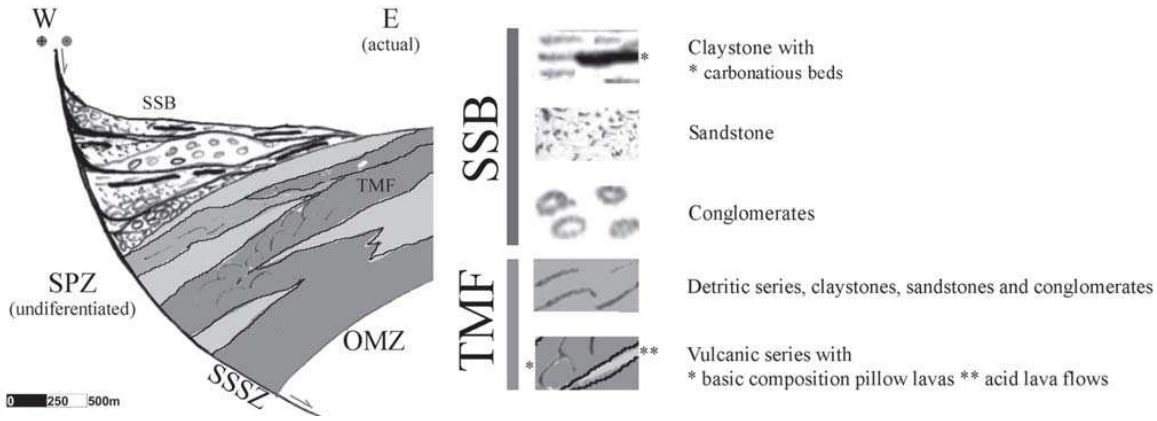

Fig. 5.1 Schematic Santa Susana Basin cross section showing the hemigraben structure with depocenter to the W. SSB – Santa Susana Basin; TMF – Toca da Moura Formation (Complex); SPZ – South Portuguese Zone; OMZ – Ossa-Morena Zone; SSSZ – Santa Susana shear zone. Adapted from Oliveira et al. (2007) and Almeida et al. (2006).

5.2 Methods and materials

As mentioned above there are few localities with sufficient exposure to construct lithological columns and properly interpret the sedimentary facies. Here 6 localities covering the 3 main outliers of the basin are described, although they certainly do not represent the whole sequence of each area (see Fig 5.2 for locations). All sections were sampled for palynology. Samples were processed using the methods described in Chapter 2. Residues were mounted on glass slides and observed under a transmitted light microscope. A mild oxidation using low concentrated bleach was performed to render some thicker-walled taxa translucent and observable under the microscope.

Several palaeobotanical specimens were collected at the Vale de Figueira classical locality (Vale Figueira 1 to 5 section). The palaeobotanical collection stored at the Museum of the Portuguese Geological Survey (LNEG) appears to come from two different localities, probably from different sampling campaigns. One part comes from the Vale de Figueira locality (precise location is given with some specimens) and another from "Moinho da Ordem" which is a local landmark. The precise location of this site is unknown and possibly is now underwater. The matrix in which the fossils are found is a pink fine siltstone which was not recognized in the Vale de Figueira site. The collection at the Natural History Museum in Lisbon is restricted to about 6 small specimens with no reference of the sampling site.

The palynological residues containing abundant phytoclasts were sieved through a 63µm mesh, mounted and polished using a similar method to the one described in Hillier & Marshall (1988). Additional residues were mounted and polished from dark grey shales and siltstones samples of the Toca da Moura/Cabrela Complex described in Pereira et al., (2006) and Oliveira et al., (2006). Random mean vitrinite reflectance (Rr%) was measured in all samples using standardized methods (performed by Paulo Fernandes, UAlg).

Further data presented here derives from the papers dealing with the extensive borehole campaign done from the 1930s up to the 1950s (Andrade 1927/30; 1955). Although executed or sponsored by the Portuguese Geological Survey there is neither record of them in the Survey's archives, nor the cuttings or cores seem available. The logs and descriptions were systematized and used to construct cross sections in several areas of the basin (Fig. 5.2). Surface mapping, dips and other cartographic information was used to produce more accurate sections.

Palaeocurrent data was collected in the several sections mentioned above. Additional data was collected in small outcrops which were not logged but had enough exposure to be measured. The data derive from cross bedding structures in sandstones and fine conglomerates and from large oriented plant debris found in bedding surfaces (Ordem1 section).

Several samples from the VFIG 1 to 5, VFIG 6, ORD (Ordem 1) and REM sections were selected for clay mineralogy analysis (same as for palynology analysis). The <4μm fraction was decanted and mounted over a glass slide and left to dry at room temperature. The X-ray diffraction pattern was recorded with a copper anode X-ray tube (Cu-Kα radiation) using a Philips PW1710, powder diffractometer and X´Pert software PC-APD 3.6 in Aveiro University and in a similar equipment in the Tropical Research Institute (IICT) Department of Natural Sciences(DCN)/ Global Development(DES) in Lisbon.

5.3 Results

5.3.1 Lithostratigraphy

The same units presented in the simplified geological map were considered with the exception of the Santa Susana basin which was separated into two laterally correlatable units:

1) Basal conglomeratic unit composed by a very coarse grained basal conglomerate with abundant “porphyry” boulders overlain by coarse sandstones and polygenic conglomerates. Finer grained rocks and coal seams are rare. Outcrops of this unit are rare, but they can be found in the Remeiras outlier and along the Eastern edge of the Vale de Figueira outlier.
2) Upper unit composed by sandstones, shales and coals. It contains all of the mined coal seams and provided all the palaeobotanical and palynological assemblages so far. Some quartz/quartzite-rich gravel conglomerates occur. Most of the surface area occupied by the Santa Susana basin corresponds to this unit.

The separation of the two units was arbitrarily defined by the dominant proportion of coarse/fine grained sedimentary rocks. Although prone to some uncertainty, the shift from a coarse-grained dominated sequence (conglomerates and sandstones) to a fine-grained one (siltstones and mudstones) seems rather abrupt (within a few meters) and clearly unidirectional in all instances, probably corresponding to a considerable and rapid change of the sedimentary environment.

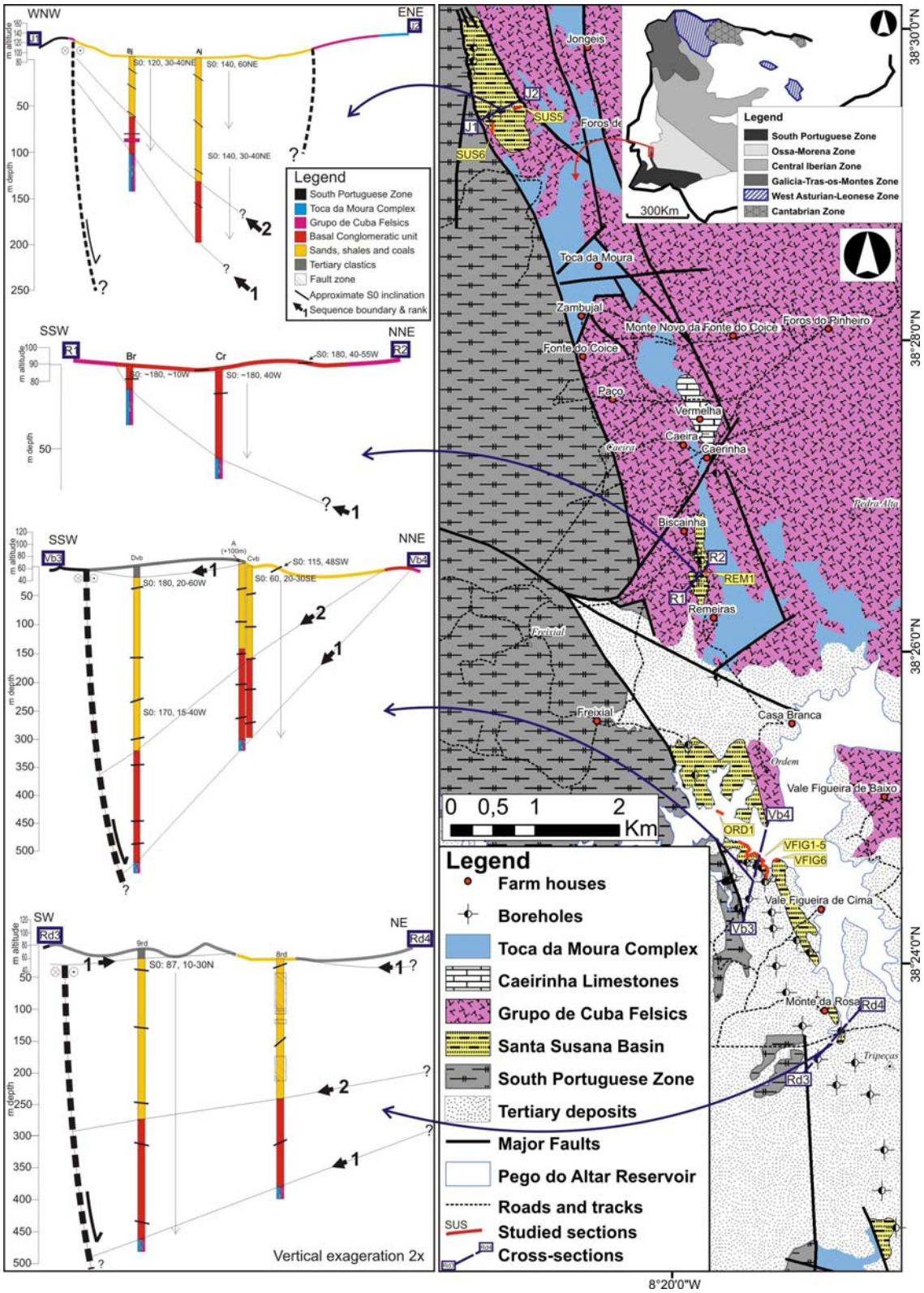

Fig. 5.2. Right: Geological sketch map of the Santa Susana basin and surrounding areas. Adapted from Andrade et al. (1955), Gonçalves (1984/5), sheet 39D of the Portuguese Geological Survey 1 / 50000 map, Oliveira et al. (2007) and Almeida et al. (2006) and unpublished data from the authors. SUS – Susana sections; REM- Remeiras section; ORD – Moinho da Ordem section; VFIG – Vale de Figueira sections. Left: Geological transverses from several locations in the basin. Compiled with data from Andrade et al. (1955) and unpublished data from the authors.

Unfortunately by the time the borehole campaign was performed and reports produced, the knowledge of the surrounding metamorphic units was scarce. Thus Andrade (1927/30; 1955) uses terms such as “Complexo Cristalofílico Ante-Cambrico” to describe the basement rocks of the basin, which basically refers to undifferentiated metamorphic and igneous rocks of the Ossa-Morena Zone. Other lithological references are “Porfirito” (which refers to the Grupo de Cuba felsic rocks (commonly referred to as Baleizão Porphyry – Ossa-Morena Zone), “Xisto Fameniano” (probably referring to the upper units of the Pulo do Lobo Group – South Portuguese Zone) and “Xistinhos” (referring to the slates of the Toca da Moura Complex – Ossa Morena Zone). Additional problems arise when the basement of Jongeis area is described as being “Xisto Fameniano”, thus South Portuguese Zone. All other wells found Ossa-Morena Zone units as the basement of the basin. No faults are described in the contact with the basement in Jongeis area. It is considered here, that this is probably a misidentification of metamorphic rocks of the Ossa-Morena Zone. Confirmation or rejection of this hypothesis is at this time impossible.

5.3.1.2 Santa Susana sections – SUS (Jongeis outlier)

As in other areas of the basin, outcrops and especially continuous sections are scarce. The Jongeis outlier has the additional problem of having large areas covered by mine tailings. Only two sections were considered to be appropriate for description and palynological sampling. Both belong to the SSB upper unit.

Susana 5

This is a small section observable along the bed of a perennial stream. Several badly defined dm-thick fining-upward cycles can be observed. Gravel conglomerates grade to sandstones and mudstones (Fig. 5.3). Within the finer, upper part of the cycles, fine conglomeratic beds or lenses are common. The sandstone and mudstone beds frequently show bedding-parallel lamination and are grouped in cm to dm-thick fining-upward cycles (Fig. 5.3; Pl. 5.8D). The classification of these cycles and its bounding surfaces according to ranks or orders (e.g. Miall, 1996) and the discussion on the geological processes that originated them is difficult due the limited extent and poor preservation of the section. This is probably a fluvial sequence.

Susana 6

This is a long section logged on a vegetated hill slope. Observational gaps are extensive. The little information available derives from relatively resistant conglomeratic and sandstone beds and a few mudstone levels (Fig. 5.3). Although uncertain it seems the meter scale fining-upward cycles are present, as observed in other sections across the basin. The extensive gaps preclude further interpretations.

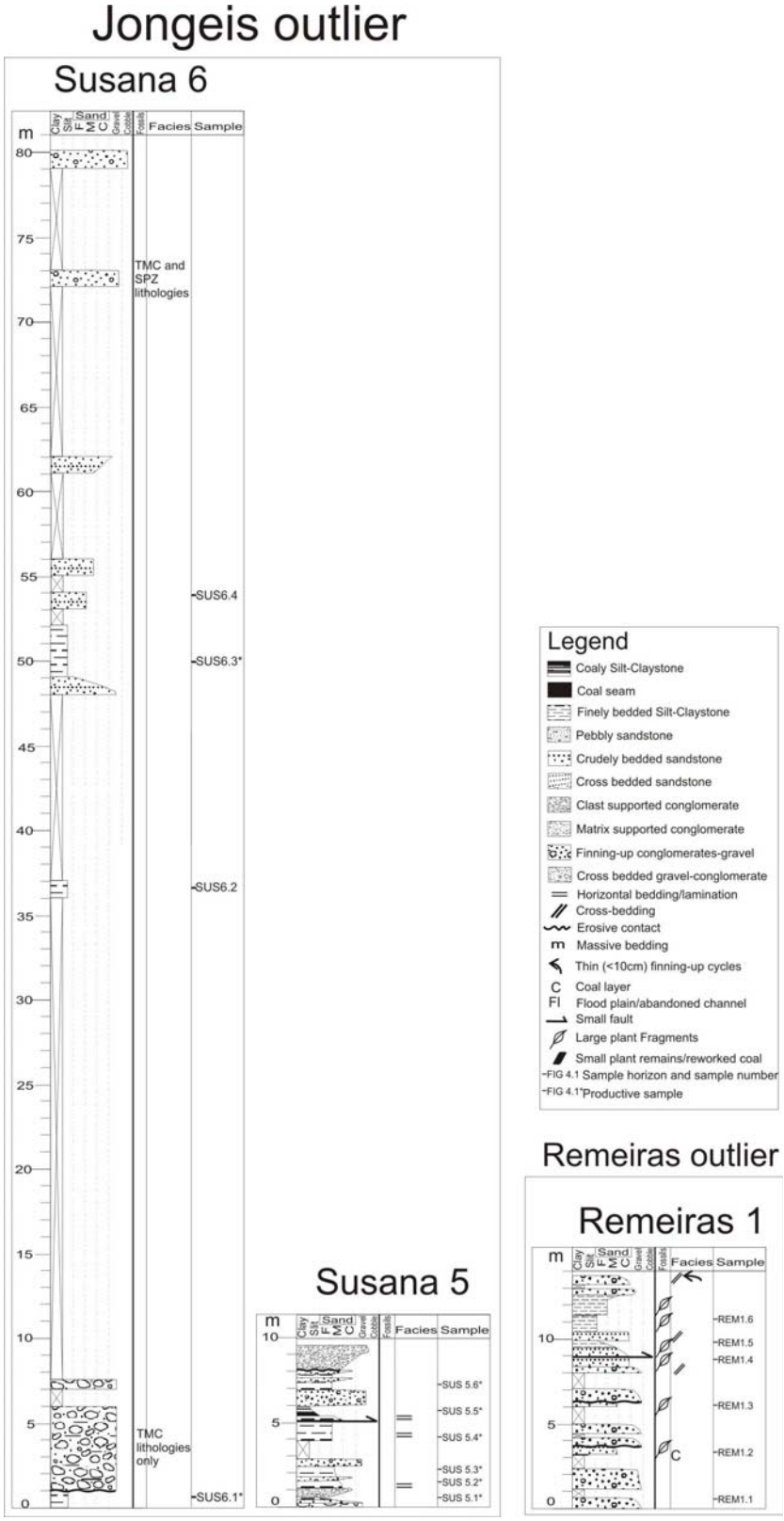

Fig. 5.3 - Lithostratigraphic columns of selected localities of the Jongeis and Remeiras outliers. Susana 5 and 6 – (?)Fluvial sequences in the Jongeis outlier. Remeiras 1 – (?)Fluvial sequence with highly diversified sources of clasts and common small plant remains.

5.3.1.3 Remeiras section - REM (Remeiras outlier)

This is a small section observable along the bed of a perennial stream. The section is considerably weathered. Observational gaps are common, especially at the top of conglomeratic beds. These probably correspond to fine sandstone and mudstone levels that erode more easily. It seems that the same fining-upward cycles observed in other sections are present, but on a sub-metrical scale. The conglomerates' clasts have an extremely varied origin: greenish slate, black slate, porphyry, psamitic metasediments, quartz, quartzite, basic rocks and coal fragments. Maximum clast size varies little throughout the section (2-4cm). A thin coal seam is observable at ca. 3m and plant fragments are commonly found in sandstone and mudstone beds. Cm- to dm-thick cycles can be observed, especially at the top of the section. These have a conglomeratic or coarse sand base and grade to fine sand at the top (Fig. 5.3).

This sequence is probably fluvial, but with some differences to other sections. The greater diversity of lithologies and the presence of reworked coal in the conglomerates suggests that the source areas are quite diversified, extending to both Ossa-Morena and South Portuguese Zones and probably the basin itself.

This is the only section attributable to the SSB lower unit, but it is uncertain if it is representative of the rest of the unit. Along the Eastern edge of the basin, where the lower unit is expected to be found, one can easily find outcrops of very coarse, porphyry rich conglomerates. The same is described from the borehole data (Andrade et al., 1955).

5.3.1.3 Moinho da Ordem section - ORD (Vale de Figueira outlier)

A small section was logged in the northern bank of the Pego do Altar reservoir which is only observable during summer months. Outcrops in the area are not rare, but continuous sections do not abound.

The section is composed by a few 1 to 3m cycles of coarse conglomerates that grade into sandstones and occasionally topped by finely laminated fine sandstone to mudstone. The clast lithologies include slate, psamitic metasediments and porphyry, but quartz and quartzite dominate throughout. Clasts are generally sub-rounded and maximum size varies considerably within and between beds (from 20cm to 2cm). This section has abundant, very large, heavily oxidized plant remains, mostly impressions, preserved on sandstones over bedding surfaces. There is a clear coherent alignment of the remains (see palaeocurrents section). The reduced size and poor preservation preclude further interpretations. This section belongs to the SSB upper unit.

5.3.1.4 Vale de Figueira Locality and sections - VFIG (Vale de Figueira outlier)

The Vale de Figueira locality is referenced in the palaeobotanical collections of the Portuguese Geological Survey Museum that were probably sampled by Lima (or his field assistants) and later by Teixeira. At this locality there are several continuous sections (up to 100m thick) usually bounded by faults, but with slight internal deformation. Strong lateral variations in bed thickness and facies (few meters) can be observed where there is enough exposure.

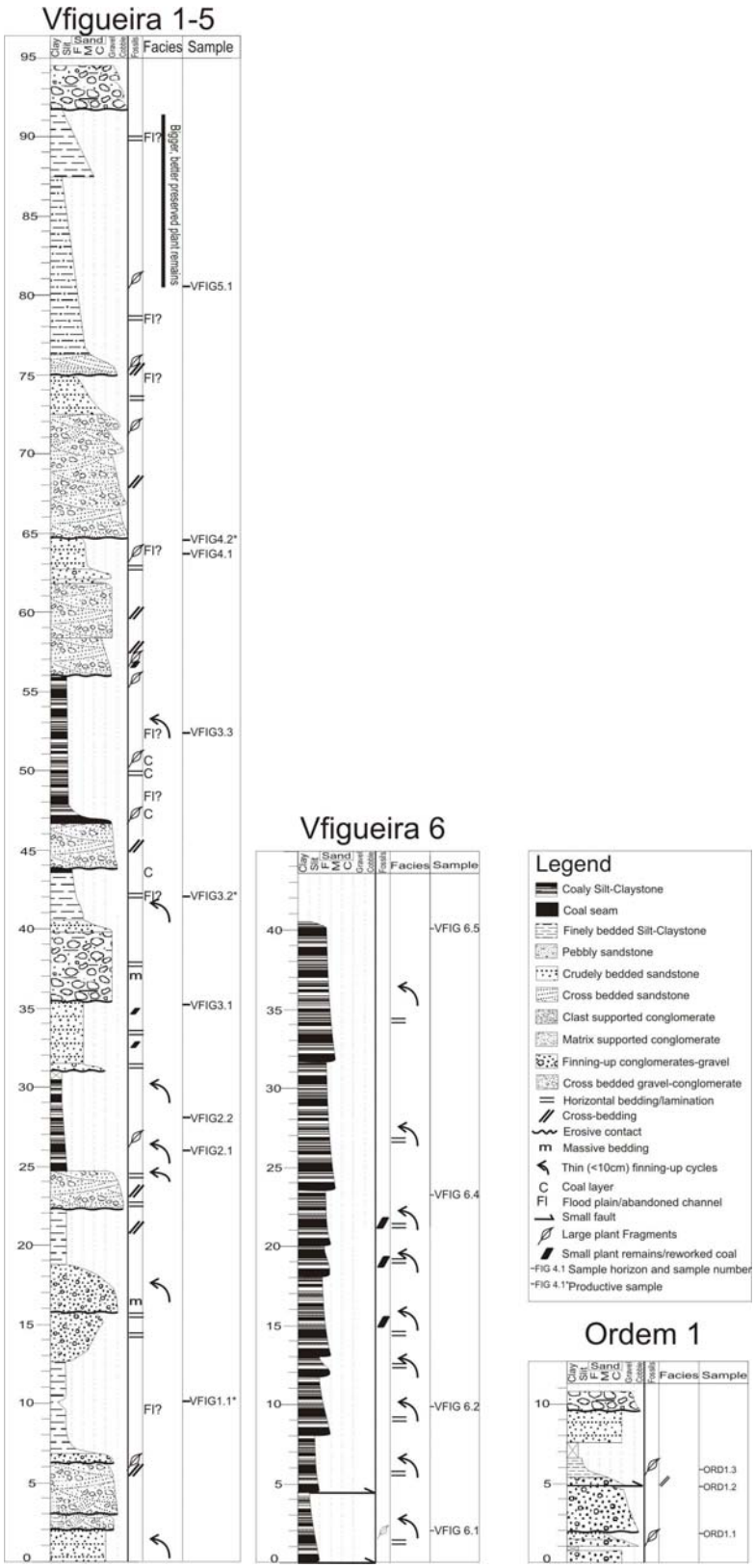

Fig. 5.4 – Lithostratigraphic columns of selected localities of the Vale de Figueira outlier. VFigueira 1-5 - Fluvial sequence with flood plain/abandoned channel levels where most of the large plant remains are found, especially between the 81-91m interval. VFigueira 6 – Lacustrine sequence with monotonous finely bedded mudstones. Ordem 1 – A small section with very large, heavily oxidized, plant remains. This section is flooded during most of the year.

VFigueira 1 to 5

Several fining-upward cycles can be observed, starting with pebbly gravel conglomerates grading up to sandstones and topped by fine dark grey siltstones and shales, occasionally with coal seams (Fig.5.4; Pl. 5.8B, E, F). At the base of the section, the clasts of the conglomerates have a poor roundness (angulose to sub-angulose), grains are badly sorted and several lithologies make up the clasts in similar proportion (undifferentiated slate, quartzite, quartz, micas). Matrix content is high, although all conglomerates are clast-supported. To the top of the sequence, roundness becomes gradually better (up to rounded), with a marked increase of the proportion of quartz and quartzite clasts and decrease of matrix content. This gradual change is very irregular, with some conglomeratic beds (breccias) having very-angulose clasts, erosive bases, high diversity of clast lithologies and high matrix content (e.g. intervals 65-72m and 92-94m, Fig.5.4). Maximum grain size remains fairly constant throughout the sequence (3 to 4cm). Often mudstone, sandstone and even finer conglomeratic beds show very thin fining-upward cycles. These are 10 to 20cm thick in finer conglomeratic beds, ca. 5cm in sandstones and <5cm in mudstones, down to ca. 1cm (Pl. 5.8H). This sequence is interpreted as deposits of a fluvial meandering system and associated flood plain and/or abandoned channel deposits. This section belongs to the SSB upper unit.

Plant remains are found in all lithologies, but are concentrated in the siltstones and shales, frequently as fine debris, but occasionally as large (centrimetrical to decimetrical) remains (Pl. 5.8G). The top of the sequence is dominated by fossiliferous silts and shales which define the Vale de Figueira palaeobotanical site *sensu stricto*.

VFigueira 6

Another continuous section (over 30m) in the same area is composed solely of coaly siltstones and shales. Beds are laterally continuous and often have fine bedding-parallel lamination (VFigueira 6 – Fig.5.4). This sequence is interpreted as deposits of a lacustrine environment. This section did not provide large, identifiable, plant remains so far. The section is bounded by faults in its base and top. This section belongs to the SSB upper unit.

5.3.2 Geometry and architectural elements analysis

To the South of the Remeiras outlier, borehole data show that both units of the basin are thicker in the West, i.e. closer to the SSSZ separating the SPZ and OMZ. Bedding (S0 in Fig5.2.) generally dips mildly to the W. This is very much in accordance with the model proposed by Oliveira et al. (2007) and Almeida et al. (2006) that considers a depocenter close to the SSSZ. However, in Remeiras and Jongeis outliers, the geometry is quite different: the thickest sequences (preserved) are to the E and, at least in Jongeis, bedding generally dips to the E. The thickness of the basin's sedimentary sequences is considerably different when compared to the Southern parts of the basin: <200m in Jongeis and <75m in Remeiras, compared to the ~500m of the Vale de Figueira outlier Moreover, the whole area between Jongeis and Remeiras is composed by basement rocks and the Remeiras outlier is composed solely by the basal conglomeratic unit. It is plausible to assume that tectonics played a very important role in the post-sedimentary evolution of the basin, namely late Variscan and Alpine as suggested by Gonçalves (1983) and Oliveira et al. (2007). The reactivation of tectonic structures with ca. E-W alignment as

compressive faults probably promoted the exhumation and erosion of significant parts of the SSB, especially in the areas to the North (Jongeis and Remeiras). The same fault system probably controlled sedimentation during the Tertiary that covered most of the SSB in its Southern parts. The reactivation of the SSSZ with a reverse component in its Northern segment would easily explain the geometry observed in Jongeis and Remeiras, but evidence of this kinematics is unknown.

The interpretation of the available data from the architectural elements perspective is difficult due to the limited knowledge of the borehole data, poor exposure but also because some of the proposed methods for describing bounding surfaces and orders of sequences (e.g. Miall, 1996) are not directly applicable. The suggestion of Catuneanu (2006) is followed here and orders or ranks are defined for the bounding surfaces and groups of sedimentary packages/sequences according to the available data and characteristics of the basin. In this sense the following bounding surfaces are defined:

Rank	Definition of boundaries	Sequences bounded	Possible origin	Correlation with Miall's boundary classification (Miall, 1982 in Miall, 1996)
1st	Lower (with basement) and upper (with Tertiary deposits) boundaries of the basin	Whole basin sedimentary sequence	Major regional tectonic processes	8th order
2nd	Basal unit (conglomeratic) to Upper unit (sands, shales, coals) transition	Basal and upper units	Local tectonic stasis or geomorphologic evolution of surrounding area	6th or 7th order
3rd	Erosional surfaces at the base of meter-scale fining-upward sequences	Meter scale fining-upward sequences	Small local tectonic pulses or channel avulsion	4th or 5th
4th	Bedding surfaces of intra-bed fining-upward cycles (cm- to dm-scale)	cm- to dm-scale fining-upward sequences	Seasonal events (year to 10s year scale)	3rd

Table 5.2 – Summary table of the bounding surfaces and corresponding sequences defined for the SSB. Possible origin and the correlation with Miall's classification scheme are tentative.

The surface corresponding to the contact of the basin with the basement is defined as a 1st rank boundary. It can be described from the sub-surface data for the whole basin (Fig. 5.2). Its origin is linked to a major regional tectonic process during of late Variscan orogeny that promoted the appearance of topographic highs and trenches along the SSSZ (Oliveira et al., 2007; Almeida et al., 2006; see geological setting above). This surface can rarely be observed outcropping and is frequently tectonized. A discontinuous outcrop ca. 50m to the NW of the Vale de Figueira de Baixo farm house is possibly the best example of this surface, where the basal conglomerate seems to rest over porphyry rocks (Pl. 5.8C). The erosional surface at the base of the Tertiary sequence is also defined as a 1st rank boundary. It is defined solely in the Vale de Figueira outlier and the southernmost outcrops (Fig. 5.2). Although this boundary corresponds to a defined cartographic geological limit, it was not observed outcropping. Its origin is related to the uplift and erosion of the basin and surrounding area. The regional uplift can be related with the

SSSZ, but the possible E-W strike group of compressive faults discussed above probably had a major role in the post-Pennsylvanian evolution of this area (see Gonçalves, 1983 maps and interpretation). Considering Miall's boundary classification scheme these 2 boundaries would be 8th order boundaries.

The boundary between the two units within the SSB is only tentatively defined as it is a rapid shift of the sedimentation characteristics and not a boundary or surface s.s. Furthermore, it can only be generally described from the data provided by Andrade et al. (1955) in their summarized descriptions of the borehole cores (Fig. 5.2). It is classified as a 2nd rank boundary. Its origin is probably due to a tectonic stasis or period of milder activity that promoted a shift from a sedimentation stage considerably dependant on the orographic characteristics of the surrounding area to a stage of more distal fluvial and lacustrine sedimentation. This change can also reflect a simple geomorphological change of the surrounding area as the main topographic highs were eroded. This surface can be tentatively associated with 6th or 7th order sequence boundaries (*sensu* Miall, 1982 in Miall 1996).

At the outcrop scale, the erosional surfaces bounding the m-scale conglomerate to mudstone cycles (often incomplete) are present in nearly all studied sections from both basal and upper units. These are classified as 3rd rank boundaries (Pl. 5.8B, E). Their origin is uncertain but can be connected with small tectonic pulses affecting the area. The changes in the clasts' lithologies and roundness from one cycle to the next suggest changes of source areas. Alternatively these cycles and corresponding erosional surfaces can merely be related with the processes of the fluvial system such as channel avulsion (Jones & Schumm, 1999)

These surfaces can be classified as 4th or 5th order bounding surfaces (sensu Miall, 1982 in Miall, 1996).

The bounding surfaces of the intra-bed cycles are classified as 4th rank boundaries. These are observed in all sections studied, mainly in sandstone, siltstone and shale beds, although some finer conglomeratic beds also showed this cyclicity (Pl. 5.8D, H). These are probably related with seasonal cycles and/or with year or 10s year-scale events such as floods. These surfaces are probably equivalent to the 3rd order boundaries of Miall (1982) in Miall (1996).

Higher rank boundaries can be defined such as sets and cosets of cross-bedding structures and specific levels within beds, but this is outside the scope of this study.

5.3.3 Palaeocurrents and provenance data

The several sections measured are probably not coeval, distance several kilometres from each other and are questionably representative of each area and time interval. The reduced number of measurements, due to the poor exposure, precludes comprehensive interpretations and firm conclusions. The upper unit with sandstones and coals is over represented due to the scarcity of outcrops of the basal unit. Two main trends seem to exist. One, approximately E-W, possibly representing relatively proximal sediment transport from source areas located around the edges of the basin. The other, to the South, may represent more distal transport along the strike of the basin.

The dextral sense of the SSSZ which limits the current extent of the basin to the W very likely altered the original orientation of the measured planes and lineaments. The amount of rotational (clock-wise) movement is uncertain.

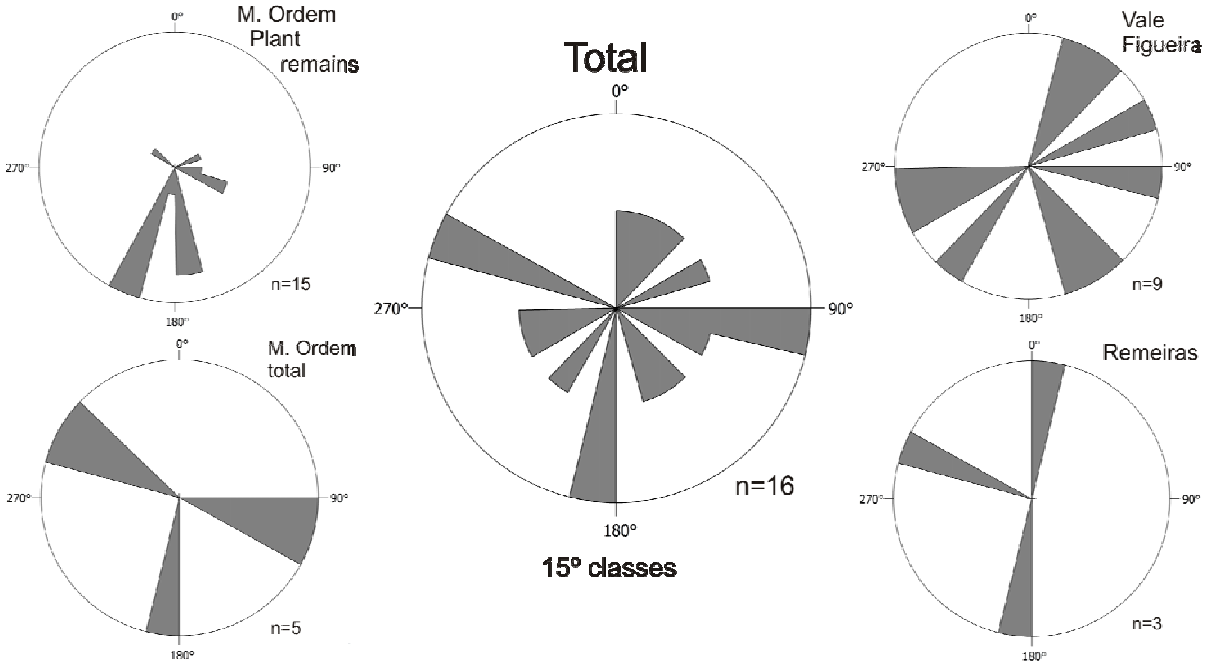

Fig. 5.5 - Rose diagrams showing palaeocurrent directions of several localities in Santa Susana Basin. The Moinho da Ordem total diagram considered the averages of the two main directions of the oriented plant remains horizon as single measurements. Bulk results from all the sections and additional measurements in smaller outcrops are shown in the central diagram. The averages of multiple measurements from the same horizon where considered as single measurements.

The lithologies eroded and deposited in the basin are easily recognizable in the conglomeratic beds that dominate the basal unit but also appear in the upper unit. The lithologies can be associated with known units and formations in Ossa-Morena and South Portuguese Zones. The basal conglomeratic unit rarely outcrops, but it very commonly shows large rounded boulders (up to 50cm) of the Grupo de Cuba Porphyry rocks. Several mine reports state that sills and dykes of this porphyry unit were observed to cut the basin's sediments. Indeed one of the boreholes describes two sills cutting the basal conglomeratic unit. This was never observed by us. It seems that the magmatic activity that originated the porphyry unit was, at least in part, coeval with the initial stages of sedimentation. Porphyry and porphyry-derived rocks (possibly sub-aerial equivalents – see Gonçalves, 1983) probably dominated the landscape in this area and seem to have been the main source of material during initial basinal development. The conglomerates in the upper unit are dominated by quartz and quartzite clasts, but other lithologies are common. These include black and greenish slates, black cherts and psamitic metasediments. The following table links the lithologies found and the units and formations from which they derived

The polygenic nature of the conglomerates shows that during the deposition of the SSB both South Portuguese Zone (to W current coordinates) and Ossa-Morena Zone (to E current coordinates) were exposed and being eroded, coherent with the palaeocurrent data.

Lithology	Probable source
Black slate	Série Negra – Ossa Morena Zone
Black chert	Série Negra – Ossa Morena Zone
Greenish slate	Toca da Moura Complex – Ossa Morena Zone
Pink and green porphyry rocks	Grupo de Cuba Felsics - Ossa Morena Zone
Quartz (magmatic or hydrothermal origin)	Pulo do Lobo Group – South Portuguese Zone (?)Silurian metasediments – Ossa Morena Zone
Quartzite	Ordovician units – Ossa Morena Zone Pulo do Lobo Group – South Portuguese Zone
Psamitic metasediments	Pulo do Lobo Group – South Portuguese Zone

Table 5.3 – Lithologies of the clasts found in the SSB conglomerates and their probable origin

5.3.4 Clay fraction mineralogy

Most samples showed a strong distortion of the X-ray diffractogram due to the high content of very fine organic matter and probably organic acids that settled with the clay fraction. These samples were treated with low concentrated H_2O_2 for several days and remounted. All samples show a Quartz-Illite-Kaolinite composition, with varying proportions. Illite dominated in many samples (30 to 50%), but most had equal amounts of the 3 components. Vermiculite appeared in several samples as a minor component (<10%). Its presence in fluvial/lacustrine sedimentary environments is difficult to explain. Weaver (1989, p.137-141) presents several case studies available in the literature were microbial (mostly fungal) activity in organic matter-rich settings promotes the transformation of clay minerals to vermiculite. Areas with stagnant water in flood plains could possibly provide an appropriate setting.

Feldspars were also found in minor amounts (up to 11%) in the Ordem1 section. This may reflect a poorly mature nature of some of the deposits.

No significant differences were found between the diffraction pattern of the samples from the VFigueira 6 section (interpreted as lacustrine) and the remaining fluvial sections.

5.3.5 Palaeobotany

The palaeobotanical site (Vale de Figueira) is composed of several levels of siltstone and shales with abundant large (decimetrical) plant remains at the top of a fluvial sequence. Fossils are found in the outcrop and associated floats. Other levels in lower parts of the sequence are also fossiliferous, but these usually have a worse preservation and lower abundance (Pl.5.8G).

Most plant fossils are preserved as thin coaly films, but there are also low relief impressions and iron oxide replacement. Intermediate situations are common. 3D

preservation of stems, usually by silicification, is occasionally found in more coarse sediments such as sandstones and fine conglomerates (Pl.5.8G).

The taxa described in the literature (Sousa and Wagner, 1983; 1985) are summarized in the following table.

The fossil diversity analysis indicates that Lycophytes were probably the dominant group of the sedimentation area. All kind of lycophyte organs have been preserved in Santa Susana fossil record: leaves, stems, reproductive structures, recently rhizophores (*Stigmaria* sp.) were found.

In terms of palaeoecology, Lycophytes dominated the peat-forming swamps of Carboniferous times (Taylor, 1981; Raven et. al, 1999). Others specimens present in Santa Susana fossil record can also be found in this type of environment. *Sphenophyllum* sp. could occur both in lycophyte forest, as an understory shrub, or in over bank flood plain and lake deposits as a climbing plant which was locally abundant (Arens et al., 1998). *Cordaites* existed in the edges of lycophytes forests (Arens et al., 1998; Raven et al. 1999), although it is thought to be ecological diverse and widely distributed (Raven et al., 1999). Considering this, the possibility of downstream transportation of *Cordaites* cannot be excluded, since they are also common in other environments (Gall 1995; Taylor, 1981; Raven et al., 1999).

It is also relevant that arborescent sphenopsids and specimens belonging to *Medullosales* (*Pteridospermophyta* division) occurred in different environments. The arborescent sphenopsid *Calamites* sp. found at Vale de Figueira locality, are normally associated with moist and damp environments such as surrounding areas of lakes and streams and on point bars, along the edge of forest areas (Gall, 1995; Taylor, 1981; Raven et al. 1999). The Medullosans grew on levee banks of wandering rivers and streams (Gall, 1995; Taylor, 1981).

Since information about fossil site locations and abundance in Santa Susana basin is scarce it is difficult to infer on the initial source area of the plants. Organ diversity of Lycophytes can also imply that transport was not long, because the fragile reproductive structures were preserved (Gall, 1995). Environment divergence between arborescent sphenopsids and medullosans may possibly imply that there is more than one source area of plant remains or a single large area with different environments and their transitions (Gall, 1995).

Division	Class	Order	Family	Genus	Species
Lycophyta		Lepidodendrales		*Lepidodendron*	*Lepidodendron* cf. *aculeatum*
				Lepidophloios	*Lepidophloios* ? sp. nov.?
				Lepidocarpon	*Lepidocarpon major*
				Lepidoslrobophyllum	*Lepidoslrobophyllum hastatum*
				Siqillaria	*Siqillaria* cf. *tessellata*
		Lycopodiales		*Lycopodites*	*Lycopodites sp.*
Sphenophyta		Sphenophyllales		*Sphenophyllum*	*Sphenophyllum emarginatum*
					Sphenophyllum emarginatum forma *truncatum*
					Sphenophyllum querreiroi
		Equisetales		*Annularia*	*Annularia sphenophylloides*
					Annularia stellata
				Asterophyllites	*Asterophyllites equisetiforms*
					Asterophyllites longifolius
				Calamites	*Calamites carinatus*
					Calamites suckowi
Pteridophyta	Coenopteridopsida		Zygopteridaceae	*Alloiopteris*	cf. *Alloiopteris* sp.
	Filicopsida	Marattiales		*Pecopteris*	cf. *Pecopteris avoldensis*
					Pecopteris (Lobapteris) cf. *camertonensis*
					Pecopteris daubreei sensu
					Pecopteris dentata
					Pecopteris haussei
					Pecopteris monyi
					Pecopteris nyranensis
					Pecopteris cf. *obliquenervis*
					Pecopteris plumosa
					Pecopteris raconensis
					Pecopteris cf. *saraefolia*
					Pecopteris unita
					Pecopteris sp.
		Filicales		*Dicksonites*	*Dicksonites plueckeneti*
Pteridospermophyta		Medullosales		*Alethopteris*	*Alethopteris lesquereuxi*
				Linopteris	*Linopteris palentina*
				Mariopteris	*Mariopteris rotundata*
				Neuropteris	*Neuropteris flexuosa*
					Neuropteris scheuchzeri
				Sphenopteris	*Sphenopteris alentajana*
					Sphenopteris cf. *pecopteroides*
					Sphenopteris sewardi
					Sphenopteris (Palmatopteris?) spinosa
					Sphenopteris sp. nov. ? (cf. *douvillei* Zeiller)
Conipherophyta	Cordaitopsida			*Cordaites*	*Cordaites* sp.

Table 5.4 - List of taxa described in the literature from Santa Susana basin. Adapted from Mattioli et al. (2009)

5.3.6 Palynology and age of the assemblages

Most of the processed samples were barren in terms of sporomorphs, although all yielded a significant amount of organic matter. Phytoclasts were dominant in all samples. Organic residues consistently showed signs of corrosion, probably due to weathering that promoted oxidation of organic matter. Only some samples from VFigueira 1 to 5 and Susana 5 and 6 sections provided recognizable palynomorphs.

The biostratigraphical division of the Late Westphalian and Early Stephanian in terms of palaeobotany and palynology has been discussed for a long time (e.g. Cleal et al. 2003). Wagner (1966a, b) discussed the existence of a "Cantabrian" stage in NW Spain with characteristic macroflora that was not represented elsewhere in Europe. He argued that the base of the Stephanian corresponding to the Holz conglomerate (Saar-Lorraine coal field) represented a hiatus and that probably the upper part of the Westphalian D and the lower part of the Stephanian were missing. The same hiatus seemed to be present in other paralic basins across Europe. The later macrofloral biozonation of the Westphalian and Stephanian (Wagner, 1984), revised by Cleal (1991) included considerable detail of the Westphalian-Stephanian boundary. Further refinement of the floral succession in this time interval was conducted by Cleal et al. (2003) who also discussed the application of the zonal scheme to areas outside the classical locality in NW Spain.

The palynostratigraphical subdivision of this time interval was conducted in several areas in Europe a North America, mainly in basins containing coal fields and in some cases restricted to coal bearing intervals (e.g. Kosanke, 1950, Peppers, 1970). Regional zonal schemes were developed (e.g. Smith and Butterworth, 1967; Alpern et al., 1967a, b), but their correlation was not always completed. Clayton et al. (1977) proposed a Western Europe Carboniferous Miospore biostratigraphical scheme, compiling the available data from several basins in Europe. It is still in use today. The scheme was revised for the Mississippian and part of the Pennsylvanian sub-systems for some areas (e.g. Clayton et al., 2003; Mclean et al., 2005; Owens et al., 2004, 2005). The official subdivision of the Carboniferous System (Heckel & Clayton, 2003) considered the Upper Carboniferous East European stages as the global stages. This artificially solved the problem of naming Westphalian or Cantabrian/Stephanian to sequences in Western Europe but did not facilitate the correlation of the several basins, especially when these are strictly terrestrial. The middle upper part of the Pennsylvanian sub-system (Stephanian = uppermost Moscovian, Kasimovian and Gzhelian) is currently under revision (Clayton et al., 2008). In recent years, two important lines of work have shed some light on the palynostratigraphical division of the Moscovian-Kasimovian in Europe. Mclean et al. (2005) produced a very detailed zonation of the North Sea Carboniferous strata from the uppermost Tournaisian up to Westphalian D based on first and last occurrences of miospore species. For the Westphalian the scheme has been applied to some extent in offshore and onshore areas in The Netherlands, northern Germany and northern France (Mclean et al., 2005). Ties with marine biota were made in several points but none in the Westphalian D. In parallel, several papers by Dimitrova and Cleal (Cleal et al., 2003; Dimitrova & Cleal 2008, 2007; Dimitrova et al., 2005; Dimitrova, 2004a, b) studied the Westphalian-Stephanian microfloral succession of terrestrial basins in Bulgaria and the UK and revised some of the published data from other basins across Europe and North America. The ties with the macrofloral record were made for most of the studied areas. Although these studies did not refine the existing zonation schemes, they provided valuable information on ranges of several taxa that can be used to correlate different basins. Unfortunately there are some apparent discrepancies in the ranges and boundary defining taxa between the available biozonation

schemes. For example, the range bases of *Lundbladispora gigantea* (Alpern) Doubinger, 1968 and *Schopfites dimorphus* Kosanke, 1950 is at the base of biozone W7b (Westphalian D see Fig.5.6) according to Mclean et al. (2005), but is said to be marking the base of the Stephanian by Dimitrova & Cleal (2008). *L. gigantea* (Alpern) Doubinger, 1968 is represented in Clayton et al. (1977) range chart as having its range base in upper SL biozone (Westphalian C). Additionally Mclean et al. (2005) also considers the range top of *Westphalensisporites irregularis* Alpern, 1959 to be near the base of biozone W7b while it is reported in several basins in Europe to extend well into the Stephanian (lower N.BM zone) (Clayton et al., 1977). A similar situation occurs with *Florinites junior* Potonié & Kremp, 1954.

For the Santa Susana basin assemblages, one may ask what scheme is more appropriate. The work by Cleal (2008a, b) suggests that macrofloral associations of Pennsylvanian Portuguese basins, including the SSB, are closely associated with the Silesian and Rhine palaeoprovinces which includes the assemblages from NW Spain, Upper Silesia, NW Germany, Dobrudzha Coalfield (Bulgaria), N Turkey, Pennines (Silesian) and SW Britain and Canadian Maritimes (Rhine). During the Cantabrian Portuguese and NW Spanish assemblages develop some degree of provincialism, but remain closely related with Silesian and Rhine palaeoprovinces (Cleal, 2008a, b). Thus it seems appropriate to use the scheme proposed by Clayton et al., (1977) with the refinements proposed by Cleal et al., (2003) and Dimitrova & Cleal (2008). The use of the scheme by Mclean et al., (2005) may not be readily applicable as it may reflect a floral succession of a different palaeoprovince, it does not cover the Stephanian and the fact that it is based on marine sequences may introduce other variables that limit its application to a terrestrial basin such as the SSB.

Fernandes (1998, 2001) attributed the SSB assemblage studied by him to the OT or ST Miospore Biozones. He found (?)*Angulisporites splendidus* Bharadwaj 1954, *Latensina trileta* Alpern 1958 (index taxa for the ST Miospore Biozone), *Cheidelonites* sp. and *Candidispora candida* Venkatachala, 1963, indicative of the ST Miospore Biozone. In his analysis of the assemblage the positioning of the Westphalian/Stephanian boundary in terms of microflora is discussed and it is suggested that the assemblage might in fact belong to the ST Miospore Biozone.

VFigueira 1 to 5 sections

Several samples were collected from grey shales and silts of the sequence underlying the fossiliferous levels (Fig. 5.4). From the 4 samples processed by standard palynological methods, 3 provided observable palynomorphs from which several slides were produced. The forth sample collected within the top fossiliferous levels provided only dark brown and black phytoclasts. Samples were observed mainly from unoxidized residues, but low concentrated bleach was used to clear darker sporomorphs (mainly thick-walled ones).

The organic residues from the 3 productive samples were dominated by light to dark brown phytoclasts with subordinate amounts of sporomorphs. Rare algal remains were found in all samples. Within the sporomorphs, large (>80μm), thin walled, laevigate and finely sculptured trilete and monolete forms were clearly dominant (ca. 45%) Most of these forms are assignable to genera *Schopfipollenites* (ca. 30%), *Wilsonites* and *Florinites*. Other numerically important sporomorphs within the assemblages are Cingulicavati and Crassiti infraturmae spores, namely the genera *Densosporites*, *Lycospora* and *Crassispora* (all around 7-8%). Considering the parent plants described for these taxa (e.g. Balme, 1995; Bek & Oplustil, 1998; Traverse, 2007 and references there in), it seems plausible that the surrounding palaeobotanical assemblage was dominated by Medullosaceae, Cycadofilicales and Cordaitales forms along with lycopsid trees. Qualitatively this is in accordance with the

palaeobotanical finds in the same section, although lycopsids are more abundant than any other group (see palaeobotanical section for discussion).

Sporomorph wall colour was yellow in thin walled forms (e.g. *Schopfipollenites* spp.) and medium brown in thick walled taxa (e.g. *Crassispora* spp.). Preservation of sporomorphs is moderate to good, but nearly all specimens had some corrosion features such as pitting of the wall surface, enhancement/modification of simple ornamentation (laevigate, granulate, verrucate, punctuate, etc.) or partial destruction of thin exine layers (mostly the exoexine) which often made difficult the recognition of trilete and monolete marks. Over 80 spore and pollen taxa were identified, although a significant number of these are left in open nomenclature due to the moderate preservation. The basal sample (VFIG 1.1) provided only a few determinable specimens while samples VFIG 3.2 and VFIG 4.2 provided over 300 grains per slide.

The VFigueira 1 to 5 section assemblages contain *Cadiospora magna* Kosanke, 1950 which appears in the upper OT miospore biozone and extends into the Stephanian. Significant numbers of the ST miospore biozone index species *Latensina trileta* Alpern 1958 are found and many other specimens appear to be *L. trileta*, but the poor preservation limits specific determination. The presence of *Latensina trileta* Alpern 1958 is recorded rarely from the *Torispora securis–Torispora laevigata* (SL) Miospore Biozone onwards (Clayton et al., 1977; Pittau et al., 2008), but it only becomes frequent or common in the ST zone. *Angulisporites splendidus* Bharadwaj 1954 was not found. Auxiliary taxa such as *Cheidelonites* sp. is represented by a several specimens. *Lundbladispora gigantea* (Alpern) Doubinger, 1968 is present and could indicate a Stephanian age, but is reported from the North Sea from the mid Westphalian D (see discussion above). The presence of cf. *Reticulatisporites reticulatus* Ibrahim, 1933, is problematic as the reported range top is in the middle-upper part of the OT miospore biozone. In general terms the assemblage is more characteristic of the Stephanian, considering the abundance of pollen grains and the presence of typical spore taxa of this age.

There is an apparent discrepancy with the biostratigraphical results derived from the palaeobotanical data (Wagner & Sousa, 1983) which point to an older age: *Neuropteris ovata* zones or *Dicksonites plueckeneti* sub zone – corresponding to upper OT Miospore Biozone of Clayton *et al*., 1977; 2003 (Moscovian age). All of the fossil plant taxa described from the locality have biostratigraphical ranges that reach the Cantabrian (uppermost OT – lowermost ST biozones). Wagner and Sousa, 1983 could not exclude the possibility that the fossil plant assemblage was in fact Cantabrian in age.

It thus seems plausible to conclude that the VFigueira 1 to 5 section is truly Stephanian in age (see Fig. 5.6).

The assemblage described by Fernandes (1998, 2001) from borehole cuttings may indeed belong to the ST Miospore Biozone. His results are coherent with ours.

Revision of the macroflora is underway and the preliminary results (Mattioli *et al*., 2009) show the existence of previously undescribed taxa from the site which may lead to a reassessment of its age. The publication of a revised Western Europe Upper Pennsylvanian Miospore Biozonation scheme (especially for the Stephanian) will certainly facilitate a more definitive biostratigraphical conclusion.

Susana 5 and 6 sections

As mentioned above the samples from Susana 5 and 6 sections provided few recognizable palynomorphs. Although considerably impoverished and thus difficult to interpret, it is interesting to note that pollen grains are almost absent (few specimens of *Florinites* sp. and *Schopfipollenites* sp. are present). *Verrucosisporites* spp. and

Laevigatosporites spp. are dominant in both sections. The presence of *Vestispora* cf. *costata* (Balme, 1952) Spode in Smith & Buterworth 1967; *Raistrickia fulva* Artuz, 1957 and *Convolutispora* sp. could indicate that the assemblage is significantly older than the ST zone proposed for the VFigueira 1 to 5 assemblages (see Fig. 5.6). Other recorded taxa such as *Crassispora* cf. *maculosa*, *Raistrickia* cf. *corynoges*, *Verrucosisporites* cf. *cerosus*, *Trinidulus diamphidios* Felix & Paden, 1964 and *Microreticulatisporites microreticulatus* Knox, 1950 have range tops in lower Westphalian or even the Mississippian. Due to the reduced number of specimens and moderate to poor preservation it is uncertain if these are reworked from older rocks or autochtonous palynomorphs. Several reworked palynomorphs were observed, mainly acritarchs (e.g. *Veryhachyum* sp., *Gorgonisphaeridium* sp.) but these clearly have a different degree of maturation and stand out in the slides (see Pl. 5.7). These reworked acritarchs very likely originate from the surrounding Toca da Moura complex metasedimentary rocks (OMZ) or the SPZ Grupo do Lobo units (Santa Iria and Horta da Torre Fms.). *Westphalensisporites* cf. *irregularis* and *Triquitrites* cf. *sculptilis* are also present limiting the age of the assemblage to the Westphalian B.

The assemblages from the Susana 5 and 6 are considered to be, possibly, of Westphalian C or D age, but further investigation of the basin's palynology is needed to assess the true temporal extent of the sedimentation.

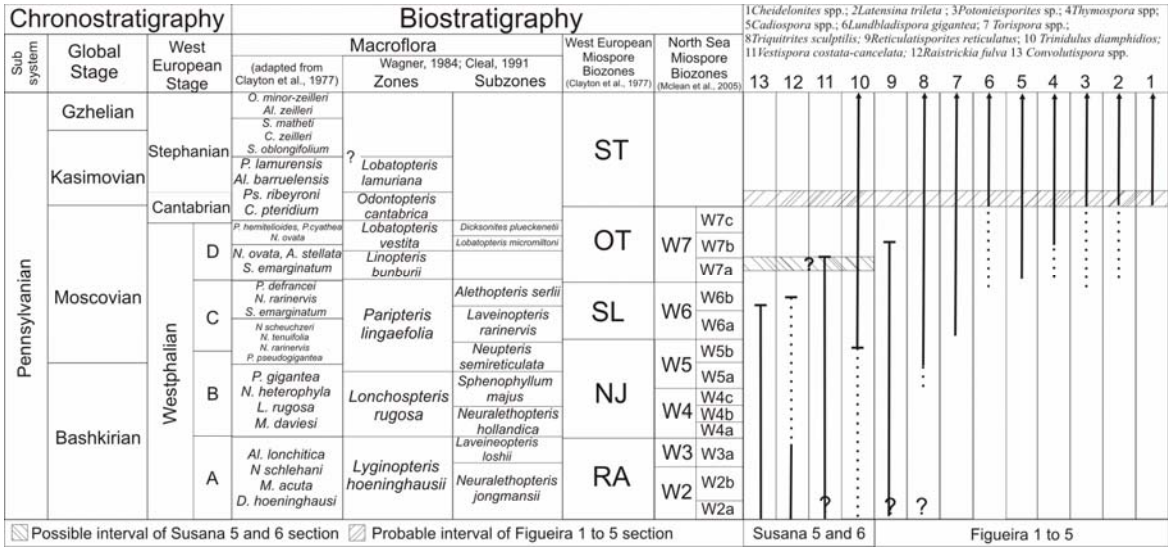

Fig. 5.6 – Range of selected taxa from the VFigueira 1 to 5 and Susana 5 and 6 sections and possible biostratigraphical positioning (cross hatch). "?" denotes taxon in open nomenclature. Dashed line denotes infrequent occurrence or discrepancy between ranges reported by different authors. Ranges and biozonations compiled from Alpern et al. (1967); Alpern & Liabeauf (1967); Clayton et al. (1977); Cleal (1991) in Cleal & Thomas (1996); Wagner (1984) and Mclean et al. (2005).

5.3.7 Thermal and burial history

The results obtained from the vitrinite reflectance measurements are summarized in Table 5.5. All the maceral particles from the SSB are altered, probably due to outcrop weathering, causing a decrease in the Rr% values. Sample VFIG 6.1 did not provide unaltered particles and the measured Rr% (1,1%) can be used is as a reference for the values expected for weathered samples. Significantly higher values such as the ones measured in VFIG 3.2 are associated with semifusinite particles which are difficult to distinguish from vitrinite in palynological residues. The remaining values in Table 5.5 refer to unaltered vitrinite particles.

Toca da Moura/Cabrela Complex						
Outcrop/section	**Sample**	**Biozone/Age**	**%Rm**	**Std. Dev.**	**#particles**	**Palaeotemp**
Estação de Cabrela	C5	CM – Up. Tournaisian	3,79	0,22	100	286,6
Pedreira Monte da Chaminé	PQ3	CM – Up. Tournaisian	4,16	0,35	100	296,3
	PQ5	Pu – L. Viséan	4,22	0,4	100	297,7
	PQ6	Pu – L. Viséan	4,15	0,34	100	296
	PQ7	TS – L. Viséan	3,49	0,23	100	278
	PQ8	TS – L. Viséan	4,24	0,5	100	298,2
	PQ9	TS – L. Viséan	4,08	0,24	100	294,2
Corte Pereiro	CP15	NM – Up. Viséan	3,66	0,32	100	282,9
	CP16	NM – Up. Viséan	3,33	0,29	100	273,1
	CP17	NM – Up. Viséan	3,03	0,22	100	263,3
Cai Água	CBCA3	CM/Pu – Tournasian-Viséan	3,27	0,35	100	274,4
	CBCA4	Pu – L. Viséan	3,09	0,25	100	265,3
Pedreira da Ribeira dos Marmelos	PRM6	Pu – L. Viséan	3,19	0,35	100	268,6
	PRM7	Pu – L. Viséan	3,61	0,42	95	281,5
	PRM8	Pu – L. Viséan	3,8	0,33	100	286,8
	PRM9	Pu – L. Viséan	3,32	0,45	100	272,8
	PRM10	Pu – L. Viséan	3,78	0,29	80	286,3
Santa Susana Basin						
Jongeis	SUS 3	Moscovian(?)	1,69	0,11	70	203
	SUS 6	Moscovian(?)	1,48	0,12	31	189
Vfigueira 1 to 5	VFIG 1.1	ST – Lower Kasimovian	1,44	0,17	63	186
	VFIG 3.2	ST – Lower Kasimovian	1,87	0,18	70	213
	VFIG 4.2	ST – Lower Kasimovian	1,55	0,23	70	194
Vfigueira 6	VFIG 6.1	Kasimovian (?)	1,15	0,14	30	163
	VFIG 6.5	Kasimovian (?)	1,51	0,29	62	191
Remeiras	REM 1.6	Moscovian(?)	1,58	0,13	71	196

Table 5.5 – Random mean vitrinite reflectance values and corresponding palaeotemperatures of the SSB and Toca da Moura/Cabrela Complex. Palaeotemperatures obtained from equation in Barker (1988). Data from Paulo Fernandes (unpublished).

Thus, the representative Rr% values for the SSB are around 1,55%, corresponding to a maximum temperature of ca. 193ºC using Barker's equation (Barker, 1988). This is coherent with the values obtained by Sousa et al. (2009) in museum coal samples from the SSB.

The samples from the Toca de Moura/Cabrela Complex have Rr% values between 3,02 and 4,24%. Many of the outcrops of these complexes have igneous intrusions, which produce higher Rr% values. The representative Rr% value of these complexes, unaffected by igneous intrusion is probably between 3 and 3,8%Rr (260 – 290ºC). Despite its age (Tournaisian –

Viséan) these are significantly higher values than the ones obtained for the SSB that rests unconformably over the Toca da Moura Complex.

The results show that the BSS and Toca da Moura/Cabrela complex had different thermal histories. The processes of subsidence, organic maturation and exhumation of the Toca da Moura/Cabrela complex occurred during a considerably short time interval, between the Upper Viséan and the Lower Kasimovian (possibly Moscovian). This is a maximum time span of 34Ma. The results also show that the thermal evolution of the SSB is post-Kasimovian and never reached the same magnitude of temperatures attained by the Toca da Moura/Cabrela complex. The maturation of this complex was not affected by its re-burial under the SSB.

The stratigraphical and organic maturation data point to the synorogenic character of these basins and rapid subsidence with elevated geothermal gradients. The effect of igneous activity on the maturation of the SSB is unknown but cannot be excluded.

5.4 Discussion and Conclusions

The basin's sedimentary facies and its evolution can only be generally considered due to the limited exposure and restricted knowledge of the basal unit. A fluvial system probably controlled sedimentation of the basin, although the basal unit was probably more dependant on the surrounding topography, possibly with a considerable alluvial component. During later stages of the basin evolution (corresponding to the upper unit), perennial lakes developed in some areas (e.g. VFigueira 6 section), but a fluvial meandering system and associated flood plain and/or abandoned channel deposits seems to have defined the sedimentation characteristics of most of the temporal and spatial extent of the basin.

Considering the geometry of the basin, palaeocurrent and provenance data, it is evident that both SPZ and OMZ rocks were exposed, being eroded during the time sedimentation was occurring in the SSB. During the initial stages of the basin filling, the surrounding landscape was very likely dominated by the Grupo de Cuba felsic rocks as they make up the vast majority of the clasts of the basal conglomerate. The magmatic activity that originated them extended at least to the lower part of the basin's sedimentation history. The main palaeocurrent directions probably reflect the sediment transport from the areas to the W and E to the central areas of the basin and along the strike, mainly to S.

Several controls acted on the basin sedimentation. Large scale tectonic events and periods promoted the formation of a depocenter along the SSSZ and consequent onset of sedimentation. The same tectonic kinematics allowed the continuation of the sedimentation. A period of tectonic stasis (or milder activity) is probably associated with the shift from an essentially conglomeratic sedimentation (basal unit) to a stage dominated by finer grained material and the development of peat in some areas (upper unit). The cyclic characteristics of the sedimentation (at the meter scale) may be associated with small tectonic pulses, but may simply reflect autogenic processes of the fluvial system (Catuneanu, 2006).

The post-Pennsylvanian evolution of the basin was controlled, at an early stage, by the same tectonic activity that originated the basin (late Variscan). During the Cainozoic (and Mesozoic?) the basin was exposed and eroded, especially the northern parts. The southern parts of the basin were covered during the Tertiary by a thin sequence (<20m) of sediments. The original extent of the basin was probably much bigger and it was probably connected to the flysch sedimentation occurring to the S during the Mississippian and Pennsylvanian (at least to the OT miospore biozone, Pereira et al. (2008), in the SPZ. The increased preservation potential of a basin along a structural-originated trench and the partial cover by Tertiary sediments allowed its perpetuation to the current day.

The plant fossil assemblage found at Vale de Figueira locality is probably a combination of transported plant remains from several areas of a river system (corresponding to different ecological settings), with a greater predominance of peat forming plants which seem to have been transported only for short distances (para-autochthonous assemblage?). The different lithologies found at the site indicate a river system with strong lateral and vertical variations (in time and space) which is in accordance with the observed mixing of plant remains from different areas of the system.

Additional collecting will allow a detailed revision of the plant taxonomy. The interpretation the section in terms of coupled lithofacies – plant taxonomy analysis is also planed. The abundance, proportions and taphonomy of each group and the relation with the lithology in which it is found will hopefully allow to infer on the palaeoecology of different groups of plants and shed some light on the apparent discrepancies between palaeobotanical and palynological records.

The age of the basin can only be bracketed for a part of the upper unit. The VFigueira 1 to 5 section provided a sporomorph assemblage assignable to the ST miospore biozone of Clayton et al., (1977) (Kasimovian = "Lower Stephanian"). Previous records from another locality (Fernandes, 1998, 2001) provided the same results. The assemblages from Susana 5 and 6 suggest that significantly older sediments may be present, but the poor quality of the residues preclude further interpretations.

5.5 Systematic Palynology

For the systematic palynology the Turmal System proposed by Potonié (1970) with modifications by Traverse (2007) is followed. The frequency of each taxon is indicated as well as the section where it occurs. The statistical significance of the frequency of sporomorphs in VFigueira 1 to 5 section is high as several hundreds of specimens were counted. For the Susana 5 and 6 sections, the significance is much lower as the total number of specimens in each section is lower than 100 and thus the abundance categorization is not shown for these sections. The frequency ranges of Smith and Butterworth (1967) were applied and are summarized in the following table:

Rare	<0,5%
Frequent	0,5-2%
Common	2,1-5%
Very common	5,1-10%
Abundant	>10%

Anteturma SPORITES Potonié, 1893

Turma TRILETES (Reinsch) Dettmann, 1963

Subturma AZONOTRILETES (Luber) Dettmann, 1963

Infraturma LAEVIGATI (Bennie & Kiston) Potonié, 1956

Genus *Calamospora* Schopf, Wilson & Bentall, 1944

Occurrence: Frequent in all sections
Calamospora cf. *microrugosa* (Ibrahim) Schopf, Wilson & Bentall, 1944 (Pl. 5.1a)
Occurrence: rare in VFigueira 1-5
Calamospora cf. *parva* Guennel, 1958 (Pl. 5.1b)
Occurrence: rare in VFigueira 1-5
Calamospora aff. *pusilla* Peppers, 1970 (Pl. 5.1c)
Occurrence: rare in VFigueira 1-5
Calamospora spp.
Occurrence: rare in VFigueira 1-5 and present in Susana 5

Genus *Leiotriletes* (Naumova) Potonié & Kremp, 1954
Occurrence: frequent in VFigueira 1-5, present in Susana 5
Leiotriletes levis (Kosanke) Potonié & Kremp, 1955 (Pl. 5.1d)
Occurrence: rare in VFigueira 1-5
Leiotriletes sp (Pl. 5.6r)
Occurrence: rare in VFigueira 1-5, present in Susana 5

Genus *Punctatisporites* (Ibrahim) Potonié & Kremp, 1954
Occurrence: rare in VFigueira 1-5, present in Susana 5
Punctatisporites provectus Kosanke, 1950 (Pl. 5.1e)
Occurrence: rare in VFigueira 1-5
Punctatisporites sp. (Pl. 5.6s)
Occurrence: present in Susana 5

Infraturma APICULATI (Bennie & Kidston) Potonié, 1956

Subinfraturma GRANULATI Dybová & Jachowicz, 1957
Genus *Cyclogranisporites* Potonié & Kremp, 1954
Occurrence: rare in VFigueira 1-5, present in Susana 6
aff. *Cyclogranisporites breviradiatus* Peppers, 1970 (Pl. 5.1f)
Occurrence: rare in VFigueira 1-5
Cyclogranisporites sp. (Pl. 5.6a)
Occurrence: present in Susana 6

Genus *Granulatisporites* (Ibrahim) Potonié & Kremp, 1954
Occurrence: frequent in VFigueira 1-5 and present in Susana 5
Granulatisporites cf. *granularis* Kosanke, 1950 (Pl. 5.1i)
Occurrence: rare in VFigueira 1-5
Granulatisporites spp. (Pl. 5.1j, k, l; Pl. 5.6t)
Occurrence: frequent in VFigueira 1-5 and present in Susana 5

Subinfraturma VERRUCATI Dybová & Jachowicz, 1957

Genus *Converrucosisporites* Potonié & Kremp, 1954
Occurrence: frequent in VFigueira 1-5
Converrucosisporites aff. *armatus* (Dybóva & Jachowicz) Smith & Butterworth, 1967 (Pl. 5.1g, h)
Occurrence: frequent in VFigueira 1-5

Genus *Schopfites* Kosanke, 1950
Occurrence: rare in VFigueira 1-5
Schopfites sp. (Pl. 5.1m)
Occurrence: rare in VFigueira 1-5

Genus *Verrucosisporites* (Ibrahim) Smith & Butterworth, 1967
Occurrence: common in VFigueira 1-5 and present in Susana 5 and 6
Verrucosisporites cerosus (Hoffmeister, Staplin & Maloy) Butterworth & Williams, 1958 (Pl. 5.6u)
Occurrence: frequent Susana 5
Verrucosisporites cf. *microtuberosus* (Loose) Smith & Butterworth, 1967
Occurrence: rare in VFigueira 1-5
Verrucosisporite papulosus Hacquebard, 1957 (Pl. 5.1q)
Occurrence: rare in VFigueira 1-5
Verrucosisporites cf. *pergranulus* (Alpern) Smith & Alpern, 1971(Pl. 5.1n, o; Pl. 5.6v)
Occurrence: rare in VFigueira 1-5 and present in Susana 5
Verrucosisporites cf. *verrucosus* (Ibrahim) Smith & Butterworth, 1967 (Pl. 5.1p)
Occurrence: common in VFigueira 1-5
Verrucosisporites spp. (Pl. 5.6b, w)
Occurrence: common in VFigueira 1-5 and present in Susana 5 and 6

Subinfraturma NODATI Dybová & Jachowicz, 1957

Genus *Lophotriletes* (Naumova) Potonié & Kremp, 1954
Occurrence: rare in VFigueira 1-5
aff. *Lophotriletes gibbosus* (Ibrahim, 1933) Potonié & Kremp, 1955 (Pl. 5.1r)
Occurrence: rare in VFigueira 1-5

Subinfraturma BACULATI Dybová & Jachowicz, 1957

Genus *Raistrickia* (Schopf,Wilson & Bentall) Potonié & Kremp, 1954
Occurrence: frequent in VFigueira 1-5 and present in Susana 5 and 6
Raistrickia carbondalensis Peppers, 1970 (Pl. 5.2a)
Occurrence: rare in VFigueira 1-5
Raistrickia fulva Artuz, 1957 (Pl. 5.6x)
Occurrence: present in Susana 5
Raistrickia aff. *corynoges* Sullivan, 1968 (Pl. 5.6y)
Occurrence: present in Susana 5
Raistrickia spp. (Pl. 5.2b; Pl. 5.6c)
Occurrence: frequent in VFigueira 1-5 and present in Susana 5 and 6

Infraturma MURORNATI Potonié & Kremp, 1954

Genus *Microreticulatisporites* (Knox) Potonié & Kremp 1954
Occurrence: rare in VFigueira 1-5
Microreticulatisporites microreticulatus Knox, 1950 (Pl. 5.6d)
Occurrence: present in Susana 6

aff. *Microreticulatisporites* sp.
Occurrence: rare in VFigueira 1-5

Genus *Convolutispora* Hoffmeister, Staplin & Malloy, 1955
Occurrence: present in Susana 6
Convolutispora sp. (Pl. 5.6e)
Occurrence: present in Susana 6

Subturma ZONOTRILETES Waltz, 1935

Infraturma AURICULATI (Schopf) Dettmann, 1963

Genus *Triquitrites* (Wilson & Coe) Potonié & Kremp, 1954
Occurrence: common in VFigueira 1-5 and present in Susana 5 and 6
Triquitrites cf. *desperatus* Potonié & Kremp, 1955 (Pl. 5.2c)
Occurrence: rare in VFigueira 1-5
Triquitrites priscus Kosanke 1950 (Pl. 5.2d)
Occurrence: rare in VFigueira 1-5
Triquitrites cf. *sculptilis* Balme, 1952 (Pl. 5.2e; Pl5.6z)
Occurrence: rare in VFigueira 1-5, present in Susana 6
Triquitrites aff. *triturgidus* (Loose) Schopf, Wilson & Bentall, 1944 (Pl. 5.2f)
Occurrence: rare in VFigueira 1-5
Triquitrites spp (Pl. 5.2g; Pl. 5.6f, aa)
Occurrence: common in VFigueira 1-5 and present in Susana 5 and 6

Infraturma TRICRASSATI Dettmann, 1963

Genus *Reinschospora* Schopf, Wilson & Bentall, 1944
Occurrence: rare in VFigueira 1-5
Reinschospora sp. (Pl. 5.2h)
Occurrence: rare in VFigueira 1-5

Infraturma CINGULATI (Potonié & Klaus) Dettmann, 1963

Genus *Cadiospora* (Kosanke) Turner, 1993
Occurrence: frequent in VFigueira 1-5
Cadiospora magna Kosanke, 1950 (Pl. 5.2i, j)
Occurrence: frequent in VFigueira 1-5

Genus *Reticulatisporites* (Ibrahim) Neves, 1964
Occurrence: frequent in VFigueira 1-5
aff. *Reticulatisporites lacunosus* Kosanke, 1950 (Pl. 5.2k)
Occurrence: rare in VFigueira 1-5
Reticulatisporites cf. *reticulatus* Ibrahim, 1933 (Pl. 5.2n, o)
Occurrence: frequent in VFigueira 1-5

Genus *Savitrisporites* Bharadwaj, 1955
Occurrence: present in Susana 5

? *Savitrisporites* sp. (Pl. 5.6bb)
Occurrence: present in Susana 5

Subturma ZONOLAMINATITRILETES Smith & Butterworth, 1967

Infraturmae CRASSITI (Bharadwaj & Venkatachala) Smith & Butterworth, 1967 and CINGULICAVATI Smith & Butterworth, 1967

Genus *Cirratriradites* Wilson & Coe, 1940
Occurrence: frequent in VFigueira 1-5
Cirratriradites cf. *elegans* (Waltz) Potonié & Kremp, 1956 (Pl. 5.2l)
Occurrence: rare in VFigueira 1-5
Cirratriradites sp. (Pl. 5.2m)
Occurrence: frequent in VFigueira 1-5

Genus *Crassispora* Bharadwaj, 1957
Occurrence: Very common in VFigueira 1-5 and present in Susana 5 and 6
Crassispora kosankei (Potonié & Kremp) Bharadwaj, 1957 (Pl. 5.2p, q; Pl. 5.6g)
Occurrence: Very common in VFigueira 1-5 and present in Susana 5 and 6
Crassispora cf. *maculosa* (Knox) Sullivan, 1968 (Pl. 5.7a)
Occurrence: present in Susana 5
Crassispora sp. (Pl. 5.7b)
Occurrence: present in Susana 5 and 6

Genus *Densosporites* (Berry) Butterworth et al., 1964
Occurrence: Very common in all sections
Densosporites cf. *anulatus* (Loose) Smith & Butterworth, 1967 (Pl. 5.3d)
Occurrence: rare in VFigueira 1-5
Densosporites crassigranifer Artuz, 1957 (Pl. 5.3c)
Occurrence: rare in VFigueira 1-5
Densosporites cf. *lobatus* Kosanke, 1950 (Pl. 5.3a, b; Pl. 5.6h)
Occurrence: frequent in VFigueira 1-5 and present in Susana 6
Densosporites gracilis Smith & Butterworth. 1967 (Pl. 5.3f)
Occurrence: rare in VFigueira 1-5
Densosporites cf. *pseudoanulatus* Kosanke, 1950 (Pl. 5.3g)
Occurrence: rare in VFigueira 1-5
Densosporites cf. *sphaerotriangularis* Kosanke, 1950 (Pl. 5.3e)
Occurrence: frequent in VFigueira 1-5
Densosporites spp. (Pl. 5.7c)
Occurrence: Very common in VFigueira 1-5 and present in Susana 5

Genus *Lundbladispora* (Balme) Playford, 1965
Occurrence: common in VFigueira 1-5
Lundbladispora gigantea (Alpern) Doubinger, 1968 (Pl. 5.3m, n)
Occurrence: frequent in VFigueira 1-5
Lundbladispora sp
Occurrence: frequent in VFigueira 1-5

Genus *Lycospora* (Schopf, Wilson & Bentall) Somers, 1972
Occurrence: very common in VFigueira 1-5 and present in Susana 5 and 6
Lycospora parva Kosanke, 1950 (Pl. 5.3j)
Occurrence: rare in VFigueira 1-5
Lycospora pusilla (Ibrahim) Somers, 1972 (Pl. 5.3h, I; Pl. 5.6i; Pl. 5.7d)
Occurrence: common in all sections
Lycospora sp. (Pl. 5.3k; Pl. 5.6j)
Occurrence: common in VFigueira 1-5 and present in Susana 6

Genus *Radiizonates* Staplin & Jansonius, 1964
Occurrence: rare in VFigueira 1-5
Radiizonates tenuis (Loose) Butterworth & Smith, 1964 (Pl. 5.3o)
Occurrence: rare in VFigueira 1-5

Genus *Westphalensisporites* Alpern, 1959
Occurrence: frequent in VFigueira 1-5 and present in Susana 5
Westphalensisporites irregularis Alpern, 1959 (Pl. 5.3l; Pl. 5.7e)
Occurrence: frequent in VFigueira 1-5 and present in Susana 5

Supersubturma PSEUDOSACCITRILETES Richardson, 1965

Infraturma MONOPSEUDOSACCITI Smith & Butterworth, 1967

Genus *Endosporites* Wilson & Coe, 1940
Occurrence: frequent in VFigueira 1-5
Endosporites globiformis (Ibrahim) Schopf, Wilson & Bentall, 1944 (Pl. 5.3p)
Occurrence: frequent in VFigueira 1-5

Subturma PERINOTRILETES Erdtman, 1947

Genus Vestispora (Wilson & Hoffmeister). Wilson & Venkatachala, 1963
Occurrence: rare in VFigueira 1-5, present in Susana 6
Vestispora cf. *costata* (Balme, 1952) Spode in Smith & Buterworth, 1967 (Pl. 5.6k, l)
Occurrence: present in Susana 6
Vestispora sp.
Occurrence: rare in VFigueira 1-5

Turma MONOLETES Ibrahim, 1933

Subturma AZONOMONOLETES Luber, 1935

Infraturma LAEVIGATOMONOLETI Dybová & Jachowicz, 1957

Genus *Laevigatosporites* Ibrahim, 1933
Occurrence: common in VFigueira 1-5
Laevigatosporites maximus (Loose) Potonié & Kremp, 1954 (Pl. 5.3q)
Occurrence: frequent in VFigueira 1-5
Laevigatosporites medius Kosanke, 1950 (Pl. 5.7f)

Occurrence: present in Susana 5
Laevigatosporites minimus (Wilson & Coe) Schopf, Wilson & Bentall, 1944 (Pl. 5.7g)
Occurrence: present in Susana 5
Laevigatosporites cf. *perminutus* Alpern, 1958 (Pl. 5.6m; Pl.5.7h)
Occurrence: present in Susana 5 and 6
Laevigatosporites cf. *ovalis* Kosanke, 1950 (Pl.5.7i)
Occurrence: present in Susana 5
Laevigatosporites cf. *robustus* Kosanke, 1950 (Pl. 5.3r)
Occurrence: rare in VFigueira 1-5
Laevigatosporites cf. *vulgaris* (Ibrahim) Alpern & Doubinger, 1973 (Pl. 5.3t; Pl.5.7j)
Occurrence: frequent in VFigueira 1-5 and present in Susana 5
Laevigatosporites spp. (Pl. 5.3s; Pl. 5.6n; Pl. 5.7k)
Occurrence: frequent in VFigueira 1-5, very common is Susana 5 and present in Susana 6

Infraturma SCULPTATOMONOLETI Dybová & Jachowicz, 1957

Genus *Cheiledonites* Doubinger, 1957
Occurrence: frequent in VFigueira 1-5
Cheiledonites sp. (Pl. 5.3x, y)
Occurrence: frequent in VFigueira 1-5

Genus *Punctatosporites* Ibrahim, 1933
Occurrence: rare in VFigueira 1-5, present in Susana 5 and present in Susana 6
Puntactosporites cf. *minutus* (Pl. 5.6o)
Occurrence: rare in VFigueira 1-5 and present in Susana 6
Punctatosporites sp. (Pl. 5.3u; Pl 5.7l)
Occurrence: rare in VFigueira 1-5, present in Susana 5 and present in Susana 6

Genus *Torispora* Balme, 1952
Occurrence: rare in VFigueira 1-5
cf. *Torispora securis* (Balme) Alpern, Doubinger & Horst, 1973 (Pl. 5.3v)
Occurrence: rare in VFigueira 1-5

Genus *Thymospora* (Wilson & Venkatachala) Alpern & Doubinger, 1973
Occurrence: frequent in VFigueira 1-5
Thymospora cf. *pseudothiessenii* (Kosanke) Alpern & Doubinger, 1973 (Pl. 5.3w)
Occurrence: frequent in VFigueira 1-5

Anteturma POLLENITES Potonié, 1931

Turma SACCITES Erdtmann, 1947

Subturma MONOSACCITES (Chitaley) Potonié & Kremp, 1954

Infraturma TRILETESACCITI Leschik, 1955

Genus *Cordaitina* (Samoilovich) Hart, 1965
Occurrence: rare in VFigueira 1-5

Cordaitina sp. (Pl. 5.3bb, cc)
Occurrence: rare in VFigueira 1-5

Genus *Latensina* Alpern, 1958
Occurrence: common in VFigueira 1-5
Latensina trileta Alpern, 1958 (Pl. 5.3z, aa)
Occurrence: frequent in VFigueira 1-5
Latensina sp.
Occurrence: frequent in VFigueira 1-5

Genus *Wilsonites* Kosanke, 1950
Occurrence: very common in VFigueira 1-5
Wilsonites aff. *delicatus* Kosanke, 1950 (Pl. 5.4a)
Occurrence: frequent in VFigueira 1-5
Wilsonites cf. *vagus* Inossova, 1976 (Pl. 5.4b)
Occurrence: frequent in VFigueira 1-5
Wilsonites spp. (Pl. 5.4c)
Occurrence: common in VFigueira 1-5

Infraturma ALETESACCITI Leschik, 1955

Genus *Florinites* Schopf, Wilson & Bentall, 1944
Occurrence: very common in VFigueira 1-5 and present in Susana 5
Florinites cf. *bederi* Pittau et al, 2008 (Pl. 5.4f)
Occurrence: frequent in VFigueira 1-5
Florinites cf. *diversiformis* Kosanke, 1950 (Pl. 5.4g)
Occurrence: frequent in VFigueira 1-5
Florinites sp.cf. Florinites junior Potonié & Kremp, 1954 (Pl. 5.4h)
Occurrence: frequent in VFigueira 1-5
aff. *Florinites pellucidus* (Wilson & Coe) Wilson, 1958 (Pl. 5.4e)
Occurrence: rare in VFigueira 1-5
Florinites cf. *similis* Kosanke, 1950
Occurrence: frequent in VFigueira 1-5
Florinites visendus (Ibrahim) Schopf, Wilson & Bentall, 1944 (Pl. 5.4d)
Occurrence: frequent in VFigueira 1-5
Florinites spp. (eg. Pl. 5.4i; Pl. 5.7m)
Occurrence: common in VFigueira 1-5 and present in Susana 5

Infraturma VESICULOMONORADITI Pant, 1954

Genus *Potonieisporites* (Bharadwaj) Bharadwaj, 1964
Occurrence: frequent in VFigueira 1-5
Potonieisporites sp.
Occurrence: frequent in VFigueira 1-5

Subturma DISACCITES Cookson, 1947

Disaccites non striatti (Pl. 5.4j)

Occurrence: rare in VFigueira 1-5

Infraturma DISACCITRILETI Leschik, 1955

Genus *Pityosporites* Seward, 1914
Occurrence: frequent in VFigueira 1-5
Pityosporites sp. (Pl. 5.4l)
Occurrence: frequent in VFigueira 1-5

Subturma POLYSACCITES Cookson, 1947

Genus *Alatisporites* Ibrahim, 1933
Occurrence: frequent in VFigueira 1-5
Alatisporites sp. (Pl. 5.4l)
Occurrence: frequent in VFigueira 1-5

Turma PLICATES (Naumova) Potonié & Kremp, 1954

Subturma PRAECOLPATES Potonié & Kremp, 1954

Genus *Schopfipollenites* Potonié & Kremp, 1954
Occurrence: abundant in VFigueira 1-5, present in Susana 5 and present in Susana 6
Schopfipollenites ellipsoides (Ibrahim) Potonié & Kremp, 1954. (Pl. 5.5a, e, f)
Occurrence: abundant in VFigueira 1-5
Schopfipollenites ovalis Schwartsman, 1976 (Pl. 5.5g, h, i)
Occurrence: very common in VFigueira 1-5
Schopfipollenites parvus Schwartsman, 1976 (Pl. 5.5b, c)
Occurrence: common in VFigueira 1-5
Schopfipollenites sp. (Pl. 5.5d; Pl. 5.6p; Pl. 5.7n)
Occurrence: common in VFigueira 1-5, present in Susana 5 and present in Susana 6

Unknown morphological affinity
Trinidulus Felix & Paden 1964
Occurrence: present in Susana 6
Trinidulus diamphidios Felix & Paden, 1964 (pl. 5.6q)
Occurrence: present in Susana 6

Acknowledgements

Ícaro Silva and Pedro Almeida for the joint field work and brainstorming (this is also their work). Mário Cachão and Carlos Marques da Silva of the Centro de Geologia of the University of Lisbon for the logistical support. We acknowledge LNEG (Portuguese Geological Survey), especially Miguel Ramalho and Jorge Sequeira from the Geological Museum and the National Museum of Natural History, especially Liliana Póvoas for the access to the palaeobotanical collections. Zélia Pereira (LNEG) and Paulo Fernandes (UAlg) for the joint work on the organic petrology.

References

ALMEIDA, P., DIAS DA SILVA, I. & OLIVEIRA, H., 2006. Caracterização Tectono-Estratigráfica da Zona de Cisalhamento de Santa Susana (ZCSS) no Bordo SW da Zona de Ossa Morena (ZOM), (Portugal). VII Cong. Nac. de Geol., Livro de Resumos, I: 49-53.

ALPERN, B., LACHKAR, G. & LIABEUFF, J. J., 1967. Le bassin houiller Lorrain peut-il fournir un stratotype pour le Westphalien supérieur. Review of Palaeobotany and Palynology 5: 75-91.

ALPERN, B. AND LIABEAUF, J. J., 1967. Considérations palynologiques sur le Westphàlien et le Stéphanien: propositions pour un parastratotype. C. R. Acad. Sc. Paris serie D, 265: 840-843.

ANDRADE, C., 1927-30. Alguns Elementos para o Estudo dos Depósitos de Carvão do Moinho da Ordem. Comunicações Geológicas. Tomo XVI: 3-28.

ANDRADE, C., SANTOS, R., CABRAL GUERREIRO, A., 1955. Estudo por sondagens da região carbonífera do Moinho da Ordem. Comunicações dos Serviços Geológicos de Portugal. Tomo XXXVI: 199-255.

ARENS, C., STRÖMBERG, C. & THOMPSON, A., 1998. Virtual Paleobotany http://www.ucmp.berkeley.edu/IB181/VPL/Dir.html

BALME, B.E., 1995. Fossil in situ spores and pollen grains: an annotated catalogue. Review of Palaeobotany and Palynology 87: 81–323.

BARKER, C. E., 1988. Geothermics of petroleum systems: implications of the stabilisation of kerogen thermal maturation after a geologically brief heating duration at peak temperature. In: Magoon, L. B. (ed.) Petroleum systems of the United States. United States Geological Survey Bulletin, 1870: 26 - 29.

BEK, J., OPLUSTIL, S., 1998. Some lycopsid, sphenopsid and pteropsid fructifications and their miospores from the Upper Carboniferous basins of the Bohemian Massif. Palaeontographica B, 248: 127–161.

CATUNEANU, O., 2006. Principles of Sequence Stratigraphy. Elsevier. 375p.

CARVALHOSA, A., ZBYSZEWSKY, G., 1994. Carta Geológica de Portugal, na escala 1:50000. Notícia Explicativa da folha 35-D (Montemor-o-Novo). Instituto Geológico e Mineiro. 86 p.

CLAYTON, G., COQUEL, R., DOUBINGER, J., GUEINN K.J., LOBOZIAK, S., OWENS, B. & STREEL, M., 1977. Carboniferous Miospores of Western Europe: illustration and zonation. Meded. Rijks Geol. Dienst, 29: 1-71.

CLAYTON, G., MCCLEAN, D. & OWENS, B., 2003. Carboniferous palinostratigraphy: recent developments in Europe (Abstract 103). International Congress on Carboniferous and Permian Stratigraphy, Utrecht, August 2003.

CLAYTON, G., HIGGS, K., MCCLEAN, D. & OWENS, B., 2008. Carboniferous miospore biostratrigraphy in Western Europe. 12th International Palynological Congress, 8th International Organisation of Palaeobotany Conference Bonn, Germany. Terra Nostra, 2. Abstract no. 117: 51-52.

CLEAL, C.J., 1991. Plant fossils in geological investigation: the Palaeozoic. Ellis Horwood, Chichester. 233 p.

CLEAL, C. J., 2008a. Palaeofloristics of Middle Pennsylvanian lyginopteridaleans in Variscan Euramerica. Palaeogeography, Palaeoclimatology, Palaeoecology 261(1-2):1-14.

CLEAL, C. J., 2008b. Palaeofloristics of Middle Pennsylvanian medullosaleans in Variscan Euramerica. Palaeogeography, Palaeoclimatology, Palaeoecology 268(3-4): 164-180.

CLEAL, C., DIMITROVA, T. K. & ZODROW, E. L., 2003. Macrofloral and palynological criteria for recognising the Westphalian-Stephanian boundary. Newsletters on Stratigraphy 39(2-3): 181-208.

DIMITROVA, T. 2004a. Microfloral biostratigraphy and vegetation change of the late Westphalian in the Dobrudzha Basin, NE Bulgaria. Geologica Balcanica 34 (1-2): 21-29.

DIMITROVA, T. 2004b. Palynological study of the Gurkovo Formation (Westphalian D/Cantabrian), Dobrudzha Basin, Bulgaria. Geologica Balcanica. 34 (3-4): 29-43.

DIMITROVA, T. K., CLEAL, C. J. & THOMAS, B. A., 2005. Palynology of late Westphalian-early Stephanian coal-bearing deposits in the eastern South Wales Coalfield. Geological Magazine 142 (6): 809-821.

DIMITROVA, T., C., CLEAL , 2007. Palynological evidence for late Westphalian - early Stephanian vegetation change in the Dobrudzha Coalfield, NE Bulgaria. Geol. Mag. 144, 513-524.

DIMITROVA, T. & CLEAL, C, 2008. The late Westphalian D - Early Cantabrian palynology of Europe and the Canadian maritimes. GEOSCIENCES: 61-62.

DOMINGOS, L. C. G., FREIRE, J. L. S., SILVA, F. G., GONÇALVES, F.; PEREIRA, E. & RIBEIRO, A., 1983. The Structure of the Intramontane Upper Carboniferous Basins in Portugal. In The Carboniferous of Portugal. Memórias - Nova Série. 29: 187-194

FERNANDES, J.P., 1998. Resultados preliminares del estudio palinológico de la Cuenca de Santa Susana (Alcácer do Sal, Portugal), Estudios palinológicos – Actas XI Simposio de Palinología A.P.L.E. – Alcalá de Heranes, p. 3.

FERNANDES, J.P., 2001. Nuevos resultados del estudio palinológico de la Cuenca de Santa Susana (Alcácer do Sal, Portugal). In: M.A.FOMBELLA BLANCO, D.FERNÁNDEZ GONZÁLEZ & R.M.VALENÇA BARRERA (Editors) - Palinología: Diversidad y

Aplicaciones, Trabajos del XII Simposio de Palinología (A.P.L.E.), León, 1998, Universidad de León: 95-99.

GALL, J.C., 1995. Paléoécologie – Paysages et environnements diparus. Masson. Paris. 239 p.

GARCIA-ALCALDE, J., CARLS, P.; PARDO-ALONSO, M.; SANZ-LOPEZ, J.; SOTO, F.; TRUYOLS-MASSONI, M. & VALENZUELA-RÍOS, J. 2002. Devonian. In Gibbons, W., Moreno, T. The Geology of Spain. Geological Society: 67-92.

GOMES, B. A., 1865. Flora fóssil do terreno carbonífero das visinhanças do Porto, Serra do Bussaco e Moinho d'Ordem próximo de Alcácer do Sal. Commissão Geológica de Portugal. Memória. Lisboa.

GONÇALVES, F., 1983. Formações Precâmbricas e do Paleozóico Superior do Flanco Meridional do Anticlinório de Évora – Moura, Dia 29 de Setembro (Excursão nº2), Guia das Excursões no bordo sudoeste da Zona de Ossa-Morena. Comun. Serv. Geol. Portugal. 69 (2): 267-282.

GONÇALVES, F., 1984/85. Contribuição para o conhecimento geológico do complexo vulcano-sedimentar de Toca da Moura, Alcácer do Sal. Memórias da Academia das Ciências de Lisboa. Tomo XXVI: 263-267.

HECKEL, P. H. & CLAYTON, G., 2006. The Carboniferous System. Use of the new official names for the subsystems, series, and stages. Geologica Acta 4(3): 403-407.

HILLIER, S. & MARSHALL, J., 1988. A rapid technique to make polished thin sections of sedimentary organic matter concentrates. Journal of Sedimentary Petrology, 58: 754-755.

JONES, L. S. & SCHUMM, S. A., 1999. Causes of avulsion: an overview. In: Dwight, N. S. & Rogers, J., Fluvial sedimentology. Special Pub. International Association of Sedimentologists 28: 171-178.

KOSANKE, R. M.,1950. Pennsylvanian spores of Illinois and their use in correlation. Bulletin Geological Survey Illinois 74. 128p.

LIMA, W., 1895-1898. Estudo sobre o carbónico do Alemtejo . Communicações da Direcção dos Trabalhos Geológicos de Portugal. Tomo III: 34-54

MATTIOLI, M., MACHADO, G., SILVA, I. & ALMEIDA, P. 2009. Revision of the stratigraphy and palaeobotany of the Moscovian (Upper Carboniferous intramontane Santa Susana Basin (SW Portugal). Paleolusitana 1: 269-275.

MCLEAN, D., OWENS, B. & NEVES, R., 2005. Carboniferous miospore biostratigraphy of the North Sea. In: Carboniferous hydrocarbon geology: the southern North Sea and surrounding onshore areas. Collinson, J. D., Evans, D. J., Holliday, D. W. and Jones, N. S. (eds) Yorkshire Geological Society 7: 13-24.

MIALL, A., 1996. The geology of fluvial deposits: sedimentary facies, basin analysis and petroleum geology. Springer-Verlag, Berlin. 582 p.

NEIVA, J.M., 1943. Os conglomerados antracolíticos e a idade de algumas formações eruptivas portuguesas. Boletim da Sociedade Geológica de Portugal 3: 71-80.

OLIVEIRA, J.T., 1983. The marine Carboniferous of south Portugal: A stratigraphic and sedimentological approach. In: Lemos de Sousa, MJ & Oliveira, J.T. JT (eds). The Carboniferous of Portugal. Serviços Geológicos de Portugal, Lisboa, Memorias, 29: 3-38.

OLIVEIRA, J. T., RELVAS, J. M. R. S., PEREIRA, Z., MUNHÁ, J. M., MATOS, J. X., BARRIGA, F. J. A. S. & ROSA, C. J., 2006. O complexo vulcano-sedimentar de Toca da Moura-Cabrela, Zona de Ossa Morena : evolução tectono-estratigráfica e mineralizações associadas. Geologia de Portugal: 1-13.

OLIVEIRA, H., SILVA, I. & ALMEIDA, P., 2007. Tectonic and Stratigraphic Description and Mapping of the Santa Susana Shear Zone (SSSZ), the SW Border of Ossa Morena Zone (OMZ), Barrancão – Ribeira de S. Cristóvão Sector (Portugal): Theoretical Implications. Geogaceta 41(3-6): 151-154.

OWENS, B., MCLEAN, D. & BODMAN, D., 2004. A revised palynozonation of British Namurian deposits and comparisons with Eastern Europe. Micropaleontology 50(1): 89-103.

OWENS, B., MCLEAN, D., SIMPSON, K. R. M., SHELL, P. M. J. & ROBINSON, R., 2005. Reappraisal of the Mississippian palynostratigraphy of the East Fife coast, Scotland, United Kingdom. Palynology 29(1): 23-47.

PEPPERS, R. A., 1970. Correlation and Palynology of Coals in the Carbondale and Spoon Formations (Pennsylvanian) of the Northeastern Part Of the Illinois Basin. Illinois State Geological Survey Bulletin, 93: 1-173.

PEREIRA, Z., MATOS, J. X. D., FERNANDES, P. & OLIVEIRA, T., 2008. Palynostratigraphy and systematic palynology of the Devonian and Carboniferous Successions of the South Portuguese Zone, Portugal. Memórias Geológicas 34: 181p.

PEREIRA, Z., OLIVEIRA, V., & OLIVEIRA, J. T., 2006. Palynostratigraphy of the Toca da Moura and Cabrela Complexes, Ossa Morena Zone, Portugal. Geodynamic implications. Review of Palaeobotany and Palynology 139(1-4): 227-240.

PITTAU, P., DEL RIO, M., COTZA, F., RONCHI, A., SANTI, G. & GIANNOTTI, R., 2008. Pennsylvanian miospore assemblages from the Bèdero Section, Varese, Italian Southern Alps. Revue de Micropaleontologie 51(2): 133-166.

POTONIÉ, R., 1970. Synopsis der Gattungen der Sporae dispersae V. Nachträge zu allen Gruppen (Turmae). Beihefte zum Geologischen Jahrbuch, 87: 1–22.

PRIEM, H.N.A., BOELRIJK, N.A.I.M., HEBEDA, E.H., VERDUMEN, E.A.TH. & VERCHURE, R.A., 1976. Isotopic dating in Southern Portugal. E.CO.G. IV Meeting.

RAVEN, P., EVERT, R., EICHHORN, S., 1999. Biology of Plants. W.H. Freeman and Company. New York: 243pp.

SANTOS, J., MATA, J., GONÇALVES, F. & MUNHÁ, J., 1987. Contribuição para o conhecimento Geológico-Petrológico da Região de Santa Susana: O Complexo Vulcano-sedimentar da Toca da Moura. Comunicações dos Serviços Geológicos de Portugal 73 (1-2): 29-48.

SMITH, A. H. V. & BUTTERWORTH, M. A., 1967. Miospores in the coal seams of the Carboniferous of Great Britain. Special Papers in Palaeontology 1: 1-324.

SOUSA, M. J., MARQUES, M., FLORES, D., RODRIGUES, C.F., 2009. Carvões portugueses: Petrologia e Geoquímica. In: J.M. Cotelo Neiva, António Ribeiro, Mendes Victor, Fernando Noronha, Magalhães Ramalho, Eds, Ciências Geológicas - Ensino e Investigação e sua História, 2009, Porto, I: 291-311.

DE SOUSA, J. L. & WAGNER, R. H., 1983. General Description of the Terrestrial Carboniferous Basins in Portugal and History of Investigations. In The Carboniferous of Portugal. Memórias - Nova Série. 29: 117-126.

DE SOUSA, J. L. & WAGNER, R. H., 1985. Annoted Catalogue of the Bernardino António Gomes fossil plant collection on Lisbon. Anais da Faculdade de Ciências. Universidade do Porto. Papers on the Carboniferous of the Iberian Peninsula. Supplement to volume 64 (1983): 411- 434.

TAYLOR, T. N., 1981. Paleobotany – an introdution to Fossil plant Biology. McGraw-Hill. 583p.

TEIXEIRA, C., 1938/40. Sobre a flora fossil do Carbónico alentejano. Bol. Mus. Labor. Miner. Geol. Univ. Lisboa. 3ª série. 7/8: 83-100.

TEIXEIRA, C., 1940. Notas para o estudo da flora fóssil do Carbónico alentejano. Prisma (Porto), 4(1): 67-72.

TEIXEIRA, C., 1944. O Antracolítico continental Português (Estratigrafia e Tectónica). PhD thesis. Universidade do Porto. Porto. 135 pp.

TEIXEIRA, C., 1945. O Antracolítico continental Português (Estratigrafia e Tectónica). Bol. Soc. Geol. Portug. Porto. 5(1/2): 1-139.

TRAVERSE, A., 2007. Paleopalynology. Topics in Geobiology, 28. 2nd ed. Springer. 814p.

WAGNER, R. H., 1966a. La succession des séries cantabriennes et leur limite supérieur. Comptes rendus de l'Académie des Sciences, Paris Serie D(262): 1419-1422.

WAGNER, R. H., 1966b. Sur l'existence, dans la Cordillère Cantabrique, de séries de passage entre Westphalien et Stéphanien : la limite inférieure de ces formations «cantabriennes». Comptes rendus de l'Académie des Sciences, Série D 262: 1337-1340.

WAGNER, R. H. & DE SOUSA, M. J., 1983. The Carboniferous Megafloras of Portugal – A revision of identifications and discussion of stratigraphic ages. In The Carboniferous of Portugal. Memórias - Nova Série. 29: 127-152.

WAGNER, R.H., 1984. Megafloral zones of the Carboniferous. Compte rendu 9e Congrès International de Stratigraphie et de Géologie du Carbonifère (Washington, 1979) 2: 109-134.

WEAVER, R. (1989). Clays, Muds, and Shales, Elsevier. 837p.

Plates

Plate 5.1 – Sporomorphs from the VFigueira 1 to 5 section

a *Calamospora* cf. *microrugosa* (Ibrahim) Schopf, Wilson & Bentall, 1944
b *Calamospora* cf. *parva* Guennel, 1958
c *Calamospora* aff. *pusilla* Peppers, 1970
d *Leiotriletes levis* (Kosanke) Potonié & Kremp, 1955
e *Punctatisporites provectus* Kosanke, 1950
f aff. *Cyclogranisporites breviradiatus* Peppers, 1970
g, h *Converrucosisporites* aff. *armatus* (Dybóva & Jachowicz) Smith & Butterworth, 1967
i *Granulatisporites* cf. *granularis* Kosanke, 1950
j, k, l *Granulatisporites* spp.
m *Schopfites* sp.
n, o *Verrucosisporites* cf. *pergranulus* (Alpern) Smith & Alpern, 1971
p *Verrucosisporites* cf. *verrucosus* (Ibrahim) Smith & Butterworth, 1967
q *Verrucosisporites* cf. *papulosus* Hacquebard, 1957
r aff. *Lophotriletes gibbosus* (Ibrahim, 1933) Potonié & Kremp, 1955

Plate 5.1

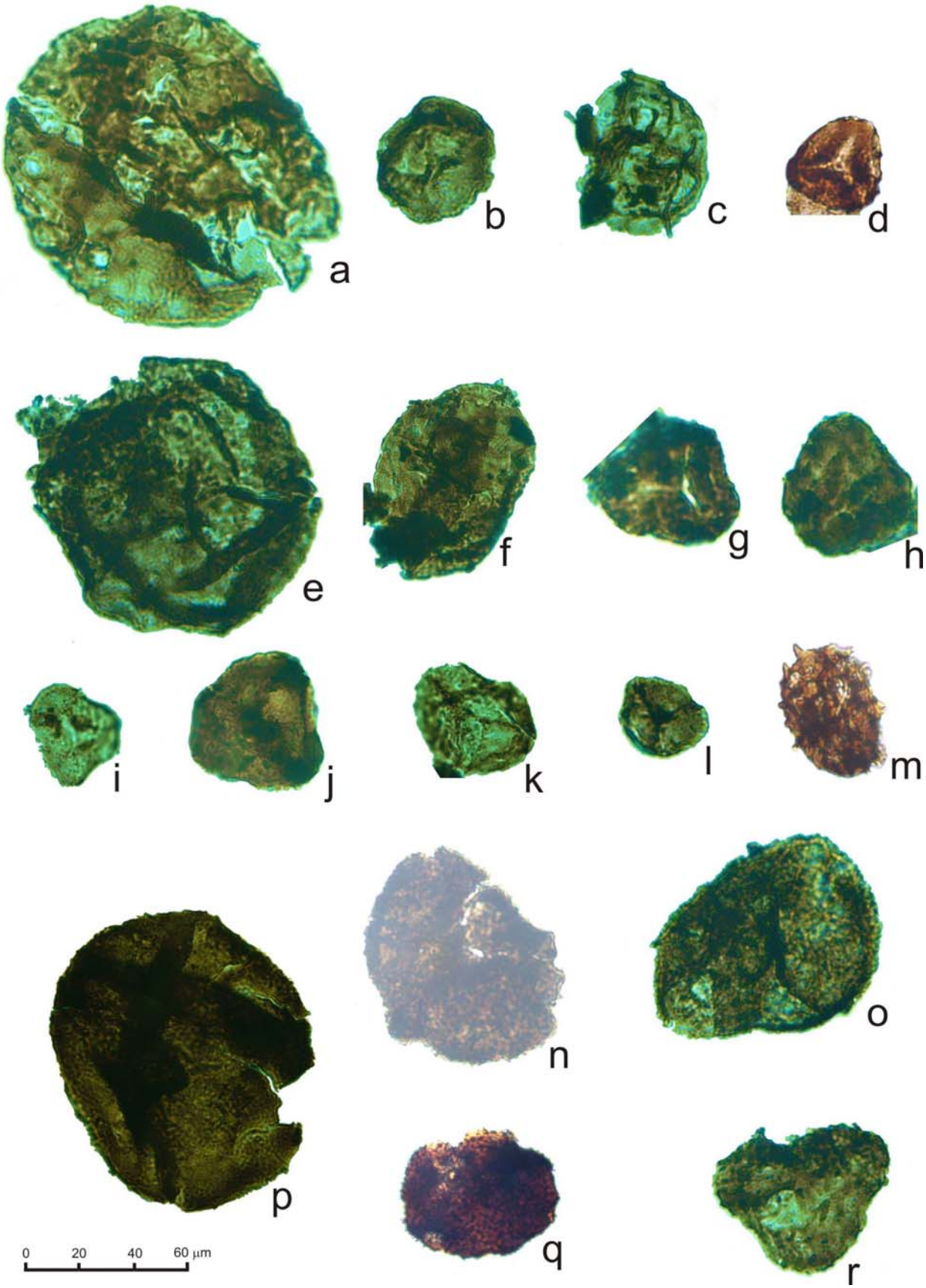

Plate 5.2 – Sporomorphs from the VFigueira 1 to 5 section

a *Raistrickia carbondalensis* Peppers, 1970
b *Raistrickia* sp.
c *Triquitrites* cf. *desperatus* Potonié & Kremp, 1955
d *Triquitrites* priscus Kosanke, 1950
e *Triquitrites* aff. *sculptilis* Balme, 1952
f *Triquitrites* aff. *triturgidus* (Loose) Schopf, Wilson & Bentall, 1944
g *Triquitrites* sp.
h *Reinschospora* sp.
i, j *Cadiospora magna* Kosanke, 1950
k *Reticulatisporites* cf. *lacunosus* Kosanke, 1950
l *Cirratriradites* cf. *elegans* (Waltz) Potonié & Kremp, 1956
m *Cirratriradites* sp.
n, o cf. *Reticulatisporites reticulatus* Ibrahim, 1933
p, q *Crassispora kosankei* (Potonié & Kremp) Bharadwaj, 1957

Plate 5.2

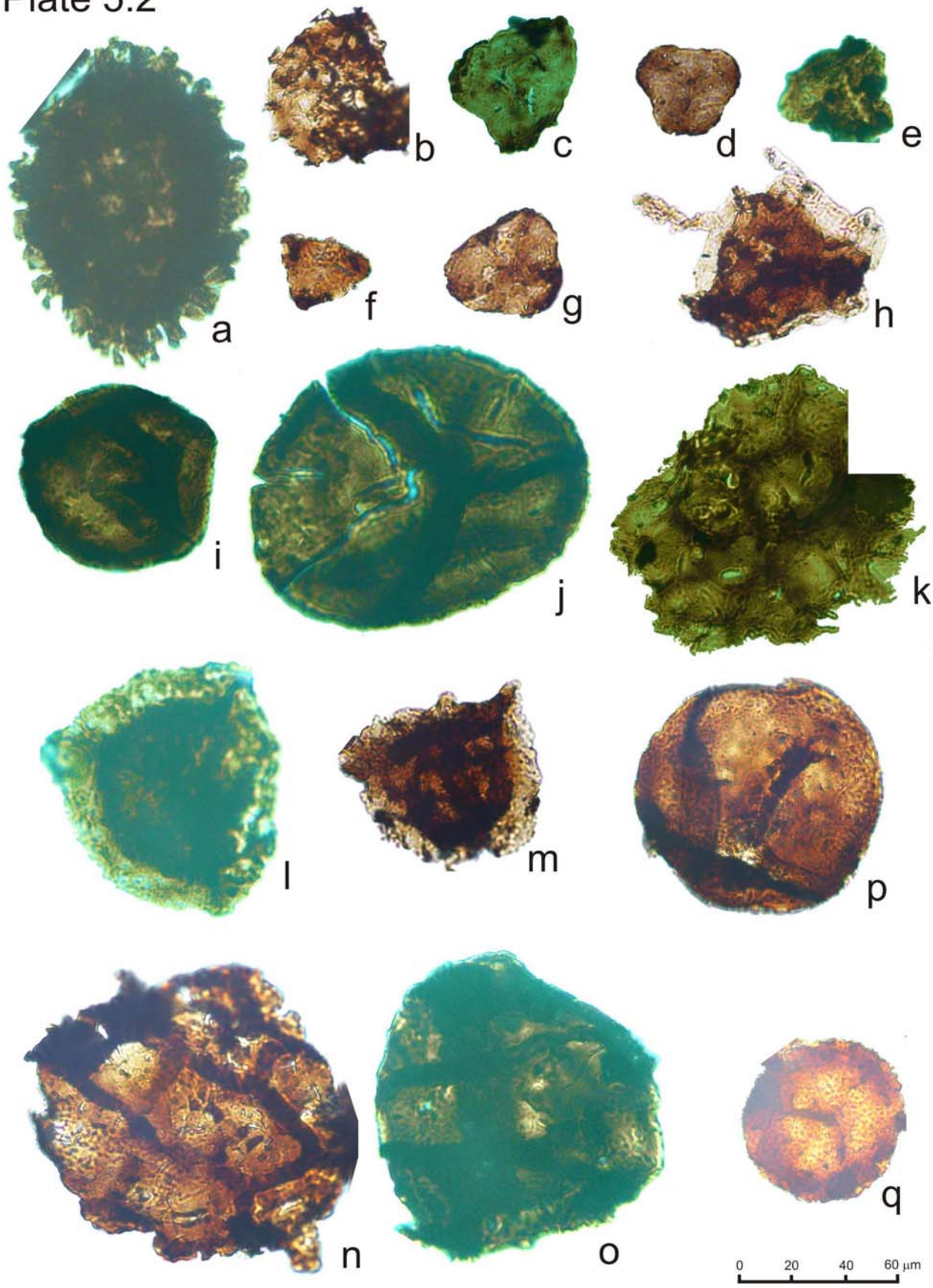

Plate 5.3 – Sporomorphs from the VFigueira 1 to 5 section

a, b *Densosporites* cf. *lobatus* Kosanke, 1950
c *Densosporites crassigranifer* Artuz, 1957
d *Densosporites* cf. *anulatus* (Loose) Smith & Butterworth, 1967
e *Densosporites* cf. *sphaerotriangularis* Kosanke, 1950
f *Densosporites gracilis* Smith & Butterworth, 1967
g *Densosporites* cf. *pseudoanulatus*
h, i *Lycospora pusilla* (Ibrahim) Somers, 1972
j *Lycospora parva* Kosanke, 1950
k *Lycospora* sp.
l *Westphalensisporites irregularis* Alpern, 1959
m, n *Lundbladispora gigantea* (Alpern) Doubinger, 1968 (same specimen, different focus)
o *Radiizonates tenuis* (Loose) Butterworth & Smith, 1964
p *Endosporites globiformis* (Ibrahim) Schopf, Wilson & Bentall, 1944
q *Laevigatosporites maximus* (Loose) Potonié & Kremp, 1954
r *Laevigatosporites robustus* Kosanke, 1950
s *Laevigatosporites* sp.
t *Laevigatosporites* cf. *vulgaris* (Ibrahim) Alpern & Doubinger, 1973
u *Punctatosporites* sp.
v cf. *Torispora securis* (Balme) Alpern, Doubinger & Horst, 1973
w *Thymospora* cf. *pseudothiessenii* (Kosanke) Alpern & Doubinger, 1973
x, y *Cheiledonites* spp.
z, aa *Latensina* trileta Alpern, 1958
bb, cc *Cordaitina* sp.

Plate 5.3

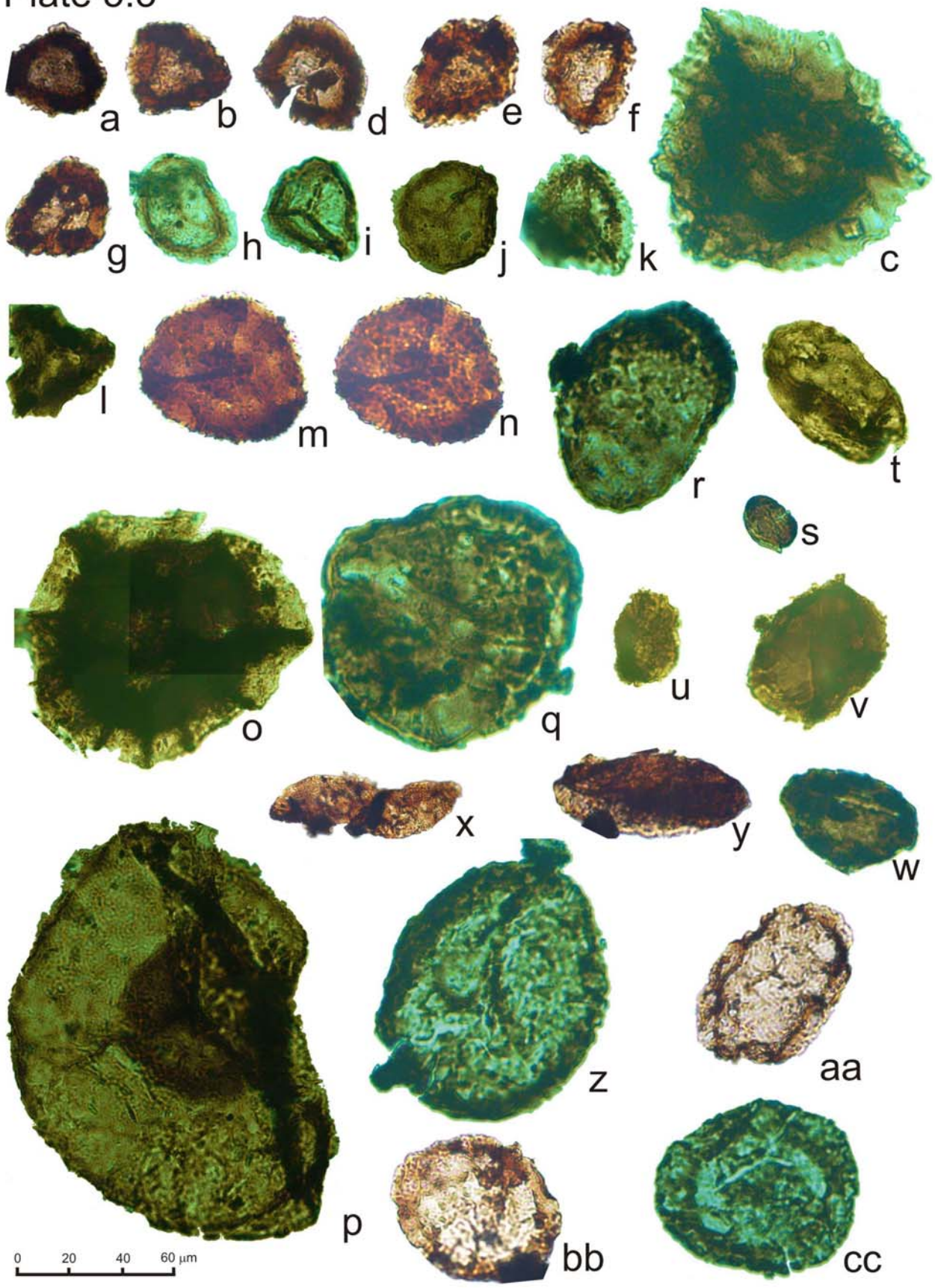

Plate 5.4 – Sporomorphs from the VFigueira 1 to 5 section

a *Wilsonites* aff. *delicatus* Kosanke, 1950
b *Wilsonites* cf. *vagus* Inossova, 1976
c *Wilsonites* spp
d *Florinites visendus* (Ibrahim) Schopf, Wilson & Bentall, 1944
e aff. *Florinites pellucidus* (Wilson & Coe) Wilson, 1958
f *Florinites* cf. *bederi* Pittau et al, 2008
g *Florinites* cf. *diversiformis* Kosanke, 1950
h *Florinites* sp.cf. *Florinites junior* Potonié & Kremp, 1954
i *Florinites* sp.
j *Disaccites* non striatti
k *Potonieisporites* sp.
l *Pityosporites* sp
m *Alatisporites* sp

Plate 6.4

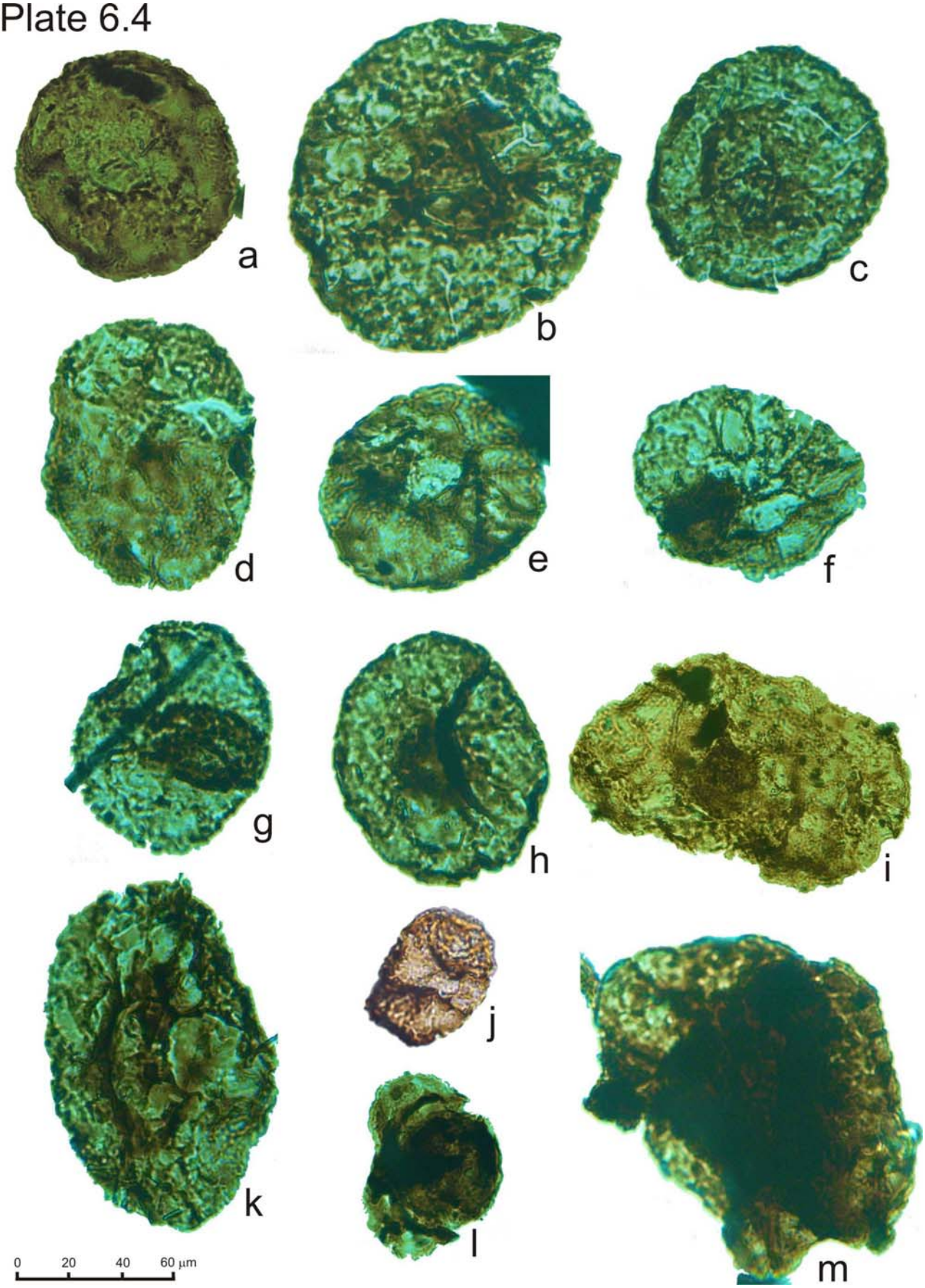

Plate 5.5 – Sporomorphs from the VFigueira 1 to 5 section

a, e, f *Schopfipollenite ellipsoides* (Ibrahim) Potonié & Kremp, 1954.
b, c *Schopfipollenites parvus* Schwartsman, 1976
d *Schopfipollenites* sp.
g,h, i *Schopfipollenites ovalis* Schwartsman, 1976

Plate 5.5

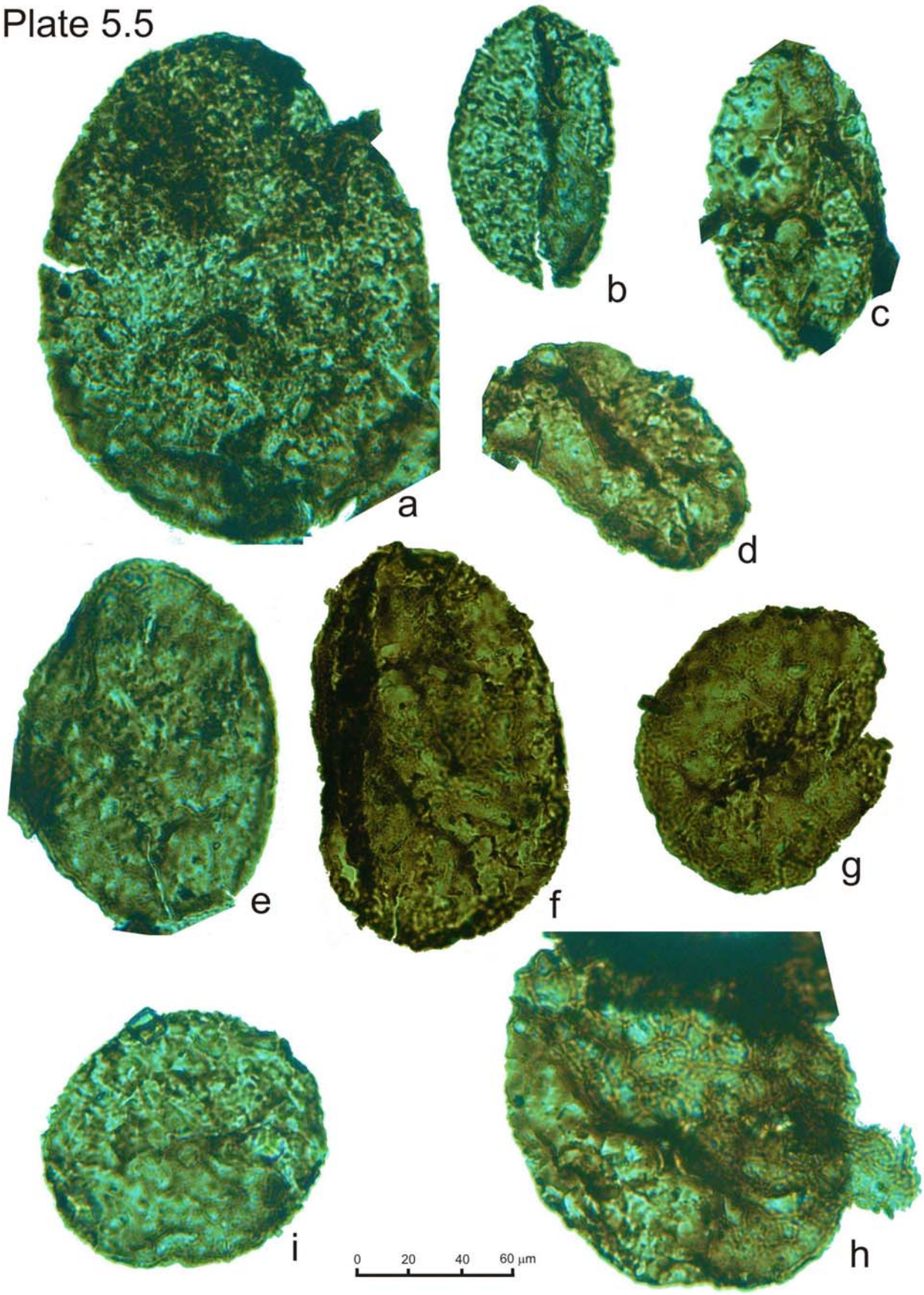

Plate 5.6 – a to p Sporomorphs from the Susana 6 section and Susana 5 (q to cc)

Susana 6

a *Cyclogranisporites* sp.
b *Verrucosisporites* sp.
c *Raistrickia* sp.
d *Microreticulatisporites microreticulatus* Knox, 1950
e *Convolutispora* sp.
f *Triquitrites* sp.
g *Crassispora kosankei* (Potonié & Kremp) Bharadwaj, 1957
h *Densosporites* cf. *lobatus* Kosanke, 1950
i *Lycospora* aff. *pusilla* (Ibrahim) Somers, 1972
j *Lycospora* sp.
k, l *Vestispora* cf. *costata* (Balme, 1952) Spode in Smith & Buterworth 1967
m *Laevigatosporites* cf. *perminutus* Alpern, 1958
n *Laevigatosporites* sp.
o *Puntactosporites* cf. *minutus*
p *Schopfipollenites* sp.
q *Trinidulus diamphidios* Felix & Paden, 1964

Susana 5

r *Leiotriletes* sp
s *Punctatisporites* sp.
t *Granulatisporites* sp.
u *Verrucosisporites cerosus* (Hoffmeister, Staplin & Maloy) Butterworth & Williams, 1958
v *Verrucosisporites* cf. *pergranulus* (Alpern) Smith & Alpern, 1971
w *Verrucosisporites* sp.
x *Raistrickia fulva* Artuz, 1957
y *Raistrickia* aff. *corynoges* Sullivan, 1968
z *Triquitrites* cf. *sculptilis* Balme, 1952
aa *Triquitrites* sp.
bb ? Savitrisporites sp.
cc *Crassispora kosankei* (Potonié & Kremp) Bharadwaj, 1957

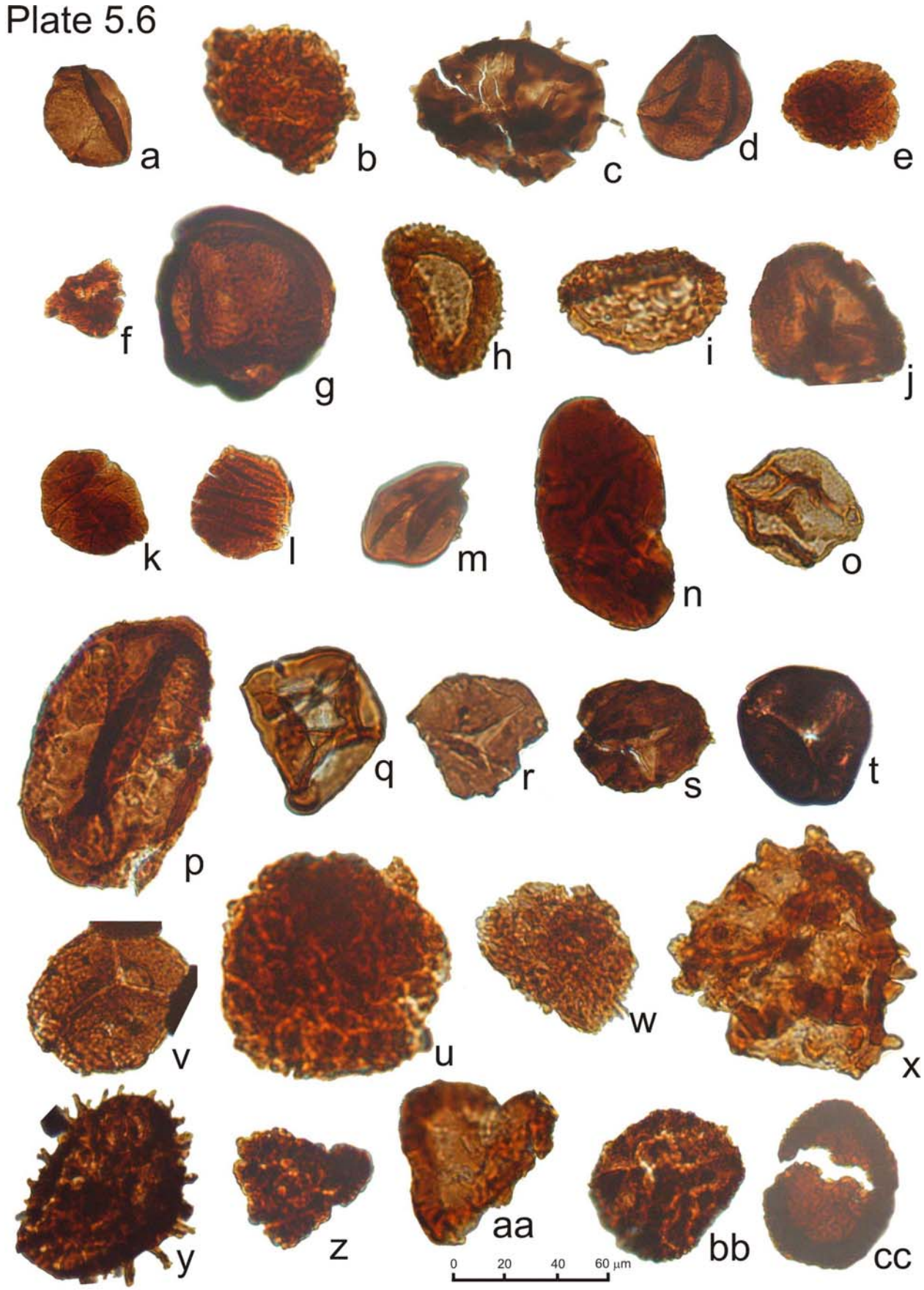
Plate 5.6
a
b
c
d
e
f
g
h
i
j
k
l
m
n
o
p
q
r
s
t
u
v
w
x
y
z
aa
bb
cc
0 20 40 60 µm

Plate 5.7 –Sporomorphs from the Susana 5 section. r and s from Susana 6.

a *Crassispora* cf. *maculosa* (Knox) Sullivan, 1968
b *Crassispora* sp.
c *Densosporites* sp.
d *Lycospora pusilla* (Ibrahim) Somers, 1972
e aff. *Westphalensisporites irregularis* Alpern, 1959
f *Laevigatosporites* cf. *medius* Kosanke, 1950
g *Laevigatosporites minimus* (Wilson & Coe) Schopf, Wilson & Bentall, 1944
h *Laevigatosporites* cf. *perminutus* Alpern, 1958
i *Laevigatosporites* cf. *ovalis* Kosanke, 1950
j *Laevigatosporites* cf. *vulgaris* (Ibrahim) Alpern & Doubinger, 1973
k *Laevigatosporites* sp.
l *Punctatosporites* sp.
m *Florinites* sp.
n *Schopfipollenites* sp.
o ? *Leiosphaeridia* sp. (reworked)
p *Veryhachyum* sp. (reworked)
q *Gorgonisphaeridium* sp. (reworked)
r Arthropod fragment (note different scale)
s same as r, right lower corner enlarged (note different scale)

Plate 5.7

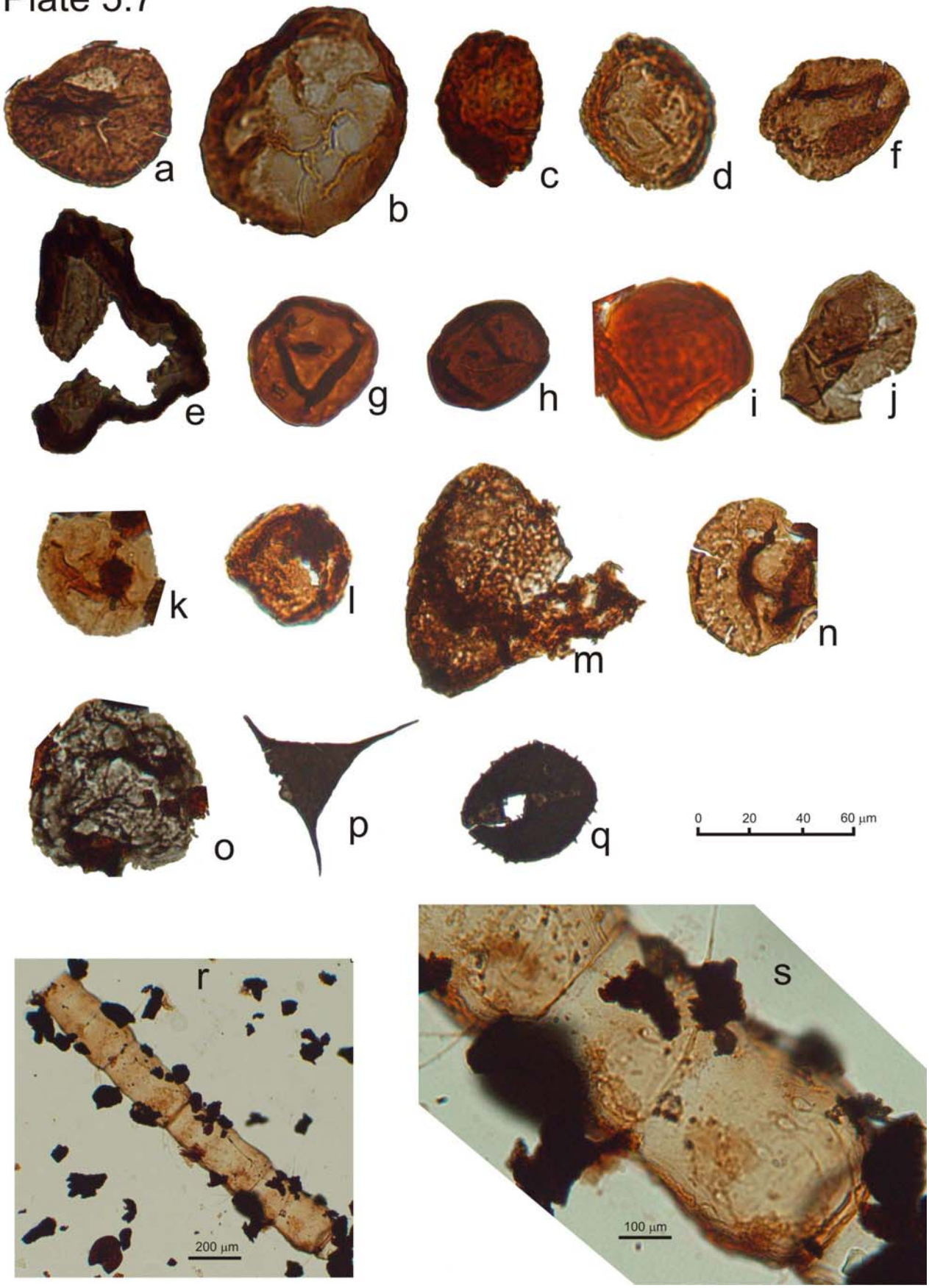

Plate 5.8 – Field photos and sedimentary features of the Santa Susana Basin. Arrows and numbers represent bounding surfaces and their rank

A View to South of the VFigueira 1 to 5 and VFigueira 6 sections in the banks of the Pego do Altar reservoir.
B VFigueira 1 to 5 section between 55 and 60m (see Fig 5.4). Note the successive erosional contacts of the gravel conglomerate beds. Hammer at the base of first conglomeratic bed for scale
C Basal conglomerate near the Vale de Figueira de Baixo farm house. Note the abundant porphyry clasts (pinkish colours).
D Decimetrical fining-upward cycles (sandstone to shale) in Susana 5 section.
E M-scale fining-upward cycle between 75 and 76m of the VFigueira 1 to 5 section. Cross lamination is visible at the top of the gravel-conglomerate bed.
F Incipient cross lamination within a gravel conglomerate bed in VFigueira 1 to 5 section.
G Large plant remain imprint on a bedding surface of a conglomeratic bed.
H Polished surface of sample VFig2.2 showing one complete and one incomplete centimetrical fining-upward cycles (sandstone to siltstone).

Plate 5.8

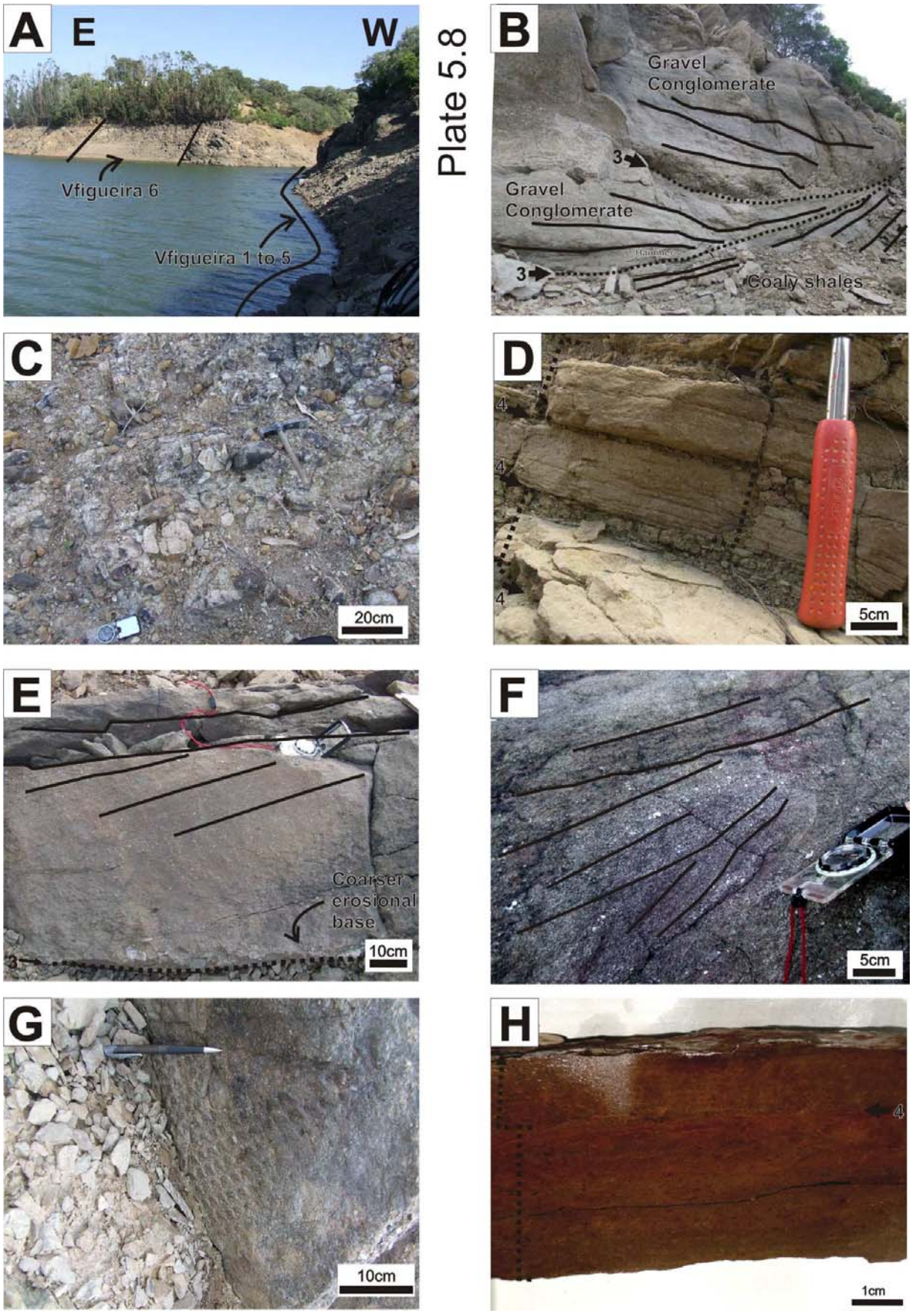
A
E
W
Vfigueira 6
Vfigueira 1 to 5
B
Gravel Conglomerate
3
Gravel Conglomerate
3
Coaly shales
C
20cm
D
4
4
4
5cm
E
Coarser erosional base
3
10cm
F
5cm
G
10cm
H
4
1cm

Chapter 6

Lower and Middle Devonian Limestone units of Western Ossa-Morena Zone

This chapter includes work published in:

MACHADO, G., HLADIL, J., KOPTIKOVA, L., FONSECA, P. E., GALLE, A. & ROCHA, F. T., 2008. Middle Devonian reef fauna and co-occurring acritarchs from volcanosedimentary sequences within the Beja Igneous Complex (SW Ossa-Morena Zone, Portugal). IGCP 497 & IGCP 499 Final Meeting. Frankfurt. Germany.

MACHADO, G., HLADIL, J., KOPTÍKOVÁ, L., FONSECA, P., ROCHA, F. & GALLE, A., 2009a. The Odivelas Limestone: evidence for a Middle Devonian reef system in western Ossa-Morena Zone (Portugal). Geologica Carpathica 60(2): 121-137.

MACHADO, G., SLAVIK, L., KOPTIKOVA, L., HLADIL, J. & FONSECA, P., 2009b. Emsian-Eifelian mixed carbonate-volcaniclastic sequence in western Ossa-Morena zone (Odivelas limestone). First IGCP 580 MAGNETIC SUSCEPTIBILITY, CORRELATIONS AND PALEOENVIRONMENTS meeting. Liège University, B20, Sart Tilman, Belgium: 37.

MACHADO, G., HLADIL, J., SLAVIK, L., KOPTIKOVA, L., MOREIRA, N., FONSECA, M. & FONSECA, P., 2010. An Emsian-Eifelian carbonate- volcaniclastic sequence and the possible correlatable pattern of the Basal Choteč event in Western Ossa-Morena Zone, Portugal (Odivelas Limestone). Geologica Belgica 13 (4): 431-446.

MACHADO, G., HLADIL, J., 2010 On the age and significance of the limestone localities included in the Toca da Moura volcano-sedimentary complex: preliminary results. III Congresso Ibérico de Paleontologia e as XXVI Jornadas de la SEP. Lisbon, Portugal. Publicaciones del Seminario de Paleontología de Zaragoza 9: 153-156.

LOWER AND MIDDLE DEVONIAN LIMESTONE UNITS OF WESTERN OSSA-MORENA ZONE

Chapter Index

Abstract 250
6.1 Introduction 251
6.1.2 Upper Palaeozoic sedimentation in Ossa-Morena Zone 253
6.1.3 The Basal Choteč Event 254
6.2 Covas Ruivas Locality 255
6.2.1 Local Geological setting and previous work 255
6.2.2 Materials and Methods 256
6.2.2.1 Conodonts 256
6.2.2.2 Reef fauna 256
6.2.2.3 Thin sections, XRD and palynology analysis 256
6.2.2.4 Magnetic susceptibility 257
6.2.3 Results 257
6.2.3.1 Litho- and bio-facies and TOC 257
6.2.3.2 Conodonts 262
6.2.3.3 Reef Fauna 263
6.2.3.4 Magnetic susceptibility stratigraphy 264
6.2.4 Discussion and conclusions 265
6.3 Cortes Locality 267
6.3.1 Local Geological setting 267
6.3.2 Previous work 268
6.3.3 Lithotypes and stratigraphy 268
6.3.3.1 Petrographic and geochemical analyses 268
6.3.3.2 Magnetic susceptibility 269
6.3.4 Palaeontological record 271
6.3.4.1 Macrofauna 271
6.3.4.2 Micropalaeontology 276
6.3.5 Discussion and conclusions 276
6.4 Limestone units included in the Toca da Moura Volcano-Sedimentary complex 277
6.4.1 Local geological setting 277
6.4.2 Monte da Pena locality 278
6.4.2.1 Macropalaeontology and facies 278
6.4.3 Caeirinha locality 280
6.4.3.1 Macropalaeontology, micropalaeontology and facies 280
6.4.4 Age and interpretation of Monte da Pena and Caeirinha localities 281
Acknowledgements 281
References 282
Plates 294

Abstract

Several late Early Devonian and Middle Devonian limestone occurrences in Western Ossa-Morena are described here (Odivelas Limestone). These occur within the

oldest volcanic rocks of the Beja Igneous Complex (BIC) and along important shear zones within and bordering the Ossa-Morena Zone.

One of these occurrences (Covas Ruivas locality) was studied in terms of reef fauna, conodont biostratigraphy, macro- and micro-facies and magnetic susceptibility stratigraphy. The results point to a bracketing between the *Po. patulus* and *T. australis* conodont biozones (uppermost Emsian – middle-late Eifelian). The field data, facies analysis and reef fauna indicate that the sequence is composed entirely of calciturbidite and debris-flow deposits (intercalated with hemipelagic tuffites) related to a (up-slope) reefal system resting on top of volcanic buildings within a large volcanic complex. The purity of the limestones does not seem to be generally influenced by volcanic contributions. Although with some uncertainties, the first part of the section seems to show pre-, syn- and post-Basal Choteč Event (BCE) beds as recorded by significant shifts in lithofacies and magnetic susceptibility signal. A tentative interregional correlation is suggested with sections in Morocco, Nevada (USA), Czech Republic and Uzbekistan.

The Cortes locality, also in the Odivelas reservoir area, although deformed and metamorphosed provided an abundant fossil recored which allows their positioning as late Eifelian/early Givetian in age and to relate the reef fauna with the typical Rhenish facies for the same time period. Magnetic susceptibility analysis was attempted and is in agreement with the biostratigraphy, but the limited extent of sections and the metamorphism precludes firm correlations. The field evidence, petrographic and geochemical analysis point to a close palaeogeographical relation and dependence of the reef system on volcanic structures which are included in the Beja Igneous Complex

Several limestone occurrences are known from the Toca da Moura complex (TMC), which are probably correlatable with the Odivelas Limestone but their stratigraphic and structural relation with the surrounding pelitic and volcanic rocks of this complex is not known in detail. The finding of crinoidal fragments in samples from two of these limestone bodies is reported. These suggest a Mid Devonian sedimentation age, although some taxonomic and biostratigraphic uncertainties remain. The previously reported Early Carboniferous age of the pelitic sediments of the TMC is confirmed by palynology from one of the sites.

Key words: Ossa-Morena Zone, Beja Igneous Complex, Odivelas limestone, Emsian-Eifelian-Givetian, Magnetic susceptibility Stratigraphy, reef fauna, conodonts, crinoids.

6.1 Introduction

The Ossa-Morena Zone (OMZ) is a major geotectonic unit located in the southern sector of the Iberian Massif (Lötze, 1945; Julivert & Martínez,1983, see Fig.6.1), forming, together with the Central-Iberian Zone, the Iberian Autochthon (IA) of the so-called Iberian Massif (e.g. Ribeiro et al., 1990). The Iberian Massif, located in the western half of Iberian Peninsula, represents the largest and one of the most complete and continuous exposures of Variscan Belt in Western Europe. The OMZ involves a complex tectonic scenario with a development and closure of an ophiolitic complex – the so-called Beja-Acebuches Ophiolitic Complex (BAOC, Fonseca & Ribeiro, 1993; Fonseca et al., 1999; Figueiras et al. 2002; Mateus et al., 1999). Moreover, the OMZ southern border comprises highly deformed exotic terranes of oceanic nature (including the "Pulo do Lobo" Accretionary Terrane (PLAT) and the BAOC), as complex tectonic melanges (Almeida et al., 2001; Araújo et al., 2005; Booth-Rea et al., 2006). These formations are rimming an early main Variscan suture in southwest of Iberian Massif and they accreted to the Iberian

Autochthon before the Middle/Upper Devonian times (Fonseca & Ribeiro, 1993; Fonseca et al., 1999).

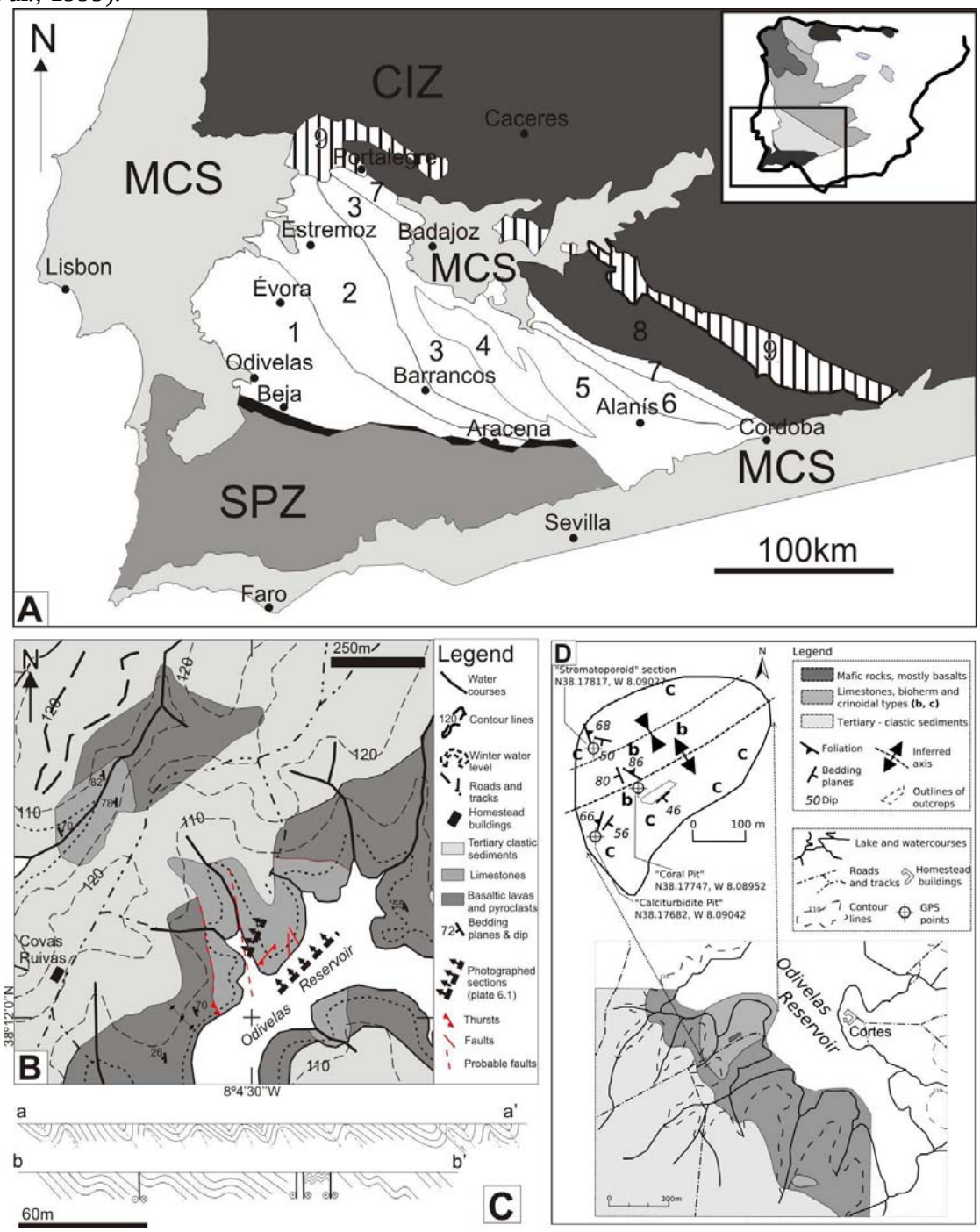

Fig. 6.1 - Geological setting of the Cortes and Covas Ruivas localities, Odivelas Reservoir. A - Geological sketch of southern Iberian Peninsula (adapeted from Robardet & Gutierrez-Marco, 2004 and Oliveira et al. 1991); CIZ: Central Iberian Zone (8 – Obejo-Valsequillo-puebla de la Reina Unit; 9 - Los Pedroches batolith and other granitoids); SPZ: South Portuguese Zone (Beja-Acebuches Ophiolitic complex in black); MCS: Meso-Cenozoic sediments; Ossa-Morena Units or domains: 1 - Beja Aracena Massif; 2 – Montemor-Ficalho Unit; 3 – Alter-do-Chão – Elvas Unit; 4 – Olivenza-Monesterio Antiform; 5 – Zafra – Cordoba – Alanís Unit; 6 – Sierra Albarrana Unit; 7 – Cordoba – Badajoz shear zone (milonitic zone); B - local geological map of the Covas Ruivas locality. C - Schematic structural cross-sections from lines aa' and bb' indicated in B; D – local geological map of the Cortes locality. From Machado et al., 2009a and Machado et al. 2010.

The BAOC separates the OMZ and the South-Portuguese Zone (SPZ), which is regarded as another exotic terrain, originated from a so-called "Southern Palaeo-continent" and accreted to the IA during Carboniferous times (Dallmeyer et al., 1993).

It has been proposed (Crespo-Blanc & Orozco, 1988; Crespo-Blanc, 2007; Fonseca, 1995, 1997; Fonseca et al., 1999) that a major ocean (Rheic Ocean) was closed by subduction/obduction leaving some remainder ophiolitic slices: the Lizard suture in SW England and the Beja-Acebuches suture zone, represent, respectively, the northern and southern branches of the same ocean (Fonseca et al., 1999; Ribeiro et al., 2007).
Data acquired during different research projects clearly shows new dismembered ophiolitic slices into the OMZ (Internal Ossa-Morena Zone Ophiolitic Sequences – IOMZOS, Fonseca et al, 1999), which corresponds to allochthonous klippen resting on top of the lower Palaeozoic sequences (Ribeiro et al., 2007).

6.1.2 Upper Palaeozoic sedimentation in Ossa-Morena Zone

During the Lower Devonian, as well as for most of the Lower Palaeozoic (except for the Cambrian), the sedimentation in the OMZ was generally occurring in a passive margin setting (Quesada, 1990; Robardet & Gutiérrez-Marco, 1990, 2004). These rocks occur in wide areas from Portalegre to Cordoba (Robardet & Gutiérrez-Marco, 1990, 2004) and more to the South in the Barrancos-Estremoz area (Robardet & Gutiérrez-Marco, 1990, 2004; Oliveira et al., 1991; Piçarra, 2000), Terena syncline (Piçarra, 2000) and Valle synclines, Venta de Ciervo and Cerron del Hornillo in Spain (Robardet & Gutiérrez-Marco, 1990, 2004). Fine siliciclastics dominate the sequences but some calcareous levels occur (Robardet & Gutiérrez-Marco, 1990, 2004) characterising proximal deposits to deep fan turbidites (Oliveira et al., 1991; Piçarra, 2000; Borrego et al., 2005).

Lower Devonian sediments are known from several sectors of the Ossa-Morena Zone (OMZ), namely the Estremoz-Barrancos area (Montemor-Ficalho Unit) where several Formations (Terena, Xistos Raiados and Russianas Fms) have been dated by spores (Pereira et al., 1998, 1999), graptolites (Piçarra, 1997, 1998, 2000) and trilobites (Perdigão, 1973; Perdigão et al., 1982). The whole sequence is siliciclastic and the lithological variations probably reflect a palaeogeographical change from proximal deposits to deep fan turbidites (Oliveira et al., 1991; Piçarra, 2000; Borrego et al., 2005). The youngest sediments described from this area are from the Terena Fm. which reach the DE miospore biozone of Richardson & McGregor, 1986 (Upper Emsian-lowermost Eifelian) (Pereira et al., 1999). Several fossiliferous limestone occurrences in this area have been reported by Piçarra & Le Menn (1994), Piçarra et al. (1999), Sarmiento et al. (2000) and Piçarra & Sarmiento (2006). The age is still uncertain due to the considerable deformation and metamorphic grade, but in view of the crinoidal remains and rare conodonts extracted from the limestones the authors suggested an Upper Silurian to Devonian age, questioning the true age of the Estremoz Marbles, so far considered as being Cambrian (Sarmiento et al., 2000; Piçarra & Sarmiento,2006).

Further East, in the Zafra-Córdoba-Alanís sector of the OMZ, the Valle and Cerrón del Hornillo synclines comprise fossiliferous Silurian-Lower Devonian siliciclastic sequences (Robardet & Gutiérrez-Marco, 1990, 2004 and references therein).

Emsian reefal sedimentation in the OMZ was described by May (1999) and Rodríguez et al. (2007). It should also be mentioned the occurrence of several Lower Devonian carbonate sediments in the Obejo-Valsequillo-Puebla de la Reina Domain of the Central Iberian Zone (CIZ) (Liao et al., 2001; May, 2006). Also in the CIZ, near

Portalegre, Perdigão (1967, 1974) described a long succession and several fossiliferous sites of Late Silurian to "Couvinian" age. The sequence is mostly siliciclastic, grading to impure limestones in the upper part of the "Geddinian". Folding and faulting of the sections limited firm conclusions concerning the age of the sediments. Both studies were based on brachiopods which were regarded as being of an "Ardenne type" of fauna (Perdigão 1967, 1974). The same affinity was considered for the contemporaneous faunas described from Barrancos (Ossa-Morena Zone) (Perdigão, 1973). The palaeobiogeographical relation of the CIZ sediments with the contemporaneous occurrences in OMZ was suggested to be significantly different by Robardet & Gutiérrez-Marco (2004). These authors refer a more "Rhenish" affinity of the CIZ contrasting with the more "Bohemian" affinity of the OMZ.

The Middle Devonian is generally absent in the OMZ. This has been interpreted as a consequence of the first pulses of the Hercynian orogeny and generalized uplift of this area during the Middle Devonian (Robardet & Gutiérrez-Marco, 1990, 2004; Oliveira et al. 1991). In the Évora-Beja Domain, the Pedreira de Engenharia calciturbidite outcrops (near Montemor-o-Novo) provided Eifelian conodonts (van den Boogaard, 1973), but the relation of these with the surrounding siliciclastic sediments remains unclear (van den Boogaard, 1973; Pereira et al., 2006). The overlying limestone lenses interbedded with shales of the Cabrela Complex dated as Frasnian (van den Boogaard, 1983) have been shown to be olistoliths in Viséan shales (Pereira & Oliveira, 2003, Pereira et al., 2006). In the same sector and within the BIC, the only known Middle Devonian sediments are the Odivelas limestones (Conde & Andrade, 1974) which are the subject of the present work. Other rare occurrences of limestones in the same domain are reported in the contact area with the South Portuguese Zone near the Caeirinha mine, Pena, Atalaia, Monte das Cortes and Alfundão (Pereira et al., 2006; Oliveira et al., 2006), but the age of these lenses is unknown and the relation with the surrounding Carboniferous Toca da Moura volcano-sedimentary complex remains obscure.

The Upper Devonian and Carboniferous sedimentation is controlled by the pulses and geometry of the oblique collision occurring between the SPZ and the OMZ in a clear synorogenic phase (Quesada et al., 1990). According to the same authors these sediments can be divided in foreland basin flysches and molasses (mostly Upper Devonian and Lower Carboniferous), synorogenic intermontane terrestrial deposits (Upper Carboniferous) and late orogenic intermontane deposits (uppermost Carboniferous and Permian), all of which have a greater development to the eastern areas of the OMZ. Close to the studied area (western OMZ) the Cabrela and Toca-da-Moura complexes are the representatives of the Lower Carboniferous foreland basin deposits (Pereira et al., 2006) and the Santa Susana coal basin of the intermontane Pennsylvanian deposits (Wagner & Sousa, 1983; Sousa & Wagner, 1983; Wagner, 1983; Chapter 5 of this work)

Other Devonian and Carboniferous sediments (mostly black shales) are present in the northern parts of the OMZ along the Porto-Tomar shear zone but their deposition seems to be controlled by a quite different geodynamic setting (e.g. Chaminé et al., 2003; Fernandes et al., 2001; Fernández et al., 2003; Vázquez et al., 2007) and are dealt with elsewhere in this work.

6.1.3 The Basal Choteč Event

The Basal Choteč Event (BCE) is regarded as a global bioevent which corresponds to a transgressive pulse within a series of moderate to strongly manifested fluctuations of

sea level closely above the Emsian-Eifelian boundary. In carbonate slope conditions, these environmental changes are often (but not always) manifested by the presence of "blackish" suboxic sediments and reduced carbonate accumulation rate, typically with an overlying series of rapidly accumulated coarse litho- and bioclastic calciturbidites (e.g. Berkyová et al., 2008; Chlupáč & Kukal, 1986).

This event was originally defined in the Barrandian area (Chlupáč & Kukal, 1986) and has been reported from many other basins world wide (Berkyová et al., 2008) e.g. in Southern Europe, North Africa, North America (Appalachians), South America and Asia (Siberian Platform, Ural Mountains). In MS-GRS records (Koptíková et al. 2007), the BCE usually corresponds to a zone with low amplitude MS records, whereas the immediately overlying intervals show broadly oscillatory patterns, and the BCE level is typically followed by the shift of Th/U ratio and uranium concentration peak (burial of organic matter, hiatuses). The glacigenic origin of a sea level fall and subsequent sea level rise around and after the BCE, respectively, was proposed according to oxygen isotope trends (Elrick et al., 2009).

6.2 Covas Ruivas Locality

6.2.1 Local Geological setting and previous work

The Covas Ruivas group of outcrops is located in the southernmost sector of the Ossa-Morena Zone, specifically in the Évora- Beja Domain (Fig.6.1A). These limestones are capped by volcanic rocks belonging in Beja Igneous Complex – Sta. Susana-Odivelas Subsector (Oliveira et al., 1991). Volcanic rocks have a porphyritic texture, with plagioclase phenocrysts, and more rarely, clinopyroxenes changed and transformed to epidote, still with some chlorite and calcite (Santos et al., 1990). A typical mineral paragenesis of low-grade metamorphism (green schists facies), with chlorite + actinolite + epidote (in occurrence order) is observed.

Andrade et al. (1976) grouped these volcanic rocks in the Peroguarda Complex, and named them Rebolado Basalts. This author described the rocks as (meta)basalts that range from pyroclastic to effusive rocks. Santos et al. (1990), states that the Rebolado Basalts (referred as OD-6 unit) consist of basic to intermediate volcanites.

The limestones are bounded by two major faults that connect the volcanic rocks with the limestones, although the eastern fault is interpreted. Internally the limestone body presents folding (Fig.6.1B), which is attributed to regional variscan deformation (episodes D2b and D3) and so there is some uncertainty on the existence of small repetitions and/or gaps in the section. The folding assigned to D2b shows vergency to the NW with axial planes with general direction NNE-SSW dipping 70º to the SE and the fold axis dipping to the NE. Folds are open (opening angle of around 80º), cylindrical and asymmetrical with short limb to tilt about 70 to the N-NW and along limb about 45 to the NE-E.

In turn, the folding assigned to D3 presents vergency to the SW with axial planes nearly vertical, dipping to the NE, with axes plunging 40° to the NW quadrant. Folds are cylindrical, open and usually symmetrical. The flanks tilt between 40º and 60º to the NE and NW.

The name of the locality – Covas Ruivas – derives from the name given to a local farm house referred in topographic maps of the 1950's and 1960's used in Andrade et al. (1976) and Andrade (1983). Unfortunately the name was not used in more recent

topographic coverage of the area. The original name is kept to avoid contradicting referencing of the site.

The site is composed by two groups of outcrops (Fig.6.1B). The westernmost (Covas Ruivas I) is restricted to a few, small and badly preserved, natural outcrops and abundant floats. The second group, to the East, (Covas Ruivas II) is composed of extensive and continuous natural outcrops and a several small abandoned quarries. Most of our study is dedicated to this second group of outcrops. Both groups of outcrops are over- and underlain by fine tuffites that grade to coarser pyroclastic "true volcanic" deposits and basaltic lava flows. Tertiary deposits cover discordantly the whole area so that outcrops of older rocks are restricted to valleys and low land zones.

6.2.2 Materials and Methods

The Covas Ruivas II site was logged and the limestone beds sampled for magnetic susceptibility and conodont analyses. Lithology, fossil content and relevant sedimentary structures are described. Additional samples of the limestones and interbedded tuffites were taken for thin-sectioning, palynology processing and XRD analyses.

6.2.2.1 Conodonts

33 limestone samples weighting between 1,5kg and 4kg were collected in regular intervals. Limestones composed of sand-sized particles were preferably chosen, which normally corresponded to the base of beds. Each sample was washed with running water and brush and crushed to pieces of about 4cm in diameter. Dissolution was done using 10% acetic acid in ca. 20L plastic buckets in laboratories in Aveiro University and in Prague (Institute of Geology, Academy of Sciences). The acid was replaced when reaction halted and the <1mm undissolved residue separated. The residue was further sieved to discard the <125μm fraction. After drying, the residue was observed under a binocular microscope and conodont elements picked into a cell. The dissolution of some samples resulted in a large amount of residue. In these cases heavy liquid and magnetic separation were performed. Selected conodont elements were observed and photographed by SEM CAMECA SX 100 at the Institute of Geology of the Academy of Sciences of the Czech Republic (see Pl. 6.3).

6.2.2.2 Reef fauna

One thick limestone bed between 58 and 61,5m (Fig. 6.2; Pl. 6.2) was particularly rich in macroscopic (up to a few centimetres) bioclasts of corals, stromatoporoids and crinoids. Weathered surfaces revealing fossils were photographed and floats deriving from this bed were sampled for thin section analysis.

6.2.2.3 Thin sections, XRD and palynology analysis

Conodont samples were thin-sectioned for semi-quantitative petrographic description. Additional samples closely below and above the Emsian-Eifelian boundary were thin-sectioned and described. Besides standard petrographic characterization, the proportions of selected components were quantified. Counting of particles (> 100 μm) along successive, randomly chosen, lines on thin sections was performed. Particles were grouped according to their origin: reef and platform derived (crinoid skeletal remains, bryozoa, corals, stromatoporoids, etc.); pelagic origin (tentaculites and radiolarians);

peloids; intraclasts; volcanic grains; other non-carbonate grains (micas, quartz, feldspars, etc.) and pyrite and oxides (mostly diagenetic). These groups were assembled in bar charts and plotted on Fig. 6.2. This method overestimates the purity of limestones as it does not consider smaller non-carbonate particles. Roughly the same samples were processed for determination of total organic and inorganic carbon concentrations in rocks (TOC, TIC) in the Infra-Red Laboratory of the Institute of Geology SAS, Banská Bystrica, Slovakia. The results are plotted in Fig. 6.2.

Tuffite and limestone samples were crushed and sieved to obtain the smaller than 63 μm fraction. A small amount was placed over a glass slide and homogenized by mixing with distilled water and was left to dry. The X-ray diffraction pattern was recorded with a copper anode X-ray tube (Cu-Kα radiation) using a Philips PW1710, powder diffractometer and X´Pert software PC-APD 3.6 at the Tropical Research Institute (IICT) Department of Natural Sciences(DCN) / Global Development (DES) in Lisbon. Six samples of dark grey tuffites were also processed for palynology using standard HCl + HF attacks.

6.2.2.4 Magnetic susceptibility

The top of each calciturbidite bed was preferably sampled avoiding the overlying tuffite bed. Each calciturbidite bed was considered to be a single turbidity event and thus quasi-instantaneous. Several beds were sampled at different levels and the resulting MS values varied very little (< 2.10^{-9} [$m^3.kg^{-1}$]) within a single bed, even for thicker (> 2 m) beds. This method resulted in a sampling spacing dependant on the thicknesses of each limestone bed and tuffite interbed. In practice the spacing varies between 10 cm and ca. 50 cm. At the base and top of the sequence, tuffites are dominant over the limestones (mostly lenses) and the spacing between two samples can reach several meters (Fig. 6.2). All samples were measured using a Kappabridge KLY-2 (Agico s.r.o.) at the Rock Magnetism Laboratory of the Instituto D. Luiz (Faculty of Sciences of the University of Lisbon).

6.2.3 Results

6.2.3.1 Litho- and bio-facies and TOC

The Covas Ruivas II site has a long exposure of mildly deformed volcanic rocks, mostly coarse pyroclastic deposits and subordinate basaltic lava flows (Pl. 6.1B). Rare black chert beds up to ca. 2 m thick occur within the finer pyroclastic material. The sequence fines up to silt-sized, very finely laminated tuffs/tuffites where the first limestone beds appear. The term tuffite is used here in a broad sense. It refers to the rocks usually forming thin laminated beds, which have, invariably, a large proportion of volcanic-derived material (Pl. 6.1C; Pl. 6.1E). These seem to be, in most instances, hemipelagites.

All limestone beds have visible recrystalization, observed both macroscopically and in thin sections (the detail of some grains is frequently obliterated). The bio- and litho-facies are described and categorized as observed macroscopically and in thin sections. Facies codes are ca1, ca2, … for limestones and t1, t2, … for tuffites. The data are summarized in Table 1.

Name	Texture	Mesoscale features	Main bioclasts	Distribution	Interpretation
ca1	Wst - gst abundant bioclasts.	Laterally thin (<30cm) continuous beds, coarse-grained (sand) bases.	Crinoidal fragments (up to 90%). Rare tentaculites, ostracods, bryozoans, corals.	> 0 to 5m of part A (lower *patulus* zone) > 58m of part A to top of part C (*costatus* zone).	High-energy calciturbidites and rare debris flow deposits.
ca2	Calcimudstones with abundant peloids (up to 75%). Occasional mixing of coarser carbonate grains.	Frequently laterally discontinuous. Fine lamination. Very fine grained with occasional mixing of coarser carbonate grains and possibly highly altered volcanic material. Common convolute bedding.	Crinoidal fragments ca. 25%, rare foram/algae, tentaculites and radiolarians.	> 14 to 31 meters of part A (upper *patulus* and lower *partitus* zones).	Reworked (?) organic-rich hemipelagic sediments and rare calciturbidites.
ca3	Wst - gst with significant proportion of peloids. Frequent presence of calcimudstone clasts.	Variable bed thickness (from 10cm to 4m). Convolute bedding. Coarse- to very coarse-grained bases (sand to cobble-sized grains).	Crinoidal fragments (up to 80%). Frequent corals, stromatoporoids, crinoids, bryozoans, algae.	> 47 to 57 meters of part A (basal *costatus* zone).	Low density calciturbidites with reworked material.
t1	Cryptocrystaline texture, fine micas and other silicate grains. Rare carbonate-rich laminae.	Fine lamination. Brown, slightly coarser laminae and dark grey finer laminae.	Rare tentaculites and radiolarians.	> 0 to 24m of part A (*patulus* and lowermost *partitus* zones) and 55m of part C (uppermost *costatus* and *australis* zones).	Hemipelagic deposits mainly of volcanic-derived material.
t2	Cryptocrystaline texture, fine micas and other silicate grains. Significant amount of organic matter. Often cherty.	Dark grey and black, with mm- to cm-thick chert or cherty lenses, often with py. Fine lamination.	Radiolarians and tentaculites are common, may form thin radiolarite.	> 24m to 47m of part A (*patulus* zone).	Hemipelagic siliceous ooze
t3	Microcrystaline with very small carbonate grains (up to 80%) and quartz and micas grains. Carbonate-rich laminae alternate with siliceous laminae or mix of silicate grains.	Grey, pink coloured. Silt-sized (silt to fine sand). Fine lamination.	Tentaculites, radiolarians and ostracod shells common is some siliceous and carbonate laminae. Dark grey organic tissues.	> 47m to 81m of part A and 0 to 60m of part B of the section (*costatus* zone).	Hemipelagic deposits and reworked (?) siliceous and calcareous ooze.

Table 6.1 – Summary of the main characteristics of the limestone (ca) and tuffite (t) lithofacies and their distribution.

The first 5m of sequence (Section part A) are within the *patulus* Zone and are characterized by continuous beds of wackestones and grainstones with very abundant crinoidal fragments (lithofacies ca1). These are interbedded with finely laminated tuffites which are dominant over the limestones (lithofacies t1). The following 42m (5 to 47m) correspond to the *patulus* and *partitus* Zones. The limestone beds become generally thinner, laterally discontinuous and rarer (lithofacies ca2) (Pl. 6.1D). Between 20 and 27m, there are thicker, laterally continuous limestone beds, but these have the same characteristics as the limestone lenses just above and below. In the same interval and up to 31m, there are several limestone beds and lenses with convolute bedding. One of these beds has abundant friable green shally clasts up to 2 cm in diameter. XRD analysis of these clasts show a composition dominated by calcite, but with relevant amounts of feldspars (ca. 15%), quartz (ca. 5%), clay minerals (illite, chlorite and smectite) and small amounts of Fe oxides. These clasts are interpreted as weathered tuffs/tuffites resting on the marine floor that were eroded during a particularly energetic turbidity event.

Between 25 and 47 m the interbeded tuffites become dominant over the limestones. The tuffites become progressively darker with dark grey and black chert and cherty laminae (and radiolarians) increasing in proportion (lithofacies t2). The large gaps between 35 and 47 m correspond to a part of the section covered by rubble derived solely from dark grey and black cherty tuffites with rare outcrops. This part of the section is very probably a continuous sequence of cherty tuffites (lithofacies t2) which erode and disaggregate more easily than limestone beds.

Above these initial 47 m and up to 81 m, in the basal *costatus* Zone, the tuffites become suddenly subordinate in relation to the limestones and the section becomes carbonate rich (up to 80%) with few cherty mm lenses (lithofacies t3).

Between 47 and 57 m limestone beds characteristically have a coarser massive base and fine up to a finely laminated top with silt sized grains (Pl. 6.1I). Synsedimentary deformation features such as small scale slumping and more commonly convolute bedding are observable occasionally throughout this part of the sequence (lower *costatus* Zone) (Pl. 6.1H). Most of beds have a significant amount of peloids (up to 40%) (lithofacies ca3).

Above 57 m and to the top of part A of the section (80 m) all limestone beds can be classified as belonging to facies ca1, with a variable but generally decreasing proportion of peloids and pelagic grains (Pl. 6.1F). Within this interval the thick coarse breccia bed (57 to 61,5 m) allows a closer description of the bio- and lithoclastic material and its characteristics. The debris is highly polydisperse and contains fragments from millimetre size up to several centimetres size. Variable alterations are indicative of an extensive mixing of the material delivered with the 'coral breccia'. Fresh or slightly reworked crinoidal debris are relatively common, from about 5 to 40 vol. % of the rock, and crinoidal pluricolumnals are also present. Brachiopods, bryozoans, ostracods, foraminifers, algae and other shell/skeleton forming organisms are also observed, but they never represent the dominant rock components. The coarsest 'breccia' types have the lowest contents of crinoids, and amount of sediment matrix is reduced in general, so that the large clasts have mostly stylolitic, pressure solution contacts. Intraclasts are also highly diversified. The spectrum of their compositions encompasses the rock types from partly cemented grainstones of platform and upper slope environments to compacted calcisiltites and muds of slope (e.g. Pl. 6.2D), as marked by sponge spiculae, styliolinid and rare cephalopod shells. The intraclasts of lithified limestones contain a variety of rocks types, which are ranging from coarse and well-washed grainstones to medium- to fine grained, well-sorted grainstones containing unaltered bioclasts together with

micritized chips and peloids, both in roughly equal amounts. Besides the grainstones and packstones of reef and upper slope environments, the basal parts of the channelized breccia flow sediments and coarse calciturbidites also contain blackish intraclasts of hemipelagic calcimudstones (rarely wackestones-packstones), which have angular to subrounded shapes and cm sizes. These were presumably reworked from older parts of the sequence (*patulus* and *partitus* zones?), and may originate from deeply dissected slopes (similarly as in the case of the younger Kačák Event and its post-event breccia flows (e.g. Hladil, 1993).

The coral and stromatoporoid skeletons are fragmentary, broken into mm to cm (max. dm) sized parts; complete coral colonies are almost absent. Some skeletons have a fresh appearance and were filled by cements after their breccia- or turbulent flow redeposition into a deeper water environments, but many of them do not. In the latter, the silicification/desilicification and dolomitization/dedolomitization spots together with micritized rims and bands are commonly observed, and these altered spots in skeletons (partly also in early cements) were cut by abraded/crushed surfaces. Further, these surfaces were often micritized or coated by cryptalgal structures, and sometimes repeatedly. The intensity of this early change varies depending upon time of exposure and burial in the original sediment, differently on specimens or sides of the clasts. This type of alteration resembles the shoals with coral gravel on repeatedly abraded islands in Eastern Moravia (Hladil et al., 1994; Bosák et al., 2002).

Parts B and C of the sequence (within the *costatus* Zone) (Pl. 6.1K) are generally monotonous in terms of facies, bioclast content, thicknesses, proportion of tuffites/limestones, etc. and very similar to the upper 24 m (57 to 81 m) of part A of the sequence (lower *costatus* Zone) and can be generally included in the limestone facies ca1 (more rarely ca3) and tuffite facies t3 (Pl. 6.1G, Pl. 6.1H).

The top of the sequence (part C), starting near the base of the *australis* Zone (Pl. 6.1K), is marked by an increase of the thickness and relative abundance of the tuffite beds. Limestone beds become rarer and laterally discontinuous, but are still grainstones/wackstones with abundant crinoid fragments – limestone facies ca1 and more rarely ca3. The composition of the tuffites becomes more siliceous, with quartz dominating (up to 90%) and very small amounts of calcite, feldspars and micas. Organic matter is present in minor amounts and its composition and maturity remains the same as for the rest of the sequence – tuffite facies t1.

Results from TIC/TOC analysis show an inverse proportional relation between organic and inorganic carbon content for all the analyzed samples. The higher TOC values are associated with lithofacies ca2, coherent with the darker colour and higher organic matter content observed in thin sections. There is, nevertheless, a sharp drop in TOC within this interval (ca. 15 to 31 m of part A) at 24,5 m. This drop is mimicked by the MS signal and the same roughly parallel curve is observed in the remaining section, with few, but noteworthy exceptions. After the sharp drop at 24,5 m there is sharp increase and a second sharp drop and the TOC values seem to remain low, contrary to the high MS values for the same interval (28-31 m). The gap above and significantly different sampling intervals preclude further correlations. The MS values at the base of the *costatus* zone (47-48 m of part A) are not mimicked by the TOC curve. An inverse correlation is observed in the topmost part of the sequence (*australis* zone – part C) with a general decrease of the MS values and a general increase of TOC values.

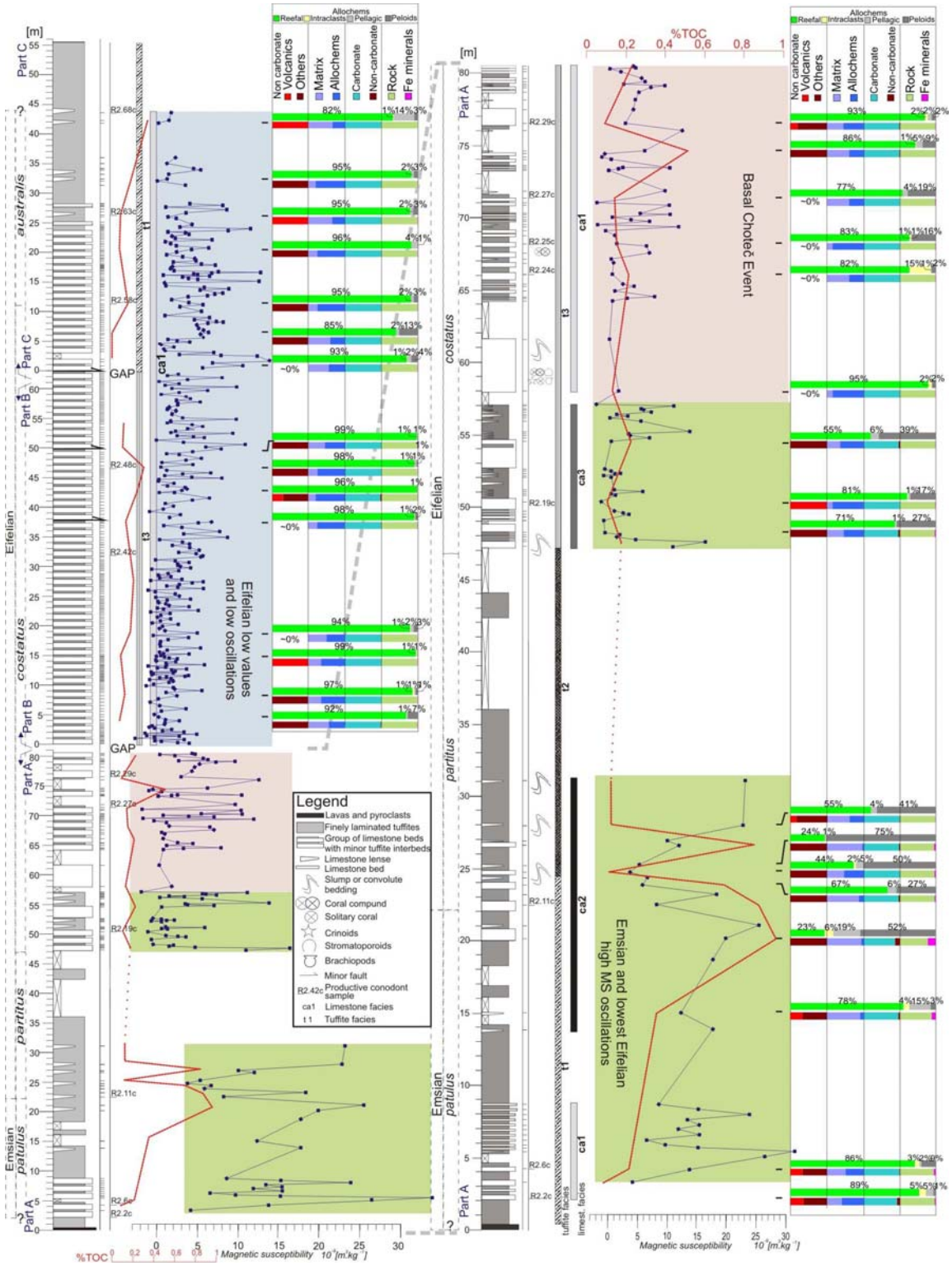

Fig. 6.2 - Lithological column of the Covas Ruivas II site. On the left a simplified column of the whole sequence with the indication of productive conodont samples; "tuffite" and limestone facies; corresponding MS signal, TOC content and quantification of main components (based on thin sections). On the right side a detailed column of the first part of the sequence with the same data plus macroscopically recognizable bioclasts and relevant sedimentary structures. Note that particles counted on thin sections are all greater than 250µm (with some tolerance on peloids) and thus the purity of limestones is most likely overestimated as it does not take into account smaller particles. From Machado et al. (2010).

6.2.3.2 Conodonts

31 of the 33 samples collected and processed provided more than one hundred, mainly platform conodont elements. Only a few samples, however, provided well preserved specimens for identification and documentation including stratigraphically significant taxa regarding the current zonal concept. The CAI is estimated to be between 4 and 5 corresponding to ca. 300ºC, coherent with the results obtained from the maturation of the organic matter.

There are several problems with taxonomical delimitation in the *Polygnathus* stock just around the Emsian-Eifelian boundary. These are mostly expressed by difficulties in identification of taxa in the critical (boundary-defining) part of the *Polygnathus costatus* lineage (*Po. cost. patulus – Po. cost. partitus – Po. cost. costatus*). The lineage suffers from lack of pronounced morphological change that would clearly characterize the succession of taxa whose stratigraphic ranges largely overlap (see Klapper et al., 1978; Berkyová, 2009). The zonally diagnostic taxa are also accompanied by a great number of morphologically variable forms appearing in short time-spans that preclude clear identification of the conodont indexes. In spite of these problems the platform conodont elements obtained from samples from Covas Ruivas, enabled to observe a moderate morphological progress in the *costatus* lineage and compare it successfully with the material figured from type localities in New York and the Barrandian. Some associated taxa (e.g. "*Pandorinellina*" cf. *expansa* Uyeno & Mason 1975 and *Polygnathus* aff. *P. trigonicus* Bischoff & Ziegler 1957) provided further biostratigraphical control. Many determinations out of 31 selected and photographed platform elements were left in open nomenclature due to breakage or uncertainties regarding some morphological features.

The age of this sequence of the Odivelas Limestone is most probably latest Emsian to middle-late Eifelian (*patulus – australis* Zones). The clear morphology of *Polygnathus serotinus* Telford, 1975 found in two samples would point to an "earlier" late Emsian age, but in regard of stratigraphic precision, there is a certain limitation due to its overlap with the stratigraphic range of all three problematic members of the *costatus* lineage (the Emsian "*patulus*" and the Eifelian "*partitus*" and "*costatus*" taxa). However the faunal succession in the Covas Ruivas locality indicates a high probability of late Emsian age of the lower part of the section (part A) (there are no associated "*partitus*" and "*costatus*" in samples with *P. patulus*). The Emsian/Eifelian boundary is probably at the level of sample R2.11c (22m) or closely below this level. The precision is affected by the density of successful conodont samples (see Fig. 6.2). Sample R2.19c (50 m) is already within the *costatus* Zone. The base of this zone is however obscured by the underlying gap.

The record of *Polygnathus* aff. *P. cooperi cooperi* Klapper et al., 1978 and *Icriodus* cf. *beckmanni sinuatus* Klapper et al., 1978 (i.e., typical taxa for the *serotinus* Zone) in sample R2.48c which is already deep within the *costatus* Zone might be caused by repetition in the section or reworking, although there is no colour change or wear out of the respective specimens, neither significant faults, nor any other suggestion of repetition of the sequence in that part of the section (samples below and above are well within the *costatus* Zone).

An important guiding conodont – *Tortodus kockelianus australis* Jackson, 1970 appears in sample R2.58c. It is associated with typically middle-late Eifelian – early Givetian taxa as *Polygnathus eiflius* Bischoff & Ziegler, 1957, *Polygnathus* cf. *pseudofoliatus* Wittekindt 1966 and *Polygnathus* aff. *ansatus* Ziegler & Klapper, 1976. Due to stratigraphical overlap of *T. k. australis* Jackson, 1970 with subsequent zonal indexes and the above mentioned associated taxa (although some were left in open

nomenclature) that are characterized by a rather long range, an earliest Givetian age of the last sample R2.68c (top of part C) cannot be excluded.

6.2.3.3 Reef Fauna

The exact determination of coral and stromatoporoid fauna is complicated by several factors related to the mode of preservation. First of all it is almost impossible to achieve the precise orientation of the sections, and it is due to strong fragmentation of colonies, as well as to the growth distortion within the small fragments and, occasionally, also to deformation (compaction or shear deformation). In addition, the early diagenetic changes caused that a significant part of original microstructures was changed or erased completely. Although many significant features in morphologies and microarchitecture of the skeletons remain, all the determinations had to be classified as being uncertain, at about a 60 to 80% level of reliability, so that the taxa in the approximate lists of faunas, as follows, must be used with question marks. In spite of this unavoidable degree of uncertainty, the rough outlines of the studied coral and stromatoporoid assemblages are remarkably wide:

Tetracorals: *Disphyllum* sp., *Grypophyllum* sp., *Neospongophyllum* sp., *Parasociophyllum isactis* Frech, 1886, *Petronella* sp., *Pseudamplexus* sp., *Solipetra* sp., *Spinophyllum* sp., *Stringophyllum* sp., *Syringaxon* sp., and about 7 other, undetermined taxa (17 together).

Tabulate corals: *Alveolitella* sp., *Alveolites edwardsi* Lecompte, 1939, *A. nalivkini* Sokolov, 1952, *Axuolites* sp., *Bainbridgia* sp., *Caliapora* (*Luciaella*) sp., *Caliapora venusta* Yanet, 1972, *Celechopora* sp., *Celechopora devonica* Schlüter, 1885, *Cladopora* sp., *Coenites* sp., *Dualipora* sp., *Hillaepora circulipora* Kayser, 1879, *Hillaepora* sp., *Lecomptia* sp., *Microalveolites* sp., *Planocoenites* sp., *Platyaxum* sp., *Remesia* sp., *Roemerolites* sp., *Scoliopora cruciformis* Yanet, 1959, *Scoliopora serpentina* Yanet, 1972, *Spongioalveolites* sp., *Squameoalveolites fornicatus* Schlüter, 1889, *Squameoalveolites robustus* Pradáčová 1938, *Squameoalveolites* sp., *Striatopora* sp., *Striatopora* ex gr. *zeaporoides* Dubatolov, 1963 , *Taouzia* sp., *Thamnopora* sp., and about 3 other, undetermined taxa (33 together).

Heliolitids: *Heliolites barrandei* Penecke, 1887, *H. porosus bilsteinensis* Iven, 1980, *H. porosus intermedius* Le Maître, 1947, *H. porosus porosus* Goldfuss, 1826, *Heliolites* sp., *H. vulgaris* Tchernyshev, 1951, and 2 problematic forms (8 together).

Rhapidoporids ('chaetetids'): *Rhapidopora crinalis* Schlüter, 1880, *Rhapidopora* sp., and 2 undetermined, possible rhapidoporid taxa (4 together).

Stromatoporoids: *Actinostroma perspicuum* Nicholson, 1886, *Actinostroma* sp., *Amphipora* sp., *Atelodictyon* sp., *Atopostroma* sp., *Bifariostroma* sp., *Clavidictyon* sp., *Dendrostroma* sp., *Ferestromatopora* sp., *Habrostroma* sp., *Hermatoporella* sp., *Hermatostroma* sp., *Hermatostromella* sp., *Labechia* sp., *Parallelopora* sp., *Plectostroma* sp., *Pseudoactinodictyon* sp., *Salairella* sp., *Stachyodes* (*Sphaerostroma*) sp., *Stachyodes* (*Stachyodes*) sp., *Stictostroma* sp., *Stromatopora* sp., *Syringostromella* sp., *Trupetostroma* sp., and about 7 difficultly classifiable taxa (31 together).

The majority of above listed genera and possible species have European and territorially widespread Asian terrane records. Many of them also reach to north American realm (e.g., *Grypophyllum*) (Pl. 6.2G) or, on the other hand, are linked even to Australian basins (e.g., *Pseudamplexus*). Some taxa may be considered as being mostly the representatives of typically peri-Laurussian and Rhenish faunas (e.g., *Alveolites edwardsi*)

(Pl. 6.2B), but some taxa which are regularly connected with the peri-Gondwanan areas are also involved (e.g., *Taouzia* –an Ibarmaghian marker, Plusquellec & Hladil, 2001) (Pl. 6.2H). The markers of the types as represented by *Bainbrigia-Dualipora* association or numerous forms of *Heliolites* (Pl. 6.2F) are indicative of settlements coming with open-ocean migration routes (Tourneur, 1991), because these markers primarily contribute to coral colonizations on off-shore volcanic mounds, elsewhere. The stratigraphic significance of this faunal assemblage is only modest. It must be noted that the precise biostratigraphic correlation based on corals and stromatoporoids is basically impossible due to absence of specialized studies on coral assemblages which are strictly related to this BCE time window in particular. On the other hand, the prevailing 'Middle Devonian' character of the faunas puts significant constraints on any stratigraphically deeper recycling of older Emsian coral-stromatoporoid limestones.

6.2.3.4 Magnetic susceptibility stratigraphy

Hypothetically the volcanic-sedimentary setting of this section could preclude the application of magnetic susceptibility stratigraphy to it. The MS values are generally very low, indicative that the volcanic-derived admixture is very low and probably negligible (opposed to the carbonate-rich interbedded tuffites that had MS values one or two orders of magnitude higher). The insoluble residues from acetic acid and also hydrochloric acid show extremely rare particles that could have a volcanic origin (<1mm, black rounded microgranular particles) but again the samples where these particles are slightly more common do not correspond to higher MS values. Pyrite is present, although rare, in samples with greater amount of organic matter. However, the proportion of this non-volcanic accessory material is known only approximately as it was estimated from the counts of diagenetically affected mineral aggregates and grains of 100 μm and larger sizes. The possibility that extremely fine volcanic-derived material (ashes) are present cannot be excluded. These are difficult to observe or detect and could affect the MS signal. There is an evident absence of terrigenous clastics in this facies association in general.

There seems to be no relation between the amount of non-carbonate material (volcanic or non-volcanic) with the MS values in this section (compare MS values to proportions of carbonate and non-carbonate particles in Fig. 6.2). The sensitivity of magnetic rock properties to background sedimentation components together with prevailingly low magnetism of volcanic admixtures in these limestones suggest that there is a good opportunity to trace general MS stratigraphic patterns which are not fully masked by noise from local volcanic and sedimentary regimes. These conclusions corroborate the observed similarities with inter-regionally juxtaposed MS stratigraphic curves (see below).

The upper Emsian and the lowest Eifelian MS records (part A) show an alternation of periods with high amplitude oscillations with highly oscillating intervals (between 0–10 and 20–30 m), and the mean MS values are visibly elevated (14,25 and 11,8 $m^3.kg^{-1}$ respectively, contrasting with an overall section average of 3,57 $m^3.kg^{-1}$). Koptikova et al. (2007, 2008) described a coherent pattern of low MS values in different sections (Nevada – Lone Mountain section and Barrandian – Na Škrábku Quarry, Prastav Quarry and Red Quarry or Červený lom Quarry), occurring just before the BCE. In the Covas Ruivas section, this decrease was not observed but could correspond to the major gap in part A (Fig. 6.2 and Fig. 6.3, 36-47 m), as well as to the first sets of calciclastic (skeletal, lithoclastic and peloidal), rhythmically arranged beds above this lacuna. An abrupt

positive shift on MS values which ends the interval with low values occurs within these calciclastic series (around 47m). This shift is continued by irregularly structured patterns with high mean MS values (47–57 m). Above, a markedly developed decrease of MS values (from 11,17 to -1,9 $m^3.kg^{-1}$around 58 m) is observed, which might be considered as the starting of the BCE. However this interval of low MS values is not as significant as the pre-BCE low. Also the amplitudes of oscillations in this interval are higher than during the former low (68–80m of part A).

6.2.4 Discussion and conclusions

Conodont data point to a limestone deposition which can be most probably bracketed between the *patulus* and the *australis* Zones (latest Emsian – middle-late Eifelian). These results also indicate that there are no relevant gaps or repetitions within the sequence due to faulting. The volcanic activity of this part of the Beja Igneous Complex occurred before and after this time span as can be seen by the field stratigraphical relation. Volcanic activity in the immediate vicinity of the sedimentation area must have stopped to allow the development of the reef system and was probably extremely reduced in the region, as this was probably not an isolated reef (see below).

The close palaeogeographical relation between the volcanic buildings of the oldest part of the Beja Igneous Complex and the limestone deposition is inferred by the gradual passage at the base and top of the section to tuffs/tuffites and by the existence of interbedded hemipelagites with a significant volcaniclastic component.

The general abundance of reef- (or platform-) derived bioclasts indicates that sedimentation took place in a peri-reefal environment. The coarser, usually massive base and the finer laminated top (and the intermediate cross bedded interval occasionally seen) suggest a low density calciturbidite type of sedimentation. Convolute bedding and slump structures are further indications of sedimentation on a slope. The fact that most beds show relatively fine grained and well sorted material (silt-sand, rarely coarser) indicates a considerable transport distance, implying that the deposition area is not in the close vicinity of a bioherm/biostrome. The intercalation of tuffites with hemipelagic characteristics constrain the sedimentation setting to the base of slope where basinal sedimentation is recorded between turbidity current events.

The reef fauna diversity is quite unusual when compared with Middle Devonian faunas which are known from analogous tectonosedimentary settings, e.g., from the basalt heights of Horní Benešov, Moravia (Galle et al., 1995), Maly Bozkow, Central Sudetes (Hladil et al., 1999), or Ještěd Ridge, western Sudetes (Chlupáč & Hladil, 1992). The number of taxa for corals and stromatoporoids is about three times smaller at the localities which are used for comparison. However, a higher diversity was reported in the studies on corals and stromatoporoids of NW Sauerland (May, 1987, 1993). This unusually large spectrum of corals and stromatoporoids in Early Eifelian 'breccia' must be related to sources in complex, large and long-term surviving reefs, because only the large and complex platforms and reefs may provide numerous possible guilds and environments which do not represent only ephemeral or short-term colonizations. In addition, the faunal remains found in the 'breccia' bed are characteristic of various types of settings (calm water, inner backreef colonizers (e.g., *Amphipora*) to high energy water conditions of outer lagoon or reef-front (e.g. *Stachyodes*) or open-ocean colonizers (e.g., *Bainbridgia*, partly heliolitids) (Pl. 6.3A). Such a diversity and overlapping complexity of faunas can be either explained by possible existence of a really large volcanic complex, or may suggest a possible

juxtaposition of such a volcanic complex with some large crustal block beneath or in neighbourhood. However, the latter possibility seems to be constrained by lack of detrital quartz in these sedimentary rocks.

The wide and complex palaeogeographical relationships of these faunas suggest that connection of this area with open ocean territories was good. A continuous, strong and diverse colonization flux of coral and stromatoporoid planulae and larvae was, most likely, an unavoidable precondition for the development of these high-diversity faunas.

The MS signal does not seem to be related to the amount of observed non-carbonate material and there is no evidence of relevant detritism – no quartz or other minerals associated with siliclastic input were observed. Thus a scenario where the major part of this impurity was delivered by atmospheric transport seems likely. Possible delivery of dust into the basin waters is almost regularly connected to enrichment of these marine areas in dissolved Fe-bearing solute species, and consequently, the fertilised aquatic conditions and also (bio)precipitation of highly magnetic phases may follow (Jickells, et al. 2005; Kaspari et al., 2009).

The intensity of magnetic signal is contrasting to small amounts of impurity in limestone and, therefore, is almost certainly associated with hematite or magnetite (Hladil et al., 2006).

In spite of a considerable uncertainty in conodont based correlation, which is highly indicative of stratigraphic levels but not describing them in detail, the arrangements of MS stratigraphic patterns in the section suggest the possibility for interregional comparison, even with distant places like Nevada, Uzbekistan or Morocco (Fig. 6.3).

It is interesting to note that the onset of syn- to post-BCE calciclastites is a very important lithological marker inter-regionally (Koptikova et al., 2007; 2008), and the development of pre-BCE MS low with rapidly evolving spikes on MS curves within these calciclastites is a potentially applicable marker, at least for part of the Emsian-Eifelian sections and lithologies. The prospective application of these tentatively defined patterns and MS curve alignments seems to be strengthened by the common occurrence of MS oscillatory and stepwise decrease which occurs still within the levels with *Po. costatus costatus*. (Koptikova et al., 2007; 2008) The deposition of coarse bioclastic and intraclastic, calciturbidites just after a pronounced period of deposition of low-carbonated hemipelagites is indicative of the record of the BCE in this section (Berkyová et al., 2008; Elrick et al., 2009). The richly bioclastic beds occur exclusively in the coral breccia interval, (between 58 and 61 m), and may relate to a typical, early *costatus*-Zone facies change (syn- to post-BCE calciclastites).

The TOC curve roughly follows the overall trends which are seen in the MS curves which can be explained by the increased organic productivity (and consequent organic matter accumulation) induced by an increased delivery of dust (Kawahata et al., 2000). In detail there are many differences between the two curves. However, these differences can also be caused by natural variability of rock compositions or occurrence of inhomogenities. This variability must be considered between samples which are cm apart or even two parts of a sample with ~20-40 g. Considering the significant degree of similarity between TOC and MS, but an obvious dissimilarity between these two parameters and the amount of volcanic-derived impurities in the limestones (Fig. 6.2), one can infer that the burial of organic matter (or also increased primary productivity in open sea) was particularly linked to increased contents of non-volcanic clayey/silty components. The process when increased transport of aerosol with mineral dust into the oceans (MS on paramagnetic and ferri-/ferromagnetic minerals) causes increased organic

oceans (MS on paramagnetic and ferri-/ferromagnetic minerals) causes increased organic productivity and organic carbon burial (MS on diagenetic Fe-mineral phases) would be relevant to this case (e.g. Kawahata et al., 2000; Saltzman, 2005).

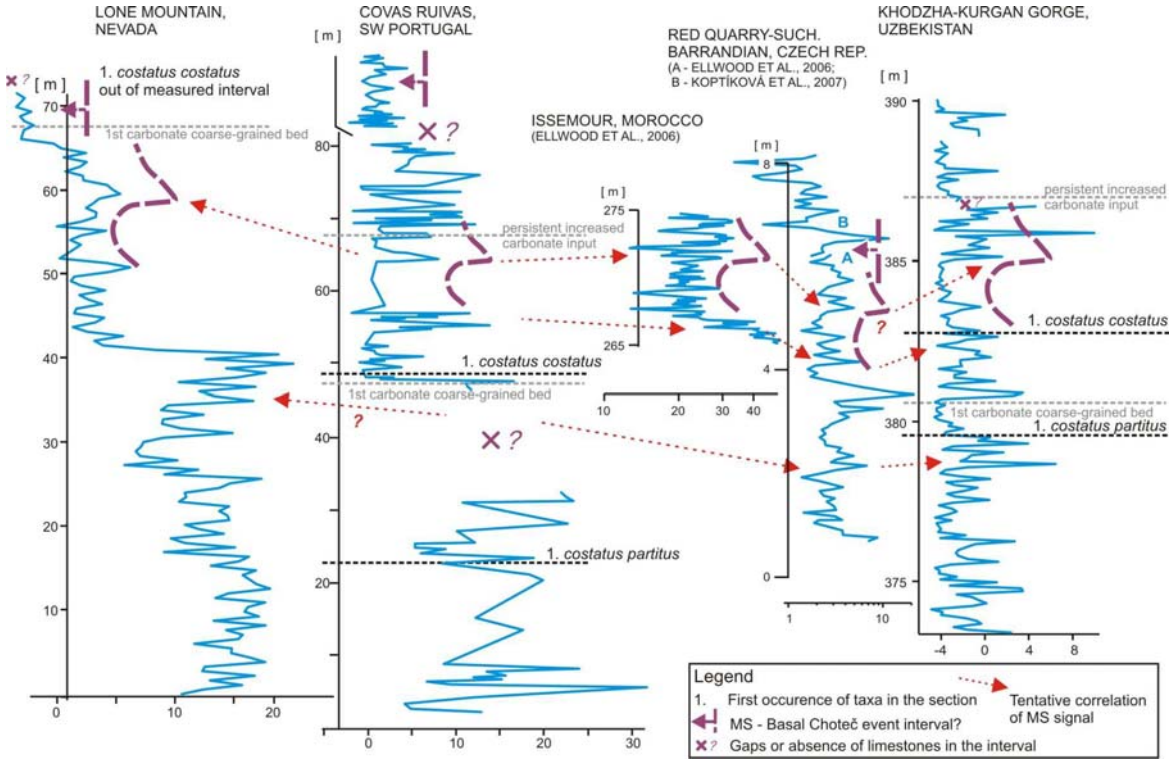

Fig. 6.3 - Tentative correlation of the MS curve from Covas Ruivas II section with other MS curves from Lone Mountain, Nevada USA (Elrick & Hinnov, 1996, Klapper & Johnson, 1975 and unpublished data); Issemour, Morocco (Ellwood et al., 2006) and Hodzha-Kurgan Gorge, Uzbekistan (unpublished data). All MS data (x axes) are in 10^{-9} [$m^3.kg^{-1}$] values. From Machado et al. (2010).

6.3 Cortes Locality

6.3.1 Local Geological setting

The Odivelas Limestone site near Cortes is composed of several natural and artificial outcrops and wide area of abundant loose boulders. The limestone was quarried and processed locally as can be seen by the ruins of an old lime mill. Nearly all the outcrops and most of the loose boulder area is flooded during the winter season. Although outcrops are scarce a limestone zonation is observable with bioherm limestones mainly in the centre and calicturbidite with crinoid fragments on the edges of the body (Fig.6.1D). Together with geometric information from bedding planes and foliation it is possible to infer that the limestone body corresponds to a small, badly defined, anticline structure.

The main limestone body is surrounded by massive lava flows and rare pyroclastic deposits comprised in the Rebolado Basalts (Andrade *et al.*, 1976). The same authors considered these to be the volcanic equivalents of the Casa Branca Dolerites that crop out to the W and SW due to the similar chemistry. These dolerites were studied in more detail by Jesus *et al*. (2003, 2007) and Mateus *et al*., 2001 who refer the relatively young ages in the 355-320 Ma interval (~ Famennian/ Tournaisian to Visean).

The chronological relation between the basalts and limestones is unclear. Field evidence of the contacts is scarce, but the structural interpretation (and also facies) suggests that the limestones overlay the basalts. The presence of a small dyke intruding the limestones is indicative that at least the final part of the magmatic activity that generated the volcanic and sub-volcanic suite of the BIC is posterior (clearly intruding) to the limestone deposition. Chemical analyses show that limestones deposited contemporaneously with extrusive volcanic activity (see geochemical and petrographic analysis).

A second, smaller, sector with limestone occurrences is present to the SE of the main one (Fig.6.1C). No outcrops are visible, just abundant loose limestone boulders, mainly calciturbidites. It is possible that this location is an old quarry or lime mill filled in with tailings and local detritus.

The Tertiary deposits cover most of the northern area of the Odivelas reservoir and significant parts of the southern area. They are unconformably overlaying the volcanic suite and seem to have a topographic control leading to a local restriction of Beja Massif outcrops to valleys and other low land areas.

6.3.2 Previous work

Several short communications, papers and regional field trip guides (e.g. Andrade *et al*., 1991), mention the Odivelas limestones and also the carbonates that occur near the reservoir wall but all of them refer to the original work by Conde & Andrade (1974). This was, therefore, the only work so far that described the palaeontology and location of the site and proposed a tentative limestone zonation. The fossil content described in Conde & Andrade (1974) includes stromatoporoids, corals, crinoids, brachiopods, bryozoans, conodonts and trilobites. The presence of fossils compared with *Athyris concentrica* and *Thamnopora boloniensis* (brachiopod and tabulate coral) was then regarded as evidence of a Middle or Upper Devonian age. The only described conodont taxa was *Polygnathus* sp. and no stratigraphical implication for this finding was made.

6.3.3 Lithotypes and stratigraphy

6.3.3.1 Petrographic and geochemical analyses

Several outcrop samples were cut to produce thin sections and polished hand samples to be observed optically and to perform EDX and microprobe analyses. The bioherm limestone is dominated by biogenic particles in a micritic matrix (see palaeontological record section). The calciturbidite limestone has a homogeneous crypto- to microcristalline texture (Pl. 6.4E). In both lithotypes six main petrographic features were observed: 1) lamination (marked by ghosts of often well recognizable bioclasts and a first generation of stylolites); 2) feldspar sub-euhedral crystals; 3) second generation stylolites (Pl. 6.4G); 4) white and grey coarsely recrystallized areas and small veins, 5) Pumpellyite/prehnite and quartz rosettes (Pl. 6.4H); 6) late generations of veins with carbonate and feldspar, and finally but only in calciturbidites, 7) prismatic black particles (Pl. 6.4B to D and F) in size range from tenths of millimetre to centimetres. Original sedimentary features seem to be the abundant, mostly non-authigenic feldspar crystals and the lamination, later marked by a sub-parallel generation of stylolites. The WDS microprobe and EDX analyses indicate that up to 30% of the finer and darker limestones are composed of volcanic derived minerals such as chlorite, albite, oligoclase, microcline,

titanite, rare micas and altered pyrite, although only the feldspars and pyrite were observed optically.

The black prismatic crystalloclasts which occur only in the calciturbidites can (in some levels only) constitute up to 20% of the limestone; their length ranges from 0.1 mm to 5 cm long (Pl. 6.4C and D), but the width of these elongated, partly or often euhedral specimens, exceeds 2.5– 3 mm. Usually they form single prisms, but occasionally also complex shapes are present (Pl. 6.4D). The transverse section is square, rhombic or irregularly hexagonal. The microprobe analyses show a core composed of hexagonal platelets of phlogopite retaining compositions as well as a very faint cleavage plane [001] which is sub-perpendicular to the prism axis. The high content of Al (up to 25%) is tentatively explained due to nanometric inclusions or mixtures between the mica layers, although this could not be confirmed. This core is interpreted as a forming in an early heating stage due to the contact metamorphism of the surrounding subvolcanic suite. The core is surrounded by an irregular, partially hollow cylinder composed by Mg-rich muscovite and biotite. The outer envelope defining the hexagonal prism is composed by chlorite and tosudite. These two outer layers are interpreted as diachronically forming or pseudomorphosing during late diagenesis and metamorphism. Some of the prisms have a porous structure which is filled by calcite, hematite and other minerals. Occasionally planar cracks and fissures (sub-perpendicular to the axis of the needle) are filled by calcite. This fracturing correspond to otherwise plastic shear deformation which is parallel to original lamination and can be compared to that which was observed on rarely thinsectioned conodonts. This deformation can start as early as with compaction of the rocks and early burial diagenesis.

The major recrystalization areas and second generation of stylolites cut or affect the previous features. These represent a second phase of pressure solution and recrystallization of carbonate, contemporaneous with the main deformation phase as can be seen by the delta and sigmoid structures formed around the prismatic particles (Pl. 6.4E and F, Fig. 6.4). Finally, a second generation of veins (carbonates, perthitic alkali feldspars and rare quartz) cut the entire structure. They are usually thicker and with a more regular orientation which suggests fracture filling formed during a late deformational event (Pl. 6.4E and F, Fig. 6.4)or by adiabatic decompression.

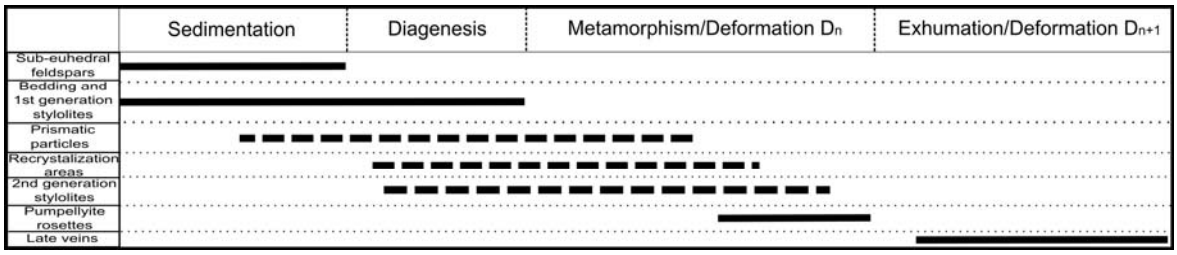

Fig. 6.4 - Graphical chronology of the observed petrographic features. Solid lines refer to chronologically well defined processes and dashed lines to doubtful chronologies. From Machado et al., 2009a.

6.3.3.2 Magnetic susceptibility

In one of the artificial outcrops a small mostly undeformed sequence (ca. 2.4 m) of thin-bedded crinoidal calciturbidites was preserved. This section was sampled for magnetosusceptibility stratigraphy in ca. 10 cm intervals and for palynology in more spaced intervals. The results are summarized in Fig 6.5. According to the structural

interpretation the measured section (light grey shade) would be overlaying the bioherm beds (dark grey shade, Fig. 6.5), but the positioning is merely tentative.

The data obtained from a short section with condensed stratigraphy can be tentatively be assigned to the end-Eifelian segment 37-43 of the MS Reference Section Moravian Karst (Hladil *et al.*, 2006; Fig. 6.5 herein). This position seems to be determined by extremely low MS magnitudes together with medium amplitude "coarse brush patterns". The compared point in the reference section was originally held close to the base of *Polygnathus ensensis* stratigraphic correlatives (Hladil *et al.*, 2006), but the most recent Belgian data (F. Boulvain et al., pers. commun. 2008) are highly indicative of little younger ages for this point, i.e. with *Polygnathus hemiansatus* age correlatives.

Although the latter is quite concordant with the palaeontological record, several concurrent problems exist. A crude visual estimation of the proportion of the small black prisms in the magnetic susceptibility samples show a good correlation with the obtained MS curve. The measured MS values in isolated prims varies from 6.9 for complete specimens to 84.6 ($\cdot 10^{-9}$ [$m^3 \cdot kg^{-1}$]) for the minute flakes composing their outer envelopes (Pl. 6.4D). Additionally, the not negligible proportion of fine-grained, mostly altered volcanic admixture (?volcanic ash and recycled microdetrital material) is expected to modify the MS record. In this context, however, the mean MS values which are smaller than 1 $\cdot 10^{-9}$ are very surprising and this can be explained by early diagenetic trapping of iron by pyrite and its late weathering alteration to iron oxyhydroxidic subcrystalline mixtures. Metamorphism, although low grade probably adds other noise or overprints the sedimentary MS variations. The obtained curve can, therefore, reflect the combination of several processes which may have modified the comparability of the original, wide regional to global (climatically induced) magnetosusceptibility stratigraphic record.

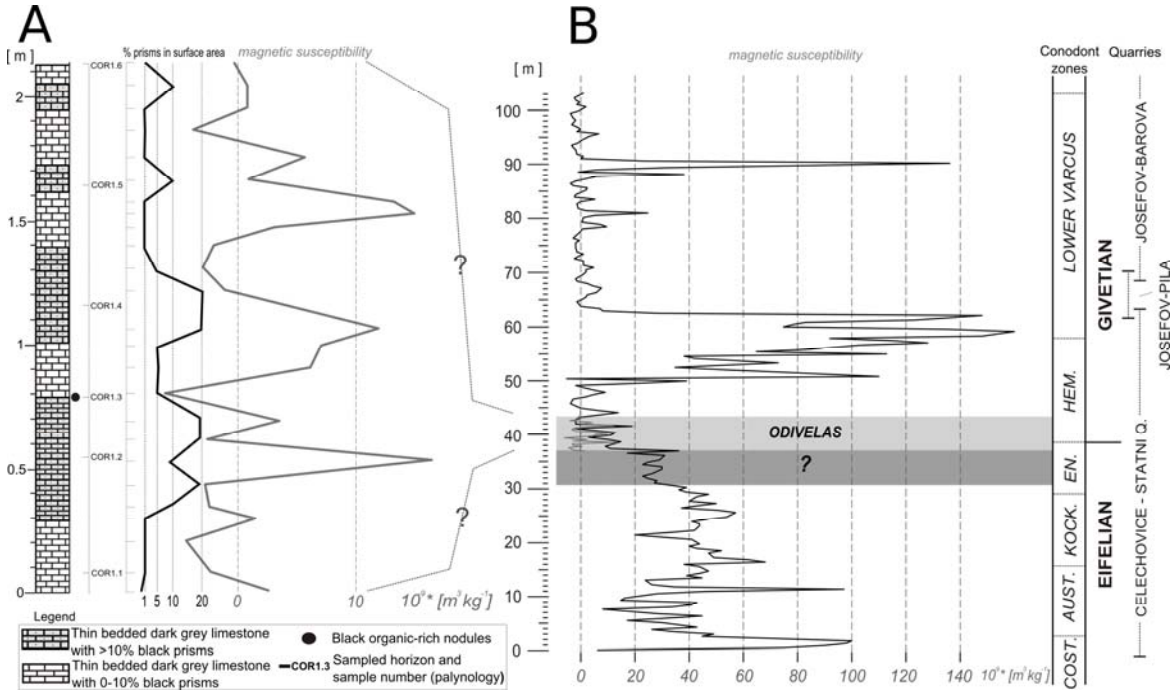

Fig. 6.5 - Sampled section for magnetic susceptibility and palynology with reference to the sampled horizons and possible correlation with the published magnetic susceptibility curves for the same time interval (Hladil et al., 2006) and estimated conodont zone time equivalents (still under improvement by interregional correlation). The biostratigraphic correlatives for indicated point (base of Polygnathus ensensis Z.) can be updated by means of the most recent Belgian results (slightly younger, in Pol. hemiansatus Z.; Bultynck et al., pers. Commun. 2008). From Machado et al., 2009a

6.3.4 Palaeontological record

6.3.4.1 Macrofauna

Crinoids: Very common columnals of the crinoid genus *Cupressocrinites* are visible on the weathered rock surfaces or in slabs of the limestone sampled from relatively well preserved layers and boudins. These remarkable fossils are present across all discernible original sedimentary facies of the Odivelas Limestone on its type occurrence outcrops (i.e., from bioherms to calciturbidites). The largest about 5-7 mm wide columnals were regularly found with the coral-crinoid-brachiopod bioherm and biostrome relict structures. The large and medium sized columnals can be compared, according to their rough morphology, with *Cupressocrinites* cf. *crassus* ? (Goldfuss, 1831) or at least very similar forms – Pl. 6.5A–C. Some of small columnals having well separated peripheral canals may also be compared with *Cupressocrinites* sp. M ? Le Menn, 1999 (in Ureš et al., 1999). The columnals having similarity to the latter taxon are found mainly in tempestites–calciturbidites which are interpreted as an original cover of the underlying biohermal-biostromal facies. These *Cupressocrinites* species occur together, for example, in the lowermost Givetian part of the Celechovice Limestone in Moravia, Czech Republic (e.g., Bouček, 1931; Remes, 1939; Ureš et al., 1999; V. Petr, internet comments on the *C. crassus* 2007). They are especially abundant in the Middle Devonian and particularly Eifelian–Givetian strata worldwide (i.e., among North Gondwana, South Baltica, Urals and Siberia basins and terranes) but they typically mark the Rhenish facies together with parallel, closely adjacent Variscan facies-tectonic belts on the inner side of the former and having a partial resemblance to pre-closure Rheic passages. Such a high abundance of *Cupressocrinites* remnants coupled with the presence of dark-grey coloured coral and stromatoporoid limestones is, therefore, a not negligible indication in order to prove that these sediments deposited in the middle of Variscan belts, and according to stratigraphic position close to the Eifelian/Givetian stratigraphic boundary. In spite of the predominance of these crinoid columnals, the presence of other crinoid genera is quite possible. Most of these genera, however, cannot be seriously determined on the base of the random sections, due to imperfectly preserved features of facet, areola, latus, etc. The only exception is for *Gasterocoma* ? sp. because its "rounded, double-axial-canal" in columnals and cirral ossicles which is well visible in the sections.

Tabulate corals: Owing the local thickening of originally calcite corallite walls the branches of *Thamnopora* tabulate corals belong to the most spectacular fossils which can be found in the less deformed layers and boudins of biohermal limestone facies. Whitish colour and positive weathering surfaces of these corals are eyecatching during collecting of the fossils, and this may lead to a slight overestimation of their relative abundances in comparison with other coral–stromatoporoid fauna of softer, Mg-calcite or aragonitic and thus less preservable skeletons. The present analysis of newly collected *Thamnopora* specimens does not confirm the previous determinations (Conde & Andrade 1974) but suggests that majority of these branched coralla and their fragments most likely belong to *Thamnopora* cf. *irregularis* Lecompte, 1939 (Pl. 6.5D–L). The main evidence for the revision of the previous determination as *T. boloniensis* (Gosselet, 1877) consists in the capability of this coral for frequent rejuvenations and irregular arrangement of the corallites as well as irregular budding and often imperfectly developed (or missing) separation of the thick-walled peripheral zone. The other supportive arguments for this determination are based on full agreement of the coralla and corallite shapes and mural

pore dimensions with the type populations of *T. irregularis* which were described from the "Gi*a*" levels (Lecompte 1939) [in the present stratigraphic terms: Hanonet Formation / Trois Fontaines Member in the Dinant Synclinorium, Belgium ~ *Polygnathus hemiansatus* Zone]. Besides this dominant species also some small and rare forms and one medium-sized form are present, but their determination is very difficult. These forms resemble in some of their poorly preserved features *T.* cf. *compacta minima* ? Sharkova, 1981, *T.* cf. *incerta perpussila* Hladil, 1984, *T.* cf. *vermicularis* ? (McCoy, 1850) and *T.* cf. *bilamellosa* ? Ermakova, 1960. Although the presence of these species remain highly problematic, it is interesting that all these possible links are also focused to the Eifelian–Givetian ages, and palaeogeographically are also indicative of the same space as the above mentioned high abundance of the *Cupressocrinites* crinoid remains.

Other prominent component among tabulatomorphic (but not tabulate) corals are colonies of *Heliolites*. Domical and short cylindrical colonies prevail. Also the colonies with several centimetres thick overgrowths by undetermined massive coenostea of stromatoporoids are commonly seen in the bioherm–biostrome facies in central part of the Odivelas Limestone type occurrence outcrops, but their subtle skeletons were often and considerably damaged by recrystallization. A few uncoated colonies with at least partial preservation of visible internal structures (Pl. 6.6A–F) were classified as *Heliolites* cf. *porosus bilsteinensis* ? Iven, 1980, but also a certain similarity to *Heliolites* "Typus C" Hubmann, 1991 must be considered and partly also to the youngest forms of problematically defined *H.* cf. *vulgaris* Tchernyshev, 1951 (e.g., Hladil & Lang 1985). The morphologies like *H. porosus bilsteinensis*, and considering also these three morphologically related forms are quite indicative of the Eifelian–Givetian and particularly the earliest Givetian ages. On the other hand, there is no evidence for the presence of the typical septate heliolites as *H. porosus porosus* (Goldfuss, 1826) or *H.* "*intermedius*" Le Maitre, 1947 which are also typical for these stratigraphic levels but occur rather in thicker limestones around platforms than in thin limestone layers on volcanic substrates. Despite of a certain tendency for the reduction of coenenchymatic tubulae, the possible comparison with *H. barrandei* Penecke, 1887 is hindered by the absence of rudimentary but thickened bases of septa as well as local thickenings of the parts of the skeleton as a whole (compare, e.g., Fernández-Martínez 1999).

The small favositid-like, nodularly or domically shaped centimetre-sized coralla often have characteristics of caliaporids (rotation of parallel corallites, presence of battens, indications of squamulae). However, the presence of *Calipora battersbyi* (Milne-Edwards & Haime, 1851), *Mariusilites chaetetoides* (Lecompte, 1939) or their Eifelian precursor species lack unambiguous evidence in this recrystallized coral material. In contrast to this, several colony remains (perhaps randomly preserved?) provided sufficient indications that one of these caliaporids can be labelled as *Caliapora* ? cf. *plagiosquamata* Hladil, 1981 (Pl. 6.6G–I). This coral has all the evident though moderately reduced *Caliapora* type features. Its occurrence is typical for the Givetian stage, ranging in Moravia from the Eifelian–Givetian to Middle Givetian strata.

Many observed and analysed colonies must likely be encompassed within alveolitids, specifically between the genera *Squameoalveolites* and *Spongioalveolites*. The best evidence was found for several coating to low domical colonies of relatively compact skeleton which were determined as *Squameoalveolites* cf. *fornicatus* (Schluter, 1889) – Pl. 6.6J–M. Corallite have an evident alveolitid shape where densely spaced and well opened mural pores are on the lateral sides and are regularly alternated by couples of thick, tongue-shaped skeletal protrusions which resemble formations of "squamulae or spines".

Again, the species is very typical for the Eifelian–Givetian and lowermost Givetian strata worldwide and mainly in Rhenish and adjacent marine basins.

Other fossils apparent among well preserved, thick skeleton branched tabulate corals are scolioporids with subdominant *Scoliopora denticulata denticulata* (Milne-Edwards & Haime, 1851) cf. alpha morfotype Hladil, 1984 – Pl. 6.7A–D. The corallites elongated in the transverse section have flattened, rounded-rectangular to bean shapes, and despite and in spite of the corallite rotation after the budding they tend again to be sub-parallel near the colony surface. Septal ridges are always well visible, as well as the typical galleries of tube-like pores. The morphology of these corals is in agreement with that of the old Givetian populations from the Lazanky-Zrcadla locality in Moravia. The presence of this species is quite interesting from two points. First, this coral in Moravia usually occurs on platforms and their slopes and, second, it is rather indicative of earliest Givetian ages than the Late Eifelian. As this coral most likely belongs to very slowly and consistently growing microsuspension feeders which can also considerably exceed from the territorial ranges of typical reef communities (e.g., settling on slopes, and vice versa, in the sheltered environments only with amphiporids) it is not surprising that these *Scoliopora* branches were also here preferentially embedded in originally ?micritic–micropeloidal sediments that have relatively low admixture of the skeletal debris.

Rugose corals: There was a rich, moderately diversified assemblage of these corals in the materials collected from the fragmentary bioherm–biostrome structures in the centre of the type Odivelas Limestone locality. Corals which were determined as *Pseudamplexus* ? sp. (Pl. 6.7F–I) are slightly dominant. Most of these corals occur in clusters and accumulated in lenses, where complete specimens are more abundant than millimetre to centimetre detritus of their calices. Typical original sediments were most likely ? ostracod packstones/wackestones, although more diversified skeletal packstone varieties occur as well. It seems that some populations differ in the shape, as longer conical shapes with less cemented skeleton can be found and also forms with deeper and more opened calices where the skeletons were filled and coated by early cements, but the more detailed taxonomic conclusions are restricted by poor preservation of most of the internal structures.

Among well represented groups mainly the Digonophyllinae must be mentioned. Large conical to keg-shaped corals filled by large dissepiments are labelled as *Cystiphylloides* ? sp. (Pl. 6.7K). Large rugose corals with relatively well indicated length and arrangement of septa were determined as Mesophyllum ? sp. (Pl. 6.7L).
Presence of other genera, e.g. phillipsastreids *Disphyllum* ? sp., locally also *Thamnophyllum* ? sp. and *Peneckiella* ? sp. is quite possible due to observed general growth forms but lack the evidence based on preserved internal skeletal structures. The same is true for possible but not definitely confirmed occurrences of *Acanthophyllum* ? sp.

On the other hand, the sub random preservation and sectioning of limestones provided a tentative evidence for the presence of various other rugose corals: for example, *Calceola* cf. *sandalina* (Linne, 1771) – Pl. 6.7M, *Pseudodigonophyllum* ? sp. – Pl. 6.7N, *Holmophyllum* ? sp. (*Holmophyllum* ? cf. *uralicum* Zhavoronkova, 1972) – Pl. 6.8A, or *Cyathopaedium* ? sp. – Pl. 6.8B.

Occurrences of *Pseudamplexus*, *Cystiphylloides* and *Mesophyllum* correspond well to the Eifelian–Givetian ages, and the occurrences of other very briefly mentioned genera are not in conflict with this age determination. In addition, the single finds and determinations of other rugose corals support these ideas about age of these faunas.

Calceola sandalina, although relatively rare, is an important cosmopolitan marker for these ages and a very characteristic species of Rhenish and adjacent seas. *Pseudodigonophyllum* ? sp. and *Holmophyllum* ? cf. *uralicum* also confirm these ages, and *Cyathopaedium* ? sp. shows a parallel to occurrences of *Cyathopaedium paucitabulatum* (Schluter, 1879) in the upper part of the Newberria Formation, lower Givetian of western Sauerland, Germany (May 2003).

Stromatoporoids (and amphiporids): The stromatoporoids are certainly an important faunal component of the bioherm–biostrome structures in the central part of the Odivelas Limestone type locality, but their originally aragonitic to Mg-calcitic skeletons were recrystallized during both the diagenesis and slight metamorphosis to a degree which even precludes their generic identification. Only some of the observed relict structures allow speculating about possible occurrence of *Actinostroma* ? (or *Plectostroma* ?) [thick, well separated pillars], *Salairella* ? [preponderance of regular coenosteles], *Atelodictyon* ? [strongly expressed laminated features of coenosteum] and *Clathrocoilona* ? [very densely structured coatings on corals]. However, this must be considered only in a category of tentative and disputable opinions, not bringing the facts which could be supported by unequivocal evidence.

It is significant that the abundance of stromatoporoids and their overall shape diversity rapidly increased at the transition between the bioherm–biostrome structures and overlying tempestites and calciturbidites. Judging only on the base of coenosteal outer morphologies in the rock slabs, one can speculate about the possible presence of ?*Stachyodes* together with massive and coating coenostea of the genera with easily recrystallizable skeletons (e.g., ?*Stromatopora*, ?*Taleastroma*, ?*Stromatoporella*, ?*Anostylostroma*, etc.).

The poor preservation of this fauna therefore means nothing more than that stromatoporoids are certainly present, but they can hardly be used for any detailed estimates in terms of systematics, stratigraphy and palaeogeography.

In comparison with the major part of these undeterminable stromatoporoid skeletons, the preservation of some rare amphiporids is better. They occur only in relicts of some biostromal structures, in the centre of the limestone body and close to the basalts, and they were locally preserved in a very specific way. The coating by algal–bacteria? "stockings" together with burial in the lime-mud led to a post-mortem concentration of the organic matter in the porous but closed skeleton with resulting in a reduced carbonate cementation and increased silicification. The analysis of weathered silicified fragments in combination with unsilicified accumulations of these fossils in rock slabs and thin sections suggests the presence of *Amphipora* ? cf. *spissa* Yavorsky, 1957 (Pl. 6.8C–K). Concerning the stocking-like coatings both the cyanobacteria and algal coatings must be considered, i.e., *Wetheredella* ? sp. (*sensu* Kazmierczak & Kempe 1992) and *Gymnocodium* ? sp, respectively. Relicts of both structures were preserved. Particularly the silicified fragments and some of the appropriately weathered surfaces provided an undoubted image of the amphiporid skeleton structures. The quite regular internal structures, large size of these branches and irregular occurrences of axial canals in them are actually pointing to *Amphipora* ? *spissa* or closely related forms. These forms are particularly common in the Eifelian–Givetian limestones, where they are either accompanied or alternated by the cosmopolitan species *A. ramosa* (Phillips, 1841). Several small silicified fragments of thin cylindrical specimens with roughly structured skeleton tissues (indicating the "sabre"-shaped pillars), regular axial canal and well separated outer gallery of chambers were also

found, but it is difficult to decide whether they really represent *A. ramosa* or only some morphological extremes within the population of *A. spissa* (or other amphiporid). It is possible, that also a few stachyodid or coral branches were admixed in the more recrystallized accumulations of these ca. 0.5cm wide cylindrical fossils.

Amphiporids dominated the sheltered areas of platforms, but in small amounts they were found also on isolated, drowning elevations with basalts (e.g. at Horni Benesov in Moravia; Galle et al. 1995).

Brachiopods: The accumulations of brachiopod shells are relatively common at the base of biohermal structures, and were observed in several places in the centre of the type locality. Rare fragments of these coquinas (together with coral and coral–stromatoporoid facies) were found also in rock fragments around the eastern Odivelas limestone body, although this body is characteristic by preponderance of crinoidal calciturbidites. In spite of their relatively common occurrences according to our newly collected material the presence of *Athyris concentrica* (von Buch, 1834) reported by Conde & Andrade (1974) cannot be confirmed.

Especially the largest and thickest brachiopod shells (7 to 12 cm long specimens) have internal structures which cannot be compared with this species, and in addition they do not correspond to the basic structures of many of the commonly known brachiopod genera (consulted with by U. Jansen, 2007). These brachiopod shells are reported under the working name Brachiopoda gen. et sp. indet. (Type Y) – compare Pl. 6.8L–O. These very thick shells are preferentially preserved, and this corresponds to the assumption that they were thicker and larger than the opposite valves, i.e., one can speculatively infer that they most likely were pedicle valves on ventral its side of this brachiopod. The most spectacular feature of these valves is the presence of extremely thick ventral medium septa. The cross sections of their posterior parts, where these shells have typically a width of 3–5 cm, show commonly a thick septum which is closely connected with other connate skeletal elements, forming typical bulky shapes of "capital upsilon". It is interesting that these brachiopod shells were not yet documented by the systematic palaeontology. These shapes were observed on two localities of the Czech and Polish Sudetes, and both of these localities have very similar successions of the Givetian limestones which deposited on submerging basalt seafloor highs (Padouchov in the Ještěd Mountain Ridge, Chlupáč & Hladil, 1992; and Mały Bożków in Klodzko area, Hladil et al., 1999). Similarity of these brachiopods within this Variscan belt structure resembles the conclusions which can be made on the base of the Odivelas coral faunas.

The small brachiopod shells found as a positive relief on the weathered rock surfaces (Pl. 6.8P–Q) were left without determination, because there is no more than one shell. Very speculatively, there is a possibility to compare these shells with *Cranaena* ? sp. or similar brachiopods. With similarly low validity of assumptions one can speculate about presence of *Kaplex* or *Stringocephalus* shells in the deformed brachiopod coquinas (e.g. Pl. 6.8R), but also without any direct evidence. It is caused mainly by the tectonic deformation of these shell accumulations which make it difficult to successfully reconstruct the shapes of the valves on the basis of such haphazardly oriented and deformed sections.

6.3.4.2 Micropalaeontology

A small preserved sequence of the calciturbidite deposits was sampled for palynology analysis. HCl attack destroyed nearly all the mineral fraction. Concentrated HF attack was preformed but it had little effect on the residue. The organic residue was quite abundant. Black opaque heavily thermally altered (sensu Batten, 1983) amorphous organic matter was the most abundant component of the residue. Rare complete leiosphere-type palynomorphs were observed. Skeletal remains of acritarchs and grey organic tissues were more commonly seen. In some of the samples skeletal remains of acritarchs were quite common, attributable to spheromorphs, acantomorphs and polygonomorphs (Fig.6.6). Long grey branching filaments were also found in some of the samples (Fig.6.6). Although poorly preserved, this assemblage suggests a relatively high initial diversity that was subsequently destroyed by diagenetic and metamorphic activity.

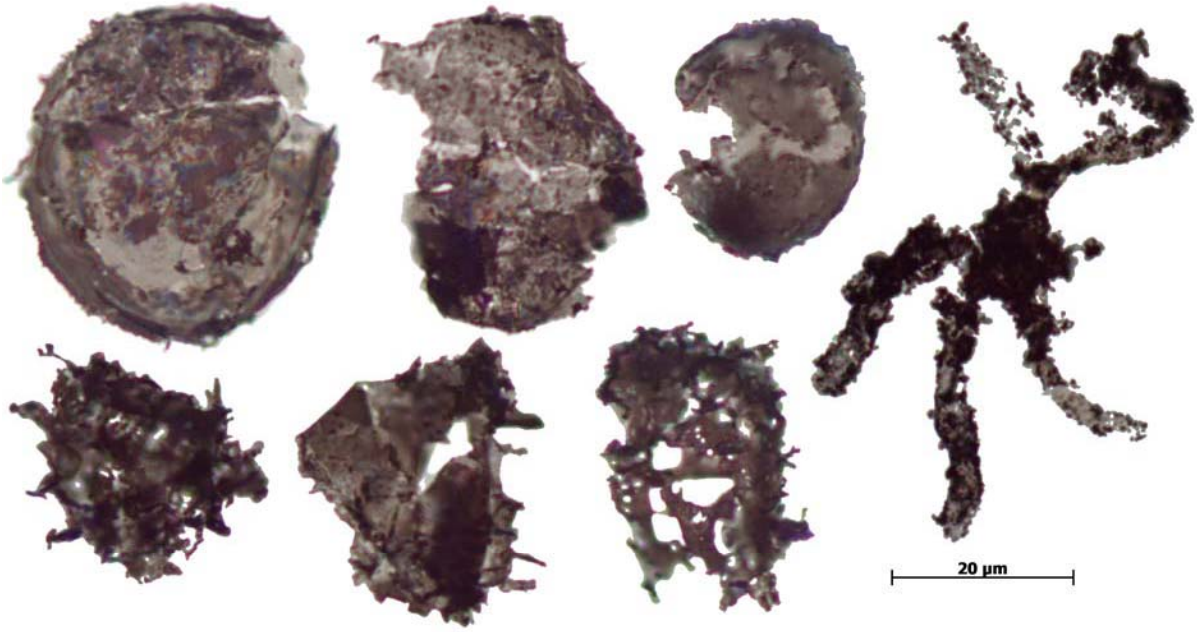

Fig. 6.6 - Acritarchs and filaments from the Middle Devonian Odivelas Limestone, Cortes locality. From Machado et al., 2008

Three samples from different outcrops (two from the bioherm type and one from the calciturbidite type) were collected for conodont studies and dissolved with 10% acetic acid. The 30 and 120µm fractions were thoroughly examined after acetic acid dissolution and a single Icriodus sp. specimen was found which does provide useful biostratigraphic information. Rare ghosts of conodont elements found by means of thinsectioning were partly dephosphatized and fragmented. The residue was composed by a carbonaceous material, probably organic matter. Small amounts of quartz crystals were present as well as pyrite (heavily corroded). From the calciturbidite sample, the coarser fraction (>120µm) was dominated by black prismatic particles, usually with less than 2 cm in length (see petrographic analyses).

6.3.5 Discussion and conclusions

From the described fauna it is possible to constrain the age of the Odivelas limestones to an interval between the uppermost Eifelian and lowermost Givetian. The

most frequently indicated ages of the sediments dominated the main body of the classical Odivelas Limestone seem to be centred roughly about stratigraphic equivalents of the *Polygnathus hemiansatus* Zone. However, it cannot be completely excluded that closely adjacent limestone occurrences would contain also some subordinated, stratigraphically condensed partial sequences (or lenses) of older (?Eifelian) and younger (?Givetian) ages.

The magnetic susceptibility results do not clarify the stratigraphical positioning and their correlation with the Kačak-Event lowest MS magnitudes and possible patterns is only tentative, having only slight supportive weight in comparison with biostratigraphical indications. It is mainly due to volcanic admixture in limestones and their slight metamorphosis.

The field, petrographic and geochemical data are indicative that volcanic and subvolcanic activity took place before, during and after the limestone deposition and that at least part of subvolcanic activity was syn or post-deformational.

The deposition of limestone was most likely dependant on a volcanic building, with the shallower areas supporting a bioherm-biostromal system with calciturbidite-type sedimentation on the flanks and in the surrounding deeper areas. The described faunal assemblages dominated by crinoids, heliolitids, solitary rugose corals and brachiopods are suggestive of sedimentation on basalt seafloor highs developed along the inner side of the central Variscan facies-tectonic belts as recorded elsewhere in Europe and particularly in Rhenish facies areas. The relevant palaeogeographical constraints are inferred, e.g. from the occurrences of *Cupressocrinites*, *Calceola* and spectrum of possible tabulate coral taxa.

The Pedreira de Engenharia formation (Évora-Beja Domain, Ossa-Morena Zone), comprising calciturbidites and providing Eifelian conodonts can tentatively be compared with the Odivelas Limestone setting, but the palaeogeography and palaeoenvironmental conditions of the latter are unknown and contemporaneous volcanic activity in the area as not been recognized. Further work in the Pedreira de Engenharia area is needed to assess the relation between the two areas.

The new data presented here contributes to the better understanding of the palaeogeography of the southern border of the Ossa-Morena Zone and the Variscan deformation in SW Europe.

6.4 Limestone units included in the Toca da Moura Volcano-Sedimentary complex

6.4.1 Local geological setting

The Toca da Moura unit was rightfully called a volcano-sedimentary complex (e.g. Santos et al., 1987; Pereira et al., 2006; Oliveira et al., 2006) considering the variety of lithologies that crop out in a restricted area and the complexity of their geometrical relations. In older literature the slates of this complex are informally called “Xistinhos”. The better defined and described part are the marine sediments and associated basalts and pyroclastic deposits (and pyroclastic derived material) from the Corte Pereiro locality, Cai-Água and other localities which were dated using miospores by Pereira & Oliveira (2001) and Pereira et al., 2006 and described in a subsequent work in Oliveira et al., 2001. The age was bracketed between the late Tournaisian CM and late Viséan NM miospore Biozones of Clayton et al. (1977) (Pereira et al., 2006). The latter work also showed that

the Cabrela complex that crops out further North is coeval in age and probably belongs to the same volcano-sedimentary complex. The geochemistry and petrology of the basaltic parts of the complex were described in Santos et al. (1987) and more recently in Oliveira et al. (2006). Other papers were published by Gonçalves (1985) and Gonçalves & Carvalhosa (1984) that generally describe the complex and present detailed mapping of some areas. The unit also contains several Fe and Cu ore deposits (Relvas, 1987; Oliveira et al., 2006) that were commercially explored (e.g. Corte Pereiro, Caeirinha, Toca da Moura).

The complex is restricted to a few areas along the Ferreira-Ficalho fault zone, the Santa-Susana shear zone and scattered over older Ossa-Morena units (Fig.6.7A). The original extent of the unit was discussed in Santos et al. (1987) and in Pereira et al. (2006) and Oliveira et al. (2006).

Within this unit there are several limestone occurrences which are usually heavily recrystalized and silicified (most of them can be considered to be marbles and metassomatic cherts), significantly deformed and often contain or are associated with Fe and/or Cu mineralizations (Relvas, 1987; Oliveira et al., 2006). The age and nature of these limestones remained unclear for a long time, except the lenses in the Cabrela area which were dated as Frasnian by conodonts (Van den Boogaard, 1983) and later interpreted as olistoliths in Tournaisian pelitic deposits (Pereira et al., 2006).

In this work badly preserved but identifiable sections of crinoidal stems and possible algal remains are reported in two of these limestone bearing groups of outcrops.

6.4.2 Monte da Pena locality

This locality is composed of several small areas (<400m^2) with rare outcrops and very abundant loose boulders of limestones and heavily silicified lithologies, probably metasomatic cherts derived from marbles and limestones. These areas run along a WNW-ESE trend corresponding to the Ferreira Ficalho fault (Fig.6.7C). The limestones are closely associated with the volcanic rocks of the Toca da Moura complex and the felsic rocks of the Baleizão porphyry (s.l.). There is an intense oxide mineralization and silicification that replaces both limestones and volcanic rocks especially along the Northern edge of the limestone alignment.

A few limestone outcrops in old quarries (currently mostly filled with local detritus and vegetated) allow a glimpse of what seems to be the original geometry and general facies: bedded limestones intercalated with volcanic rocks. The reduced number and size of the outcrops and the intense recrystalization preclude any further interpretations.

6.4.2.1 Macropalaeontology and facies

As in other localities some loose boulders have suggestive particles on weathered surfaces although no bioclasts could be positively recognized. These occur mostly in the southern edge of the alignment where recrystalization and mineralization seem to be milder.

Cutting and later polishing of the sampled boulders allowed the identification of a limestone which was likely originally a crinoidal grainstone (Pl. 6.14), but suffered intense recrystalization with veining and replacement of carbonate by silica. Most crinoidal elements are small columnal plates (<1mm), with simple circular outline and a small circular central canal. Some rare, bigger columnal plates can be tentatively identified as Gasterocomids and possibly Cupresocrinitids (Pl. 6.14).

Several boulders of crinoidal limestones were processed for conodont analysis as a composite sample but no conodont elements were found.

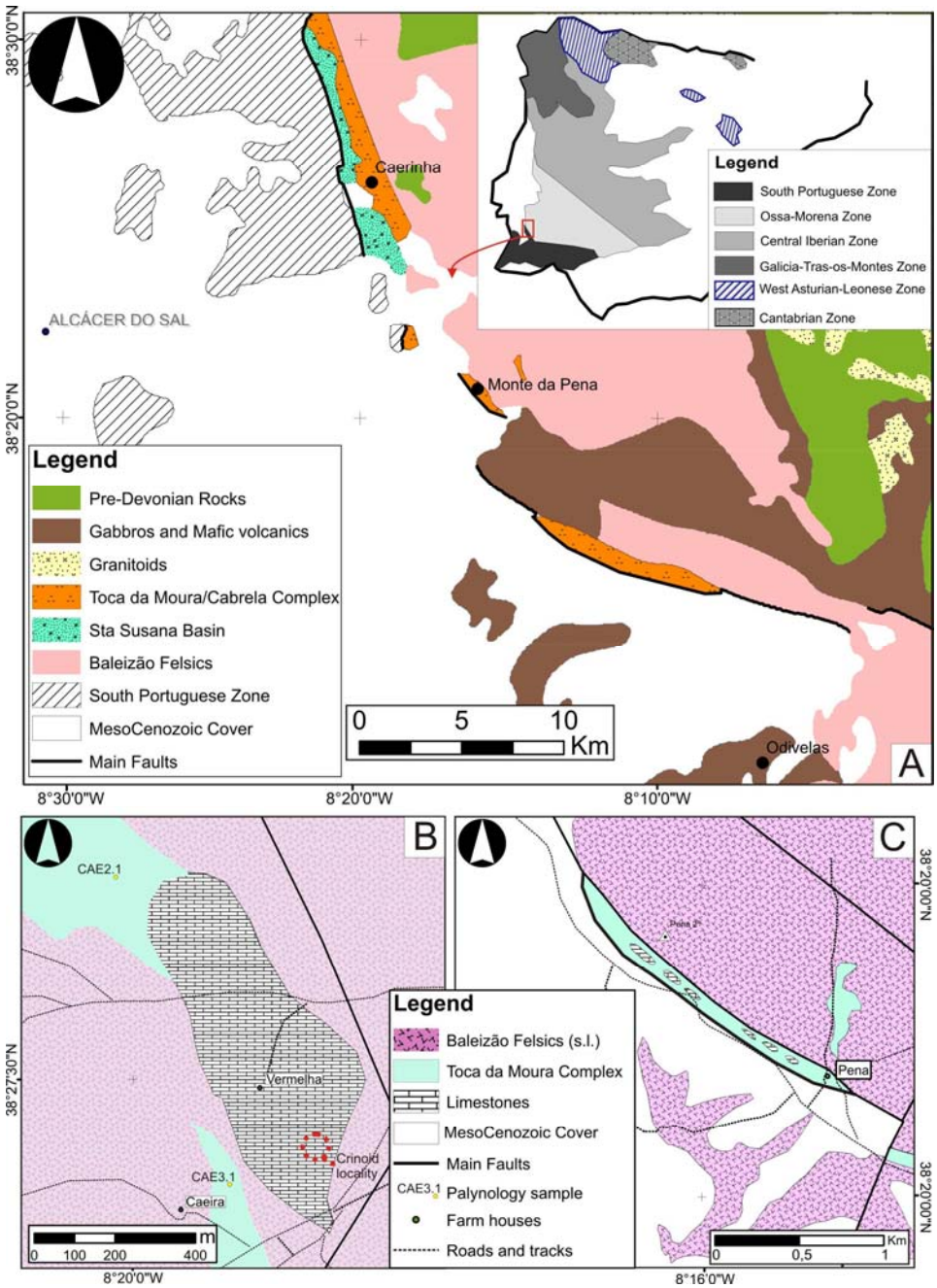

Fig. 6.7 – A - Simplified geological map of the Southwestern-most part of the Ossa-Morena Zone and Northern-most part of the South Portuguese Zone. Adapted from the Portuguese Geological Survey's 1:500.000 geological map; sheet 39D of the 1:50.000 geological map (Torrão) and unpublished data from the authors. B – Simplified geological map of the Caeira area. Data from Relvas, 1987 and unpublished field data from the authors; C - Simplified Geological map of the Pena locality, adapted from sheet 39D of the 1:50.000 geological map (Torrão).

6.4.3 Caeirinha locality

The Caeirinha locality is known in the regional geological literature as a small Cu mine within the Toca da Moura complex (Relvas, 1987; Oliveira et al., 2006) and within the Santa Susana shear zone domain. The site is also refered to as Caeira and Vermelha (local farm houses). Besides the mildly deformed basalts and associated sediments of the Toca da Moura Complex there is a relatively large limestone body (ca. 1000 X 370m maximum length and width) with oxide mineralization around it and with metassomatic replacement around the edges (Fig. 6.7B). The limestone body is heavily recrystalized and silicified. In the area there are a few natural outcrops along stream beds (basalts and pelitic sediments), a small abandoned quarry/open pit mine (silicified limestones) and abundant loose boulders (especially of the limestones and the oxide ore). The geometrical relations between the several rock types in the area are unclear.

6.4.3.1 Macropalaeontology, micropalaeontology and facies

Loose boulders of the Caeirinha locality were preferably sampled near the central part of the limestone body where, at least apparently, the deformation, recrystalization and mineralization are milder. Some of the boulders had suggestive particles naturally etched out on weathered surfaces, although no bioclasts could be recognized. Cutting and later polishing of the boulders showed that most of the sampled limestones were originally composed, almost entirely, by crinoidal elements (mostly columnal plates), most of them very small (<1mm) and the rock has a considerably low proportion of matrix. Although uncertain it seems the original limestone was a crinoidal packstone/wackstone (Pl. 6.10). The larger and more discernible columnal plates (in transverse section) were dominated by Gasterocomids and (?)Cupresocrinitids. (Pl. 6.10, 6.11, 6.12 and 6.13). Other simple morphologies were present, namely circular outline columnal plates with a small circular axial canal. Other fossils can be tentatively identified as calcareous algae (Pl. 6.9E and F) and ostracod shells (Pl. 6.9A) but these were rare and too damaged to perform any conclusive taxonomic identification.

Several boulders of crinoidal limestones were processed for conodont analysis as a composite sample, but no conodont elements were found. The amount of insoluble residue was quite big, consisting mostly of silicates and oxides. Some rare heavily corroded columnal plates attributable to Gasterocomids were found in the residue (e.g. Pl. 6.11H).

Two samples from the pelitic sediments of the Toca da Moura Complex where collected for palynology analysis (CAE 2.1 and CAE3.1 - see Fig. 6.7B). The organic residues provided badly preserved palynomorphs, mostly miospores. The following taxa where observed *Convolutispora* sp.; *Densosporites rarispinosus* Playford, 1963; *Densosporites* sp.; *Dictyotriletes* sp.; cf. *Dibolisporites* sp., *Lophozonotriletes* cf. *bellus* Kedo 1963; *Lycospora* cf. *pussila* (Ibrahim) Somers, 1972; aff. *Raistrickia variabilis* Dolby & Neves, 1970; *Rugospora* cf. *flexuosa* (Juschko) Streel, 1974; *Spelaeotriletes balteatus* (Playford) Higgs, 1996 and *Verrucosisporites nitidus* (Naumova) Playford, 1964. Rare acritarchs assignable to (?)*Gorgonisphaeridium* sp. and *Leiosphaeridia* sp. were also recorded.

6.4.4 Age and interpretation of Monte da Pena and Caeirinha localities

The common presence and the high proportion of gasterocomids and (?)cupressocrinitids columnal plates in all observed samples are indicative of an acme of these genera in the reef biota. This acme has been described in several areas of the European Variscides, namely from Čelechovice and Konice (Czech Republic) (Ureš et al., 1999; Galle & Hladil, 1995), and Armorican Massif (Le Menn, 1985) for a time interval ranging from the uppermost Eifelian to lowermost Givetian. Additionally and perhaps more importantly, the dominant presence of Cupressocrinites sp. and common presence of Gasterocoma sp. columnals was described recently in Machado et al., (2009) for the Odivelas Limestone classical locality (some tenths of Kms to the SE) which provided a typical coral assemblage of the same time interval. As discussed by Głuchowski, (1993) the identification of several genera based solely on their stem columnals is generally valid for the Cupressocrinites genus, but this and other genera of similar morphology are present in younger Devonian and even Tournaisian sediments. The original lithofacies are difficult to interpret due to the poorly preserved sedimentary features at a meso and microscopic scale and the total absence of information at a macroscale. Nevertheless there is a striking resemblance of the petrographic characteristics and bioclasts association between the Caeirinha limestones and the crinoidal calciturbidite facies described for the Odivelas Limestone classical locality (cf.Pl. 6.5 A, C). It is likely that other lithofacies may have been originally present (e.g. biostromal/bioherm) but are now completely obliterated by the intense deformation and metasomatism.

The described miospore assemblage is coherent with the previously described assemblages for the TMC (Pereira et al., 2006) which contain reworked miospores. The presence of *Lycospora* cf. *pussila* (Ibrahim) Somers, 1972 is indicative of the Pu miospore biozone of Clayton et al. (1977) – latest Tournaisian – earliest Viséan. The remaining taxa may be, at least in part, reworked. The presence of Middle Devonian Limestones within a volcano-sedimentary complex that has been, for the most part, dated as Viséan-Tournaisian can have 2 possible explanations. Considering the previous record of olistoliths in the associated Cabrela complex (Pereira et al., 2006; Oliveira et al., 2006), one can easily assume the same setting for the Caeirinha (and possibly the Monte da Pena) locality. Despite this relatively straightforward explanation, one must consider the localities are within important shear zones. The possibility that the limestone body is merely tectonically imbricated with the surrounding (younger) rocks can not be discarded

Acknowledgements

Acknowledgements to Madalena Fonseca of the Tropical Research Institute (IICT) Department of Natural Sciences(DCN)/ Global Development(DES); The Rock Magnetism Laboratory of the Instituto Infante D. Luís – FCUL; the Museu Geológico of the Portuguese Geological survey; George Sevastopulo (Trinity College Dublin) for the support in the initial stages of the work. Jean LeMenn for the helpful discussions on crinoid taxonomy and biostratigraphy. The owners of Monte da Pena for the access to the locality.

References

ALMEIDA E., POUS J., SANTOS F.M., FONSECA P.E., MARCUELLO A., QUERALT P., NOLASCO R. & Mendes-Victor L., 2001. Electromagnetic imaging of a transpressional tectonics in SW Iberia. Geophys. Res. Lett., AGU, 28, 3, 439–442.

ANDRADE, A. A. S., 1983. Contribution à l'analyse de la suture hercynienne de Beja (Portugal): perspectives métallogéniques. Laboratoire de Métallogénie I Nancy, Institut National Polytechnique de Lorraine. PhD thesis: 137.

ANDRADE, A.A.S., PINTO, A.F.F. & CONDE L.E.N., 1976. Sur la géologie du Massif de Beja: Observations sur la Transversale d' Odivelas. Comunicações dos Serviços Geológicos de Portugal, 60: 171–202.

ARAÚJO A., FONSECA P., MUNHÁ J., MOITA P., PEDRO P. & RIBEIRO A., 2005. The Moura Phyllonitic Complex: An accretionary complex related with obduction in the Southern Iberia Variscan Suture. Geodinamica Acta 18 (5): 375–388.

BATTEN D.J., 1983. Identification of amorphous sedimentary organic matter by transmitted light microscopy. Spec. Publ. Geol. Soc. London 12 (1): 275–287.

BERKYOVÁ, S., 2009. Lower-Middle Devonian (upper Emsian-Eifelian, *serotinus-kockelianus* zones) conodont faunas from the Prague Basin, the Czech Republic. Bulletin of Geosciences 84: 667–686.

BERKYOVÁ, S., FRÝDA, J. & KOPTÍKOVÁ, L., 2008. Environmental and biotic changes close to the Emsian/Eifelian boundary in the Prague Basin, Czech Republic: paleontological, geochemical and sedimentological approach. *In* Kim, A.I., Salimova ,F.A. & Meshchankina, N.A. (eds) International Conference Global Aligments of Lower Devonian Carbonate and Clastic Sequences, SDS/IGCP Project 499 joint field meeting, 25.8.-3.9.2008, State Committee of the Republic of Uzbekistan on Geology and Resources & Kitab State Geological Reserve, Contributions, Taskhent-Novosibirsk: 18-19.

VAN DEN BOOGAARD, M., 1973. Conodont faunas from Portugal and Southwestern Spain. Part 1: A Middle Devonian fauna from near Montemor-o-Novo. Scripta Geologica 13: 1-11.

VAN DEN BOOGAARD, M., 1983. Conodont faunas from Portugal and Southwestern Spain. Part 7: A Frasnian conodont fauna near the Estação de Cabrela (Portugal). Scripta Geologica 69: 1-17.

BORREGO J., ARAÚJO A. & FONSECA P.E., 2005. A geotraverse through the south and central sectors of the Ossa-Morena Zone in Portugal (Iberian Massif). In: Carosi R., Dias R., Iacopini D. & Rosenbaum G. (Eds): The southern Variscan belt. Journal of the Virtual Explorer 19. Electronic Edition, Paper 10.

BORREGO J., ARAÚJO A. & FONSECA P.E., 2005. A geotraverse through the south and central sectors of the Ossa-Morena Zone in Portugal (Iberian Massif). In: Carosi R.,

Dias R., Iacopini D. & Rosenbaum G. (Eds): The southern Variscan belt. Journ. Virtual Explorer 19. Electronic Edition, Paper 10.

BOOTH-REA G., SIMANCAS J.F., AZOR A., AZAÑÓN J.M., GONZÁLEZ-LODEIRO F. & FONSECA P., 2006. HP–LT Variscan metamorphism in the Cubito-Moura schists (Ossa-Morena Zone, southern Iberia) Compt. Rend. Geosci 338 (16): 1260–1267.

BOSÁK, P., MYLROIE, J.E., HLADIL, J., CAREW, J.L. & SLAVÍK, L., 2002. Blow Hole Cave: An unroofed cave on San Salvador Island, the Bahamas, and its importance for detection of paleokarst caves on fossil carbonate platforms. Acta Carsologica 31 (3): 51-74.

BOULVAIN, F., DA SILVA, A.-C., HLADIL, J., GERSL, M., KOPTIKOVA, L. & SCHNABL, P., 2010. Magnetic susceptibility correlation of km-thick Eifelian–Frasnian sections (Ardennes and Moravia). Geologica Belgica, (in press)

BOUČEK B., 1931 Report about interesting new finding of the genus Cupressocrinus Goldf. in the Devonian of Celechovice (in Czech). Čas. Vlas.. spol. mus.. Olomouc 44 (3-4): 1–2.

von BUCH L., 1834 Über Terebrateln, mit einem Versuch, sie zu classificiren und zu beschrieben. Phys. Abh. Königl. Akad. Wissensch. Jahre 1833: 1–124.

CHAMINÉ H.I., GAMA PEREIRA L.C., FONSECA P.E., MOÇO L.P., FERNANDES J.P., ROCHA F.T., FLORES D., PINTO DE JESUS A., GOMES C., SOARES de ANDRADE A.A. & ARAÚJO, A., 2003. Tectonostratigraphy of Middle and upper Palaeozoic black shales from the Porto–Tomar–Ferreira do Alentejo shear zone (W Portugal): new perspectives on the Iberian Massif. Geobios 36 (6): 649–663.

CLAYTON, G., COQUEL, R., DOUBINGER, J., GUEINN K.J., LOBOZIAK, S., OWENS, B. & STREEL, M., 1977. Carboniferous Miospores of Western Europe: illustration and zonation. Meded. Rijks Geol. Dienst, 29: 1-71.

CHLUPAČ, I. & HLADIL, J., 1992. New Devonian occurrences in the Jested Mts., North Bohemia. Journal of the Czech Geological Society 37(3): 185-191.

CHLUPÁČ, I. & KUKAL, Z., 1986. Reflection of possible global Devonian events in the Barrandian area, C.S.S.R. *In* Walliser, O.H. (ed.), Global Bio-events. Lecture Notes in Earth Sciences, Springer-Verlag, Berlin 8: 169-179.

CONDE L.L. & ANDRADE A.A., 1974. Sur la faune méso et/ou néodevonienne des calcaires du Monte das Cortes, Odivelas (Massif de Beja). Memórias e Notícias, Publ. Depart. Ciênc. Terra Mus. Mineral. Geol. Univ. Coimbra 78: 141–145.

CRESPO-BLANC A. & OROZCO M. 1988: The Southern Iberian Shear Zone; a major boundary in the Hercynian folded belt. Tectonophysics 148: 221–227.

CRESPO-BLANC, A., 2007. La banda metamórfica de Aracena. In: Vera, J.A. (Ed.): Geología de España. Sociedad Geológica de España-Instituto Geológico y Minero de España, Madrid: 179-182.

DALLMEYER R.D., FONSECA P.E., QUESADA C. & RIBEIRO A., 1993. 40Ar/39Ar mineral age constraints for the tectonothermal evolution of a Variscan Suture in SW Iberia. Tectonophysics 222: 177–194.

ELRICK, M. & HINNOV, L. A., 1996. Millennial-scale climate origins for stratification in Cambrian and Devonian deep-water rhythmites, western USA. Palaeogeography, Palaeoclimatology, Palaeoecology 123: 353-372

ELRICK, M., BERKYOVÁ, S., KLAPPER, G., SHARP, Z., JOACHIMSKI, M. & FRÝDA, J., 2009. Stratigraphic and oxygen isotope evidence for My-scale glaciation driving eustasy in the Early-Middle Devonian greenhouse world. Palaeogeography, Palaeoclimatology, Palaeoecology 276: 170-181

ELLWOOD, B.B., GARCIA-ALCALDE, J.L., EL HASSANI, A., HLADIL, J., SOTO, F.M., TRUYÓLS-MASSONI, M., WEDDIGE, K., & KOPTIKOVA, L., 2006. Stratigraphy of the Middle Devonian Boundary: Formal Definition of the Susceptibility Magnetostratotype in Germany with comparisons to Sections in the Czech Republic, Morocco and Spain. Tectonophysics, 418: 31-49.

ERMAKOVA K.A., 1960. Nekotorye vidy kishechnopolostnykh devona central'nykh i vostochnykh oblastey Russkoy platformy. Tr. Vsesoyuz. nauch.-issled. geol.-razved. neft. Inst. VNIGNI 16, Paleontol. Sbor. 3: 69–91.

FERNANDES J.P., FLORES D., ROCHA F.T., GOMES C., GAMA PEREIRA L.C., FONSECA P.E. & CHAMINÉ H.I., 2001 Devonian and Carboniferous palynomorph assemblages of black shales from the Ovar-Albergaria-a-Velha-Coimbra-Tomar (W Portugal): tectonostratigraphic implications for the Iberian Terrane. Geociências, Rev. Univ. de Aveiro 15: 1–23.

FERNÁNDEZ F. J., CHAMINÉ H. I., FONSECA P. E., MUNHÁ J., RIBEIRO A., ALLER J., FUERTES-FUENTE M. & SODRÉ BORGES F., 2003. HT-fabrics in garnet-bearing quartzite from Western Portugal: geodynamic implications for the Iberian Variscan Belt. Terra Nova 15: 96-103.

FERNÁNDEZ-MARTÍNEZ E. 1999. Heliolitidae (Cnidaria, Tabulata) del Devónico de la Cordillera Cantábrica (NW de España). Trabajos Geologia 21: 97–110.

FIGUEIRAS, J., MATEUS, A., GONÇALVES, M., WAERENBORG, J. & FONSECA, P.E., 2002. Geodynamic evolution of the South Variscan Iberian Suture as recorded by mineral transformations. Geodinamica Acta 15(1): 45–61.

FONSECA, P. & RIBEIRO, A., 1993. Tectonics of the Beja-Acebuches Ophiolite: a major suture in the Iberian Variscan Foldbelt. Geologische Rundschau 82: 440–447.

FONSECA P., 1995. Estudo da Sutura Varisca no SW Ibérico nas regiões de Serpa-Beja-Torrão e Alvito-Viana do Alentejo. PhD Thesis, GeoFCUL, Univ. Lisboa: 325 pp.

FONSECA P.E., 1997. Domínios meridionais da Zona de Ossa-Morena e limites com a Zona Sul Portuguesa: Metamorfismo de Alta Pressão relacionado com a sutura Varisca Ibérica. In: Araújo A. & Pereira M. (Eds.) GEOCEV 96 - Estudo sobre a Geologia da Zona de Ossa-Morena (Maciço Ibérico), Évora: 133–168.

FONSECA, P., MUNHÁ, J., PEDRO, J., ROSAS, F., MOITA, P., ARAÚJO, A. & LEAL, N., 1999. Variscan ophiolites and high-pressure metamorphism in Southern Iberia. Ofioliti 24 (2): 259–268.

GALLE, A., HLADIL, J. AND ISAACSON, P. E., 1995. Middle Devonian biogeography of closing South Laurussia; North Gondwana Variscides; examples from the Bohemian Massif (Czech Republic), with emphasis on Horni Benesov. Palaios 10(3): 221-239.

GŁUCHOWSKI, E., 1993. Crinoid assemblages in the Polish Givetian and Frasnian. Acta Palaeontologica Polonica 38(1-2): 35-92.

GONÇALVES, F., 1985. Contribuição para o conhecimento geológico do Complexo Vulcano-sedimentar da Toca da Moura. Memórias da Academia das Ciências de Lisboa, 26: 263-267.

GONÇALVES, F., CARVALHOSA, A., 1984. Subsídios para o conhecimento geológico do Carbónico de Santa Susana. Vol. d Hommage au géologue G. Zbyszewski. Ed.Recherche de Civilisations, Paris: 109-130

GOLDFUSS G.A., 1831. Petrefacta Germaniae, et cetera. Divisio prima, secunda, tertia (1826-1833), pp. I-XV + 1-692, pls. 119, Arnz & Co. Düsseldorf (1831): 165–240.

GOSSELET, J., 1877. Le calcaire dévonien supérieur dans le Nord-Est l'arrondissement d'Avesnes. Ann. Soc. géol. Nord 4: 238–320.

HLADIL, J., 1981. The genus Caliapora Schlüter (tabulate corals), from the Devonian of Moravia. Věst. Ústřed. úst. geol. 56: 157–167.

HLADIL, J., 1984. Tabulate corals of the genus Thamnopora Steininger from the Devonian of Moravia. Věst. Ústřed. úst. geol: 59, 29–39.

HLADIL, J., 1985. Tabulate corals from the NP 824 Ostravice borehole (in Czech). Acta Univ. Carol., Geol. 3: 251–259.

HLADIL, J., 1993. Tabulatomorphs and stromatoporoids below and above the upper boundary of the Acanthopyge Limestone, Eifelian Givetian transitional interval, Central Bohemia. Věstník Českého geologického ústavu 68 (2): 27-42.

HLADIL, J. & LANG, L., 1985. Devonian limestones of the Újezd V-1 borehole in the eastern margin of the Boskovice Furrow. Věst. Ústřed. úst. geol. 60: 361–364.

HLADIL, J. HELEŠICOVÁ, K., HRUBANOVÁ, J., MÜLLER, P. & UREŠ, M., 1994. Devonian island elevations under the scope Central Europe, basement of the Carpathian Mountains in Moravia. Jahrbuch der Geologischen Bundesanstalt in Wien 136 (4): 741-750.

HLADIL, J., MAZUR, S., GALLE, A. & EBERT, J.R., 1999. Revised age of the Maly Bozkow limestone in the Klodzko metamorphic unit, early Givetian, late Middle Devonian; implications for the geology of the Sudetes, SW Poland. Neues Jahrbuch fur Geologie und Palaontologie, Abhandlungen 211: 329-353.

HLADIL, J., GERŠL, M., STRNAD, L., FRÁNA, J., LANGROVÁ, A., SPIŠIAK, J., 2006. Stratigraphic variation of complex impurities in platform limestones and possible significance of atmospheric dust: a study with emphasis on gamma-ray spectrometry and magnetic susceptibility outcrop logging (Eifelian-Frasnian, Moravia, Czech Republic). Intl. J. Earth Sci. 95 (4): 703–723.

HLADIL, J., CEJCHAN, P., BABEK, O., KOPTIKOVA, L., NAVRATIL, T. & KUBINOVA, P., 2010. Dust – a geology-orientated attempt to reappraise the natural components, amounts, inputs to sediment, and importance for correlation purposes. Geologica Belgica, in press.

IVEN, C., 1980. Alveolitiden and Heliolitiden aus dem Mittle- und Oberdevon des Bergischen Landes (Rheinisches Schiefergebirge). Palaeontographica 167: 1–179.

JESUS, A., MATEUS, A., WAERENBORGH, J., FIGUEIRAS, J., ALVES, L.C. & OLIVEIRA, V., 2003. Hypogene titanian, vanadian maghemite in reworked oxide cumulates in the beja layered gabbro complex, Odivelas, southeastern Portugal. Canad. Mineral. 41 (5): 1105–1124.

JESUS, A., MUNHÁ, J., MATEUS, A., TASSINARI, C. & NUTMAN, A., 2007. The Beja layered gabbroic sequence (Ossa-Morena Zone, Southern Portugal): geochronology and geodynamic implications. Geodinamica Acta 20 (3): 139–157.

JICKELLS, T.D. et al., 2005. Global Iron connections between desert dust, ocean biogeochemistry and climate. Science 308: 67-71.

JULIVERT, M. & MARTÍNEZ, F., 1983. Estructura de conjunto y visión global de la Cordillera Herciniana. Libro Jubilar J. M. Rios. Geología de España 1: 607-630.

KASPARI, S., MAYEWSKI, P. A., HANDLEY, M., KANG, S., HOU, S., SNEED. S., MAASCH, K. & QIN, D. 2009. A High-Resolution Record of Atmospheric Dust Composition and Variability since a.d. 1650 from a Mount Everest Ice Core. Journal of Climate 22: 3910-3925.

KAWAHATA, H., OKAMOTO, T., MATSUMOTO, E. & UJIIE, H., 2000. Fluctuations of eolian flux and ocean productivity in the mid-latitude north Pacific during the last 200 kyr. Quaternary Science Reviews 19: 1279-1291.

KAZMIERCZAK J. & KEMPE S., 1992. Recent cyanobacterial counterparts of Paleozoic Wetheredella and related problematic fossils. Palaios 7: 294–304.

KLAPPER, G. & JOHNSON, D. B., 1975. Sequence in conodont genus Polygnathus in Lower Devonian at Lone Mountain, Nevada. Geologica et Palaeontologica 9: 65-83.

KLAPPER, G., ZIEGLER, W. & MASHKOVA, T. V., 1978. Conodonts and correlation of Lower Middle Devonian boundary beds in the Barrandian area of Czechoslovakia. Geologica et Palaeontologica, 12: 102-116.

KOPTÍKOVÁ, L., HLADIL, J., SLAVÍK, L., & FRÁNA, J., 2007. The precise position and structure of the Basal Choteč Event: lithological, MS-and-GRS and geochemical characterisation of the Emsian-Eifelian carbonate stratal successions in the Prague Syncline (Tepla-Barrandian unit, central Europe). In Over, D. & Morrow, J. (eds): Subcommission on Devonian Stratigraphy and IGCP 499 Devonian Land Sea Interaction, Eureka, NV, 2007, San Diego State University & SUNY-Geneseo, Eureka, September 9-18. SDS & IGCP 499 Eureka NV 2007 Program and Abstracts, Geneseo: 55-57.

KOPTÍKOVÁ, L., BERKYOVÁ, S., HLADIL, J., SLAVÍK, L., SCHNABL, P., FRÁNA, J. & BÖHMOVÁ, V., 2008. Long-distance correlation of Basal Chotec Event sections using magnetic susceptibility (Barrandian –vs– Nevada) and lateral and vertical variations in fine-grained non-carbonate mineral phases. In Kim, A.I., Salimova, F.A. & Meshchankina, N.A. (eds): International Conference Global Aligments of Lower Devonian Carbonate and Clastic Sequences, SDS/IGCP Project 499 joint field meeting, 25.8. - 3.9. 2008, State Committee of the Republic of Uzbekistan on Geology and Resources, Kitab State Geological Reserve Contributions: 60-62.

KOPTÍKOVÁ, L., HLADIL, J., SLAVÍK, L., ČEJCHAN, P. & BÁBEK, O., 2010. Fine-grained non-carbonate particles embedded in neritic to pelagic limestones (Lochkovian to Emsian, Prague synform, Czech Republic): composition, provenance and links to magnetic susceptibility and gamma-ray logs. Geologica Belgica, in press.

LE MAÎTRE, D., 1947. Le récif coralligène de Ouihalane. Protect. Republ. Franç. Maroc, Serv. géol. Maroc, Not. Mém. 67: 1–112.

LECOMPTE, M., 1939. Les Tabulés du Dévonien moyen et supérieur du bord sud du bassin de Dinant. Mém. Mus. Roy. Hist. Natur. 90: 1–230.

LE MENN, J., 1985. Les crinoides du Devonien inferieur et moyen du massif Armoricain: Memoires de la Societe Geologique et Mineralogique de Bretagne, 30: 1-268

LINNÉ, C. 1771,. Mantissa plantarum altera. Generum editionis VI. & Specierum editionis II (1767-1771), Laurentius Salvius, Holmiae (Stockholm) 1771: 143–588.

LIAO, J. C., RODRÍGUEZ, S. & VALENZUELA-RÍOS, J. I., 2001. Conodontos del Devónico Inferior de Arroyo del Pozo del Rincón, Sierra Morena, Cordoba. Los fósiles y la paleogeografía y simposios de los proyectos del Programa Internacional de Correlación

Geológica, UNESCO-IUGS, Nº 410 y Nº 421 : XVII Jornadas de la Sociedad Española de Paleontología. Ayuntamiento de Albarracín. - Albarracín, Universidad de Zaragoza. II: 551-556.

LÖTZE, F. 1945. Zur Gliederung der Variszíden in der Iberischen Meseta. Geotektonische Forschungen 6: 78–92.

MACHADO, G., HLADIL, J., KOPTÍKOVÁ, L., FONSECA, P. E., ROCHA, F. T. & GALLE, A., 2009. The Odivelas Limestone: evidence for a Middle Devonian reef system in western Ossa-Morena Zone (Portugal). Geologica Carpathica, 60(2): 121-137.

MACHADO, G., HLADIL, J., KOPTÍKOVÁ, L., FONSECA, P. E., ROCHA, F. T., 2008. Middle Devonian reef fauna and co-occurring acritarchs from volcanosedimentary sequences within the Beja Igneous Complex (SW Ossa-Morena Zone, Portugal). IGCP 497 & IGCP 499 Final Meeting. Frankfurt. Germany.

MACHADO, G., SLAVIK, L., KOPTÍKOVÁ, L., HLADIL, J. & FONSECA, P., 2009b. Emsian-Eifelian mixed carbonate-volcaniclastic sequence in western Ossa-Morena zone (Odivelas limestone). First IGCP 580 MAGNETIC SUSCEPTIBILITY, CORRELATIONS AND PALEOENVIRONMENTS meeting. Liège University, B20, Sart Tilman, Belgium: 37.

MACHADO, G., HLADIL, J., SLAVIK, L., KOPTIKOVA, L., MOREIRA, N., FONSECA, M. & FONSECA, P., 2010. An Emsian-Eifelian carbonate- volcaniclastic sequence and the possible correlatable pattern of the Basal Choteč event in Western Ossa-Morena Zone, Portugal (Odivelas Limestone). Geologica Belgica 13 (4): 425-440

MACHADO, G., HLADIL, J., 2010 On the age and significance of the limestone localities included in the Toca da Moura volcano-sedimentary complex: preliminary results. III Congresso Ibérico de Paleontologia e as XXVI Jornadas de la SEP. Lisboa. In press.

MATEUS, A., FIGUEIRAS, J., GONÇALVES, M. & FONSECA, P.E., 1999. Evolving fluid circulation within the Beja-Acebuches Variscan Ophiolite Complex (SE, Portugal), Ofioliti 24 (2) (Sp. Iss.): 269–282.

MATEUS, A., JESUS, A.P., OLIVEIRA, V., GONÇALVES, M.A. & ROSA, C., 2001. Vanadiferous iron-titanium ores in Gabbroic Series of the Beja Igneous Complex (Odivelas, Portugal); remarks on their possible economic interest. Estud. Not. Trabal. Inst. Geol. Min. 43: 3–16.

MAY, A., 1987. Der Massenkalk (Devon) nördlich von Brilon (Sauerland). Geologie und Paläontologie in Westfalen 10: 51-84.

MAY, A., 1993. Korallen aus dem höheren Eifelium und unteren Givetium (Devon) des nordwestlichen Sauerlandes (Rheinisches Schiefergebirge). Teil I: Tabulate Korallen. Palaeontographica, Abt. A 227: 87-224.

MAY, A., 1999. Stromatoporen aus dem Ober-Emsium (Unter-Devon) der Sierra Morena (Süd-Spanien). Münstersche Forschungen für Geologie und Paläontologie 86: 97–105.

MAY, A., 2003. Die Fossilführung des Mitteldevons im Raum Attendorn-Olpe (West-Sauerland; Rechtsrheinisches Schiefergebirge). Geol. Paläont. Westfalen 60: 47–79.

MAY, A., 2006. Lower Devonian Stromatoporoids from the northern Obejo-Valsequillo-Puebla de la Reina Domain (Badajoz and Córdoba Provinces, Southern Spain. Revista Española de Paleontología 21 (1): 29-38.

MCCOY, F., 1850. On some new genera and species of Silurian Radiata in the collection of the University of Cambridge. Ann. Mag. Nat. Hist., 2nd Ser. 6: 270–290.

MILNE-EDWARDS, H. & HAIME, J., 1851. Monographie des polypiers fossiles des terrains palaeozoiques, palaeozoîques, précédé d'un tableau général de la classification des polypes. Arch. Mus. Hist. Natur. 5: 1–502.

OLIVEIRA, J. T., OLIVEIRA, V. & PIÇARRA, J. M., 1991. Traços gerais da evolução tectono-estratigráfica da Zona de Ossa-Morena, em Portugal: síntese critica do estado actual dos conhecimentos. Comunicações dos Serviços Geológicos de Portugal 77: 3-26.

OLIVEIRA J.T., RELVAS J.M.R.S., PEREIRA Z., MUNHÁ J.M., MATOS J.X., BARRIGA F.J.A.S. & ROSA C.J. 2006: O complexo Vulcano-sedimentar de Toca da Moura-Cabrela (Zona de Ossa-Morena); Evolução tectono-estratigráfica e mineralizações associadas. In: Dias R., Araújo A., Terrinha P. & Kullberg J.C. (Eds.) Geologia de Portugal: 1–13.

PENECKE K.A., 1887. Über die Fauna und das Alter einiger paläozoischer Korallenriffe der Ostalpen. Z. Deutsch. Geol. Gesel. 39: 267–276.

PERDIGÃO, J. C., 1967. Descoberta de Mesodevónico em Portugal (Portalegre). Comunicações dos Serviços Geológicos de Portugal 52: 55-78.

PERDIGÃO, J. C., 1973. O Devónico de Barrancos (Paleontologia e Estratigrafia). Comunicações dos Serviços Geológicos de Portugal 56: 33-54.

PERDIGÃO, J. C., 1974. O Devónico de Portalegre. Comunicações dos Serviços Geológicos de Portugal 57: 28-68

PERDIGÃO, J. C., OLIVEIRA, J. T. & RIBEIRO, A. 1982. Notícia explicativa da folha 44-B (Barrancos). Carta Geológica de Portugal na escala 1:50 000. Serviços Geológicos de Portugal, Lisboa.

PEREIRA, Z., PIÇARRA, J. M. & OLIVEIRA, J. T., 1998. Palinomorfos do Devónico inferior da região de Barrancos (Zona de Ossa Morena). Actas do V Congresso Nacional de Geologia, Comunicações do Instituto Geológico e Mineiro 84: A 18-21.

PEREIRA, Z., PIÇARRA, J. M. & OLIVEIRA, J. T., 1999. Lower Devonian palynomorphs from the Barrancos region, Ossa-Morena Zone, Portugal. Bolletino della Società Paleontologica Italiana 38: 239-245.

PEREIRA, Z. AND OLIVEIRA, J. T., 2001. Palinomorfos do Viseano do Complexo vulcânico da Toca da Moura, Zona de Ossa Morena. VI Congresso Nacional de Geologia. UNL, Portugal, Ciências da Terra V: A120-A121.

PEREIRA, Z. & OLIVEIRA, J.T. 2003. Estudo palinostratigráfico do sinclinal da Estação de Cabrela. Implicações tectonostratigráficas. Congr. Nac. Geol., Lisboa, Ciênc. Terra (UNL) VI: A118–A119.

PEREIRA, Z., OLIVEIRA, V., & OLIVEIRA, J. T., 2006. Palynostratigraphy of the Toca da Moura and Cabrela Complexes, Ossa Morena Zone, Portugal. Geodynamic implications. Review of Palaeobotany and Palynology 139(1-4): 227-240.

PETR V., 2007. Crinoidea – Lilijice. Web pages http://sweb.cz/new.petr/, part http://www.sweb.cz/new.petr/Galerie/Cupressocrinites.html (10.7.2007).

PHILLIPS, J., 1841. Figures and descriptions of the Palaeozoic fossils of Cornwall, Devon, and West Somerset; observed in the course of the Ordnance Geological Survey of that district. Longman, Brown, Green & Longmans, London: 1–231.

PIÇARRA, J. M., 1997. Nota sobre a descoberta de graptólitos do Devónico inferior na Formação de Terena, em Barrancos (Zona de Ossa Morena). In: A. V. Araújo, M. F. Pereira (eds.) Estudo sobre a Geologia da Zona de Ossa Morena (Maciço Ibérico). Livro de homenagem ao Professor Francisco Gonçalves, Universidade de Évora: 27-36.

PIÇARRA, J. M., 1998. First Devonian graptolites from Portugal. Temas Geológico-Mineros, ITGE, 23: 242-243.

PIÇARRA, J.M., 2000, Estudo estratigráfico do sector de Estremoz-Barrancos, Zona de Ossa Morena, Portugal. Litoestratigrafia e Bioestratigrafia do intervalo Câmbrico Médio?-Devónico Inferior. PhD Thesis, Univ. Évora: 268.

PIÇARRA, J. M. & LE MENN, J., 1994. Ocorrência de crinóides em mármores do Complexo Vulcano-Sedimentar Carbonatado de Estremoz: implicações estratigráficas: Comunicações Instituto Geológico e Mineiro, 80: 15-25.

PIÇARRA, J. M., LE MENN, J., PEREIRA, Z., GOURVENNEC, R., OLIVEIRA, J. T. & ROBARDET, M., 1999. Novos dados sobre o Devónico inferior de Barrancos (Zona de Ossa Morena, Portugal): Temas Geológico-Mineros ITGE 26: 628-631

PIÇARRA, J. M. & SARMENTO, G., 2006. Problemas de posicionamento estratigráfico dos Calcários Paleozóicos da Zona de Ossa Morena (Portugal). VII Congresso Nacional de Geologia, Lisboa. Resumos 2: 657-660.

PLUSQUELLEC, Y. & HLADIL, J., 2001. Tabulate corals of Ibarmaghian affinities in the Upper Emsian of Bohemia. Geologica et Palaeontologica 35: 31-51.

QUESADA, C., 1990. Introduction of the Ossa-Morena Zone (part V). In: Dallmeyer R.D. & Martínez García E. (Eds.) Pre-Mesozoic Geology of Iberia. Springer Verlag, Berlin Heidelberg: 249–251.

QUESADA, C., ROBARDET, M. & GABALDÓN, V. 1990. Synorogenic phase (Upper Devonian-Carboniferous-Lower Permian). In: Dallmeyer R.D. & Martínez García E. (Eds.) Pre-Mesozoic Geology of Iberia. Springer Verlag, Berlin Heidelberg: 249–251

RELVAS, J., 1987. Alteração hidrotermal na área da Mina da Caeirinha (Santa Susana): perspectiva metalogenética. Unpublished BsC thesis. Universidade de Lisboa: 254pp.

REMEŠ, M., 1939. Some rare findings in the Celechovice Devonian (in Czech). Čas.Vlasten. spol. mus. Olomouc 52, 195-196: 1–5.

RIBEIRO A., QUESADA C. & DALLMEYER R.D., 1990. Geodynamic Evolution of the Iberian Massif. In: Dallmeyer R.D. & Martínez Garcia E. (Eds) Pre-Mesozoic Geology of Iberia, Springer-Verlag: 398–409.

RIBEIRO A., SANDERSON D. & SW-Iberia Colleagues, 1996: SW Iberia: transpressional orogey in the Variscides. In: Gee D. &Zeyen H.J. (Eds) Europrobe '96 - Litosphere Dynamics: Origin and Evolution of Continents. European Science Foundation. Uppsala Univ.: 91–98.

RIBEIRO, A., MUNHÁ, J., DIAS, R., MATEUS, A., PEREIRA, E., RIBEIRO, M.L., FONSECA, P. E., ARAUJO, A., OLIVEIRA, J.T., ROMÃO, J., CHAMINÉ, H., COKE, C. & PEDRO, J.C., 2007. Geodynamic evolution of SW Europe Variscides. Tectonics 26, 6. TC6009, doi:10.1029/2006TC002058

RIBEIRO, A.; MUNHÁ, J.; FONSECA, P.E.; ARAÚJO, A.; PEDRO, J.; MATEUS, A.; TASSINARI, C.; MACHADO, G. & JESUS, A., 2009. Variscan Ophiolite Belts in the Ossa-Morena Zone (Southwest Iberia): geological characterization and geodynamic significance. IGCP Project 497, Ocean Rheic Special Volume, Gondwana Research 17: 408-421

RICHARDSON, J.B. & MCGREGOR, D.C., 1986. Silurian and Devonian spore zones of the Old Red Sandstone continent and adjacent regions. Geological Survey of Canada Bulletin 364: 1-79.

ROBARDET M. & GUTIÉRREZ-MARCO J.C., 1990. Passive margin phase (Ordovician-Silurian-Devonian). In: Dallmeyer R.D. and Martínez García E. (Eds) Pre-Mesozoic Geology of Iberia. Springer Verlag: 249–251.

ROBARDET M. & GUTIÉRREZ-MARCO J.C., 2004. The Ordovician, Silurian and Devonian sedimentary rocks of the Ossa-Morena Zone (SW Iberian Peninsula, Spain). Journal of Iberian Geology 30: 73-92.

RODRÍGUEZ, S., FERNÁNDEZ-MARTÍNEZ, E., CÓZAR, P., VALENZUELA-RÍOS, J. I., LIAO, J-CH., PARDO, M.V. & MAY, A., 2007. Emsian reefal development in Ossa-Morena Zone (SW Spain): Stratigraphic succession, microfacies, fauna and depositional environment. Abstracts of the X Internacional Congress on Fossil Cnidaria and Porifera, Saint Petersburg: 76-77.

SALTZMAN, M.R., 2005. Phosphorus, nitrogen, and the redox evolution of the Paleozoic oceans. Geology 33: 573–576.

SANTOS, J., MATA, J., GONÇALVES, F. & MUNHÁ, J., 1987. Contribuição para o conhecimento Geológico-Petrológico da Região de Santa Susana: O Complexo Vulcano-sedimentar da Toca da Moura. Comunicações dos Serviços Geológicos de Portugal 73(1-2): 29-48.

SANTOS, J.F.; ANDRADE, A.S. & MUNHÁ, J.M., 1990. Magmatismo Orogénico Varisco no limite meridional da Zona de Ossa-Morena. Comunicações dos Serviços Geológicos de Portugal, 76: 91-124.

SARMIENTO G.N., PIÇARRA, J.M. & OLIVEIRA, J.T., 2000. Conodontes do Silúrico (superior?)-Devónico nos "Mármores de Estremoz", sector de Estremoz-Barrancos (Zona de Ossa-Morena, Portugal). Implicações estratigráficas e estruturais a nível regional. I Congresso Ibérico de Paleontologia/VIII International meeting of IGCP 421. Évora. Abstracts: 284-285.

SHARKOVA, T.T., 1981. Silurian and Devonian tabulate corals of Mongolia (in Russian). Tr, Sovmest. sovet.-mongol. eksp. 14, Nauka Moscow: 1–103.

SCHLÜTER, C., 1879. Devonische Korallen und Dünschliffe von Spongophyllum Kunthi und Calophyllum paucitabulatum. Sitzungsber. Naturhist. Vereins Rheinl. Westph., Bd. 1879: 402.

SCHLÜTER C., 1889. Anthozoen des rheinischen Mittel-Devon. Abh. geol. Specialkarte Preussen Thüring. Staaten 8 4: 1–207.

SOUSA, J.L. & WAGNER, R.H., 1983. General description of the Terrestrial Carboniferous Basins in Portugal and History of investigations. In: Sousa J.L. & Oliveira J.T. (Eds) The Carboniferous of Portugal. Mem. Serv. Geol. Portugal 29: 117–126.

TCHERNYSHEV, B.B., 1951. Silurian and Devonian Tabulata and Heliolitida from margins of Kuznetsk Coal Basin (in Russian). Vsesoyuz. nauch.-issled. geol. inst. (VSEGEI) Ministr. geol., Gosgeolizdat Moskva: 1–160.

TOURNEUR, F., 1991. The *Bainbridgia – Dualipora* association (Cnidaria, Tabulata): palaeogeographical and palaeoecological implications. Hydrobiologia 216/217: 419-425.

UREŠ, M., LE MENN, J. & HLADIL, J., 1999. Middle Devonian crinoid columnals from Čelechovice in Moravia, Czech Republic. Bull. Czech Geol. Surv. 74: 323–333.

VÁZQUEZ, M., ABAD, I., JIMÉNEZ MILLÁN, J., ROCHA, F. T., FONSECA, P. E. & CHAMINÉ, H. I., 2007. Prograde epizonal clay mineral assemblages and retrograde alteration in tectonic basins controlled by major strike-slip zones (W Iberian Variscan Chain). Clay Minerals 42: 109-128.

WAGNER, R.H., 1983. The palaeogeographical and age relationships of the Portuguese Carboniferous floras with those of other parts of the Western Iberian Peninsula. In: Sousa J.L. & Oliveira J.T. (Eds) The Carboniferous of Portugal. Mem. Serv. Geol. Portugal 29: 153–177.

WAGNER, R.H. & SOUSA J.L., 1983. The Carboniferous megafloras of Portugal - a revision of identifications and discussion of stratigraphic ages. In: Sousa J.L. & Oliveira J.T. (Eds) The Carboniferous of Portugal. Mem. Serv. Geol. Portugal 29: 127–151.

YAVORSKY 1957. Stromatoporoids of the Sovetskyi Soyuz (in Russian). 2nd part. Tr. Vsesoyuz. nauch.-issled. geol. inst. (VSEGEI) 18: 1–168.

ZHAVORONKOVA, R.A., 1972. Description of corals, subclass Tabulata. In: Tyazheva A.P. & Zhavoronkova R.A. (Eds) Corals and brachiopods from the boundary beds of the Silurian and Devonian of the Southern Ural (in Russian). Nauka Moskva: 17–33.

Plates

Plate 6.1 - Field and microscopic images of the Covas Ruivas II locality. From Machado et al. (2010).

A Panorama of part A of the section (0-80m) with the approximate extension of the conodont biozones.
B Detail of a coarse pyroclastic deposit a few meters below the first limestone beds.
C Hand specimen scale image of a finely laminated tuffite (facies t1) in the *patulus* zone where the limestones are subordinate to tuffites. Note the dark grey organic mater-rich laminae alternating with the coarser and lighter laminae.
D Microscopic image (white transmitted light) of limestone facies ca1 in basal *partitus* zone. Note the (locally) common radiolarians and peloids.
E Limestone lense (arrows) interbeded with finely laminated tuffites within the lower *partitus* zone.
F Microscopic image (white transmitted light) of a grainstone belonging to facies ca1 within *costatus* zone. Note the abundant crinoid skeletal elements (cri) and the rare intraclasts (int) and tentaculites (tent).
G General appearance of the section within the *costatus* zone (part B). Note the thicker limestone beds (grainstones) and the subordinate, much thinner, interbeded tuffites.
H Slumped bed in lower *costatus* zone. The slump "head" contains reworked material from both tuffite and limestone beds.
I Small scale trough cross-bedding at the top of a limestone bed, overlaid by a tuffite bed.
J General appearance of the section in lower *australis* zone (part C). Note the thicker limestone beds and the subordinate tuffites, as in most of the *costatus* zone below. Compare with G.
K Panorama of parts B and C of the section, separated by a faulted zone. The approximate extension of the conodont biozones is shown. The first part of the section is seen in the background in the upper left.

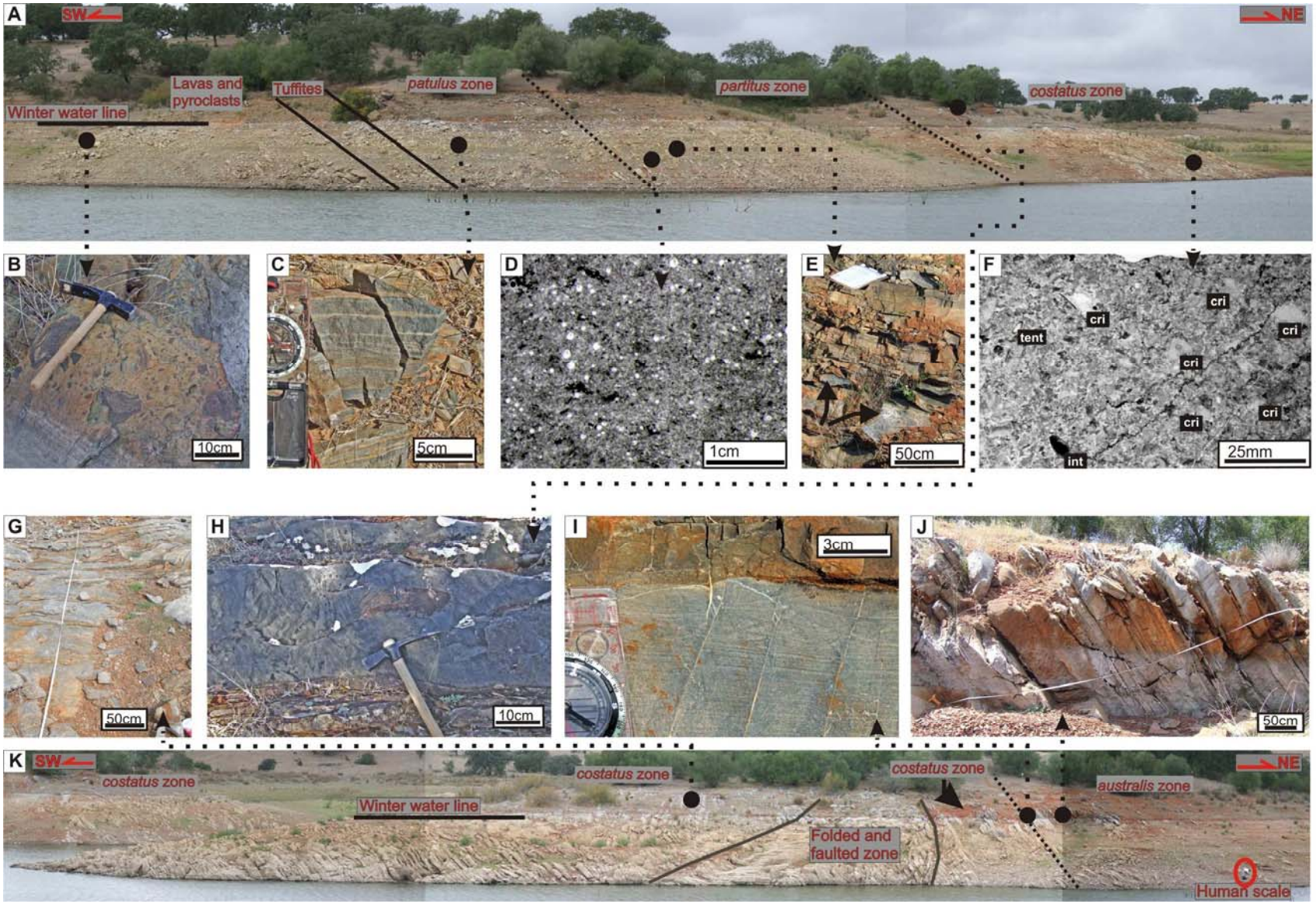
A
SW
NE
Lavas and pyroclasts
Tuffites
patulus zone
partitus zone
costatus zone
Winter water line
B
10cm
C
5cm
D
1cm
E
50cm
F
cri
tent
int
25mm
G
50cm
H
10cm
I
3cm
J
50cm
K
SW
costatus zone
costatus zone
costatus zone
australis zone
NE
Winter water line
Folded and faulted zone
Human scale

Plate 6.2 - Selected thin section and natural weathering images of the fauna from the breccia bed at 58-61,5m of the Covas Ruivas II section. From Machado et al. (2010).

A to D – Microscopic views, thin sections, transmitted white light, photographs by J. Hladil.

A Diversified coral and stromatoporoid bioclasts, all being altered to various degree; crinoid columnals and ostracods are scattered in this material. 'Sol' - rugose coral *Solipetra*; 'Hil' - tabulate coral *Hillaepora*; Sta - stromatoporoid *Stachyodes*. Erosional contact with an interleaving bed of finer calciturbidite is seen at the base (above the lower edge of the picture).

B A part of rock, where fragments of stromatoporoids prevail, occurring together with *Rhapidopora*, *Hillaepora* and amphiporids. 'Spi' - rugose coral *Spinophyllum*, 'Ple' - stromatoporoid *Plectostroma*. Note the early diagenetic, silicified and partly desilicified patches in cemented skeleton of *Plectostroma.*

C Densely packed coral detritus is mixed with originally semi-lithified intraclasts of different compositions: from grainstones (upper right corner) to dark grey calcisiltites (lower part of this picture). 'Cel '- tabulate coral *Celechopora*, 'Str' - tabulate coral *Striatopora.*

D Coarse grained calciturbidite with crinoidal debris contains a medium large, sub-rounded intraclast of calcisiltitic-mud sedimentary rock. The rock has evidently a deeper and pelagic environmental affinity if compared with shallow water debris of reef builders in 'breccia'. Photographs taken directly in field, by G. Machado. 'Int' – intraclast; 'Cep' - two small cephalopod shells, with telescopic insertion of one shell into another.

E to H – Macroscopic views. Natural weathering of these rocks has very selective effect on altered and 'fresh', pure calcite bioclasts; i.e., the most of 'fresh' bioclasts are not so nicely seen in the relief.

E Str - rugose coral, possibly *Stringophyllum* (or *Neostringophyllum*?), Alv - *Alveolites edwardsi*. Note that slightly visible skeleton structures (in grey colour hues, just above the alveolitid colony as marked) may suggest a presence of a 'fresh' heliolitid skeletal fragment .

F A medium large fragment of a colony of *Heliolites porosus* is embedded mostly in fine grained calciturbiditic grainstone. The weathering-resistant margins typically contain increased amounts of silica and dolomite.

G Gry - rugose coral *Grypophyllum*. This coral is embedded in diversified detritus of millimetre sized clasts of pure calcite compositions, where only few crinoid ossicles are selectively weathered and have positive relief and brownish colour hues (because of slight dolomite and silica contents; mix of differently altered clasts from different parts of the reef and slope areas).

H A partly abraded branch of tabulate coral *Taouzia*, marked as Tao in the picture. This coral is present in the layers where also intraclasts richer in original clayey and silica components occur; see the fractured intraclast in the upper right corner of the picture, for example.

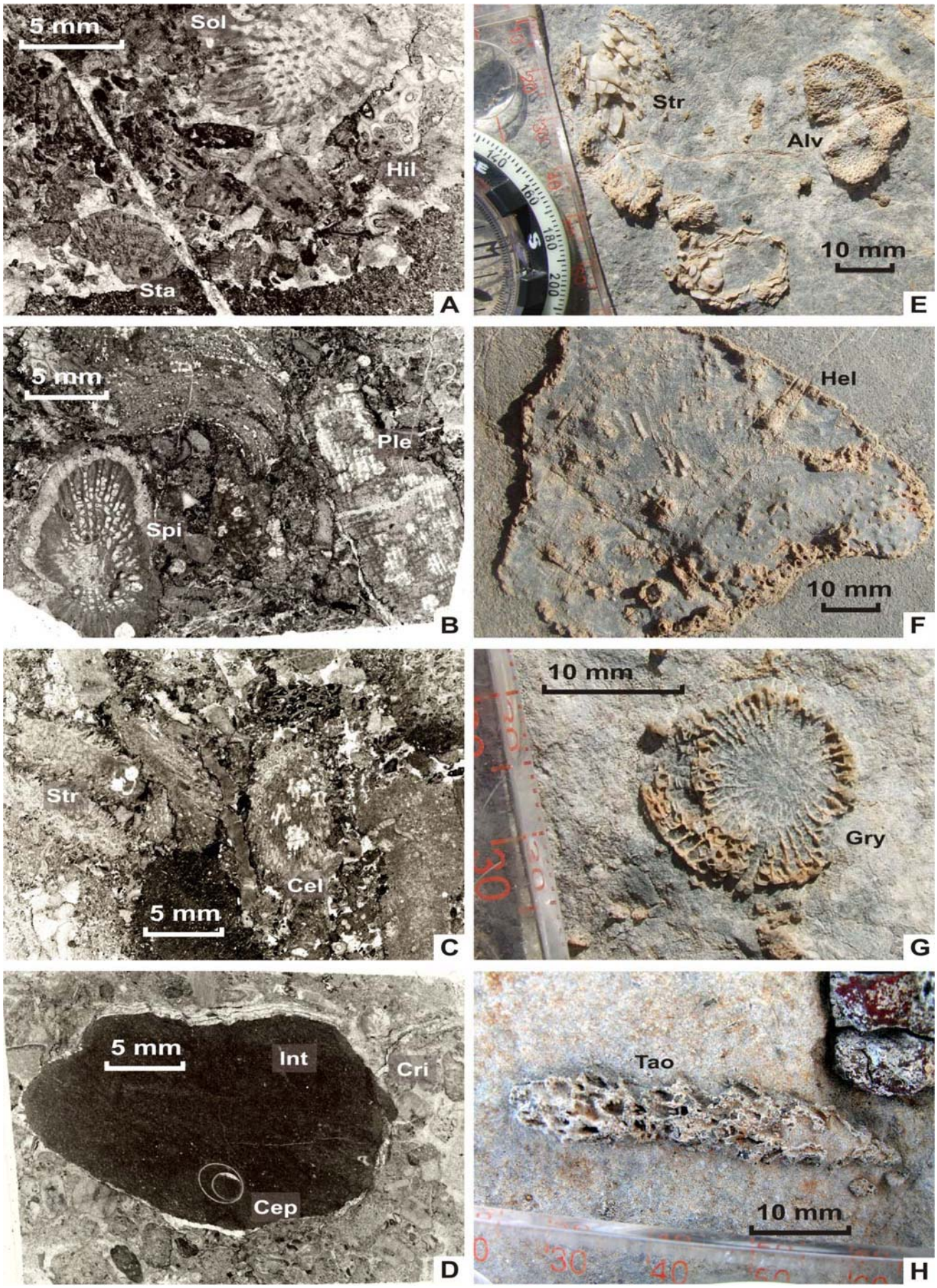
5 mm
Sol
Hil
Sta
A
Str
Alv
10 mm
E
5 mm
Ple
Spi
B
Hel
10 mm
F
Str
Cel
5 mm
C
10 mm
Gry
G
5 mm
Int
Cri
Cep
D
Tao
10 mm
H

Plate 6.3 - Selected conodont specimens from Covas Ruivas II site (SEM images, all specimens are the same scale, corresponding to the 500µm scale bar on the plate) Figured conodont specimens and additional material is stored on one slide at the Museu Geológico of the Portuguese Geological Survey, inventory number 25926. From Machado et al. 2010. Microphotographs by L. Slavik.

A to B *Polygnathus serotinus* Telford; A - sample R2.2c, upper view; B - R2.6c, upper view of broken specimen

C to D *Polygnathus costatus patulus* Klapper 1971; both specimens from sample R2.2c, upper view

E *Polygnathus costatus* cf. *partitus* Klapper, Ziegler & Mashkova 1978; sample R2.11c, upper view

F to G *Polygnathus* cf. *costatus costatus* Klapper 1971; F - broken specimen from sample R2.27c, G - incomplete specimen from sample R2.19c, upper view

H to I *Polygnathus costatus costatus* Klapper 1971; H - sample R2.27c, upper view, I - sample R2.42c, lower view

J *Polygnathus* aff. *P. trigonicus* Bischoff & Ziegler 1957, sample R2.42c, upper view

K *Polygnathus* aff. *P. cooperi cooperi* Klapper et al. 1978, sample R2.48c, upper view

L *Pandorinellina* cf. *expansa* Uyeno & Mason 1975, broken specimen from sample R2.2c, lateral view

M *Polygnathus eiflius* Bischoff & Ziegler 1957, sample R2.58c, upper view

N to P *Tortodus kockelianus australis* (Jackson 1970) (in Pedder, Jackson & Ellenor, 1970); N - sample R2.68c, upper view; O - sample R2.58c, upper view; P - sample R2.68c, upper view of deformed specimen, all specimens incomplete

Q *Icriodus* cf. *beckmanni sinuatus* Klapper, Ziegler & Mashkova 1978, incomplete specimen from sample R2.48c, upper view

R *Polygnathus* aff. *ansatus* Ziegler & Klapper 1976, sample R2.68c, upper view

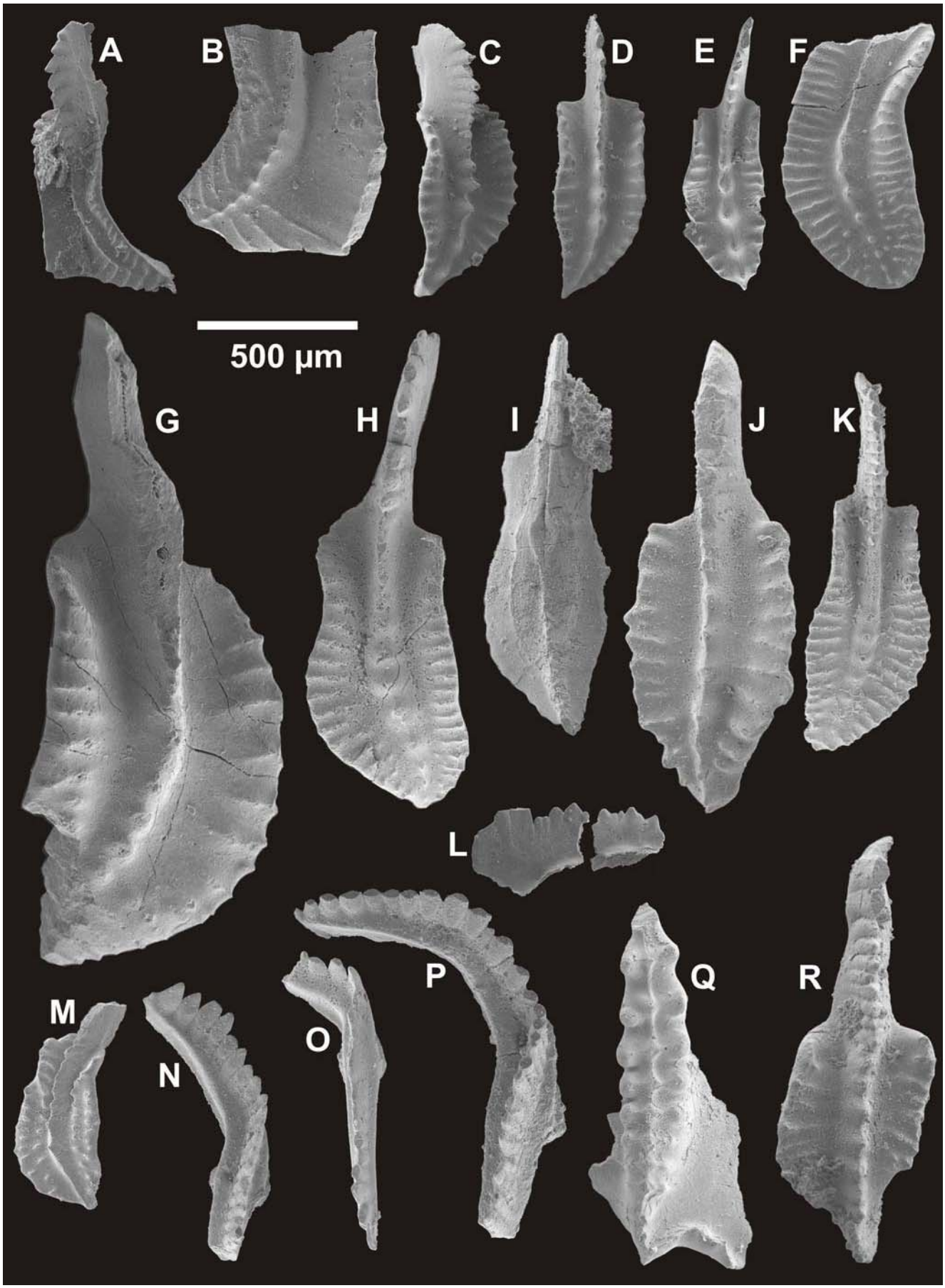
A
B
C
D
E
F
500 µm
G
H
I
J
K
L
M
N
O
P
Q
R

Plate 6.4 Outcrop and hand sample images and photomicrographs of thin sections. Legend: bd bedding (emphasized by first order stylolites); cr probable crinoid element fragment; LV late carbonate vein; pr black prismatic particle; pu pumpellyite crystals; sg sigmoid structure shadows; st1 first generation stylolite; st2 second generation stylolite. From Machado et al. 2009a.

A Natural outcrop and surrounding landscape.
B Partially undissolved calciturbidite limestone block after acetic acid treatment. Note the black prismatic particles.
C Isolated prismatic particles (from acetic acid residue) showing overall shape and texture. Note the inner area and outer envelope in some of the particles.
D Finner fraction of the acetic acid residue showing the dismembered outer envelope fragments of larger prisms and very small prisms.
E Thin section image showing the general appearance of the calciturbidite limestone. Note the scattered prismatic particles acting as centres for delta and sigmoid structures. Late carbonate veins cut all the previous structures.
F Photomicrograph of a sigmoid structure around a prismatic graphitic particle. Note the latter vein cutting all the previous structures. Calciturbidite limestone. Crossed polars.
G Photomicrograph of a large scale stylolite (second generation). Subsidiary stylolites are visible (same stage) and previous ones (marking the bedding fabric). Crinoid(?) skeletal pieces are visible in the upper part of the image. Bioherm limestone. Crossed polars.
H Photomicrograph of a pumpellyite rosette surrounded by calcite crystals and a recrystalization area. Crossed polars.


A


2cm
B


C
1mm

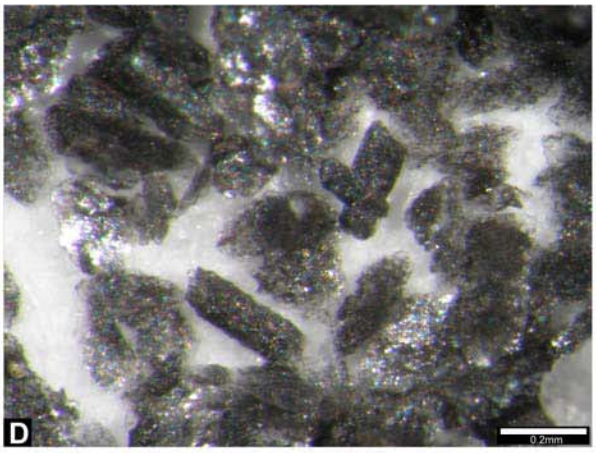
D
0.2mm

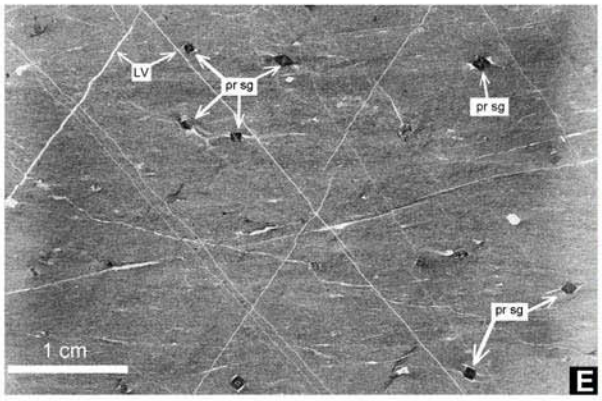
LV
pr sg
pr sg
pr sg
1 cm
E

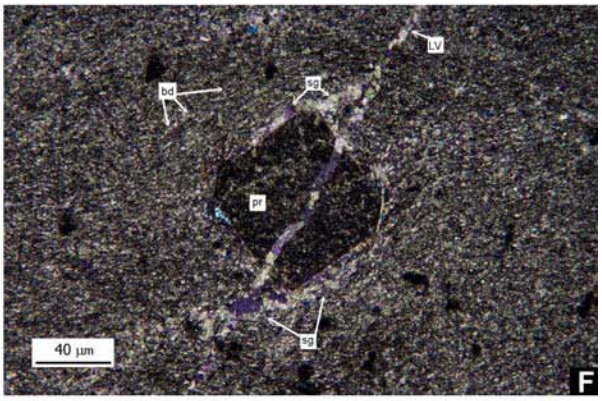
LV
bd
sg
pr
sg
40 µm
F

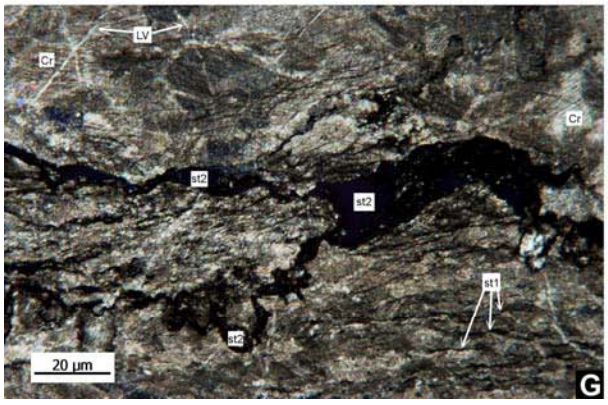
LV
Cr
Cr
st2
st2
st1
st2
20 µm
G

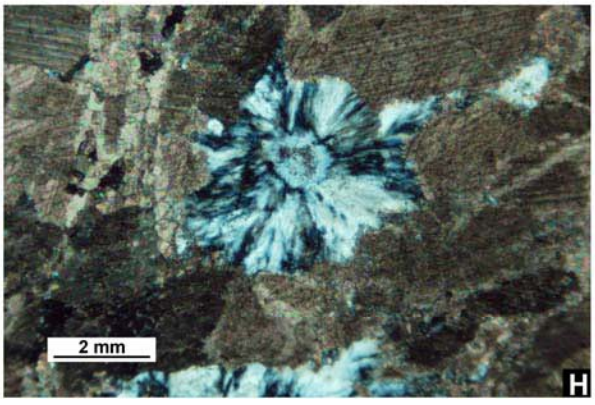
2 mm
H

Plate 6.5 - Crinoids and corals from the Cortes locality. From Machado et al. 2009a.

A–C – *Cupressocrinites* sp. remains, echinoderms.

A A wide but low columnal has an extremely opened lumen that originated due to interconnection of the axial and four peripheral canals. The specimen shape is indicative of a distal internodal. The obliteration of the articular facet was caused by recrystallization of the calcite-filled skeleton tissue, as well as by recent corrosion/erosion of the rock surface. The porous, 1-5 mm thick, dark grey coloured fossils with positive relief are silicified fragments of amphiporid stems.

B A middle sized but high crinoid columnal corresponds to a nodal from a middle part of the stem. Cirrus with dichotomically branched cirral canals was inserted on the latus. This nodal was embedded in packstone where detritus of shelly fauna, crinoids and corals prevail.

C Assemblage of numerous, small cupressocrinitid and/or gasterocomids columnals, accompanied by less abundant *Gasterocoma*, together with detritus of other, mainly brachial crinoid parts.

D–L – *Thamnopora* cf. *irregularis* Lecompte, 1939. Tabulate coral. The variability of the colony and corallite growth shapes is illustrated using eleven, relatively undeformed coral fragments in rock slabs.

D The thamnoporid displays its former capability of easily overgrowing of damaged/attacked parts in the apical part of the branch as well as on its sides.

E A considerable irregularity in budding and arrangement of corallites is regularly present, and according to these relatively well preserved specimens this cannot be alternatively ascribed only to possible environmental extremes or effects of tectonic deformation.

F–G The irregularity of budding is directly reflected by irregular shapes of the corallites that differ also in the number of neighbouring corallites (number of wall parts) and also in corallite diameters.

H–I Also the pseudo-arching of parts of corallite walls in transverse or oblique sections is indicative of incongruent growth domains and layers in the skeleton of the colony.

J–L The terminal parts of the densely branched coralla have regularly the shapes and lengths which can be best described as a shape of "human thumb".

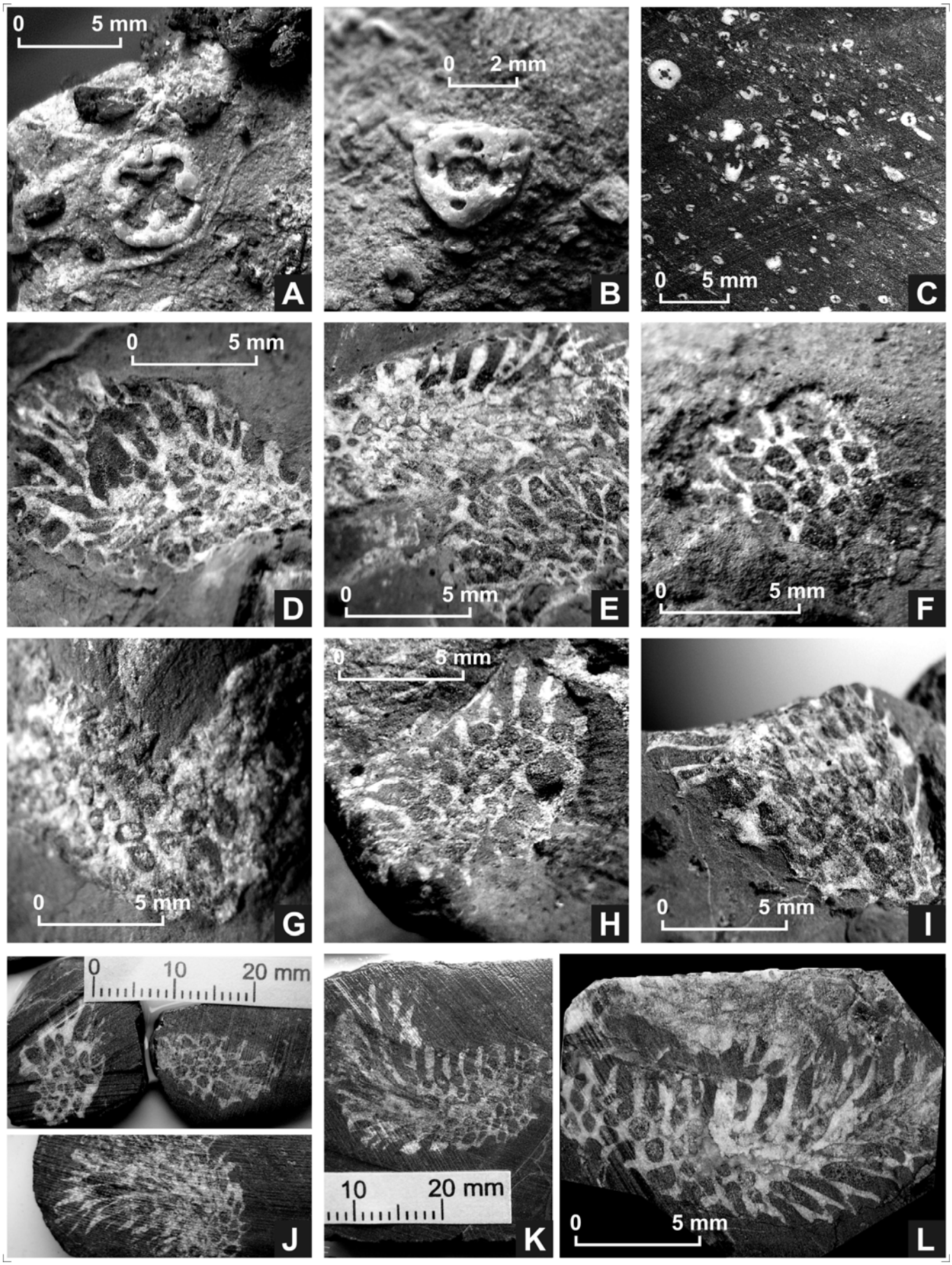
0 5 mm
A
0 2 mm
B
0 5 mm
C
0 5 mm
D
0 5 mm
E
0 5 mm
F
0 5 mm
G
0 5 mm
H
0 5 mm
I
0 10 20 mm
J
10 20 mm
K
0 5 mm
L

Plate 6.6 - Corals from the Cortes locality From Machado et al. 2009a.

A–F – *Heliolites* cf. *porosus bilsteinensis* ? Iven, 1980 (? = *Heliolites* Typus C Hubmann, 1991). Small bulbous and domical colony shapes prevail, both usually little protracted, as it is seen in their longitudinal, oblique and transverse sections (A, B and C), A and C are slabs, B is broken and weathered colony.

D Close views on two other weathered sections (transverse and longitudinal, left and right in this picture.

E–F Rare silicified areas found in the thin sectioned colonies give more contrast on the skeleton details, but there is also evident that the deformation locally caused certain breakage and secondary reduction of the coenenchyme width.

G–I – *Caliapora* ? cf. *plagiosquamata* Hladil, 1981. Tabulate coral.

G The transverse section shows regular arrangement of corallites with only slight rotation of corallites, so that an overall appearance is somewhere among usual favositid, caliaporid and alveolitid appearances.

H The slabs are indicative of presence of pores in short distances and only rudimental squamulae (longitudinal sections) and some transverse sections have rotated, four to six walled corallites, even though they grew parallel to the growth of their neighbours, without any strong lateral increase of the colony.

I Some slightly bent parts of the wall seem to be thicker than the other parts, resembling the "batten" structures of caliaporids.

J–M – *Squameoalveolites* cf. *fornicatus* (Schlüter, 1889). Tabulate coral. Coating and low domical colonies.

J–K The bent upper walls are undoubtedly dominant, being regularly, unidirectionally arranged in the colony.

L The longitudinal section cutting the lateral walls with pores suggests the regular presence of the couples of squamula-like swellings of wall, alternating with these mural pores.

M An oblique section of a colony gives other evidence about presence of thick spines and squamula-like swellings on the corallite walls.

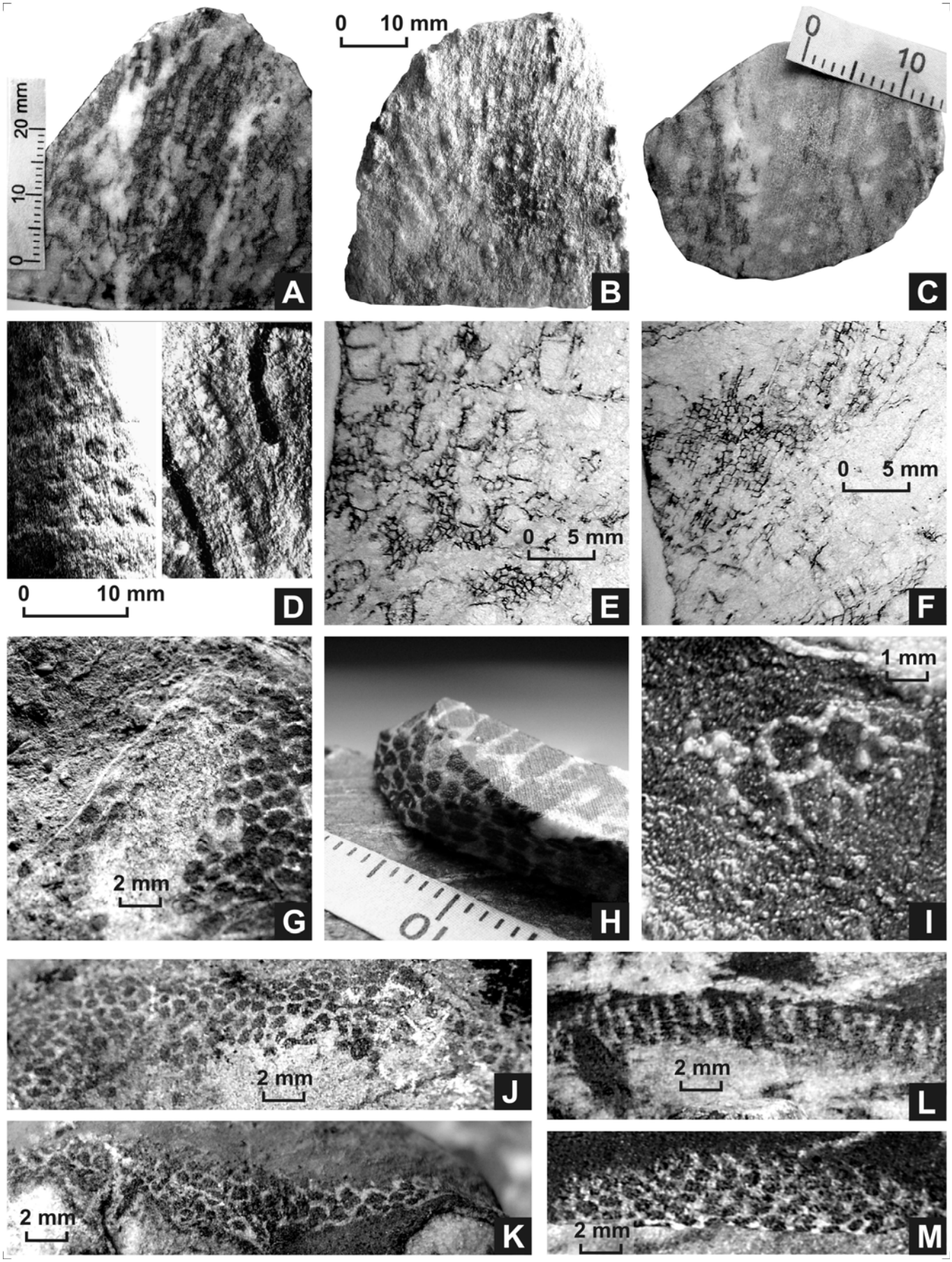
0 20 mm 10 0
A
0 10 mm
B
0 10
C
0 10 mm
D
0 5 mm
E
0 5 mm
F
2 mm
G
H
1 mm
I
2 mm
J
2 mm
L
2 mm
K
2 mm
M

Plate 6.7 - Corals from the Cortes locality. From Machado et al. 2009a.

A–D *Scoliopora denticulata denticulata* (Milne-Edwards & Haime, 1851) cf. "alpha morphotype" Hladil, 1985). Tabulate coral. Small, thick-walled corallites are elongated to 0.5 ratio in the transverse section and tend to be sub-parallel near colony surface. Wall thickenning from axial to peripheral zone of the branch is gradual. Arrangement of pores in galleries is visible, as well as swelling of walls between them. Rugose corals.

E–I – *Pseudamplexus* ? sp.

E–F Sparite-filled calicional parts of this coral in brachiopod skeletal packstone. Slab and weathered rock surface (E), weathered surface (F).

G–I The higher and not so steeply conical specimens from ostracod packstones/wackestones are congeneric but do not need necessarily belong to the same species.

K–L Examples of two possible digonophyllids (*Digonophyllinae* Wedekind, 1923).

K *Cystiphylloides* ? sp.; a conical (and then keg-shaped) coral specimen on weathered rock surface typically shows large and dish arranged, bubble shaped dissepiments.

L *Mesophyllum* ? sp. Transverse section, weathered surface.

M–N Other fragmentary rugose corals.

M *Calceola* cf. *sandalina* (Linné, 1771).

N An oblique section across a calicional margin of a coral. Possibly *Pseudodigonophyllum* ? sp.

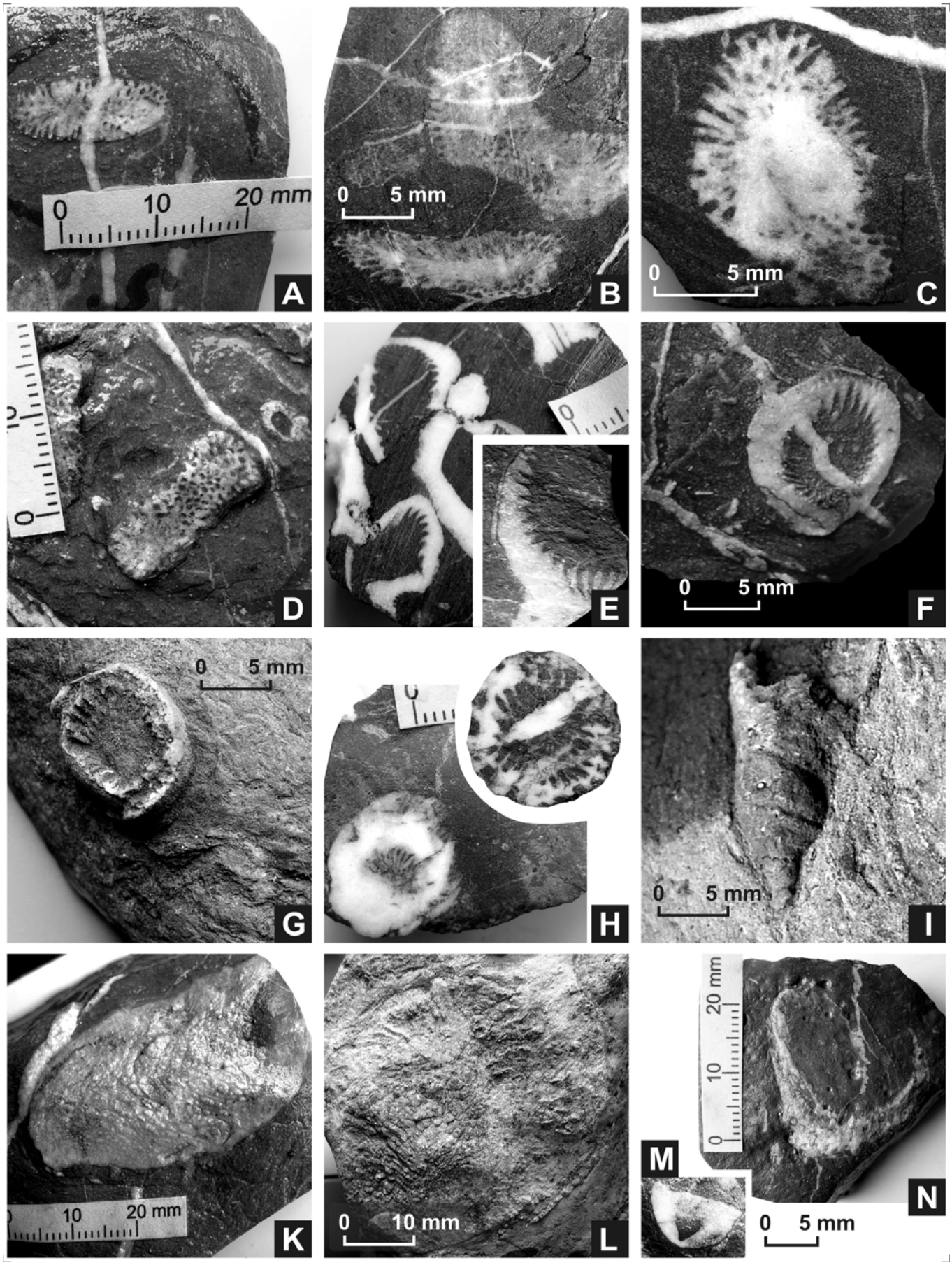
0 10 20 mm
A
0 5 mm
B
0 5 mm
C
D
E
0 5 mm
F
0 5 mm
G
H
0 5 mm
I
10 20 mm
K
0 10 mm
L
0 10 20 mm
M
N
0 5 mm

Plate 6.8 - Corals and brachiopods from the Cortes locality. From Machado et al. 2009a.

A–B – Other fragmentary rugose corals (continuation).

A *Holmophyllum* ? sp. (*Holmophyllum* ? cf. *uralicum* Zhavoronkova, 1972). Well separated, flabellacanthine-like trabeculae are indicated on the images

B An undeterminable rugose coral, tentatively a young specimen of *Cyathopaedium* ? sp. attached on a broken part of amphiporid stem. Amphiporids

C–K – *Amphipora* ? cf. *spissa* Yavorsky, 1957.

C Some broken parts of amphiporid stems were silicified.

D–E The stems (branches) of typical 5 mm width are locally coated by thickened vesicular and/or multiple-tube structures which may be compared with cyanobacteria and algal products *Wetheredella* ? sp. (sensu Kazmierczak & Kempe 1992) and *Gymnocodium* ? sp., respectively. Separation of these coatings is seen on figure E.

F–I Four slabs illustrate that growth of such a bacteria-algal stocking can continue also on necrotic amphiporid tissues.

J–K Some terminations of these stockings show features of dividing. This morphology must rather be ascribed to unknown temporary inhabitants of these hollows than to self-organizing capability of the bacteria-algal structures. Brachiopods

L–O rachiopoda gen. et sp. indet. (Type Y).

P–Q Small, undetermined brachiopod valves as they were leached by natural weathering on the rocksurfaces.

R An accumulation of thick brachiopod shells. Different types of shell morphologies prevail. Presence of fragmentary *Kaplex* and *Stringocephalus* shells is possible, but any strong evidence for this assumption is absent.

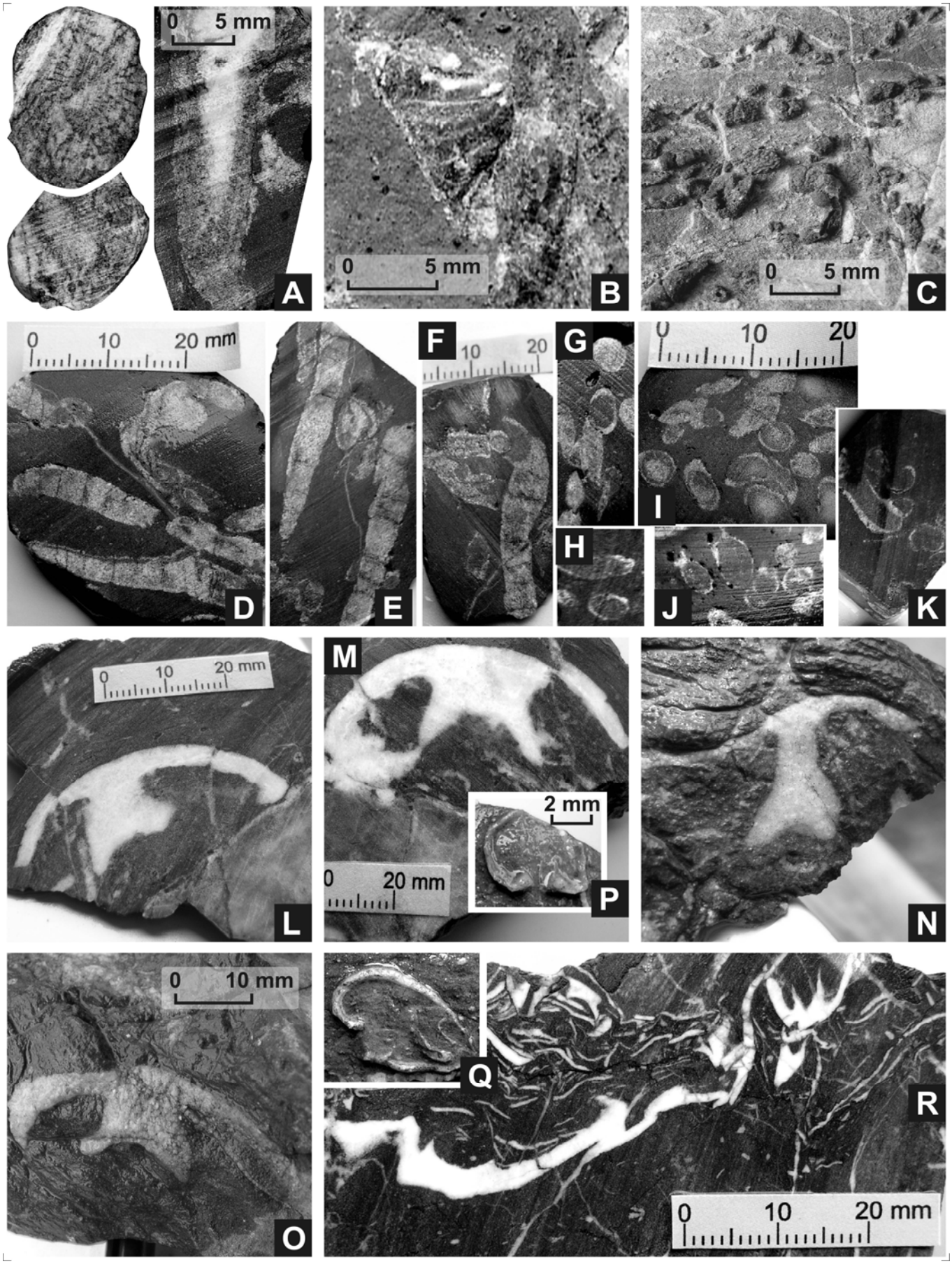
0 5 mm
A
0 5 mm
B
0 5 mm
C
0 10 20 mm
D
E
F
10 20
G
H
0 10 20
I
J
K
0 10 20 mm
L
M
2 mm
0 20 mm
P
N
0 10 mm
O
Q
R
0 10 20 mm

Plate 6.9- Selected bioclasts from polished surfaces of hand samples from Caeirinha site (binocular microscope photographs)

A (?)Ostracod valves in dorsal-ventral section;
B Transverse section of a (?) rugose coral;
C, D Transverse sections of juvenile rugose coral(?)
E to H (?) Calcareous algae structures.

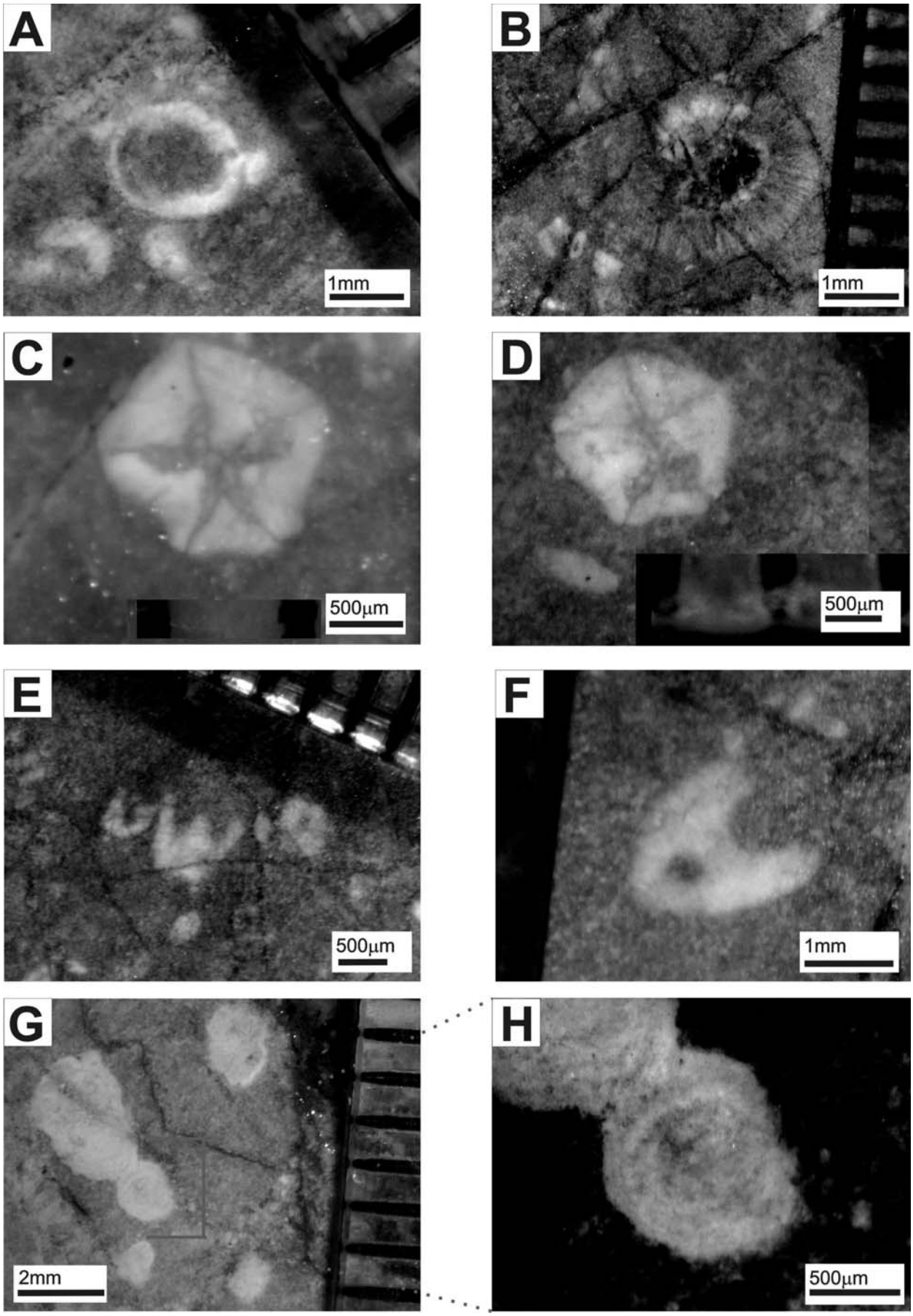
A
1mm
B
1mm
C
500µm
D
500µm
E
500µm
F
1mm
G
2mm
H
500µm

Plate 6.10– Microphotographs of selected bioclastic (crinoidal) packstone/wackestone samples from the Caeirinha site.

A to D Thin sections under a binocular microscope on a black background. E to H - polished surfaces of hand samples under a binocular microscope.

A Crinoidal wackestone;
B Detail showing a tranverse section of a columnal plate of a (?)gasterocomid.
C Crinoidal wackestone;
D Detail showing a tranverse section of a columnal plate of (?)gastercomid.
E to F Crinoidal wackestones. Note the dominant presence of (?)gasterocomids. and possibly cupressocrinitids crinoidal elements.

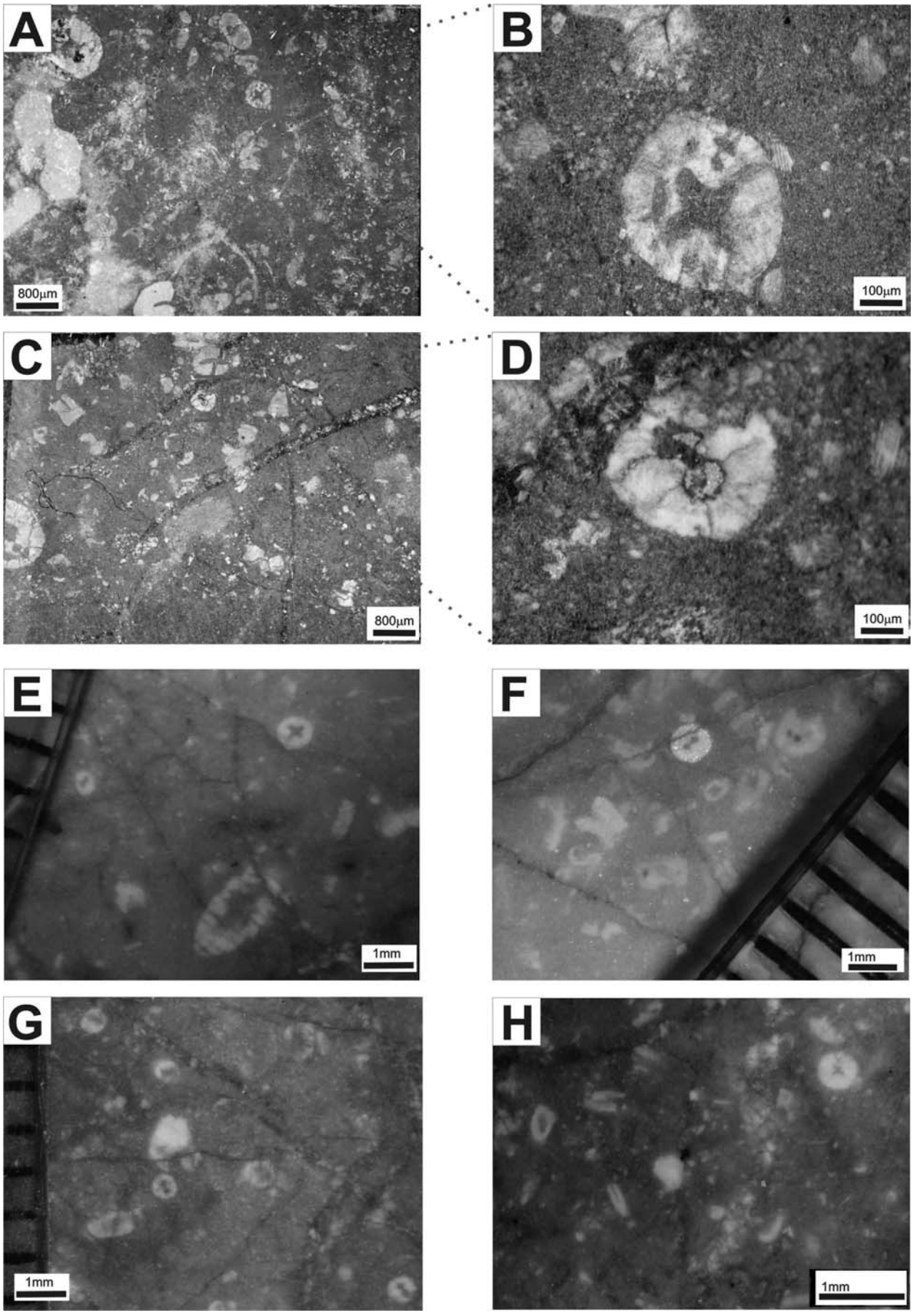
A
800µm
B
100µm
C
800µm
D
100µm
E
1mm
F
1mm
G
1mm
H
1mm

Plate 6.11– Selected microphotographs of several crinoidal elements from the Caeirinha site (binocular microscope photographs).

A to G - Polished surfaces of hand samples; H – Isolated columnal plate extracted from acetic acid insoluble residue.

A to C (?)Gasterocomids transverse sections of columnal plates from different parts of the crinoid stem or ontogenic stage;
D (?)Gasterocomid transverse section of a columnal plate;
E longitudinal section of a set of columnal plates;
F Unidentified transverse section of a columnal plate of a crinoid;
G Oblique section of a columnal plate of an unidentified crinoid;
H (?)Gasterocomid isolated columnal plate.

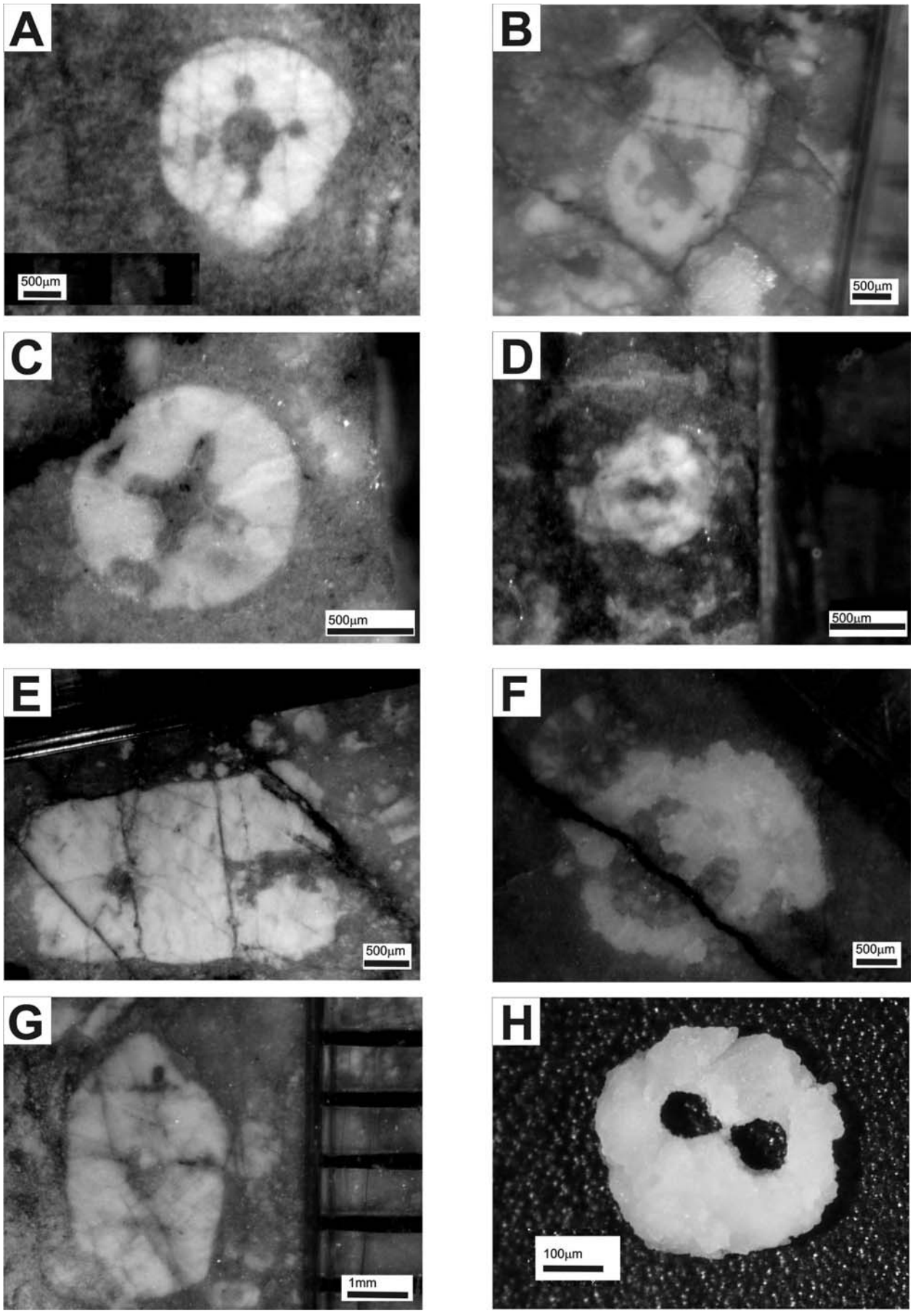
A
500µm
B
500µm
C
500µm
D
500µm
E
500µm
F
500µm
G
1mm
H
100µm

Plate 6.12 – Selected microphotographs of several crinoidal elements from the Caeirinha site (binocular microscope photographs).

A to H Polished surfaces of hand samples;
A to H Cupressocrinitids transverse (or slightly oblique) sections of columnal plates from different parts of the crinoid stem or ontogenic stage.

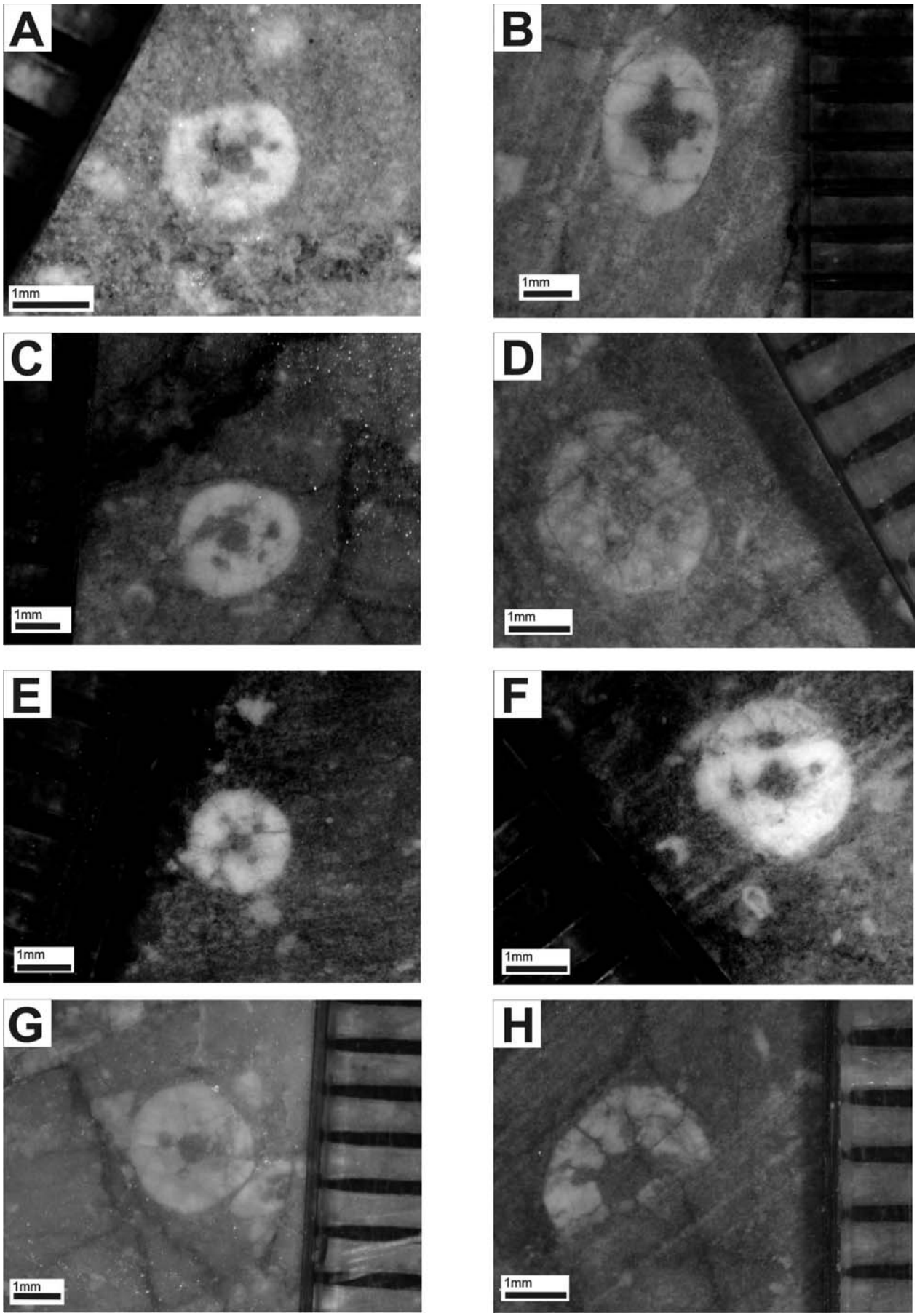
A
1mm
B
1mm
C
1mm
D
1mm
E
1mm
F
1mm
G
1mm
H
1mm

Plate 6.13 – Selected microphotographs of several crinoidal elements from the Caeirinha site (binocular microscope photographs).

A and B - Polished surfaces of hand samples;
C to H – Thin sections under a binocular microscope on a black background.

A, B, D and F	Cupressocrinitids transverse sections of columnal plates;
C	Unidentified transverse section of a columnal plate of a crinoid;
E, H	Unidentified transverse sections of a columnal plate of a crinoid;
G	(?)Gasterocomid transverse section of a columnal plate.

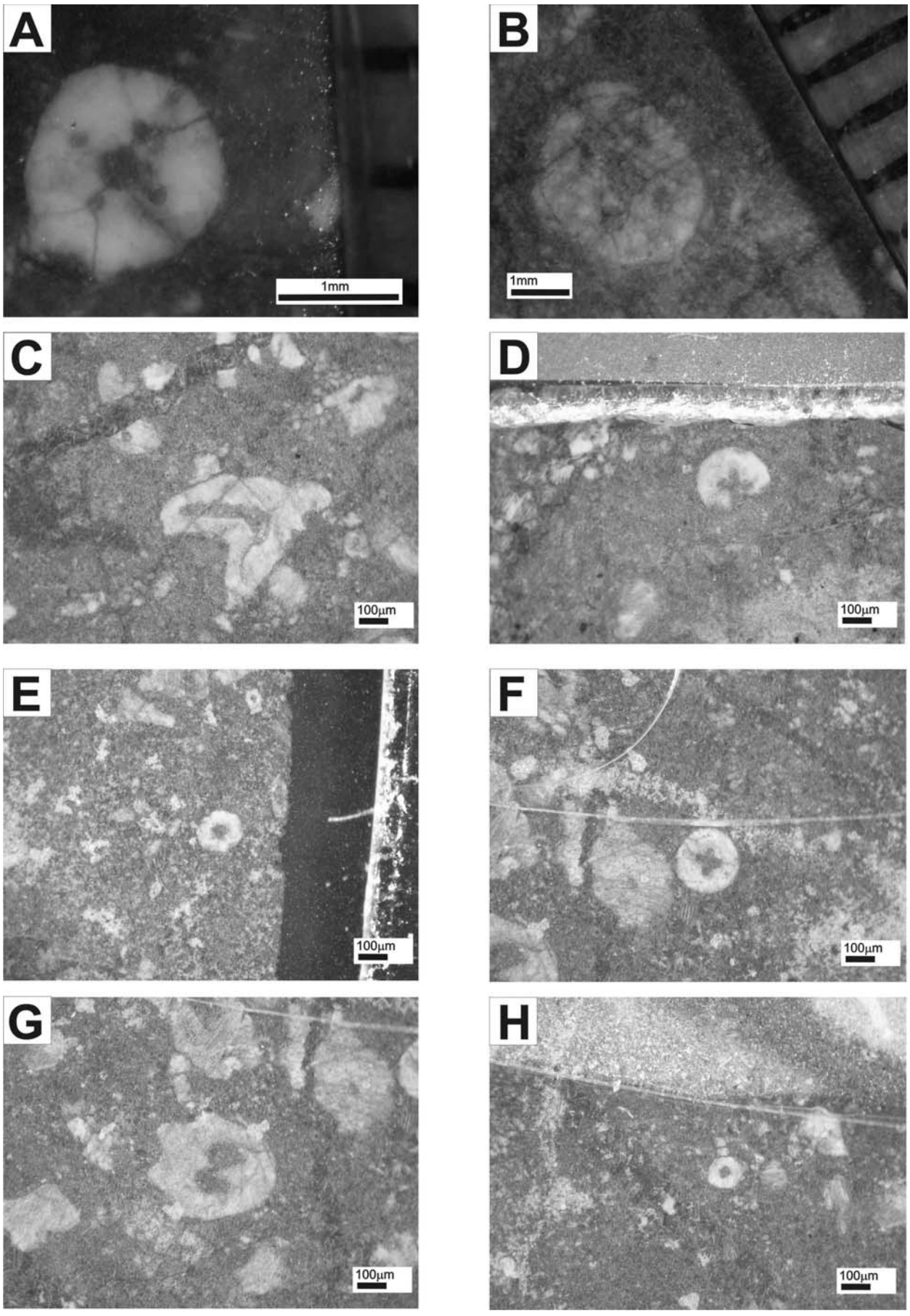
A
1mm
B
1mm
C
100µm
D
100µm
E
100µm
F
100µm
G
100µm
H
100µm

Plate 6.14 – Selected microphotographs of several crinoidal elements from the Monte da Pena site.

A to F - Polished surfaces of hand samples;
G and H – Thin sections under a polarizing microscope.
A, G (?)Gasterocomids transverse sections of a columnal plate;
B, D, E Cupressocrinitids transverse sections of columnal plates;
C, F Unidentified transverse section of a columnal plate of a crinoid;
H Unidentified oblique section of a columnal plate of a crinoid;

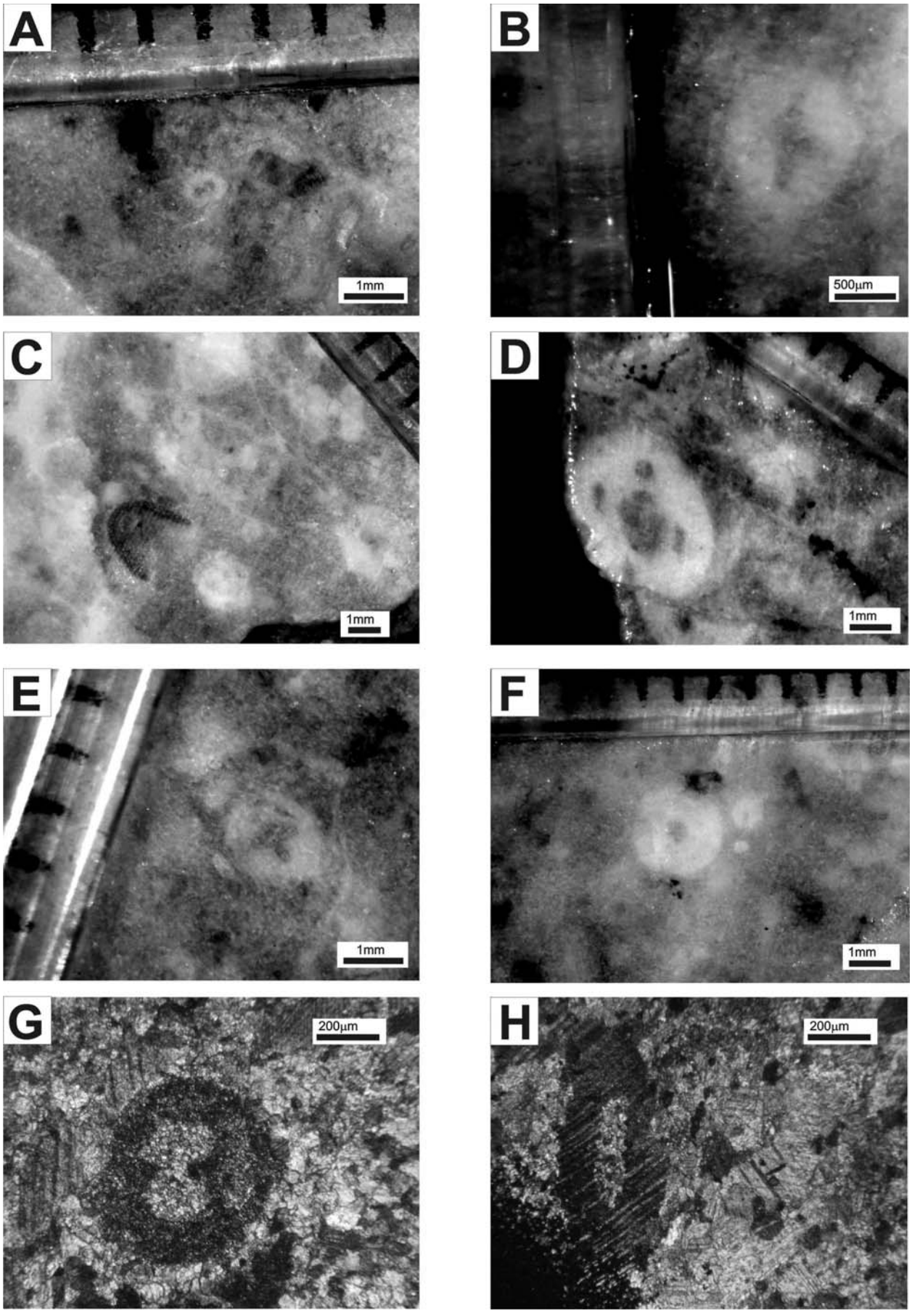
A
1mm
B
500µm
C
1mm
D
1mm
E
1mm
F
1mm
G
200µm
H
200µm

Chapter 7

Final remarks and future work

FINAL REMARKS AND FUTURE WORK

Chapter Index

Future work 325
References 326

The Porto-Tomar shear zone is an important structural domain in the context of the NW Iberian variscides, but also to the interpretation of the geodynamic evolution of the whole Variscan belt. The magnitude and chronology of the activity of this structure is thus vital.

The Albergaria-a-Velha Unit constitutes one of the few opportunities to constrain sedimentary, metamorphic and deformation events in this context. The data collected suggests the presence of a cratonic area acting as a sediment source area, which can be tentatively identified as the Central Iberian Zone (CIZ). This sedimentary setting lasted from the Frasnian (Late Devonian) to the Serpukovian (Late Mississippian). However several questions remain unanswered: 1) what unit, or even what geotectonic zone, was the basement on which the Albergaria-a-Velha unit deposited on? ; 2) was the Porto-Tomar shear zone active and controlling sedimentation?

The strong deformation does not allow the first question to be answered. The Arada unit would be a possible candidate, but stratigraphical contacts between the two where never found. If some kind of important structure, which later would become the Porto-Tomar dextral mega shear zone, was present, it certainly did not have the same magnitude and probably not the same type of activity as it had during Pennsylvanian times. It is plausible to assume that some kind of important structural feature was limiting the CIZ, controlling a shore line and possibly triggering turbidity current events. This structure could have evolved to the Porto-Tomar shear zone after the Serpukovian. The major tectono-thermal event bracketed between the Serpukovian and the Gzhelian can be tentatively linked to the onset of the Porto-Tomar dextral shear movement.

The data collected does not support the idea that the AVU represents pull-apart basins (e.g. Chaminé et al., 2003; 2007). This interpretation was based on the apparent scattered disposition of the AVU and the possible association with the PTSZ, analogous to the terrestrial Pennsylvanian Buçaco basin. Although it is impossible to state that there was a single basin, with no sub-basins, the sedimentary and biostratigraphical evidences suggest a single sedimentary system. The significant tectonic activity invariably related to pull-apart basins would result in significantly different sedimentological and palynological characteristics: extensive reworking, presence of intraclasts, varied sediment source areas, etc.. The current spatial disposition of the AVU is most likely a result of its post-sedimentary evolution, certainly related with the movement of the PTSZ.

The Buçaco and Santa Susana basins have very similar tectonosedimentary settings. The analysis of the thermal evolution of both basins and surrounding units, coupled with the biostratigraphical, geological and structural evidences suggest that a major regional (Iberian scale) tectono-thermal event occurred sometime (or during) after the Viséan/Serpukovian (younger sediments of the Toca da Moura Fm. and the AVU respectively) and the Middle-Late Pennsylvanian (ages of the Santa Susana and Buçaco basins respectively). In both cases this event can be correlated with the onset of dextral movements of major ~N-S trending shear zones: the Santa Susana shear zone and Porto-

Tomar shear zone. The pre-existence of important structures in these areas is uncertain. The timing of events and correlation of these N-S trending shear zones with associated ESE-WNW trending ones (Tomar-Córdoba and Ferreira-Ficalho) cannot be clarified with the present data.

It is worth to mention that the Odivelas Limestone and correlatable marble and silicified limestone occurrences in the southern areas of the OMZ are affected and probably tectonically transported along the Ferreira-Ficalho fault and also along the Santa Susana shear zone, limiting the age of the movement of these structures (or part of it) to post-Middle Devonian times.

The occurrence of spatially (and most likely genetically) related Middle Devonian volcanic intermediate rocks, iron-silica ores and reef-related limestones at the Covas Ruivas site (and generally for the older volcanic part of the Beja Igneous Complex - BIC) can be compared with other occurrences elsewhere in the European Variscides. The Lahn and Dill synclines in the Rheno-Hercynian zone (Germany) show extensive Devonian volcanic rocks mostly of submarine facies (Breitkreuz & Flick, 1997; Flick et al., 2008; Nesbor et al., 1993). During the Middle Devonian several reefs developed in areas of volcanic islands and sea mounts (Flick et al., 2008; Königshof et al., 2010), recorded as reef and peri-reefal facies. Several iron ore occurrences are known from the same synclines (Lahn-Dill ores) (Flick et al., 1990, 2008). The resemblance of the petrology of these ores with the ones from the BIC is striking. The same type of ores is also present in the Moravian – Silesian part of the Bohemian massif within thick Middle Devonian volcanic successions (Václav Kachlík, pers. com.). It thus seems that a similar tectono-magmatic-sedimentary setting prevailed during the Middle Devonian in wide spread areas of what are now the European Variscides.

Future work

The complete thermal history of the AVU and its hydrocarbon generation potential can only be completely understood if further data is available. The on-shore and off-shore extension of the basin represented by the AVU under the Lusitanian basin (and other Palaeozoic units?) can be further ascertained with the examination of 1) the available wells and dredges of the several ODP and IODP that collected pre-Mesozoic rocks; 2) the available and future deep exploration wells performed by oil companies; 3) the available and future seismic profiles of the Lusitanian basin.

The thermal history of pre-Mesozoic sedimentary and metasedimentary rocks (be it the AVU or others) in this area can be further investigated by using apatite and zircon fission track analysis. This would be extremely useful to date thermal and geological events and determine if (and where and when) hydrocarbon generation, migration and accumulation occurred.

The palaeobiogeography of the Late Devonian organic-walled microplankton of the AVU suggests stronger affinities to the Laurussian realm, while the South Portuguese Zone (SPZ) ones are more comparable with a North-Gondwanan realm. It would be extremely interesting to obtain organic-walled microplankton assemblages from Upper Devonian sediments of the southern parts of the OMZ and compare them to the AVU, SPZ and Gondwanan and Laurussian realms assemblages. This study would shed light on the palaeogeography of the collisional setting supposedly occurring during the Devonian between the OMZ and SPZ in this area and the closure of the Rheic ocean in general.

The detailed study of the vitrinite reflectance along the Buçaco basin sequence and of available borehole samples of the Santa Susana basin will probably allow the

definition, even if only crudely, of geothermal gradients that prevailed during their deposition. This determination can have a significant impact on the interpretation of the tectonosedimentary setting of these basins. If these are truly pull-apart basins, high geothermal gradients are expected.

The recent discovery of an ash bed-like layer in an outcrop of the Buçaco basin may prove to be a significant find if radiometric dating can be performed. The calibration of the West-European Carboniferous time scale is far from complete and the correlation with the globally defined stages of the Pennsylvanian (mostly based on Eastern Europe sections) is still in its early stages. The direct correlation between a radiometric date and miospore biostratigraphy would be a significant contribution for the desired calibration.

Further study of the stratigraphy of the Odivelas Limestone and correlatable marbles and silicified limestones along with study of the petrology of the volcanic rocks and iron ores surrounding the limestones will allow a better understanding of processes that originated these rocks and why they occur together. This is vital to understand the possible connections with other geotectonic zones elsewhere in Europe.

References

BREITKREUZ, C. & FLICK, H., 1997. Sedimentation am trachytisch/ alkalirhyolithischen Inselvulkan von Katzenelnbogen-Steinkopf (Devon/ Rheinisches Schiefergebirge). Geol. Jb. Hessen 125: 5-16.

CHAMINÉ, H. I., GAMA PEREIRA L. C., FONSECA P. E., MOÇO L. P., FERNANDES J. P., ROCHA F T., FLORES D., PINTO de JESUS A., GOMES C., SOARES de ANDRADE A. A. & ARAÚJO, A., 2003. Tectonostratigraphy of middle and upper Palaeozoic black shales from the Porto–Tomar–Ferreira do Alentejo shear zone (W Portugal): new perspectives on the Iberian Massif. Geobios 36 (6): 649-663.

CHAMINÉ, H. I., FONSECA, P. E., PINTO DE JESUS, A., GAMA PEREIRA, L. C., FERNANDES, J. P., FLORES, D. MOÇO, L. P., DIAS DE CASTRO, R., GOMES, A., TEIXEIRA, J., ARAÚJO, M. A., SOARES de ANDRADE, A. A., GOMES C. & ROCHA, F. T., 2007. Tectonostratigraphic imbrications along strike-slip major shear zones: an example from the early Carboniferous of SW European Variscides (Ossa-Morena Zone, Portugal). In: Theo E. Wong (Ed.), XVth International Congress on Carboniferous and Permian Stratigraphy (Utrecht, 2003). Royal Dutch Academy of Arts and Sciences, Amsterdam, Edita NKAW: 405-416.

FLICK, H., NESBOR, H. D. & BEHNISCH, R., 1990. Iron ore of the Lahn-Dill type formed by diagenetic seeping of pyroclastic sequences — a case study on the Schalstein section at Gänsberg (Weilburg). International Journal of Earth Sciences 79 (2): 401-415.

FLICK, H., NESBOR, H. D. & KÖNIGSHOF, P., 2008. Volcanism and reef development in the Devonian: A case study from the Rheinisches Schiefergebirge (Lahn syncline, Germany). In: KÖNIGSHOF, P. & Linnemann, U. Final Meeting of the IGCP 497 & IGCP 499 Excursion Guide: 159pp.

KÖNIGSHOF, P., NESBOR, H. D. & FLICK, H., 2010. Volcanism and reef development in the Devonian: A case study from the Lahn syncline, Rheinisches Schiefergebirge (Germany). Gondwana Research 17 (2-3): 264-280.

NESBOR, H. D., BUGGISH, W., FLICK, H., HORN, M., LIPPERT H. J., 1993. Vulkanismus im Devon des Rhenoherzynikums. Fazielle und Paläogeographische entwicklung vulkanish geprägter mariner Becken am Beispiel des Lahn-Dill Gebietes. Geol. Abh. Hessen 98: 3-87.

Appendix 1

Sample details

SAMPLE DETAILS

All GPS coordinates are datum WGS84

Albergaria-a-Velha Unit samples

Sample	Lithology	Colour	Alteration	Deformation	Mineralization	Outcrop type	GPS Coordinates	Reference
Aço 1.1	Shale	Dark grey	Light	Light foliation Faint bedding		Road cut	40°40'54.79"N 8°27'47.18"O	Sernada do Vouga SND-comb
AG 1.1	Coal	Brown	Medium	Clear Bedding		Float	40°33'58.97"N 8°27'16.31"O	Agueda
AG 1.2	Siltstone	Green	Medium	Clear Bedding		Float	40°33'58.97"N 8°27'16.31"O	Agueda
AG 2.1	Shale	Black	Light	Clear Bedding	Pyrite and sulfides Small quartz veins	Road cut	40°34'45.90"N 8°25'33.60"O	Águeda
ALH 1.1	Shale	Dark grey	Light		Ox Fe Extensive silicification	Road cut	40°33'50.94"N 8°24'57.84"O	Alhandra
ALH 1.2	Shale	Dark grey	Light		Ox Fe Extensive silicification	Road cut	40°33'51.12"N 8°24'57.00"O	Alhandra
ALH 1.3	Siltstone	Dark grey	Light	Clear Bedding	Ox Fe	Road cut	40°33'51.39"N 8°24'54.12"O	Alhandra
ALH 1.4	Siltstone	Dark grey	Light	Faint bedding	Ox Fe	Road cut	40°33'51.96"N 8°24'52.02"O	Alhandra
ALH 1.5	Shale	Dark grey	Light		Ox Fe Extensive silicification	Road cut	40°33'51.07"N 8°24'49.50"O	Alhandra
ALH 2.1	Shale	Black	Medium	Very penetrative foliation	Ox Fe	Road cut	40°33'42.78"N 8°25'31.50"O	Alhandra
ALH 3.1	Siltstone	Dark grey	Medium	Faint bedding	Ox Fe	Road cut	40°33'45.78"N 8°25'17.76"O	Alhandra
ALH 3.2	Siltstone	Dark grey	Light	Faint bedding	Ox Fe	Road cut	40°33'49.50"N 8°25'21.06"O	Alhandra
ALH 3.3	Shale	Dark grey	Light	Clear Bedding	Ox Fe	Road cut	40°33'49.74"N 8°25'21.54"O	Alhandra
ALH 3.4	Siltstone	Dark grey	Light	Clear Bedding	Ox Fe	Road cut	40°33'53.46"N 8°25'23.46"O	Alhandra

ALH 3.5	SiltstoneShale	Dark grey	Light	Clear Bedding Light foliation	Ox Fe	Road cut	40°33'45.60"N 8°25'22.74"O	Alhandra
ALH 3.6	Shale	Black	Light	Clear Bedding Light foliation	Ox Fe	Road cut	40°33'44.40"N 8°25'25.62"O	Alhandra
ALV 1.1	Shale	Dark grey	Light	Very penetrative foliation		Road cut	40°32'38.10"N 8°22'55.68"O	Alvarim
AM18	Shale	Black	Light	Very penetrative foliation	Ox Fe	Road cut	40°52'47.76"N 8°34'47.42"O	
Ang1	Shale	Dark grey	Light	Clear Bedding Folding Along S0	Extensive silicification Fe Ox	Road cut	40°40'48.05"N 8°33'4.12"W	Angeja
Ang10	Siltstone	Light grey	Light	Clear Bedding Folding Kink	Extensive silicification Fe Ox	Road cut	40°40'48.84"N 8°32'59.88"W	Angeja
Ang11	Shale	Dark grey	Light	Clear Bedding Folding strong thining along S0	Fe Ox	Road cut	40°40'48.84"N 8°32'59.88"W	Angeja
Ang12	Siltstone	Dark grey	Light	Folding strong thining along S0 Clear Bedding	Fe Ox Extensive silicification	Road cut	40°40'48.84"N 8°32'59.88"W	Angeja
Ang13	Shale	Light grey	Light	Folding thining along S0 Clear Bedding	Small quartz veins	Road cut	40°40'47.94"N 8°32'57.60"W	Angeja
Ang14	Shale	Light grey	Light	Folding thining along S0 Clear Bedding	Extensive silicification Ox Fe	Road cut	40°40'47.94"N 8°32'57.60"W	Angeja
Ang15	Oil shale	Black	Light	Folding thining along S0 Clear Bedding		Road cut	40°40'48.05"N 8°33'4.12"W	Angeja
Ang2	Siltstone	Light grey	Light	Clear Bedding Folding Along S0	Extensive silicification Fe Ox	Road cut	40°40'48.05"N 8°33'4.12"W	Angeja
Ang3	Siltstone	Dark grey	Light	Clear Bedding Folding Along S0	Extensive silicification	Road cut	40°40'48.05"N 8°33'4.12"W	Angeja
Ang4	Shale	Dark grey	Light	Clear Bedding Folding Thinning Along S0	Extensive silicification Small quartz veins	Road cut	40°40'48.05"N 8°33'4.12"W	Angeja
Ang5	Shale	Light grey	Light	Clear Bedding Folding Thinning Along S0	Extensive silicification	Road cut	40°40'48.05"N 8°33'4.12"W	Angeja
Ang6	Shale	Light grey	Light	Clear Bedding Folding Thinning Along S0	Extensive silicification	Road cut	40°40'48.05"N 8°33'4.12"W	Angeja
Ang7	Shale	Light grey	Light	Clear Bedding Folding Thinning Along S0	Extensive silicification	Road cut	40°40'48.05"N 8°33'4.12"W	Angeja
Ang8	Shale	Dark grey	Light	Clear Bedding	Extensive silicification	Road cut	40°40'48.84"N	Angeja

				Folding Thinning Along S0			8°32'59.88"W	
Ang9	Shale	Dark grey	Light	Clear Bedding Folding Thinning Along S0	Extensive silicification	Road cut	40°40'48.84"N 8°32'59.88"W	Angeja
ASS1	Shale	Brown	Light	Faint bedding		Road cut	40°40'59.52"N 8°28'54.24"W	Assilhó
ASS10	Shale	Black	Light	Faint bedding Folding	Pyrite and sulfides	Road cut	40°41'0.38"N 8°28'53.15"W	Assilhó
ASS11	Shale	Black	Light	Faint bedding		Road cut	40°41'1.20"N 8°28'53.34"W	Assilhó
ASS12	Other	Green	Light		Small quartz veins	Road cut	40°41'1.20"N 8°28'53.34"W	Assilhó
ASS13	Shale	Black	Light	Faint bedding Folding	Small quartz veins	Road cut	40°41'1.20"N 8°28'53.34"W	Assilhó
ASS14	Shale	Black	Medium	Faint bedding	Extensive silicification	Road cut	40°41'2.70"N 8°28'53.40"W	Assilhó
ASS2	Shale	Black	Light	Faint bedding		Road cut	40°40'59.94"N 8°28'53.64"W	Assilhó
ASS3	Shale	Black	Light	Faint bedding		Road cut	40°40'59.94"N 8°28'53.64"W	Assilhó
ASS4	Shale	Black	Light	Faint bedding	Pyrite and sulfides	Road cut	40°41'0.38"N 8°28'53.15"W	Assilhó
ASS5	Shale	Black	Light	Faint bedding	Pyrite and sulfides	Road cut	40°41'0.38"N 8°28'53.15"W	Assilhó
ASS6	Shale	Black	Light	Faint bedding Folding	Pyrite and sulfides	Road cut	40°41'0.38"N 8°28'53.15"W	Assilhó
ASS7	Shale	Black	Light	Faint bedding Folding	Pyrite and sulfides Extensive silicification	Road cut	40°41'0.38"N 8°28'53.15"W	Assilhó
ASS8	Shale	Black	Light	Faint bedding Folding	Pyrite and sulfides Extensive silicification	Road cut	40°41'0.38"N 8°28'53.15"W	Assilhó
ASS9	Shale	Black	Light	Faint bedding Folding	Pyrite and sulfides	Road cut	40°41'0.38"N 8°28'53.15"W	Assilhó
AUT1.1	Shale	Black	Light	Very penetrative foliation		Road cut	40°42'54.96"N 8°31'58.74"O	Autoestrada
AUT2.1	Shale	Black	Light	Very penetrative foliation		Road cut	40°42'48.72"N 8°31'58.02"O	Autoestrada

AUT3.1	Shale	Black	None	Very penetrative foliation	Pyrite and sulfides	Road cut	40°42'46.14"N 8°31'57.60"O	Autoestrada
AUT4.1	Shale	Black	Light	Very penetrative foliation		Road cut	40°43'28.86"N 8°32'0.78"O	Autoestrada
BOS1.1	Siltstone	Dark grey	Light	Faint bedding Light foliation	Small quartz veins Ox Fe	Road cut	40°16'29.12"N 8°22'52.50"W	Bostelin
BOS2.1	Siltstone	Dark grey	Light	Clear Bedding Light foliation		Road cut	40°16'35.31"N 8°22'46.25"W	Bostelim
BOS2.2	Shale	Dark grey	Light	Clear Bedding Light foliation		Road cut	40°16'35.31"N 8°22'46.25"W	Bostelim
BOS2.3	Sandstone	Light grey	Light	Clear Bedding Light foliation	Ox Fe	Road cut	40°16'35.31"N 8°22'46.25"W	Bostelim
BOS3.1	Shale	Dark grey	Light	Clear Bedding Light foliation		Road cut	40°16'47.09"N 8°22'41.56"W	Bostelim
BOS4.1	Sandstone	Black	Light	Clear Bedding Light foliation	Ox Fe	Road cut	40°16'50.82"N 8°22'32.76"W	Bostelim
BOS5.1	Siltstone	Dark grey	Light			Road cut	40°16'56.64"N 8°22'28.84"W	Bostelim
BOU1.1	Shale	Dark grey	Light	Very penetrative foliation	Ox Fe Small quartz veins	Road cut	40°10'26.16"N 8°22'53.88"W	Bouça
BRU1	Shale	Black	Medium	Very penetrative foliation Folding	Ox Fe	Floor	40°37'29.15"N 8°25'16.26"W	Brunhido
BRU2	Siltstone	Black	Light	Faint bedding		Floor	40°37'29.15"N 8°25'16.26"W	Brunhido
BRU3.1	Shale	Dark grey	Light	Light foliation	Small quartz veins	Float	40°38'21.30"N 8°25'25.56"W	Brunhido
BUÇ 1.1	Shale	Black	Light	Folding Clear Bedding Light foliation	?	Road cut	40°22'42.94"N 8°21'59.40"W	Buçaco
BUÇ 2.1	Shale	Black	Light	Folding Very penetrative foliation	Ox Fe Small quartz veins	Road cut	40°22'38.61"N 8°21'42.55"W	Buçaco
BUÇ 2.2	Siltstone	Dark grey	Light	Folding Clear Bedding		Road cut	40°22'38.61"N 8°21'42.55"W	Buçaco
BUÇ 2.3	Shale	Black	Medium	Very penetrative foliation Folding	Extensive silicification Ox Fe veins	Road cut	40°22'38.61"N 8°21'42.55"W	Buçaco
BUÇ 3.1	Shale	Black	None	Very penetrative foliation Folding	Ox Fe Small quartz veins	Road cut	40°22'44.59"N 8°21'42.51"W	Buçaco

CAE 2.1	Shale	Dark grey	Medium	Clear Bedding Faulting	Ox Fe e Mn?	Floor	38°27'56.42"N 8°20'6.68"O	Caeira
CAE 2.2	Siltstone	Dark grey	Medium	Clear Bedding	Ox Fe e Mn?	Floor	38°28'4.30"N 8°20'10.43"O	Caeira
CAE 3.1	Shale	Dark grey	Medium	Clear Bedding Faulting	Ox Fe e Mn?	Floor	38°27'24.09"N 8°19'53.64"O	Caeira
CAN 1	Siltstone	Dark grey	None	Compaction	Extensive silicification	Road cut	40°12'34.82"N 8°22'33.29"W	Vale de Canas
CAN 2.1	Shale	Black	Light	Very penetrative foliation	Small quartz veins	Floor	40°12'38.64"N 8°22'39.12"W	Vale de Canas
CAT1.1	Siltstone	Light grey	Light			Road cut	40°18'31.18"N 8°22'39.99"W	Botão
CAT2.1	Shale	Black	Light	Very penetrative foliation	Small quartz veins Ox Fe	Road cut	40°18'31.93"N 8°22'49.35"W	Botão
CAT3.1	Shale	Light grey	Light	Very penetrative foliation Boudin no meio de shales	Small quartz veins Ox Fe	Road cut	40°18'31.85"N 8°22'54.30"W	Botão
CAT4.1	Shale	Black	Light	Light foliation Clear Bedding		Road cut	40°18'26.59"N 8°23'2.69"W	Botão
CAT4.2	Sandstone	Light grey	Light	Light foliation Clear Bedding		Road cut	40°18'26.59"N 8°23'2.69"W	Botão
CAT5.1	Shale	Black	Light	Light foliation Clear Bedding		Road cut	40°18'22.90"N 8°23'7.25"W	Botão
CEI1	Shale	Black	None	Compaction	Extensive silicification Ox Fe	Road cut	40°10'48.41"N 8°23'29.35"W	Ceira
CEI2.1	Siltstone	Black	Light	Very penetrative foliation	Small quartz veins Extensive silicification Pyrite and sulfides	Road cut	40°10'24.89"N 8°23'36.34"W	Ceira
CER1.1	Sandstone	White	Light	Clear Bedding		Road cut	40° 1'25.59"N 8°20'46.10"W	Cerejeiras
CHA1.1	Shale	Dark grey	Light	Light foliation		FloorRoad cut	40°40'47.52"N 8°25'12.54"W	Chãs
CHA2.1	Shale	Black	Light	Light foliation	ox fe	FloorRoad cut	40°41'0.06"N 8°25'34.89"W	Chãs
CHE1.1	Shale	Black	Light	Very penetrative foliation		Road cut	40° 3'11.34"N 8°21'55.78"W	Cheira
CHE1.2	Shale	Black	Light	Very penetrative foliation	Extensive silicification	Road cut	40° 3'11.34"N	Cheira

							8°21'55.78"W	
CHE2.1	Sandstone	White	Light	Clear Bedding		Road cut	40° 3'35.13"N 8°21'42.80"W	Cheira
CND 1.1	Shale	Dark grey	Light	Clear Bedding	Ox Fe	Road cut	40°33'40.95"N 8°25'1.98"O	Candam
CND 1.2	Sandstone	Dark grey	Light	Clear Bedding		Road cut	40°33'39.94"N 8°25'2.00"O	Candam
CND 2.1	Shale	Dark grey	Light	Clear Bedding	Ox Fe	Road cut	40°33'42.48"N 8°25'5.61"O	Candam
CND 3.1	Shale	Dark grey	Light	Clear Bedding	Ox Fe	Road cut	40°33'42.07"N 8°25'10.39"O	Candam
CND 4.1	Siltstone	Dark grey	Light	Clear Bedding	Ox Fe	Road cut	40°33'35.84"N 8°25'41.38"O	Candam
CND 4.2	Shale	Dark grey	Light		Ox Fe	Road cut	40°33'36.48"N 8°25'45.96"O	Candam
CND 5.1	Siltstone	Dark grey	Light	Clear Bedding	Ox Fe	Road cut	40°33'37.56"N 8°25'49.38"O	Candam
CRT 1.1	Shale	Dark grey	Light	Very penetrative foliation	Ox Fe	Floor	40°45'13.82"N 8°30'52.17"O	Cristelo
DUP1	Shale	Black	Light	Folding Very penetrative foliation thining	Small quartz veins	Road cut	40°23'17.16"N 8°23'7.93"W	Villa Duparchy
Fon-C-1	Shale	Dark grey	None	Very penetrative foliation	Ox Fe	Road cut	40°40'9.50"N 8°32'14.57"W	Fontão
Fon-C-2	Shale	Dark grey	None	Very penetrative foliation	Ox Fe	Road cut	40°40'9.50"N 8°32'14.57"W	Fontão
Fon-C-3	Shale	Black	None	Very penetrative foliation Folding	Ox Fe	Road cut	40°40'9.50"N 8°32'14.57"W	Fontão
Fon-C-4	Shale	Black	None	Very penetrative foliation	Ox Fe	Road cut	40°40'9.50"N 8°32'14.57"W	Fontão
Fon-D-1	Shale	Black	None	Very penetrative foliation	Ox Fe	Road cut	40°40'10.64"N 8°32'16.69"W	Fontão
Fon-D-2	Shale	Black	None	Very penetrative foliation	Ox Fe	Road cut	40°40'10.64"N 8°32'16.69"W	Fontão
Fon-D-3	Shale	Black	None	Very penetrative foliation	Ox Fe Extensive silicification	Road cut	40°40'10.64"N 8°32'16.69"W	Fontão

Fon-D-4	Shale	Dark grey	None	Very penetrative foliation	Ox Fe	Road cut	40°40'10.64"N 8°32'16.69"W	Fontão
Fon-D-5	Shale	Dark grey	None	Very penetrative foliation	Ox Fe	Road cut	40°40'12.08"N 8°32'18.21"W	Fontão
Fon-E-1	Shale	Black	Light	Very penetrative foliation	Ox Fe sobre S1	Road cut	40°40'13.37"N 8°32'16.76"O	Fontão
Fon-E-2	Shale	Black	Light	Very penetrative foliation	Ox Fe sobre S1	Road cut	40°40'13.74"N 8°32'16.21"O	Fontão
Fon-E-3	Shale	Black	Light	Very penetrative foliation	Ox Fe sobre S1	Road cut	40°40'14.56"N 8°32'15.61"O	Fontão
Fon-E-4	Shale	Dark grey	Light	Very penetrative foliation	Ox Fe veios	Road cut	40°40'15.18"N 8°32'15.35"O	Fontão
Fon-F-1	Shale	Dark grey	Light	Very penetrative foliation	Ox Fe sobre S1	Road cut	40°40'17.65"N 8°32'16.29"O	Fontão
Fon-F-2	Shale	Black	Light	Very penetrative foliation	Ox Fe sobre S1	Road cut	40°40'18.00"N 8°32'17.04"O	Fontão
Fon-F-3	Shale	Black	Light	Very penetrative foliation	Ox Fe sobre S1	Road cut	40°40'18.00"N 8°32'17.04"O	Fontão
Fon-F-4	Shale	Dark grey	Light	Very penetrative foliation	Ox Fe sobre S1	Road cut	40°40'18.45"N 8°32'18.10"O	Fontão
Fon-G-0	Shale	Dark grey	Light	Very penetrative foliation	Ox Fe sobre S1	Road cut	40°40'22.63"N 8°32'26.07"O	Fontão
Fon-G-1	Shale	Dark grey	Light	Very penetrative foliation	Ox Fe sobre S1	Road cut	40°40'22.63"N 8°32'26.07"O	Fontão
Fon-G-2	Shale	Dark grey	Light	Very penetrative foliation	Ox Fe sobre S1	Road cut	40°40'22.63"N 8°32'26.07"O	Fontão
Fon-G-3	Shale	Dark grey	Light	Very penetrative foliation	Ox Fe sobre S1	Road cut	40°40'22.63"N 8°32'26.07"O	Fontão
Fon-G-4	Shale	Dark grey	Light	Very penetrative foliation	Ox Fe sobre S1	Road cut	40°40'22.63"N 8°32'26.07"O	Fontão
Fon-G-5	Shale	Dark grey	Light	Very penetrative foliation	Ox Fe sobre S1	Road cut	40°40'22.63"N 8°32'26.07"O	Fontão
Fon-H-1	Shale	Dark grey	Light	Clear Bedding Light foliation	Ox Fe sobre S1	Road cut	40°40'26.82"N 8°32'25.15"O	Fontão
Fon-H-2	Shale	Dark grey	Light	Clear Bedding Light foliation	Ox Fe sobre S1	Road cut	40°40'27.47"N 8°32'26.20"O	Fontão

Fon-H-3	Shale	Black	Light	Light foliation Faint bedding	Ox Fe sobre S1	Road cut	40°40'24.72"N 8°32'26.28"O	Fontão
Fon-H-4	Shale	Dark grey	Light	Light foliation	Ox Fe raros	Road cut	40°40'24.90"N 8°32'26.10"O	Fontão
Fon-H-5	Shale	Dark grey	Light	Light foliation	Ox Fe sobre S1	Road cut	mal tirado	Fontão
Fon-H-6	Shale	Light grey	Medium	Light foliation Faint bedding	Ox Fe sobre S1	Road cut	40°40'25.20"N 8°32'26.04"O	Fontão
Fon-I-0	Siltstone	Light grey	Light	Clear Bedding	Ox Fe sobre S1	Road cut	40°40'27.66"N 8°32'27.00"O	Fontão
Fon-I-00	Siltstone	Light grey	Light	Clear Bedding	Ox disseminados	Road cut	40°40'27.78"N 8°32'27.18"O	Fontão
Fon-I-1	Shale	Dark grey	None	Clear Bedding		Road cut	40°40'27.72"N 8°32'27.00"O	Fontão
Fon-I-2	Shale	Black	None	Clear Bedding	Ox sobre S0	Road cut	40°40'27.90"N 8°32'27.24"O	Fontão
Fon-I-3	Shale	Dark grey	None	Clear Bedding	Ox Fe	Road cut	40°40'28.02"N 8°32'27.30"O	Fontão
Fon-I-4	Shale	Dark grey	None	Clear Bedding		Road cut	40°40'28.32"N 8°32'27.36"O	Fontão
Fon-I-5	Shale	Dark grey	Medium	Clear Bedding		Road cut	40°40'28.44"N 8°32'27.42"O	Fontão
Fon-J-1	Shale	Black	None	Very penetrative foliation	Extensive silicification	Road cut	40°40'30.72"N 8°32'38.10"O	Fontão
Fon-J-2	Shale	Dark grey	None	Very penetrative foliation	Ox Fe+Mn sobre S1	Road cut	40°40'31.02"N 8°32'38.64"O	Fontão
Fon-J-3	Siltstone	Black	Light	Very penetrative foliation	Ox Fe+Mn sobre S1	Road cut	40°40'32.16"N 8°32'39.18"O	Fontão
Fon-L-1	Shale	Dark grey	Light	Very penetrative foliation	Ox Fe+Mn sobre S1	Road cut	40°40'36.48"N 8°32'38.04"O	Fontão
Fon-L-2	Shale	Dark grey	Light	Very penetrative foliation	Ox Fe+Mn sobre S1	Road cut	40°40'37.68"N 8°32'39.12"O	Fontão
Fon-M-1	Shale	Black	Light	Very penetrative foliation		Road cut	40°40'39.33"N 8°32'42.23"O	Fontão
Fon-M-2	Shale	Dark grey	Light	Very penetrative foliation	poucos ox Fe+Mn sobre S1	Road cut	40°40'40.74"N 8°32'44.76"O	Fontão

Fon-M-3	Shale	Dark grey	Light	Very penetrative foliation	poucos ox Fe+Mn sobre S1	Road cut	40°40'41.10"N 8°32'44.82"O	Fontão
Fon-M-4	Sandstone	Dark grey	Light	Very penetrative foliation	light oxidation	Road cut	40°40'41.40"N 8°32'44.94"O	Fontão
Fon-M-5	Shale	Dark grey	Light	Very penetrative foliation	poucos ox Fe+Mn sobre S1	Road cut	40°40'41.82"N 8°32'45.13"O	Fontão
Fon1	Shale	Dark grey	Light	Folding thining along S0 Compaction	Ox Fe	Road cut	40°40'9.76"N 8°32'8.79"W	Fontão
Fon10	Shale	Dark grey	Light	Folding Very penetrative foliation	Ox Fe Extensive silicification	Road cut	40°40'6.79"N 8°32'8.79"W	Fontão
Fon2	Shale	Dark grey	Light	Folding thining along S0 Compaction	Ox Fe	Road cut	40°40'9.76"N 8°32'8.79"W	Fontão
Fon3	Shale	Black	Light	Folding thining along S0 Compaction	Ox Fe	Road cut	40°40'9.76"N 8°32'8.79"W	Fontão
Fon4	Shale	Dark grey	Light	Folding Very penetrative foliation	Ox Fe Extensive silicification	Road cut	40°40'6.79"N 8°32'8.79"W	Fontão
Fon5	Shale	Dark grey	Light	Folding Very penetrative foliation	Ox Fe Extensive silicification	Road cut	40°40'6.79"N 8°32'8.79"W	Fontão
Fon6	Shale	Dark grey	Light	Folding Very penetrative foliation	Ox Fe Extensive silicification	Road cut	40°40'6.79"N 8°32'8.79"W	Fontão
Fon7	Shale	Dark grey	Light	Folding Very penetrative foliation	Ox Fe Extensive silicification	Road cut	40°40'6.79"N 8°32'8.79"W	Fontão
Fon8	Shale	Dark grey	Light	Folding Very penetrative foliation	Ox Fe Extensive silicification	Road cut	40°40'6.79"N 8°32'8.79"W	Fontão
Fon9	Shale	Dark grey	Light	Folding Very penetrative foliation	Ox Fe Extensive silicification	Road cut	40°40'6.79"N 8°32'8.79"W	Fontão
FRA1	Siltstone	Dark grey	Light	Clear Bedding	Extensive silicification	Road cut	40°14'52.35"N 8°23'25.83"W	S. Paulo de Frades
FRA1.2	Shale	Black	Light	Very penetrative foliation	Extensive silicification	Road cut	40°14'52.35"N 8°23'25.83"W	S. Paulo de Frades
FRA1.3	Shale	Black	Light	Very penetrative foliation	Extensive silicification Ox Fe	Road cut	40°14'51.26"N 8°23'30.74"W	S. Paulo de Frades
FRA2	Shale	Black	None	Faint bedding	Small quartz veins Carbonate veins	Road cut	40°15'4.17"N 8°22'51.99"W	S. Paulo de Frades
FRA3.1	Shale	Dark grey	Light	Very penetrative foliation	Extensive silicification	Road cut	40°15'1.51"N	S. Paulo de

				Faint bedding			8°23'16.02"W	Frades
FRO 1.1	Siltstone	Dark grey	Light	Clear Bedding Light foliation		Road cut	40°40'5.55"N 8°33'18.25"O	Frossos
FRO 1.2	Shale	Black	Light	Clear Bedding Light foliation		Road cut	40°40'4.68"N 8°33'16.68"O	Fontão
FRU-1.1	Shale	Dark grey	None	Clear Bedding Folding	Extensive silicification	Road cut	40°11'0.33"N 8°21'39.67"W	S. Frutuoso
GEN1.1	Shale	Black	Medium	Very penetrative foliation	Ox Fe	Road cut	40° 3'14.56"N 8°20'44.83"W	Moinhos
GOL1.1	Siltstone	Light grey	Light	Very penetrative foliation Faint bedding	Extensive silicification	Road cut	40°14'53.19"N 8°22'10.15"W	Golpe
LOB1.1	Shale	Black	Light	Very penetrative foliation Faint bedding		Float	40°13'8.80"N 8°22'27.26"W	Casal do Lobo
LOU1.1	Shale	Black	MediumLight	Clear Bedding Folding		Road cut	40°21'4.80"N 8°21'49.62"W	Louredo
LUS 2.1	Shale	Dark grey	None	Very penetrative foliation		Road cut	40°23'5.70"N 8°22'57.90"W	Luso
LUS 2.2	Shale	Dark grey	Light	Very penetrative foliation	Extensive silicification Ox Fe	Road cut	40°23'5.70"N 8°22'57.90"W	Luso
LUS 2.3	Shale	Black	Light	Very penetrative foliation		Road cut	40°23'5.70"N 8°22'57.90"W	Luso
LUS 2.4	Shale	Black	Light	Very penetrative foliation		Road cut	40°23'5.70"N 8°22'57.90"W	Luso
LUS 2.5	Shale	Black	Light	Very penetrative foliation		Road cut	40°23'5.70"N 8°22'57.90"W	Luso
MAN1	Shale	Black	Light	Folding Very penetrative foliation	Small quartz veins	Road cut	40°24'46.74"N 8°23'1.86"W	V.N. Monsarros
MAN3.1	Sandstone	Dark grey	Light	Folding Very penetrative foliation	Small quartz veins	Road cut	40°24'46.74"N 8°23'1.86"W	V.N. Monsarros
MAR 1.1	Siltstone	Dark grey	Light	Light foliation	Small quartz veins Pyrite and sulfides	Float	40°40'44.70"N 8°30'42.78"O	S. Marcos
MIN1	Shale	Black	None	Folding Very penetrative foliation	Small quartz veins	Road cut	40°46'49.49"N 8°30'38.88"W	Minhoteira
MIN10	Shale	Dark grey	None	Very penetrative foliation	Extensive silicification Ox Fe	Road cut	40°46'52.94"N 8°30'32.80"W	Minhoteira

MIN10.2	Shale	Dark grey	None	Very penetrative foliation	Extensive silicification Ox Fe	Road cut	40°46'53.64"N 8°30'31.26"W	Minhoteira
MIN11.1	Shale	Dark grey	Medium	Very penetrative foliation	Small quartz veins ox fe	Road cut	40°46'13.80"N 8°31'8.70"W	Minhoteira
MIN11.2	Shale	Dark grey	Medium	Very penetrative foliation	Small quartz veins ox fe	Road cut	40°46'15.06"N 8°31'8.70"W	Minhoteira
MIN11.3	Shale	Dark grey	Light	Very penetrative foliation Faint bedding	ox fe	Road cut	40°46'20.10"N 8°31'6.30"W	Minhoteira
MIN11.4	Shale	Dark grey	Light	Very penetrative foliation	Ox fe	Road cut	40°46'24.29"N 8°31'5.18"W	Minhoteira
MIN11.5	Shale	Dark grey	Light	Very penetrative foliation Faint bedding	Small quartz veins ox fe	Road cut	40°46'24.29"N 8°31'5.18"W	Minhoteira
MIN11.6	Shale	Dark grey	Light	Very penetrative foliation Faint bedding	Small quartz veins	Road cut	40°46'24.29"N 8°31'5.18"W	Minhoteira
MIN12.1	Shale	Black	Light	Very penetrative foliation Faint bedding	ox fe Small quartz veins	Road cut	40°46'24.91"N 8°31'4.99"W	Minhoteira
MIN12.2	Shale	Dark grey	Medium	Very penetrative foliation Faint bedding	ox fe	Road cut	40°46'26.96"N 8°31'2.83"W	Minhoteira
MIN12.3	Shale	Dark grey	Light	Very penetrative foliation Faint bedding	ox fe Small quartz veins	Road cut	40°46'28.79"N 8°31'1.93"W	Minhoteira
MIN12.4	Shale	Light grey	Light	Very penetrative foliation	ox fe	Road cut	40°46'29.72"N 8°31'1.80"W	Minhoteira
MIN13.1	Shale	Dark grey	Light	Very penetrative foliation	ox fe	Road cut	40°46'31.29"N 8°31'1.53"W	Minhoteira
MIN14.1	Shale	Light grey	Light	Very penetrative foliation Faint bedding	ox fe	Road cut	40°46'33.55"N 8°31'0.90"W	Minhoteira
MIN14.2	Shale	Black	Light	Very penetrative foliation	ox fe	Road cut	40°46'35.00"N 8°30'59.99"W	Minhoteira
MIN14.3	Shale	Black	Light	Very penetrative foliation	ox fe Small quartz veins	Road cut	40°46'35.47"N 8°30'59.35"W	Minhoteira
MIN16.1	Shale	Light grey	Light	Very penetrative foliation Faint bedding		Road cut	40°46'54.36"N 8°30'32.94"W	Minhoteira
MIN16.2	Shale	Dark grey	Light	Very penetrative foliation Faint bedding		Road cut	40°46'54.66"N 8°30'32.70"W	Minhoteira
MIN16.3	Shale	Dark grey	Light	Very penetrative foliation		Road cut	40°46'55.08"N 8°30'31.98"W	Minhoteira

MIN16.4	Shale	Dark grey	Light	Very penetrative foliation	Small quartz veins	Road cut	40°46'55.08"N 8°30'31.98"W	Minhoteira
MIN16.5	Shale	Dark grey	Light	Very penetrative foliation	Small quartz veins ox fe	Road cut	40°46'56.28"N 8°30'31.08"W	Minhoteira
MIN16.6	Shale	Light grey	Light	Very penetrative foliation		Road cut	40°46'56.76"N 8°30'30.66"W	Minhoteira
MIN16.7	Shale	Light grey	Light	Very penetrative foliation		Road cut	40°46'57.36"N 8°30'30.06"W	Minhoteira
MIN17.1	Shale	Light grey	Light	Very penetrative foliation	ox fe	Road cut	40°46'58.44"N 8°30'28.68"W	Minhoteira
MIN17.2	Shale	Light grey	Light	Very penetrative foliation	ox fe	Road cut	40°46'58.44"N 8°30'28.68"W	Minhoteira
MIN2	Shale	Black	None	Folding Very penetrative foliation	Small quartz veins	Road cut	40°46'49.49"N 8°30'38.88"W	Minhoteira
MIN3	Shale	Black	None	Folding Very penetrative foliation	Small quartz veins	Road cut	40°46'49.49"N 8°30'38.88"W	Minhoteira
MIN4	Shale	Black	None	Folding Very penetrative foliation	Small quartz veins	Road cut	40°46'49.49"N 8°30'38.88"W	Minhoteira
MIN5	Shale	Black	None	Folding Very penetrative foliation	Small quartz veins	Road cut	40°46'49.49"N 8°30'38.88"W	Minhoteira
MIN5.2	Shale	Dark grey	None	Very penetrative foliation	Ox Fe	Road cut	40°46'56.46"N 8°30'33.84"W	Minhoteira
MIN5.3	Shale	Black	None	Very penetrative foliation	Ox Fe Extensive silicification	Floor	40°47'10.68"N 8°30'45.78"W	Minhoteira
MIN6	Shale	Dark grey	None	Folding Very penetrative foliation	Extensive silicification Ox Fe	Road cut	40°46'48.67"N 8°30'36.87"W	Minhoteira
MIN7	Shale	Black	None	Folding Very penetrative foliation	Extensive silicification Ox Fe	Road cut	40°46'48.67"N 8°30'36.87"W	Minhoteira
MIN8	Shale	Black	None	Folding Very penetrative foliation	Extensive silicification Ox Fe	Road cut	40°46'49.46"N 8°30'35.97"W	Minhoteira
MIN9	Shale	Dark grey	None	Very penetrative foliation	Extensive silicification Ox Fe	Road cut	40°46'52.35"N 8°30'33.85"W	Minhoteira
MIR1.1	Siltstone	Dark grey	Light		Extensive silicification Ox Fe	Road cut	40° 5'47.02"N 8°20'20.26"W	Miranda do Corvo
MIR2.1	Shale	Black	Light	Very penetrative foliation	Ox Fe Small quartz veins	Road cut	40° 5'44.39"N 8°20'7.25"W	Miranda do Corvo

MIR3.1	Shale	Black	Light	Very penetrative foliation	Small quartz veins Extensive silicification	Road cut	40° 5'23.92"N 8°20'13.08"W	Miranda do Corvo
MIR4.1	Shale	Dark grey	Light	Very penetrative foliation Faint bedding	Ox Fe	Road cut	40° 5'21.17"N 8°20'31.58"W	Miranda do Corvo
MIR4.2	Siltstone	Light grey	Light	Very penetrative foliation Faint bedding	Ox Fe	Road cut	40° 5'20.94"N 8°20'33.53"W	Miranda do Corvo
MIR4.3	Shale	Black	Light	Faint bedding Light foliation		Road cut	40° 5'20.88"N 8°20'36.80"W	Miranda do Corvo
MIR4.4	Shale	Black	Light	Faint bedding Light foliation		Road cut	40° 5'20.70"N 8°20'37.61"W	Miranda do Corvo
MIS1.1	Shale	Black	Light	Very penetrative foliation	Ox Fe	Road cut	40°12'21.30"N 8°21'24.45"W	Casal da Misarela
MOI1.1	Siltstone	Dark grey	Light	Very penetrative foliation Faint bedding	Ox Fe	Float	40° 7'13.93"N 8°21'28.78"W	Moinhos
MON 2.1	Shale	Dark grey	Light	Folding Clear Bedding	Fe em capas sobre S0	Road cut	40°24'49.11"N 8°22'54.76"W	Monsarros 2
MON 2.2	Shale	Black	Light	Folding Clear Bedding	Fe e Mn	Road cut	40°24'49.11"N 8°22'54.76"W	Monsarros 2
MON 2.3	Shale	Black	Light	Folding Clear Bedding		Road cut	40°24'49.11"N 8°22'54.76"W	Monsarros 2
MON 2.4	Oil shale	Black	Medium	Folding Clear Bedding		Road cut	40°24'49.11"N 8°22'54.76"W	Monsarros 2
MON 2.5	Shale	Black	Light	Folding Clear Bedding	Small quartz veins Fe e Mn	Road cut	40°24'49.11"N 8°22'54.76"W	Monsarros 2
MON 2.6	Siltstone	Dark grey	Light	Folding Clear Bedding	Fe e Mn	Road cut	40°24'49.11"N 8°22'54.76"W	Monsarros 2
MON1.1	Sandstone	Light grey	Light			Road cut	40°24'57.03"N 8°22'16.02"W	Monsarros
MTN-1.1	Shale	Black	Medium	Very penetrative foliation	Ox Fe e Mn Small quartz veins	Floor	40°23'0.66"N 8°21'41.58"W	Monte Novo
MTN-1.2	Shale	Black	Medium	Very penetrative foliation	Ox Fe e Mn Small quartz veins	Floor	40°23'0.66"N 8°21'41.58"W	Monte Novo
MTN-1.3	Shale	Black	Medium	Very penetrative foliation	Ox Fe e Mn Small quartz veins Sulfur	Floor	40°23'0.66"N 8°21'41.58"W	Monte Novo
MTN-1.4	Shale	Black	Medium	Very penetrative foliation	Ox Fe e Mn small quartz veins Sulfur	Floor	40°23'0.66"N 8°21'41.58"W	Monte Novo

PEQ1.1	Shale	Black	Light	Very penetrative foliation	Ox Fe Extensive silicification thick quartz veins	Road cut	40° 8'41.88"N 8°21'55.80"W	Casal Pequeno
PIC 1.1	Shale	Dark grey	Light	Very penetrative foliation	Extensive silicification Pyrite and sulfides	Road cut	40°21'9.54"N 8°22'32.19"W	Picoto
PIC2.1	Shale	Dark grey	Light	Very penetrative foliation		Road cut	40°11'8.98"N 8°23'25.78"W	Picoito
POR 1.1	Shale	Black	Light	Very penetrative foliation	Ox Fe	Float	40°43'17.41"N 8°30'34.40"O	Portos
QUI 1.1	Siltstone	Yellow	Light	Clear Bedding Folding	Ox Fe	Road cut	40°21'9.54"N 8°22'32.19"W	Quintinha
QUI 2.1	Shale	Dark grey	Light	Very penetrative foliation	Ox Fe	Road cut	40°11'10.86"N 8°23'44.22"W	Quintinha
QUI3.1	Sandstone	Dark grey	Light	Faint bedding Light foliation	Ox Fe Pyrite and sulfides	Road cut	40°11'14.56"N 8°23'41.59"W	Quintinha
RED1.1	Shale	Dark grey	Light	Light foliation		Floor	40°39'8.70"N 8°25'22.80"W	Redonda
RET1.1	Shale	Black	Light	Very penetrative foliation		Road cut	40° 3'46.58"N 8°21'39.52"W	Retorta
RET2.1	Shale	Black	Light	Very penetrative foliation		Road cut	40° 3'59.51"N 8°21'32.59"W	Retorta
SAL 3.1	Siltstone	Black	Light	Folding	OxFe	Road cut	40°23'36.51"N 8°22'17.56"W	Salgueiral 3
SAL 3.2	Shale	Black	Medium	Folding Light foliation	Small quartz veins Carbonatos verdes e py	Road cut	40°23'38.36"N 8°22'11.46"W	Salgueiral 3
SAL1.1	Shale	Dark grey	Light	Clear Bedding Folding	Ox Fe S	Road cut	40°23'32.16"N 8°21'20.59"W	Salgueiral 1
SAL1.2	Siltstone	Dark grey	Light	Clear Bedding Folding	Ferruginização	Road cut	40°23'32.16"N 8°21'20.59"W	Salgueiral 1
SAL2.1	Siltstone	Light grey	Light	Clear Bedding Folding	Ferruginização	Road cut	40°23'44.44"N 8°21'28.10"W	Salgueiral 2
SAL3.3	Shale	Black	Medium	Very penetrative foliation	Small quartz veins	Road cut	40°23'38.36"N 8°22'11.46"W	Salgueiral 3
SAL3.4	Shale	Black	Light	Folding Very penetrative foliation	Small quartz veins	Road cut	40°23'43.51"N 8°22'0.59"W	Salgueiral 3
SEN1.1	Sandstone	Dark grey	Light	Very penetrative foliation	Small quartz veins	Road cut	40° 9'56.43"N	Senhor da Serra

					Extensive silicification Pyrite and sulfides		8°20'50.87"W	
Ser1	Shale	Black	Light	Folding Great compaction Clear Bedding	Ox Fe Small quartz veins	Road cut	40°39'29.28"N 8°28'0.24"W	Serém E2
Ser2	Shale	Black	Light	Folding Great compaction Clear Bedding	Extensive silicification	Road cut	40°39'29.28"N 8°28'0.24"W	Serém E2
Ser3	Shale	Black	Light	Folding Great compaction Clear Bedding	Small quartz veins	Road cut	40°39'29.28"N 8°28'0.24"W	Serém E2
Ser4	Shale	Black	Light	Folding Great compaction Clear Bedding	Small quartz veins	Road cut	40°39'29.28"N 8°28'0.24"W	Serém E2
Ser5.1	Shale	Light grey	Light	Very penetrative foliation	Small quartz veins	Road cut	40°39'21.78"N 8°28'1.11"W	Serém convento
Ser6.1	Shale	Dark grey	Light	Very penetrative foliation	Extensive silicification Ox Fe	Road cut	40°39'26.14"N 8°28'1.86"W	Serém
Ser6.2	Shale	Dark grey	None	Very penetrative foliation	Extensive silicification Ox Fe	Road cut	40°39'22.15"N 8°28'2.36"W	Serém
Ser7.1	Shale	Dark grey	None	Folding Clear Bedding Beding folded in closely packed folds	Extensive silicification Ox Fe	Road cut	40°39'36.85"N 8°28'10.69"W	Serém
SND 20.1	Shale	Black	None		Small quartz veins oxidation	Road cut	40°40'31.45"N 8°26'47.99"O	Sernada do Vouga SND 20
SND 20.2	Shale	Black	None	Folding Clear Bedding	Small quartz veins	Road cut	40°40'36.72"N 8°26'46.96"O	Sernada do Vouga SND 20
SND 21.1	Shale	Black	Light	Folding Clear Bedding Very penetrative foliation	Small quartz veins	Road cut	40°40'22.61"N 8°26'54.18"O	Sernada do Vouga SND 21
SND 22.1	Shale	Dark grey	Medium	Folding Clear Bedding Very penetrative foliation	Small quartz veins oxidos	Road cutFloat	40°40'56.16"N 8°27'18.30"O	Sernada do Vouga SND 22
SND 23.1	Shale	Dark grey	Medium	Folding Very penetrative foliation	Small quartz veins oxidos	Floor	40°41'0.31"N 8°27'17.33"O	Sernada do Vouga SND 23
SND 23.2	Shale	Black	Medium	Folding Very penetrative foliation	Small quartz veins oxidos	Floor	40°40'59.64"N 8°27'18.35"O	Sernada do Vouga SND 23
SND 24.1	Shale	Dark grey	Light	Folding Very penetrative foliation	oxidos	Road cut	40°40'49.82"N 8°27'22.01"O	Sernada do Vouga SND 24
SND-A-1	Siltstone	Light grey	Medium	Folding Clear Bedding	Ox Fe	Road cut	40°40'34.66"N 8°27'33.66"W	Sernada do Vouga SND-A
SND-B-1	Shale	Black	Medium	Very penetrative foliation	Ox Fe veins	Road cut	40°40'30.86"N	Sernada do Vouga

					Small quartz veins		8°27'33.97"W	SND-B
SND-B-2	Shale	Black	Light	Clear Bedding	Ox Fe veins Small quartz veins	Road cut	40°40'30.86"N 8°27'33.97"W	Sernada do Vouga SND-B
SND-B-3	Sandstone	Dark grey	None	Very penetrative foliation		Road cut	40°40'30.86"N 8°27'33.97"W	Sernada do Vouga SND-B
SND-B-4	Siltstone	Dark grey	Light	Clear Bedding	Ox Fe	Road cut	40°40'30.86"N 8°27'33.97"W	Sernada do Vouga SND-B
SND-B-5	Shale	Dark grey	Light	Very penetrative foliation	Ox Fe Extensive silicification	Road cut	40°40'30.86"N 8°27'33.97"W	Sernada do Vouga SND-B
SND-C-1	Shale	Black	Light	Folding Clear Bedding	Extensive silicification	Road cut	40°40'28.38"N 8°27'29.28"W	Sernada do Vouga SND-C
SND-C-2	Shale	Black	Light	Folding Clear Bedding Estiramento Compactação	Extensive silicification Ox Fe	Road cut	40°40'28.38"N 8°27'29.28"W	Sernada do Vouga SND-C
SND-C-3	Shale	Black	Light	Folding Clear Bedding Estiramento Compactação	Extensive silicification Ox Fe	Road cut	40°40'28.38"N 8°27'29.28"W	Sernada do Vouga SND-C
SND-C-4	Shale	Dark grey	Light	Folding Clear Bedding Estiramento compactação	Extensive silicification Ox Fe	Road cut	40°40'28.50"N 8°27'26.52"W	Sernada do Vouga SND-C
SND-C-5	Shale	Dark grey	Light	Folding Clear Bedding Estiramento compactação	Extensive silicification Ox Fe	Road cut	40°40'28.50"N 8°27'26.52"W	Sernada do Vouga SND-C
SND-comb-1.1	Shale	Black	Light		Small quartz veins	Road cut	40°40'48.54"N 8°27'44.58"W	Sernada do Vouga SND-comb
SND-comb-2.1	Shale	Dark grey	Light		Ox Fe	Road cut	40°40'48.77"N 8°27'50.29"W	Sernada do Vouga SND-comb
SND-comb-2.2	Shale	Black	Light		Small quartz veins Ox Fe	Road cut	40°40'48.77"N 8°27'50.29"W	Sernada do Vouga SND-comb
SND-comb-3.1	Shale	Black	LightNone		Ox Fe Extensive silicification	Road cut	40°40'46.56"N 8°27'55.96"W	Sernada do Vouga SND-comb
SND-comb-4.1	Shale	Black	None		Ox Fe Extensive silicification	Road cut	40°40'45.58"N 8°28'0.05"W	Sernada do Vouga SND-comb
SND-comb-4.2	Shale	Dark grey	Light		Extensive silicification	Road cut	40°40'44.46"N 8°28'3.90"W	Sernada do Vouga SND-comb
SND-comb-4.3	Siltstone	Yellow	None			Road cut	40°40'45.60"N 8°28'0.06"O	Sernada do Vouga SND-comb
SND-comb-5.1	Shale	Black	Light	Faint bedding		Road cut	40°40'37.92"N 8°27'30.06"O	Sernada do Vouga SND-comb

SND-comb-6.1	Shale	Dark grey	Light	Faint bedding	Small quartz veins ox fe	Road cut	40°40'38.22"N 8°27'25.20"O	Sernada do Vouga SND-comb
SND-comb-8.1	Shale	Dark grey	Light	Clear Bedding Light foliation		Road cut	40°40'46.80"N 8°27'28.92"O	Sernada do Vouga SND-comb
SND-comb-8.2	Shale	Dark grey	Light	Clear Bedding Light foliation		Road cut	40°40'45.54"N 8°27'28.32"O	Sernada do Vouga SND-comb
SND-comb-8.3	Siltstone	Green	Light	Clear Bedding Light foliation		Road cut	40°40'45.66"N 8°27'29.04"O	Sernada do Vouga SND-comb
SND-comb10.1	Shale	Dark grey	Medium	Clear Bedding Light foliation		Road cut	40°40'49.96"N 8°27'41.53"O	Sernada do Vouga SND-comb
SND-comb11.1	Shale	Dark grey	Light	Light foliation		Road cut	40°40'56.48"N 8°27'43.60"O	Sernada do Vouga SND-comb
SND-comb13.1	Shale	Dark grey	Light	Light foliation		Road cut	40°40'50.26"N 8°27'26.41"O	Sernada do Vouga SND-comb
SND-comb13.2	Shale	Dark grey	Light	Light foliation		Road cut	40°40'50.26"N 8°27'26.41"O	Sernada do Vouga SND-comb
SND-comb13.3	Shale	Dark grey	Light	Light foliation		Road cut	40°40'50.26"N 8°27'26.41"O	Sernada do Vouga SND-comb
SND-comb14.1	ShaleSiltstone	Yellow	Light	Light foliation		Road cut	40°40'47.40"N 8°27'22.05"O	Sernada do Vouga SND-comb
SND-comb15.1	Shale	Dark grey	Light	Very penetrative foliation		Road cut	40°40'45.81"N 8°27'20.09"O	Sernada do Vouga SND-comb
SND-E-1	Siltstone	Dark grey	None	Clear Bedding	Ox Fe Extensive silicification	Road cut	40°40'27.00"N 8°27'22.32"W	Sernada do Vouga SND-E
SND-E-2	Siltstone	Dark grey	None	Clear Bedding	Ox Fe Extensive silicification	Road cut	40°40'27.00"N 8°27'22.32"W	Sernada do Vouga SND-E
SND-E-3	Siltstone	Dark grey	None	Clear Bedding	Ox Fe Extensive silicification	Road cut	40°40'27.00"N 8°27'22.32"W	Sernada do Vouga SND-E
SND-E-4	Shale	Dark grey	None	Very penetrative foliation	Ox Fe Extensive silicification	Road cut	40°40'27.00"N 8°27'22.32"W	Sernada do Vouga SND-E
SND-E-5	Siltstone	Dark grey	None	Folding	Ox Fe Extensive silicification	Road cut	40°40'27.00"N 8°27'22.32"W	Sernada do Vouga SND-E
SND-E-6	Shale	Black	None	Folding	Ox Fe Extensive silicification	Road cut	40°40'25.86"N 8°27'18.72"W	Sernada do Vouga SND-E
SND-E-7	Shale	Dark grey	None	Folding	Ox Fe Extensive silicification	Road cut	40°40'25.86"N 8°27'18.72"W	Sernada do Vouga SND-E

SND-E-8	Shale	Dark grey	None	Clear Bedding	Ox Fe Extensive silicification	Road cut	40°40'25.86"N 8°27'18.72"W	Sernada do Vouga SND-E
SND-F-1	Shale	Black	None	Clear Bedding	Ox Fe Extensive silicification	Road cut	40°40'25.17"N 8°27'17.93"W	Sernada do Vouga SND-F
SND-F-2	Shale	Black	None	Clear Bedding	Ox Fe Extensive silicification	Road cut	40°40'24.02"N 8°27'18.35"W	Sernada do Vouga SND-F
SND-F-3	Shale	Dark grey	None	Clear Bedding	Extensive silicification	Road cut	40°40'22.14"N 8°27'16.98"W	Sernada do Vouga SND-F
SND-G1.1	Shale	Black	Medium	Very penetrative foliation		Road cut	40°40'43.68"N 8°27'36.36"O	Sernada do Vouga SND G
SOB 1.1	Shale	Dark grey	Light	Very penetrative foliation	Ox Fe	Road cut	40°41'11.89"N 8°30'43.15"W	Sobreiro
SPD1	Shale	Black	None	Folding Very penetrative foliation	Small quartz veins	Road cut	40°23'16.03"N 8°23'29.64"W	Lameira de S Pedro
SPD2	Shale	Black	Light	Folding Very penetrative foliation	Small quartz veins	Road cut	40°23'16.03"N 8°23'29.64"W	Lameira de S Pedro
SPD3	Shale	Black	Medium	Folding Very penetrative foliation	Small quartz veins	Road cut	40°23'16.03"N 8°23'29.64"W	Lameira de S Pedro
TAP1.1	Shale	Black	Light		Ox Fe Small quartz veins	Road cut	40°10'32.88"N 8°22'26.28"W	Tapada
TOR1.1	Sandstone	Dark grey	Light	Very penetrative foliation	Ox Fe	Road cut	40°11'38.49"N 8°22'59.06"W	Torres do Mondego
TOV-1.1	Shale	Black	None		Ox Fe Extensive silicification	Road cut	40°12'50.71"N 8°23'0.44"W	Tovim
TOV-2.1	Shale	Dark grey	None	Folding Clear Bedding Very penetrative foliation	Ox Fe Small quartz veins	Road cut	40°12'41.40"N 8°22'57.30"W	Tovim
TRE1.1	Shale	Black	Light	Very penetrative foliation	Ox Fe	Float	40° 7'56.96"N 8°21'26.35"W	Tremoa
Val1	Shale	Dark grey	Light	Folding Great compaction Clear Bedding	Small quartz veins	Road cut	40°41'37.23"N 8°28'35.75"W	IC2 E5
Val10.1	Shale	Black	Medium	Very penetrative foliation		Road cut	40°41'49.21"N 8°28'24.07"W	Albergaria-a-Velha
Val11.1	Shale	Black	Light	Very penetrative foliation	Extensive silicification Ox Fe	Road cut	40°41'56.76"N 8°28'28.08"W	Albergaria-a-Velha

Val2	Shale	Dark grey	Light	Folding Great compaction Clear Bedding	Small quartz veins	Road cut	40°41'37.23"N 8°28'35.75"W	IC2 E5
Val3	Shale	Black	Light	Folding Great compaction Clear Bedding	Small quartz veins	Road cut	40°41'37.23"N 8°28'35.75"W	IC2 E5
Val4	Shale	Black	Light	Folding Great compaction Clear Bedding	Small quartz veins Carbonate veins	Road cut	40°41'37.23"N 8°28'35.75"W	IC2 E5
Val5.1	Shale	Black	Light	Folding Great compaction Clear Bedding	Small quartz veins Carbonate veins Extensive silicification	Floor	40°41'43.74"N 8°28'28.32"W	Corta Fogo
Val5.2	Shale	Black	Light	Folding Clear Bedding Very penetrative foliation	Small quartz veins Carbonate veins Extensive silicification	Floor	40°41'43.74"N 8°28'28.32"W	Corta Fogo
Val5.3	Shale	Black	Light	Folding Clear Bedding Very penetrative foliation	Small quartz veins Carbonate veins Extensive silicification	Floor	40°41'43.74"N 8°28'28.32"W	Corta Fogo
Val5.4	Shale	Black	Light	Folding Clear Bedding Very penetrative foliation	Small quartz veins Carbonate veins Extensive silicification	Floor	40°41'43.74"N 8°28'28.32"W	Corta Fogo
Val5.5	Shale	Black	Light	Folding Clear Bedding Very penetrative foliation	Small quartz veins Carbonate veins Extensive silicification	Floor	40°41'43.74"N 8°28'28.32"W	Corta Fogo
Val6.1	Shale	Black	Light	Very penetrative foliation	Extensive silicification	Building foundations	40°41'40.24"N 8°28'28.51"W	Nova urbanização
Val7.1	Shale	Black	Medium	Very penetrative foliation	Small quartz veins Carbonate veins Ox Fe	Float	40°41'35.40"N 8°28'8.70"W	Albergaria-a-Velha
Val8.1	Shale	Black	Medium	Very penetrative foliation	Small quartz veins Carbonate veins Ox Fe	Steep hill	40°41'26.52"N 8°28'5.28"W	Albergaria-a-Velha
Val9.1	Shale	Black	Light	Very penetrative foliation		Road cut	40°41'37.74"N 8°28'40.92"W	Albergaria-a-Velha
VAR 1.1	Shale	Black	Medium	Very penetrative foliation Folding	Ox Fe Small quartz veins Oxidação Triássica?	Road cut	40°23'30.63"N 8°23'24.98"W	Varzea
VAR 1.2	Shale	Dark grey	Light	Very penetrative foliation Folding	Ox Fe Extensive silicification	Road cut	40°23'29.58"N 8°23'18.72"W	Varzea
VAR 2.1	Shale	Dark grey	None	Very penetrative foliation Folding Clear Bedding	Extensive silicification	Road cut	40°23'33.96"N 8°23'40.86"W	Varzea
VAR 2.2	Shale	Dark grey	None	Very penetrative foliation Folding clear Bedding		Road cut	40°23'34.50"N 8°23'42.24"W	Varzea

VAR 3.1	Shale	Dark grey	None	Very penetrative foliation Folding Clear Bedding		Floor	40°23'21.25"N 8°23'23.25"W	Varzea
VAR 4.1	Shale	Dark grey	None	Very penetrative foliation Folding Clear Bedding		Road cut	40°23'21.77"N 8°22'45.82"W	Varzea
VEI 1.1	Shale	Black	Light	Light foliation		Float	40°36'33.34"N 8°25'25.03"O	Veiga
VEN-1.1	Shale	Dark grey	None	Folding Very penetrative foliation	Ox Fe e Mn Small quartz veins	Road cut	40°12'4.92"N 8°22'6.42"W	Venda Nova
ZOR1.1	Sandstone	Dark grey	Light	Very penetrative foliation	Ox Fe	Road cut	40°12'5.26"N 8°21'12.70"W	Zorro
ZOR1.2	Siltstone	Dark grey	Light	Very penetrative foliation		Road cut	40°12'5.24"N 8°21'13.59"W	Zorro

Borehole samples (AVU samples recovered from shallow and deep wells in the Lusitanian basin)

Sample	Lithology	Colour	Alteration	Deformation	Mineralization	Outcrop type	GPS Coordinates	Reference
17C1 2400m	Other	Rose	Light	Folding Very penetrative foliation	Small quartz veins	Cutting	39º28´1,8´´N 9º22'0,2" W	sondagem 17C1 2400m prof
5A1 S111 2595-2625	Shale	Dark grey	Light			Cutting	48º8'0,2"N 9º7'45"W	sondagem 5A1 S111 2595-2625prof
AC 15 80-82m	Shale	Dark grey	Light			Cutting		Sondagem AC15 (para Ampor)
AC 51 84m	Shale	Dark grey	Light			Cutting		Sondagem AC51 (para C.F.C.?)
ACC01	Shale	Dark grey	Light	Very penetrative foliation	Ox Fe S	Cutting	relatorio de sondagem	Sondagem ACC01 3ª coleção
ALJ 1/1A 2670-2685m	Shale	Dark grey	Light			Cutting	39º37'54,339´´N 8º58"51,395"	sondagem ALJ 1/1A 2670-2685m

Golfinho1 5800-5870pés	Shale	Dark grey	Light			Cutting	38º20'35,242"N 8º57'12,349´´W	sondagem Golfinho1 5800-5870pés prof
JK Torreira-Murtosa 272-274	Siltstone	Dark grey	Medium			Cutting		Sondagem JK Torreira-Murtosa
MONT1 T 1667-1669	Limestone	Black	Light			Cutting	M + 76714,06 P + 76 891,06	sondagem Montalegre1 1667-1669m
MONT1 X carote24	Shale	Light grey	Light			Cutting	M + 76714,06 P + 76 891,06	sondagem Montalegre1 1746m
Montepaio1	Shale	Rose	Light	Clear Bedding		Cutting	não sei local	sondagem Montepaio1 1140m
S1 - 14 8,4m	Shale	Dark grey	Medium	Very penetrative foliation		Cutting		Sondagem S1-14
S4 - 7 7m	Shale	Black	Light	Very penetrative foliation		Cutting		Sondagem S4-7
Sobral1 2704-2718	Shale	Dark grey	Light			Cutting	38º57´28,29N 9º11'39,00"W	sondagem Sobral1 2704-2718prof

Buçaco Basin samples

Sample	Lithology	Colour	Alteration	Deformation	Mineralization	Outcrop type	GPS Coordinates	Reference
ALG1	Sandstone	Dark grey	None			Road cut	40°25'8.46"N 8°21'47.64"W	Algeriz
ALG1.1	Sandstone	Dark grey	None			Road cut	40°25'8.46"N 8°21'47.64"W	Algeriz
ALG10.1	Coal	Black	Light	Clear Bedding Folding		Road cut		Algeriz 10
ALG10.2	Shale	Dark grey	Light	Clear Bedding Folding		Road cut		Algeriz 10
ALG10.3	Sandstone	Red	Light	Clear Bedding Folding		Road cut		Algeriz 10
ALG2.1	Shale	Dark grey	Light	Clear Bedding Folding	ferruginização	Road cutFloor	40°25'8.74"N 8°21'47.59"W	Algeriz 2
ALG2.2	Siltstone	Light grey	Light	Clear Bedding Folding		Road cut	40°25'8.74"N 8°21'47.59"W	Algeriz 2
ALG2.3	Siltstone	Dark grey	Light	Clear Bedding Folding	ferruginização	Road cut	40°25'8.74"N 8°21'47.59"W	Algeriz 2

ALG2.4	Siltstone	Dark grey	Light	Clear Bedding Folding		Road cut	40°25'8.74"N 8°21'47.59"W	Algeriz 2
ALG2.5	Siltstone	Dark grey	Light	Clear Bedding Folding		Road cut	40°25'8.74"N 8°21'47.59"W	Algeriz 2
ALG2.6	Siltstone	Dark grey	Light	Clear Bedding Folding		Road cut	40°25'8.74"N 8°21'47.59"W	Algeriz 2
ALG2.7	Siltstone	Dark grey	Light	Clear Bedding Folding		Road cut	40°25'8.74"N 8°21'47.59"W	Algeriz 2
ALG3.1	Sandstone	Light grey	Light	Clear Bedding Folding		Road cut	40°25'9.22"N 8°22'2.36"W	Algeriz 3
ALG3.2	Siltstone	Dark grey	Light	Clear Bedding Folding	capas Fe	Road cut	40°25'9.22"N 8°22'2.36"W	Algeriz 3
ALG3.3	Siltstone	Light grey	Light	Clear Bedding Folding		Road cut	40°25'9.22"N 8°22'2.36"W	Algeriz 3
ALG4.1	Siltstone	Light grey	Light	Clear Bedding Folding	capas Fe	Road cut	40°25'2.35"N 8°22'7.97"W	Algeriz 4
ALG4.2	Siltstone	Light grey	Light	Clear Bedding Folding	capas Fe	Road cut	40°25'2.35"N 8°22'7.97"W	Algeriz 4
ALG5.1	Siltstone	Dark grey	Light	Clear Bedding Folding	ferruginização	Road cut	40°25'1.06"N 8°22'11.08"W	Algeriz 5
ALG5.2	Sandstone	Dark grey	Light	Clear Bedding Folding	pouca ferruginização	Road cut	40°25'1.06"N 8°22'11.08"W	Algeriz 5
ALG6.1	Siltstone	Dark grey	Light	Clear Bedding Folding	Enxofre Fe	Road cut	40°24'57.09"N 8°22'15.08"W	Algeriz 6
ALG6.2	Shale	Dark grey	Light	Clear Bedding Folding	Enxofre Fe	Road cut	40°24'57.09"N 8°22'15.08"W	Algeriz 6
ALG6.3	Sandstone	Light grey	Light	Clear Bedding Folding		Road cut	40°24'57.09"N 8°22'15.08"W	Algeriz 6
ALG6.4	Siltstone	Light grey	Light	Clear Bedding Folding	Ferruginização	Road cut	40°24'57.09"N 8°22'15.08"W	Algeriz 6
ALG6.5	Sandstone	Light grey	Light	Clear Bedding Folding		Road cut	40°24'57.09"N 8°22'15.08"W	Algeriz 6
ALG6.6	Siltstone	Light grey	Light	Clear Bedding Folding	Fe	Road cut	40°24'57.09"N 8°22'15.08"W	Algeriz 6
ALG6.7	Coal	Black	Light	Clear Bedding Folding	Fe	Road cut	40°24'57.09"N 8°22'15.08"W	Algeriz 6

				Faultig				
ALG6.8	Shale	Black	Light	Light foliation	Fe	Road cut	40°24'57.09"N 8°22'15.08"W	Algeriz 6
ALG6.9	Sandstone	Dark grey	Light	Clear Bedding Folding	Fe	Road cut	40°24'57.09"N 8°22'15.08"W	Algeriz 6
ALG7.1	Siltstone	Light grey	Medium	Clear Bedding Folding	Ferruginização	Road cut	40°24'56.52"N 8°22'19.73"W	Algeriz 7
ALG7.10	Shale	Dark grey	Light	Clear Bedding Folding	Ox Fe	Road cut	40°24'57.87"N 8°22'25.08"O	Algeriz 7
ALG7.11	Shale	Rose	Light	Clear Bedding Folding	Ox Fe	Road cut	40°24'57.87"N 8°22'25.08"O	Algeriz 7
ALG7.12	Shale	Yellow	Light	Clear Bedding Folding		Road cut	40°24'57.87"N 8°22'25.08"O	Algeriz 7
ALG7.13	Siltstone	Brown	Medium	Clear Bedding Folding	Ox Fe	Road cut	40°24'57.87"N 8°22'25.08"O	Algeriz 7
ALG7.14	Siltstone	Brown	Medium	Clear Bedding Folding	Mn	Road cut	40°24'57.87"N 8°22'25.08"O	Algeriz 7
ALG7.2	Siltstone	Light grey	Light	Clear Bedding Folding	Ferruginização	Road cut	40°24'56.88"N 8°22'21.26"W	Algeriz 7
ALG7.3	Sandstone	Light grey	Light	Clear Bedding Folding	Ferruginização	Road cut	40°24'56.88"N 8°22'21.26"W	Algeriz 7
ALG7.4	Sandstone	Light grey	Light	Clear Bedding Folding	Ferruginização	Road cut	40°24'57.52"N 8°22'23.93"W	Algeriz 7
ALG7.5	Siltstone	Light grey	Light	Clear Bedding Folding	Ferruginização	Road cut	40°24'57.52"N 8°22'23.93"W	Algeriz 7
ALG7.6	Siltstone	Light grey	Light	Clear Bedding Folding		Road cut	40°24'57.87"N 8°22'25.08"O	Algeriz 7
ALG7.7	Sandstone	Light grey	Light	Clear Bedding Folding	Ox Fe	Road cut	40°24'57.87"N 8°22'25.08"O	Algeriz 7
ALG7.8	Sandstone	Light grey	Light	Clear Bedding Folding	Ox Fe	Road cut	40°24'57.87"N 8°22'25.08"O	Algeriz 7
ALG7.9	Sandstone	Light grey	Light	Clear Bedding Folding	Ox Fe	Road cut	40°24'57.87"N 8°22'25.08"O	Algeriz 7
ALG8.1	Coal	Dark grey	Light	Clear Bedding Folding		Road cut		Algeriz 8

ALG9.1	Siltstone	Red	Light	Clear Bedding Folding		Road cut		Algeriz 9
BOL 1.1	Siltstone	Dark grey	Light	Clear Bedding		Road cut	40°34'4.23"N 8°24'4.86"O	Bolfiar
CRI 1.1	Siltstone	Dark grey	Light	Clear Bedding Folding		Road cut	40°21'9.54"N 8°22'32.19"W	St. Cristina
CRI 1.2	Siltstone	Dark grey	Light	Clear Bedding Folding		Road cut	40°21'9.54"N 8°22'32.19"W	St. Cristina
CRI 1.3	Siltstone	Dark grey	Light	Clear Bedding Folding		Road cut	40°21'9.54"N 8°22'32.19"W	St. Cristina
CRI2.1	Sandstone	Light grey	Light	Clear Bedding Folding	Ox Fe	Road cut	40°21'10.29"N 8°22'28.48"O	Cristina 2
CRI2.2	Sandstone	Light grey	Light	Clear Bedding Folding	Ox Fe	Road cut	40°21'10.29"N 8°22'28.48"O	Cristina 2
CRI3.1	Siltstone	Light grey	Medium	Clear Bedding Folding Light foliation		Road cut	40°21'9.61"N 8°22'31.92"O	Cristina 3
CRI3.2	Siltstone	Dark grey	Light	Clear Bedding Folding		Road cut	40°21'9.61"N 8°22'31.92"O	Cristina 3
CRI3.3	Sandstone	Light grey	Light	Clear Bedding Folding		Road cut	40°21'9.61"N 8°22'31.92"O	Cristina 3
CRI3.4	Sandstone	Light grey	Light	Clear Bedding Folding		Road cut	40°21'9.61"N 8°22'31.92"O	Cristina 3
CRI3.5	Siltstone	Dark grey	Light	Clear Bedding Folding		Road cut	40°21'9.61"N 8°22'31.92"O	Cristina 3
CRI3.6	Siltstone	Dark grey	Light	Clear Bedding Folding		Road cut	40°21'9.61"N 8°22'31.92"O	Cristina 3
CRI5.1	Sandstone	Light grey	Light	Clear Bedding Folding	Ox Fe	Road cut		Cristina 5
GRA1.1	Sandstone	Red	Light	Clear Bedding Folding		Road cut	40°27'8.66"N 8°22'15.59"W	Gralheira
GRA1.2	Sandstone	Red	Light	Clear Bedding Folding		Road cut	40°27'8.66"N 8°22'15.59"W	Gralheira
GRA2.1	Shale	Light grey	Light	Clear Bedding Folding		Road cut	40°27'25.16"N 8°22'43.75"W	Gralheira
GRA5.1	Sandstone	Red	Light	Clear Bedding		Road cut	40°27'14.56"N	Gralheira

				Folding			8°22'21.09"W	
GRA5.2	Sandstone	Red	Light	Clear Bedding Folding		Road cut	40°27'14.20"N 8°22'22.86"W	Gralheira
GRA5.3	Sandstone	Red	Light	Clear Bedding Folding		Road cut	40°27'13.34"N 8°22'24.24"W	Gralheira
MON1	Sandstone	Light grey	Light			Road cut	40°24'57.03"N 8°22'16.02"W	Monsarros
MO1	Siltstone	Dark grey	Light			Road cut	40°25'11.34"N 8°22'2.88"W	Vale de Mó
MO1.1	Siltstone	Dark grey	Light			Road cut	40°25'11.34"N 8°22'2.88"W	Vale de Mó
MTN-1.5	Siltstone	Red	Medium	Very penetrative foliation	Ox Fe e Mn Small quartz veins	Floor	40°23'0.66"N 8°21'41.58"W	Monte Novo
MTN-1.6	Siltstone	Red	Medium	Clear Bedding	Ox Mn	Floor	40°23'0.66"N 8°21'41.58"W	Monte Novo
MTN-1.7	Siltstone	Red	Medium	Clear Bedding	Ox Mn	Floor	40°23'0.66"N 8°21'41.58"W	Monte Novo
MTN-1.8	Siltstone	Red	Medium	Clear Bedding	Ox Mn	Floor	40°23'0.66"N 8°21'41.58"W	Monte Novo
MTN-1.9	Siltstone	Red	Medium	Clear Bedding	Ox Mn	Floor	40°23'0.66"N 8°21'41.58"W	Monte Novo
VMO1.1	Sandstone	Red	Light	Clear Bedding Folding		Road cut	40°26'32.88"N 8°22'1.82"W	Vale da Mó 1
VMO2.1	Sandstone	Red	Light	Clear Bedding Folding		Road cut	40°26'39.05"N 8°22'7.15"W	Vale da Mó 2
VMO3.1	Sandstone	Red	Light	Clear Bedding Folding		Road cut	40°26'40.55"N 8°22'12.79"W	Vale da Mó 3
VMO4.1	Sandstone	Red	Light	Clear Bedding Folding		Road cut	40°26'38.08"N 8°22'14.72"W	Vale da Mó 4
VMO5.1	Siltstone	Light grey	Light	Clear Bedding Folding		Road cut	40°26'30.05"N 8°22'28.85"W	Vale da Mó 5A
VMO5.2	Sandstone	Dark grey	Light	Clear Bedding Folding		Road cut	40°26'31.57"N 8°22'31.44"W	Vale da Mó 5B
VMO5.3	Shale	Dark grey	Light	Clear Bedding Folding		Road cut	40°26'31.80"N 8°22'33.43"W	Vale da Mó 5C

VMO6.1	Shale	Light grey	Light	Clear Bedding Folding		Road cut	40°26'26.63"N 8°22'38.85"W	Vale da Mó 6A
VMO6.2	Siltstone	Light grey	Light	Clear Bedding Folding		Road cut	40°26'26.69"N 8°22'39.06"W	Vale da Mó 6B
VMO6.3	Shale	Light grey	Light	Clear Bedding Folding		Road cut	40°26'27.38"N 8°22'40.64"W	Vale da Mó 6B
VMO7.1	Siltstone	Light grey	Light	Clear Bedding Folding		Road cut	40°26'27.61"N 8°22'44.37"W	Vale da Mó 7A
VMO7.2	Siltstone	Light grey	Light	Clear Bedding Folding		Road cut	40°26'27.35"N 8°22'46.03"W	Vale da Mó 7B
VMO7.3	Siltstone	Light grey	Light	Clear Bedding Folding		Road cut	40°26'27.26"N 8°22'47.86"W	Vale da Mó 7C
VMO7.4	Shale	Light grey	Light	Clear Bedding Folding	Ox Fe	Road cut	40°26'27.95"N 8°22'54.76"W	Vale da Mó 8B
VMO7.5	Shale	Light grey	Light	Clear Bedding Folding		Road cut	40°26'28.13"N 8°22'56.04"W	Vale da Mó 8C
VMO9.1	Siltstone	Light grey	Light	Clear Bedding Folding		Road cut	40°26'28.00"N 8°23'2.83"W	Vale da Mó 9A
VMO9b	Siltstone	Light grey	Light	Clear Bedding Folding		Road cut	40°26'28.00"N 8°23'2.83"W	Vale da Mó 9B

Triassic samples surrounding the AVU

Sample	Lithology	Colour	Alteration	Deformation	Mineralization	Outcrop type	GPS Coordinates	Reference
ABE1.1	Siltstone	WhiteGreen	Light	Clear Bedding		Road cut	40° 8'59.52"N 8°22'49.25"W	Abelheira
CAR1.1	Sandstone	White	Light	Clear Bedding		Road cut	40° 9'19.88"N 8°23'29.74"W	Conraria
CAR1.2	Siltstone	Dark grey	Light	Clear Bedding		Road cut	40° 9'19.88"N 8°23'29.74"W	Conraria
COU1.1	Sandstone	White	Light	Clear Bedding		Road cut	40°10'27.42"N 8°24'0.71"W	Conraria
EIR 1.1	Coal	Black	Light	Clear Bedding		Road cut	40°36'27.32"N 8°31'49.48"O	Eirol

ESP1.1	Sandstone	RedWhite	Light	Clear Bedding		Road cut	40°33'58.08"N 8°29'41.46"O	Espinhel
ESP1.2	Sandstone	White	Light	Clear Bedding		Road cut	40°33'58.08"N 8°29'41.46"O	Espinhel
ESP1.3	Sandstone	White	Light	Clear Bedding		Road cut	40°33'58.08"N 8°29'41.46"O	Espinhel
ESP1.4	Siltstone	White	Light	Clear Bedding		Road cut	40°34'3.00"N 8°29'35.28"O	Espinhel
ESP1.5	Shale	White	Light	Clear Bedding		Road cut	40°33'51.06"N 8°29'40.14"O	Espinhel
ESP1.6	Siltstone	Yellow	Light	Clear Bedding		Road cut	40°33'48.18"N 8°29'29.10"O	Espinhel
Jaf1	Shale	Light grey	Light	Folding Faint bedding Strong foliation	Ferruginização (subaérea?)	Road cut	40°39'43.69"N 8°27'39.78"W	Jafafe E3
Jaf10.1	Siltstone	Red	Medium	Clear Bedding		Road cut	40°39'35.32"N 8°27'37.83"O	jafafe-macinhata
Jaf11.1	Sandstone	Red	Medium	Clear Bedding		Road cut	40°39'35.32"N 8°27'37.83"O	jafafe-macinhata
Jaf12.1	Sandstone	Red	Medium	Clear Bedding		Road cut	40°39'39.27"N 8°27'38.47"O	jafafe-macinhata
Jaf13.1	Siltstone	Red	Medium	Clear Bedding		Road cut	?	jafafe-macinhata
Jaf2	Sandstone	Yellow	Light		Ferruginização (subaérea?)	Road cut	40°39'43.69"N 8°27'39.78"W	Jafafe E3
Jaf3	Sandstone	Red	Light		Ferruginização (subaérea?)	Road cut	40°39'43.69"N 8°27'39.78"W	Jafafe E3
Jaf4	Shale	Light grey	Light	Folding Clear Bedding Ox Fe over bedding	Ferruginização (subaérea?)	Road cut	40°39'43.69"N 8°27'39.78"W	Jafafe E3
Jaf5	Shale	Black	LightNone	Very penetrative foliation	Extensive silicification	Road cut	40°39'43.67"N 8°27'40.18"W	Jafafe E3
Jaf6	Sandstone	Yellow	Medium	Clear Bedding		Road cut	40°39'38.30"N 8°27'38.33"W	Jafafe E3
Jaf8.1	Siltstone	Red	Light	Clear Bedding		Road cut	40°39'23.76"N 8°27'39.36"O	entrada de macinhata
Jaf8.2	Sandstone	Yellow	Medium	Clear Bedding		Road cut	40°39'23.76"N 8°27'39.36"O	entrada de macinhata

Jaf9.1	Siltstone	Red	Medium	Clear Bedding		Road cut	40°39'26.08"N 8°27'39.27"O	jafafe-macinhata
LAR1.1	Siltstone	Light grey	Light			Road cut	40°19'34.48"N 8°23'14.03"W	Larçã
OUT1.1	Siltstone	Light grey	Light	Clear Bedding		Road cut	40°17'45.29"N 8°23'51.66"W	Outeiro do Botão
VIL1.1	Siltstone	Green	Light	Clear Bedding		Building foundations	40°15'21.65"N 8°24'14.52"W	Vilarinho de cima

Santa Susana Basin samples

Sample	Lithology	Colour	Alteration	Deformation	Mineralization	Outcrop type	GPS Coordinates	Reference
FIG1.1	Shale	Dark grey	Light	Clear Bedding Folding		Steep hill	38°24'54.99"N 8°19'35.99"W	Vale de Figueira de Baixo
FIG2.1	Siltstone	Brown	Medium	Clear Bedding Folding		Steep hill	38°24'50.57"N 8°19'27.41"W	Vale de Figueira de Baixo
FIG2.2	Sandstone	Brown	Medium	Clear Bedding Folding		Steep hill	38°24'50.57"N 8°19'27.41"W	Vale de Figueira de Baixo
FIG3.1	Siltstone	Brown	Medium	Clear Bedding Folding		Steep hill	38°24'46.35"N 8°19'21.71"W	Vale de Figueira de Baixo
FIG3.2	Siltstone	Light grey	Medium	Clear Bedding Folding		Steep hill	38°24'46.35"N 8°19'21.71"W	Vale de Figueira de Baixo
FIG3.3	Siltstone	Light grey	Light	Clear Bedding Folding		Steep hill	38°24'46.35"N 8°19'21.71"W	Vale de Figueira de Baixo
FIG3.4	Siltstone	Dark grey	Light	Clear Bedding Folding		Steep hill	38°24'46.35"N 8°19'21.71"W	Vale de Figueira de Baixo
FIG4.1	Siltstone	Dark grey	Light	Clear Bedding Folding		Steep hill	38°24'45.21"N 8°19'19.81"W	Vale de Figueira de Baixo
FIG4.2	Siltstone	Dark	Light	Clear Bedding		Steep	38°24'45.21"N	Vale de Figueira de

		grey		Folding		hill	8°19'19.81"W	Baixo
FIG5.1	Siltstone	Dark grey	Light	Clear Bedding Folding		Steep hill	38°24'44.49"N 8°19'19.53"W	Vale de Figueira de Baixo
FIG6.1	Shale	Dark grey	Light	Clear Bedding Folding	Ox Fe	Steep hill	38°24'45.36"N 8°19'14.51"W	Vale de Figueira de Baixo
FIG6.2	Shale	Dark grey	Light	Clear Bedding Folding	Ox Fe	Steep hill	38°24'45.14"N 8°19'15.39"W	Vale de Figueira de Baixo
FIG6.3	Sandstone	Light grey	Light	Clear Bedding Folding	Ox Fe	Steep hill	38°24'45.14"N 8°19'15.39"W	Vale de Figueira de Baixo
FIG6.4	Siltstone	Dark grey	Light	Clear Bedding Folding	Ox Fe	Steep hill	38°24'45.04"N 8°19'15.90"W	Vale de Figueira de Baixo
FIG6.5	Shale	Light grey	Light	Clear Bedding Folding	Ox Fe	Steep hill	38°24'44.88"N 8°19'16.42"W	Vale de Figueira de Baixo
ORD-1.1			None					Santa Susana
ORD-1.2			None					Santa Susana
ORD-1.3			None					Santa Susana
REM-1.1			None					Santa Susana
REM-1.2			None					Santa Susana
REM-1.3			None					Santa Susana
REM-1.4			None					Santa Susana
REM-1.6			None					Santa Susana
SUS 5.1	Sandstone	Dark grey	Light	Clear Bedding		Floor	38º29.625N 08º21.255W	Santa Susana Ribeira
SUS 5.2	Sandstone	Dark grey	Light	Clear Bedding		Floor	38º29.625N 08º21.255W	Santa Susana Ribeira
SUS 5.3	Sandstone	Dark grey	Light	Clear Bedding		Floor	38º29.625N 08º21.255W	Santa Susana Ribeira
SUS 5.4	Sandstone	Dark grey	Light	Clear Bedding		Floor	38º29.625N 08º21.255W	Santa Susana Ribeira
SUS 5.5	Sandstone	Dark	Light	Clear Bedding		Floor	38º29.625N	Santa Susana Ribeira

		grey					08º21.255W	
SUS 5.6	Sandstone	Dark grey	Light	Clear Bedding		Floor	38º29.625N 08º21.255W	Santa Susana Ribeira
SUS 5.7	Sandstone	Dark grey	Light	Clear Bedding		Floor	38º29.625N 08º21.255W	Santa Susana Ribeira
SUS 6.1	Shale	Black	Heavy	Clear Bedding Faulting	Small quartz veins	Steep hill	38°29'25.38"N 8°21'34.44"W	Santa Susana topo Sul
SUS 6.2	Sandstone	Dark grey	Light	Clear Bedding		Steep hill	38°29'25.38"N 8°21'34.44"W	Santa Susana topo Sul
SUS 6.3	Shale	Dark grey	Light	Clear Bedding	Ox. Mn	Steep hill	38°29'26.40"N 8°21'31.80"W	Santa Susana topo Sul
SUS 6.4	Siltstone	Dark grey	Light	Clear Bedding Faulting		Steep hill	38°29'26.40"N 8°21'31.80"W	Santa Susana topo Sul
SUS-1	Shale	Black	None	Folding Clear Bedding	Ox Fe e Mn?	Floor	38°29'25.98"N 8°21'31.14"W	Santa Susana
SUS-2	Siltstone	Black	None				38°29'40.26"N 8°21'29.64"W	Santa Susana
SUS-3	Shale	Black	None				38°29'40.26"N 8°21'29.64"W	Santa Susana
SUS-4	Coal	Black	None		Ox Fe e Mn?		38°29'40.26"N 8°21'29.64"W	Santa Susana

Odivelas Limestone Samples (including the Caeirinha and Monte da Pena localities)

Sample	**Lithology**	**Colour**	**Alteration**	**Deformation**	**Mineralization**	**Outcrop type**	**GPS Coordinates**	**Reference**
CAE-1	Limestone	Light grey	None		Ox Fe e Mn?	Floor	38°27'29.94"N 8°19'51.90"W	Caeira
CAE4	Limestone	Light grey	Light		veios calcite	Float	38°27'31.92"N	Caeira

					estilolitos		8°19'47.88"O	
COR1.1	Limestone	Dark grey	None	Clear Bedding	Calcite veins stylolites	Quarry wall		Cortes
COR1.2	Limestone	Dark grey	None	Clear Bedding	Calcite veins stylolites	Quarry wall		Cortes
COR1.3	Other	Black	Light			Quarry wall		Cortes
COR1.4	Limestone	Dark grey	None			Quarry wall		Cortes
COR1.5	Limestone	Dark grey	None			Quarry wall		Cortes
COR1.6	Limestone	Dark grey	None			Quarry wall		Cortes
Cortes 7	Limestone	Dark grey	Light	Faint bedding	Stylolites calcite veins	Floor	38°10'40.81"N 8° 5'24.42"W	Cortes
COV 1	Other	Red	None		Small quartz veins	Floor	38°12'09.639"N 8° 4'16.588"W	Covas Ruivas
COV 2	Other	Black	None		Small quartz veins	Floor	38°11'59.775"N 8° 4'34.617"W	Covas Ruivas
COV 3	Tuff	Green	None		Ox Mn	Floor	38°12'23.49"N 8° 3'48.89"W	Covas Ruivas
PEN 1.1	Limestone	Light grey	Light		Extensive silicification	Float	38°20'34.50"N 8°15'46.68"W	PEN
PEN 1.2	Limestone	Light grey	Light		Extensive silicification	Float	38°20'34.50"N 8°15'46.68"W	PEN
PEN 2	Limestone	Light grey	Light		veios calcite	Float		PEN
RUI 1.1	Limestone	Dark grey	Light	Clear Bedding	Stylolites calcite veins	Float	38°10'40.81"N 8° 5'24.42"W	Covas Ruivas
RUI 1.2	Limestone	Dark grey	Light	Clear Bedding	Stylolites calcite veins	Float		Covas Ruivas

RUI 1.3	Limestone	Black	Light	Clear Bedding recrystalization	Stylolites calcite veins	Float		Covas Ruivas
RUI 1.4	Limestone	Black	Light	Clear Bedding		Floor	38°12'22.90"N 8° 4'49.46"W	Covas Ruivas
RUI 1.5	Limestone	Black	Light	Clear Bedding recrystalization	calcite veins Fe Ox.	Floor	38°12'22.90"N 8° 4'49.46"W	Covas Ruivas
RUI 1.6	Limestone	Black	Light	Clear Bedding recrystalization	calcite veins Fe Ox.	Floor	38°12'22.90"N 8° 4'49.46"W	Covas Ruivas
RUI 2.1	Tuff	Black	Light	Clear Bedding recrystalization		Floor	38°12'13.02"N 8° 4'40.81"W	Covas Ruivas
RUI 2.10	Tuff	Dark grey	Light	Clear Bedding recrystalization	ox Fe	Floor	38°12'13.02"N 8° 4'40.81"W	Covas Ruivas
RUI 2.11c	Limestone	Dark grey	Light	Clear Bedding recrystalization	calcite veins Fe Ox.	Floor	38°12'13.02"N 8° 4'40.81"W	Covas Ruivas
RUI 2.12c	Limestone	Dark grey	Light	Clear Bedding recrystalization	calcite veins Fe Ox.	Floor	38°12'13.02"N 8° 4'40.81"W	Covas Ruivas
RUI 2.13	Tuff	Dark grey	Medium	Clear Bedding recrystalization	Ferruginização	Floor	38°12'13.02"N 8° 4'40.81"W	Covas Ruivas
RUI 2.14	Tuff	Dark grey	Light	Clear Bedding recrystalization	Ferruginização Mn	Floor	38°12'13.02"N 8° 4'40.81"W	Covas Ruivas
RUI 2.15c	Limestone	Dark grey	Light	Clear Bedding recrystalization	calcite veins Fe Ox.	Floor	38°12'13.02"N 8° 4'40.81"W	Covas Ruivas
RUI 2.16	Tuff	Dark grey	Light	Clear Bedding recrystalization		Floor	38°12'13.02"N 8° 4'40.81"W	Covas Ruivas
RUI 2.18	Tuff	Light grey	Light	Clear Bedding recrystalization		Floor	38°12'13.02"N 8° 4'40.81"W	Covas Ruivas
RUI 2.19c	Limestone	Dark grey	Light	Clear Bedding recrystalization	calcite veins Fe Ox.	Floor	38°12'13.02"N 8° 4'40.81"W	Covas Ruivas
RUI 2.20	Tuff	Light grey	Medium	Clear Bedding recrystalization	Ox Fe Mn	Floor	38°12'13.02"N 8° 4'40.81"W	Covas Ruivas

RUI 2.21c	Limestone	Dark grey	Light	Clear Bedding recrystalization	calcite veins Fe Ox.	Floor	38°12'13.02"N 8° 4'40.81"W	Covas Ruivas
RUI 2.22c	Limestone	Dark grey	Light	Clear Bedding recrystalization	calcite veins Fe Ox.	Floor	38°12'13.02"N 8° 4'40.81"W	Covas Ruivas
RUI 2.23	Tuff	Light grey	Light	Clear Bedding recrystalization	?	Floor	38°12'13.02"N 8° 4'40.81"W	Covas Ruivas
RUI 2.24c	Limestone	Dark grey	Light	Clear Bedding recrystalization	calcite veins Fe Ox.	Floor	38°12'13.02"N 8° 4'40.81"W	Covas Ruivas
RUI 2.25c	Limestone	Dark grey	Light	Clear Bedding recrystalization	calcite veins Fe Ox.	Floor	38°12'13.02"N 8° 4'40.81"W	Covas Ruivas
RUI 2.26	Tuff	Dark grey	Light	Clear Bedding recrystalization		Floor	38°12'13.02"N 8° 4'40.81"W	Covas Ruivas
RUI 2.27c	Limestone	Dark grey	Light	Clear Bedding recrystalization	calcite veins Fe Ox.	Floor	38°12'13.02"N 8° 4'40.81"W	Covas Ruivas
RUI 2.28	Tuff	Dark grey	Medium	Clear Bedding recrystalization		Floor	38°12'13.02"N 8° 4'40.81"W	Covas Ruivas
RUI 2.29c	Limestone	Dark grey	Light	Clear Bedding recrystalization	calcite veins Fe Ox.	Floor	38°12'13.02"N 8° 4'40.81"W	Covas Ruivas
RUI 2.2c	Limestone	Dark grey	Light	Clear Bedding recrystalization	calcite veins Fe Ox.	Floor	38°12'13.02"N 8° 4'40.81"W	Covas Ruivas
RUI 2.3	Tuff	Black	Light	Clear Bedding recrystalization		Floor	38°12'13.02"N 8° 4'40.81"W	Covas Ruivas
RUI 2.30	Tuff	Dark grey	Medium	Clear Bedding recrystalization		Floor	38°12'13.02"N 8° 4'40.81"W	Covas Ruivas
RUI 2.31c	Limestone	Dark grey	Light	Clear Bedding recrystalization	calcite veins Fe Ox.	Floor	38°12'13.02"N 8° 4'40.81"W	Covas Ruivas
RUI 2.32c	Limestone	Dark grey	Light	Clear Bedding recrystalization	calcite veins Fe Ox.	Floor	38°12'12.19"N 8° 4'33.52"W	Covas Ruivas
RUI 2.33	Tuff	Dark grey	Medium	Clear Bedding recrystalization	ox fe	Floor	38°12'12.19"N 8° 4'33.52"W	Covas Ruivas

RUI 2.34c	Limestone	Dark grey	Light	Clear Bedding recrystalization	calcite veins Fe Ox.	Floor	38°12'12.19"N 8° 4'33.52"W	Covas Ruivas
RUI 2.35	Tuff	Black	MediumLight	Clear Bedding recrystalization		Floor	38°12'12.19"N 8° 4'33.52"W	Covas Ruivas
RUI 2.36c	Limestone	Dark grey	Light	Clear Bedding recrystalization	calcite veins Fe Ox.	Floor	38°12'12.19"N 8° 4'33.52"W	Covas Ruivas
RUI 2.37	Tuff	Dark grey	Medium	Clear Bedding recrystalization	Ox Fe	Floor	38°12'12.19"N 8° 4'33.52"W	Covas Ruivas
RUI 2.38	Tuff	Dark grey	Light	Clear Bedding recrystalization	Ox Fe	Floor	38°12'12.19"N 8° 4'33.52"W	Covas Ruivas
RUI 2.39c	Limestone	Dark grey	Light	Clear Bedding recrystalization	calcite veins Fe Ox.	Floor	38°12'12.19"N 8° 4'33.52"W	Covas Ruivas
RUI 2.40	Siltstone	Rose	Medium	Clear Bedding		Floor	38°12'12.19"N 8° 4'33.52"W	Covas Ruivas
RUI 2.41c	Limestone	Dark grey	Light	Clear Bedding recrystalization		Floor	38°12'12.19"N 8° 4'33.52"W	Covas Ruivas
RUI 2.42c	Limestone	Dark grey	Light	Clear Bedding recrystalization		Floor	38°12'12.19"N 8° 4'33.52"W	Covas Ruivas
RUI 2.43	Siltstone	Rose	Medium	Clear Bedding		Floor	38°12'12.19"N 8° 4'33.52"W	Covas Ruivas
RUI 2.44	Tuff	Rose	Medium	Clear Bedding		Floor	38°12'12.19"N 8° 4'33.52"W	Covas Ruivas
RUI 2.45c	Limestone	Dark grey	Light	Clear Bedding recrystalization		Floor	38°12'12.19"N 8° 4'33.52"W	Covas Ruivas
RUI 2.46	Limestone	RoseBlack	Light	Clear Bedding		Floor	38°12'12.19"N 8° 4'33.52"W	Covas Ruivas
RUI 2.47c	Limestone	Dark grey	Light	Clear Bedding recrystalization		Floor	38°12'12.19"N 8° 4'33.52"W	Covas Ruivas
RUI 2.48c	Limestone	Dark grey	Light	Clear Bedding recrystalization		Floor	38°12'12.19"N 8° 4'33.52"W	Covas Ruivas

RUI 2.49	Limestone	Black	Light	Clear Bedding		Floor	38°12'12.19"N 8° 4'33.52"W	Covas Ruivas
RUI 2.4c	Limestone	Dark grey	Light	Clear Bedding recrystalization	calcite veins Fe Ox.	Floor	38°12'13.02"N 8° 4'40.81"W	Covas Ruivas
RUI 2.50c	Limestone	Dark grey	Light	Clear Bedding recrystalization	Calcite veins	Floor	38°12'12.19"N 8° 4'33.52"W	Covas Ruivas
RUI 2.51	Limestone	Black	Light	Clear Bedding		Floor	38°12'12.19"N 8° 4'33.52"W	Covas Ruivas
RUI 2.52c	Limestone	Dark grey	Light	Clear Bedding recrystalization	Calcite veins	Floor	38°12'12.19"N 8° 4'33.52"W	Covas Ruivas
RUI 2.53	Tuff	Dark grey	Light	Clear Bedding		Floor	38°12'12.19"N 8° 4'33.52"W	Covas Ruivas
RUI 2.54c	Limestone	Dark grey	Light	Clear Bedding recrystalization	Calcite veins	Floor	38°12'12.19"N 8° 4'33.52"W	Covas Ruivas
RUI 2.55	Tuff	Dark grey	Light	Clear Bedding		Floor	38°12'12.19"N 8° 4'33.52"W	Covas Ruivas
RUI 2.56c	Limestone	Dark grey	Light	Clear Bedding recrystalization	Calcite veins	Floor	38°12'12.19"N 8° 4'33.52"W	Covas Ruivas
RUI 2.57	Tuff	Black	Light	Clear Bedding		Floor	38°12'12.19"N 8° 4'33.52"W	Covas Ruivas
RUI 2.58c	Limestone	Dark grey	Light	Clear Bedding recrystalization	Calcite veins	Floor	38°12'12.19"N 8° 4'33.52"W	Covas Ruivas
RUI 2.59	Limestone	Black	Light	Clear Bedding		Floor	38°12'12.19"N 8° 4'33.52"W	Covas Ruivas
RUI 2.5c	Limestone	Dark grey	Light	Clear Bedding recrystalization	calcite veins Fe Ox.	Floor	38°12'13.02"N 8° 4'40.81"W	Covas Ruivas
RUI 2.60c	Limestone	Dark grey	Light	Clear Bedding recrystalization	Calcite veins	Floor	38°12'12.19"N 8° 4'33.52"W	Covas Ruivas
RUI 2.61	Tuff	Black	Light	Clear Bedding		Floor	38°12'12.19"N 8° 4'33.52"W	Covas Ruivas

RUI 2.62	Tuff	Black	Light	Clear Bedding		Floor	38°12'12.19"N 8° 4'33.52"W	Covas Ruivas
RUI 2.63c	Limestone	Dark grey	Light	Clear Bedding recrystalization	Calcite veins	Floor	38°12'12.19"N 8° 4'33.52"W	Covas Ruivas
RUI 2.64c	Limestone	Dark grey	Light	Clear Bedding recrystalization	Calcite veins	Floor	38°12'12.19"N 8° 4'33.52"W	Covas Ruivas
RUI 2.65	Tuff	Black	Light	Clear Bedding		Floor	38°12'12.19"N 8° 4'33.52"W	Covas Ruivas
RUI 2.66	Tuff	Black	Light	Clear Bedding		Floor	38°12'12.19"N 8° 4'33.52"W	Covas Ruivas
RUI 2.67c	Limestone	Dark grey	Light	Clear Bedding recrystalization	Calcite veins	Floor	38°12'12.19"N 8° 4'33.52"W	Covas Ruivas
RUI 2.68c	Limestone	Dark grey	Light	Clear Bedding recrystalization	Calcite veins	Floor	38°12'12.19"N 8° 4'33.52"W	Covas Ruivas
RUI 2.69	Tuff	Black	Light	Clear Bedding	ox fe	Floor	38°12'12.19"N 8° 4'33.52"W	Covas Ruivas
RUI 2.6c	Limestone	Dark grey	Light	Clear Bedding recrystalization	calcite veins Fe Ox.	Floor	38°12'13.02"N 8° 4'40.81"W	Covas Ruivas
RUI 2.7	Tuff	Black	Light	Clear Bedding recrystalization	ox Fe	Floor	38°12'13.02"N 8° 4'40.81"W	Covas Ruivas
RUI 2.9	Tuff	Dark grey	Light	Clear Bedding recrystalization	ox Fe	Floor	38°12'13.02"N 8° 4'40.81"W	Covas Ruivas